STREPTOCOCCUS SPP. AND *CORYNEBACTERIUM SPP.*: CLINICAL AND ZOONOTIC EPIDEMIOLOGY, VIRULENCE POTENTIAL, ANTIMICROBIAL RESISTANCE AND GENOMIC TRENDS AND APPROACHES,

2nd Edition

EDITED BY: Prescilla Emy Nagao, Andreas Burkovski and Ana Luíza Mattos Guaraldi

PUBLISHED IN: Frontiers in Microbiology

frontiers Research Topics

ISSN 1664-8714
ISBN 978-2-83251-039-1
DOI 10.3389/978-2-83251-039-1

About Frontiers

Frontiers is more than just an open-access publisher of scholarly articles: it is a pioneering approach to the world of academia, radically improving the way scholarly research is managed. The grand vision of Frontiers is a world where all people have an equal opportunity to seek, share and generate knowledge. Frontiers provides immediate and permanent online open access to all its publications, but this alone is not enough to realize our grand goals.

Frontiers Journal Series

The Frontiers Journal Series is a multi-tier and interdisciplinary set of open-access, online journals, promising a paradigm shift from the current review, selection and dissemination processes in academic publishing. All Frontiers journals are driven by researchers for researchers; therefore, they constitute a service to the scholarly community. At the same time, the Frontiers Journal Series operates on a revolutionary invention, the tiered publishing system, initially addressing specific communities of scholars, and gradually climbing up to broader public understanding, thus serving the interests of the lay society, too.

Dedication to Quality

Each Frontiers article is a landmark of the highest quality, thanks to genuinely collaborative interactions between authors and review editors, who include some of the world's best academicians. Research must be certified by peers before entering a stream of knowledge that may eventually reach the public - and shape society; therefore, Frontiers only applies the most rigorous and unbiased reviews.
Frontiers revolutionizes research publishing by freely delivering the most outstanding research, evaluated with no bias from both the academic and social point of view. By applying the most advanced information technologies, Frontiers is catapulting scholarly publishing into a new generation.

What are Frontiers Research Topics?

Frontiers Research Topics are very popular trademarks of the Frontiers Journals Series: they are collections of at least ten articles, all centered on a particular subject. With their unique mix of varied contributions from Original Research to Review Articles, Frontiers Research Topics unify the most influential researchers, the latest key findings and historical advances in a hot research area! Find out more on how to host your own Frontiers Research Topic or contribute to one as an author by contacting the Frontiers Editorial Office: frontiersin.org/about/contact

STREPTOCOCCUS SPP. AND *CORYNEBACTERIUM SPP.*: CLINICAL AND ZOONOTIC EPIDEMIOLOGY, VIRULENCE POTENTIAL, ANTIMICROBIAL RESISTANCE AND GENOMIC TRENDS AND APPROACHES,
2nd Edition

Topic Editors:
Prescilla Emy Nagao, Rio de Janeiro State University, Brazil
Andreas Burkovski, University of Erlangen Nuremberg, Germany
Ana Luíza Mattos Guaraldi, Rio de Janeiro State University, Brazil

Publisher's note: In this 2nd edition, the following articles have been removed: Shi H, Li T, Xu J, Yu J, Yang S, Zhang X-E, Tao S, Gu J and Deng J-Y (2021) MgrB Inactivation Confers Trimethoprim Resistance in *Escherichia coli. Front. Microbiol*. 12:682205. doi: 10.3389/fmicb.2021.682205 and Liu Z, Liu Y, Xi W, Liu S, Liu J, Mu H, Chen B, He H, Fan Y, Ma W, Zhang W, Fu M, Wang J and Song X (2021) Genetic Features of Plasmid- and Chromosome-Mediated *mcr-1* in *Escherichia coli* Isolates From Animal Organs With Lesions. *Front. Microbiol.* 12:707332. doi: 10.3389/fmicb.2021.707332

Citation: Nagao, P. E., Burkovski, A., Guaraldi, A. L. M., eds. (2022). *Streptococcus spp*. and *Corynebacterium spp*.: Clinical and Zoonotic Epidemiology, Virulence Potential, Antimicrobial Resistance and Genomic Trends and Approaches, 2nd Edition. Lausanne: Frontiers Media SA. doi: 10.3389/978-2-83251-039-1

Table of Contents

frontiers in Microbiology

EDITORIAL
published: 28 February 2022
doi: 10.3389/fmicb.2022.867210

Editorial: *Streptococcus* spp. and *Corynebacterium* spp.: Clinical and Zoonotic Epidemiology, Virulence Potential, Antimicrobial Resistance, and Genomic Trends and Approaches

Prescilla Emy Nagao[1], Andreas Burkovski[2] and Ana Luíza Mattos-Guaraldi[3]*

[1] *Laboratory of Molecular Biology and Physiology of Streptococci, Institute of Biology Roberto Alcantara Gomes, Rio de Janeiro State University – UERJ, Rio de Janeiro, Brazil,* [2] *Microbiology Division, Department of Biology, Friedrich-Alexander-Universität Erlangen-Nürnberg, Erlangen, Germany,* [3] *Laboratory of Diphtheria and Corynebacteria of Clinical Relevance, Faculty of Medical Sciences, Rio de Janeiro State University – UERJ, Rio de Janeiro, Brazil*

Keywords: ***Streptococcus*** **spp.,** ***Corynebacterium*** **spp., epidemiology, virulence, antimicrobial resistance, genomic features**

Edited and reviewed by:
Rustam Aminov,
University of Aberdeen,
United Kingdom

****Correspondence:***
Prescilla Emy Nagao
pnagao@uol.com.br

Specialty section:
This article was submitted to Antimicrobials, Resistance and Chemotherapy, a section of the journal Frontiers in Microbiology

Received: *31 January 2022*
Accepted: *03 February 2022*
Published: *28 February 2022*

Citation:
Nagao PE, Burkovski A and Mattos-Guaraldi AL (2022) Editorial: Streptococcus spp. and Corynebacterium spp.: Clinical and Zoonotic Epidemiology, Virulence Potential, Antimicrobial Resistance, and Genomic Trends and Approaches. Front. Microbiol. 13:867210. doi: 10.3389/fmicb.2022.867210

Editorial on the Research Topic

Streptococcus spp. and *Corynebacterium* spp.: Clinical and Zoonotic Epidemiology, Virulence Potential, Antimicrobial Resistance, and Genomic Trends and Approaches

Streptococcus genus comprises pathogens implicated in human and animal diseases, economic losses to agriculture, in addition to species employed in dairy industry. Molecular genetics, taxonomic approaches, and phylogenomic investigations detected more than 100 *Streptococcus* spp. and more than nine subspecies. Studies also contributed to the understanding of highly complex features of pathogenic potential and multiple virulence mechanisms (Lannes-Costa et al., 2021), in addition to antimicrobial resistance with impact on health systems worldwide (Haenni et al., 2018).

Nowadays, *Corynebacterium* has more than 132 species, including at least 50 species of medical, veterinary, and/or biotechnological relevance. Despite global immunization programs, diphtheria outbreaks and atypical cases of diphtheria, localized, and/or systemic infections independent of diphtheria toxin production by *Corynebacterium diphtheriae* and *Corynebacterium ulcerans* zoonotic pathogen, still occur in industrialized and developing countries. Cases of infections related to different and new non-diphtherial *Corynebacterium* species have been favored by genotyping, virulence, taxonomy studies, and/or laboratorial identification techniques (Zasada and Mosiej, 2018; Silva-Santana et al., 2021).

Streptococcus spp. and non-diphtherial *Corynebacterium* species expressing multidrug-resistance profiles (MDR) have been reported with increased frequency as pathogens of invasive infections and/or nosocomial outbreaks. A detailed understanding of multifactorial pathogenic mechanisms is essential to develop new therapeutic approaches, surveillance and control strategies of streptococcal, diphtheria, and non-diphtherial corynebacterial diseases, including adhesive activities, biofilm formation, metabolite exchange, cellular communication, protection to antimicrobials, and against host immune attacks. Therefore, additional studies remain necessary to investigate phenotypic and genotypic properties of virulence mechanisms and resistance

to antimicrobial agents involved in multifactorial and complex adaptation strategies to host environmental conditions. Invasive medical devices and/or empirical antibiotic therapy may contribute to dissemination of invasive infection in hospitalized patients (Ramos et al., 2019; Figueiredo et al., 2021; Henares et al., 2021).

We thank all the authors who provided relevant aspects of *Streptococcus* spp. and *Corynebacterium* spp. to this Research Topic by analyzing different features concerning virulence, multidrug resistance, biofilm production, potential target, genetic, and environmental factors.

Streptococcus pneumoniae is an important human pathogen that can cause severe invasive pneumococcal diseases (IPDs). In a multicenter study of Zhou et al. investigated serotypes, sequence type distribution, antimicrobial susceptibility, and virulence of *S. pneumoniae* invasive strains causing IPD in China. Data provided insight into the epidemiology and virulence diversity of *S. pneumoniae* strains, including capsular polysaccharide and non-capsular virulence factors. The isolation rate of serogroup 15 *S. pneumoniae* has been increasing since developing countries began administering the 13-valent pneumococcal conjugate vaccine. Shi et al. verified that serogroup 15 *S. pneumoniae* presenting 78.57% multidrug resistance rate is common among children in China, and consequently, these strains should be continuously monitored.

Streptococcus agalactiae (group B *Streptococcus*) is one of the most important agent of bovine mastitis and causes remarkable direct and indirect economic losses to the livestock sector. Moreover, this species can cause severe human diseases in susceptible individuals. The study conducted by Carra et al. showed that human and bovine isolates strains shared the same antibiotic resistance profiles supporting the hypothesis of interspecies transmission of *S. agalactiae* between bovines and humans.

Streptococcus pyogenes (group A *Streptococcus*; GAS) is an important pathogen for humans often associated with severe and invasive diseases. No vaccine exists, so antibiotics are essential for effective treatment. Even though this pathogen remains universally susceptible to penicillin, therapeutic failures have been reported in some GAS illnesses. Additional studies remain necessary to fully explain and elucidate the mechanisms of antibiotic-unresponsive infections. Martini et al. showed that some GAS strains could form antimicrobial persisters during biofilm formation on abiotic surfaces. Gene expression assays showed upregulation of some genes associated with efflux pumps in persisters strains arising in the presence of penicillin. This event was due to non-inherited resistance mechanisms. Multifactorial mechanisms involving protein synthesis inhibition, cell growth impairment, and efflux pumps seemed to play roles in the formation of antimicrobial persisters in *S. pyogenes*. In their review, Johnson and LaRock discussed the challenges of treating GAS infection, mechanisms that contribute to antibiotic failure, and adjunctive therapeutics for improving the treatment of high-risk GAS infections by non-susceptible or resistant isolates.

Streptococcus mutans is considered the prime pathogen of dental caries. Li et al. provided new insights into the thoroughly investigated mechanism of microbial fluoride tolerance, and suggested F0F1-ATPase as a potential target for suppressing fluoride resistant strains. Moreover, *S. mutans* can secrete glucosyltransferases (GTFs) to synthesize extracellular polysaccharides, which are the virulence determinants of cariogenic biofilms. Ursolic acid, a type of pentacyclic tri terpene natural compound, was verified to decrease bacterial viability and prevent *S. mutans* biofilm formation by binding and inhibiting the activity of GTFs (Liu et al.).

In recent years, reports of infections and nosocomial outbreaks caused by antimicrobial multidrug-resistant *Corynebacterium striatum* strains have been increasing worldwide. Despite the different existing mobile genomic elements, there is evidence that acquired resistance genes are coupled to insertion sequences in *C. striatum*. This perspective article reviewed the insertion sequences linked to resistance genes, their relationship to evolutionary lineages, epidemiological characteristics, and the niches the strains inhabit. The potential of the insertion sequences for their application as a descriptor of epidemiological scenarios, allowing us to anticipate the emergence of multidrug-resistant lineages was also discussed (Leyton-Carcaman and Abanto). Dover et al. reported phylogenomic reappraisal of fatty acid biosynthesis, mycolic acid biosynthesis and clinical relevance among members of the genus *Corynebacterium*. Data suggested that although a mycolic acid-based mycomembrane is widely considered the target for interventions by the immune system and chemotherapeutics, the structure is not essential in corynebacteria and is not a prerequisite for pathogenicity or colonization of animal hosts. In the investigation using a mouse model for *Corynebacterium* in which colonization with either *Corynebacterium accolens* or *Corynebacterium amycolatum*, significantly reduced *S. pneumoniae* acquisition in the upper airway and infection in the lung. The lungs of co-infected mice had reduced pro-inflammatory cytokines and inflammatory myeloid cells, indicating resolution of infection-associated inflammation. Lipase-dependent and independent effects, indicating that both this and other bacterial factors contribute to inhibitory effects of *C. accolens* and *C. amycolatum* on *S. pneumoniae* (Horn et al.).

Finally, we would like to thank the people that supported this Research Topic and the reviewers for their time and comments that helped to improve the manuscripts.

AUTHOR CONTRIBUTIONS

PN, AB, and AM-G wrote and edited the manuscript. All authors have made substantial contributions to the article and approved the manuscript for publication.

FUNDING

The authors and their work were supported by Fundação de Amparo à Pesquisa do Estado do Rio de Janeiro

(FAPERJ), Conselho Nacional de Desenvolvimento Científico e Tecnológico (CNPq, Brazil), Sub Reitoria de Pós-Graduação e Pesquisa da Universidade do Estado do Rio de Janeiro (SR-2/UERJ), and Coordenação de Aperfeiçoamento de Pessoal de Nível Superior–Brasil (CAPES)–Finance Code 001.

ACKNOWLEDGMENTS

The editors would like to thank the authors for their contributions, and all the reviewers for their effort, expertise and constructive suggestions that significantly contributed to the quality of this Research Topic.

REFERENCES

Figueiredo, S. G., Lannes-Costa, P. S., Cristoforêto, M. C., Doran, K. S., Mattos-Guaraldi, A. L., and Nagao, P. E. (2021). *Streptococcus agalactiae* strains isolated from cancer patients in Rio de Janeiro, Brazil. *Braz. J. Microbiol.* 52, 303–310. doi: 10.1007/s42770-020-00419-6

Haenni, M., Lupo, A., and Madec, J. Y. (2018). Antimicrobial resistance in *Streptococcus* spp. *Microbiol. Spectr.* 6, 2. doi: 10.1128/microbiolspec.ARBA-0008-2017

Henares, D., Rocafort, M., Brotons, P., de Sevilla, M. F., Mira, A., Launes, C., et al. (2021). Rapid increase of oral bacteria in nasopharyngeal microbiota after antibiotic treatment in children with invasive pneumococcal disease. *Front. Cell Infect. Microbiol.* 11, 744727. doi: 10.3389/fcimb.2021.744727

Lannes-Costa, P. S., Oliveira, J. S. S., Silva, S. G., and Nagao, P. E. (2021). A current review of pathogenicity determinants of *Streptococcus* spp. *J. Appl. Microbiol.* 131, 1600–1620. doi: 10.1111/jam.15090

Ramos, J. N., Souza, C., Faria, Y. V., Silva, E. C., Veras, J. F. C., Baio, P. V. P., et al. (2019). Bloodstream and catheter-related infections due to different clones of multi-drug resistant and biofilm producer *Corynebacterium striatum*. *BMC Infect. Dis.* 19, 672. doi: 10.1186/s12879-019-4294-7

Silva-Santana, G., Silva, C. M. F., Olivella, J. G. B., Silva, I. F., Fernandes, L. M. O., Sued-Karam, B. R., et al. (2021). Worldwide survey of *Corynebacterium striatum* increasingly associated with human invasive infections, nosocomial outbreak, and antimicrobial multidrug-resistance, 1976-2020. *Arch. Microbiol.* 203, 1863–1880. doi: 10.1007/s00203-021-02246-1

Zasada, A. A., and Mosiej, E. (2018). Contemporary microbiology and identifcation of *Corynebacteria* spp. causing infections in human. *Lett. Appl. Microbiol.* 66, 472–483. doi: 10.1111/lam.12883

Conflict of Interest: The authors declare that the research was conducted in the absence of any commercial or financial relationships that could be construed as a potential conflict of interest.

Publisher's Note: All claims expressed in this article are solely those of the authors and do not necessarily represent those of their affiliated organizations, or those of the publisher, the editors and the reviewers. Any product that may be evaluated in this article, or claim that may be made by its manufacturer, is not guaranteed or endorsed by the publisher.

frontiers in Microbiology

ORIGINAL RESEARCH
published: 11 June 2021
doi: 10.3389/fmicb.2021.673126

Evidence of Common Isolates of *Streptococcus agalactiae* in Bovines and Humans in Emilia Romagna Region (Northern Italy)

Elena Carra[1], Simone Russo[1], Alessia Micheli[1], Chiara Garbarino[1], Matteo Ricchi[1], Federica Bergamini[1], Patrizia Bassi[1], Alice Prosperi[1], Silvia Piva[2], Monica Cricca[3,4], Roberta Schiavo[5], Giuseppe Merialdi[1], Andrea Serraino[2] and Norma Arrigoni[1]*

[1] Experimental Zooprophylactic Institute in Lombardy and Emilia Romagna, Brescia, Italy, [2] Department of Veterinary Medical Sciences, University of Bologna, Bologna, Italy, [3] Microbiology, DIMES, Alma Mater Studiorum, University of Bologna, Bologna, Italy, [4] Center for Applied Biomedical Research, St. Orsola-Malpighi University Hospital, Bologna, Italy, [5] Microbiology, Department of Clinical Pathology, "Guglielmo da Saliceto" Hospital, Piacenza, Italy

OPEN ACCESS

Edited by:
Prescilla Emy Nagao, Rio de Janeiro State University, Brazil

Reviewed by:
Lucia Martins Teixeira, Federal University of Rio de Janeiro, Brazil
Claudia Andrea Daubenberger, Swiss Tropical and Public Health Institute (Swiss TPH), Switzerland

***Correspondence:**
Elena Carra
elena.carra@izsler.it

Specialty section:
This article was submitted to Antimicrobials, Resistance and Chemotherapy, a section of the journal Frontiers in Microbiology

Received: *26 February 2021*
Accepted: *17 May 2021*
Published: *11 June 2021*

Citation:
Carra E, Russo S, Micheli A, Garbarino C, Ricchi M, Bergamini F, Bassi P, Prosperi A, Piva S, Cricca M, Schiavo R, Merialdi G, Serraino A and Arrigoni N (2021) Evidence of Common Isolates of Streptococcus agalactiae in Bovines and Humans in Emilia Romagna Region (Northern Italy). Front. Microbiol. 12:673126. doi: 10.3389/fmicb.2021.673126

Streptococcus agalactiae (group B *Streptococcus*, GBS) is one of the most important agents of bovine mastitis and causes remarkable direct and indirect economic losses to the livestock sector. Moreover, this species can cause severe human diseases in susceptible individuals. To investigate the zoonotic potential of *S. agalactiae*, 203 sympatric isolates from both humans and cattle, isolated in the same time frame (2018) and in the same geographic area (Emilia Romagna region, Northern Italy), were characterized by molecular capsular typing (MCT), pilus island typing (PI), and multi-locus sequence typing (MLST). In addition, antibiotic-resistant phenotypes were investigated. The distribution of the allelic profiles obtained by combining the three genotyping methods (MCT-PI-MLST) resulted in 64 possible genotypes, with greater genetic variability among the human compared to the bovine isolates. Although the combined methods had a high discriminatory power (>96,2%), five genotypes were observed in both species (20,9% of the total isolates). Furthermore, some of these strains shared the same antibiotic resistance profiles. The finding of human and bovine isolates with common genotypes and antibiotic resistance profiles supports the hypothesis of interspecies transmission of *S. agalactiae* between bovines and humans.

Keywords: *Streptococcus agalactiae*, bovines, humans, genotyping, MLST, pilus island, molecular capsular typing, antimicrobial resistance

INTRODUCTION

Streptococcus agalactiae (Group B Streptococcus, GBS) is one of the etiological agents of bovine contagious mastitis. The disease causes considerable direct and indirect economic losses to the livestock sector (Hogeveen et al., 2011; Åkerstedt et al., 2012). During the 1950s, this bacterium was the leading cause of mastitis in Europe (Katholm et al., 2012; Mweu et al., 2012). After the

application of control plans from 1960–2000, the prevalence of the infection gradually decreased, leading to disease eradication in some countries (Skoff et al., 2009; Lambertsen et al., 2010; Katholm et al., 2012).

In the 21st century, due to major changes in dairy farm management in most European countries, such as reductions in the number of farms, increased herd sizes, introduction of robotic milking systems, and selective antibiotic treatments at drying off, the prevalence of *S. agalactiae* infection in cattle has increased, and is thus considered a re-emerging problem (Skoff et al., 2009; Lambertsen et al., 2010; Katholm et al., 2012).

In Italy, the infection is widespread in the bovine population, with an estimated herd-level prevalence of 7–10% in Lombardy and Emilia-Romagna (personal data).

Streptococcus agalactiae is a commensal species of human gastrointestinal and genitourinary flora and colonizes the gastrointestinal and genitourinary tracts of 10–35% of the adult human population. The asymptomatic colonization of the large intestine and genitourinary tract of pregnant women is the main cause of infection in new-borns during childbirth (Le Doare and Heath, 2013). Moreover, it can also cause bacteremia, skin and soft tissue infections, urinary tract infections, and occasionally necrotizing fasciitis, arthritis, toxic shock syndrome, endocarditis, meningitis, and pneumonia (Sendi et al., 2008, 2011; Sunkara et al., 2012).

In this context, epidemiological studies have excluded the transmission of *S. agalactiae* between humans and cattle (Bisharat et al., 2004; Richards et al., 2011; Bergal et al., 2015; Emaneini et al., 2016); however, a recent study (Lyhs et al., 2016) that analyzed a large number of sympatric field isolates from humans and cattle highlighted how the same subtypes were present in both species, bringing back the attention of the scientific community about possible interspecies transmission of GBS. In this regard, another recent study employing a phylogenetic approach confirmed that some GBS can be transmitted between cattle and humans (Botelho et al., 2018). The same authors hypothesized that transmission to humans can occur during milking, drinking contaminated milk, or through environmental contamination.

Several methods for identifying and characterizing GBS for diagnostic and epidemiological purposes have been described. These include molecular capsular typing (MCT), multi-locus sequence typing (MLST), typing of surface proteins (such as virulence factors), and typing of surface pili that mediate interactions with host cells (Shabayek and Spellerberg, 2018). Three pilus islands (PI), PI-1, PI-2a, and PI-2b, which encode distinct pilus structures that mediate interactions with host cells, have been identified on the GBS surface (Springman et al., 2014). The MLST profiling scheme is publicly available and regularly updated (Springman et al., 2014; Furfaro et al., 2018), allowing the worldwide comparison of GBS field isolates (Jones et al., 2003).

Our research aimed to investigate whether *S. agalactiae* isolates circulating in cattle and humans shared the same genotyping profiles and the same antibiotic-resistant phenotypes. For this purpose, sympatric field isolates from dairy cattle and human patients from hospitals located in the same territorial area (Emilia Romagna Region, Northern Italy) were compared using combined molecular subtyping methods.

MATERIALS AND METHODS

Bovine and Human Isolates

From January to September 2018, during routine diagnostic activity at the Istituto Zooprofilattico Sperimentale della Lombardia and Emilia Romagna (IZSLER) Laboratories, 191 *S. agalactiae* isolates were collected from the milk of individual cows from 49 different herds from five provinces of the Emilia-Romagna region (Piacenza, Parma, Reggio Emilia, Modena, Bologna). Phenotypic identification was performed according to the recommendations of the National Mastitis Council (Adkins et al., 2017). At least three isolates were selected for each herd, choosing those showing different serotypes (for the definition see below), except for two herds located in the Parma province, in which four isolates were selected because they all belonged to different serotypes. All isolates came from the diagnostic activity of all lactating cows of infected herds submitted to eradication plans. The sampled animals were affected by subclinical infections and were only characterized by high somatic cell counts (SCC). This presentation of the disease is most common in cattle (Adkins et al., 2017). For the purposes of the eradication plans, the SCC data were not collected and were not relevant for subsequent actions (isolation, separate milking, or antimicrobial therapy). Based on this criterion, 103 isolates were selected for molecular typing: 53 isolates from 28 herds in Parma province, 20 isolates from nine herds in Reggio Emilia province, 15 isolates from seven herds in Piacenza province, 12 isolates from four herds in Modena province, and three isolates from one herd in Bologna province (**Table 1**).

In the same period (February–July 2018), 100 *S. agalactiae* isolates of human origin were collected. In detail, 49 patients were from the Guglielmo da Saliceto Hospital, in Piacenza province, and 51 from patients of the Polyclinic S. Orsola-Malpighi in Bologna province. These isolates were from different sources, mainly vaginal swabs and vaginal–rectal swabs (71,0%), collected in the context of surveillance of pregnant women, and from urine, urethral swabs, and other sources (29,0%) from symptomatic patients.

Human urines and genital swabs were processed as follow: one μL of urine was seeded in Horse Blood Agar media (Vacutest Kima, Italy), selective (Chrome Candida, Vacutest Kima, Italy) and non-selective chromogenic media (Chrome Orientation, Vacutest Kima, Italy) and incubated at 37°C for 24 and 48, respectively. Genital swabs were directly streaked in the above described media. Ano-genital swabs were collected for *S. agalactiae* screening during late pregnancy, enriched in Lim Broth (Copan, Italy) and incubated at 37°C for 16–24 h, then 10 μL of broth were seeded in chromogenic agar plate (ChromeAgar StrepB, Vacutest Kima, Italy or in ChromID® Strepto B agar, Biomeriéux, Italia) and incubated at 37°C for 24 h.

Streptococcus agalactiae suspected colonies were sub-cultured onto tryptone soy agar media with sheep blood (Vacutest Kima, Italy) for 16 h of incubation, then the bacterial isolates

TABLE 1 | Origin and characteristics of *Streptococcus agalactiae* isolates included in this study.

Host	Number of isolates	Geographical origin (province)	Number of herds	Number of MCT-PI-MLST profiles
Bovine	53	Parma	28	18*
	20	Reggio Emilia	9	7
	15	Piacenza	7	8
	12	Modena	4	4
	3	Bologna	1	1
TOTAL	**103**		**49**	
Host	**Number of isolates**	**Geographical origin (province)**	**Number of hospitals**	**Number of MCT-PI-MLST profiles**
Humans	49	Piacenza	1	24*
	51	Bologna	1	27
TOTAL	**100**		**2**	

**With the exclusion of one isolate from an incomplete MLST profile.*
MCT, molecular capsular typing; PI, pilus island typing; MLST, multi-locus sequence typing.
The numbers in bold represent the total of bovine and human Isolates in the second column, respectively, and the numbers of herds and hospitals in the fourth column.

were identified by MALDI-TOF Mass Spectrometry (Bruker, Milan, Italy). Finally, the clinical isolates were frozen at −70°C using MicroBank vials (Pro-Lab Diagnostics, Round Rock, TX, United States).

The details of the isolation matrices and the characteristics of all bovine and human isolates included in this study are listed in **Supplementary Tables 1, 2**, respectively.

Species Identification and Lactose Typing

DNA was extracted from each isolate using a semi-automatic method. Briefly, a few colonies were suspended in 100 μL of distilled water and then processed according to the One-For-All-Vet kit (Qiagen, Milan, Italy).

To confirm the phenotypic identification of *S. agalactiae*, the extracted DNA was subjected to species-specific PCR (Lyhs et al., 2016).

Subsequently, all isolates were subjected to phenotypic lactose typing (LT), testing the ability of each GBS to metabolize lactose. For this purpose, some colonies of each isolate were suspended in phenol red broth (BioLife, Milan, Italy) supplemented with lactose monohydrate (Carlo Erba, Val de Reuil, France) and incubated for up to 7 days at 37°C (Lyhs et al., 2016).

Molecular Capsular Typing

A multiplex MCT PCR assay was performed to detect all known GBS capsular polysaccharides (s) according to Poyart et al. (2007).

Pilus Island Typing

Multiplex PCR was used to screen for the presence of PI genes in a final volume of 25 μL with three primer pairs (PI-1: SAG647_F496, SAG647_R889; PI 2a: SAG1406_F356, SAG1406_R598; PI 2b: SAN1517_F57, SAN1517_R575) as previously described (Springman et al., 2014), using the Mastermix GoTaq® G2 Hot Start Colorless (Promega, Madison, WI). The amplification products were electrophoresed on a 1.8% agarose gel stained with Midori Green Advance (NIPPON Genetics Europe, Deuren, Germany) in 0.5× TBE running buffer (Sigma-Aldrich, St. Louis, MO, United States) at a constant voltage (90 V) in the presence of a 100-bp DNA ladder (Invitrogen, Carlsbad, CA, United States) and visualized on an ultraviolet trans-illuminator. The expected size fragments were 394, 243, and 519 bp for PI-1, PI-2a, and PI-2b, respectively (**Figure 1**). For PI-1, the presence of a 684-bp amplicon indicated an intact integration site; otherwise, the absence of an amplicon indicated occupation by an alternative, uncharacterized genetic element (Springman et al., 2014). The method was also applied to the ATCC 13813 *S. agalactiae* strain (**Figure 1**) as a positive control.

Multi-Locus Sequence Typing

The MLST genotyping protocol of the selected *S. agalactiae* isolates was performed according to a previous study (Jones et al., 2003). In detail, seven housekeeping genes encoding alcohol dehydrogenase (adhP), phenylalanine tRNA synthetase (pheS), amino acid transporter (atr), glutamine synthetase (glnA), serine dehydratase (sdhA), glucose kinase (glcK), and transketolase (tkt) were genotyped. PCR reactions were performed in 10 μL volumes using the Mastermix GoTaq® G2 Hot Start Colorless (Promega). The PCR conditions were 95°C for 2 min, followed by 30 cycles at 94°C for 1 min, 55°C for 45 s, and 72°C for 1 min, and 5 min at 72°C before cooling at 4°C. PCR products were purified by enzyme treatment with a mixture of exonuclease I and shrimp alkaline phosphatase (GE Healthcare, Little Chalfont, United Kingdom). Purified PCR products were sequenced in both directions using the GenomeLab DTCS Quick Start Kit (Beckman Coulter, Indianapolis, IN, United States) in a final volume of 10 μL using sequencing primers according to the above reference (Jones et al., 2003). Sequencing was performed with a Sciex GenomeLab™ GeXP sequencer (Beckman Coulter), and the results were analyzed and assembled using the "Sequencing" and "Investigator" packages of GenomeLab™ System software, version 11.0.24. Alleles and sequence type (ST) were assigned

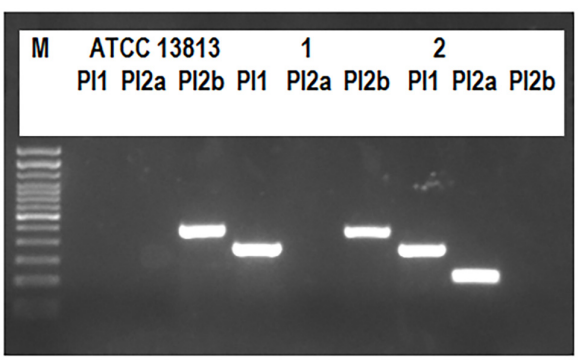

FIGURE 1 | Pilus island typing. The expected fragment sizes were 394, 243, and 519 bp for PI-1, PI-2a, or PI-2b, respectively. The image shows the pilus island profiles obtained for the ATCC 13813 strain, and for the human 1–109 (1) and 2–109 (2) isolates.

using the *S. agalactiae* database[1] (Jolley et al., 2018). Isolates were assigned an ST according to their allelic profiles. New alleles were submitted to the database curator for quality control and the allocation of allele numbers and STs. Novel allele combinations were also submitted for ST assignment.

Data Analysis

Global eBURST analysis was performed using PHYLOVIZ software (available online) (Francisco et al., 2012): isolates sharing the same alleles in at least five of seven loci were included in the same clonal complex (CC) (Furfaro et al., 2018).

The evolutionary relationships among STs, representing 3,456 nucleotides of the seven MLST genes, were inferred using the neighbor-joining (NJ) method. Evolutionary distances were calculated using the *p*-distance method, which considers the number of different nucleotides out of the total, and an NJ tree with 1,000 bootstrap replications was constructed using MEGA5 software (Tamura et al., 2011).

The discriminatory power of the different methods, alone or in association, was evaluated using the Simpson's index of diversity (Mokrousov, 2017), using a free online tool[2].

Antimicrobial Susceptibility Testing

The susceptibility of the isolates was analyzed using the disc diffusion method according to the Clinical and Laboratory Standard Institute (CLSI) guidelines (Clinical and Laboratory Standard Institute (CLSI), 2018b). The zone diameter interpretative standards of CLSI-M100 Ed29 and CLSI-VET08 Ed4 (Clinical and Laboratory Standard Institute (CLSI), 2018a, Clinical and Laboratory Standard Institute (CLSI), 2019) were used for interpretation.

The antimicrobial tests were those included in the laboratory panel for mastitis Gram-positive pathogens of IZSLER. The molecules used are representative antimicrobials that can predict susceptibility to other members of the same class, according to the guidelines of the Italian Reference Centre for Antimicrobial Resistance[3].

The following antimicrobials were tested: amoxicillin-clavulanic acid (20–10 μg), ampicillin (10 μg), cephalothin (30 μg), ceftiofur (30 μg), erythromycin (15 μg), kanamycin (30 μg), penicillin G (10 IU, International Units), pirlimycin (2 μg), rifampicin (5 μg), sulfisoxazole (300 μg), tetracycline (30 μg), and trimethoprim-sulfamethoxazole (1.25–23.75 μg).

RESULTS

MCT and LT

All Selected Isolates Were Confirmed to Be *S. agalactiae* Using Species-Specific PCR

The results of MCT on the selected cattle and human isolates are reported in **Supplementary Tables 1, 2**, respectively. The MCT results summarized in **Table 2** show that serotypes Ia, Ib, II, III, IV, and V were common to human and bovine isolates, while there were no isolates with serotypes VI, VII, and VIII in either cattle or humans.

In bovines, serotype IV was predominant in 39 out of 103 (37.9%) isolates, followed by Ia in 26 out of 103 (25.2%), while three isolates (2.9%) did not return any PCR results (**Supplementary Table 1**). In humans, the predominant serotype was V in 31 out of 100 cases (31.0%) (**Supplementary Table 2**).

The ability to ferment lactose was common in cattle (98.1%) and rare (9.0%) in human isolates.

PI Typing

The PI-1/2b profile was the most common type among bovine isolates (44.7%), while the PI-1/2a profile was the most common among human isolates (46.0%) (**Table 2** and **Supplementary Tables 1, 2**).

MLST

A Total of 45 Different STs Were Obtained From MLST Analysis of All 203 Isolates

Specifically, 27 different STs were obtained among the 103 bovine isolates, 11 of which were new and deposited in PubMLST (ST1363-ST1368, ST1389-ST1391, and ST1397-ST1398). The most frequent profiles were ST103 (16/103, 15.5%), ST297 (13/103, 12.6%), ST1363 (13/103, 12.6%), and ST591 (12/103, 11.7%) (**Supplementary Table 1**). In five bovine isolates, indicated with an asterisk in **Supplementary Table 1**, PCR amplification of the *glcK* gene produced a 3.0-kb band instead of the expected 0.5-kb band. This increase in the fragment size was found to be due to a mobile genetic element which was inserted at an identical point in the *glcK* gene in each of these five isolates. As MLST analysis creates concatenated sequences, the nucleotide sequence of the mobile element was ignored and removed, leaving the intact *glcK* sequence corresponding to allele 1 for all isolates.

Among the 100 human isolates, 25 different STs already described were obtained (Jolley et al., 2018), and the most frequent STs were ST17 (21/100, 21.0%), ST1 (14/100, 14.0%), ST19 (10/100, 10.0%), and ST23 (9/100, 9.0%) (**Supplementary Table 2**). The most frequent STs were isolates from both symptomatic and asymptomatic human cases.

The common STs in both groups were ST1, ST2, ST4, ST12, ST19, ST23, and ST498 (**Table 2** and **Supplementary Tables 1, 2**).

Global eBURST analysis (**Figure 2**) showed that 13 STs were singletons, not belonging to any CC, eight of which were from cattle and five from humans (**Table 2**). The remaining 32 STs, with single- and double-locus variants, were grouped into seven CCs: CC17 was exclusively found in human isolates, while the other six (CC1, CC19, CC23, CC358, CC498, and CC932) were common to both groups.

The evolutionary relationships of the 45 ST profiles are shown in an NJ phylogenetic tree (**Figure 3**), where we have underlined how the different genotypes are related to each other. This may explain, for example, the presence in the same herd (PC06) of isolates with different sequence types (ST19 and ST27),

[1] http://pubmlst.org/sagalactiae/

[2] http://www.comparingpartitions.info/?link=Tool

[3] www.izslt.it./crab/linee-guida-per-linterpretazione-delle-prove-di-sensibilita-ai-chemioantibiotici-*in vitro*-per-un-utilizzo-nella-terapia-clinica/

TABLE 2 | Results of the molecular capsular typing, pilus island typing, and multi-locus sequence typing of 201 *Streptococcus agalactiae* isolates.

MCT	PI	ST	S/CC	Number of isolates
BOVINE				
0	2a	2	CC1	3
Ib	1 2a	1	CC1	1
IV	1 2a	459	CC1	1
IV	1 2a	1390	CC1	1
IV	**1 2b**	**297**	**CC1**	**13**
IV	**1 2b**	**1363**	**CC1**	**13**
IV	1 2b	1364	CC1	3
IV	1 2b	1365	CC1	2
IV	1 2b	1367	CC1	1
IV	2b	1391	CC1	1
IV	2b	1398	CC1	3
V	**1 2a**	**1**	**CC1**	**5**
III	**1 2a**	**19**	**CC19**	**1**
III	1 2a	27	CC19	2
III	1 2a	1397	CC19	1
Ia	**2a**	**23**	**CC23**	**1**
Ia	2a	1002	CC23	2
III	1 2a	23	CC23	3
Ia	2a	12	CC358	1
V	**2a**	**498**	**CC498**	**3**
Ia	**1 2b**	**4**	**CC932**	**1**
Ia	1 2a	1366	S	2
Ia	1 2b	591	S	1
Ia	**2b**	**103**	**S**	**16**
Ia	2b	314	S	2
Ib	2a	6	S	3
II	**1 2b**	**591**	**S**	**11**
II	2b	310	S	1
III	2b	1389	S	3
IV	1 2b	1368	S	1
HUMAN				
II	1 2a	1	CC1	1
II	1 2a	139	CC1	1
II	2a	2	CC1	1
IV	1 2a	196	CC1	1
IV	1 2b	196	CC1	2
V	**1 2a**	**1**	**CC1**	**13**
III	1 2a	17	CC17	1
III	**1 2b**	**17**	**CC17**	**18**
III	1 2b	126	CC17	1
III	2b	17	CC17	2
II	1 2a	19	CC19	1
II	1 2a	28	CC19	4
II	2a	19	CC19	2
II	2a	28	CC19	2
III	**1 2a**	**19**	**CC19**	**3**
V	1 2a	19	CC19	6
V	1 2a	28	CC19	1
V	1 2a	109	CC19	1
Ia	**2a**	**23**	**CC23**	**9**
Ia	2a	55	CC23	1
Ia	2a	144	CC23	2
Ib	1 2a	8	CC358	1
Ib	1 2a	10	CC358	1
Ib	1 2a	12	CC358	1
II	1 2a	10	CC358	1
II	1 2a	12	CC358	1
II	2a	358	CC358	1
Ia	2a	24	CC498	1
Ia	2a	498	CC498	1
V	**2a**	**498**	**CC498**	**5**
Ia	**1 2b**	**4**	**CC932**	**1**
II	1 2b	932	CC932	1
II	1 2a	569	S	2
II	2a	22	S	1
III	1 2a	529	S	3
III	2a	529	S	1
V	1 2a	529	S	1
V	1 2a	832	S	1
V	2a	26	S	2

The most frequently combined genotypes are in bold. Common combined genotypes between bovines and humans are put in evidence by the same color.

which, although different, are evolutionarily related and belong to the same CC (CC19).

Combination of Typing Methods

Considering the combination of the three typing methods (MCT-PI-MLST), it was possible to obtain 64 combined profiles for 201 out of 203 isolates; two isolates were excluded because their MLST profiles were incomplete (**Supplementary Tables 1, 2**).

Simpson's index of diversity was 0.962 (95% CI: 0.953–0.971). The most frequent combined profiles are shown in bold in **Table 2**, where the five allelic profiles common to bovines and humans (V-1 2a-ST1, III-1 2a-ST19, Ia-2a-ST23, V-2a-ST498, and Ia-12b-ST4) are marked in the same colors.

By analyzing the MCT results, we found the presence of sympatric field isolates belonging to different serotypes in two herds: serotypes Ia and IV in herd PR2, and serotypes Ib and V in herd PR15. This observation was confirmed by the MLST analysis. In herd PR2, we observed the presence of isolates ST103 and ST297, which were associated with serotypes Ia and IV, respectively, whereas in herd PR15, ST1, and ST498 were associated with serotypes Ib and V, respectively.

Antimicrobial Susceptibility Testing

Table 3 Shows the Percentages of Isolates Resistant to the Main Classes of Antibiotics

All field isolates were sensitive to beta-lactam antibiotics (amoxicillin-clavulanic acid, ampicillin, cephalothin, ceftiofur, and penicillin G) and rifampicin.

All field isolates were resistant to aminoglycosides (representative molecule: kanamycin) because of the intrinsic resistance of *Streptococcus* to this category of molecules.

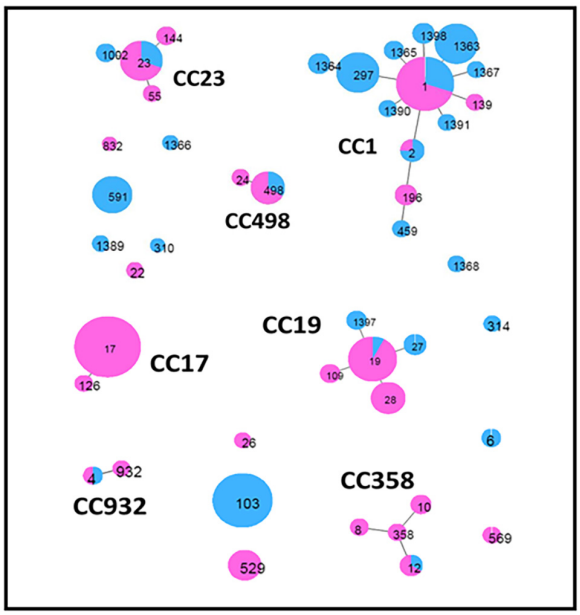

FIGURE 2 | Minimum spanning tree obtained by global eBurst analysis using PHYLOVIZ software. This shows the distribution of host species across clusters of *Streptococcus agalactiae* sequence types (STs) obtained in the present study. Each circle represents an ST. The size of the circle and its colored segments are proportional to the number and origin of isolates, where pink refers to humans and blue refers to bovines, respectively. Clusters, including single- and double-locus variants, are indicated by the corresponding clonal complex (CC).

Different proportions of isolates resistant to erythromycin, pirlimycin, sulfisoxazole, and tetracycline were observed in both groups. In particular, resistance to sulfisoxazole and tetracycline was the most widespread in both groups.

The resistance of human and bovine GBSs to these antibiotics was associated with many different serotypes and STs, as reported in **Table 4**. We observed two bovine III-ST23 and eight human Ia-ST23 isolates that were resistant to sulfisoxazole and/or tetracycline. In addition, many human and bovine 1 2a-ST1 and 2a-ST498 isolates, in combination with serotype V, are often resistant to one or more of the following antibiotics: erythromycin, pirlimycin, sulfisoxazole, and tetracycline.

Human ST19 isolates associated with serotype II or V showed multi-resistance, while all bovine ST19 isolates were susceptible to all antibiotics.

Notably, we observed one human and one bovine isolate, both from the same province, with the same combined Ia-1 2b-ST4 profile, showing resistance to sulfisoxazole.

Finally, among the most common human and bovine isolates (those showing profiles III-ST17 and Ia-ST103, respectively), we often observed resistance to sulfisoxazole and/or tetracycline.

DISCUSSION

To investigate the zoonotic potential of *S. agalactiae* in Italy, a collection of 203 sympatric *S. agalactiae* isolates from both humans and cattle, isolated in the same time frame (2018) and in the same geographic area (Emilia Romagna region, Northern Italy), were characterized.

Previously, Gherardi et al. (2007) and De Francesco et al. (2012) provided insight into the correlation among clonal types, serotypes, surface proteins, and antibiotic resistance of many Italian human isolates, highlighting clonal spread of the Italian GBSs. On the contrary, no studies on cattle isolates from Italian herds are so far available in the international literature.

Recently Lyhs et al. (2016) analyzed many sympatric isolates from humans and cattle in Finland and Sweden and highlighted how the same GBS subtypes were present in both species.

With regard to serotypes, serotype V was the most widespread in both species in Finland and Sweden (Lyhs et al., 2016). In Spain (Rojo-Bezares et al., 2016), serotype III (associated with serious infections in humans) was predominant in humans, while in Iran (Emaneini et al., 2016), serotype III was predominant in both humans and cattle, followed by serotype V in humans. In Algeria and France, serotype V was the most prevalent among human isolates (Bergal et al., 2015). In the United States, there was an increase in the prevalence of human isolates with serotype IV from 1990–2010 (Diedrick et al., 2010); moreover, they observed a higher representation of serotype Ia compared to the rest of the world (Ippolito et al., 2010). In our study, serotypes IV and Ia were the most prevalent in cattle, whereas serotype V was prevalent in humans, confirming the widespread diffusion of this serotype in humans (Gherardi et al., 2007; De Francesco et al., 2012; Bergal et al., 2015; Emaneini et al., 2016; Lyhs et al., 2016; Furfaro et al., 2018). We found three cattle isolates that could not be typed by MCT, as previously observed (Diedrick et al., 2010). This could be related to mutations in the alignment region of primers, the presence of non-specific capsular types, or absence of the capsule, as hypothesized by Carvalho-Castro et al. (2017). In contrast, the presence of mobile genetic elements in five bovine isolates recovered in the present study seems to be related to a particular bovine GBS lineage (Bisharat et al., 2004; Martins et al., 2010).

Notably, the ability to ferment lactose by almost all the cattle isolates may be due to a host adaptation mechanism in the cattle udder environment, as suggested by Lyhs et al. (2016).

PI typing was performed to verify the assignment of the field isolates to the possible profiles (PI-1, PI-1/2a, PI-1/2b, PI 2a, and PI 2b). Given the role of pili in GBS colonization and disease progression, the type of pilus affects GBS colonization and invasion of host cells (Richards et al., 2011). In this regard, we observed that the PI-1/2b profile and PI-1/2a were the most common types among bovine and human isolates, respectively, in line with previous reports (Springman et al., 2014; Lyhs et al., 2016; Shabayek and Spellerberg, 2018).

Out of the 45 different STs obtained by MLST analysis, 32 STs (corresponding to 74,6% of total) were grouped into seven CCs, with large differences within groups of clones. The most prevalent CCs were CC1, CC19, CC17, and CC23, as previously observed (Lyhs et al., 2016). Interestingly, ST1 (CC1), ST2 (CC1), ST4 (CC932), ST12 (CC358), ST19 (CC19), ST23 (CC23), and ST498 (CC498) profiles were common in cattle and humans. ST498, which has so far been isolated only in humans, was found in three

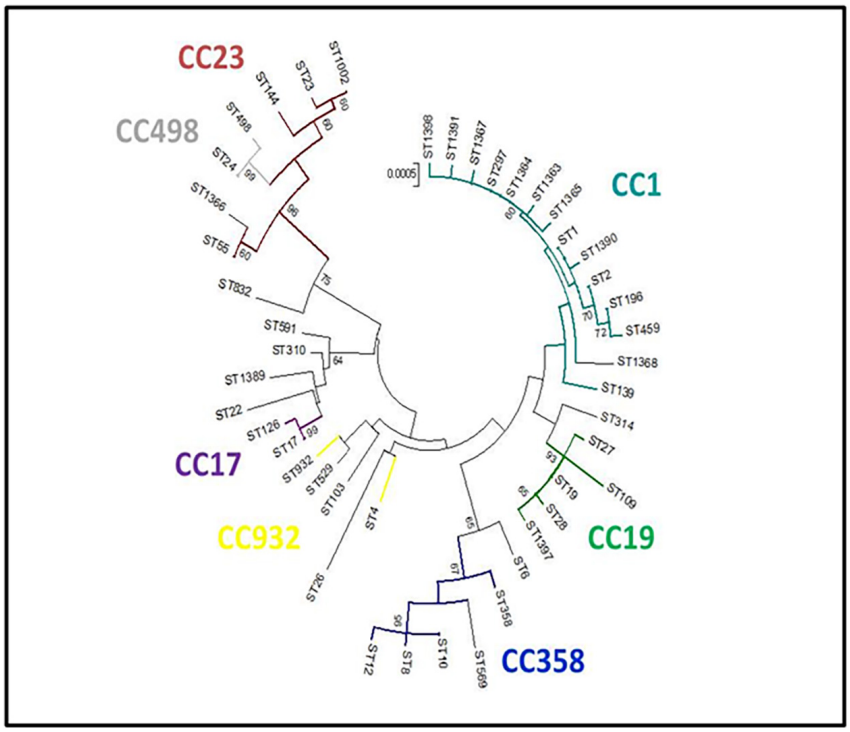

FIGURE 3 | Neighbor-joining (NJ) tree. Genetic relationships among the 45 *S. agalactiae* sequence types (STs) obtained in the present study were inferred with MEGA5 software [14]. Evolutionary distances were calculated using the *p*-distance method, which considers the number of different nucleotides out of the total (3,456). A NJ tree with 1,000 bootstrap replications was constructed. The clonal complexes (CCs) obtained by the global eBURST analysis are reported.

cattle isolates in our study, suggesting a possible transfer between the two species.

Among human isolates, four STs (ST17, ST1, ST19, and ST23), corresponding to 56,6% of all STs, were the most widespread, as previously reported (Bisharat et al., 2004; Gherardi et al., 2007; De Francesco et al., 2012; Botelho et al., 2018; Furfaro et al., 2018). Notably, the main STs included in CC1 (ST1) and CC19 (ST19), in combination with different serotypes, have been associated with healthy carriers of Guillain-Barré syndrome and are responsible for the majority of GBS infections (Poyart et al., 2007; Bergal et al., 2015). The data obtained confirm that ST17, which is associated with capsular type III, has a known host-specific human profile, is associated with invasive neonatal diseases (Martins et al., 2010; Bergal et al., 2015; Lyhs et al., 2016; Lannes-Costa et al., 2020), and is one of the most frequent human STs, mainly in asymptomatic pregnant women. ST196 (serotype IV) was found in only three human isolates: one from a biopsy and two from vaginal swabs. These findings are relevant because GBSs with ST196 profiles are currently recognized as emerging pathogens for humans and have also been reported in cattle, which may therefore represent a potential reservoir (Lyhs et al., 2016).

TABLE 3 | Antimicrobial susceptibility testing.

	Bovine isolates not susceptible (intermediated or resistant) *N* = 103	Human isolates not susceptible (intermediated or resistant) *N* = 100
Amoxicillin-clavulanic acid	0	0
Ampicillin	0	0
Cephalothin	0	0
Ceftiofur	0	0
Erythromycin	11 (10.7%)	15 (15%)
Kanamycin	103 (100%)	100 (100%)
Penicillin G	0	0
Pirlimycin	9 (8.7%)	12 (12%)
Rifampicin	0	0
Sulfisoxazole	23 (22.3%)	44 (44%)
Tetracycline	32 (31.1%)	36 (36%)
Trimethoprim – sulfamethoxazole	1 (1.0%)	0

The percentages of isolates by origin (bovine and human) resistant to representative molecules of the main classes of antibiotics.

Among bovine isolates, ST103 (S), ST297 (CC1), ST1363 (CC1), and ST591 (S) were the most prevalent, accounting for 52.4% of all bovine isolates. ST103 (serotype Ia), commonly reported among bovine isolates (Ippolito et al., 2010; Zadoks et al., 2011; Jørgensen et al., 2016; Lyhs et al., 2016; Botelho et al., 2018), was confirmed to be the most common type in cattle. Moreover, in some countries, ST103 has been circulating for a longer time (Zadoks et al., 2011) than elsewhere. In particular, in Brazil, ST103 was recovered from bovine and human isolates in the 1980s (Oliveira et al., 2006), where it

TABLE 4 | Molecular capsular typing and sequence types of the bovine and human resistant isolates.

	Bovine isolates		Human isolates	
	MCT	**ST**	**MCT**	**ST**
Erythromycin	Ia	12, 1,366		
	Ib	1	Ib	10
	II	591 (2)	II	19, 22, 28
	V	1, 498 (3)	V	1 (7), 19, 109, 498, NT
	NT	2		
Kanamycin		All strains		All strains
Pirlimycin	Ib	1	Ib	10
	III	1,397	II	19, 22
	IV	459, 1,363		
	V	1 (2), 498	V	1 (7), 19, NT
	NT	2 (2)		
Sulfisoxazole	Ia	4, 103 (4), 591, 1002, 1366	Ia	4, 23 (8), 55, 144
			Ib	8, 12
	II	591 (7)	II	10, 12, 19 (2), 22, 28 (4), 932
	III	23 (2)	III	17 (10), 19 (2)
	IV	297 (3), 1363, 1365	IV	196
	V	1	V	1 (2), 19 (2), 26, 498, 832, NT
Tetracycline	Ia	12, 23, 103 (11), 314 (2), 1002 (2)	Ia	23 (4), 24, 498
	Ib	1, 6 (3)	Ib	12
			II	1, 12, 19 (2), 22, 28 (2), 569, 932
	III	27, NT	III	17 (5), 529 (2)
	IV	297, 459, 1363, 1398,	IV	196 (2)
	V	498 (3)	V	1 (4), 19, 26 (2), 498, 529, 832, NT
	NT	2 (2)		
Trimethoprim – sulfamethoxazole	V	1		

MCT, molecular capsular typing; ST, sequence type.

has been reported to colonize the gastrointestinal tract of cattle, survive in the environment, and adapt well to the fecal-oral transmission pathway. These characteristics could be a critical point for *S. agalactiae* eradication in infected herds, unless appropriate environmental sanitation measures are put in place (Jørgensen et al., 2016). In Denmark, ST103 has only recently been detected as a consequence of the re-emergence of GBS as a significant cause of bovine mastitis (Zadoks et al., 2011). In the present study, ST103, even if it is the most frequent ST among bovine isolates, is not included in any CC and was detected only in this species, possibly because it was only recently introduced in cattle in this area.

In addition, we observed the circulation of isolates with different serotypes, PIs, and STs within the same farm. This observation highlights the possibility of co-infection caused by multiple genetically distinct isolates within the same herd. This may be attributed to the lack of biosecurity programs, or because of the introduction of cows with *S. agalactiae* infection or to different reservoirs of this pathogen other than infected mammary glands (Jørgensen et al., 2016; Tomazi et al., 2018).

Notably, previous studies (Lyhs et al., 2016; Botelho et al., 2018) did not report a Simpson's index of diversity, while in the present study, the combination of MCT, PI typing, and MLST resulted in a Simpson's index of diversity of 0.962 (95% CI: 0.953–0.971). This underlines the possibility of recovery of isolates with the same allelic profile in both cattle and humans, reinforcing the possibility of transmission between these two groups.

This hypothesis is supported by the observation that isolates from both groups not only share the same genotypes, but also the same antibiotic resistance profiles.

In addition, we noticed that human isolates always showed a higher rate of resistance to sulphamidic and tetracycline antibiotics than cattle strains, independent of their allelic profiles. In accordance with other studies (Gherardi et al., 2007; De Francesco et al., 2012; Bergal et al., 2015), most resistant isolates in the present study belonged to serotype V and CC-1, CC-498, and CC-19 clonal groups. Moreover, the resistance of *S. agalactiae* to erythromycin seems to be lower in cattle than in human isolates, with some differences among clusters, as previously reported (Lyhs et al., 2016; Tomazi et al., 2018). The resistance to erythromycin (10.7% and 15.0% in bovine and human isolates, respectively) seems to agree with the 15% of resistant isolates reported in a previous Italian study in humans (De Francesco et al., 2012), but lower than 29% and 40% recently observed by Tomazi et al. (2018) in bovine isolates from Brazil and by Bergal et al. (2015) in isolates recovered from clinical human cases in Algeria and France, respectively.

In conclusion, by analyzing sympatric GBS isolates, we found common isolates of *S. agalactiae* circulating both in cattle and human groups in the Emilia Romagna region, for a total of 20,9% (42/201) of common isolates. These results are supported by the high discriminatory power (>96.2%) of the combined typing methods used in this study.

DATA AVAILABILITY STATEMENT

The datasets presented in this study can be found in online repositories. The names of the repository/repositories and accession number(s) can be found in the article/**Supplementary Material**.

AUTHOR CONTRIBUTIONS

NA, GM, and AS: conceptualization. EC, CG, MC, and RS: data input and cleaning. EC and AM: data collection and analysis. NA, GM, and EC: funding acquisition. SR, AM, FB, CG, MC, RS, PB, and AP: investigation. NA, MR, EC, and AS: supervision. EC and NA: writing the original draft. EC, MR, NA, and AS: writing, review, and editing. All authors contributed to the article and approved the submitted version.

FUNDING

This work was supported by the Public Health Service of the Ministry of Health, Italy (grant E89I17000130001-PRC2017003).

SUPPLEMENTARY MATERIAL

The Supplementary Material for this article can be found online at: https://www.frontiersin.org/articles/10.3389/fmicb.2021.673126/full#supplementary-material

REFERENCES

Adkins, P., Fox, L. K., Godden, S., Brusham, M., Keefe, G., Kelton, D. et al. (2017). *Laboratory Handbook on Bovine Mastitis*, 3rd Edn, New Prague, MN: National Mastitis Council.

Åkerstedt, M., Wredle, E., Lam, V., and Johansson, M. (2012). Protein degradation in bovine milk caused by *Streptococcus agalactiae*. *J. Dairy Res.* 79, 297–303. doi: 10.1017/s0022029912000301

Bergal, A., Loucif, L., Benouareth, D. E., Bentorki, A. A., Abat, C., and Rolain, J. M. (2015). Molecular epidemiology and distribution of serotypes, genotypes, and antibiotic resistance genes of *Streptococcus agalactiae* clinical isolates from Guelma, Algeria and Marseille, France. *Eur. J. Clin. Microbiol. Infect. Dis.* 34, 2339–2348. doi: 10.1007/s10096-015-2487-6

Bisharat, N., Crook, D., Leigh, J., Harding, R., Ward, P., Coffey, T., et al. (2004). Hyperinvasive neonatal group B *Streptococcus* has arisen from a bovine ancestor. *J. Clin. Microbiol.* 42, 2161–2167. doi: 10.1128/jcm.42.5.2161-2167.2004

Botelho, A. C. N., Ferreira, A. F. M., Fracalanzza, S. E. L., Teixeira, L. M., and Pinto, T. C. A. (2018). A perspective on the potential zoonotic role of *Streptococcus agalactiae*: searching for a missing link in alternative transmission routes. *Front. Microbiol.* 9:608. doi: 10.3389/fmicb.2018.00608

Carvalho-Castro, G. A., Silva, J. R., Paiva, L. V., Custódio, D. A. C., Moreira, R. O., Mian, G. F. I., et al. (2017). Molecular epidemiology of *Streptococcus Agalactiae* isolated from mastitis in brazilian dairy herds. *Braz. J. Microbiol.* 48, 551–559. doi: 10.1016/j.bjm.2017.02.004

Clinical and Laboratory Standards Institute (CLSI) (2018a). *Performance Standards for Antimicrobial Disk and Dilution Susceptibility Tests for Bacteria Isolated From Animals Approved Standard*. 4th Edn, Pittsburgh, PA: CLSI. CLSI VET 08.

Clinical and Laboratory Standards Institute (CLSI) (2018b). *Performance Standards for Antimicrobial Disk and Dilution Susceptibility Tests for Bacteria Isolated From Animals Approved Standard*. 5th Edn, Pittsburgh, PA: CLSI. CLSI VET 01.

Clinical and Laboratory Standards Institute (CLSI) (2019). *Performance Standards for Antimicrobial Disk and Dilution Susceptibility Testing, Approved Standard*. 29th Edn, Pittsburgh, PA: CLSI. CLSI M100.

De Francesco, M. A., Caracciolo, S., Gargiulo, F., and Manca, N. (2012). Phenotypes, genotypes, serotypes and molecular epidemiology of erythromycin-resistant *Streptococcus agalactiae* in Italy. *Eur. J. Clin. Microbiol. Infect. Dis.* 31, 1741–1747. doi: 10.1007/s10096-011-1495-4

Diedrick, M. J., Flores, A. E., Hillier, S. L., Creti, R., and Ferrieri, P. (2010). Clonal analysis of colonizing group B *Streptococcus*, serotype IV, an emerging pathogen in the United States. *J. Clin. Microbiol.* 48, 3100–3104. doi: 10.1128/jcm.00277-10

Emaneini, M., Khoramian, B., Jabalameli, F., Abani, S., Dabiri, H., and Beigverdi, R. (2016). Comparison of virulence factors and capsular types of *Streptococcus agalactiae* isolated from human and bovine infections. *Microb. Pathog.* 91, 1–4. doi: 10.1016/j.micpath.2015.11.016

Francisco, A., Vaz, C., Monteiro, P., Melo-Cristino, J., Ramirez, M., and Carriço, J. (2012). PHYLOViZ: phylogenetic inference and data visualization for sequence based typing methods. *BMC Bioinform.* 13:87. doi: 10.1186/1471-2105-13-87

Furfaro, L., Chang, B., and Payne, M. (2018). Perinatal *Streptococcus agalactiae* epidemiology and surveillance targets. *Clin. Microbiol. Rev.* 31:e0049-18.

Gherardi, G., Imperi, M., Baldassarri, L., Pataracchia, M., Alfarone, G., Recchia, S., et al. (2007). Molecular epidemiology and distribution of serotypes, surface proteins, and antibiotic resistance among group B *Streptococci* in Italy. *J. Clin. Microbiol.* 45, 2909–2916. doi: 10.1128/jcm.00999-07

Hogeveen, H., Huijps, K., and Lam, T. J. (2011). Economic aspects of mastitis: new developments. *N. Z. Vet. J.* 59, 16–23. doi: 10.1080/00480169.2011.547165

Ippolito, D. L., James, W. A., Tinnemore, D., Huang, R. R., Dehart, M. J., Williams, J., et al. (2010). Group B *Streptococcus* serotype prevalence in reproductive-age women at a tertiary care military medical center relative to global serotype distribution. *BMC Infect. Dis.* 10:336. doi: 10.1186/1471-2334-10-336

Jolley, K., Bray, J., and Maiden, M. (2018). Open-access bacterial population genomics: BIGSdb software, the PubMLST.org website and their applications. *Wellcome Open Res.* 3:124. doi: 10.12688/wellcomeopenres.14826.1

Jones, N., Bohnsack, J., Takahashi, S., Oliver, K., Chan, M., Kunst, F., et al. (2003). Multilocus sequence typing system for Group B *Streptococcus*. *J. Clin. Microbiol.* 41, 2530–2536.

Jørgensen, H. J., Nordstoga, A. B., Sviland, S., Zadoks, R. N., Sølverød, L., Kvitle, B., et al. (2016). *Streptococcus agalactiae* in the environment of bovine dairy herds–rewriting the textbooks? *Vet. Microbiol.* 184, 64–72. doi: 10.1016/j.vetmic.2015.12.014

Katholm, J., Bennedsgaard, T. W., Koskinen, M. T., and Rattenborg, E. (2012). Quality of bulk tank milk samples from Danish dairy herds based on real-time polymerase chain reaction identification of mastitis pathogens. *J. Dairy Sci.* 95, 5702–5708. doi: 10.3168/jds.2011-5307

Lambertsen, L., Ekelund, K. I, Skovsted, C., Liboriussen, A., and Slotved, H. C. (2010). Characterisation of invasive group B *Streptococci* from adults in Denmark 1999 to 2004. *Eur. J. Clin. Microbiol. Infect. Dis.* 29, 1071–1077. doi: 10.1007/s10096-010-0941-z

Lannes-Costa, P. S., Baraúna, R. A., Ramos, J. N., Veras, J. F. C., Conceição, M. V. R., Vieira, V. V., et al. (2020). Comparative genomic analysis and identification of pathogenicity islands of hypervirulent ST-17 *Streptococcus agalactiae* Brazilian strain. *Infect. Genet. Evol.* 80:104195. doi: 10.1016/j.meegid.2020.104195

Le Doare, K., and Heath, P. T. (2013). An overview of global GBS epidemiology. *Vaccine* 31(Suppl. 4), D7–D12.

Lyhs, U., Kulkas, L., Katholm, J., Waller, K. P., Saha, K., Tomusk, R. J., et al. (2016). *Streptococcus agalactiae* serotype IV in humans and Cattle, Northern Europe. *Emerg. Infect. Dis.* 22, 2097–2103. doi: 10.3201/eid2212.151447

Martins, E. R., Melo-Cristino, J., and Ramirez, M. (2010). Evidence for rare capsular switching in *Streptococcus agalactiae*. *J. Bacteriol.* 192, 1361–1369. doi: 10.1128/jb.01130-09

Mokrousov, I. (2017). Revisiting the hunter gaston discriminatory index: note of caution and courses of change. *Tuberculosis* 104, 20–23. doi: 10.1016/j.tube.2017.02.002

Mweu, M. M., Nielsen, S. S., Halasa, T., and Toft, N. (2012). Annual incidence, prevalence and transmission characteristics of *Streptococcus agalactiae* in Danish dairy herds. *Prev. Vet. Med.* 106, 244–250. doi: 10.1016/j.prevetmed.2012.04.002

Oliveira, I. C., de Mattos, M. C., Pinto, T. A., Ferreira-Carvalho, B. T., Benchetrit, L. C., Whiting, A. A., et al. (2006). Genetic relatedness between group B *Streptococci* originating from bovine mastitis and a human group B *Streptococcus* type V cluster displaying an identical pulsed-field gel electrophoresis pattern. *Clin. Microbiol. Infect.* 12, 887–893. doi: 10.1111/j.1469-0691.2006.01508.x

Poyart, C., Tazi, A., églier-Poupet, H. R., Billoët, A., Tavares, N., Raymond, J., et al. (2007). Multiplex PCR assay for rapid and accurate capsular typing of group B *Streptococci*. *J. Clin. Microbiol.* 45, 1985–1988. doi: 10.1128/jcm.00159-07

Richards, V. P., Lang, P., Bitar, P. D., Lefébure, T., Schukken, Y. H., Zadoks, R. N., et al. (2011). Comparative genomics and the role of lateral gene transfer in the evolution of bovine adapted *Streptococcus agalactiae*. *Infect. Genet. Evol.* 11, 1263–1275. doi: 10.1016/j.meegid.2011.04.019

Rojo-Bezares, B., Azcona-Gutiérrez, J. M., Martin, C., Jareño, M. S., Torres, C., and Sáenz, Y. (2016). *Streptococcus agalactiae* from pregnant women: antibiotic and heavy-metal resistance mechanisms and molecular typing. *Epidemiol. Infect.* 144, 3205–3214. doi: 10.1017/s0950268816001692

Sendi, P., Christensson, B., Uçkay, I., Trampuz, A., Achermann, Y., Boggian, K., et al. (2011). Group B *Streptococcus* in prosthetic hip and knee joint-associated infections. *J. Hosp. Infect.* 79, 64–69. doi: 10.1016/j.jhin.2011.04.022

Sendi, P., Johansson, L., and Norrby-Teglund, A. (2008). Invasive group B *Streptococcal* disease in non-pregnant adults : a review with emphasis on skin and soft-tissue infections. *Infection* 36, 100–111. doi: 10.1007/s15010-007-7251-0

Shabayek, S., and Spellerberg, B. (2018). Group B streptococcal colonization, molecular characteristics, and epidemiology. *Front. Microbiol.* 9:437. doi: 10.3389/fmicb.2018.00437

Skoff, T., Farley, M., Petit, S., Craig, A., Schaffner, W., Gershman, K., et al. (2009). Increasing burden of invasive group B streptococcal disease in nonpregnant adults, 1990-2007. *Clin. Infect. Dis.* 49, 85–92. doi: 10.1086/599369

Springman, A., Lacher, D., Waymire, E., Wengert, S., Singh, P., Zadoks, R., et al. (2014). Pilus distribution among lineages of Group B *Streptococcus*: an evolutionary and clinical perspective. *BMC Microbiol.* 14:159. doi: 10.1186/1471-2180-14-159

Sunkara, B., Bheemreddy, S., Lorber, B., Lephart, P. R., Hayakawa, K., Sobel, J. D., et al. (2012). Group B *Streptococcus* infections in non-pregnant adults: the role of immunosuppression. *Int. J. Infect. Dis.* 16:e00182-86.

Tamura, K., Peterson, D., Peterson, N., Stecher, G., Nei, M., and Kumar, S. (2011). MEGA5: molecular evolutionary genetics analysis using maximum likelihood, evolutionary distance, and maximum parsimony methods. *Mol. Biol. Evol.* 28, 2731–2739. doi: 10.1093/molbev/msr121

Tomazi, T., de Souza Filho, A., Heinemann, M., and Dos Santos, M. (2018). Molecular characterization and antimicrobial susceptibility pattern of *Streptococcus agalactiae* isolated from clinical mastitis in dairy cattle. *PLoS One* 13:e0199561. doi: 10.1371/journal.pone.0199561

Zadoks, R. N., Middleton, J. R., McDougall, S., Katholm, J., and Schukken, Y. H. (2011). Molecular epidemiology of mastitis pathogens of dairy cattle and comparative relevance to humans. *J. Mamm. Gland Biol. Neoplas.* 16, 357–372. doi: 10.1007/s10911-011-9236-y

Conflict of Interest: The authors declare that the research was conducted in the absence of any commercial or financial relationships that could be construed as a potential conflict of interest.

frontiers in Microbiology

ORIGINAL RESEARCH
published: 03 September 2021
doi: 10.3389/fmicb.2021.709826

Anthraquinones as Potential Antibiofilm Agents Against Methicillin-Resistant *Staphylococcus aureus*

Zhi-Man Song[1,2,3], Jun-Liang Zhang[1], Kun Zhou[1], Lu-Ming Yue[1], Yu Zhang[1], Chang-Yun Wang[4,5,6], Kai-Ling Wang[3] and Ying Xu[1]**

[1] Shenzhen Key Laboratory of Marine Bioresource and Eco-Environmental Science, Shenzhen Engineering Laboratory for Marine Algal Biotechnology, College of Life Sciences and Oceanography, Shenzhen University, Shenzhen, China, [2] Department of Chemistry, The University of Hong Kong, Pokfulam, Hong Kong, China, [3] College of Pharmacy, Institute of Materia Medica, Dali University, Dali, China, [4] Key Laboratory of Marine Drugs, The Ministry of Education of China, School of Medicine and Pharmacy, Ocean University of China, Qingdao, China, [5] Laboratory for Marine Drugs and Bioproducts, Qingdao National Laboratory for Marine Science and Technology, Qingdao, China, [6] Institute of Evolution and Marine Biodiversity, Ocean University of China, Qingdao, China

OPEN ACCESS

Edited by:
Ana Luíza Mattos Guaraldi, Rio de Janeiro State University, Brazil

Reviewed by:
Jessica Amber Jennings, University of Memphis, United States
Marc Maresca, Aix-Marseille Université, France

***Correspondence:**
Kai-Ling Wang
kailingw@dali.edu.cn
Ying Xu
boxuying@szu.edu.cn

Specialty section:
This article was submitted to Antimicrobials, Resistance and Chemotherapy, a section of the journal Frontiers in Microbiology

Received: *14 May 2021*
Accepted: *04 August 2021*
Published: *03 September 2021*

Citation:
Song Z-M, Zhang J-L, Zhou K, Yue L-M, Zhang Y, Wang C-Y, Wang K-L and Xu Y (2021) Anthraquinones as Potential Antibiofilm Agents Against Methicillin-Resistant Staphylococcus aureus. Front. Microbiol. 12:709826. doi: 10.3389/fmicb.2021.709826

Biofilms formed by methicillin-resistant *Staphylococcus aureus* (MRSA) are one of the contributing factors to recurrent nosocomial infection in humans. There is currently no specific treatment targeting on biofilms in clinical trials approved by FDA, and antibiotics remain the primary therapeutic strategy. In this study, two anthraquinone compounds isolated from a rare actinobacterial strain *Kitasatospora albolonga* R62, 3,8-dihydroxy-l-methylanthraquinon-2-carboxylic acid (**1**) and 3,6,8-trihydroxy-1-methylanthraquinone-2-carboxylic acid (**2**), together with their 10 commercial analogs **3**–**12** were evaluated for antibacterial and antibiofilm activities against MRSA, which led to the discovery of two potential antibiofilm anthraquinone compounds anthraquinone-2-carboxlic acid (**6**) and rhein (**12**). The structure-activity relationship analysis of these anthraquinones indicated that the hydroxyl group at the C-2 position of the anthraquinone skeleton played an important role in inhibiting biofilm formation at high concentrations, while the carboxyl group at the same C-2 position had a great influence on the antibacterial activity and biofilm eradication activity. The results of crystal violet and methyl thiazolyl tetrazolium staining assays, as well as scanning electron microscope and confocal scanning laser microscopy imaging of compounds **6** and **12** treatment groups showed that both compounds could disrupt preformed MRSA biofilms possibly by killing or dispersing biofilm cells. RNA-Seq was subsequently used for the preliminary elucidation of the mechanism of biofilm eradication, and the results showed upregulation of phosphate transport-related genes in the overlapping differentially expressed genes of both compound treatment groups. Herein, we propose that anthraquinone compounds **6** and **12** could be considered promising candidates for the development of antibiofilm agents.

Keywords: anthraquinones, antibiofilm agents, *Kitasatospora albolonga*, RNA-Seq, antibiotics, Pst system

INTRODUCTION

Bacterial biofilms are surface or interphase-attached microbial communities that are encapsulated in self-secreted extracellular matrix comprising largely of proteins, polysaccharides, nucleic acids, and lipids (Costerton et al., 1999; Flemming and Wingender, 2010). Bacteria growing inside biofilms are more extremely resistant to hostile environment, antimicrobial agents, and mechanical stresses than their planktonic counterparts (Gilbert et al., 2002; Fux et al., 2005; Hoiby et al., 2010, 2011). It is reported that more than 80% of chronic infections are related with the formation of biofilms by pathogens and very difficult to tackle (Potera, 1999; Lebeaux et al., 2013).

Antimicrobial resistance of *Staphylococcus aureus* has become a global health threat. As a notorious member of the drug-resistant *S. aureus* family, methicillin-resistant *S. aureus* (MRSA) causes various diseases, ranging from minor skin infections to fatal necrotizing pneumonias (Boyce et al., 2005; Calo et al., 2007; DeLeo et al., 2010). Conventional antibiotics are becoming ineffective in the treatment of biofilm-forming MRSA and their biofilms (Laplante and Mermel, 2009; Kelley et al., 2011; Gu et al., 2013; Hall Snyder et al., 2014; Meeker et al., 2016). There is an urgent need to explore new antibiofilm agents that prevent the formation of MRSA biofilms and/or disrupt the preformed biofilms (Brady et al., 2011; Craigen et al., 2011; Kaplan et al., 2012; Ranall et al., 2012; Bjarnsholt et al., 2013; Alves et al., 2014; Bhattacharya et al., 2015).

Natural products cannot be ignored as a potential source for the exploitation of bioactive substances (Gunatilaka, 2006; Li and Vederas, 2009; Ranall et al., 2012; Fletcher et al., 2014). Some natural compounds isolated from plants [resveratrol (Augustine et al., 2014), quercetin (Lee et al., 2013), magnolol (Wang et al., 2011), baicalein (Zeng et al., 2008), ellagic acid (Quave et al., 2012), phloretin (Lee et al., 2011), oroidin (Richards et al., 2008), etc.] and microbes [4-phenylbutanoic acid (Nithya et al., 2011), glycolipid (Dusane et al., 2011), butanolide (Yin et al., 2019), etc.] have been reported to exhibit excellent antibiofilm activity (Gunatilaka, 2006; Wang et al., 2011). Anthraquinones (AQs), as a big family of natural products, have been demonstrated to have antibacterial, antibiofilm, anti-inflammatory, antioxidative, anticancer, and antiviral activities (Barnard et al., 1992; Galasinski et al., 1996; Agarwal et al., 2000; Yen et al., 2000; Bashir et al., 2011; Lin et al., 2015; Nam et al., 2017). Among them, four AQs have been proved to be able to reduce biofilm formation efficiently (Coenye et al., 2007; Lee et al., 2016; Farooq et al., 2017; Manoharan et al., 2017). Two alkyl-substituted anthraquinone derivatives, symploquinones A and C, inhibited the biofilm formation of *Streptococcus mutans*, *S. aureus*, and *Proteus mirabilis* with low minimal inhibitory concentration (MICs) (83–160 μg/ml) (Farooq et al., 2017). Emodin could significantly reduce biofilm formation of *S. mutans* and *S. aureus* (Coenye et al., 2007) and alizarin at 10 μg/ml inhibited biofilm formation of *S. aureus* significantly (Lee et al., 2016). These studies suggested that some AQs could be considered promising inhibitors of biofilms. Unfortunately, most of them are only capable of inhibiting initial biofilm formation instead of eradicating existing biofilms, although the latter is more relevant in clinical infection. Until now, to our best knowledge, biofilm eradication function of AQs has not been reported yet.

In this study, two known natural anthraquinone compounds 3,8-dihydroxy-1-methylanthraquinone-2-carboxylic acid (**1**) and 3,6,8-trihydroxy-1- methylanthra-quinone-2-carboxylic acid (**2**) from the actinomycete *Kitasatospora albolonga* R62, together with their 10 commercial analogs **3**–**12** were screened for antibacterial and antibiofilm activity against MRSA, and then analyzed for their structure-activity relationships (SARs). It was found that anthraquinone-2-carboxlic acid (**6**) and rhein (**12**) could effectively eradicate biofilms formed by MRSA strain ATCC43300. Stanning method [crystal violet (CV) and methyl thiazolyl tetrazolium (MTT)] and microscopic technology [scanning electron microscope (SEM) and confocal scanning laser microscopy (CLSM)] were employed to determine the potential eradication activity of these two compounds against the preformed MRSA biofilms. Based on transcriptome profiling and quantitative reverse transcription polymerase chain reaction (qRT-PCR) validation, we propose that the antibiofilm mechanism of compounds **6** and **12** might involve dispersing biofilm cells and upregulation of phosphate transport-related genes.

MATERIALS AND METHODS

Sample Collection and Bacterial Identification

The soil sample was collected from the rhizosphere sediment of the mangrove plant *Kandelia candel* (L.) Druce in Mai Po Nature Reserve, Hong Kong (114.05°E, 22.49°N). Strain R62 was isolated from the sample through stepwise purification. The 16S rRNA gene of strain R62 was amplified by two universal primers of 27F (5′-AGAGTTTGATCMTGGCTCAG-3′) and 1492R (5′-TACGGYTACCTTGTTACGACTT-3′). The 16S rRNA gene sequence displayed 100% similarity with *K. albolonga* NBRC 13465.

Fermentation, Extraction, and Compound Isolation

The actinobacterial strain *K. albolonga* R62 was distributed to 250 ml Erlenmeyer flask containing 80 ml SGTYP medium (5 g of starch, 5 g of glucose, 1 g of peptone, 1 g of tryptone, 1 g of yeast extract, and 17 g artificial sea salt is dissolved in 1 L double-distilled water, pH 7.4–7.6) and fermented at 28°C, 200 rpm for 5 days. In total, nearly 15 L of culture broth was centrifuged at 10,000 × *g* for 15 min to remove cells. The supernatant was extracted using ethyl acetate (ν/ν 1:3) three times to yield an EtOAc extract (3.0 g) after concentration. The extract was separated by ODS open column elution with a gradient of MeOH-H_2O (20–100%, at intervals of 10%) to afford nine fractions (Fr. 1–Fr. 9). HPLC-MS analysis of these fractions showed that natural products are mainly concentrated in Fr. 3 and Fr. 4. Both fractions were isolated and purified by semipreparative HPLC (Waters, Parsippany, NJ, United States)

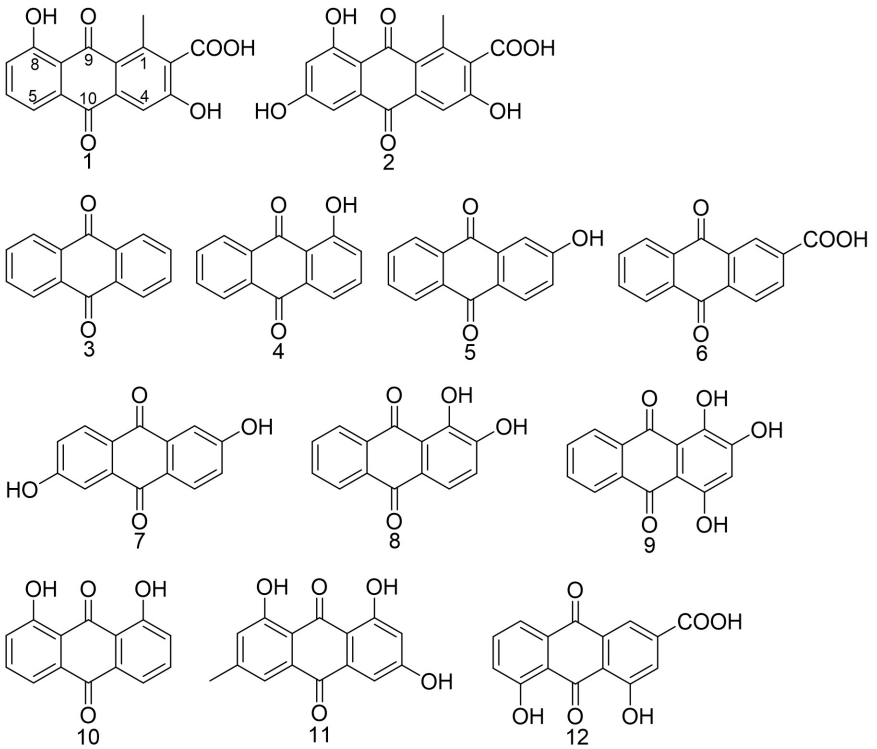

FIGURE 1 | Chemical structures of anthraquinones mentioned in the article. Compounds **1** and **2** were isolated from *Kitasatospora albolonga* R62 and compounds **3**–**12** were commercially obtained.

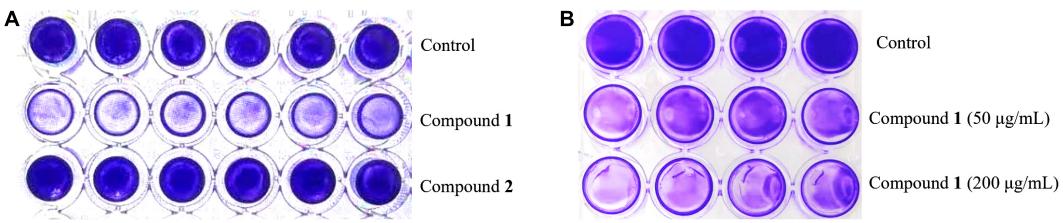

FIGURE 2 | The formation of MRSA biofilms after treatment with compound **1** or **2** staining by CV. The biofilm inhibition activity results after treatment with compound **1** or **2** (200 μg/ml) in a 96-well plate **(A)** and different concentrations of compound **1** (50 and 200 μg/ml) in a 24-well plate **(B)**. The same volume of DMSO was used as negative control.

TABLE 1 | Minimum inhibitory concentrations of anthraquinones.

Compound	MIC (μg/ml)	Compound	MIC (μg/ml)
DMCA (**1**)	>200	2,6-Dihydroxyanthraquinone (**7**)	>200
TMCA (**2**)	>200	Alizarin (**8**)	>200
Anthraquinone (**3**)	>200	Purpurin (**9**)	>200
1-Hydroxyanthraquinone (**4**)	>200	1,8-Dihydroxyanthraquinone (**10**)	>200
2-Hydroxyanthraquinone (**5**)	>200	Emodin (**11**)	>200
Anthraquinone-2-carboxlic acid (**6**)	100	Rhein (**12**)	12.5

*DMCA, 3,8-dihydroxy-1-methylanthraquinone-2-carboxylic acid (**1**); TMCA, 3,6,8-trihydroxy-1-methylanthraquinone-2-carboxylic acid (**2**).*
*The bold value behind the compound indicates the compound number corresponding to **Figure 1** and the entire article.*

using semipreparative reverse-phase Phenomenex C18 columns (5 μm, 250 × 10 mm in size) with a gradient mobile phase of ACN-H_2O (40–60%) to yield compounds **1** and **2**.

Experimental Strain and Compounds

Methicillin-resistant *Staphylococcus aureus* strain ATCC 43300 was used as biofilm model organism. Anthraquinone

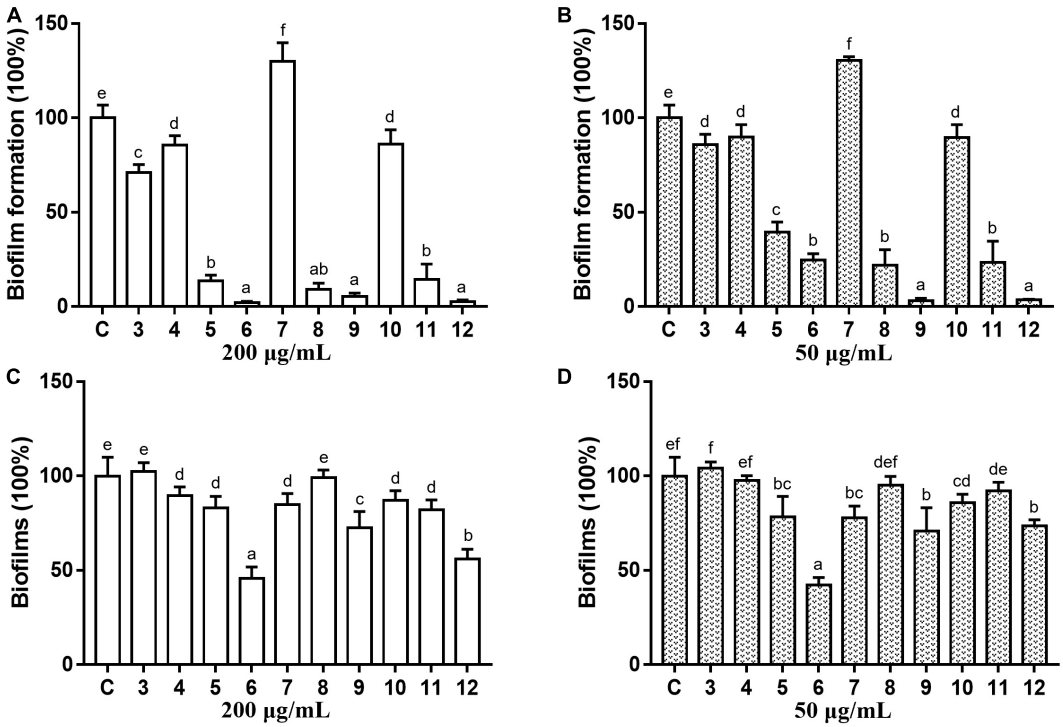

FIGURE 3 | Antibiofilm activity of commercial anthraquinones **3–12** against MRSA. The MRSA biofilm inhibitory activity **(A,B)** and the biofilm eradication activity **(C,D)** of each compound at two different concentrations (**A,C** 200 μg/ml; **B,D** 50 μg/ml). The same volume of DMSO was used as negative control. C, control. Results are presented as percentages of the control group. The data represent mean ± SD (n = 9). Means in a group with different letters are significant differences based on Ryan-Einot-Gabriel-Welsch multiple F-test, $p < 0.001$.

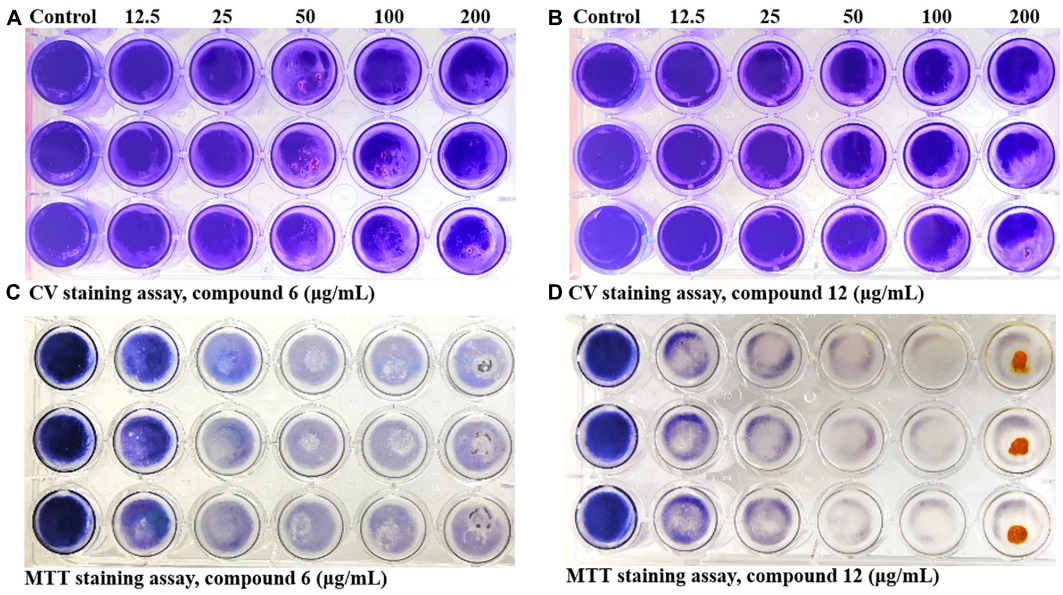

FIGURE 4 | Dose-dependent effects of compounds **6** and **12** against MRSA biofilms qualified by two different staining methods. The 24-h preformed MRSA biofilms were treated with increasing concentrations of compounds **6** and **12** (12.5–200 μg/ml) for another 24 h before staining with CV **(A,B)** or MTT **(C,D)** solution. The same volume of DMSO was used as negative control. At least three independent experiments were conducted, and there were three biological replicates each time.

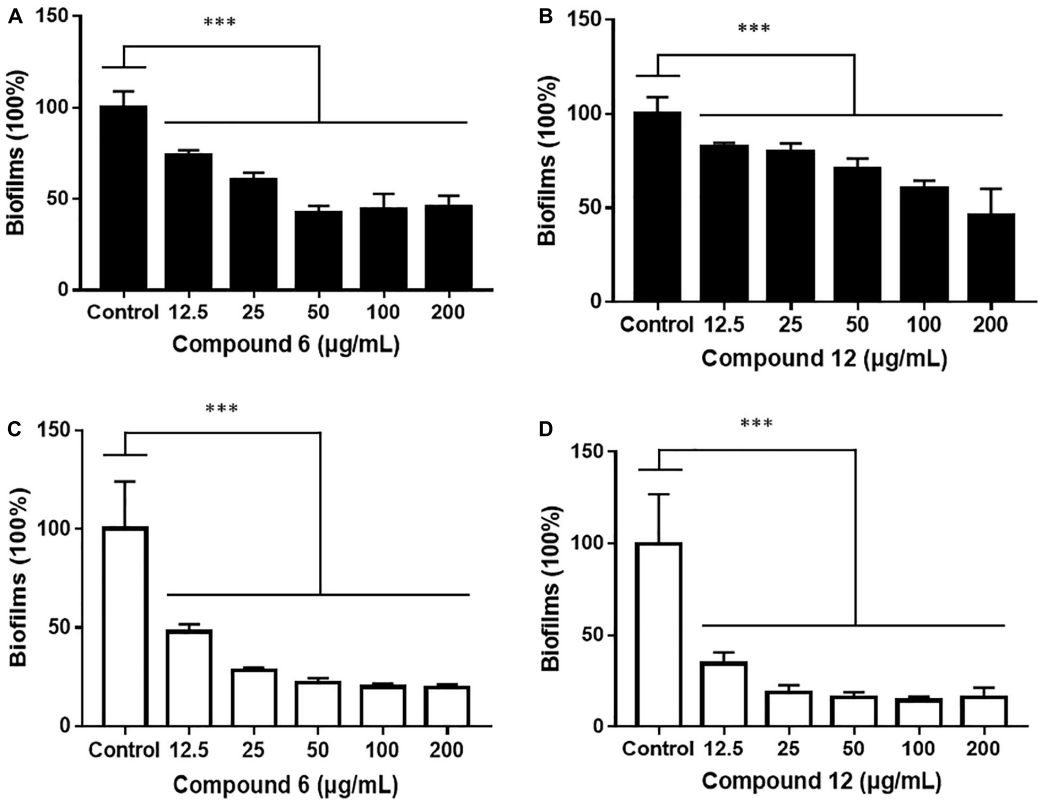

FIGURE 5 | Relative values of dose-response effects of compounds **6** and **12** against MRSA biofilms qualified by two different staining methods. The 24-h preformed biofilms were treated with different concentrations of compounds **6 (A,C)** and **12 (B,D)** using CV staining **(A,B)** and MTT staining **(C,D)** methods. The same volume of DMSO was used as negative control. Results are presented as percentages of the control. The data represent mean ± SD ($n = 9$); ***$p < 0.001$.

(**3**, MCKLIN, China), 1-hyrdroxyanthraquanone (**4**, Yuanye Biotechnology, China), 2-hydroxyanthraquanone (**5**, Yuanye Biotechnology, China), anthraquinone-2-carboxlic acid (**6**, Sigma-Aldrich, Japan), 2,6-dihydroxyanthraquinone (**7**, Energy Chemical, China), alizarine (**8**, Aladdin, China), purpurin (**9**, Solarbio, China), 1,8-dihydroxyanthraquinone (**10**, Aladdin, China), emodin (**11**, Aladdin, China), and rhein (**12**, MCKLIN, China) were all commercially available. All compounds tested were dissolved in DMSO to get the stock solution. The structure of commercially obtained AQs is shown in **Figure 1**, and their LC-MS data are shown in **Supplementary Figure 1**.

The Determination of Minimum Inhibitory Concentration

The minimum inhibitory concentrations (MICs) of AQs were determined according to the Clinical and Laboratory Standards Institute (CLSI) guideline. The experiment was conducted in 96-well microplates (Corning, Corning, NY, United States). In brief, a stock solution of 20 μg/μl of each compound was prepared in DMSO, diluted 100 times with bacterial culture (∼5 × 10^5 CFU/ml) to 200 μg/ml, and further diluted by a serial twofold dilution to obtain the tested solutions with five concentrations ranging from 100 to 6.25 μg/ml. One microliter of DMSO was used as the negative control. Cell growth was monitored by the absorbance at OD_{595} using the spectrophotometer (Varioskan Flash, Thermo Scientific, Waltham, MA, United States).

The Evaluation of Inhibitory Activity Against MRSA Biofilm Formation

The inhibition of static biofilm formation was tested as previously described (Stepanovic et al., 2007; Nair et al., 2016; Yin et al., 2019). After overnight cultivation, 100 μl/well of the bacterial culture, diluted in LB broth with 0.5% glucose (about 5 × 10^6 CFU/ml), was aliquoted into 96-well microplates (Corning, United States) with 1 μl of different concentrations (20 or 5 μg/μl) of each compound or DMSO and incubated at 37°C for 24 h. Using the same method, 1 ml/well of the diluted culture was added into 24-well microplates (Corning, United States) with 2 μl of compounds (100 or 25 μg/μl) or DMSO. After incubation, each well was rinsed with 1 × PBS to remove non-adherent cells and then dried at 37°C. CV staining was used to determine the remaining total biofilm biomass. Biofilms were stained with 0.5% CV for 10 min before washing. The washed biofilm mass was then dissolved in 30% acetic acid, and then the absorbance was measured at 550 nm.

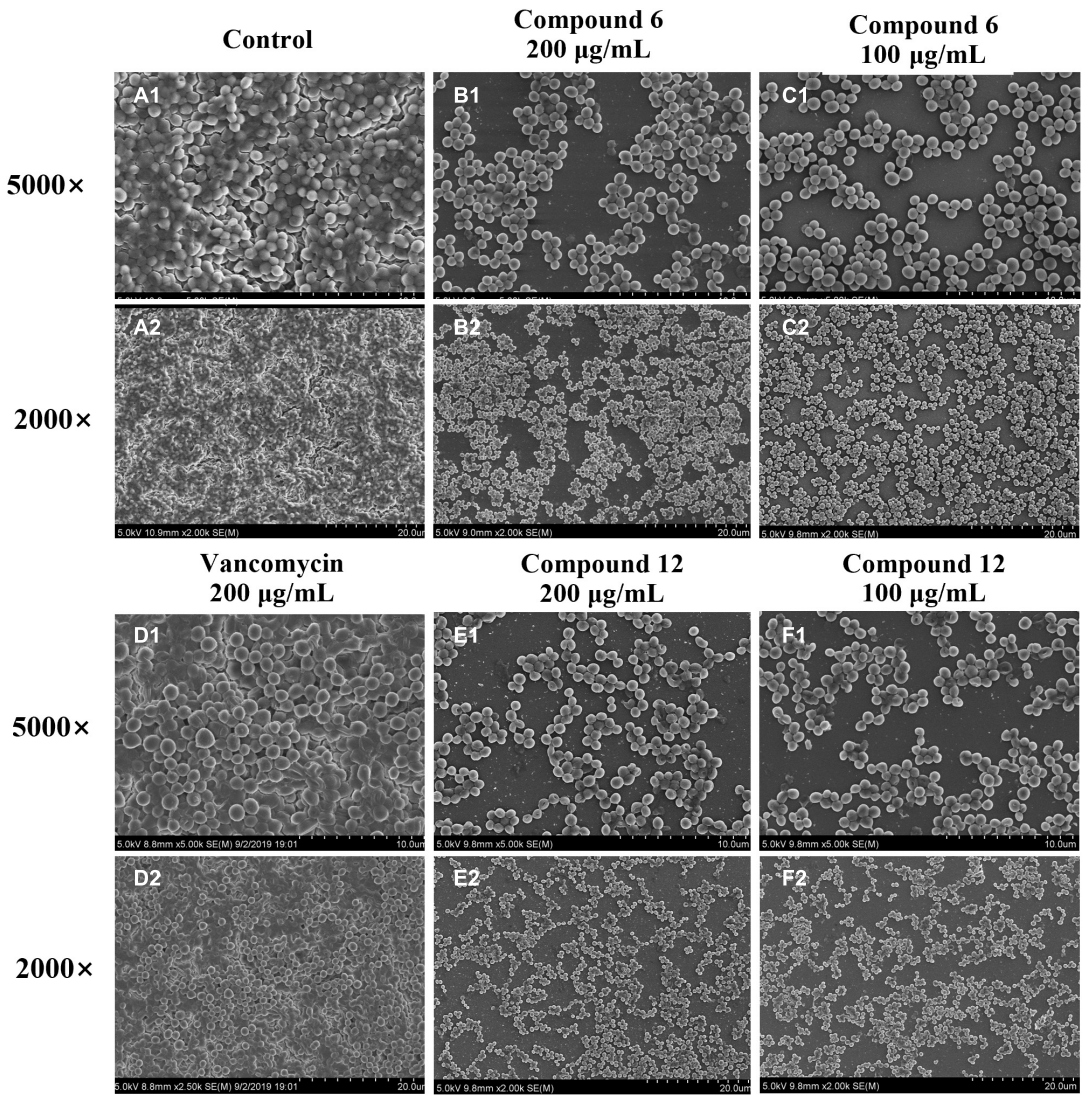

FIGURE 6 | Scanning electron micrographs of 24-h preformed MRSA biofilms treated with different concentrations of compounds **6** and **12**. **(A1–F2)** Different treatment groups (**A1,A2** DMSO control; **B1,B2** 200 μg/ml of compound **6**; **C1,C2** 100 μg/ml of compound **6**; **D1,D2** 200 μg/ml of vancomycin; **E1,E2** 200 μg/ml of compound **12**; **F1,F2** 100 μg/ml of compound **12**). Series 1 and 2 were different magnifications with ×5,000 and ×2,000, respectively.

Biofilm Eradication Assay

The 24-h mature biofilms containing no compounds or DMSO preformed in 24-well microplates according to the described method (Nair et al., 2016; Yin et al., 2019). Each well was rinsed twice by 1 × PBS, followed by adding fresh LB broth with 0.5% glucose and 2 μl of different concentrations (25 and 100 μg/ml) of each compound or DMSO, respectively, then incubated at 37°C for another 24 h. The rest of the washing and CV staining steps were the same as the static biofilm formation assay. Additionally, 3-(4,5-dimethyl-2-thiazolyl)-2,5-diphenyl-2H-tetrazoliumbromide (MTT; HiMedia, West Chester, PA, United States) staining was conducted to show the number of viable cells in the remaining biofilms at 550 nm. Both CV staining and MTT staining assay were used to determine the eradication assay of compounds **6** and **12** in the gradient-diluted concentrations (6.25, 12.5, 25, 50, and 100 μ g/ml).

Biofilm Eradication Imaging

Bacterial biofilms were grown on the glass coverslips which were at the bottom of 24-well microplates at the beginning. The biofilm eradication assay was then carried out according to the method described in Yin et al. (2019) and Nair et al. (2016). For SEM imaging (Nithya et al., 2010; Sultana et al., 2016; Yin et al., 2019), before drying, the biofilms were fixed by 2.5% glutaraldehyde in 0.1 M phosphate for 24 h, followed by rinsing with 1 × PBS and dehydrated by a gradient of ethanol (50, 70, 80, 90, 95, and 100% ethanol for 10 min each). The biofilms were then subjected to analysis using a SEM (SU-70, HITACHI, Japan) after air drying and sputter

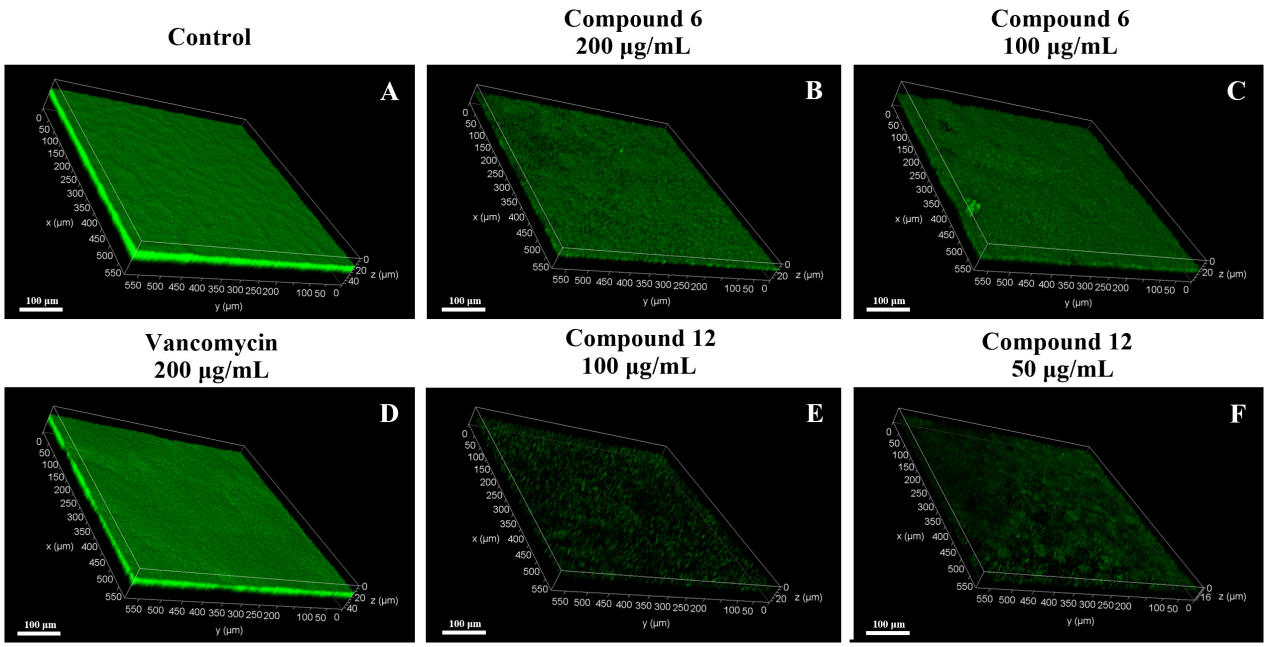

FIGURE 7 | Confocal scanning laser micrographs of 24-h preformed MRSA biofilms treated with different concentrations of compounds **6** and **12**. **(A–F)** Different treatment groups (**A** DMSO control; **B** 200 μg/ml of compound **6**; **C** 100 μg/ml of compound **6**; **D** 200 μg/ml of vancomycin; **E** 100 μg/ml of compound **12**; **F** 50 μg/ml of compound **12**). Scale bars represent 100 μm.

coating with gold (50 s). The CSLM (TCS SP8, Leica, Germany) analysis was implemented as describe by the reported articles (Nithya et al., 2010; Dusane et al., 2011; Yin et al., 2019). In brief, the biofilms were washed with 1 × PBS after 24 h of treatment and dried at 37°C for 30 min, then stained with the LIVE/DEAD *Bac*Light Bacterial Viability Kit (L7007, Invitrogen, Carlsbad, CA, United States) in the dark. The biofilms were observed using a ×20 objective, and images were acquired with 1,024 × 1,024 resolutions. The CLSM was conducted at 488 and 561 nm.

RNA Extraction, Library Construction, Sequencing, and Data Analysis

Samples were collected according to the method mentioned in the biofilm eradication assay. Mature MRSA biofilms were treated with compound **6** or **12** at the concentration of 100 μg/ml and washed by 1 × PBS three times after 8 h. The same volume of DMSO-treated mature biofilms was used as control. Total RNA of all the samples was extracted using Trizol reagent (Invitrogen) according to the manufacturer's instructions. RNA qualification was examined by 1% agarose gel electrophoresis and the NanoDrop spectrophotometer (Thermo Fisher Scientific). Strand-specific libraries were constructed using the TruSeq RNA sample preparation kit (Illumina, San Diego, CA, United States) and sequencing with Illumina nova-seq6000.

The quality of raw data was checked by FastQC version 0.11.2.[1] High-quality clean reads were mapped to reference gene *S. aureus* A9754 sequence (genome assembly: ASM17799v1) using STAR (2.5.3a) (Dobin et al., 2013). All mapped reads were then annotated by BLASTX against NCBI non-redundant protein database (nr) and Swiss-Prot. Gene IDs of the whole detected sequence were named according to the information on the ensemble bacterial database for analysis.[2] The fragments per kilobase of transcript per million mapped reads (FPKM) for the mapped sequences of each sample were calculated and normalized by Cuffnorm (Trapnell et al., 2012), and the differential expression of genes between control and compound treatment groups were analyzed with DESeq2 (version 1.16.1) (Love et al., 2014). Some differentially expressed genes (DEGs; $p < 0.05$ and absolute fold change ≥ 2) were chosen for subsequent analysis of gene function and signaling pathway enrichment based on searching against Gene Ontology (GO) and Kyoto Encyclopedia of Genes and Genomes (KEGG) database (Sun et al., 2017; Wang et al., 2018). The GO functional annotation of the DEGs was determined with topGO package (Alexa and Rahnenfuhrer, 2010) for each gene clusters, and the KEGG pathway enrichment analysis was performed using phyper algorithm in R 3.6.1[3] against the KEGG database. Significantly enriched GO terms and KEGG pathways were selected using a threshold of p-value of ≤ 0.05.

qRT-PCR

To confirm the RNA-Seq data, the relative expression of some related genes was assessed by qRT-PCR. Total RNA was extracted

[1]http://www.bioinformatics.babraham.ac.uk/projects/fastqc/

[2]http://bacteria.ensembl.org/

[3]https://cran.r-project.org/doc/FAQ/R-FAQ.html#Citing-R

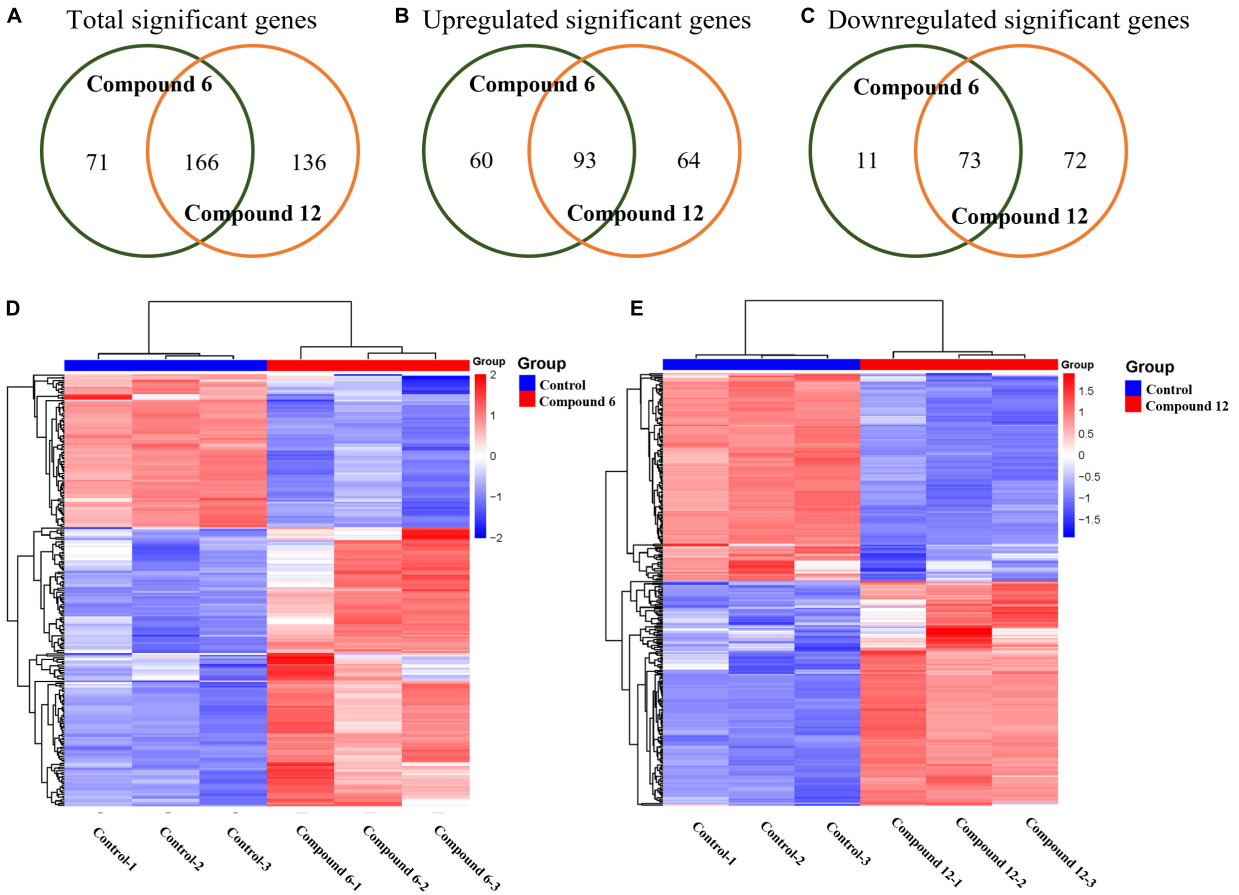

FIGURE 8 | Gene expression analysis of MRSA biofilm cells treated with compounds **6** and **12** at concentration of 100 μg/ml. **(A–C)** Venn diagrams of total significant, upregulated, and downregulated significant genes in MRSA biofilm cells due to compounds **6** and **12** treatments. Heatmaps of the cluster analysis of differentially expressed genes between control group compared with compounds **6 (D)** and **12** treatment group **(E)**. Numbers 1–3 represent the three replicates. The normalized log-transformed counts are indicated by the color key. Red indicates upregulations, white represents intermediate expression, and blue indicates downregulations in the heatmaps.

by the E.Z.N.A.® Bacterial RNA Kit (Omega Bio-Tec, Norcross, GA, United States). cDNA was synthesized using a PrimeScript RT reagent kit with a gDNA Eraser (TaKaRa, Tokyo, Japan). qRT-PCR reactions (20 μl in total volume with 4 μl of cDNA product) were carried out using TaKaRa SYBR Premix Ex Taq (Tli RNaseH Plus) in a CFX96 Real-Time System (BioRad, Hercules, CA, United States). All the primers used in the present study had been listed in the **Supplementary Table 1**. Housekeeping gene *pyk* was used as an internal reference to normalize the qRT-PCR date (Tan et al., 2015). Three independent replicates with four replications were tested in each qRT-PCR run.

Statistical Analysis

All the experiments were performed in at least three independent experiments and three biological replicates each time. Single-factor analysis of variances followed with Ryan-Einot-Gabriel-Welsch *F*-test as the *post hoc* method were performed to test the differences of the antibiofilm activity between 12 different compounds using SPSS software 16.0 in **Figure 4**. One-way ANOVA and Multiple *t*-tests in GraphPad Prism 7.0 were performed to check the other statistical comparisons in **Figures 5**, **11** ($p < 0.001$ and 0.01).

RESULTS

Identification of Compounds 1 and 2

Compound **1** (2.5 mg), orange powder, was identified as 3,8-dihydroxyl-methylanthraquinon-2-carboxylic acid (DMCA; **Figure 1**) by the NMR data and LC-MS data (**Supplementary Figures 2–4**) according to the reported data (Krupa et al., 1989). ESI-MS m/z: 299.055 $[M+H]^+$ (calculated for $C_{16}H_{10}O_6$ 299.055), 297.041 $[M-H]^-$ (calculated, 297.040). ^{1}H NMR (600 MHz, d_6-DMSO) δ: 12.90 (s, 1H), 7.72 (t, J = 7.9 Hz, 1H), 7.64 (d, J = 7.4 Hz, 1H), 7.58 (s, 1H), 7.34 (d, J = 8.2 Hz, 1H), 2.71 (s, 3H); ^{13}C NMR (DMSO-*d*6, 150 MHz) δ: 189.8, 182.6, 168.7, 161.9, 141.6, 136.8, 136.5, 133.0, 131.3, 124.9, 122.7, 118.8, 117.4, 112.8, and 20.4.

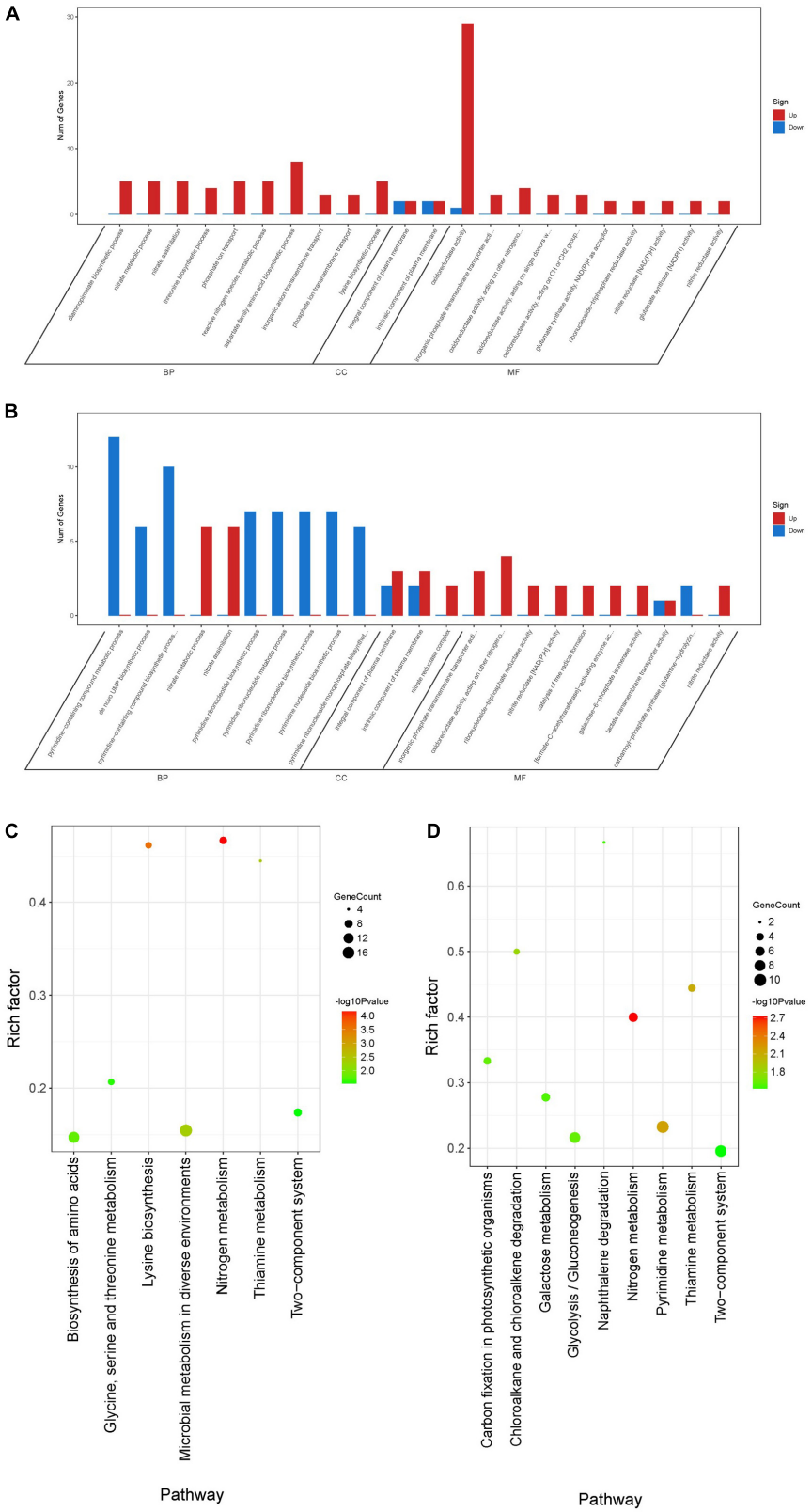

FIGURE 9 | Differentially expressed genes annotated in GO terms and KEGG pathway. **(A,B)** Genes annotated in three main categories: biological process, cellular component, and molecular function after treatment with compounds **6 (A)** and **12 (B)**. **(C,D)** The KEGG pathway enrichment results of compounds **6 (C)** and **12 (D)** treatment groups. BP, biological process; CC, cellular component; MF, molecular function.

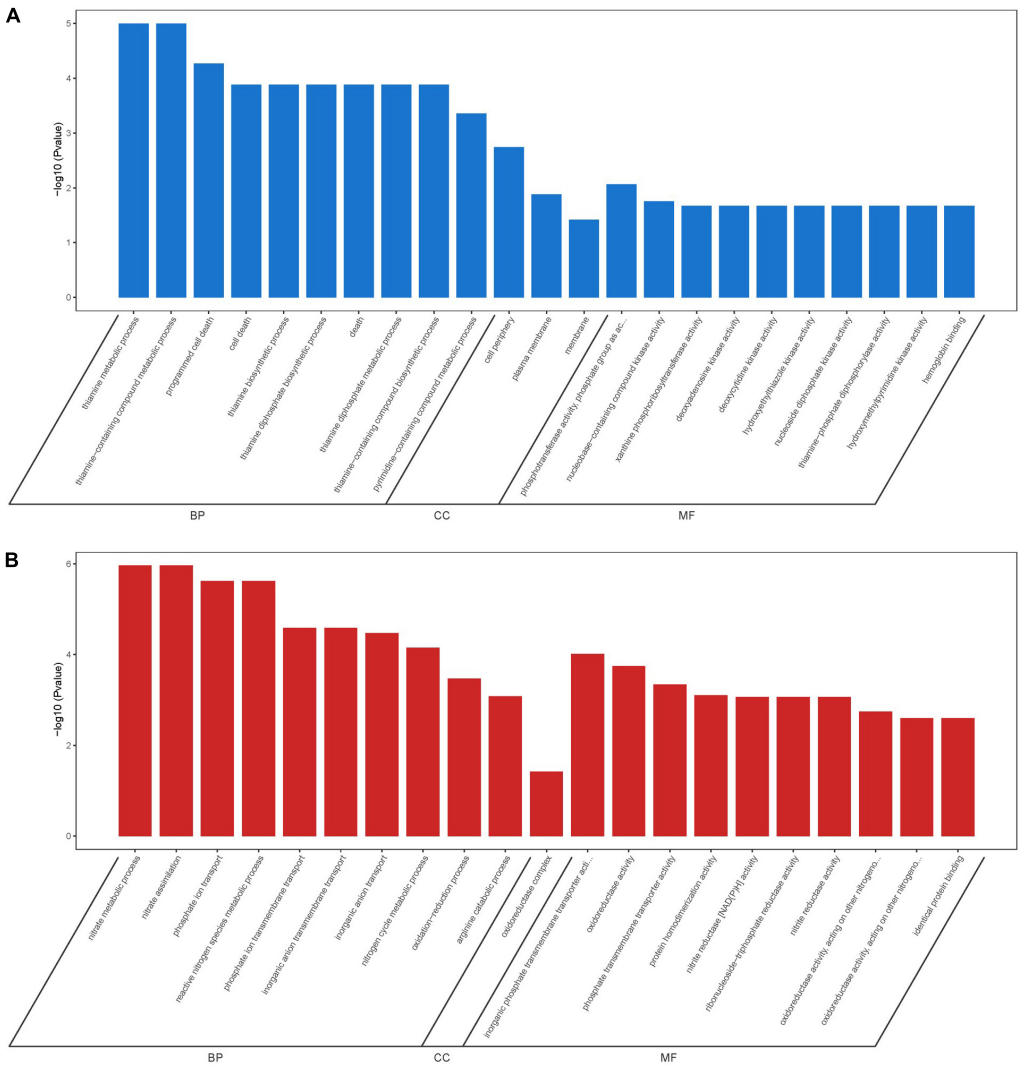

FIGURE 10 | GO enrichment analysis of overlapping DEGs in both compounds **6** and **12** treatment groups. Significantly downregulated GO terms **(A)** are shown in blue, and significantly upregulated GO terms **(B)** are in red. BP, biological process; CC, cellular component; MF, molecular function.

Compound **2** (2.0 mg), orange powder, was identified as 3,6,8-trihydroxy-1-methylanthraquinone-2-carboxylic acid (TMCA; **Figure 1**) by the NMR data and LC-MS data (**Supplementary Figures 5**, **6**) according to the reported data (Hawas et al., 2006). ESI-MS m/z: 313.036 $[M-H]^-$ (calculated, 313.035), 315.050 $[M+H]^+$ (calculated, 315.050). ^1H NMR (600 MHz, d_6-DMSO) δ: 13.14 (s, 1H), 11.11 (s, 1H), 7.58 (s, 1H), 7.07 (d, J = 2.4 Hz, 1H), 6.60 (d, J = 2.4 Hz, 1H), 2.68 (s, 3H).

Biofilm Inhibition Activity of Natural Products 1 and 2 at Concentrations Lower Than MIC Values

The preliminary screening results of antibiofilm activities of compounds **1** and **2** revealed that compound **1** had a significant effect on decreasing MRSA biofilm formation by >50% at the concentration of 200 μg/ml while its MIC value was higher than 200 μg/ml (**Figure 2**), but compound **2** showed no obvious bactericidal activity or antibiofilm activity at the same concentration.

Antibacterial and Antibiofilm Activities of Anthraquinones

The antibacterial and antibiofilm activities of the other 10 commercial AQs **3**–**12** (**Figure 1**) against MRSA ATCC43300 were investigated to analyze their SARs. Among them, compounds **6** and **12** displayed antibacterial activity with MIC values of 100 and 12.5 μg/ml, respectively. The other compounds did not show antimicrobial activity against planktonic MRSA cells at the concentration of 200 μg/ml (**Table 1**). Meanwhile, antibiofilm activities (including the inhibitory effects on the formation of MRSA biofilms and the eradication abilities against preformed biofilms) of compounds **3**–**12** were evaluated

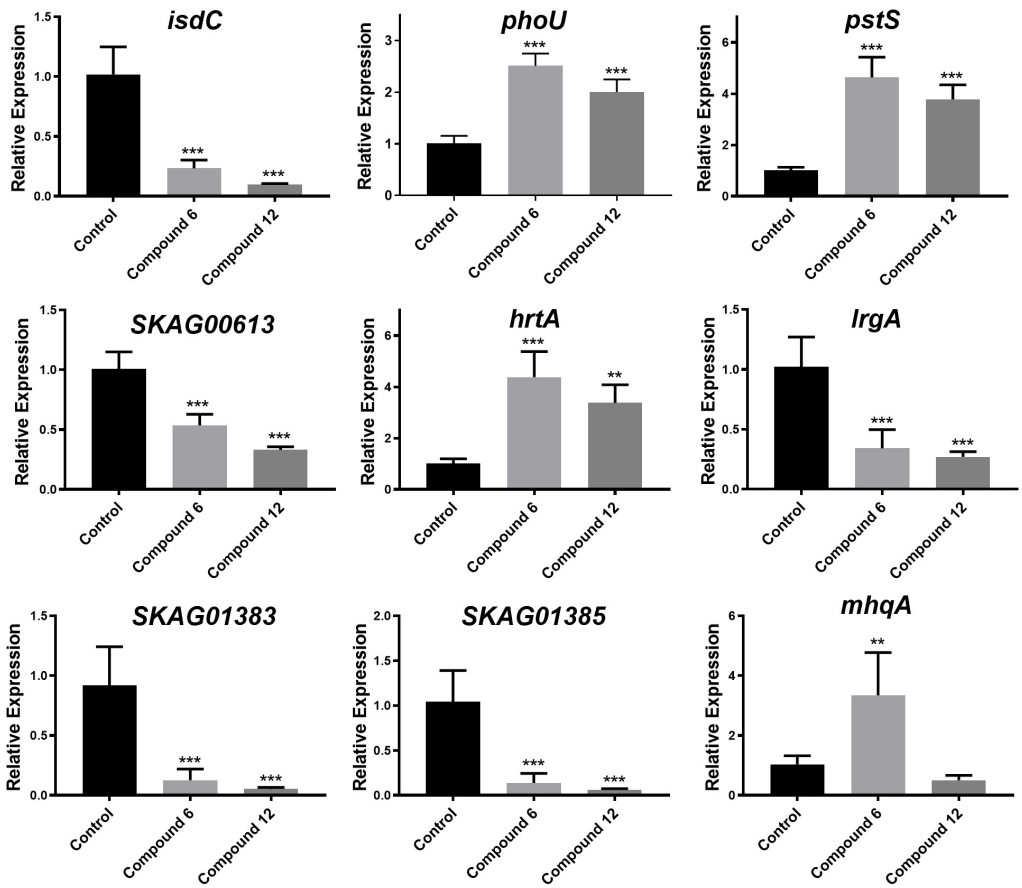

FIGURE 11 | Relative expression of nine selected genes. The data represent mean ± SD ($n = 4$); $^{***}p < 0.001$, $^{**}p < 0.01$.

at concentrations of 200 and 50 μg/ml by the CV staining method (**Figure 3**). Compounds **5**, **6**, **8**, **9**, **11**, and **12** could all strongly inhibit the formation of MRSA biofilms by >50% at the concentration of 50 μg/ml. It is worth noting that the inhibition rates were 75.2% (±3.3%) and 96.4% (±0.3%) for compounds **6** and **12**, respectively. On the contrary, compound **7** promoted biofilm forming which was not parallel to the trend of this class of compounds (**Figure 3A**). In addition to their good biofilm formation inhibitory activities, compounds **6** and **12** also showed good eradication activity against mature MRSA biofilms. Compound **6** could eradicate 54.2% (±5.9%) and 57.7% (±3.8%) of the mature MRSA biofilms at 200 and 50 μg/ml, and compound **12** could eradicate 44.0% (±3.8%) and 26.5% (±3.2%) at 200 and 50 μg/ml, respectively (**Figure 3B**). Based on their outstanding performance in both inhibiting and eradicating MRSA biofilms, we therefore chose compounds **6** and **12** as representatives for further antibiofilm study.

Biofilm Eradication Activity of Compounds 6 and 12

Two kinds of staining methods were conducted to further qualify the dose-dependent effects of compounds **6** and **12** against MRSA biofilms. The remaining total biomass in biofilms was determined by the CV staining method, while the metabolic activity of the viable cells was investigated by MTT staining method. Both compounds displayed only weak to moderate effect on reducing the total biomass of 24 h mature MRSA biofilms at concentrations ranging from 12.5 to 200 μg/ml (**Figures 4A,B**, **5A,B**). However, these two compounds could significantly disperse the living cells inside biofilms and showed strong eradicating efficiency with concentrations ranging from 12.5 to 200 μg/ml (**Figures 4C,D, 5C,D**). The remaining rates of viable biofilm cells were 47.9% (±3.8%) and 34.5% (±6.1%) at the lowest tested concentration of 12.5 μg/ml, respectively.

SEM and CLSM Analysis of Biofilm Structures After Treatment With Compounds 6 or 12

SEM and CLSM were used to analyze the 24 h preformed mature MRSA biofilm structures after treatment with compounds **6** and **12** for another 24 h. The images of SEM showed that the total MRSA biofilm biomass was significantly reduced when treated with compounds **6** and **12** at concentrations of 200 and 100 μg/ml (**Figure 6**). There were not many differences between compounds **6**- and **12**-treated groups. It also should be noticed that the cell

walls and membranes of the biofilm cells after treatment with both compounds remained as intact as those in the negative control group. Meanwhile, the viable bacteria within biofilms could be represented by the thickness and fluorescence intensity of the three-dimensional structures of MRSA biofilms in CLSM images (**Figure 7**), which showed that compound **12** at 50 and 100 μg/ml was highly effective in removing viable cells, and compound **6** at 100 and 200 μg/ml could also remove most of living bacteria.

Gene Expression Analysis

All the sequencing reads of gene expression of MRSA cells under treatment with 100 μg/ml of compounds **6** and **12** have been submitted to the NCBI Gene Expression Omnibus (GEO) with accession number GSE147157. Overall, among 3,050 unigenes of the reference strain *S. aureus* A9754, 2,989 unigenes (98%) matched those in the NR database and 2,088 (68.46%) matched those in Swiss-Prot. After treatment with compounds **6** and **12**, 237 and 302 DEGs were detected compared with the control group, respectively (**Figure 8A**). A total of 84 and 153 genes were down- and up-regulated respectively in compound **6**-treated group, while there were 145 downregulated and 157 upregulated genes in compound **12**-treated group (**Figures 8B,C**). The Venn diagrams showed that 166 DEGs (including 73 downregulated and 93 upregulated) had the same expression trend in both treatment groups (**Figures 8A–C**). The heatmaps revealed the induced and suppressed transcripts in the treatment groups compared with the control group (**Figures 8D,E**).

Functional Analyses of Differentially Expressed Genes

To further understand the function of DEGs, GO enrichment and KEGG pathway analyses of two treatment groups were performed respectively (**Figure 9**). According to GO classification analysis, DEGs were classified into three categories: biological process, cellular component, and molecular function. The GO enrichment analyses showed that the treatment groups had great different effects on the transcriptome of biofilm cells (**Figures 9A,B**). As in the biological process, all the GO term-related genes in the compound **6** treatment group were upregulated while only 2 out of 10 term-related genes were upregulated in the compound **12** treatment group. On the other hand, there were also similar changes in both treatment groups, such as the upregulation of nitrate metabolic process (GO: 0042126) and nitrate assimilation (GO: 0042128) in biological processes and the four terms enriched in molecular function were the same in both treatment groups. KEGG pathway analysis was used to clarify the biological function of genes (**Figures 9C,D**). A total of seven and nine pathways were significantly enriched in the compounds **6** and **12** treatment group, respectively. Among the pathway enrichment in the compound **6** treatment group, there were 17, 14, and 8 DEGs belonging to microbial metabolism in diverse environments, biosynthesis of amino acids, and two-component system, respectively. In the compound **12** treatment group, there were 10 DEGs that belonged to pyrimidine metabolism, 9 DEGs belonged to two-component system, and 8 DEGs belonged to glycolysis/gluconeogenesis pathway.

Overlapped Differentially Expressed Genes of Two Treatments

A total of 166 DEGs, including 73 downregulated and 93 upregulated, overlapped in compounds **6** and **12** treatment groups. As shown in **Figure 10A**, the majority of downregulated DEGs were enriched to cellular component ontology, of which 26 genes were enriched in cell periphery (GO:0071944), 23 genes in plasma membrane (GO:0005886), and 23 genes in membrane (GO:0016020). The GO terms related to compound biosynthesis and metabolic processes were frequently shown in biological process category, and the kinase- and transferase-related terms were mainly enriched in molecular function category. Meanwhile, the upregulated categories (**Figure 10B**) showed that metabolic process- and carbolic process-related GO terms were prevalent in the biological process category, oxidoreductase activity, and binding and transporter activity in the molecular function category. Among these three categories, most of DEGs were enriched in biological process with 30 genes enriched in single-organism metabolic process (GO:0044710), followed by 22 genes in small molecule metabolic process (GO:0044281) and 16 genes in oxidation-reduction process (GO:0055114); 16 genes enriched in oxidoreductase activity (GO:0016491) were the largest group in molecular function category; oxidoreductase complex (GO:1990204) with two significant genes was annotated in cellular component category.

qRT-PCR Validation

To validate the RNA-Seq results, some genes involved in phosphate-specific transport system (*phoU* and *pstS*), iron-acquisition/transport (*isdC*, *SKAG_01383* and *SKAG_001385*), and other genes (*lrgA*, *mhqA*, *hrtA*, and *SKAG_00613*) were selected to conduct the qRT-PCR analysis (**Figure 11** and **Supplementary Tables 1**, **2**). The results showed that *isdC*, *lrgA*, *SKAG_00613*, *SKAG_01383*, and *SKAG_001385* genes were significantly downregulated in two groups. On the contrary, *phoU*, *pstS*, and *hrtA* were significantly upregulated in both groups. What is more, *mhqA* was significantly upregulated in compound **6** treatment group, while it had no significant change in compound **12** treatment group. In general, most of the qRT-PCR results of these selected genes were consistent with the RNA-Seq results, indicating that the RNA-Seq data were reliable.

DISCUSSION

In this study, a total of 10 structurally related AQs including two microbe-derived natural products DMCA (**1**) and TMCA (**2**) and their eight analogs were tested for antibiofilm activity. Among these compounds, only anthraquinone-2-carboxlic acid (**6**) and rhein (**12**) exhibited bactericidal activity with MIC values lower than 200 μg/ml. Both compounds had a carboxyl group attached to the C-2 position of the anthraquinone skeleton, which is different from other tested anthraquinones. For antibiofilm activity, some of the hydroxy-anthraquinones

have been reported for their biofilm-inhibiting activity, and previous SAR analysis suggested that the hydroxyl groups at the C-1 and C-2 positions of the anthraquinone skeleton should play an important role in inhibiting biofilm formation at low concentrations (lower than 10 μg/ml) (Manoharan et al., 2017). Herein, it is interesting to note that the single hydroxyl group at the C-1 and C-2 positions exerted different biofilm inhibition activities at high concentrations (50 and 200 μg/ml). When comparing compounds **3**–**5**, compound **5** showed a higher rate of biofilm inhibition than compounds **3** and **4**, suggesting that the substitution of a hydroxyl group at the C-2 position was more important than the C-1 position in enhancing the prevention capability of MRSA biofilm formation. This was also supported by the good biofilm inhibitory activity of compounds **8** and **9**, both of which also have a C-2 hydroxyl group. Surprisingly, compound **7** with two symmetric hydroxyl groups at C-2 promoted biofilm formation instead, which was different from all the other compounds and requires further investigation. Consistent with the literature (Manoharan et al., 2017), at high concentrations, compounds **8**, **9**, and **11** still had excellent inhibitory performance for MRSA biofilm, but compounds **3**, **4**, **7**, and **10** could not suppress biofilm formation.

The biofilm eradication activity of these hydroxy- and carboxy-substituted AQs was then analyzed, and the SAR study revealed that: (i) for the hydroxyl AQs **5**, **7**, and **9**, the biofilm eradication rates of these three compounds were all around 20–30% at the concentration of 200 μg/ml, suggesting that the number of hydroxyl substitutions might not have much correlation with their activity; (ii) for the carboxylic AQs **3**, **6**, and **12**, compounds **6** and **12** showed higher biofilm eradication efficiency (the respective eradication rate of 54.2 ± 5.9 and 44.0 ± 5.3% at 200 μg/ml, and 57.7 ± 3.8 and 26.5 ± 3.2% at 50 μg/ml for compounds **6** and **12**, respectively) than that of compound **3**, indicating that the carboxyl group at C-2 position of the anthraquinone skeleton might be very important for improving eradication activity against MRSA biofilm; and (iii) combining the results of all the SAR analysis of hydroxy- and carboxy-AQs, we could conclude that the AQs including the carboxyl group at C-2 position of anthraquinone mother nucleus exhibited better MRSA biofilm eradication activity than the hydroxyl ones. Therefore, we suggest that the carboxyl substitution attached at C-2 position of anthraquinone should be considered a key group for further chemical design and development of antibiofilm AQs. In addition, it is particularly noteworthy that the biofilm eradication activity of carboxyl-substituted anthraquinone compounds **6** and **12** was reported for the first time in this study.

Since compounds **6** and **12** displayed promising eradication activity against MRSA biofilm, different staining methods, microscopy images, and RNA-Seq analysis were employed for more in-depth study. It was found that the MTT staining test always displayed a higher biofilm eradication rate than the CV staining test under the same concentrations of both compounds, which lead us to wonder whether their biofilm eradication effects against the preformed MRSA biofilms mostly involved decreasing the viable cells within biofilms rather than reducing the total biomass. Thus, the SEM imaging of the biofilm structures treated with these two compounds was carried out, and results showed visibly structural disruption of the treated biofilms. And the CLSM imaging analysis revealed that a significant decrease of the living biofilm cells in both treatment groups. All these results indicated that compounds **6** and **12** could gently reduce the total biofilm biomass but effectively remove the viable biofilm cells when exerting their antibiofilm activity.

For RNA-Seq analysis, we focused on the comparison of our transcriptomic results with those reported in literature (Monds et al., 2001; O'May et al., 2009; Neznansky and Opatowsky, 2014; Wang et al., 2017; Abouelhassan et al., 2018) due to the currently ambiguous and incomplete mechanism of the MRSA biofilm eradication. Recently, a halogenated phenazine has been reported to eradicate MRSA biofilms depending on an iron-starvation mechanism (Abouelhassan et al., 2018). The RNA-Seq results of compounds **6** and **12** treatment groups showed that most of the iron-acquisition– and iron-transport–related genes (*isdABCEFGHI*, *sbnAEI*, and *mntAB*) were downregulated or insignificantly differentially expressed instead of upregulated (**Supplementary Table 2**). Even though the iron ion might not be involved with the working mechanism of our compounds, it provided us a clue to analyze other ions. Meanwhile, among the overlapped DEGs of the two experimental groups, except for those involved in metabolic- and catabolic-related progress or function, many of the other upregulated genes belonged to transport GO terms: anion transport (GO:0006820), inorganic phosphate transmembrane transporter activity (GO:0005315), and phosphate transmembrane transporter activity (GO:1901677). It has been reported that the phosphate-specific transport system (Pst system; **Supplementary Table 2**), including five genes *pstSCAB-phoU*, has a high affinity for uptake of inorganic phosphate (P_i) and is very important for cell growth. What is more, the *pst* mutants revealed that these genes are necessary for the biofilm formation of different bacteria (Monds et al., 2001; O'May et al., 2009; Neznansky and Opatowsky, 2014; Wang et al., 2017). In our study, the upregulation of these genes suggested that P_i uptake was increased after treatment of compound **6** or **12**. The redundant P_i may be used to synthesize high-molecular-weight inorganic polyphosphate to store energy for cell metabolism and other purpose (Monds et al., 2001; Wang et al., 2017). We speculated that compounds **6** and **12** might influence phosphate homeostasis in MRSA which in turn led to the disassembly of biofilms, and more experiments are required to confirm this hypothesis.

As for the safety of compounds **6** and **12**, numerous studies have been carried out to study their biological activities and related molecular mechanisms (Sheng et al., 2011; Zhao et al., 2011; KoraMagazi et al., 2016; Panigrahi et al., 2016; Park et al., 2016a,b; Yuan et al., 2016). Take the cytotoxicity for instance, compound **6** had been demonstrated to have anti-inflammatory activity without cellular toxicity at concentrations below 26.8 μg/ml (Park et al., 2016a,b). On the contrary, compound **12**, which has been well studied in liver diseases, could trigger liver cytotoxicity in the long-term use, and the cytotoxicity

could take place quickly when used over 2.8 μg/ml (Sheng et al., 2011; Zhao et al., 2011; KoraMagazi et al., 2016; Panigrahi et al., 2016; Yuan et al., 2016). Herein, although both compounds displayed biofilm eradication activity at the lowest effective concentration of 12.5 μg/ml, it seems that compound **6** might be safer than compound **12** when used as an antibiofilm agent.

In our study, the antibacterial and antibiofilm activities against MRSA of a series of structurally related AQs have been well evaluated. The SAR analysis demonstrated that different positions of carboxyl and hydroxyl substitutions of the anthraquinone skeleton can significantly affect antibiofilm activity of these compounds. A hydroxyl group at the C-2 position of the anthraquinone skeleton was much more important than the C-1 position for improving their inhibitory activity against MRSA biofilm formation. Carboxylic AQs were more effective in the eradication of MRSA biofilms than the hydroxyl ones. The results of MTT staining and CV staining test, SEM and CLSM images, and RNA sequencing revealed that the MRSA biofilm eradication mechanism of compounds **6** and **12** might involve dispersion of biofilm cells and disruption of phosphate homeostasis.

DATA AVAILABILITY STATEMENT

The datasets presented in this study can be found in online repositories. The names of the repository/repositories and accession number(s) can be found in the article/ **Supplementary Material**.

AUTHOR CONTRIBUTIONS

Z-MS and YX designed the project. Z-MS and K-LW carried out experiments, interpreted the results, and wrote the manuscript. K-LW, YX, and C-YW funded the research and revised the manuscript. KZ, L-MY, and YZ helped in the RNA-Seq analysis. J-LZ provided a lot of help during the experiment. All authors contributed to the article and approved the submitted version.

FUNDING

This work was financially supported by the National Key R&D Program of China (2018YFA0902500), National Natural Science Foundations of China (Nos. 32060032 and 41830535), Natural Science Foundation of Yunnan Province (No. 202001AT070022), the Development and Utilization of Characteristic Medicinal Plants in Western Yunnan and Bai Nationality Medicines (No. ZKLX2019106), the Taishan Scholars Program of China and the Shenzhen Bureau of Science, Technology, and Information (JCYJ20180305123659726).

ACKNOWLEDGMENTS

The authors are very grateful to the instrumentation equipment provided by the Instrumental Analysis Center of Shenzhen University (Xili Campus). The authors also thank Chi Xu (Shenzhen University, Shenzhen, China) for his help in CLSM imaging, Hong Liu (Shenzhen University, Shenzhen, China) in SEM imaging, and Si Chen for helping to analyze the experimental data in the SPSS software (Shenzhen University, Shenzhen, China).

SUPPLEMENTARY MATERIAL

The Supplementary Material for this article can be found online at: https://www.frontiersin.org/articles/10.3389/fmicb.2021.709826/full#supplementary-material

REFERENCES

Abouelhassan, Y., Zhang, Y., Jin, S., and Huigens, R. W. III (2018). Transcript Profiling of MRSA biofilms treated with a halogenated phenazine eradicating agent: a platform for defining cellular targets and pathways critical to Biofilm Survival. *Angew. Chem. Int. Ed. Engl.* 57, 15523–15528. doi: 10.1002/anie.201809785

Agarwal, S. K., Singh, S. S., Verma, S., and Kumar, S. (2000). Antifungal activity of anthraquinone derivatives from *Rheum emodi*. *J. Ethnopharmacol.* 72, 43–46. doi: 10.1016/s0378-8741(00)00195-1

Alexa, A., and Rahnenfuhrer, J. (2010). *topGO: Enrichment analysis for Gene Ontology. R package version 2.22.0*. Available online at: https://bioconductor.org/packages/release/bioc/html/topGO.html (accessed September 1, 2020)

Alves, D. R., Gaudion, A., Bean, J. E., Perez Esteban, P., Arnot, T. C., Harper, D. R., et al. (2014). Combined use of bacteriophage K and a novel bacteriophage to reduce *Staphylococcus aureus* biofilm formation. *Appl. Environ. Microbiol.* 80, 6694–6703. doi: 10.1128/AEM.01789-14

Augustine, N., Goel, A. K., Sivakumar, K. C., Kumar, R. A., and Thomas, S. (2014). Resveratrol–a potential inhibitor of biofilm formation in *Vibrio cholerae*. *Phytomedicine* 21, 286–289. doi: 10.1016/j.phymed.2013.09.010

Barnard, D. L., Huffman, J. H., Morris, J. L., Wood, S. G., Hughes, B. G., and Sidwell, R. W. (1992). Evaluation of the antiviral activity of anthraquinones, anthrones and anthraquinone derivatives against human cytomegalovirus. *Antiviral Res.* 17, 63–77. doi: 10.1016/0166-3542(92)90091-i

Bashir, A., Saeed, B., Mujahid, T. Y., and Jehan, N. (2011). Comparative study of antimicrobial activities of *Aloe vera* extracts and antibiotics against isolates from skin infections. *Afr. J. Biotechnol.* 10, 3835–3840.

Bhattacharya, M., Wozniak, D. J., Stoodley, P., and Hall-Stoodley, L. (2015). Prevention and treatment of *Staphylococcus aureus* biofilms. *Expert Rev Anti Infect. Ther.* 13, 1499–1516. doi: 10.1586/14787210.2015.1100533

Bjarnsholt, T., Ciofu, O., Molin, S., Givskov, M., and Hoiby, N. (2013). Applying insights from biofilm biology to drug development - can a new approach be developed? *Nat. Rev. Drug Discov.* 12, 791–808. doi: 10.1038/nrd4000

Boyce, J. M., Cookson, B., Christiansen, K., Hori, S., and Pittet, D. (2005). Methicillin-resistant *Staphylococcus aureus*. *Lancet Infect. Dis.* 5, 653–663.

Brady, R. A., O'may, G. A., Leid, J. G., Prior, M. L., Costerton, J. W., and Shirtliff, M. E. (2011). Resolution of *Staphylococcus aureus* biofilm infection using vaccination and antibiotic treatment. *Infect. Immun.* 79, 1797–1803. doi: 10.1128/IAI.00451-10

Calo, M., Kinnaert, X., and Dorbath, C. (2007). Update on prevalence and treatment of methicillin-resistant *Staphylococcus aureus* infections. *Expert Rev. Anti Infect. Ther.* 5, 961–981.

Coenye, T., Honraet, K., Rigole, P., Nadal Jimenez, P., and Nelis, H. J. (2007). *In vitro* inhibition of *Streptococcus mutans* biofilm formation on hydroxyapatite

by subinhibitory concentrations of anthraquinones. *Antimicrob. Agents Chemother.* 51, 1541–1544. doi: 10.1128/AAC.00999-06

Costerton, J. W., Stewart, P. S., and Greenberg, E. P. (1999). Bacterial biofilms: a common cause of persistent infections. *Science* 284, 1318–1322. doi: 10.1126/science.284.5418.1318

Craigen, B., Dashiff, A., and Kadouri, D. E. (2011). The use of commercially available alpha-amylase compounds to inhibit and remove *Staphylococcus aureus* Biofilms. *Open Microbiol. J.* 5, 21–31. doi: 10.2174/1874285801105010021

DeLeo, F. R., Otto, M., Kreiswirth, B. N., and Chambers, H. F. (2010). Community-associated methicillin-resistant *Staphylococcus aureus*. *Lancet* 375, 1557–1568. doi: 10.1016/S0140-6736(09)61999-1

Dobin, A., Davis, C. A., Schlesinger, F., Drenkow, J., Zaleski, C., Jha, S., et al. (2013). STAR: ultrafast universal RNA-seq aligner. *Bioinformatics* 29, 15–21. doi: 10.1093/bioinformatics/bts635

Dusane, D. H., Pawar, V. S., Nancharaiah, Y. V., Venugopalan, V. P., Kumar, A. R., and Zinjarde, S. S. (2011). Anti-biofilm potential of a glycolipid surfactant produced by a tropical marine strain of *Serratia marcescens*. *Biofouling* 27, 645–654. doi: 10.1080/08927014.2011.594883

Farooq, U., Khan, S., Naz, S., Khan, A., Khan, A., Ahmed, A., et al. (2017). Three new anthraquinone derivatives isolated from *Symplocos racemosa* and their antibiofilm activity. *Chin. J. Nat. Med.* 15, 944–949. doi: 10.1016/S1875-5364(18)30011-6

Flemming, H. C., and Wingender, J. (2010). The biofilm matrix. *Nat. Rev. Microbiol.* 8, 623–633. doi: 10.1038/nrmicro2415

Fletcher, M. H., Jennings, M. C., and Wuest, W. M. (2014). Draining the moat: disrupting bacterial biofilms with natural products. *Tetrahedron* 70, 6373–6383. doi: 10.1016/j.tet.2014.06.055

Fux, C. A., Costerton, J. W., Stewart, P. S., and Stoodley, P. (2005). Survival strategies of infectious biofilms. *Trends Microbiol.* 13, 34–40. doi: 10.1016/j.tim.2004.11.010

Galasinski, W., Chlabicz, J., Paszkiewicz-Gadek, A., Marcinkiewicz, C., and Gindzienski, A. (1996). The substances of plant origin that inhibit protein biosynthesis. *Acta Pol. Pharm.* 53, 311–318.

Gilbert, P., Allison, D. G., and Mcbain, A. J. (2002). Biofilms *in vitro* and *in vivo*: do singular mechanisms imply cross-resistance? *Symp. Ser. Soc. Appl. Microbiol.* 92(Suppl.), 98S–110S.

Gu, B., Kelesidis, T., Tsiodras, S., Hindler, J., and Humphries, R. M. (2013). The emerging problem of linezolid-resistant *Staphylococcus*. *J. Antimicrob. Chemother.* 68, 4–11. doi: 10.1093/jac/dks354

Gunatilaka, A. A. (2006). Natural products from plant-associated microorganisms: distribution, structural diversity, bioactivity, and implications of their occurrence. *J. Nat. Prod.* 69, 509–526. doi: 10.1021/np058128n

Hall Snyder, A. D., Vidaillac, C., Rose, W., Mcroberts, J. P., and Rybak, M. J. (2014). Evaluation of high-dose daptomycin versus vancomycin alone or combined with clarithromycin or rifampin against *Staphylococcus aureus* and *S. epidermidis* in a novel *in vitro* PK/PD model of bacterial biofilm. *Infect. Dis. Ther.* 4, 51–65. doi: 10.1007/s40121-014-0055-5

Hawas, U. W., El-Ansari, M. A., and Laatsch, H. (2006). A new alpha-methylanthraquinone glucoside from *Emex spinosus*. *Nat. Prod. Res.* 20, 742–747. doi: 10.1080/14786410500281789

Hoiby, N., Bjarnsholt, T., Givskov, M., Molin, S., and Ciofu, O. (2010). Antibiotic resistance of bacterial biofilms. *Int. J. Antimicrob. Agents* 35, 322–332. doi: 10.1016/j.ijantimicag.2009.12.011

Hoiby, N., Ciofu, O., Johansen, H. K., Song, Z. J., Moser, C., Jensen, P. O., et al. (2011). The clinical impact of bacterial biofilms. *Int. J. Oral Sci.* 3, 55–65. doi: 10.4248/IJOS11026

Kaplan, J. B., Lovetri, K., Cardona, S. T., Madhyastha, S., Sadovskaya, I., Jabbouri, S., et al. (2012). Recombinant human DNase I decreases biofilm and increases antimicrobial susceptibility in *Staphylococci*. *J. Antibiot.* 65, 73–77. doi: 10.1038/ja.2011.113

Kelley, P. G., Gao, W., Ward, P. B., and Howden, B. P. (2011). Daptomycin non-susceptibility in vancomycin-intermediate *Staphylococcus aureus* (VISA) and heterogeneous-VISA (hVISA): implications for therapy after vancomycin treatment failure. *J. Antimicrob. Chemother.* 66, 1057–1060. doi: 10.1093/jac/dkr066

KoraMagazi, A., Wang, D., Yousef, B., Guerram, M., and Yu, F. (2016). Rhein triggers apoptosis via induction of endoplasmic reticulum stress, caspase-4 and intracellular calcium in primary human hepatic HL-7702 cells. *Biochem. Biophys. Res. Commun.* 473, 230–236. doi: 10.1016/j.bbrc.2016.03.084

Krupa, J., Lessmann, H., and Lackner, H. (1989). Ein α-Methylanthrachinon aus Streptomyceten. *Liebigs Ann. Chem.* 7, 699–701. doi: 10.1002/jlac.198919890217

Laplante, K. L., and Mermel, L. A. (2009). *In vitro* activities of telavancin and vancomycin against biofilm-producing *Staphylococcus aureus*, *S. epidermidis*, and *Enterococcus faecalis* strains. *Antimicrob. Agents Chemother.* 53, 3166–3169. doi: 10.1128/AAC.01642-08

Lebeaux, D., Chauhan, A., Rendueles, O., and Beloin, C. (2013). From *in vitro* to *in vivo* models of bacterial biofilm-related infections. *Pathogens* 2, 288–356. doi: 10.3390/pathogens2020288

Lee, J. H., Kim, Y. G., Yong Ryu, S., and Lee, J. (2016). Calcium-chelating alizarin and other anthraquinones inhibit biofilm formation and the hemolytic activity of *Staphylococcus aureus*. *Sci. Rep.* 6:19267. doi: 10.1038/srep19267

Lee, J. H., Park, J. H., Cho, H. S., Joo, S. W., Cho, M. H., and Lee, J. (2013). Anti-biofilm activities of quercetin and tannic acid against *Staphylococcus aureus*. *Biofouling* 29, 491–499. doi: 10.1080/08927014.2013.788692

Lee, J. H., Regmi, S. C., Kim, J. A., Cho, M. H., Yun, H., Lee, C. S., et al. (2011). Apple flavonoid phloretin inhibits *Escherichia coli* O157:H7 biofilm formation and ameliorates colon inflammation in rats. *Infect. Immun.* 79, 4819–4827. doi: 10.1128/IAI.05580-11

Li, J. W., and Vederas, J. C. (2009). Drug discovery and natural products: end of an era or an endless frontier? *Science* 325, 161–165. doi: 10.1126/science.1168243

Lin, Y. Y., Tsai, S. J., Chiang, M. Y., Wen, Z. H., and Su, J. H. (2015). Anti-inflammatory anthraquinones from the crinoid *Himerometra magnipinna*. *Nat. Prod. Commun.* 10, 317–318.

Love, M. I., Huber, W., and Anders, S. (2014). Moderated estimation of fold change and dispersion for RNA-seq data with DESeq2. *Genome Biol.* 15:550. doi: 10.1186/s13059-014-0550-8

Manoharan, R. K., Lee, J. H., Kim, Y. G., and Lee, J. (2017). Alizarin and Chrysazin Inhibit Biofilm and Hyphal Formation by *Candida albicans*. *Front. Cell. Infect. Microbiol.* 7:447. doi: 10.3389/fcimb.2017.00447

Meeker, D. G., Beenken, K. E., Mills, W. B., Loughran, A. J., Spencer, H. J., Lynn, W. B., et al. (2016). Evaluation of antibiotics active against methicillin-resistant *Staphylococcus aureus* based on activity in an established biofilm. *Antimicrob. Agents Chemother.* 60, 5688–5694. doi: 10.1128/AAC.01251-16

Monds, R. D., Silby, M. W., and Mahanty, H. K. (2001). Expression of the Pho regulon negatively regulates biofilm formation by *Pseudomonas aureofaciens* PA147-2. *Mol. Microbiol.* 42, 415–426. doi: 10.1046/j.1365-2958.2001.02641.x

Nair, S., Desai, S., Poonacha, N., Vipra, A., and Sharma, U. (2016). Antibiofilm activity and synergistic inhibition of *Staphylococcus aureus* biofilms by bactericidal protein P128 in combination with antibiotics. *Antimicrob. Agents Chemother.* 60, 7280–7289. doi: 10.1128/AAC.01118-16

Nam, W., Kim, S. P., Nam, S. H., and Friedman, M. (2017). Structure-antioxidative and anti-inflammatory activity relationships of purpurin and related anthraquinones in chemical and cell assays. *Molecules* 22:265. doi: 10.3390/molecules22020265

Neznansky, A., and Opatowsky, Y. (2014). Expression, purification and crystallization of the phosphate-binding PstS protein from *Pseudomonas aeruginosa*. *Acta Crystallogr. F Struct. Biol. Commun.* 70, 906–910. doi: 10.1107/S2053230X14010279

Nithya, C., Begum, M. F., and Pandian, S. K. (2010). Marine bacterial isolates inhibit biofilm formation and disrupt mature biofilms of *Pseudomonas aeruginosa* PAO1. *Appl. Microbiol. Biotechnol.* 88, 341–358. doi: 10.1007/s00253-010-2777-y

Nithya, C., Devi, M. G., and Karutha Pandian, S. (2011). A novel compound from the marine bacterium *Bacillus pumilus* S6-15 inhibits biofilm formation in gram-positive and gram-negative species. *Biofouling* 27, 519–528. doi: 10.1080/08927014.2011.586127

O'May, G. A., Jacobsen, S. M., Longwell, M., Stoodley, P., Mobley, H. L. T., and Shirtliff, M. E. (2009). The high-affinity phosphate transporter Pst in *Proteus mirabilis* HI4320 and its importance in biofilm formation. *Microbiology* 155, 1523–1535. doi: 10.1099/mic.0.026500-0

Panigrahi, G. K., Yadav, A., Mandal, P., Tripathi, A., and Das, M. (2016). Immunomodulatory potential of Rhein, an anthraquinone moiety of Cassia occidentalis seeds. *Toxicol. Lett.* 245, 15–23. doi: 10.1016/j.toxlet.2016.01.006

Park, J. G., Kim, S. C., Kim, Y. H., Yang, W. S., Kim, Y., Hong, S., et al. (2016a). Anti-inflammatory and antinociceptive activities of anthraquinone-2-carboxylic acid. *Mediators Inflamm.* 2016:1903849. doi: 10.1155/2016/1903849

Park, J. G., Son, Y. J., Kim, M. Y., and Cho, J. Y. (2016b). Syk and IRAK1 contribute to immunopharmacological activities of anthraquinone-2-carboxlic acid. *Molecules* 21:809. doi: 10.3390/molecules21060809

Potera, C. (1999). Forging a link between biofilms and disease. *Science* 283, 1837–1839. doi: 10.1126/science.283.5409.1837

Quave, C. L., Estevez-Carmona, M., Compadre, C. M., Hobby, G., Hendrickson, H., Beenken, K. E., et al. (2012). Ellagic acid derivatives from *Rubus ulmifolius* inhibit *Staphylococcus aureus* biofilm formation and improve response to antibiotics. *PLoS One* 7:e28737. doi: 10.1371/journal.pone.0028737

Ranall, M. V., Butler, M. S., Blaskovich, M. A., and Cooper, M. A. (2012). Resolving biofilm infections: current therapy and drug discovery strategies. *Curr. Drug Targets* 13, 1375–1385. doi: 10.2174/138945012803530251

Richards, J. J., Ballard, T. E., Huigens Iii, R. W., and Melander, C. (2008). Synthesis and screening of an oroidin library against *Pseudomonas aeruginosa* Biofilms. 9, 1267–1279. doi: 10.1002/cbic.200700774

Sheng, X., Wang, M., Lu, M., Xi, B., Sheng, H., and Zang, Y. Q. (2011). Rhein ameliorates fatty liver disease through negative energy balance, hepatic lipogenic regulation, and immunomodulation in diet-induced obese mice. *Am. J. Physiol. Endocrinol. Metab.* 300, E886–E893. doi: 10.1152/ajpendo.00332.2010

Stepanovic, S., Vukovic, D., Hola, V., Di Bonaventura, G., Djukic, S., Cirkovic, I., et al. (2007). Quantification of biofilm in microtiter plates: overview of testing conditions and practical recommendations for assessment of biofilm production by staphylococci. *APMIS* 115, 891–899. doi: 10.1111/j.1600-0463.2007.apm_630.x

Sultana, S. T., Call, D. R., and Beyenal, H. (2016). Eradication of *Pseudomonas aeruginosa* biofilms and persister cells using an electrochemical scaffold and enhanced antibiotic susceptibility. *NPJ Biofilms Microbiomes* 2:2. doi: 10.1038/s41522-016-0003-0

Sun, D., Zhang, W., Mou, Z., Chen, Y., Guo, F., Yang, E., et al. (2017). Transcriptome analysis reveals silver nanoparticle-decorated quercetin antibacterial molecular mechanism. *ACS Appl. Mater. Interfaces* 9, 10047–10060. doi: 10.1021/acsami.7b02380

Tan, X., Qin, N., Wu, C., Sheng, J., Yang, R., Zheng, B., et al. (2015). Transcriptome analysis of the biofilm formed by methicillin-susceptible *Staphylococcus aureus*. *Sci. Rep.* 5:11997. doi: 10.1038/srep11997

Trapnell, C., Roberts, A., Goff, L., Pertea, G., Kim, D., Kelley, D. R., et al. (2012). Differential gene and transcript expression analysis of RNA-seq experiments with TopHat and Cufflinks. *Nat. Protoc.* 7, 562–578. doi: 10.1038/nprot.2012.016

Wang, D., Jin, Q., Xiang, H., Wang, W., Guo, N., Zhang, K., et al. (2011). Transcriptional and functional analysis of the effects of magnolol: inhibition of autolysis and biofilms in *Staphylococcus aureus*. *PLoS One* 6:e26833. doi: 10.1371/journal.pone.0026833

Wang, S., Zheng, Y., Gu, C., He, C., Yang, M., Zhang, X., et al. (2018). Bacillus cereus AR156 activates defense responses to *Pseudomonas syringae* pv. tomato in *Arabidopsis thaliana* Similarly to flg22. *Mol. Plant Microbe Interact.* 31, 311–322. doi: 10.1094/MPMI-10-17-0240-R

Wang, X., Han, H., Lv, Z., Lin, Z., Shang, Y., Xu, T., et al. (2017). PhoU2 but Not PhoU1 as an important regulator of biofilm formation and tolerance to multiple stresses by participating in various fundamental metabolic processes in *Staphylococcus epidermidis*. *J. Bacteriol.* 199:e00219-17. doi: 10.1128/JB.00219-17

Yen, G. C., Duh, P. D., and Chuang, D. Y. (2000). Antioxidant activity of anthraquinones and anthrone. *Food Chem.* 70, 437–441. doi: 10.1016/S0308-8146(00)00108-4

Yin, Q., Liang, J., Zhang, W., Zhang, L., Hu, Z. L., Zhang, Y., et al. (2019). Butenolide, a marine-derived broad-spectrum antibiofilm agent against both gram-positive and gram-negative pathogenic bacteria. *Mar. Biotechnol.* 21, 88–98. doi: 10.1007/s10126-018-9861-1

Yuan, Y., Zheng, J., Wang, M., Li, Y., Ruan, J., and Zhang, H. (2016). Metabolic Activation of Rhein: insights into the potential toxicity induced by Rhein-Containing Herbs. *J. Agric. Food Chem.* 64, 5742–5750. doi: 10.1021/acs.jafc.6b01872

Zeng, Z., Qian, L., Cao, L., Tan, H., Huang, Y., Xue, X., et al. (2008). Virtual screening for novel quorum sensing inhibitors to eradicate biofilm formation of *Pseudomonas aeruginosa*. *Appl. Microbiol. Biotechnol.* 79, 119–126. doi: 10.1007/s00253-008-1406-5

Zhao, Y. L., Zhou, G. D., Yang, H. B., Wang, J. B., Shan, L. M., Li, R. S., et al. (2011). Rhein protects against acetaminophen-induced hepatic and renal toxicity. *Food Chem. Toxicol.* 49, 1705–1710. doi: 10.1016/j.fct.2011.04.011

Conflict of Interest: The authors declare that the research was conducted in the absence of any commercial or financial relationships that could be construed as a potential conflict of interest.

Publisher's Note: All claims expressed in this article are solely those of the authors and do not necessarily represent those of their affiliated organizations, or those of the publisher, the editors and the reviewers. Any product that may be evaluated in this article, or claim that may be made by its manufacturer, is not guaranteed or endorsed by the publisher.

frontiers in Microbiology

ORIGINAL RESEARCH
published: 21 September 2021
doi: 10.3389/fmicb.2021.716628

Cellular Growth Arrest and Efflux Pumps Are Associated With Antibiotic Persisters in *Streptococcus pyogenes* Induced in Biofilm-Like Environments

Caroline Lopes Martini[1†], Amada Zambrana Coronado[1†], Maria Celeste Nunes Melo[2], Clarice Neffa Gobbi[1], Úrsula Santos Lopez[1], Marcos Correa de Mattos[1], Thais Tavares Amorim[1], Ana Maria Nunes Botelho[1], Ana Tereza Ribeiro Vasconcelos[3], Luiz Gonzaga Paula Almeida[3], Paul J. Planet[4,5,6], Russolina Benedeta Zingali[7], Agnes Marie Sá Figueiredo[1] and Bernadete Teixeira Ferreira-Carvalho[1]**

[1] Instituto de Microbiologia Paulo de Góes, Universidade Federal do Rio de Janeiro, Rio de Janeiro, Brazil, [2] Departamento de Microbiologia e Parasitologia, Universidade Federal do Rio Grande do Norte, Natal, Brazil, [3] Laboratório Nacional de Computação Científica (LNCC), Petrópolis, Brazil, [4] Department of Pediatrics, Perelman College of Medicine, University of Pennsylvania, Philadelphia, PA, United States, [5] Sackler Institute for Comparative Genomics, American Museum of Natural History, New York, NY, United States, [6] Children's Hospital of Philadelphia, Philadelphia, PA, United States, [7] Unidade de Espectrometria de Massas e Proteomica – UEMP, Instituto de Bioquímica Médica Leopoldo de Meis, Universidade Federal do Rio de Janeiro, Rio de Janeiro, Brazil

Streptococcus pyogenes (group A *Streptococcus*-GAS) is an important pathogen for humans. GAS has been associated with severe and invasive diseases. Despite the fact that these bacteria remain universally susceptible to penicillin, therapeutic failures have been reported in some GAS infections. Many hypotheses have been proposed to explain these antibiotic-unresponsive infections; however, none of them have fully elucidated this phenomenon. In this study, we show that GAS strains have the ability to form antimicrobial persisters when inoculated on abiotic surfaces to form a film of bacterial agglomerates (biofilm-like environment). Our data suggest that efflux pumps were possibly involved in this phenomenon. In fact, gene expression assays by real-time qRT-PCR showed upregulation of some genes associated with efflux pumps in persisters arising in the presence of penicillin. Phenotypic reversion assay and whole-genome sequencing indicated that this event was due to non-inherited resistance mechanisms. The persister cells showed downregulation of genes associated with protein biosynthesis and cell growth, as demonstrated by gene expression assays. Moreover, the proteomic analysis revealed that susceptible cells express higher levels of ribosome proteins. It is remarkable that previous studies have reported the recovery of *S. pyogenes* viable cells from tissue biopsies of patients presented with GAS invasive infections and submitted to therapy with antibiotics. The persistence phenomenon described herein brings new insights into the origin of therapeutic failures in *S. pyogenes* infections. Multifactorial mechanisms involving protein synthesis inhibition, cell growth impairment and efflux pumps seem to play roles in the formation of antimicrobial persisters in *S. pyogenes*.

Keywords: *Streptococcus pyogenes*, drug refractory, persisters, efflux pump, antimicrobial resistance, clinical resistance

OPEN ACCESS

Edited by:
Ana Luíza Mattos Guaraldi, Rio de Janeiro State University, Brazil

Reviewed by:
Cassius Souza, Rio de Janeiro State University, Brazil
Louisy Santos, Rio de Janeiro State University, Brazil

***Correspondence:**
Agnes Marie Sá Figueiredo
agnes@micro.ufrj.br
Bernadete Teixeira Ferreira-Carvalho
bernadete@micro.ufrj.br

[†] These authors have contributed equally to this work and share first authorship

Specialty section:
This article was submitted to Antimicrobials, Resistance and Chemotherapy, a section of the journal Frontiers in Microbiology

Received: *28 May 2021*
Accepted: *23 August 2021*
Published: *21 September 2021*

Citation:
Martini CL, Coronado AZ, Melo MCN, Gobbi CN, Lopez ÚS, de Mattos MC, Amorim TT, Botelho AMN, Vasconcelos ATR, Almeida LGP, Planet PJ, Zingali RB, Figueiredo AMS and Ferreira-Carvalho BT (2021) Cellular Growth Arrest and Efflux Pumps Are Associated With Antibiotic Persisters in Streptococcus pyogenes Induced in Biofilm-Like Environments. Front. Microbiol. 12:716628. doi: 10.3389/fmicb.2021.716628

INTRODUCTION

Group A streptococci (GAS) has long been recognized as one of the most important disease-causing bacteria in humans. These bacteria are associated with different types of infections, including pharyngitis, impetigo, scarlet fever, cellulitis and abscesses. GAS is also involved in severe invasive infections such as myositis and necrotizing fasciitis, and cases of toxic shock syndrome. Additionally, some post infectious sequelae have been reported (Avire et al., 2021).

GAS strains are typically susceptible to penicillin (Oppegaard et al., 2020). However, studies have reported treatment failures of patients receiving β-lactam therapy (Gidengil et al., 2013; Brook, 2017; Randhawa et al., 2018). Many explanations have been proposed to elucidate clinical failures of penicillin treatment, including protection of GAS-susceptible isolates by β-lactamase producers in the pharyngeal microbiota, penicillin tolerance, biofilm formation, bacterial internalization in host cells among others (Thulin et al., 2006; Walker et al., 2014; Fiedler et al., 2015; Brook, 2017). However, the contribution of each of these mechanisms for drug failures remains unclear (Walker et al., 2014; Brook, 2017).

Several mechanisms have also been described in other bacterial species to explain phenotypic drug resistance including tolerance, small colony variants (SVCs), heteroresistance and persisters (Brauner et al., 2016; Balaban et al., 2019; Proctor, 2019; Yu et al., 2019; Lee et al., 2020). The phenomenon of tolerance is defined for bactericidal antibiotics when the minimum inhibitory concentration (MIC) of the tolerant is equal to that of the susceptible strain, but the minimal bactericidal concentration (MBC) and the time required for bacterial death to occur are considerably higher (Brauner et al., 2016; Balaban et al., 2019). SCVs are characterized by their slow growth resulting in small colony sizes, which show mutations in genes often associated with auxotrophic phenotypes, electron transportation chain, and biosynthetic pathways (Proctor, 2019; Lee et al., 2020). Heteroresistance defines a mechanism by which cell subpopulations in a bacterial culture are killed by different antibiotic concentrations. Therefore, although most cells are eliminated at the MIC value, a few can survive. Nevertheless, they are often killed at certain drug concentration not far from MIC, leading to low-level (borderline) resistance. Additionally, heteroresistance is generally defined for an antimicrobial class while persisters are often resistant to different classes and remain viable in antimicrobial concentrations far above the MIC (Balaban et al., 2019). In the mechanism of persister generation, fraction of the bacterial population switches stochastically to the persister phenotype during the growth phase. An important characteristic of the persisters is the occurrence of slow- or non-growing bacterial cells that remain viable during exposure to antibiotics. Despite that, antibiotic susceptibility is regained after bacterial growth in the absence of the drug (Pontes and Groisman, 2019; Yu et al., 2019; Huemer et al., 2020). Therefore, the demonstration of growth impairment in the presence of antibiotics is important before they can be classified as persisters (Yu et al., 2019; Pontes and Groisman, 2019).

In the study herein we report the generation of antimicrobial-persisters by GAS cells in a biofilm-like environment and investigate some mechanisms known to be associated with persisters in other bacterial pathogens. The formation of GAS persisters may be also a mechanism behind antimicrobial failures that has been overlooked.

MATERIALS AND METHODS

Bacterial Isolates

Two hundred-eleven GAS isolates were used to test the emergence of persister cells to β-lactam antibiotics. These isolates belong to a convenience collection obtained from infected patients and colonized individuals, in different Brazilian cities, from different clinical sites (**Supplementary Table 1**). The majority of these isolates were from outpatient cases of symptomatic oropharyngeal infections, and obtained from 1978 to 1997. Clonality were previously analyzed by pulsed-field gel electrophoresis (PFGE) for roughly half of these isolates, which displayed extensive genetic diversity (Melo et al., 2003). These GAS were identified by routine methods and confirmed by latex agglutination tests (Streptococcal Grouping Kit; Oxoid, Basingstoke, Hampshire, United Kingdom). Minimal inhibitory concentration (MIC) for all antimicrobials used in this study, except azithromycin and ethidium bromide (EtBr), was previously determined for this GAS collection (Melo et al., 2003). Since all GAS isolates analyzed were equally able to produce persisters under the experimental model used, to get some insights into the molecular mechanisms associated with antimicrobial persisters in GAS we randomly choose the GAS strain 37–97 among the isolates of this collection whose PFGE patterns were previously determined. This strain showed sequence type (ST) 62, *emm* 87 and was isolated from symptomatic oropharynx infection case, in 1997, in the outpatient clinic of the Hospital de Puericultura Martagão Gesteira, Rio de Janeiro, RJ. Additionally, nine other GAS isolates were chosen from the convenience collection based on diverse PFGE patterns, different clinical sources, and susceptibility to all antimicrobials tested (**Supplementary Table 2**). These nine isolates were used as control in the phenotypic tests to detect persisters to validate the results obtained for the representative strain 37–97. Pure cultures of the 211 GAS isolates analyzed were obtained from lyophilized stocks. One tube of each isolate was opened and after reconstitution, cultures was stored at −80°C in brain heart infusion (w/v) with 0.5% (w/v) of yeast extract and 18% (v/v) glycerol.

Minimal Inhibitory Concentration

MIC determinations for azithromycin (Azi; Sigma, St. Louis, MO, United States) and ethidium bromide (EtBr; Sigma) were done using the agar dilution method as recommended by the Clinical & Laboratory Standards Institute (CLSI, 2021) with concentrations ranging from 0.06 to 4 μg/mL and 0.015 to 4 μg/mL; respectively. Two biological experiments were performed ($N = 2$).

Development of GAS-Persister Cells to β-Lactams

The model used in this study to generate persisters was based on previous work done with *Staphylococcus aureus* strains

(Novais et al., 2020). In this system (here called biofilm like-environment) high bacterial load is inoculated in order to allow the formation of an initial bacterial film on the smooth surface of a cellophane membrane placed onto agar media containing antibiotics to mimic bacterial agglomeration found in some environments such as those encountered in biofilms. Persisters were indirectly detected in the system containing antibiotic by CFU counting (Orman and Brynildsen, 2015; Yu et al., 2019). To prepare the bacterial inoculum, GAS isolates (n = 211) were grown in Todd Hewitt broth containing 0.5% (w/v) of yeast extract (THB-Y) at 37°C/6 h in order to reach the exponential phase. After centrifugation, the pellet was adjusted ($\sim$ 1–2 $\times$ 10^{10} colony forming unit-CFU/mL) using the same broth. To form a bacterial film, a 100-μL volume ($\sim$ 2–4 $\times$ 10^7 CFU/cm^2) was homogeneously spread on the surface of a cellophane membrane placed onto THB-Y agar containing 5% defibrinated sheep blood (BAB) and supplemented with 0.005–8 μg/mL penicillin (Pen; Wyeth-Whitehall Ltda, Itapevi, SP, Brazil) or 0.25–4 μg/mL cephalexin (Cep; Sigma). After 37°C/18 h, persisters were removed from the cellophane membranes at the highest drug concentration in which growth was detected for CFU counting. To test whether defibrinated sheep blood interfered with the analysis, the experiments were also performed in the absence of blood. Antimicrobial susceptible control cells were obtained exactly as described above but using inoculum size adjusted to concentrations recommended by CLSI ($\sim$$10^6$ CFU/plate; condition that does not allow the generation of persisters). Four biological experiments were performed with two technical replicates each. CFU determinations were carried out for the representative strain 37-97. Two CFU determinations were carried out for each dilution (N = 4).

Proteomic Analysis

A proteomic analysis was done to assess protein differential expression between cells grown in biofilm-like environment (condition that allows generation of persisters) and GAS susceptible cells (inoculum size adjusted to $\sim$$10^6$ CFU/plate, condition that does not promote antibiotic persistence). Bacterial cells from strain 37–97 were collected from the cellophane membrane, suspended in phosphate buffered saline (PBS) (140 mM NaCl; 2.7 mM KCl; 8 mM Na_2HPO_4, and KH_2PO_4 1.5 mM; pH 7.2) using vigorous shaking, and adjusted to $OD_{600\ nm}$ = 0.4. Pellet was washed twice, resuspended in PBS and lysed with 106 μm beads (Sigma) in a Bio101 Fast Prep system (BioSavant, Qbiogene, Carslbad, CA, United States) using six cycles (5 speeds/30 s pulse). After centrifugation, the protein concentration was estimated using a Qubit 2.0 (Invitrogen Life Technologies, CA, United States), and lysates diluted in sodium dodecyl sulfate polyacrylamide Gel (SDS-PAGE) sample buffer (1:1, v/v) (Laemmli, 1970). Proteins were separated using a 12.5% SDS-PAGE gel electrophoresis, and individual bands were isolated from the gels. All procedures used for the treatment of gel slices and trypsin digestion were performed as previously described (Shevchenko et al., 1996). The resulting peptides were desalted using an in-house reverse-phase microcolumn (POROS R2 resin, Applied Biosystems, Carlsbad, CA, United States) and dried by vacuum centrifugation (Rodrigues et al., 2011). Peptides were solubilized in 20 μL of 0.1% (v/v) formic acid (FA), and 10 μL were injected into a trap column (Opti-Pak C18, Waters, Milford, MA, United States). Liquid chromatography separation was performed using a reverse-phase capillary column (nanoEase C18, 100 mm $\times$ 100 μm, Waters) connected to a nano-HPLC system (Waters UPLC, Waters). The eluted peptides were introduced into an ESI-Q-TOF-MS/MS (Q-TOF Micro, Waters) controlled by MassLynx software (Version 4.1, Waters). Mass spectra (MS) were collected in the 50–2,000 m/z range, and the three most abundant ions (charges +2, +3, and +4) were submitted for collision-induced dissociation (CID) using argon gas at 13 psi and 18–45 V. The raw data were converted to a peak list using the ProteinLynx Global software (version 4.0, Waters). Protein identification was considered valid if at least one peptide with minimum of 10 amino acids was observed with a maximum error tolerance of 50 ppm and Mascot score $\geq$ 46 ($p \leq 0.05$). The GenBank (Acc) access number, locus tag, and gene and protein names were determined using BLASTp.[1] In addition, Uniprot BLAST analysis[2] was performed in order to identify homologs in *S. pyogenes* MGAS10750. Only *e*-values $\leq$ 1.0 e–3 were considered in the database search.

Detection of Ethidium Bromide-Refractory Cells

The increase in ethidium bromide (EtBr) MIC values is highly sensitive and specific in identifying efflux-proficient strains in *S. aureus* (Patel et al., 2010). Therefore, we evaluated the occurrence of EtBr-refractory cells in the biofilm-like environment. Different EtBr concentrations (0.015–4.0 μg/mL) were added to BAB agar that was covered with cellophane membranes. High-bacterial load was placed onto the surface of cellophane membranes to produce a biofilm-like environment as described before. After 18 h incubation (37°C), GAS cells were recovered from the cellophane membranes at the highest EtBr concentration in which growth was detected for CFU determinations. Controls were performed exactly as above but with susceptible cells ($\sim$$10^6$ CFU/plate). Four biological experiments were performed with two technical replicates each. CFU determinations were carried out for the representative strain 37–97. Two CFU determinations were carried out for each dilution (N = 4).

Persistence to Non-β-Lactam Antibiotics

These experiments were performed to assess if the persistence observed for GAS cells was associate to β-lactams only, or to universal mechanisms as those involving efflux pumps. The ability of GAS strain 37–97 to become refractory to different antimicrobials was tested in concentrations ranging from 0.01 to 4 μg/mL erythromycin (Ery; Sigma), 0.06–4 μg/mL azithromycin (Azi; Sigma), 0.01–1 μg/mL clindamycin (Cli; Sigma), 0.25–16 μg/mL chloramphenicol (Chl; Sigma), or 0.125–16 μg/mL tetracycline (Tet; Sigma). Plates were examined after incubation for 18 h at 37°C. Controls were also performed exactly as above but with susceptible cells ($\sim$$10^6$ CFU/plate).

[1] http://blast.ncbi.nlm.nih.gov/Blast.cgi

[2] www.uniprot.org/blast

Additionally, for control purposes, these experiments were also done with additional nine GAS isolates (**Supplementary Table 2**), using the highest concentration of antibiotic in which bacterial growth was detected for the representative strain 37–97. For each antimicrobial tested, two to six biological experiments were performed with two technical replicates each. CFU determinations were carried out for the representative strain 37–97. Two CFU determinations were carried out for each dilution. Ery ($N = 2$), Azi ($N = 4$), Cli ($N = 6$), Chl ($N = 6$), Tet ($N = 6$).

Effect of Cyanide 3-Chlorophenylhydrazone (CCCP) Efflux Pump Inhibitor in Antimicrobial Refractory

Because CCCP inhibits proton motive force and also the transcription of some transport associated genes (Baron and Rolain, 2018), the ability of this compound to inhibit the formation of persister cells was tested. The CCCP (Sigma) at 100 μM final concentration (Clancy et al., 1996) was incorporated to BAB (covered or not with a cellophane membrane) supplemented with 8 μg/mL penicillin (MIC = 0.01 μg/mL), 4 μg/mL cephalexin (MIC = 0.5), 4 μg/mL erythromycin (MIC = 0.12 μg/mL), 4 μg/mL azithromycin (MIC = 0.12 μg/mL), 1 μg/mL clindamycin (MIC = 0.01 μg/mL), 16 μg/mL chloramphenicol (MIC = 1.0 μg/mL), 16 μg/mL tetracycline (MIC = 0.12 μg/mL), or 4 μg/mL EtBr (MIC = 0.06 μg/mL). BAB plates without CCCP were used to control bacterial growth. High bacterial load was placed onto the surface of cellophane membranes or uncovered BAB plates. After 18 h incubation (37°C), all plates were examined and GAS cells recovered from the cellophane membranes at the highest drug concentration in which growth was detected for CFU determinations. Controls were performed exactly as above but with susceptible cells ($\sim 10^6$ CFU/plate). Three biological experiments were performed with two technical replicates each for the representative strain 37–97. Two CFU determinations were carried out for each dilution ($N = 3$).

Phenotypic Switching Test

GAS persister cells of the strain 37–97 recovered from the cellophane membranes covering BAB plates with 8 μg/mL penicillin were subjected to successive passages (up to 500 generations) on BAB without antibiotics. After passaging, bacterial growth was adjusted to concentrations recommended by CLSI ($\sim 10^6$ CFU/plate), and the penicillin MIC was determined using the agar dilution method (CLSI, 2021). Two biological experiments were performed ($N = 2$).

Whole-Genome Sequencing

For total DNA preparation, penicillin-persister (8 μg/mL penicillin plates; MIC 0.01 μg/mL) and -susceptible cells of the strain 37–97 were recovered from cellophane membranes. An aliquot of the cell suspension was inoculated in THB-Y (1:200 dilution). After incubation (37°C/18 h), DNA was obtained using the Wizard Genomic DNA Purification Kit (Promega; Madison, WI, United States). Genomic libraries were prepared using the Nextera XT kit (Illumina, San Diego, CA, United States) and sequenced on an Illumina HiSeq (125 pb reads). Reads were trimmed using BBDuk Trimmer (version 1.0) and genome assembly was carried out using Newber v3.0 (Margulies et al., 2005). Scaffolds were aligned against a reference genome (*S. pyogenes* strain NGAS743; Acc: CP007560) using cross match (version 0.990329).[3] Intra-scaffold and inter-scaffold gaps resulting from repetitive sequences were resolved by *in silico* gap filling. Any remaining gaps in the genomic sequence from penicillin-persister cells of the 37–97 strains (37–97P) were filled with "N" with estimated sizes based on the complete sequence of the susceptible cells of the strain 37–97 (37–97S). The sequenced genomes were annotated using RAST 2.0v (Overbeek et al., 2014). Taxonomic analysis was performed by calculating average nucleotide identity (ANI) for whole genomes using OrthoANIu tool.[4] Multi locus sequence typing (MLST) was performed for the genome sequences using MLST 2.4.0 software.[5] Differences in single nucleotide polymorphisms (SNPs) between samples 37–97S and 37–97P were evaluated using cross match with parameter discrep lists. The generated list was compared to the Newbler assembly ace file and genome annotation. SNPs were verified by resequencing on an ABI 3730 DNA Analyzer (Life Technologies—Applied Biosystem; Carlsbad, CA, United States). Reactions were performed using the BigDye Terminator v3.1 Cycle Sequencing Kit in 36-cm capillaries with POP7 polymer according to the manufacturer's instructions.

Gene Expression Analysis

Total RNA from penicillin-persisters and -susceptible cells obtained from 37–97 strain was prepared from a suspension of cells directly recovered from cellophane membranes as described in the item "Development of GAS-persister cells to β-lactams." The RNeasy Mini kit (Qiagen; Germantown, MD, United States) was used for RNA preparation that was quantified by a Qubit 2.0 Fluorometer (Thermo Fisher Scientific Brasil; São Paulo, SP, Brazil). RNA quality was analyzed by gel electrophoresis. For some experiments, gene expression was also performed in presence of 100 μM CCCP. To test the effect of clindamycin in the expression of the efflux-associated locus *MGAS10750_Spy1819*, total RNA was prepared from GAS persister cells recovered from cellophane membranes on BAB plates containing 1 μg/mL clindamycin (MIC = 0.01 μg/mL). The real-time quantitative reverse transcriptase PCR (real-time RT-qPCR) was performed using Power SYBR Green RNA-to-CT™ 1-Step Kit (Applied Biosystems) as recommended ("Guide to Performing Relative Quantitation of Gene Expression Using Real-Time Quantitative PCR"; Applied Biosystems). The rRNA 16S gene was used as an endogenous control. The calibrator sample was total RNA from susceptible cells of strain 37–97. The reaction was performed in a Step One™ Real Time PCR System (Applied Biosystems). Data were analyzed using Step One Software 2.2 (Applied Biosystems). All primers were validated as recommended in the cited guide and listed in **Supplementary**

[3] www.phrap.org/phrap.docs/phrap.html

[4] https://www.ezbiocloud.net/tools/ani

[5] https://cge.cbs.dtu.dk/services/MLST/

Table 3. Three biological replicates were performed with three technical replicates each ($N = 3$).

Statistical Tests

To analyze the quantity of persister cells recovering in presence of β-lactams and other antimicrobial classes, one way ANOVA was applied followed by *post hoc* Tukey's test for multiple comparisons. Two-tailed unpaired Student's *t*-test was used to analyze most the binary experiments of gene expression. To analyze the hypothesis that the expression of efflux pump-associated genes increases in the persister GAS cells, one-tailed unpaired *t*-test was performed. All statistical tests were calculated using GraphPad Prism version 9.2.0 for Windows (GraphPad Software, La Jolla, CA, United States). In addition, to confront the null hypothesis, Scaled Jeffreys–Zellner–Siow (JZS) Bayes Factor for two-samples *t*-test was calculated to test the alternative hypothesis for $r = 0.707$ (Rouder et al., 2009).

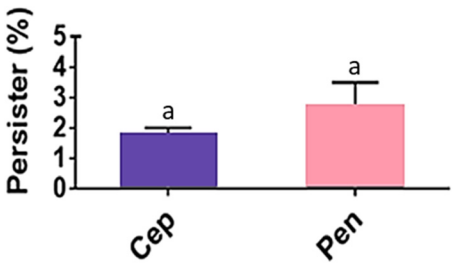

FIGURE 1 | *Streptococcus pyogenes* persisters recovered from biofilm-like environments at concentrations of 4 μg/mL cephalexin (Cep; MIC = 0.5 μg/mL) or 8 μg/mL penicillin (Pen; MIC = 0.01 μg/mL). The average CFU/mL of the control cells (no antibiotic) was 6.0×10^{10} and corresponded to 100%. One way ANOVA ($p < 0.001$; $F = 16.81$; $DF_{total} = 11$) was applied for CFU values. *Post hoc* Tukey's test was performed followed ANOVA for multiple comparisons between the control and antibiotics ($^{a}p < 0.01$) and between antibiotics (there was no significant difference in the amount of persister cells recovered when Cep and Pen were compared; $p = 0.9712$).

RESULTS

Persistence to β-Lactam Antibiotics

Despite the susceptible MIC values for penicillin (MIC range = 0.0025–0.02 μg/mL; MIC50 and MIC90 = 0.01 μg/mL), persisters were detected for the 211 GAS isolates in all penicillin concentrations tested including those far above MIC and as high as 8 μg/mL. To observe a possible influence of defibrinated sheep blood on the formation of persisters, GAS strain 37–97 was inoculated on BAB plates with and without blood supplementation, both containing 8 μg/mL penicillin, covered or not with cellophane membranes. Persister cells were equally formed when high bacterial load was inoculated. The average detection of persister corresponded to 2.7% ($p = 0.0022$) of the total cell population grown in the absence of penicillin ($6.0 \pm 2.4 \times 10^{10}$ CFU/mL) (**Figure 1**). When uncovered BAB plates were examined, persisters formed almost invisible (very tiny) hemolytic colonies, which returned to the normal size after passage in fresh media without antibiotics. Similar to the results obtained for penicillin, persisters could also arise on BAB plates containing 4 μg/mL cephalexin (MIC50 and MIC90 = 0.5 μg/mL). The mean percentage of persisters for 4 μg/mL cephalexin was 1.8% ($p = 0.0016$) of the total cell population grown in the absence of the drug ($6.0 \pm 2.4 \times 10^{10}$ CFU/mL) (**Figure 1**).

Drug susceptibility could be reverted when persister cells were submitted to serial passaging on BAB plates without penicillin, with the antibiotic persistent cells returning to their original state of drug susceptibility (MIC = 0.01 μg/mL). To assess whether this persistence phenotype was actually induced by the biofilm-like environment or due to preexistent heterogeneous resistant subpopulations present in the high bacterial load provided by the heavy inoculum size ($\sim 1–2 \times 10^9$ CFU/100 μL), this inoculum was divided in 100 parts. To each part, 99.9 μL of THB-Y was added and the total 100 μL inoculated onto a cellophane membrane on the BAB plate containing 8 μg/mL penicillin. To control this experiment, the total inoculum ($\sim 1–2 \times 10^9$ CFU/100 μL) was also inoculated onto a cellophane membrane on the BAB plate with 8 μg/mL penicillin. After 18 h at 37°C, persisters were only generated in the environment of cell agglomeration of the control. No growth was detected in the 100 plates inoculated with part of the inoculum, clearly ruling out the presence of heteroresistant subpopulations in the GAS culture.

Additionally, DNA samples from penicillin-persister (37–97P) and susceptible cells of the strain 37–97 (37–97S) underwent whole-genome sequencing (WGS). Both genomes have a GC content of 38.5% and 1.92 Mb in size. More details on the genome attributes for 37–97S (Acc: CP041408.1) and 37–97P (Acc: CP041615.1) are listed in the **Supplementary Table 4**. Both sequences were classified as ST62 by the MLST software. To calculate the ANI value, we used the genome sequence of a ST62 *S. pyogenes*, strain NGAS743, available in the GenBank (Acc: CP007560.1). The ANI value was 99.95% (coverage 37–97S = 78.66% and coverage NGAS743 = 78.83%). This value was higher than the optimal genome-wide ANI threshold for species delineation (ANI 95%; coverage 70%). WGS alignments generated in MAUVE showed high identity and perfect synteny of collinear blocks (**Figure 2A**). There was also no difference in the absence or presence of mobile genetic elements, genomic islands, or unique genes in the persister cells of the strain 37–97 (37–97P) compared with that of susceptible ones (37–97S). The ANI value for the genomes of 37–97S and 37–97P was 99.99% (coverage 37–97S = 99.89% and coverage 37–97P = 99.89%). Despite some differences in SNPs observed in the WGS, these could not be confirmed by Sanger resequencing of these regions, thus mutations were not associated with the emergence of persisters (**Figure 2B**) ruling out the phenomenon known as SCVs.

Proteomic Analysis

A total of 61 proteins were only detected in bacterial cells recovered from the biofilm-like environment of the strain 37–97, a condition that led to the formation of antimicrobial persisters (**Supplementary Table 5**). The most remarkable feature was the low frequency of L ribosomal proteins (LRP) in these

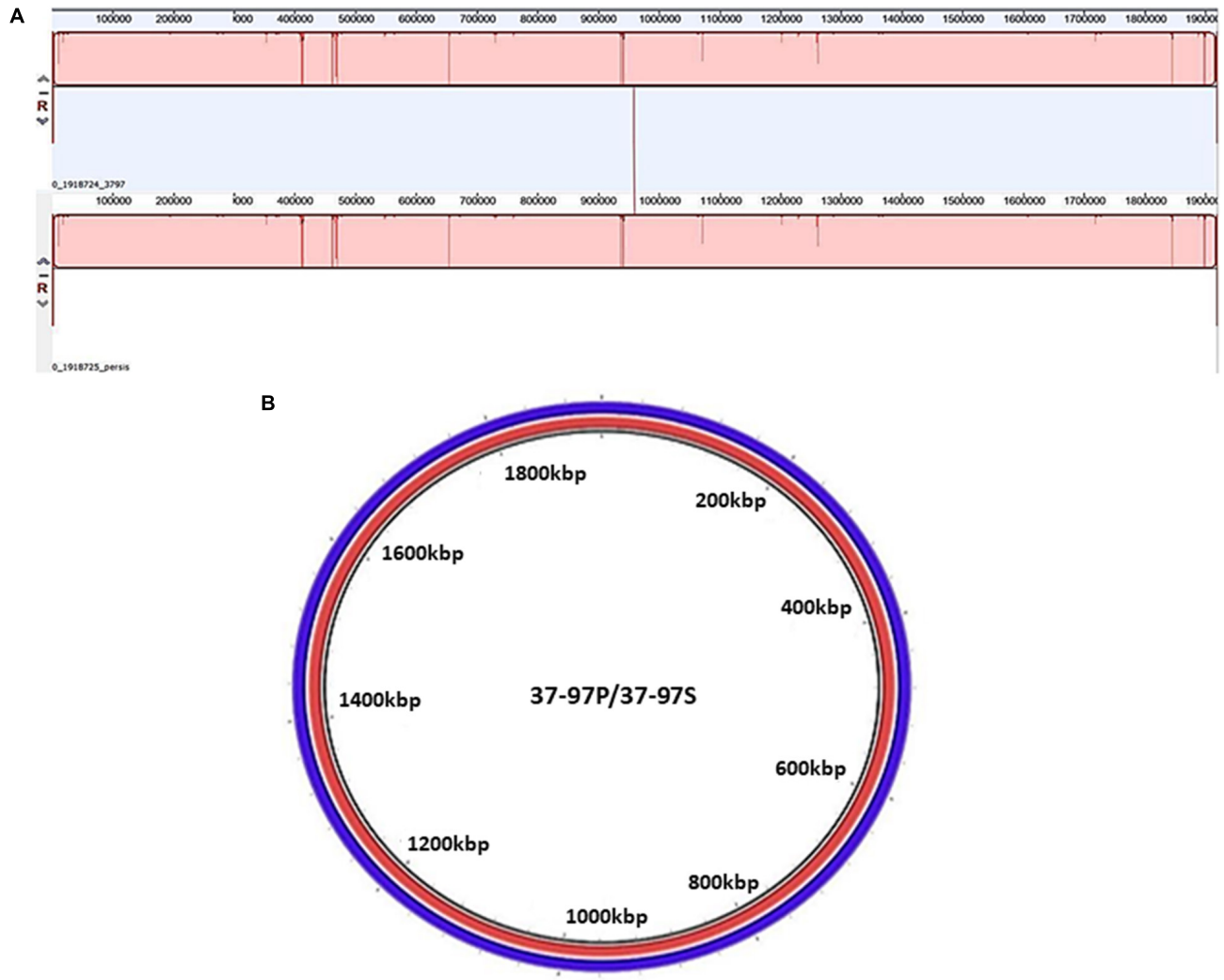

FIGURE 2 | Analysis of synteny and circular comparison of the chromosomes. **(A)** Genome alignments were performed using MAUVE. **37–97P**: DNA sequence of the penicillin persister cells of the *Streptococcus pyogenes* strain 37-97 generated in 8 μg/mL penicillin (MIC = 0.01 μg/mL), and **37–97S**: DNA sequence of the susceptible cells of strain 37–97. **(B)**. Circular comparison of the chromosomes was generated by Blast Ring Image Generator (BRIG) using genome sequences obtained from 37–97P **(red)** and 37–97S **(blue)**.

GAS cells (3.3%). Seventy-nine proteins were only detected when GAS strain 37–97 was grown using an inoculum size recommended for MIC determination (**Supplementary Table 6**), a condition for susceptibility. However, the most frequently detected proteins under this condition were the LRP proteins (31.6%), which play essential roles in ribosome assembly and are crucial for protein synthesis and cell growth (**Figure 3**). These data clearly suggest a decrease in growth activity for cells grown in biofilm-like environments. Some multidrug resistance (MDR) efflux pump components were only detected under condition of cell agglomeration, including a protein associated with the periplasmic component of the efflux system that belongs to the root-nodulation-cell-division (RND) family (Uniprot access: Q1J790). Multiple sugar transport ATP-binding protein MsmK (Uniprot access: Q1J4L0) and the multidrug resistant ABC transporter ATP-binding and permease protein (Uniprot access: Q1J8L9) were also observed under this condition (**Supplementary Table 5**). A total of 128 proteins were detected in both conditions (**Supplementary Table 7**).

Implication of Efflux Pumps

Efflux pump substrates (EtBr and different classes of antimicrobials) were used to assess the role of efflux pump activity in the formation of persisters. The MIC value of strain 37–97 for EtBr was 0.06 μg/mL. However, in the condition used to allow persister formation, growth was observed at concentrations of EtBr as high as 4 μg/mL, possibly indicating intense efflux activity. The percentage of EtBr-refractory cells recovered at concentration of 4 μg/mL was about 6% ($p = 0.001$) of the GAS cell population grown in biofilm-like environments in the absence of EtBr ($5.5 \pm 2.0 \times 10^{10}$ CFU/mL) (**Figure 4A**).

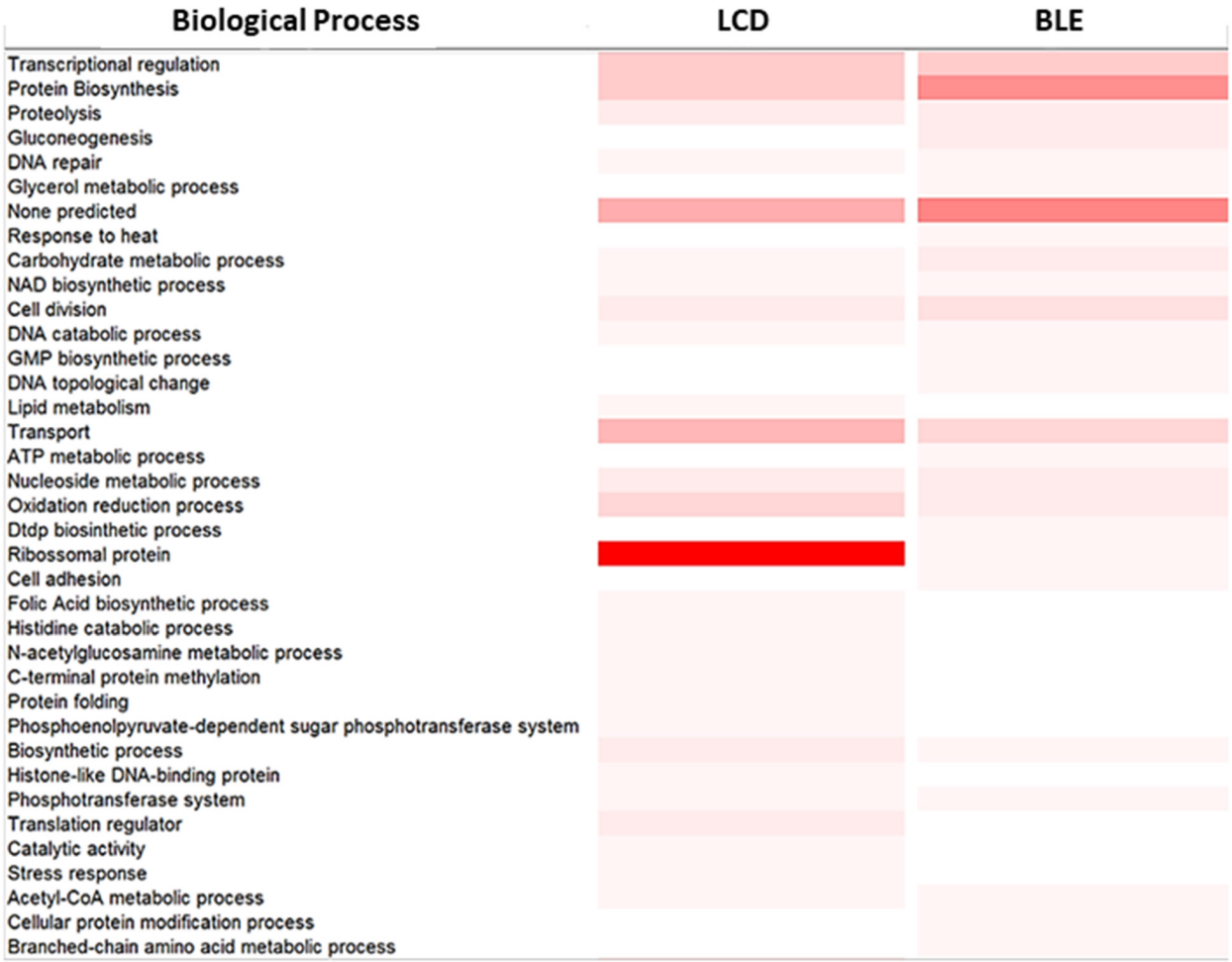

FIGURE 3 | Proteomic analysis of the *Streptococcus pyogenes* strain 37–97 in biofilm-like environment (**BLE**) and at condition of low cell density (**LCD**). Color gradient indicates the frequency of proteins involved in a biological process according to InterPro (www.ebi.ac.uk/interpro). *More intense color*: Highest number of proteins. *Lightest color*: smallest number of proteins. *White color*: absence of proteins.

Our data show that persisters were formed not only for the GAS representative strain 37–97 but similarly for the nine additional strains used as control, independent on the antibiotic classes analyzed, demonstrating that this phenomenon is a common feature in *S. pyogenes*. Persister cells were generated at MIC levels and at concentrations as high as 4 μg/mL erythromycin (MIC = 0.12 μg/mL), 4 μg/mL azithromycin (MIC = 0.12 μg/mL), 1 μg/mL clindamycin (MIC = 0.01 μg/mL), 16 μg/mL chloramphenicol (MIC = 1 μg/mL), and 16 μg/mL tetracycline (MIC = 0.12 μg/mL). The percentage of persisters recovered for 37–97 strain, considering all antimicrobials tested, ranged from 0.32 to 4.62% ($p < 0.001$) of the cell population grown in the absence of antimicrobials ($5.5 \pm 2.0 \times 10^{10}$ CFU/mL) (**Figure 4A**).

Since the resistance-nodulation-division (RND) family of efflux pumps was one of the drug/proton antiporters detected in the proteome performed with cell grown under agglomeration condition, we used the pump inhibitor CCCP to dissipate the proton-motive force. Control plates with CCCP (100 μM) without antibiotic caused no effect on bacterial growth of 37–97. Despite the inhibition of chloramphenicol and clindamycin persisters by CCCP (**Figure 4B**), this compound did not inhibit the generation of persisters by β-lactams or other antimicrobials tested.

Gene Expression Analysis

Of the 15 genes analyzed that were associated with the efflux pumps, seven showed some levels of upregulation in penicillin-persister cells compared with those of susceptible GAS cells (**Figure 5A**). Among these, genes of an operon associated with efflux pumps of the RND family showed increases of ≥4-fold, which included *MGAS10750_Spy1817* (gene product: ABC transporter ATP binding protein; $p = 0.0156$), *MGAS10750_Spy1818* (gene product: ABC transporter permease protein; $p = 0.0088$), and *MGAS10750_Spy1819* (gene product: periplasmic component of efflux system, $p < 0.001$). An increase in transcripts >4-fold was also observed for a gene product annotated as belonging to a major facilitator superfamily, the

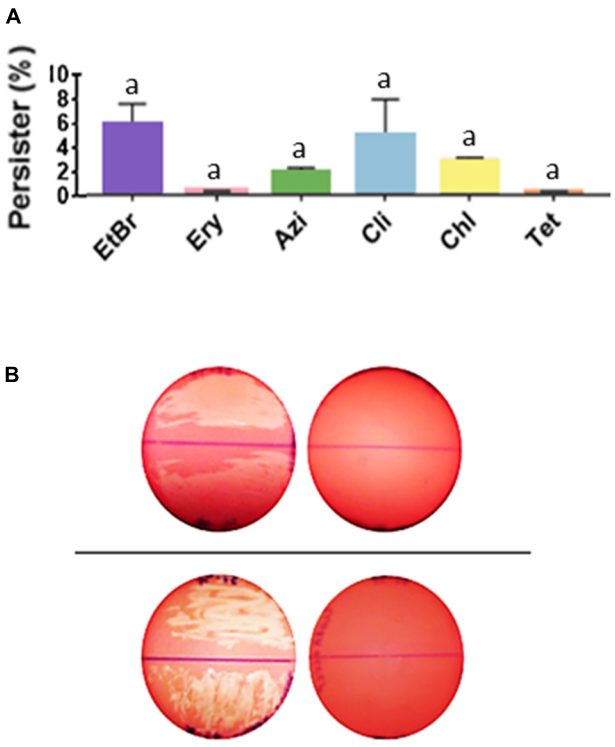

FIGURE 4 | *Streptococcus pyogenes* cells in biofilm-like environments show persistence to ethidium bromide and to a number of non-β-lactam antimicrobials. **(A)** Persisters recovered from biofilm-like environments at concentrations of 4 μg/mL ethidium bromide (EtBr; MIC = 0.06 μg/mL), 4 μg/mL erythromycin (Ery; MIC = 0.12 μg/mL), 4 μg/mL azithromycin (Azi; MIC = 0.12 μg/mL), 1 μg/mL clindamycin (Cli; MIC = 0.01 μg/mL), 16 μg/mL chloramphenicol (Chl; MIC = 1 μg/mL), or 16 μg/mL tetracycline (Tet; MIC = 0.12 μg/mL). The average CFU/mL of the control cells (no antibiotic) was 5.5×10^{10} and corresponded to 100%. One way ANOVA was applied using CFU values ($p < 0.001$; $F = 24.55$; $DF_{total} = 37$). *Post hoc* Tukey's test followed ANOVA was performed for multiple comparisons between the control and each condition ($^{a}p < 0.001$) and between the different conditions (there was no significant difference in the amount of persister cells recovered, p range = 0.995 to > 0.999). **(B)** Inhibition of antimicrobial persisters by the efflux pump inhibitor, cyanide 3-chlorophenylhydrazone (CCCP). *Top panel*; *left plate*: uncovered BAB plate was supplemented with 1 μg/mL Cli, and *right plate*: with 1 μg/mL Cli and 100 μM/mL CCCP. *Bottom panel*; *left plate*: uncovered BAB plate was supplemented with 16 μg/mL Chl, and *right plate*: with 16 μg/mL Chl and 100 μM/mL CCCP. Note the hemolysis that was produced by tiny (almost invisible) colonies for GAS cells in biofilm-like environments. Persisters for these antibiotics was completely inhibited in the presence of CCCP.

multidrug resistance protein B (*MGAS10750_Spy0495*) ($p = 0.04$). Another gene upregulated was a homolog of the multiple sugar transport ATP-binding protein MsmK (*MGAS10750_Spy1776*), which displayed a 2.2-fold increase in expression levels. Despite this difference was not very expressive ($p = 0.1490$), protein of this same family was detected only on the proteome of cells grown in the biofilm-like environment. The loci *MGAS10750_Spy0043* and *MGAS10750_Spy1633* (*norA* homolog) showed about twofold increase ($p < 0.001$ and $p = 0.0031$, respectively, **Figure 5A**).

Because clindamycin was one of the antibiotics completely inhibited by CCCP, we also investigated the effect of this antibiotic in the overexpression of *MGAS10750_Spy1819*, which is part of the ABC transport operon. Our data showed an overexpression of about ninefold in these gene transcripts. It was observed that CCCP had simultaneously affected the transcript levels of this ABC operon and two gene homologs to *ihk* (*MGAS10750_Spy1815*) and *irr* (*MGAS10750_ Spy1816*) encoding the two-component regulatory system (TCS) Ihk/Irr, which are adjacent to and upstream this operon. Our data also demonstrated that both the operon and TCS were downregulated in the presence of CCCP (ABC operon: $p = 0.03$, $p = 0.021$, $p < 0.001$ and *ihk/irr*: $p = 0.0057$, $p = 0.0389$, respectively, **Figure 5B**). Similar to the downstream genes belonging to the ABC operon, *ihk/irr* homologs also displayed increased levels of transcripts (fourfold) for persisters formed in the absence of CCCP ($p < 0.001$ and $p = 0.01$), compared with the susceptible GAS cells (**Figure 5B**). These data suggest that the *Ihk/Irr* system could be acting as a regulator of this operon. Indeed, consistent with an increase in pump activity, genes (M*GAS10750_Spy1765* and M*GAS10750_Spy1120*) annotated as belonging to the MarR and GntR families (pump negative transcriptional regulators) were downregulated in the persister cells ($p = 0.0032$ and $p = 0.0137$; **Figure 5C**).

Additionally, the expression of genes associated with protein biosynthesis and cell growth/division were evaluated. For all these genes, the transcript levels decreased, but for *bcaT* homolog (gene product: branched-chain-amino acid aminotransferase) this decrease was less than twofold. The *guaA* homolog (gene product: GMP synthesis [glutamine hydrolyzing]), which is involved in the GTP pathway, was twofold down-regulated ($p = 0.016$). Decreased expression was also observed for *relA* (gene product: GTP pyrophosphokinase; $p = 0.003$) and *typA* (gene product: GTP-binding protein TypA/BipA; $p = 0.0314$). Finally, the *ftsA* homolog, which is essential for cell division, was reduced threefold ($p = 0.0187$) (**Figure 5D**).

Among the genes associated with the stress conditions studied, which includes some genes related to oxidative stress, the majority was down-regulated in penicillin-persisters. An increase was only observed for a *dpr* homolog (gene product: hydrogen peroxide resistance regulator), which was about twofold ($p = 0.03$) more expressed compared with the susceptible GAS cells (**Figure 5E**). Finally, we examined the expression of three genes homologous to toxin-antitoxin (TA) systems found in the genome of *S. pyogenes* strain 37–97. Increased expression was observed for the *hicA/B* homologs (2.8- and 3.5-fold increase, respectively; $p = 0.007$ and $p = 0.017$, respectively) for persisters (**Figure 5F**).

DISCUSSION

The influence of high bacterial load in environments such those found in biofilms on antimicrobial persistence *in vitro* and *in vivo* has been described by others (Thulin et al., 2006; Rio-Marques et al., 2014; Karslake et al., 2016; Li et al., 2017; Vulin et al., 2018; Novais et al., 2020). Persisters have

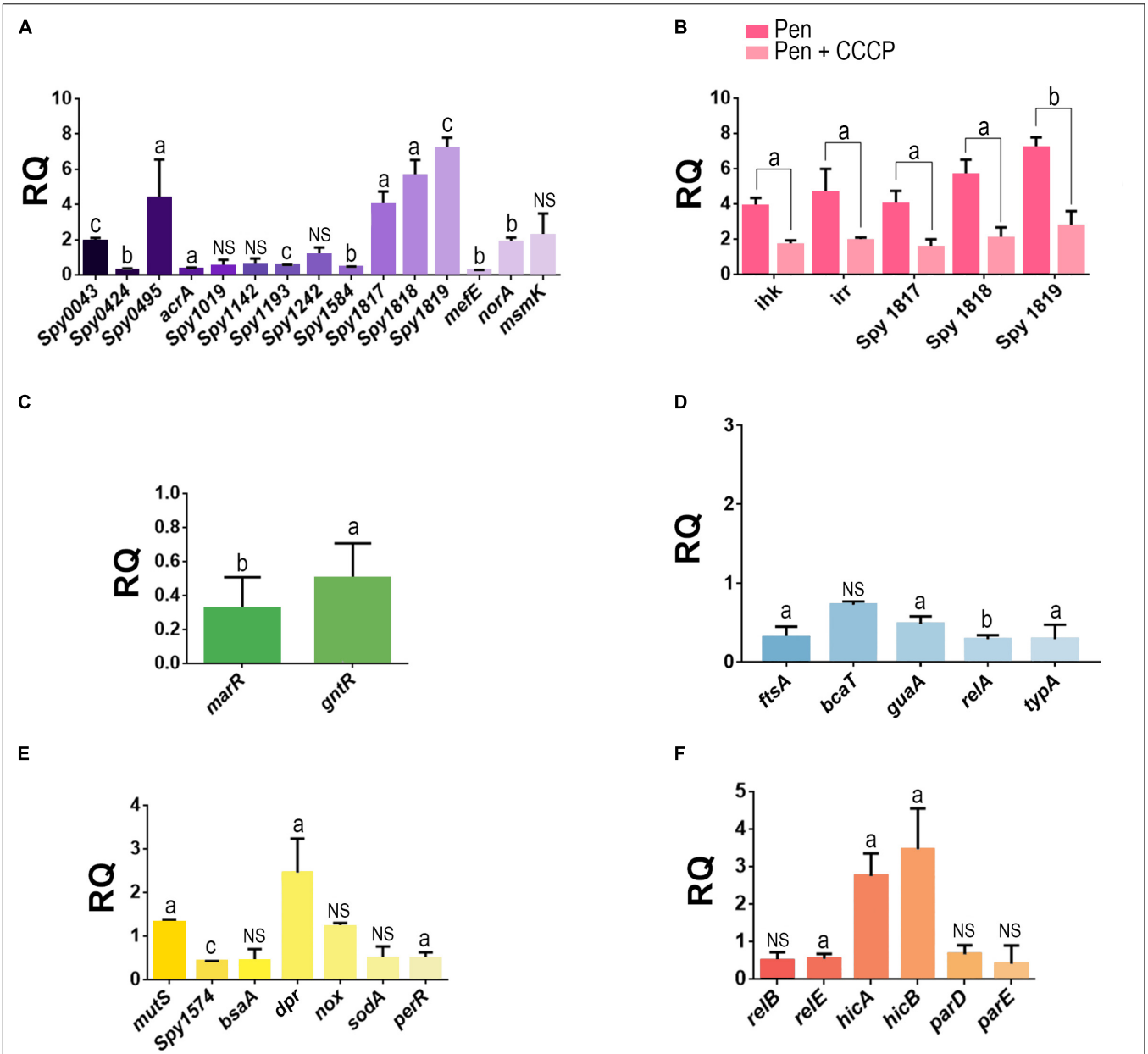

FIGURE 5 | Analysis of the gene expression in penicillin-persister cells of the *Streptococcus pyogenes* strain 37–97. **(A)** Transcript levels of genes associated with efflux pumps in penicillin persisters. **(B)** Influence of CCCP in the expression of genes associated with ABC-type efflux pump (Locus_tag: *MGAS10750_Spy1817*, *MGAS10750_Spy1818*, and *MGAS10750_Spy1819*) and *ihk/irr* regulators in penicillin persisters. **(C)** Transcript levels of genes associated with negative transcriptional regulators of efflux pump in penicillin persisters. **(D)** Transcript levels of genes associated with protein biosynthesis and cell growth in penicillin-persisters. **(E)** Transcript levels of genes associated with stress conditions in penicillin-persisters. **(F)** Transcripts levels of genes associated with toxin-antitoxin (TA) systems in penicillin-persisters. Gene locus tags annotated in the genome of the strain MGAS10750 (Acc: NC_008024) were used as a reference sequences for primer design. Student's *t*-test was applied. $^{a}p < 0.05$, $^{b}p < 0.01$, $^{c}p < 0.001$. For all gene expression assays, the respective calibrator sample (susceptible cells) was assigned relative quantification equal 1. For all tests, JZS Bayes factor agrees with Student's *t*-test, except for the gene locus *MGAS10750_Spy1019* for which the Bayes Factor (BF = 1.042144) was in favor of the alternative hypothesis, *bsaA* (BF = 1.289759, in favor of alternative hypothesis), *sodA* (BF = 1.213086, in favor of the alternative hypothesis), and *relB* (BF = 1.349216, in favor of the alternative hypothesis). RQ, Relative quantification.

conventionally been detected by indirectly determining CFUs after treating the bacterial cells with a high concentration of an antibiotic, or from bacterial cells that do not grow in the presence of the antibiotic, but regrow under a microfluidic device after drug removal (Orman and Brynildsen, 2015; Yu et al., 2019). Recently, Yu et al. (2019), detected persisters not only from 24 h stationary phase cultures treated with antibiotics but also observed increased detection of persisters from 12 to 24 h incubation, demonstrating the heterogeneous nature of the phenomenon. Additionally, their studies suggested that

multiple proteins, important for cell growth, are sequestered in reversible subcellular structures, named regrowth-delay bodies, in non-growing cells. Notably, they also demonstrated that different depths of persistence occur in persister cells (Yu et al., 2019). In our study, *S. pyogenes* persisters were developed during antibiotic exposition of a high bacterial load placed onto the surface of cellophane membranes covering BAB plates. Although the last phase of biofilm accumulation does not occur in this model, due to the presence of antibiotics, the cell accumulation in the initially formed bacterial film (due the high bacterial load applied onto the membrane surface) led to generation of GAS persisters by possibly inducing growth impairment, as demonstrated by the proteome and gene expression data.

Despite the fact that it might be a reason for failures in the drug therapy, antimicrobial persistence remains unexplored in *S. pyogenes*. Here, we showed that GAS cells in an agglomerated condition persist not only to β-lactams but also to various classes of antimicrobials, corresponding to about 0.3–6.0% of the total bacterial population, depending on the drug tested. It is important to emphasize that drug persistence was not a particular characteristic of only one or few representatives of GAS since different isolates with distinct PFGE patterns were tested.

Phenotypic reversion was observed, indicating the involvement of non-inherited antimicrobial resistance mechanisms. Also, no mutation was detected in the tiny colonies formed by persister cells. In addition, the colony size returned to normal after growth in antibiotic-free medium, discarding the phenomenon of SVCs (Proctor, 2019; Huemer et al., 2020). In addition, no heterogeneous subpopulation displaying distinct penicillin MIC value was detected in the cell culture of the 37–97 strain ruling out heteroresistance phenotype. Also, penicillin tolerance was not observed for this strain (MCB/MIC = 1) (Melo et al., 2003). It is important to note that Vulin et al. (2018) found that various environmental signals might trigger the entry of *S. aureus* into a phenotypic state of growth arrest, including high bacterial density. Corroborating our finds, they found that persisters formed tiny colonies similar to SCVs that reverted to normal size after regrowth in fresh media (instable SVC phenotype). Also, they clearly demonstrated, using live-imaging microscopy, that persisters showed lag-phase delay and that antibiotics can even increase the proportion of instable SCV phenotypes.

There is no question that bacterial resistance acquired through genetic mechanisms is the major reason for clinical failures during antimicrobial therapy for many other pathogens. However, the importance of non-inherited resistance should not be disregarded, mainly concerning infections affecting immunocompromised patients, those associated with biofilm production, or severe and invasive infections where high number of bacterial cells can accumulate at the site of infection (Thulin et al., 2006).

It is remarkable that high bacterial load was detected in tissue biopsy specimens from 17 patients presenting with GAS disseminated infections (necrotizing fasciitis or severe cellulitis) despite intravenous antibiotic therapy (clindamycin in combination with β-lactam antibiotic) for a prolonged time (Thulin et al., 2006). Those authors suggested that GAS survival inside macrophages could represent a mechanism preventing bacterial eradication. However, patterns of purely intracellular bacteria were observed in less than half of the biopsies analyzed (Thulin et al., 2006). Some *in vitro* studies have demonstrated the effect of biofilm and high cell density in the failure of antibiotics to eliminate *Escherichia coli*, mycobacteria and methicillin-resistant *S. aureus* (Nielsen et al., 2011; Ferro et al., 2015; Coates et al., 2018; Novais et al., 2020). In fact, our findings demonstrated the generation of antimicrobial persisters for GAS in an agglomerated cell environment, which was associated with inhibition of both protein biosynthesis and cell growth, and possibly with an increased activity of intrinsic multidrug-resistant (MDR) efflux pumps.

It was observed that CCCP fully restored the susceptibility to clindamycin and chloramphenicol, suggesting the involvement of proton efflux pumps in GAS persistence/refractory to these drugs. In fact, a gene of the ABC operon of the RND family (that uses proton gradient force across inner membrane to exclude drugs; Eicher et al., 2014) was almost ninefold overexpressed in GAS-persister cells induced by clindamycin, and was detected only in the proteome of cells grown in biofilm-like environments. It is possible that additional efflux pumps, not importantly affected by CCCP, may be involved in the extrusion of the other antimicrobials tested. This assumption is supported by the fact that CCCP did not recover GAS susceptibility to the pump substrate EtBr. Indeed, about 50% of the efflux-associated genes analyzed were upregulated in penicillin-persister cells.

Typically, overexpression of efflux pumps confers resistance to different classes of antimicrobial agents and some dyes, such as EtBr, in other bacterial species (DeMarco et al., 2007; Martins et al., 2011; Sun et al., 2014; Wang et al., 2019). The involvement of conserved RND proteins in reducing *S. aureus* persistence to β-lactams and glycopeptides has also been demonstrated (Quiblier et al., 2011). Similar to our findings, Poudyal, and Sauer found increased expression of genes associated with an ABC transporter and other transport systems in *Pseudomonas aeruginosa* grown in biofilm conditions, suggesting that these mechanisms contributed to the persister phenotype of *P. aeruginosa* to tobramycin (Poudyal and Sauer, 2017). In fact, in our study, a homolog of *marR*, a negative pump regulator, was down-regulated in the persisters. In line with these data, increased resistance in *Burkholderia thailandensis* was attributed to enhanced efflux pump activity and was detected after repression of a *marR* homolog (Sabrin et al., 2019). Additionally, we found that a gene in the GntR family of regulators was also down-regulated in penicillin-persister GAS cells. It is remarkable that a *norG* knockout in *S. aureus* (a member of the GntR family) led to a threefold increase in the expression of an *abcA* gene encoding a protein of the ABC transport system with a concomitant increase in resistance to β-lactams (Truong-Bolduc and Hooper, 2007).

The Ihk/Irr two-component system is involved in the regulation of various streptococcal processes, including virulence (Han et al., 2012; Kachroo et al., 2020). It is notable that *ihk*/*irr* were overexpressed in a non-human primate model of GAS necrotizing myositis, and these genes were implicated in GAS resistance to polymorphonuclear phagocytosis

(Kachroo et al., 2020). The fact that CCCP inhibited *ihk*/*irr* gene regulators and the RND family operon concomitantly, and that both the operon and *cis* regulators displayed increased expression in GAS-persister cells, raises an interesting hypothesis about another possible role for the Ihk/Irr system beyond virulence regulation. However, despite the genes co-localization and the concomitant downregulation by CCCP of *ihk*/*irr* and genes of the ABC transport operon, molecular cloning strategies are needed to validate the hypothesis that *ihk*/*irr* may not only regulate GAS virulence but also this transport system in 37–97 strain. Corroborating this hypothesis, microarrays data from Voyich et al. (2004) obtained from an *irr* mutant of the GAS strain, JRS500, revealed that a number of ABC transport genes were downregulated in this mutant, as well as the *msmK* gene.

Oxidative stress has also been associated with antimicrobial persisters in *E. coli* (Wu et al., 2012). In this study, a *dpr* homolog was upregulated in penicillin-persister GAS cells. The *dpr* gene encodes the non-specific DNA binding protein Dps (peroxide resistance protein, Dpr), and homologs have been identified in different bacterial species associated with protection against multiple stressors (Leszczynska et al., 2013). Dps protein forms self-aggregates and an insoluble complex with DNA. In *E. coli*, the aggregates formed in the stationary growth phase correlated with increased persisters formation (Leszczynska et al., 2013). Also, the induction of *dps* in *E. coli* resulted in overexpression of the toxin/antitoxin (TA) system MqsR/MqaA (Kim et al., 2010). In fact, in our study, the TA system of the HicAB family was upregulated in GAS-persister cells. However, the contribution of TA system and (p)ppGpp in *E. coli* persisters remains controversial (Goormaghtigh et al., 2018).

In addition to efflux pumps, stress conditions, and TA systems, slow-growing cells and stringent responses have also been implicated in the generation of antimicrobial persisters (Goormaghtigh et al., 2018; Vulin et al., 2018). The GAS persisters produced tiny colonies, indicating a condition of slow growth. Actually, genes associated with protein biosynthesis were downregulated in the penicillin-persisters, including homologs of *typA*/*bipA* (important in ribosome assembly) and *guaA* (essential in GTP synthesis). The inhibition of *guaBA* operon by (p)ppGpp in *E. coli* led to low levels GTP and increased bacterial survival during amino acid starvation (Hauryliuk et al., 2015). These results agree with the proteomic data that showed increased expression of ribosome protein L in GAS cells grown at low density population (susceptible cells) compared with cells obtained from the biofilm-like environment. Indeed, the expression of the *ftsA* gene, which is essential for cell growth, was reduced in penicillin-persister GAS cells. It is notable that a substantial reduction in transcription and translation of this gene was previously observed for antimicrobial-persisters in *E. coli,* which was associated with increased expression of different RNases (including RNase E, which is involved in the specific degradation of *ftsA*-*ftsz* transcripts) (Radzikowski et al., 2016). Indeed, *ftsA* and *ftsZ* proteins are among the proteins sequestered in regrowth-delay bodies found in *Shigella flexineri* and *Salmonella* Thyphimurium persisters forming non-growing cells (Yu et al., 2019).

Bacterial persistence to antibiotics is still a controversial issue that has been attributed to several mechanisms. The discrimination between the different phenomena does not seem to be an easy task. However, the antimicrobial persistence observed in our study could not be classified as heteroresistance, tolerance or stable SCVs phenotypes and are better defined as persisters on the basis of the following features: i. the level of persistence is not greatly affected by antibiotic concentrations since persisters can grow in antibiotic levels far above the MIC; ii. when regrown in the absence of the antimicrobial, persisters completely restore drug susceptibility to MIC values; iii. not all bacterial cells in the culture are killed at the same frequency; iv. they frequently exhibit persistence to different classes of antibiotics; v. the advantage of persisters against the susceptible cells, in the bacterial population, seems to be the slow-growing/non-growing characteristic of the persister cells (Vulin et al., 2018; Yu et al., 2019; Pontes and Groisman, 2019).

In conclusion, we showed that subpopulations of GAS cells can become persistent to high concentrations of β-lactams and other antimicrobials when cells in condition of agglomeration such as those observed in high bacterial load and biofilm environments formed on biotic or abiotic surfaces. Our data suggest that growth arrest and efflux pump are mechanisms associated with this phenotypic resistance in GAS cells, which have also been observed for persisters formed by other bacterial species (Poudyal and Sauer, 2017; Vulin et al., 2018; Pontes and Groisman, 2019). It is possible that this phenomenon might have some implications for failures in antimicrobial therapy that have been reported for some GAS clinical infections (Gidengil et al., 2013; Brook, 2017), including those severe and sometimes lethal invasive diseases, for which high bacterial load ($\sim 10^7$ CFU/cm^2) can be achieved in the infected tissues, despite the use of effective antimicrobial therapy (Thulin et al., 2006), and should not be overlooked. Finally, further studies with *ihk*/*irr* are required to clarify the role of this TC system in antimicrobial clinical failures due to a possible upregulation of both intracellular survival of GAS into macrophages and efflux pump activity.

DATA AVAILABILITY STATEMENT

The datasets presented in this study can be found in online repositories. The names of the repository/repositories and accession number(s) can be found below: https://www.ncbi.nlm.nih.gov/genbank/, CP041615.1 and https://www.ncbi.nlm.nih.gov/genbank/, CP041408.1.

ETHICS STATEMENT

The studies involving human participants were reviewed and approved by the Ethics Committee of the Hospital Universitario Clementino Fraga Filho UFRJ/RJ under the # 4-485-002; the study was considered nonhuman subject research.

AUTHOR CONTRIBUTIONS

AF, BF-C, and RZ performed the conception and design of the work. AC, CM, CG, MMa, MMe, TA, and ÚL carried out the experiments. AF, AC, BF-C, CM, and RZ analyzed and interpreted the data. AB, AV, LA, and PP performed the whole genome sequencing and analysis. AF, BF-C, and CM wrote and revised the manuscript. All authors read and approved the final manuscript.

FUNDING

This work was supported in part by the Fundação Carlos Chagas Filho de Amparo à Pesquisa do Estado do Rio de Janeiro (FAPERJ) # E-26/010.001764/2014, # E-26/211-554/2019 and E-26/010.002435/2019, Conselho Nacional de Desenvolvimento Científico e Tecnológico (CNPq) # 443804/2018-4 and 202067/2015-2, and Coordenação de Aperfeiçoamento de Pessoal do Ensino Superior (CAPES) # 001.

ACKNOWLEDGMENTS

We thank Mrs. Raquel Neves for her excellent technical assistance. We are very grateful Dr. Clemente Aguilar for his assistance with the Blast2Go software, and to Ms. Ana L. Carvalho for her help with the LC-MS/MS analysis.

SUPPLEMENTARY MATERIAL

The Supplementary Material for this article can be found online at: https://www.frontiersin.org/articles/10.3389/fmicb.2021.716628/full#supplementary-material

Supplementary Table 1 | Isolation year, geographic region, clinical origin of the 211 *Streptococcus pyogenes* isolates used in this study.

Supplementary Table 2 | Characteristics of the *Streptococcus pyogenes* strains selected as controls for the experiments of persister generation for different classes of antimicrobials.

Supplementary Table 3 | Primers used for real-time quantitative reverse transcriptase PCR (real-time RT-qPCR).

Supplementary Table 4 | Characteristics of the *Streptococcus pyogenes* genomes sequenced.

Supplementary Table 5 | Proteins identified in *Streptococcus pyogenes* strain 37–97 grown in biofilm-like environments.

Supplementary Table 6 | Proteins identified in *Streptococcus pyogenes* strain 37–97 grown using low cell density.

Supplementary Table 7 | Proteins identified in *Streptococcus pyogenes* strain 37–97 grown in both biofilm-like environments and using low cell density.

REFERENCES

Avire, N. J., Whiley, H., and Ross, K. (2021). A review of *Streptococcus pyogenes*: public health risk factors, prevention and control. *Pathogens* 10:248. doi: 10.3390/pathogens10020248

Balaban, N. Q., Helaine, S., Lewis, K., Ackermann, M., Aldridge, B., Andersson, D. I., et al. (2019). Definitions and guidelines for research on antibiotic persistence. *Nat. Rev. Microbiol.* 17, 441–448. doi: 10.1038/s41579-019-0196-3

Baron, S. A., and Rolain, J. M. (2018). Efflux pump inhibitor CCCP to rescue colistin susceptibility in *mcr-1* plasmid-mediated colistin-resistant strains and Gram-negative bacteria. *J. Antimicrob. Chemother.* 73, 1862–1871. doi: 10.1093/jac/dky134

Brauner, A., Fridman, O., Gefen, O., and Balaban, N. Q. (2016). Distinguishing between resistance, tolerance and persistence to antibiotic treatment. *Nat. Rev. Microbiol.* 14, 320–330. doi: 10.1038/nrmicro.2016.34

Brook, I. (2017). Treatment challenges of group A beta-hemolytic streptococcal pharyngo-tonsillitis. *Int. Arch. Otorhinolaryngol.* 21, 286–296. doi: 10.1055/s-0036-1584294

Clancy, J., Petitpas, J., Dib-Hajj, F., Yuan, W., Cronan, M., Kamath, A. V., et al. (1996). Molecular cloning and functional analysis of a novel macrolide-resistance determinant, *mefA*, from *Streptococcus pyogenes*. *Mol. Microbiol.* 22, 867–879. doi: 10.1046/j.1365-2958.1996.01521.x

CLSI. (2021). *Performance standards for antimicrobial susceptibility testing. 31st ed. CLSI supplement M 100*. Pittsburgh: Clinical and Laboratory Standards Institute.

Coates, J., Park, B. R., Le, D., Şimşek, E., Chaudhry, W., and Kim, M. (2018). Antibiotic-induced population fluctuations and stochastic clearance of bacteria. *Elife* 7, 1–26. doi: 10.7554/eLife.32976

DeMarco, C. E., Cushing, L. A., Frempong-Manso, E., Seo, S. M., Jaravaza, T. A. A., and Kaatz, G. W. (2007). Efflux-related resistance to norfloxacin, dyes, and biocides in bloodstream isolates of *Staphylococcus aureus*. *Antimicrob. Agents Chemother.* 51, 3235–3239. doi: 10.1128/AAC.00430-07

Eicher, T., Seeger, M. A., Anselmi, C., Zhou, W., Brandstätter, L., Verrey, F., et al. (2014). Coupling of remote alternating-access transport mechanisms for protons and substrates in the multidrug efflux pump AcrB. *ELife* 3:e03145. doi: 10.7554/eLife.03145

Ferro, B. E., van Ingen, J., Wattenberg, M., van Soolingen, D., and Mouton, J. W. (2015). Time-kill kinetics of antibiotics active against rapidly growing mycobacteria. *J. Antimicrob. Chemother.* 70, 811–817. doi: 10.1093/jac/dku431

Fiedler, T., Köller, T., and Kreikemeyer, B. (2015). *Streptococcus pyogenes* biofilms formation, biology, and clinical relevance. *Front. Cell. Infect. Microbiol.* 5:15. doi: 10.3389/fcimb.2015.00015

Gidengil, C. A., Kruskal, B. A., and Lee, G. M. (2013). Initial antibiotic choice in the treatment of group A streptococcal pharyngitis and return visit rates. *J. Pediatric. Infect. Dis. Soc.* 2, 361–367. doi: 10.1093/jpids/pit043

Goormaghtigh, F., Fraikin, N., Putrinš, M., Hallaert, T., Hauryliuk, V., Garcia-Pino, A., et al. (2018). Reassessing the role of type II toxin-antitoxin systems in formation of *Escherichia coli* type II persister cells. *mBio* 9, e00640–18. doi: 10.1128/mBio.00640-18

Han, H., Liu, C., Wang, Q., Xuan, C., Zheng, B., Tang, J., et al. (2012). The two-component system Ihk/Irr contributes to the virulence of *Streptococcus suis* serotype 2 strain 05ZYH33 through alteration of the bacterial cell metabolism. *Microbiology* 158, 1852–1866. doi: 10.1099/mic.0.057448-0

Hauryliuk, V., Atkinson, G. C., Murakami, K. S., Tenson, T., and Gerdes, K. (2015). Recent functional insights into the role of (p)ppGpp in bacterial physiology. *Nat. Rev. Microbiol.* 13, 298–309. doi: 10.1038/nrmicro3448

Huemer, M., Shambat, S. M., Brugger, S. D., and Zinkernagel, A. S. (2020). Antibiotic resistance and persistence-Implications for human health and treatment perspectives. *EMBO Rep.* 21:e51034. doi: 10.15252/embr.202051034

Kachroo, P., Eraso, J. M., Olsen, R. J., Zhu, L., Kubiak, S. L., Pruittet, L., et al. (2020). New pathogenesis mechanisms and translational leads identified by multidimensional analysis of necrotizing myositis in primates. *mBio* 11, e03363–19. doi: 10.1128/mBio.03363-19

Karslake, J., Maltas, J., Brumm, P., and Wood, K. B. (2016). Population density modulates drug inhibition and gives rise to potential bistability of treatment outcomes for bacterial infections. *PLoS Comput. Biol.* 12:e1005098. doi: 10.1371/journal.pcbi.1005098

Kim, Y., Wang, X., Zhang, X. S., Grigoriu, S., Page, R., Peti, W., et al. (2010). *Escherichia coli* toxin/antitoxin pair MqsR/MqsA regulate toxin CspD. *Environ. Microbiol.* 12, 1105–1121. doi: 10.1111/j.1462-2920.2009.02147.x

Laemmli, U. (1970). Cleavage of structural proteins during the assembly of the head of bacteriophage T4. *Nature* 227, 680–685. doi: 10.1038/227680a0

Lee, J., Zilm, P. S., and Kidd, S. P. (2020). Novel research models for *Staphylococcus aureus* small colony variants (SCV) development: co-pathogenesis and growth rate. *Front. Microbiol.* 11:321. doi: 10.3389/fmicb.2020.00321

Leszczynska, D., Matuszewska, E., Kuczynska-Wisnik, D., Furmanek-Blaszk, B., and Laskowska, E. (2013). The formation of persister cells in stationary-phase cultures of *Escherichia coli* is associated with the aggregation of endogenous proteins. *PLoS One* 8:e54737. doi: 10.1371/journal.pone.0054737

Li, J., Xie, S., Ahmed, S., Wang, F., Gu, Y., and Zhang, C. (2017). Antimicrobial activity and resistance: influencing factors. *Front. Pharmacol.* 8:364. doi: 10.3389/fphar.2017.00364

Margulies, M., Egholm, M., Altman, W. E., Attiya, S., Bader, J. S., Bemben, L. A., et al. (2005). Genome sequencing in microfabricated high-density picolitre reactors. *Nature* 437, 376–380. doi: 10.1038/nature03959

Martins, M., Viveiros, M., Couto, I., Costa, S. S., Pacheco, T., Fanning, S., et al. (2011). Identification of efflux pump-mediated multidrug-resistant bacteria by the ethidium bromide-agar cartwheel method. *In Vivo* 25, 171–178.

Melo, M. C. N., Figueiredo, A. M. S., and Ferreira-Carvalho, B. T. (2003). Antimicrobial susceptibility patterns and genomic diversity in strains of *Streptococcus pyogenes* isolated in 1978-1997 in different Brazilian cities. *J. Med. Microbiol.* 52, 251–258. doi: 10.1099/jmm.0.04938-0

Nielsen, E. I., Cars, O., and Friberg, L. E. (2011). Predicting in vitro antibacterial efficacy across experimental designs with a semimechanistic pharmacokinetic-pharmacodynamic model. *Antimicrob. Agents Chemother.* 55, 1571–1579. doi: 10.1128/AAC.01286-10

Novais, J. S., Carvalho, M. F., Ramundo, M. S., Beltrame, C. O., Geraldo, R. B., Jordão, A. K., et al. (2020). Antibiofilm effects of N,O-acetals derived from 2-amino-1,4-naphthoquinone are associated with downregulation of important global virulence regulators in methicillin-resistant *Staphylococcus aureus*. *Sci. Rep.* 10:19631. doi: 10.1038/s41598-020-76372-z

Oppegaard, O., Skrede, S., Mylvaganam, H., and Kittang, B. R. (2020). Emerging threat of antimicrobial resistance in β-hemolytic streptococci. *Front. Microbiol.* 11:797. doi: 10.3389/fmicb.2020.00797

Orman, M. A., and Brynildsen, M. P. (2015). Inhibition of stationary phase respiration impairs persister formation in *E. coli*. *Nat. Commun.* 6:7983. doi: 10.1038/ncomms8983

Overbeek, R., Olson, R., Pusch, G. D., Olsen, G. J., Davis, J. J., Disz, T., et al. (2014). The SEED and the rapid annotation of microbial genomes using subsystems technology (RAST). *Nucleic Acids Res.* 42, D206–D214. doi: 10.1093/nar/gkt1226

Patel, D., Kosmidis, C., Seo, S. M., and Kaatz, G. W. (2010). Ethidium bromide MIC screening for enhanced efflux pump gene expression or efflux activity in *Staphylococcus aureus*. *Antimicrob. Agents Chemother.* 54, 5070–5073. doi: 10.1128/AAC.01058-10

Pontes, M. H., and Groisman, E. A. (2019). Slow growth determines nonheritable antibiotic resistance in *Salmonella enterica*. *Sci. Signal.* 12:eaax3938. doi: 10.1126/scisignal.aax3938

Poudyal, B., and Sauer, K. (2017). The ABC of biofilm drug tolerance: the MerR-like regulator BrlR is an activator of ABC transport systems, with PA1874-77 contributing to the tolerance of *Pseudomonas aeruginosa* biofilms to tobramycin. *Antimicrob. Agents Chemother.* 62, e01981–17. doi: 10.1128/AAC.01981-17

Proctor, R. (2019). Respiration and small colony variants of *Staphylococcus aureus*. *Microbiol. Spectr.* 7, 1–15. doi: 10.1128/microbiolspec.GPP3-0069-2019

Quiblier, C., Zinkernagel, A. S., Schuepbach, R. A., Berger-Bächi, B., and Senn, M. M. (2011). Contribution of SecDF to *Staphylococcus aureus* resistance and expression of virulence factors. *BMC Microbiol.* 11:72. doi: 10.1186/1471-2180-11-72

Radzikowski, J. L., Vedelaar, S., Siegel, D., Ortega, A. D., Schmidt, A., and Heinemann, M. (2016). Bacterial persistence is an active σ S stress response to metabolic flux limitation. *Mol. Syst. Biol.* 12:882. doi: 10.15252/msb.20166998

Randhawa, E., Woytanowski, J., Sibliss, K., and Sheffer, I. (2018). *Streptococcus pyogenes* and invasive central nervous system infection. *SAGE Open Med. Case Rep.* 6, 1–3. doi: 10.1177/2050313X18775584

Rio-Marques, L., Hartke, A., and Bizzini, A. (2014). The effect of inoculum size on selection of in vitro resistance to vancomycin, daptomycin, and linezolid in methicillin-resistant *Staphylococcus aureus*. *Microb. Drug Resist.* 20, 539–543. doi: 10.1089/mdr.2014.0059

Rodrigues, S. P., Ventura, J. A., Aguilar, C., Nakayasu, E. S., Almeida, I. C., Fernandes, P. M. B., et al. (2011). Proteomic analysis of papaya (*Carica papaya L.*) displaying typical sticky disease symptoms. *Proteomics* 11, 2592–2602. doi: 10.1002/pmic.201000757

Rouder, J. N., Speckman, P. L., Sun, D., Morey, R. D., and Iverson, G. (2009). Bayesian t-tests for accepting and rejecting the null hypothesis. *Psychon. Bull. Rev.* 16, 225–237. doi: 10.3758/PBR.16.2.225

Sabrin, A., Gioe, B. W., Gupta, A., and Grove, A. (2019). An EmrB multidrug efflux pump in *Burkholderia thailandensis* with unexpected roles in antibiotic resistance. *J. Biol. Chem.* 294, 1891–1903. doi: 10.1074/jbc.RA118.006638

Shevchenko, A., Wilm, M., Vorm, O., and Mann, M. (1996). Mass spectrometric sequencing of proteins from silver-stained polyacrylamide gels. *Anal. Chem.* 68, 850–858. doi: 10.1021/ac950914h

Sun, J., Deng, Z., and Yan, A. (2014). Bacterial multidrug efflux pumps: mechanisms, physiology and pharmacological exploitations. *Biochem. Biophys. Res. Commun.* 453, 254–267. doi: 10.1016/j.bbrc.2014.05.090

Thulin, P., Johansson, L., Low, D. E., Gan, B. S., Kotb, M., McGeer, A., et al. (2006). Viable group A Streptococci in macrophages during acute soft tissue infection. *PLoS Med.* 3:e53. doi: 10.1371/journal.pmed.0030053

Truong-Bolduc, Q. C., and Hooper, D. C. (2007). The transcriptional regulators NorG and MgrA modulate resistance to both quinolones and -lactams in *Staphylococcus aureus*. *J. Bacteriol.* 189, 2996–3005. doi: 10.1128/JB.01819-06

Voyich, J. M., Braughton, K. R., Sturdevant, D. E., Vuong, C., Kobayashi, S. D., Porcella, S. F., et al. (2004). Engagement of the pathogen survival response used by group A *Streptococcus* to avert destruction by innate host defense. *J. Immunol.* 173, 1194–1201. doi: 10.4049/jimmunol.173.2.1194

Vulin, C., Leimer, N., Huemer, M., Ackermann, M., and Zinkernagel, A. S. (2018). Prolonged bacterial lag time results in small colony variants that represent a sub-population of persisters. *Nat. Commun.* 9:4074. doi: 10.1038/s41467-018-06527-0

Walker, M. J., Barnett, T. C., McArthur, J. D., Cole, J. N., Gillen, C. M., Henningham, A., et al. (2014). Disease manifestations and pathogenic mechanisms of group A *Streptococcus*. *Clin. Microbiol. Rev.* 27, 264–301. doi: 10.1128/CMR.00101-13

Wang, Y., Liu, B., Li, J., Gong, S., Dong, X., Mao, C., et al. (2019). LuxS/AI-2 system is involved in fluoroquinolones susceptibility in *Streptococcus suis* through overexpression of efflux pump SatAB. *Vet. Microbiol.* 233, 154–158. doi: 10.1016/j.vetmic.2019.05.006

Wu, Y., Vulić, M., Keren, I., and Lewis, K. (2012). Role of oxidative stress in persister tolerance. *Antimicrob. Agents Chemother.* 56, 4922–4926. doi: 10.1128/AAC.00921-12

Yu, J., Liu, Y., Yin, H., and Chang, Z. (2019). Regrowth-delay body as a bacterial subcellular structure marking multidrug-tolerant persisters. *Cell Discov.* 5:8. doi: 10.1038/s41421-019-0080-3

Conflict of Interest: The authors declare that the research was conducted in the absence of any commercial or financial relationships that could be construed as a potential conflict of interest.

Publisher's Note: All claims expressed in this article are solely those of the authors and do not necessarily represent those of their affiliated organizations, or those of the publisher, the editors and the reviewers. Any product that may be evaluated in this article, or claim that may be made by its manufacturer, is not guaranteed or endorsed by the publisher.

frontiers in Microbiology

ORIGINAL RESEARCH
published: 27 September 2021
doi: 10.3389/fmicb.2021.743305

Ursolic Acid Targets Glucosyltransferase and Inhibits Its Activity to Prevent *Streptococcus mutans* Biofilm Formation

Yucui Liu[1,2†], Yanxin Huang[3†], Cong Fan[1,4], Zhongmei Chi[5], Miao Bai[1], Luguo Sun[3], Li Yang[5], Chunlei Yu[1], Zhenbo Song[1], Xiaoguang Yang[1,3], Jingwen Yi[1,3], Shuyue Wang[1], Lei Liu[1], Guannan Wang[1] and Lihua Zheng[1*]*

[1]National Engineering Laboratory for Druggable Gene and Protein Screening, Northeast Normal University, Changchun, China, [2]State Key Laboratory of Microbial Technology, Shandong University, Qingdao, China, [3]NMPA Key Laboratory for Quality Control of Cell and Gene Therapy Medicine Products, Northeast Normal University, Changchun, China, [4]Guangdong Provincial Key Laboratory of Malignant Tumor Epigenetics and Gene Regulation, Department of Medical Research Center, Sun Yat-Sen Memorial Hospital, Guangzhou, China, [5]Faculty of Chemistry, Northeast Normal University, Changchun, China

OPEN ACCESS

Edited by:
Prescilla Emy Nagao, Rio de Janeiro State University, Brazil

Reviewed by:
Geelsu Hwang, University of Pennsylvania, United States
Latifa Bousarghin, University of Rennes 1, France

***Correspondence:**
Luguo Sun
sunluguo01@163.com
Lihua Zheng
zhenglh015@nenu.edu.cn

†These authors have contributed equally to this work

Specialty section:
This article was submitted to Antimicrobials, Resistance and Chemotherapy, a section of journal Frontiers in Microbiology

Received: *18 July 2021*
Accepted: *24 August 2021*
Published: *27 September 2021*

Citation:
Liu Y, Huang Y, Fan C, Chi Z, Bai M, Sun L, Yang L, Yu C, Song Z, Yang X, Yi J, Wang S, Liu L, Wang G and Zheng L (2021) Ursolic Acid Targets Glucosyltransferase and Inhibits Its Activity to Prevent Streptococcus mutans Biofilm Formation. Front. Microbiol. 12:743305. doi: 10.3389/fmicb.2021.743305

Streptococcus mutans (S. mutans), the prime pathogen of dental caries, can secrete glucosyltransferases (GTFs) to synthesize extracellular polysaccharides (EPSs), which are the virulence determinants of cariogenic biofilms. Ursolic acid, a type of pentacyclic triterpene natural compound, has shown potential antibiofilm effects on *S. mutans*. To investigate the mechanisms of ursolic acid-mediated inhibition of *S. mutans* biofilm formation, we first demonstrated that ursolic acid could decrease the viability and structural integrity of biofilms, as evidenced by XTT, crystal violet, and live/dead staining assays. Then, we further revealed that ursolic acid could compete with the inherent substrate to occupy the catalytic center of GTFs to inhibit EPS formation, and this was confirmed by GTF activity assays, computer simulations, site-directed mutagenesis, and capillary electrophoresis (CE). In conclusion, ursolic acid can decrease bacterial viability and prevent *S. mutans* biofilm formation by binding and inhibiting the activity of GTFs.

Keywords: ursolic acid, biofilms, extracellular polysaccharides, glucosyltransferases, mechanism

INTRODUCTION

Most oral diseases, including periodontal diseases and especially dental caries, are prevalent and common public health problems worldwide (Jakubovics et al., 2021). Approximately 60–90% of school-aged children and almost all adults suffer from dental caries (Wong et al., 2017). Dental caries is a chronic bacterial infectious disease that occurs on the tooth surface (Taubman and Nash, 2006). Traditional methods used to prevent or cure dental caries include mechanical removal of plaque (e.g., toothbrushing), the usage of broad-spectrum antibiotics, and more comprehensive forms of clinical treatment (e.g., root canal therapy, surgery, and dental restorations; Chen et al., 2016). However, the effect of prevention can be limited by poor toothbrushing technique and drug resistance (Cummins, 2013). Dental treatment is expensive, averaging 5% of total health expenditures and 20% of out-of-pocket health expenditures in most high-income countries, and is beyond the capacity of healthcare systems in most low- and middle-income

countries (Vernazza et al., 2021). Therefore, more effective preventive and therapeutic strategies for dental caries are needed.

Dental caries is a typical biofilm induction-related disease, and cariogenic biofilms are one of the main factors leading to bacterial infection since they can protect microorganisms by enhancing microbial resistance to the host's immunologic defense and antibacterial agents (Takahashi and Nyvad, 2011; Pitts et al., 2017). *Streptococcus mutans (S. mutans)*, the prime pathogen of dental caries, is an important contributor to the formation of cariogenic biofilms (Wang et al., 2020). *S. mutans* secretes three types of glucosyltransferases (GTFs), namely, GTF-I (also known as GtfB), GTF-SI (GtfC), and GTF-S (GtfD; Bowen and Koo, 2011). These GTFs can use dietary sucrose to synthesize extracellular polysaccharides (EPSs), and EPSs are the virulence determinants of cariogenic biofilms (Tamesada et al., 2004; Bowen and Koo, 2011; Jaña et al., 2018). GTF-I and GTF-SI catalyze mainly the synthesis of water-insoluble glucans, and GTF-S produces mainly water-soluble glucans (Monchois et al., 1999; Bowen et al., 2018). Water-insoluble glucans help bacteria adhering and aggregating on the tooth surface to form biofilms, while water-soluble glucan may supply a source of metabolizable carbohydrates for plaque bacteria and induce water-insoluble glucan formation (Jakubovics et al., 2021). Therefore, GTFs play key roles in causing and forming dental caries and are an effective target for the prevention and treatment of dental caries or other related diseases (e.g., infective endocarditis; Shun et al., 2005).

Ursolic acid, a type of pentacyclic triterpene compound, can be isolated in abundance from many foods (e.g., apples, olive, and basil) and medicinal plants (e.g., *Malus pumila*, *Ocimum basiliacum*, and *Rosmarinus officinalis;* Ikeda et al., 2008; Bacanlı et al., 2017; Hui et al., 2021). Ursolic acids have been reported to have many beneficial bioactivities, such as anticancer (Patlolla and Rao, 2012), anti-inflammatory (Pádua et al., 2014), antimicrobial (Kim et al., 2012), immunity regulation (Xu et al., 2019), and antiviral activities (Kong et al., 2013). In our previous research, we confirmed that the crude extract of *Bergenia crassifolia* leaves could inhibit *S. mutans* biofilm formation (Liu et al., 2017). In a screen of the active ingredients of *Bergenia crassifolia* leaves for antibiofilm activity, we found that ursolic acid had a significant effect. Here, we confirmed the antibiofilm activities of ursolic acid against *S. mutans* and further revealed the mechanism underlying the inhibitory effect of ursolic acid on GTF-mediated synthesis of EPSs. Our study provides a potential antimicrobial agent that can be used to prevent and cure oral and other GTF-related diseases.

MATERIALS AND METHODS

Bacterial Strain, Growth Conditions, and Chemicals

S. mutans (ATCC 251175) was obtained from the Guangdong Microbiology Culture Center and was cultured in brain heart infusion (BHI) broth (Hopebio, Qingdao, China) supplemented with 1% sucrose at 37°C for 24 h under aerobic conditions. After incubation, the bacterial concentration was 10^7 cfu/ml, as determined by spectrophotometry ($OD_{630} = 0.2$). Ursolic acid was purchased from the National Institutes for Food and Drug Control with purity >98% and was dissolved in dimethyl sulfoxide.

Antimicrobial Activity Assay

The potential inhibitory activity of ursolic acid against *S. mutans* was determined by the microdilution method as described previously (Liu et al., 2017), with minor modifications. Briefly, ursolic acid was serially diluted twofold in BHI broth containing 1% sucrose, with the final concentration of ursolic acid ranging from 0.25 to 0.031 mg/ml. Twenty microliters of sterile solution of resazurin sodium per well was added to the bacterial culture and incubated at 37°C for 24 h. BHI broth alone was used as blank control, bacterial suspension alone was used as a noninhibition negative control, and chlorhexidine treatment at a final concentration of 0.6 mg/ml was used as a positive control. As bacteria grow, resazurin is reduced to resorufin, resulting in the medium color changing from blue to pink (Palomino et al., 2002; Sarker et al., 2007). The lowest concentration of ursolic acid that could inhibit the medium color change from blue to pink was defined as the minimal inhibitory concentration (Palomino et al., 2002; Süntar et al., 2016). The bacterial cultures treated with ursolic acid at concentrations equal to or higher than the minimum inhibitory concentration (MIC) were transferred to BHI agar plates and incubated at 37°C for 24 h. The lowest concentration that resulted in no visible bacterial colonies on the agar plates after incubation was defined as the minimal bactericidal concentration (MBC; Liu et al., 2017).

XTT Reduction Assay

The effect of ursolic acid on the viability of biofilms was evaluated using a 2,3-bis (2-methyloxy-4-nitro-5-sulfophenyl)-2H-tetrazolium-5-carboxanilide (XTT) reduction assay as described previously (Duque et al., 2017), with some modification. Briefly, after 24 h of incubation for cultured bacteria to form biofilms in 96-well microplates, supernatants were removed, and the wells were gently washed three times with PBS (pH 7.0) to remove nonadhered bacteria. Then, the cultures were incubated at 37°C for another 22 h in 200 µl of BHI broth including 100 µl of ursolic acid at various concentrations. After removing the supernatants, 50 µl of XTT (Sigma, St. Louis, MO, United States) reagent was added, and the microplate was kept in the dark for 2 h at 37°C. Then, the absorbance of the colored product was detected at 490 nm using an ELISA reader. Alternatively, after ursolic acid treatment, a crystal violet assay was used to evaluate the attachment of biofilm biomass as described previously (Cardoso Sá et al., 2012).

Live/Dead Bacterial Staining

Fluorescence staining was used to determine biofilm integrity as described previously (Liu et al., 2017). After biofilm formation, ursolic acid was added at a final concentration of 1/2 MIC followed by incubation at 37°C for another 18 h. The culture was then removed from the supernatant and gently washed twice with sterile water. Staining was carried out by means of the Live/Dead BacLight Bacterial Viability Kit (L13152,

Invitrogen, Carlsbad, CA, United States) for 30 min at room temperature in the dark. Stained cells were observed under a fluorescence microscope (Nikon Eclipse 80i; Nikon Co., Japan). The kit utilizes a mixture of SYTO 9, a green-fluorescent nucleic acid stains and propidium iodide (PI), a red-fluorescent nucleic acid stains. SYTO 9 is a membrane-permeable fluorescent marker that stains all cells, while PI penetrates only bacteria with damaged membranes and stains dead cells red. Twenty fields per sample were randomly selected to analyze the intensity of red and green fluorescence.

Extracellular Polysaccharide Production Assay

The method for quantification of EPS production was conducted as described previously (Packiavathy et al., 2012). Briefly, the bacterial culture was incubated with or without ursolic acid at concentrations ranging from 0.008 to 0.125 mg/ml at 37°C for 16 h, the culture was centrifuged (4°C, 12000 × *g*, 30 min), and the supernatants and cells were collected. The water-soluble and water-insoluble glucans were prepared using the method described previously (Yano et al., 2012). Briefly, water-soluble glucans were obtained by ethanol precipitation of the supernatants. The cells were resuspended in 1 M NaOH and centrifuged to collect supernatants, which were used to prepare water-insoluble glucans by ethanol precipitation. The phenol/H_2SO_4 method was used to quantify two types of EPS in the supernatant as described previously (Liu et al., 2017). The absorbance of the color was detected at 490 nm using an ELISA reader.

Molecular Dynamics Simulations

The crystal structure of glucansucrase was downloaded from the Protein Data Bank (ID: 3AIC) as the receptor, and the preparation work was done using the software Gold 5.2 and AutoDockTool 1.5.6. The MD simulation of the system was performed for 20 ns under the npt ensemble, and the data were saved every other 5 ps. CPPTRAJ was used for data analysis. The MMPBSA.py module was used to compute the binding free energy between the protein and ligand.

To further confirm the binding site between GTF-SI and ursolic acid, the amino acids in the predicted binding site were replaced by other amino acids, as shown in **Supplementary Table S1** Afterward, the mutant GTF-SI proteins were subjected to molecular docking under the same conditions as above.

GTF Activity Assay

The method for analyzing the enzymatic activity of the crude extract of GTFs was used as described previously by Koo *et al* (Koo et al., 2000). A 20-mL bacterial suspension of *S. mutans* was incubated in 200 ml of BHI broth containing 1% sucrose at 37°C. After incubation, supernatants were collected, and ammonium sulfate was added at 60% saturation for 24 h to prepare the protein. The crude enzymes were dissolved in PBS (pH 6.0). The reaction system mixture was the same as that described previously (Liu et al., 2017). The final concentration of ursolic acid ranging from 0.04 to 0.12 mg/ml was used to measure the inhibition of the synthesis of EPSs. After incubation, the method to determine the amount of the two types of glucans was applied as described above.

Preparation of Recombinant GTF and Its Mutants

cDNA fragments of wild-type GTF-SI (GenBank: M22054.1) and two mutant GTF-SI variants (**Supplementary Table S1**) were synthesized and inserted into the *Nde*I and *Xho*I sites of pCold I to generate pCold-GTF-SI recombinant plasmids with a 6× histidine tag at the N-terminus of the proteins (Ito et al., 2011). The recombinant proteins were purified by using GE metal affinity resin and dialyzed. SDS-PAGE was used to analyze recombinant GTF-SI proteins (shown in **Supplementary Figure S1**).

Capillary Electrophoresis Assay

Capillary electrophoresis (CE) was used to quantify fructose production catalyzed by GTFs as described previously (Rizelio et al., 2012). Recombinant GTF-SI was crudely extracted from recombinant transformants by ultrasonic disruption. Then, 50 µl of the crude enzyme solution together with or without ursolic acid at a final concentration of 0.03 mg/ml or 0.02 mg/ml was added to 1 ml of sucrose (0.1 M) and incubated at 37°C for 2 h. After incubation, the culture was centrifuged (4°C, 12000 × *g*, 10 min), and the supernatants were collected and filtered with a 0.22-µm nylon membrane before being subjected to the CE assay. The CE assay was conducted in a CE system, and the conditions to detect fructose were as follows: The detection wavelength was set at 254 nm; the temperature was maintained at 25°C; and fused silica capillaries had dimensions of 50 cm in total length and 40 cm in effective length, and the inner diameter and outer diameter were 50 µm and 375 µm, respectively. The sample injection was maintained at an elevation difference of 20 cm from the nearest detector for 5 s, and the separation voltage was 25 kV. The capillary system was rinsed with 0.1 M NaOH for 5 min, distilled water for 3 min, and PBS for 3 min before each run.

CE can also be used to detect the binding of drugs and proteins, which was used in this study to analyze the interaction of ursolic acid with GTF-SI and its variants as described previously (Liang et al., 2020). GTF-SI and its variants were dissolved in PBS (20 mm, pH = 6.8) and filtered with a 0.22-µm nylon membrane. Ursolic acid was dissolved in the same solution as that used to dissolve the proteins, and the final concentration was 0.3 mg/ml. Afterward, the GTF or its variants were incubated with ursolic acid for 2 h. Finally, CE was conducted as described above with a few differences: The detection wavelength was 210 nm, and the separation voltage was 20 kV.

RESULTS

Effects of Ursolic Acid on Biofilms

Biofilms are the key factors in the induction of dental caries and periodontitis. We first measured the MIC and the MBC

values of ursolic acid against *S. mutans*. The MIC value is the lowest concentration that could prevent the culture color from changing blue to pink. The MBC value is the lowest concentration that resulted in no visible bacterial colonies on the agar plates after incubation. As shown in **Supplementary Figure S2** and shown in **Table 1**, both the MIC and MBC values of ursolic acid against *S. mutans* were 0.25 mg/ml. Based on the concentration of antimicrobial activities, we evaluated the effect of ursolic acid on *S. mutans* biofilms by the XTT reduction method. As shown in **Figure 1A**, the bacterial viability within the biofilms decreased as the concentration of ursolic acid increased, while the difference was most significant at the concentration of 0.063 mg/ml. Compared with the positive control, ursolic acid showed similar inhibitory effects on the bacterial viability of biofilms at 0.125 mg/ml (**Supplementary Figure S3**). In addition, the crystal violet staining results showed that the amount of biofilm was decreased upon ursolic acid treatment, as shown in **Figure 1B**, which is consistent with the data of the XTT reduction assay.

To observe the direct effects of ursolic acid on biofilms, the Live/Dead BacLight Bacterial Viability kit was used to examine *S. mutans* bacteria within the biofilm, as shown in **Figure 1**. Compared with the control sample, the sample treated with ursolic acid had a large number of red-stained bacterial cells, indicating dead cells. Furthermore, the biofilms were thin.

TABLE 1 | The MIC and MBC values of ursolic acid against *S. mutans*.

Compound	Species/Strain	
	***S. mutans* (ATCC 25175)**	
	MIC (mg/mL)	**MBC (mg/mL)**
Ursolic acid	**0.25**	**0.25**

Negative control: the bacterial suspension alone; Positive control: chlorhexidine at a final concentration of 0.6 mg/ml.

This result confirmed that ursolic acid could significantly destroy biofilms by affecting bacterial survival and adhesion.

Effects of Ursolic Acid on GTF Activity

EPSs are the key factors contributing to bacterial colonization, biofilm formation, maturation, and caries. Because EPSs are synthesized by GTFs, we explored the effect of ursolic acid on GTF activity in crude bacterial extracts in the presence of sucrose *in vitro*. As shown in **Figure 2**, ursolic acid inhibited the activity of GTFs, resulting in a decrease in the synthesis of EPS products. The inhibition of ursolic acid on water-soluble glucan production was stronger than that on water-insoluble glucan production at low concentrations of less than 0.06 mg/ml, while this inhibition tendency was reversed at concentrations from 0.06 mg/ml to 0.12 mg/ml. Combined with the data above, these results suggest that ursolic acid could suppress the aggregation or adhesion of *S. mutans* to form cariogenic biofilms by preventing GTFs from synthesizing EPSs.

The Mode of Interaction Between Ursolic Acid and GTF-SI

The catalytic center of GTF-SI has been shown to include two subsites for EPS synthesis: Subsite+1 contains the key amino acids for sucrose to bind, and subsite-1 contains the key amino acids for glucosyl moiety polymerization to form EPSs (Ito et al., 2011). In particular, Trp517 provides a platform for the acceptor glycosyl moiety of sucrose, and Tyr430 participates in hydrophobic interactions with carbon atoms of the glycosyl moiety in subsite+1; however, Asp909 and Tyr916 are related to recognition of the glucosyl moiety of the primary sucrose and formation of the glycosyl-enzyme intermediate in subsite-1 (Ito et al., 2011). As shown in **Figure 3A**, the simulation data showed that ursolic acid formed hydrogen bonds with Tyr430 and Asp909 of GTF-SI and had hydrophobic interactions with Leu433, Leu434, Phe907, Trp517, and Tyr916, which are the key sites for catalyzing sucrose to synthesize EPSs. Furthermore, the MD simulation results showed that the binding free energy of GTF-SI to ursolic acid was similar

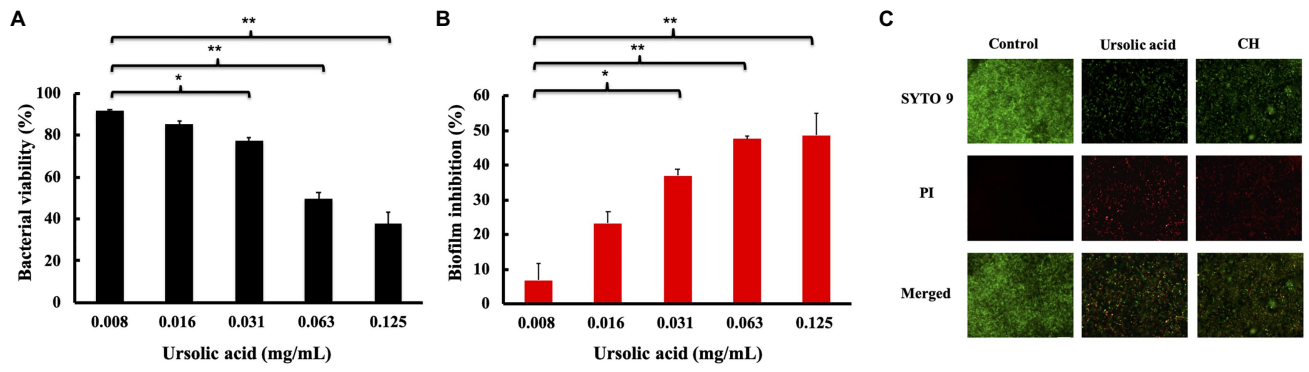

FIGURE 1 | Effects of ursolic acid on biofilms. **(A)**: Percentage of bacterial viability within biofilms detected by XTT assay; **(B)**: Inhibitory percentage of ursolic acid on biofilm formation detected by crystal violet staining. Data are presented as the mean ± standard deviation. $^{*}p < 0.05$ and $^{**}p < 0.01$. **(C)**: Effects of ursolic acid on biofilm structure. SYTO 9: green fluorescence, which stains both the dead and live bacterial cells; PI: red fluorescence, which stains dead bacterial cells. Control: ursolic acid untreated biofilms; CH: chlorhexidine (the positive control).

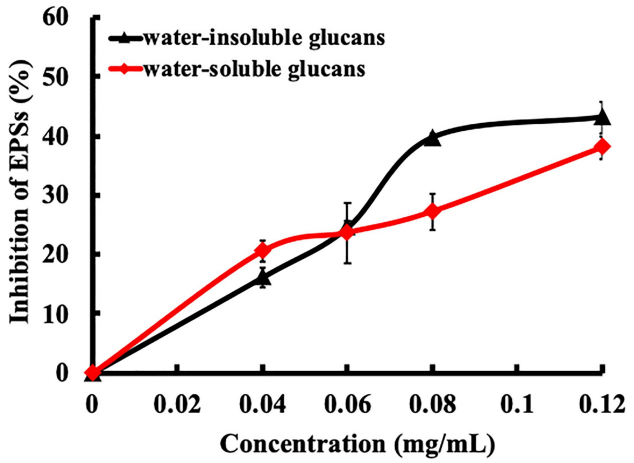

FIGURE 2 | Effect of ursolic acid on glucosyltransferase (GTF) activities. GTFs were crudely extracted from bacterial culture medium and were then used to test the effect of ursolic acid on its activities by using an *in vitro* enzymatic reaction system. The final concentration of ursolic acid ranged from 0.04 to 0.12 mg/ml. Extracellular polysaccharides (EPSs), including soluble and insoluble glucans, which are the catalytic products of GTFs, were measured as indicators of GTF activity. The data are presented as the mean ± standard deviation.

to that of sucrose (**Supplementary Table S2**). Then, we made two mutant GTF-SI variants in which the predicted amino acids that are essential for ursolic acid binding were replaced with other amino acids (**Supplementary Table S2**) to further verify the binding indicated by the simulation. The simulation showed that the number of amino acids in either GTF-SI variant that formed hydrogen bonds and hydrophobic interactions with ursolic acid decreased compared with that in wild-type GTF-SI (**Figures 3B,C**), and the interaction and binding free energy of the GTF-SI variants with ursolic acid were also decreased (**Supplementary Table S2, S3**).

Then, CE technology was used to further determine the interaction between GTFs and ursolic acid *in vitro*. As shown in **Figure 3D**, compared with that of the control, the migration time of the protein was prolonged by the addition of ursolic acid, which indicated that ursolic acid could bind with GTF-SI to change the charge-mass ratio, leading to a migration time-shift. The CE results further showed that the retention time of the variant A or variant B proteins was shorter than that of wild-type GTF-SI after the addition of ursolic acid, suggesting that the interaction between GTF-SI and ursolic acid became weaker or even lost as several key amino acids at the binding site were replaced (**Figures 3E,F**). These results indicate that ursolic acid might inhibit the enzymatic activity of GTFs through direct binding and that Phe907, Asp909 and Tyr916 in GTF-SI might be the key amino acids responsible for ursolic acid binding.

Effects of Ursolic Acid on EPSs and Fructose Production

The process of GTF synthesis of EPS includes two steps: First, the GTF enzyme binds with sucrose, and then, EPS synthesis is catalyzed. After sucrose binds with subsite+1 of the GTF, the glucosyl group of sucrose dissociates from subsite+1 and then binds subsite-1 of the GTF to form an intermediate that catalyzes EPS production, while the fructosyl group of sucrose dissociates from subsite+1 of the GTF to produce the by-product, namely, fructose (Ito et al., 2011). Therefore, the production of fructose and EPSs would decrease when the binding site and catalytic site of the GTF are occupied by a molecule other than sucrose. Since the amino acids in GTF-SI that are essential for ursolic acid binding are also indispensable for sucrose recognition and since the MD simulation results showed that the binding free energy of GTF-SI to ursolic acid was similar to that of sucrose (**Supplementary Table S2**), we hypothesized that ursolic acid may suppress GTF activity by competitively blocking sucrose binding. To test this hypothesis, we evaluated the effects of ursolic acid on the production of EPS and fructose. To confirm the effect of ursolic acid on EPS synthesis by *S. mutans*, water-soluble glucans and water-insoluble glucans were obtained from bacterial culture treated with or without ursolic acid for 16 h, and the phenol/H_2SO_4 method was used to detect the content of both types of EPSs. As shown in **Figure 4A**, ursolic acid at concentrations of 0.008 mg/ml to 0.125 mg/ml inhibited the production of both water-soluble and water-insoluble glucans. Additionally, the amount of fructose produced by crude recombinant GTF-SI was further measured in the presence of sucrose and ursolic acid for 2 h. As shown in **Figure 4B**, the amount of fructose production decreased with the addition of ursolic acid to the enzymatic reaction system, and the effect of a high concentration was more obvious than that of a low concentration. Based on this in combination with the data above, we proposed that ursolic acid could compete with sucrose to occupy the catalytic center of the GTF, which then inhibits the enzymes that synthesize EPSs and eventually prevents bacterial adhesion to form biofilms.

DISCUSSION

Dental plaque is an oral bacterial biofilm that plays a key role in oral diseases (Adler et al., 2013). Biofilm formation enhances bacterial tolerance to drugs or the environment; thus, inhibition of biofilm formation and damage to the biofilm are the effective ways to prevent or cure oral diseases (Chenicheri et al., 2017). *S. mutans* is the principal bacterium that forms biofilms by adhesion to teeth and is considered the most important pathogen for dental caries. In the present study, we investigated the effects of ursolic acid on the growth and cariogenicity of biofilms formed by *S. mutans*. The results indicated that ursolic acid could effectively prevent biofilm formation of *S. mutans* through two pathways: (i) Ursolic acid decreased the viability of planktonic and sessile bacteria; and (ii) ursolic acid inhibited GTF-mediated synthesis of EPSs by competing with sucrose to occupy the catalytic center of the enzyme, which decreased bacterial adhesion and biofilm formation. Therefore, ursolic acid has great potential to be developed as an oral protective or therapeutic drug for oral disease.

Dental caries is a secondary bacterial disease that affects the health and quality of life of half of the world's population (Hwang et al., 2014). Attention is needed to develop effective prevention

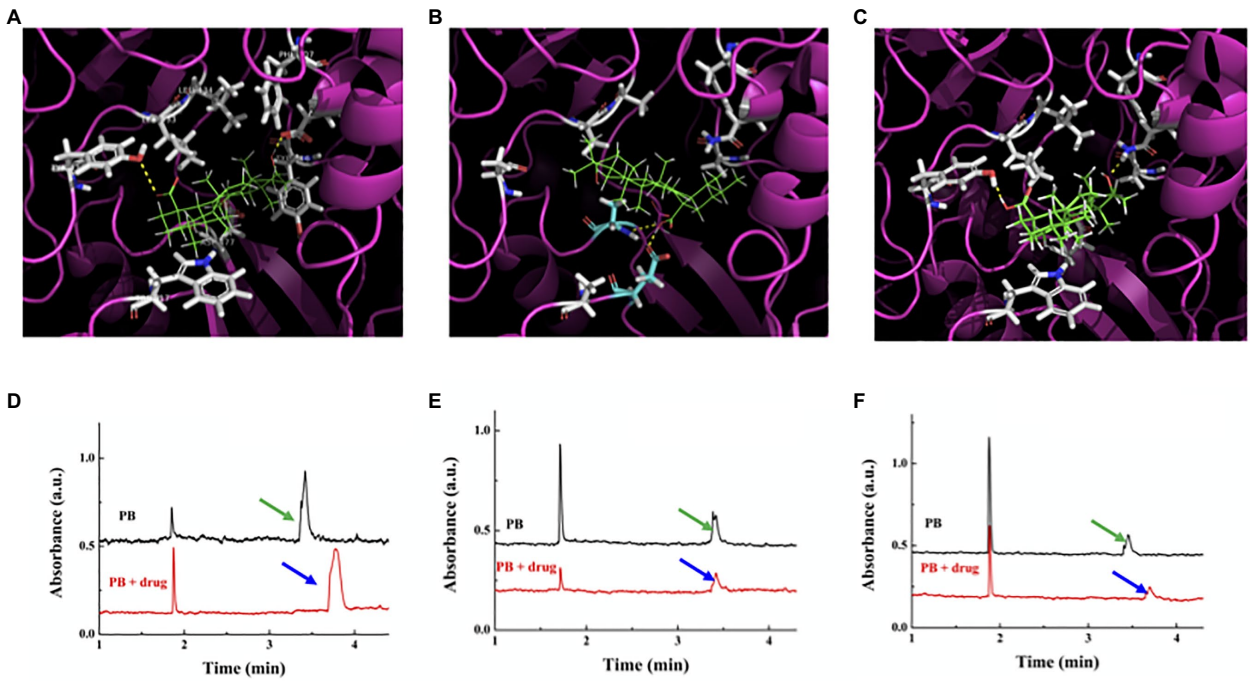

FIGURE 3 | Interaction between ursolic acid and GTF-SI. **(A-C)** Binding model of ursolic acid with GTF-SI and its variants simulated by Gold software. **(A)** Wild-type GTF-SI; **(B)** GTF-SI variant A; **(C)** GTF-SI variant B. Ursolic acid, as the ligand, is shown in green. The protein is shown as a cartoon with pink color. The yellow dotted lines represent hydrogen bonds. **(D-F)**: Interaction between ursolic acid and GTF-SI measured by CE assay. The black line represents the migration time of GTF-SI and its variants, whereas the red line is the migration time of GTF-SI or its variants together with ursolic acid. **(D)** Wild-type GTF-SI; **(E)** GTF-SI variant A; **(F)** GTF-SI variant B. Arrows point to the peak of the protein (black)/protein and ursolic acid complex (red).

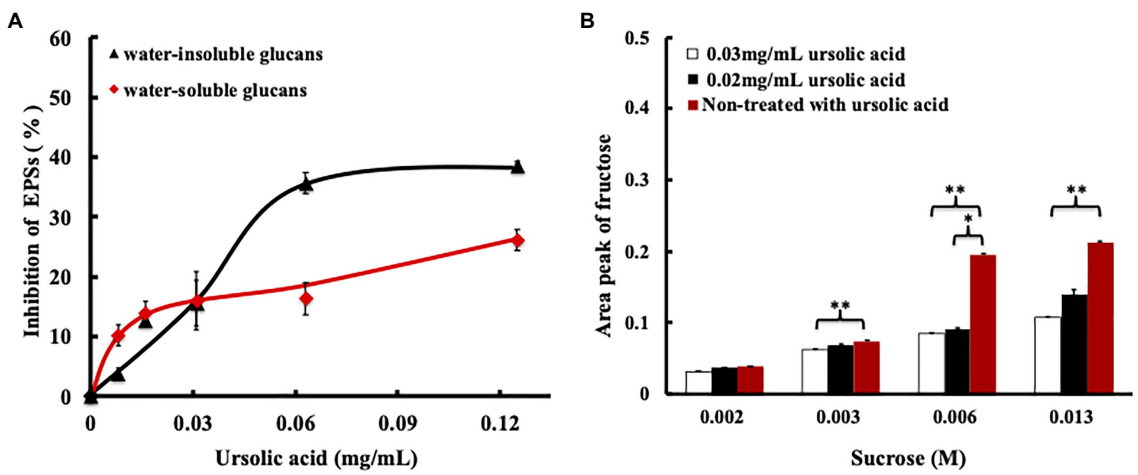

FIGURE 4 | Effect of ursolic acid on GTF catalyzed products. **(A)** Inhibitory percentage of ursolic acid on EPS production determined by phenol/H_2SO_4 analysis. After incubation with ursolic acid for 16 h, the water-soluble glucans and water-insoluble glucans were prepared from bacterial culture using the method described above. Phenol/H_2SO_4 analysis was used to quantify the two types of EPSs. Data are presented as the mean ± standard deviation; **(B)** Effect of ursolic acid on fructose production by GTFs determined *via* CE assay. Data are presented as the mean ± standard deviation. $^*p < 0.05$ and $^{**}p < 0.01$.

and treatment methods. The results of this study indicated that ursolic acid inhibits planktonic *S. mutans*. Previously, it was reported that ursolic acid could have an inhibitory effect on other cariogenic pathogens, such as *Streptococcus sobrius* (do Nascimento et al., 2014). Therefore, ursolic acid may have significant antimicrobial activity against pathogenic bacteria involved in dental caries.

Traditionally, fluoride, a common component of oral care products, is used to support oral hygiene and health. However, some studies have found that excess fluoride is unsafe for children and adults, as it may induce color nonuniformity of teeth and loss of potency (Wong et al., 2010). Chlorhexidine, a broad-spectrum antibiotic, is widely used to prevent or cure oral diseases (Charugundla et al., 2015). It was reported that *S. mutans* has some drug resistance against chlorhexidine (López-Jornet et al., 2012). Therefore, it is necessary to develop new effective components to decrease the drug resistance of oral pathogens. Interestingly, ursolic acid showed inhibitory activity on biofilms at 1/2 MIC, similar to chlorhexidine (**Supplementary Figure S3**). Moreover, ursolic acid has low toxicity and is versatile in terms of its biological activity, evidenced by its antiviral, liver protective, and whitening effects (Zou et al., 2019; Liu et al., 2021). Therefore, ursolic acid has great potential to be used as a lead compound in the development of an effective inhibitor for dental caries and as a protective agent for oral health.

Biofilm formation is a dynamic process that includes adhesion, aggregation, and maturation (Arciola et al., 2012). GTFs can synthesize EPSs by using sucrose as a substrate, which provides an adherent ability for bacterial colonization to promote biofilm formation and development (Hellmuth et al., 2008; Chen et al., 2013). Therefore, GTFs are key pathogenic factors in the induction of dental caries. It has been reported that subsite-1 and subsite+1 are the main partial catalytic centers of GTF-SI for sucrose binding and EPS formation (Ito et al., 2011). The primary bound sucrose is attacked by a proton to induce hydrolysis, and then, the glucosyl group binds to subsite-1 of GTF as an intermediate, while fructose is released from subsite+1 of the enzyme (Ito et al., 2011). Amino acid residues such as Arg475, Asp477, Glu515, Asp588, and Tyr916 construct subsite-1 of GTF for catalyzing glucan formation, while the amino acid residues located at subsite+1, such as Tyr430, Leu433, and Trp517, constitute the critical domains for recognition of the moiety (Ito et al., 2011). The molecular docking analysis showed that ursolic acid is sandwiched by Tyr430 and Asp909 to occupy the catalytic center and that the 3-hydroxyl group of ursolic acid points toward the active center. The experimental results confirmed that ursolic acid could bind with GTFs and that the binding ability disappeared as the action site was replaced by other amino acids. Quantitative analysis of EPSs and fructose showed that ursolic acid could decrease the levels of EPSs and fructose. These results confirm that ursolic acid competes with sucrose to occupy the catalytic center of GTFs, which may lead to the failure of GTFs to use sucrose as a substrate to synthesize EPSs (as shown in **Figures 2, 4**). In addition, the recognition of the glucosyl moiety of primary sucrose by GTFs and the intermediate formation at subsite-1 are well conserved in other *Streptococcus* species related to dental caries and infective endocarditis, such as *Streptococcus gordonii* (Hellmuth et al., 2008). Therefore, ursolic acid could be developed as an antimicrobial agent for dental caries or *Streptococcus*-related diseases.

CONCLUSION

We characterized the mechanism of *S. mutans* biofilm formation inhibition by ursolic acid. More importantly, ursolic acid can bind to GTFs instead of sucrose to interfere with microbial adhesion and aggregation through interactions with seven amino acids (Tyr430, Asp909, Leu433, Leu434, Phe907, Trp517, and Tyr916) of the enzyme, which is necessary for biofilm formation and even destroys mature biofilms, to prevent and cure dental caries and other oral diseases. Thus, ursolic acid has the potential to be developed as a drug or oral cleaning product to protect against and cure oral disease and other GTF-related diseases in the clinic. Finally, Leu433, Leu434, and Phe907 may serve as new target sites to screen inhibitors of GTFs to develop new antimicrobials.

DATA AVAILABILITY STATEMENT

The data sets presented in this study can be found in online repositories. The names of the repository/repositories and accession number(s) can be found in the article/**Supplementary Material**.

AUTHOR CONTRIBUTIONS

LY, BM, FC, and CZ performed the experiments. LY and SL designed the study, carried out the analysis and interpretation, and drafted and revised the manuscript. HY, YL, and ZL designed the study and analyzed the data. YC, SZ, YX, YJ, WS, LL, and WG assisted with the data analysis. All authors contributed to the article and approved the submitted version.

FUNDING

This study was supported by grants from the following foundations: the National Natural Science Foundation of China (no. 81700709), the Fundamental Research Funds for the Central Universities (nos. 135130006, 130029804, 111498001, and 131004006), the Research Foundation of Jilin Provincial Science and Technology Development (nos. 20200602023ZP, 20200901002SF, and 20200404124YY), the Foundation of Jilin Province Development and Reform Commission (no. 2020C015), the funds of the Education Department of Jilin Province (no. JJKH20201177KJ), and the Foundation of Human Resources and Social Security Department of Jilin Province (no. 2020009).

ACKNOWLEDGMENTS

This article is dedicated to my advisor Yuxin Li, who passed away last year, and commemorates his guidance in my life.

SUPPLEMENTARY MATERIAL

The Supplementary Material for this article can be found online at: https://www.frontiersin.org/articles/10.3389/fmicb.2021.743305/full#supplementary-material

REFERENCES

Adler, C. J., Dobney, K., Weyrich, L. S., Kaidonis, J., Walker, A. W., Haak, W., et al. (2013). Sequencing ancient calcified dental plaque shows changes in oral microbiota with dietary shifts of the Neolithic and industrial revolutions. *Nat. Genet.* 45, 450–455. doi: 10.1038/ng.2536

Arciola, C. R., Campoccia, D., Speziale, P., Montanaro, L., and Costerton, J. W. (2012). Biofilm formation in *staphylococcus* implant infections. a review of molecular mechanisms and implications for biofilm-resistant materials. *Biomaterials* 33, 5967–5982. doi: 10.1016/j.biomaterials.2012.05.031

Bacanlı, M., Başaran, A. A., and Başaran, N. (2017). The antioxidant, cytotoxic, and antigenotoxic effects of galangin, puerarin, and ursolic acid in mammalian cells. *Drug Chem. Toxicol.* 40, 256–262. doi: 10.1080/01480545.2016.1209680

Bowen, W. H., Burne, R. A., Wu, H., and Koo, H. (2018). Oral biofilms: pathogens, matrix, and Polymicrobial interactions in microenvironments. *Trends. Microbiol.* 26, 229–242. doi: 10.1016/j.tim.2017.09.008

Bowen, W. H., and Koo, H. (2011). Biology of Streptococcus mutans-derived glucosyltransferases: role in extracellular matrix formation of cariogenic biofilms. *Caries Res.* 5, 69–86. doi: 10.1159/000324598

Cardoso Sá, N., Cavalcante, T. T., Araújo, A. X., dos Santos, H. S., Albuquerque, M. R., Bandeira, P. N., et al. (2012). Antimicrobial and antibiofilm action of Casbane Diterpene from *croton nepetaefolius* against oral bacteria. *Arch. Oral Biol.* 57, 550–555. doi: 10.1016/j.archoralbio.2011.10.016

Charugundla, B. R., Anjum, S., and Mocherla, M. (2015). Comparative effect of fluoride, essential oil and chlorhexidine mouth rinses on dental plaque and gingivitis in patients with and without dental caries: a randomized controlled trial. *Int. J. Dent. Hyg.* 13, 104–109. doi: 10.1111/idh.12094

Chen, L., Ren, Z., Zhou, X., Zeng, J., Zou, J., and Li, Y. (2016). Inhibition of *Streptococcus mutans* biofilm formation, extracellular polysaccharide production, and virulence by an oxazole derivative. *App. Microbial. cell. physiol.* 100, 857–867. doi: 10.1007/s00253-015-7092-1

Chen, Y. P., Zhang, P., Guo, J. S., Fang, F., Gao, X., and Li, C. (2013). Functional groups characteristics of EPS in biofilm growing on different carriers. *Chemosphere* 92, 633–638. doi: 10.1016/j.chemosphere.2013.01.059

Chenicheri, S., R, U., Ramachandran, R., Thomas, V., and Wood, A. (2017). Insight into Oral biofilm: primary, secondary and residual caries and Phyto-challenged solutions. *Open Dent. J.* 11, 312–333. doi: 10.2174/1874210601711010312

Cummins, D. (2013). Dental caries: a disease which remains a public health concern in the 21st century–the exploration of a breakthrough technology for caries prevention. *J. Clin. Pediatr. Dentisitry.* 24, A1–A14.

do Nascimento, P. G., Lemos, T. L., Bizerra, A. M., Arriaga, Â. M., Ferreira, D. A., Santiago, , et al. (2014). Antibacterial and antioxidant activities of ursolic acid and derivatives. *Molecules* 19, 1317–1327. doi: 10.3390/molecules19011317

Duque, C., Aida, K. L., Pereira, J. A., Teixeira, G. S., Caldo-Teixeira, A. S., Perrone, L. R., et al. (2017). I*n vitro* and *in vivo* evaluations of glass-ionomer cement containing chlorhexidine for atraumatic restorative treatment. *J. Appl. Oral Sci.* 25, 541–550. doi: 10.1590/1678-7757-2016-0195

Hellmuth, H., Wittrock, S., Kralj, S., Dijkhuizen, L., Hofer, B., and Seibel, J. (2008). Engineering the glucan-sucrase GTFR enzyme reaction and glycosidic bond specificity: toward tailor-made polymer and oligosaccharide products. *Biochemistry* 47, 6678–6684. doi: 10.1021/bi800563r

Hui, Y., Wen, S., Lihong, W., Chuang, W., and Chaoyun, W. (2021). Molecular structures of nonvolatile components in the Haihong fruit wine and their free radical scavenging effect. *Food Chem.* 15:129298. doi: 10.1016/j.foodchem.2021.129298

Hwang, G., Klein, M. I., and Koo, H. (2014). Analysis of the mechanical stability and surface detachment of mature *Streptococcus mutans* biofilms by applying a rage of external shear forces. *Biofouling* 30, 1079–1091. doi: 10.1080/08927014.2014.969249

Ikeda, Y., Murakami, A., and Ohigashi, H. (2008). Ursolic acid: an anti-and pro-inflammatory triterpenoid. *Mol. Nutr. Food Res.* 52, 26–42. doi: 10.1002/mnfr.200700389

Ito, K., Ito, S., Shimamura, T., Weyand, S., Kawarasaki, Y., Misaka, T., et al. (2011). Crystal structure of Glucansucrase from the dental caries pathogen *Streptococcus mutans*. *J. Mol. Biol.* 408, 177–186. doi: 10.1016/j.jmb.2011.02.028

Jakubovics, N. S., Goodman, S. D., Mashburn-Warren, L., Stafford, G. P., and Cieplik, F. (2021). The dental plaque biofilm matrix. *Periodontol.* 86, 32–56. doi: 10.1111/prd.12361

Jaña, G. A., Mendoza, F., Osorio, M. I., Alderete, J. B., Fernandes, P. A., Ramos, M. J., et al. (2018). A QM/MM approach on the structural and stereoelectronic factors governing glycosylation by GTF-SI from *Streptococcus mutans*. *Org. Biomol. Chem.* 16, 2438–2447. doi: 10.1039/C8OB00284C

Kim, S. G., Min, J. K., Jin, D., Park, S. N., and Kook, J. K. (2012). Antimicrobial effect of ursolic acid and oleanolic acid against methicillin-resistant *Staphylococcus aureus*. *J. Microbiol.* 48, 212–215. doi: 10.7845/kjm.2012.029

Kong, L., Li, S., Liao, Q., Zhang, Y., Sun, R., Zhu, X., et al. (2013). Oleanolic acid and ursolic acid: novel hepatitis C virus antivirals that inhibit NS5B activity. *Antivir. Res.* 98, 44–53. doi: 10.1016/j.antiviral.2013.02.003

Koo, H., Gomes, B. P., Rosalen, P. L., Ambrosano, G. M., Park, Y. K., and Cury, J. A. (2000). *In vitro* antimicrobial activity of propolis and *Arnica Montana* against oral pathogens. *Arch. Oral Biol.* 45, 141–148. doi: 10.1016/S0003-9969(99)00117-X

Liang, C., Li, Y., Bai, M., Huang, Y., Yang, H., Liu, L., et al. (2020). Hypericin attenuates nonalcoholic fatty liver disease and abnormal lipid metabolism via the PKA-mediated AMPK signaling pathway *in vitro* and *in vivo*. *Pharmacol. Res.* 153:104657. doi: 10.1016/j.phrs.2020.104657

Liu, H. R., Ahmad, N., Lv, B., and Li, C. (2021). Advances in production and structural derivatization of the promising molecule ursolic acid. *Biotechnol. J.* 6:e2000657. doi: 10.1002/biot.202000657

Liu, Y., Xu, Y., Song, Q., Wang, F., Sun, L., Liu, L., et al. (2017). Anti-biofilm activities from *Bergenia crassifolia* leaves against *Streptococcus mutans*. *Front. Microbiol.* 8:1738. doi: 10.3389/fmicb.2017.01738

López-Jornet, P., Plana-Ramon, E., Leston, J. S., and Pons-Fuster, A. (2012). Short-term side effects of 0.2% alcohol-free chlorhexidine mouthrinse in geriatric patients: a randomized, double-blind, placebo-controlled study. *Gerodontology* 29, 292–298. doi: 10.1111/j.1741-2358.2012.00671.x

Monchois, V., Willemot, R. M., and Monsan, P. (1999). Glucansucrases: mechanism of action and structure–function relationships. *FEMS. Microbiol. Rev.* 23, 131–151. doi: 10.1016/S0168-6445(98)00041-2

Packiavathy, I. A. S. V., Agilandeswari, P., Musthafa, K. S., Pandian, S. K., and Ravi, A. V. (2012). Antibiofilm and quorum sensing inhibitory potential of *Cuminum cyminum* and its secondary metabolite methyl eugenol against gram negative bacterial pathogens. *Food Res. Int.* 45, 141–148. doi: 10.1016/j.foodres.2011.10.022

Pádua, T.A., de Abreu, B.S., Costa, T.E., Nakamura, M.J., and Valente, L.M., and Henriques, M.d., et al (2014). Anti-inflammatory effects of methyl ursolate obtained from a chemically derived crude extract of apple peels: potential use in rheumatoid arthritis. *Arch. Pharm. Res.* 37, 1487–1495. doi:10.1007/s12272-014-0345-1.

Palomino, J. C., Martin, A., Camacho, M., Guerra, H., Swings, J., and Portaels, F. (2002). Resazurin microtiter assay plate: simple and inexpensive method for detection of drug resistance in mycobacterium tuberculosis. *Antimicrob. Agents Chemother.* 46, 2720–2722. doi: 10.1128/AAC.46.8.2720-2722.2002

Patlolla, J. M., and Rao, C. V. (2012). Triterpenoids for cancer prevention and treatment: current status and future prospects. *Curr. Pharm. Biotechnol.* 13, 147–155. doi: 10.2174/138920112798868719

Pitts, N. B., Zero, D. T., Marsh, P. D., Ekstrand, K., Weintraub, J. A., Ramos-Gomez, F., et al. (2017). Dental caries. *Nature Review Disease Primers* 3:17030. doi: 10.1038/nrdp.2017.30

Rizelio, V. M., Tenfen, L., da Silveira, R., Gonzaga, L. V., Costa, A. C., and Fett, R. (2012). Development of a fast capillary electrophoresis method for determination of carbohydrates in honey samples. *Talanta* 93, 62–66. doi: 10.1016/j.talanta.2012.01.034

Sarker, S. D., Nahar, L., and Kumarasamy, Y. (2007). Microtitre plate-based antibacterial assay incorporating resazurin as an indicator of cell growth, and its application in the in vitro antibacterial screening of phytochemicals. *Methods* 42, 321–324. doi: 10.1016/j.ymeth.2007.01.006

Shun, C. T., Lu, S. Y., Yeh, C. Y., Chiang, C. P., Chia, J. S., and Chen, J. Y. (2005). Glucosyltransferases of viridans streptococci are modulins of interleukin-6 induction in infective endocarditis. *Infect. Immunnity.* 73, 3261–3270. doi: 10.1128/IAI.73.6.3261-3270.2005

Süntar, I., Oyardı, O., Akkol, E. K., and Ozçelik, B. (2016). Antimicrobial effect of the extracts from *Hypericum perforatum* against oral bacteria and biofilm formation. *Pharm. Biol.* 54, 1065–1070. doi: 10.3109/13880209.2015.1102948

Takahashi, N., and Nyvad, B. (2011). The role of bacteria in the caries process: ecological perspectives. *J. Dent. Res.* 90, 294–303. doi: 10.1177/0022034510379602

Tamesada, M., Kawabata, S., Fujiwara, T., and Hamada, S. (2004). Synergistic effects of streptococcal glucosyl-transferases on adhesive biofilm formation. *J. Dent. Res.* 83, 874–879. doi: 10.1177/154405910408301110

Taubman, M. A., and Nash, D. A. (2006). The scientific and public-health imperative for a vaccine against dental caries. *Nat. Rev. Immunol.* 6, 555–563. doi: 10.1038/nri1857

Vernazza, C. R., Birch, S., and Pitts, N. B. (2021). Reorienting Oral health services to prevention: economic perspectives. *J. Dent. Res.* 100, 576–582. doi: 10.1177/0022034520986794

Wang, C., van der Mei, H. C., Busscher, H. J., and Ren, Y. (2020). *Streptococcus mutans* adhesion force sensing in multi-species oral biofilms. *npj. Biofilms. Microbiomes.* 6, 1–9. doi: 10.1038/s41522-020-0135-0

Wong, M. C., Glenny, A. M., Tsang, B. W., Lo, E. C., Worthington, H. V., and Marinho, V. C. (2010). Topical fluoride as a cause of dental fluorosis in children. *Cochrane Database Syst. Rev.* 1:CD007693. doi: 10.1038/s41522-020-0135-0

Wong, A., Subar, P. E., and Young, D. A. (2017). Dental caries: an update on dental trends and therapy. *Adv. Pediatics.* 64, 307–330. doi: 10.1016/j.yapd.2017.03.011

Xu, H., Zhang, M., Li, X. L., Li, H., Yue, L. T., Zhang, X. X., et al. (2019). Low and high doses of ursolic acid ameliorate experimental autoimmune myasthenia gravis through different pathways. *J. Neuroimmunol.* 330, 181–183. doi: 10.1016/j.jneuroim.2019.03.016

Yano, A., Kikuchi, S., Takahashi, T., Kohama, K., and Yoshida, Y. (2012). Inhibitory effects of the phenolic fraction from the pomace of Vitis coignetiae on biofilm formation by Streptococcus mutans. *Arch. Oral Biol.* 57, 711–719. doi: 10.1016/j.archoralbio.2012.01.001

Zou, J., Lin, J., Li, C., Zhao, R., Fan, L., Yu, J., et al. (2019). Ursolic acid in cancer treatment and metastatic chemoprevention: from synthesized derivatives to Nanoformulations in preclinical studies. *Curr. Cancer Drug Targets* 19, 245–256. doi: 10.2174/1568009618666181016145940

Conflict of Interest: The authors declare that the research was conducted in the absence of any commercial or financial relationships that could be construed as a potential conflict of interest.

Publisher's Note: All claims expressed in this article are solely those of the authors and do not necessarily represent those of their affiliated organizations, or those of the publisher, the editors and the reviewers. Any product that may be evaluated in this article, or claim that may be made by its manufacturer, is not guaranteed or endorsed by the publisher.

frontiers in Microbiology

MINI REVIEW
published: 04 November 2021
doi: 10.3389/fmicb.2021.760255

Antibiotic Treatment, Mechanisms for Failure, and Adjunctive Therapies for Infections by Group A *Streptococcus*

Anders F. Johnson[1] *and Christopher N. LaRock*[1,2,3,4]*

[1] *Microbiology and Molecular Genetics Program, Graduate Division of Biological and Biomedical Sciences, Laney Graduate School, Emory University, Atlanta, GA, United States,* [2] *Department of Microbiology and Immunology, Emory University School of Medicine, Atlanta, GA, United States,* [3] *Division of Infectious Diseases, Department of Medicine, Emory University School of Medicine, Atlanta, GA, United States,* [4] *Emory Antibiotic Resistance Center, Atlanta, GA, United States*

OPEN ACCESS

Edited by:
Prescilla Emy Nagao, Rio de Janeiro State University, Brazil

Reviewed by:
Kelly Doran, University of Colorado Hospital, United States
Yoann Le Breton, Walter Reed Army Institute of Research, United States

***Correspondence:**
Christopher N. LaRock
clarock@emory.edu

Specialty section:
This article was submitted to Antimicrobials, Resistance and Chemotherapy, a section of the journal Frontiers in Microbiology

Received: *17 August 2021*
Accepted: *28 September 2021*
Published: *04 November 2021*

Citation:
Johnson AF and LaRock CN (2021) Antibiotic Treatment, Mechanisms for Failure, and Adjunctive Therapies for Infections by Group A Streptococcus. Front. Microbiol. 12:760255. doi: 10.3389/fmicb.2021.760255

Group A *Streptococcus* (GAS; *Streptococcus pyogenes*) is a nearly ubiquitous human pathogen responsible for a significant global disease burden. No vaccine exists, so antibiotics are essential for effective treatment. Despite a lower incidence of antimicrobial resistance than many pathogens, GAS is still a top 10 cause of death due to infections worldwide. The morbidity and mortality are primarily a consequence of the immune sequelae and invasive infections that are difficult to treat with antibiotics. GAS has remained susceptible to penicillin and other β-lactams, despite their widespread use for 80 years. However, the failure of treatment for invasive infections with penicillin has been consistently reported since the introduction of antibiotics, and strains with reduced susceptibility to β-lactams have emerged. Furthermore, isolates responsible for outbreaks of severe infections are increasingly resistant to other antibiotics of choice, such as clindamycin and macrolides. This review focuses on the challenges in the treatment of GAS infection, the mechanisms that contribute to antibiotic failure, and adjunctive therapeutics. Further understanding of these processes will be necessary for improving the treatment of high-risk GAS infections and surveillance for non-susceptible or resistant isolates. These insights will also help guide treatments against other leading pathogens for which conventional antibiotic strategies are increasingly failing.

Keywords: group A *Streptococcus*, *Streptococcus pyogenes*, antibiotic resistance, treatment failure, experimental therapeutics

INTRODUCTION

Streptococcus pyogenes (group A *Streptococcus*, GAS) is a ubiquitous human pathogen responsible for over half a million deaths per year worldwide (Carapetis et al., 2005). No vaccine exists, and current treatment depends on conventional antibiotics and symptom management. While the β-lactam penicillin remains the antibiotic of choice for mild to moderate infections, severe or prolonged infections require additional measures for effective clearance. The standard recommendation is to utilize the lincosamide clindamycin in combination with penicillin

(Stevens et al., 2014). Any resistance is a serious issue because of the reliance on these antibiotics, so surveillance is important. GAS has no resistance to penicillin, but treatment failure remains a major concern. Clindamycin has been very effective, but the global rates of resistance continue to rise and make the implementation of universal guidelines a challenge. Emergent challenges and opportunities for the treatment of GAS are the focus of this review.

GROUP A *STREPTOCOCCUS* INFECTIONS

GAS colonizes the nasopharynx, where it can cause disease, disseminate to other sites in the body, and transmit to other humans. GAS is isolated from this site in 12–24% of healthy children and in 37% of those with a sore throat (Shaikh et al., 2010). Pharyngitis, or strep throat, is the most common disease caused by GAS and is estimated to occur more than 600 million times per year (Carapetis et al., 2005). The common symptoms of pharyngitis are a sore throat, fever, enlarged tonsils, and coughing with throat pain, induced by pro-inflammatory exotoxins secreted by GAS (Dan et al., 2019; LaRock et al., 2020). Some individuals are susceptible to recurring pharyngitis (Dan et al., 2019), which may be prevented with tonsillectomy, although 33% of children lacking tonsils are still colonized by GAS (Roberts et al., 2012). GAS exotoxins also promote colonization of the skin and more serious invasive infections and are major drivers of pathogenesis (Wilde et al., 2021a).

Antibiotics remain necessary since fatal complications may occur from untreated infection. Famously, untreated pharyngitis can lead to scarlet fever, an inflammatory disease with resurging outbreaks (Davies et al., 2015; Park et al., 2017; Lynskey et al., 2019), and fatality rates up to 30% (Quinn, 1989). Scarlet fever is mediated by the streptococcal pyrogenic exotoxin superantigens, which induce an inflammatory cytokine storm (Shannon et al., 2019). In the bloodstream, superantigens are responsible for streptococcal toxic shock syndrome (STSS), a multi-organ disease with a fatality rate up to 44% (Lamagni et al., 2008; Wilkins et al., 2017). STSS often co-occurs with necrotizing fasciitis, an invasive infection of the skin (Low, 2013) where surgery within 24 h is often necessary for survival due to tissue damage and bacteremia (Olsen and Musser, 2010). Untreated GAS infections further have the risk of immune sequelae such as rheumatic fever, where the immune system mistakenly recognizes host tissue as foreign antigens (Cunningham, 2000; Hurst et al., 2018). When targeted toward the heart, this results in rheumatic heart disease, a chronic condition that is a major cause of GAS morbidity and mortality (Walker et al., 2014). The risk of any of these complications is thus limited when GAS infections are rapidly treated.

The β-lactam penicillin remains the gold standard of antibiotic treatment for many GAS infections (Stevens et al., 2014). β-lactams target penicillin-binding proteins (PBPs) to block peptidoglycan cross-linking in metabolically active bacteria, leading to bacterial death (**Figure 1**; Wilke et al., 2005). Despite extensive use for decades, there has been minimal change in the susceptibility of GAS to penicillin (Macris et al., 1998). Discovered in 1928 by Alexander Fleming, penicillin was brought to clinical trials in 1941. It did not take long for resistance to be observed. Penicillinase-producing *Escherichia coli* were observed in 1940, and strains of penicillin-resistant *Staphylococcus aureus* were clinically found in 1942, with 80% resistant by the end of the 1960s. Semi-synthetic versions of penicillin such as methicillin were in response; however, it would only take 20 years for methicillin resistance to become endemic (Lobanovska and Pilla, 2017).

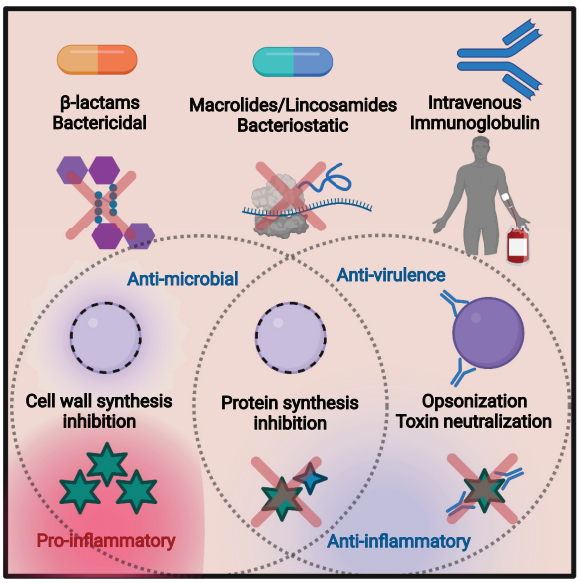

FIGURE 1 | Summary of the treatment methods discussed in this review. Bactericidal β-lactams such as penicillin target the peptidoglycan of the cell wall, leading to cell lysis. This can lead to an efflux of virulence factors and other cellular proteins, resulting in inflammation. Macrolides and lincosamides are bacteriostatic, blocking protein synthesis by targeting the bacterial ribosome. Preventing toxin synthesis works to reduce inflammation. Intravenous immunoglobulin (IVIG) is an infusion of pooled antibodies from human donors, which works to induce opsonization and neutralize toxins, reducing inflammation. Figure made in biorender.

NON-ANTIMICROBIAL ANTIBIOTIC EFFECTS

In animal models and human infection, clindamycin is also effective against severe GAS infection (Coyle, 2003; Carapetis et al., 2014). Clindamycin is a semi-synthetic lincosamide antibiotic that targets the 50S subunit of the ribosome (Spízek and Rezanka, 2004). Inhibition occurs through blocking of the peptidyl transferase reaction, preventing protein synthesis in susceptible pathogens, commonly Gram-positive cocci of *Streptococcus*, *Staphylococcus*, and *Clostridium* species (Stevens et al., 1987). Clindamycin is bacteriostatic and can limit the production of toxic proteins and virulence factors independent of its effects on growth (**Figure 1**; Schlievert and Kelly, 1984). This is also true for GAS (Mascini et al., 2001), where clindamycin inhibition of M protein synthesis promotes phagocytic killing

(Gemmell et al., 1981) and inhibition of superantigens and other toxins (Sriskandan et al., 1997; Mascini et al., 2001) can mitigate septic shock (Schlievert and Kelly, 1984). Similar anti-toxin effects have been described for *Clostridium perfringens* (Stevens et al., 1995) and *Clostridioides difficile* (Zarandi et al., 2017).

Because of their efficacy, both penicillin and clindamycin are recommended as of 2014 by the Infectious Diseases Society of America guidelines for necrotizing GAS infections (Stevens et al., 2014). They should be used in combination with surgical interventions. Due to a mortality rate of 30% or higher from severe symptoms, treatment should be rapid to minimize risk of death (Stevens et al., 1989). While penicillin and clindamycin are not antagonistic when prescribed together, there is no inherent bactericidal benefit to using both (Stevens et al., 1998). However, the added benefits of clindamycin may come from ribosome inhibition reducing the development of toxin-mediated symptoms like STSS (Sartelli et al., 2018). Since penicillin treatment can lead to lysis and toxin release (Coyle, 2003), protein synthesis inhibitors like clindamycin (Kishi et al., 1999) that decrease toxin production can help mitigate excessive immune stimulation (Coyle, 2003). It remains to be determined whether adjunctive use of additional antibiotics improves treatment (Sunderkötter et al., 2019). For clindamycin-resistant GAS, early experimental work suggests linezolid (Oppegaard and Rath, 2020) as a suitable alternative, while gentamicin is also suggested as a potential candidate, albeit with potential toxicity (Andreoni et al., 2017).

ANTIBIOTIC RESISTANCE

GAS develops resistance to clindamycin by two primary mechanisms: target site modification or efflux pumps. Methylation of clindamycin target sites on the 23S RNA by ErmA, ErmC, or enzymes are most common (Seppälä et al., 1998). Isolates with this mechanism can either have constitutive or inducible resistance to clindamycin (Lewis and Jorgensen, 2005). Inducible resistance can result in treatment failure, as inducible clindamycin resistance is undetectable unless macrolides are also present (Lewis et al., 2014). Efflux pumps are a common resistance mechanism, such as *msrA* and *mefA* involved in macrolide resistance (Clancy et al., 1996). Despite the structural similarity of clindamycin and macrolides, these pumps have shown greater efficacy against macrolides (Sutcliffe et al., 1996). *Staphylococcus* species may also enzymatically inactivate clindamycin through LinA (Matsuoka, 2000). Due to the frequency of antibiotic resistance genes being plasmid mediated, there is concern of horizontal gene transfer generating new resistant strains (Ben Zakour et al., 2015).

Clindamycin resistance in the United States is on the rise, from an estimated 0.5% in 2003 (Richter et al., 2005) to currently as high as 15% in pediatric populations (DeMuri et al., 2017). Isolates from invasive infections are more commonly resistant, increasing from 2% to over 23% in this time (Fay et al., 2021). The resistance rates are geographically variable; in China, resistance may approach 95.5% (Stevens and Bryant, 2017), where over a similar period, northern Europe rates approximated 1% (Bruun et al., 2021). Despite the rapid change in resistance trends and the emergence of potentially hypervirulent, resistant strains, the recommendation remains: continue the use of protein synthesis inhibitors such as clindamycin when necessary, but to be mindful and vigilant for resistant isolates (Stevens et al., 2014).

β-Lactams and macrolides are the drugs of choice for GAS and therefore have the highest concern for the development of resistance. Along with rapid increases in erythromycin and clindamycin resistance, tetracycline resistance is widespread and levofloxacin resistance is observed (Fay et al., 2021). However, the challenges with GAS treatment are still typically antibiotic failure, not intrinsic drug resistance. No resistance to vancomycin or β-lactams has been observed.

β-LACTAM RESISTANCE CONCERNS

The answer to why GAS has not developed resistance to β-lactams despite extensive use and widespread resistance in related species has remained elusive. A study in 1998 found no significant change in the minimum inhibitory concentration (MIC) over time (Macris et al., 1998), and this trend has continued (Fay et al., 2021). While there have been clinical isolates with elevated penicillin MIC values reported in India, Japan, and Mexico (Amábile-Cuevas et al., 2001; Capoor et al., 2006; Ogawa et al., 2011; Berwal et al., 2019), no mechanism has been provided. In other streptococci, resistance is primarily found in PBP mutations. One proposal is that PBPs with low affinity for β-lactams are poorly tolerated by GAS (Horn et al., 1998). Consistent with this, GAS engineered to express low-affinity PBPs had growth defects, poor growth rates, and morphological abnormalities (Gutmann et al., 1981; Gutmann and Tomasz, 1982). Additional work showed that decreases in the M protein production could lead to resistance, at the cost of being avirulent (Rosendal, 1958). Taken together, this suggests that PBPs are essential to GAS biology, and changes that would support resistance are either fatal or so detrimental that survival in a clinical setting is quite difficult. This has been partially backed up by recent work showing that three or fewer amino acid changes to PBP have occurred in 99% or more of the clinically relevant GAS strains (Hayes et al., 2020).

A community outbreak of GAS in Seattle recently led to the identification of two isolates with reduced susceptibility to β-lactams (Vannice et al., 2020). These isolates had a T553K substitution within *pbp2x* and a S79F substitution within *parC* of topoisomerase. The MIC values for ampicillin, amoxicillin, and cefotaxime were higher than those of isogenic isolates, while the MIC for penicillin was unchanged. The two isolates have no confirmed direct link despite their genomes being nearly identical (Vannice et al., 2020). In the wake of these findings, there were concerns that these mutations were already worldwide. Subsequent studies have identified additional natural mutations in *pbp2x* responsible for the reduced susceptibility (Musser et al., 2020). Isogenic isolates with *pbp2x* mutations show no change in virulence in a mouse model; however, they have a potential for increased fitness (Olsen et al., 2020). These mutations are concerning because of the similarities with *Streptococcus*

pneumoniae, another pathogen responsible for childhood disease (Weiser et al., 2018). Penicillin had been the antibiotic of choice for treatment, but resistance became widespread in the 1980s mutations in *pbp2x* and *pbp2b* (Grebe and Hakenbeck, 1996). One possible source of resistance was horizontal gene transfer into *S. pneumoniae* from other native oral streptococcal species such as *Streptococcus mitis* (Dowson et al., 1989). T550 in *S. pneumoniae* corresponds to T553 in GAS, suggesting that future resistance could similarly arise (Vannice et al., 2020).

ADDITIONAL CONSIDERATIONS WITH ANTIBIOTIC TREATMENT

A penicillin allergy is one of the few reasons to consider another drug for most GAS infections. This allergy is estimated in 8% of patients, but an IgE-mediated allergic response will only be visible in 1 in 20 people (Macy and Ngor, 2013; Macy, 2014). Allergy is often over-reported or self-diagnosed, leading to other antibiotics being prescribed unnecessarily (Sousa-Pinto et al., 2017). Vancomycin or linezolid are common alternatives for those with severe penicillin allergies (Stevens et al., 2014). Allergic reactions to clindamycin are rare; it has therefore become common as an alternative choice in instances of allergic reactions to other antibiotics (Lammintausta et al., 2002). Since infection is recurrent for many people, repeated use of penicillin may drive allergy, select for resistance in other species of microbes present, and give rise to a series of opportunistic infections by pathogens such as *C. difficile* (Johnson et al., 1999; Brindle et al., 2017).

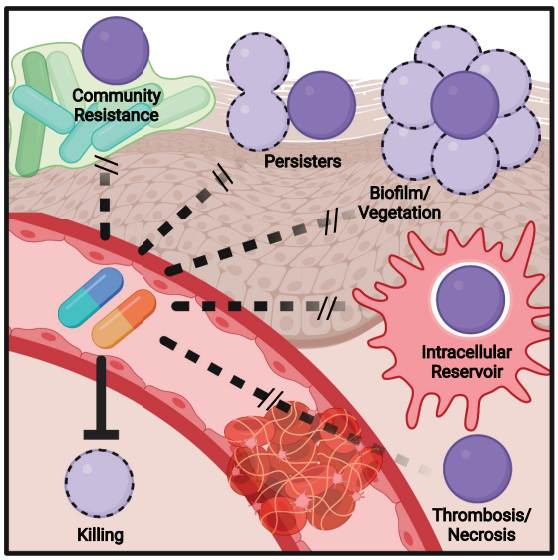

FIGURE 2 | Model of mechanisms contributing to antibiotic failure during Group A *Streptococcus* (GAS) infections. Community-mediated resistance mediated by protection by endogenous microbiota is likely most prevalent during pharyngitis and not invasive infections, where GAS most often exists as a monoculture. Persisters, resistant through altered growth rates or other epigenetic states, can contribute to treatment failure of any infection. The formation of biofilms, invasion of epithelial cells, and survival within phagocytes can similarly occur during any infection and serve to shield single bacterium from antibiotic action. During invasive infections in particular, inflammation- and toxin-mediated necrosis of tissue and thrombosis of dermal vasculature can limit antibiotic perfusion, necessitating surgical removal of the infected tissue.

MECHANISMS FOR TREATMENT FAILURE

Thus, despite *in vitro* sensitivity to many antibiotics, including universal sensitivity to penicillin, GAS remains a major public health burden. Treatment failure was first reported not long after the introduction of penicillin (Eagle, 1952) and has remained a problem ever since in both common pharyngitis and more severe invasive infections (Markowitz et al., 1993; Gillespie, 1998; Orrling et al., 2001). Death due to treatment failure is not due exclusively to lack of access to antibiotics or medical treatment because, even in resource-rich countries, invasive infections can have a high failure rate during treatment (Orrling et al., 1994). Since death is not always from overwhelming bacteremia, but rather pathological inflammation as sepsis, a bolus of antibiotic leading to massive bacterial lysis may transiently exacerbate the disease or even lead to death (Wolf et al., 2017). Individuals treated with only penicillin have also shown greater risk of recurrent tonsillitis, suggesting an inability to clear the infection fully (Brook and Hirokawa, 1985).

Bacteria can survive at antibiotic concentrations beyond a minimal bactericidal concentration (MBC) by a process known as the Eagle effect (Prasetyoputri et al., 2019). First observed in 1948 (Eagle and Musselman, 1948), it is speculated to be related to penicillin having greater efficacy on bacteria in log phase growth, as they are actively rebuilding their peptidoglycan (Eagle, 1952). During infection, resource limitation and antimicrobial immune responses slowing bacterial growth may lead to decreased antibiotic efficacy (**Figure 2**). This has manifested in treatment failure using the mouse model of GAS infection, where delaying penicillin treatment led to a significant reduction in survival (Stevens et al., 1988).

Community-mediated resistance (**Figure 2**) is another mechanism that may contribute to failure, where β-lactamases secreted by the resident microbiota in the polymicrobial environment protect sensitive pathogens, including GAS (Sorg et al., 2016; Gjonbalaj et al., 2020). One study showed that β-lactamase producers were found in 40% of pediatric patients with orofacial or respiratory tract infections (Brook, 1984), with another suggesting rates as high as 74% in the tonsils (Brook, 2009). One potential impact of clindamycin is therefore killing β-lactam-resistant species that provided protection to GAS, allowing for later reinfection (Brook and Hirokawa, 1985). The deep tissue is commonly sterile, so community resistance is more likely to play a role during pharyngitis, where there is an abundant polymicrobial community present.

Biofilms are an aggregate of bacteria encased in an extracellular matrix and contribute to the ability of many bacterial species to resist immune effectors and antibiotics. Aggregates of GAS consistent with biofilm formation have been observed in nasopharyngitis (Roberts et al., 2012) and the skin

(Akiyama et al., 2003; Siemens et al., 2016). The GAS biofilm requires cell surface-anchored proteins such as pili and the serotype-specific M protein to contribute to a hydrophobic cell surface and the aggregation of GAS chains on biotic and abiotic surfaces (Frick et al., 2000; Manetti et al., 2007; Courtney et al., 2009; Matysik et al., 2020). Host proteins recruited by cell surface-anchored virulence factors further contribute to aggregation and shield GAS from antimicrobials (LaRock et al., 2015; Döhrmann et al., 2017; Alamiri et al., 2020). This protection is also extended toward antibiotics (**Figure 2**), with biofilm formation associated with the reduced efficacy of antibiotics *in vitro* and *in vivo* (Baldassarri et al., 2006; Marks et al., 2014; Matysik et al., 2020), including a 2,500-fold increase in penicillin tolerance in one study (Vyas et al., 2020).

While the dual role of biofilms in pathogenesis and antibiotic failure is well recognized, and a target for future therapeutics, this connection is less explored with other virulence factors. GAS can invade macrophages (Hertzén et al., 2012; Wilde et al., 2021b), epithelial (Kaplan et al., 2006), and other host cells and resist autophagy and other mechanisms to promote their intracellular growth (Barnett et al., 2013). Intracellular GAS are shielded from penicillin (**Figure 2**), which cannot cross the cell envelope, and the ability to invade cells is correlated with eradication failure during the treatment of pharyngitis (Sela et al., 2000). Thus, virulence factors required for cell invasion may promote penicillin failure, but not failure of cell-penetrating antibiotics such as clindamycin or erythromycin, which are more effective against intracellular GAS (Kaplan et al., 2006). The penetration of antibiotic into tissue is also a hurdle that is worsened during severe infections (Eagle, 1952; Kiang et al., 2014; Stevens and Bryant, 2017; Thabit et al., 2019). Edema, thrombosis, and tissue necrosis are pervasive during necrotizing fasciitis and other invasive GAS infections and drastically limit antibiotic perfusion (**Figure 2**); for this reason, surgical removal of the infected tissue is often required, even for highly antibiotic-sensitive GAS (Stevens et al., 2014). This pathology is caused directly by streptolysin O and other GAS toxins (Bryant et al., 2005).

Together, these observations suggest that the virulence factors GAS uses to escape the immune system are tied to its ability to escape antibiotics. Neutralizing antibodies and small drug inhibitors of GAS virulence factors thus have the potential to not only reduce pathogenesis and restore the effectiveness of the immune response but also to work synergistically with conventional antibiotics to break the resistance/tolerance mechanisms of GAS.

ANTI-VIRULENCE TREATMENT

Since inhibiting toxin production has therapeutic benefits, neutralizing their activity may also be therapeutically useful. Intravenous immunoglobulin (IVIG) is an experimental adjunctive treatment for severe GAS infections that targets toxicity and promotes effective immune responses (Linnér et al., 2014). IVIG is generated from the pooled serum of healthy human donors and thus contains a panel of antibodies against diverse, but undefined, bacterial targets (Schwab and Nimmerjahn, 2013). These likely include major toxins and surface-anchored virulence factors (Wilde et al., 2021a). Through their neutralization (Parks et al., 2018) and increased opsonization of the bacterium, IVIG antibodies can decrease the bacterial burden and limit pro-inflammatory cytokine storms (**Figure 1**; Kaul et al., 1999). The repertoire of virulence factors produced by GAS is variable, as is the repertoire of specific antibodies between donors used for IVIG (Dhainaut et al., 2013), so the ability to neutralize toxins will vary between treatments and requires optimization (Norrby-Teglund et al., 1998; Schrage et al., 2006). Typical side effects include headaches or nausea (Katz et al., 2007), but there are risks of rare but severe complications (Pierce and Jain, 2003). Additional technical restrictions on using IVIG are the high cost of generation, storage requirements, and the risk of bloodborne pathogens found in any human blood.

In mice, IVIG has clear efficacy in models of STSS (Sriskandan et al., 2006) and necrotizing fasciitis (Tarnutzer et al., 2019). Because cases of severe GAS infections are rare, the opportunity to perform proper control trials is limited, and many findings may be underpowered. In some hospitals, IVIG is routinely used in tandem with clindamycin, although in one study this did not provide statistically significant improvement compared to clindamycin alone (Carapetis et al., 2014; de Prost et al., 2015). One trial was canceled due to limited enrollment, but the IVIG group had significant improvement compared to placebo (Darenberg et al., 2003), while another trial of 100 patients found no benefit over antibiotics alone (Madsen et al., 2017).

CLOSING COMMENTS

Until a vaccine is developed for GAS, antibiotics will remain essential for treating infection. The gold standard, penicillin, has been effective at treating GAS for over 80 years with no resistance, but low, consistent, rates of failure. Since other bacteria eventually gain resistance to the antibiotics commonly used for their treatment, it can be expected that GAS may eventually become resistant, which will lead to massive increases in morbidity and mortality. If the mutations in *pbpx2* of GAS continue to follow the same progression as that in *S. pneumoniae*, this may not be in the distant future (Grebe and Hakenbeck, 1996; Vannice et al., 2020). However, all mutations identified thus far are insufficient for non-susceptibility and carry a fitness cost, both of which will require additional compensatory mutations for GAS to overcome (Hanage and Shelburne, 2020). Therefore, dedicated surveillance is essential as the emergence of penicillin resistance by GAS would constitute a public health crisis.

Other methods of treatment beyond β-lactams are essential for handling severe GAS infections. While resistance is on the rise globally, clindamycin is one of the most effective treatments available alongside β-lactams to manage necrotizing fasciitis or STSS. With rapidly rising resistance, we lose this tool and will require new therapeutic strategies. As with penicillin, surveillance is crucial to determine current resistance trends. The properties that would be desired in these drugs, to complement the shortcomings of penicillin, include the targeting of vegetative

bacteria in biofilms and intracellular bacteria. IVIG is a promising method to improve survival during severe infections, but it may not be a replacement for clindamycin or another effective antibiotic. Understanding how resistance develops and the global profile of resistance will ensure that new drugs can be developed and deployed in the proper locations.

AUTHOR CONTRIBUTIONS

Both authors listed have made a substantial, direct and intellectual contribution to the work, and approved it for publication.

FUNDING

This work was supported by the NIH/NIAID (AI153071). The funders had no role in the study design, data collection and analysis, decision to publish, or preparation of the manuscript.

ACKNOWLEDGMENTS

We thank Dr. William Shafer and the members of the LaRock Lab for their helpful comments and discussions in the preparation of this work.

REFERENCES

Akiyama, H., Morizane, S., Yamasaki, O., Oono, T., and Iwatsuki, K. (2003). Assessment of *Streptococcus pyogenes* microcolony formation in infected skin by confocal laser scanning microscopy. *J. Dermatol. Sci.* 32, 193–199. doi: 10.1016/S0923-1811(03)00096-3

Alamiri, F., Chao, Y., Baumgarten, M., Riesbeck, K., and Hakansson, A. P. (2020). A role of epithelial cells and virulence factors in biofilm formation by *streptococcus pyogenes* in vitro. *Infect. Immun.* 88:e00133–20. doi: 10.1128/IAI.00133-20

Amábile-Cuevas, C. F., Hermida-Escobedo, C., and Vivar, R. (2001). Comparative in vitro activity of moxifloxacin by E-test against *Streptococcus pyogenes*. *Clin. Infect. Dis.* 32(Suppl_1), S30–S32. doi: 10.1086/319373

Andreoni, F., Zürcher, C., Tarnutzer, A., Schilcher, K., Neff, A., Keller, N., et al. (2017). Clindamycin affects group a *Streptococcus* virulence factors and improves clinical outcome. *J. Infect. Dis.* 215, 269–277. doi: 10.1093/infdis/jiw229

Baldassarri, L., Creti, R., Recchia, S., Imperi, M., Facinelli, B., Giovanetti, E., et al. (2006). Therapeutic failures of antibiotics used to treat macrolide-susceptible *Streptococcus pyogenes* infections may be due to biofilm formation. *J. Clin. Microbiol. Am. Soc. Microbiol. J.* 44, 2721–2727. doi: 10.1128/JCM.00512-06

Barnett, T. C., Liebl, D., Seymour, L. M., Gillen, C. M., Lim, J. Y., LaRock, C. N., et al. (2013). The globally disseminated M1T1 clone of group a *Streptococcus evades* autophagy for intracellular replication. *Cell Host Microbe* 14, 675–682. doi: 10.1016/j.chom.2013.11.003

Ben Zakour, N. L., Davies, M. R., You, Y., Chen, J. H. K., Forde, B. M., Stanton-Cook, M., et al. (2015). Transfer of scarlet fever-associated elements into the group a *Streptococcus* M1T1 clone. *Sci. Rep.* 5:15877. doi: 10.1038/srep15877

Berwal, A., Chawla, K., Shetty, S., and Gupta, A. (2019). Trend of antibiotic susceptibility of *Streptococcus pyogenes* isolated from respiratory tract infections in tertiary care hospital in south Karnataka. *Iran J. Microbiol.* 11, 13–18. doi: 10.18502/ijm.v11i1.698

Brindle, R., Williams, O. M., Davies, P., Harris, T., Jarman, H., Hay, A. D., et al. (2017). Adjunctive clindamycin for cellulitis: a clinical trial comparing flucloxacillin with or without clindamycin for the treatment of limb cellulitis. *BMJ Open* 7:e013260. doi: 10.1136/bmjopen-2016-013260

Brook, I. (1984). β-lactamase—producing bacteria recovered after clinical failures with various penicillin therapy. *Arch. Otolaryngol.* 110, 228–231. doi: 10.1001/archotol.1984.00800300020004

Brook, I. (2009). The role of beta-lactamase-producing-bacteria in mixed infections. *BMC Infect. Dis.* 9:202. doi: 10.1186/1471-2334-9-202

Brook, I., and Hirokawa, R. (1985). Treatment of patients with a history of recurrent tonsillitis due to group a beta-hemolytic *Streptococci*: a prospective randomized study comparing penicillin, erythromycin, and clindamycin. *Clin. Pediatr. (Phila)* 24, 331–336. doi: 10.1177/000992288502400606

Bruun, T., Rath, E., Madsen, M. B., Oppegaard, O., Nekludov, M., Arnell, P., et al. (2021). Risk factors and predictors of mortality in *Streptococcal* necrotizing soft-tissue infections: a multicenter prospective study. *Clin. Infect. Dis.* 72, 293–300. doi: 10.1093/cid/ciaa027

Bryant, A. E., Bayer, C. R., Chen, R. Y. Z., Guth, P. H., Wallace, R. J., and Stevens, D. L. (2005). Vascular dysfunction and ischemic destruction of tissue in *Streptococcus pyogenes* infection: the role of streptolysin O–induced platelet/neutrophil complexes. *J. Infect. Dis.* 192, 1014–1022. doi: 10.1086/432729

Capoor, M. R., Nair, D., Deb, M., Batra, K., and Aggarwal, P. (2006). Resistance to erythromycin and rising penicillin MIC in *Streptococcus pyogenes* in India. *JPN J. Infect. Dis.* 59, 334–336.

Carapetis, J. R., Jacoby, P., Carville, K., Ang, S.-J. J., Curtis, N., and Andrews, R. (2014). Effectiveness of clindamycin and intravenous immunoglobulin, and risk of disease in contacts, in invasive group a *Streptococcal* infections. *Clin. Infect. Dis. Oxford Acad.* 59, 358–365. doi: 10.1093/cid/ciu304

Carapetis, J. R., Steer, A. C., Mulholland, E. K., and Weber, M. (2005). The global burden of group a *Streptococcal* diseases. *Lancet Infect. Dis.* 5, 685–694. doi: 10.1016/S1473-3099(05)70267-X

Clancy, J., Petitpas, J., Dib-Hajj, F., Yuan, W., Cronan, M., Kamath, A. V., et al. (1996). Molecular cloning and functional analysis of a novel macrolide-resistance determinant, mefA, from *Streptococcus pyogenes*. *Mol. Microbiol.* 22, 867–879. doi: 10.1046/j.1365-2958.1996.01521.x

Courtney, H. S., Ofek, I., Penfound, T., Nizet, V., Pence, M. A., Kreikemeyer, B., et al. (2009). Relationship between expression of the family of M Proteins and lipoteichoic acid to hydrophobicity and biofilm formation in *Streptococcus pyogenes*. *PLoS One* 4:e4166. doi: 10.1371/journal.pone.0004166

Coyle, E. A. (2003). Targeting bacterial virulence: the role of protein synthesis inhibitors in severe infections. *Pharmacotherapy* 23, 638–642. doi: 10.1592/phco.23.5.638.32191

Cunningham, M. W. (2000). Pathogenesis of group A *Streptococcal* infections. *Clin. Microbiol. Rev.* 13, 470–511. doi: 10.1128/CMR.13.3.470

Dan, J. M., Havenar-Daughton, C., Kendric, K., Al-Kolla, R., Kaushik, K., Rosales, S. L., et al. (2019). Recurrent group A *Streptococcus tonsillitis* is an immunosusceptibility disease involving antibody deficiency and aberrant TFH cells. *Sci. Transl. Med.* 11, eaau3776. doi: 10.1126/scitranslmed.aau3776

Darenberg, J., Ihendyane, N., Sjölin, J., Aufwerber, E., Haidl, S., Follin, P., et al. (2003). StreptIg study group. intravenous immunoglobulin G therapy in streptococcal toxic shock syndrome: a European randomized, double-blind, placebo-controlled trial. *Clin. Infect. Dis.* 37, 333–340. doi: 10.1086/376630

Davies, M. R., Holden, M. T., Coupland, P., Chen, J. H. K., Venturini, C., Barnett, T. C., et al. (2015). Emergence of scarlet fever *Streptococcus pyogenes* emm12 clones in Hong Kong is associated with toxin acquisition and multidrug resistance. *Nat. Genet.* 47, 84–87. doi: 10.1038/ng.3147

de Prost, N., Sbidian, E., Chosidow, O., Brun-Buisson, C., and Amathieu, R. (2015). Henri mondor hospital necrotizing fasciitis group. Management of necrotizing soft tissue infections in the intensive care unit: results of an international survey. *Intensive Care Med.* 41, 1506–1508. doi: 10.1007/s00134-015-3916-9

DeMuri, G. P., Sterkel, A. K., Kubica, P. A., Duster, M. N., Reed, K. D., and Wald, E. R. (2017). Macrolide and clindamycin resistance in group a *Streptococci* isolated from children with pharyngitis. *Pediatr. Infect. Dis. J.* 36, 342–344. doi: 10.1097/INF.0000000000001442

Dhainaut, F., Guillaumat, P.-O., Dib, H., Perret, G., Sauger, A., de Coupade, C., et al. (2013). In vitro and in vivo properties differ among liquid intravenous immunoglobulin preparations. *Vox Sang.* 104, 115–126. doi: 10.1111/j.1423-0410.2012.01648.x

Döhrmann, S., LaRock, C. N., Anderson, E. L., Cole, J. N., Ryali, B., Stewart, C., et al. (2017). Group a *Streptococcal* M1 protein provides resistance against the antimicrobial activity of histones. *Sci. Rep.* 7:43039. doi: 10.1038/srep43039

Dowson, C. G., Hutchison, A., Brannigan, J. A., George, R. C., Hansman, D., Liñares, J., et al. (1989). Horizontal transfer of penicillin-binding protein genes in penicillin-resistant clinical isolates of *Streptococcus pneumoniae*. *Proc. Natl. Acad. Sci. U.S.A.* 86, 8842–8846. doi: 10.1073/pnas.86.22.8842

Eagle, H. (1952). Experimental approach to the problem of treatment failure with penicillin: I. Group a streptococcal infection in mice. *Am. J. Med.* 13, 389–399. doi: 10.1016/0002-9343(52)90293-3

Eagle, H., and Musselman, A. D. (1948). The rate of bactericidal action of penicillin in vitro as a function of its concentration, and its paradoxically reduced activity at high concentrations against certain organisms. *J. Exp. Med.* 88, 99–131. doi: 10.1084/jem.88.1.99

Fay, K., Onukwube, J., Chochua, S., Schaffner, W., Cieslak, P., Lynfield, R., et al. (2021). Patterns of antibiotic nonsusceptibility among invasive group a *Streptococcus* infections—United States, 2006–2017. *Clin. Infect. Dis.* 2021:ciab575. doi: 10.1093/cid/ciab575

Frick, I.-M., Mörgelin, M., and Björck, L. (2000). Virulent aggregates of *Streptococcus pyogenes* are generated by homophilic protein–protein interactions. *Mol. Microbiol.* 37, 1232–1247. doi: 10.1046/j.1365-2958.2000.02084.x

Gemmell, C. G., Peterson, P. K., Schmeling, D., Kim, Y., Mathews, J., Wannamaker, L., et al. (1981). Potentiation of opsonization and phagocytosis of *Streptococcus pyogenes* following growth in the presence of Clindamycin. *J. Clin. Invest.* 67, 1249–1256. doi: 10.1172/JCI110152

Gillespie, S. (1998). Failure of penicillin in *Streptococcus pyogenes* pharyngeal infection. *Lancet.* 352, 1954–1956. doi: 10.1016/S0140-6736(05)61327-X

Gjonbalaj, M., Keith, J. W., Do, M. H., Hohl, T. M., Pamer, E. G., and Becattini, S. (2020). Antibiotic degradation by commensal microbes shields pathogens. *Infect. Immun.* 88, e00012–e20. doi: 10.1128/IAI.00012-20

Grebe, T., and Hakenbeck, R. (1996). Penicillin-binding proteins 2b and 2x of *Streptococcus pneumoniae* are primary resistance determinants for different classes of beta-lactam antibiotics. *Antimicrob. Agents Chemother.* 40, 829–834. doi: 10.1128/AAC.40.4.829

Gutmann, L., and Tomasz, A. (1982). Penicillin-resistant and penicillin-tolerant mutants of group a *Streptococci*. *Antimicrob. Agents Chemother.* 22, 128–136. doi: 10.1128/AAC.22.1.128

Gutmann, L., Williamson, R., and Tomasz, A. (1981). Physiological properties of penicillin-binding proteins in group a *Streptococci*. *Antimicrob. Agents Chemother.* 19, 872–880. doi: 10.1128/AAC.19.5.872

Hanage, W. P., and Shelburne, S. A. III. (2020). *Streptococcus pyogenes* With reduced susceptibility to β-lactams: how big an alarm bell? *Clin. Infect. Dis.* 71, 205–206. doi: 10.1093/cid/ciz1006

Hayes, A., Lacey, J. A., Morris, J. M., Davies, M. R., and Tong, S. Y. C. (2020). Restricted sequence variation in *Streptococcus pyogenes* penicillin binding proteins. *mSphere* 5, e00090–e20. doi: 10.1128/mSphere.00090-20

Hertzén, E., Johansson, L., Kansal, R., Hecht, A., Dahesh, S., Janos, M., et al. (2012). Intracellular *Streptococcus pyogenes* in human macrophages display an altered gene expression profile. *PLoS One* 7:e35218. doi: 10.1371/journal.pone.0035218

Horn, D. L., Zabriskie, J. B., Austrian, R., Cleary, P. P., Ferretti, J. J., Fischetti, V. A., et al. (1998). Why have group a *Streptococci* remained susceptible to penicillin? Report on a symposium. *Clin. Infect. Dis.* 26, 1341–1345. doi: 10.1086/516375

Hurst, J. R., Kasper, K. J., Sule, A. N., and McCormick, J. K. (2018). *Streptococcal* pharyngitis and rheumatic heart disease: the superantigen hypothesis revisited. *Infec. Genet. Evol.* 61, 160–175. doi: 10.1016/j.meegid.2018.03.006

Johnson, S., Samore, M. H., Farrow, K. A., Killgore, G. E., Tenover, F. C., Lyras, D., et al. (1999). Epidemics of diarrhea caused by a clindamycin-resistant strain of clostridium difficile in four hospitals. *N. Engl. J. Med.* 341, 1645–1651. doi: 10.1056/NEJM199911253412203

Kaplan, E. L., Chhatwal, G. S., and Rohde, M. (2006). Reduced ability of penicillin to eradicate ingested group a *Streptococci* from epithelial cells: clinical and pathogenetic implications. *Clin. Infect. Dis.* 43, 1398–1406. doi: 10.1086/508773

Katz, U., Achiron, A., Sherer, Y., and Shoenfeld, Y. (2007). Safety of intravenous immunoglobulin (IVIG) therapy. *Autoimmun. Rev.* 6, 257–259. doi: 10.1016/j.autrev.2006.08.011

Kaul, R., McGeer, A., Norrby-Teglund, A., Kotb, M., Schwartz, B., O'Rourke, K., et al. (1999). Intravenous immunoglobulin therapy for streptococcal toxic shock syndrome–a comparative observational study. The Canadian *Streptococcal* Study Group. *Clin. Infect. Dis.* 28, 800–807. doi: 10.1086/515199

Kiang, T. K. L., Häfeli, U. O., and Ensom, M. H. H. A. (2014). Comprehensive review on the pharmacokinetics of antibiotics in interstitial fluid spaces in humans: implications on dosing and clinical pharmacokinetic monitoring. *Clin. Pharmacokinet.* 53, 695–730. doi: 10.1007/s40262-014-0152-3

Kishi, K., Hirai, K., Hiramatsu, K., Yamasaki, T., and Nasu, M. (1999). Clindamycin suppresses endotoxin released by ceftazidime-treated *Escherichia coli* O55:B5 and subsequent production of tumor necrosis factor alpha and interleukin-1β. *Antimicrob. Agents Chemother.* 43, 616–622. doi: 10.1128/AAC.43.3.616

Lamagni, T. L., Darenberg, J., Luca-Harari, B., Siljander, T., Efstratiou, A., Henriques-Normark, B., et al. (2008). Epidemiology of severe *Streptococcus pyogenes* disease in Europe. *J. Clin. Microbiol.* 46, 2359–2367. doi: 10.1128/JCM.00422-08

Lammintausta, K., Tokola, R., and Kalimo, K. (2002). Cutaneous adverse reactions to clindamycin: results of skin tests and oral exposure. *Br. J. Dermatol.* 146, 643–648. doi: 10.1046/j.1365-2133.2002.04665.x

LaRock, C. N., Döhrmann, S., Todd, J., Corriden, R., Olson, J., Johannssen, T., et al. (2015). Group a streptococcal M1 protein sequesters cathelicidin to evade innate immune killing. *Cell Host Microbe* 18, 471–477. doi: 10.1016/j.chom.2015.09.004

LaRock, D. L., Russell, R., Johnson, A. F., Wilde, S., and LaRock, C. N. (2020). Group A *Streptococcus* infection of the nasopharynx requires proinflammatory signaling through the interleukin-1 receptor. *Infect. Immun.* 88:e00356-20. doi: 10.1128/IAI.00356-20

Lewis, J. S. II., and Jorgensen, J. H. (2005). Inducible clindamycin resistance in staphylococci: should clinicians and microbiologists be concerned? *Clinical Infectious Diseases.* 40, 280–285. doi: 10.1086/426894

Lewis, J. S., Lepak, A. J., Thompson, G. R., Craig, W. A., Andes, D. R., Sabol-Dzintars, K. E., et al. (2014). Failure of clindamycin to eradicate infection with beta-hemolytic streptococci inducibly resistant to clindamycin in an animal model and in human infections. *Antimicrob. Agents Chemother.* 58, 1327–1331. doi: 10.1128/AAC.01877-13

Linnér, A., Darenberg, J., Sjölin, J., Henriques-Normark, B., and Norrby-Teglund, A. (2014). Clinical efficacy of polyspecific intravenous immunoglobulin therapy in patients with streptococcal toxic shock syndrome: a comparative observational study. *Clin. Infect. Dis.* 59, 851–857. doi: 10.1093/cid/ciu449

Lobanovska, M., and Pilla, G. (2017). Penicillin's discovery and antibiotic resistance: lessons for the future? *Yale J. Biol. Med.* 90, 135–145.

Low, D. E. (2013). Toxic shock syndrome: major advances in pathogenesis, but not treatment. *Crit. Care Clin.* 29, 651–675. doi: 10.1016/j.ccc.2013.03.012

Lynskey, N. N., Jauneikaite, E., Li, H. K., Zhi, X., Turner, C. E., Mosavie, M., et al. (2019). Emergence of dominant toxigenic M1T1 *Streptococcus pyogenes* clone during increased scarlet fever activity in England: a population-based molecular epidemiological study. *Lancet Infect. Dis.* 19, 1209–1218. doi: 10.1016/S1473-3099(19)30446-3

Macris, M. H., Hartman, N., Murray, B., Klein, R. F., Roberts, R. B., Kaplan, E. L., et al. (1998). Studies of the continuing susceptibility of group A streptococcal strains to penicillin during eight decades. *Pediatr. Infect. Dis. J.* 17, 377–381. doi: 10.1097/00006454-199805000-00006

Macy, E. (2014). Penicillin and beta-lactam allergy: epidemiology and diagnosis. *Curr. Allergy Asthma Rep.* 14:476. doi: 10.1007/s11882-014-0476-y

Macy, E., and Ngor, E. W. (2013). Safely diagnosing clinically significant penicillin allergy using only penicilloyl-poly-lysine, penicillin, and oral amoxicillin. *J. Allergy Clin. Immunol. Pract.* 1, 258–263. doi: 10.1016/j.jaip.2013.02.002

Madsen, M. B., Hjortrup, P. B., Hansen, M. B., Lange, T., Norrby-Teglund, A., Hyldegaard, O., et al. (2017). Immunoglobulin G for patients with necrotising soft tissue infection (INSTINCT): a randomised, blinded, placebo-controlled trial. *Intensive Care Med.* 43, 1585–1593. doi: 10.1007/s00134-017-4786-0

Manetti, A. G. O., Zingaretti, C., Falugi, F., Capo, S., Bombaci, M., Bagnoli, F., et al. (2007). *Streptococcus pyogenes* pili promote pharyngeal cell adhesion and biofilm formation. *Mol. Microbiol.* 64, 968–983. doi: 10.1111/j.1365-2958.2007.05704.x

Markowitz, M., Gerber, M. A., and Kaplan, E. L. (1993). Treatment of streptococcal pharyngotonsillitis: Reports of penicillin's demise are premature. *J. Pediatr.* 123, 679–685. doi: 10.1016/S0022-3476(05)80840-6

Marks, L. R., Mashburn-Warren, L., Federle, M. J., and Hakansson, A. P. (2014). *Streptococcus pyogenes* biofilm growth in vitro and in vivo and its role in

colonization, virulence, and genetic exchange. *J. Infect. Dis.* 210, 25–34. doi: 10.1093/infdis/jiu058

Mascini, E. M., Jansze, M., Schouls, L. M., Verhoef, J., and Van Dijk, H. (2001). Penicillin and clindamycin differentially inhibit the production of pyrogenic exotoxins A and B by group A streptococci. *Int. J. Antimicrob. Agents* 18, 395–398. doi: 10.1016/S0924-8579(01)00413-7

Matsuoka, M. (2000). Study of macrolide, lincosamide, and streptogramin B antibiotics resistance in *Staphylococcus aureus*. *Yakugaku Zasshi* 120, 374–386. doi: 10.1248/yakushi1947.120.4_374

Matysik, A., Ho, F. K., Ler Tan, A. Q., Vajjala, A., and Kline, K. A. (2020). Cellular chaining influences biofilm formation and structure in group A Streptococcus. *Biofilm* 2:100013. doi: 10.1016/j.bioflm.2019.100013

Musser, J. M., Beres, S. B., Zhu, L., Olsen, R. J., Vuopio, J., Hyyryläinen, H.-L., et al. (2020). Reduced in vitro susceptibility of *Streptococcus pyogenes* to β-lactam antibiotics associated with mutations in the pbp2x gene is geographically widespread. *J. Clin. Microbiol.* 58:e01993-19. doi: 10.1128/JCM.01993-19

Norrby-Teglund, A., Basma, H., Andersson, J., McGeer, A., Low, D. E., and Kotb, M. (1998). Varying titers of neutralizing antibodies to Streptococcal superantigens in different preparations of normal polyspecific immunoglobulin G: implications for therapeutic efficacy. *Clin. Infect. Dis.* 26, 631–638. doi: 10.1086/514588

Ogawa, T., Terao, Y., Sakata, H., Okuni, H., Ninomiya, K., Ikebe, K., et al. (2011). Epidemiological characterization of *Streptococcus pyogenes* isolated from patients with multiple onsets of pharyngitis. *FEMS Microbiol. Lett.* 318, 143–151. doi: 10.1111/j.1574-6968.2011.02252.x

Olsen, R. J., and Musser, J. M. (2010). Molecular pathogenesis of necrotizing fasciitis. *Annu. Rev. Pathol.* 5, 1–31. doi: 10.1146/annurev-pathol-121808-102135

Olsen, R. J., Zhu, L., and Musser, J. M. A. (2020). Single amino acid replacement in penicillin-binding protein 2X in *Streptococcus pyogenes* significantly increases fitness on subtherapeutic benzylpenicillin treatment in a mouse model of necrotizing myositis. *Am. J. Pathol.* 190, 1625–1631. doi: 10.1016/j.ajpath.2020.04.014

Oppegaard, O., and Rath, E. (2020). "Treatment of necrotizing soft tissue infections: antibiotics," in *Necrotizing Soft Tissue Infections: Clinical and Pathogenic Aspects*, eds A. Norrby-Teglund, M. Svensson, and S. Skrede (Cham: Springer International Publishing), 87–103. doi: 10.1007/978-3-030-57616-5_7

Orrling, A., Melhus, Å, Karlsson, E., and Stjernquist-Desatnik, A. (2001). Penicillin treatment failure in group A streptococcal tonsillopharyngitis: no genetic difference found between strains isolated from failures and nonfailures. *Ann. Otol. Rhinol. Laryngol.* 110, 690–695. doi: 10.1177/000348940111000716

Orrling, A., Stjernquist-Desatnik, A., Schalén, C., and Kamme, C. (1994). Clindamycin in persisting streptococcal pharyngotonsillitis after penicillin treatment. *Scand. J. Infect. Dis.* 26, 535–541. doi: 10.3109/00365549409011811

Park, D. W., Kim, S.-H., Park, J. W., Kim, M.-J., Cho, S. J., Park, H. J., et al. (2017). Incidence and characteristics of Scarlet Fever, South Korea, 2008-2015. *Emerg. Infect. Dis.* 23, 658–661. doi: 10.3201/eid2304.160773

Parks, T., Wilson, C., Curtis, N., Norrby-Teglund, A., and Sriskandan, S. (2018). Polyspecific intravenous immunoglobulin in clindamycin-treated patients with streptococcal toxic shock syndrome: a systematic review and meta-analysis. *Clin. Infect. Dis.* 67, 1434–1436. doi: 10.1093/cid/ciy401

Pierce, L. R., and Jain, N. (2003). Risks associated with the use of intravenous immunoglobulin. *Transfu. Med. Rev.* 17, 241–251. doi: 10.1016/S0887-7963(03)00038-5

Prasetyoputri, A., Jarrad, A. M., Cooper, M. A., and Blaskovich, M. A. T. (2019). The eagle effect and antibiotic-induced persistence: two sides of the same coin? *Trends Microbiol.* 27, 339–354. doi: 10.1016/j.tim.2018.10.007

Quinn, R. W. (1989). Comprehensive review of morbidity and mortality trends for rheumatic fever, streptococcal disease, and scarlet fever: the decline of rheumatic fever. *Rev. Infect. Dis.* 11, 928–953. doi: 10.1093/clinids/11.6.928

Richter, S. S., Heilmann, K. P., Beekmann, S. E., Miller, N. J., Miller, A. L., Rice, C. L., et al. (2005). Macrolide-resistant *Streptococcus pyogenes* in the United States, 2002–2003. *Clin. Infect. Dis.* 41, 599–608. doi: 10.1086/432473

Roberts, A. L., Connolly, K. L., Kirse, D. J., Evans, A. K., Poehling, K. A., Peters, T. R., et al. (2012). Detection of group A streptococcus in tonsils from pediatric patients reveals high rate of asymptomatic streptococcal carriage. *BMC Pediatr.* 12:3. doi: 10.1186/1471-2431-12-3

Rosendal, K. (1958). Investigations of penicillin-resistant streptococci belonging to group A. *Acta Pathol. Microbiol. Scand.* 42, 181–188. doi: 10.1111/j.1699-0463.1958.tb03183.x

Sartelli, M., Guirao, X., Hardcastle, T. C., Kluger, Y., Boermeester Marja, A., Raşa, K., et al. (2018). 2018 WSES/SIS-E consensus conference: recommendations for the management of skin and soft-tissue infections. *World J. Emerg. Surg.* 13:58. doi: 10.1186/s13017-018-0219-9

Schlievert, P. M., and Kelly, J. A. (1984). Clindamycin-induced suppression of toxic-shock syndrome-associated exotoxin production. *J. Infect. Dis.* 149, 471–471. doi: 10.1093/infdis/149.3.471

Schrage, B., Duan, G., Yang, L. P., Fraser, J. D., and Proft, T. (2006). Different preparations of intravenous immunoglobulin vary in their efficacy to neutralize streptococcal superantigens: implications for treatment of streptococcal toxic shock syndrome. *Clin. Infect. Dis.* 43, 743–746. doi: 10.1086/507037

Schwab, I., and Nimmerjahn, F. (2013). Intravenous immunoglobulin therapy: how does IgG modulate the immune system? *Nat. Rev. Immunol.* 13, 176–189. doi: 10.1038/nri3401

Sela, S., Neeman, R., Keller, N., and Barzilai, A. (2000). Relationship between asymptomatic carriage of *Streptococcus pyogenes* and the ability of the strains to adhere to and be internalised by cultured epithelial cells. *J. Med. Microbiol* 49, 499–502. doi: 10.1099/0022-1317-49-6-499

Seppälä, H., Skurnik, M., Soini, H., Roberts, M. C., and Huovinen, P. A. (1998). Novel erythromycin resistance methylase gene (ermTR) in *Streptococcus pyogenes*. *Antimicrob. Agents Chemother.* 42, 257–262. doi: 10.1128/AAC.42.2.257

Shaikh, N., Leonard, E., and Martin, J. M. (2010). Prevalence of streptococcal pharyngitis and streptococcal carriage in children: a meta-analysis. *Pediatrics* 126:e557-64. doi: 10.1542/peds.2009-2648

Shannon, B. A., McCormick, J. K., and Schlievert, P. M. (2019). Toxins and superantigens of group A streptococci. *Microbiol. Spectrum* 7, 3–6. doi: 10.1128/9781683670131.ch5

Siemens, N., Chakrakodi, B., Shambat, S. M., Morgan, M., Bergsten, H., Hyldegaard, O., et al. (2016). Biofilm in group A streptococcal necrotizing soft tissue infections. *JCI Insight* 1:e87882. doi: 10.1172/jci.insight.87882

Sorg, R. A., Lin, L., van Doorn, G. S., Sorg, M., Olson, J., Nizet, V., et al. (2016). Collective resistance in microbial communities by intracellular antibiotic deactivation. *PLoS Biol.* 14:e2000631. doi: 10.1371/journal.pbio.2000631

Sousa-Pinto, B., Fonseca, J. A., and Gomes, E. R. (2017). Frequency of self-reported drug allergy: a systematic review and meta-analysis with meta-regression. *Ann. Allergy Asthma Immunol.* 119, 362–373.e2. doi: 10.1016/j.anai.2017.07.009

Spízek, J., and Rezanka, T. (2004). Lincomycin, clindamycin and their applications. *Appl. Microbiol. Biotechnol.* 64, 455–464. doi: 10.1007/s00253-003-1545-7

Sriskandan, S., Ferguson, M., Elliot, V., Faulkner, L., and Cohen, J. (2006). Human intravenous immunoglobulin for experimental streptococcal toxic shock: bacterial clearance and modulation of inflammation. *J. Antimicrob. Chemother.* 58, 117–124. doi: 10.1093/jac/dkl173

Sriskandan, S., McKee, A., Hall, L., and Cohen, J. (1997). Comparative effects of clindamycin and ampicillin on superantigenic activity of *Streptococcus pyogenes*. *J. Antimicrob. Chemother.* 40, 275–277. doi: 10.1093/jac/40.2.275

Stevens, D. L., Bisno, A. L., Chambers, H. F., Dellinger, E. P., Goldstein, E. J. C., Gorbach, S. L., et al. (2014). Practice Guidelines for the diagnosis and management of skin and soft tissue infections: 2014 update by the infectious diseases society of America. *Clin. Infect. Dis.* 59, e10–e52. doi: 10.1093/cid/ciu296

Stevens, D. L., and Bryant, A. E. (2017). Necrotizing soft-tissue infections. *N. Engl. J. Med.* 377, 2253–2265. doi: 10.1056/NEJMra1600673

Stevens, D. L., Bryant, A. E., and Hackett, S. P. (1995). Antibiotic effects on bacterial viability, toxin production, and host response. *Clin. Infect. Dis.* 20(Suppl. 2), S154–S157. doi: 10.1093/clinids/20.Supplement_2.S154

Stevens, D. L., Gibbons, A. E., Bergstrom, R., and Winn, V. (1988). The Eagle effect revisited: efficacy of clindamycin, erythromycin, and penicillin in the treatment of streptococcal myositis. *J. Infect. Dis.* 158, 23–28. doi: 10.1093/infdis/158.1.23

Stevens, D. L., Madaras-Kelly, K. J., and Richards, D. M. (1998). In vitro antimicrobial effects of various combinations of penicillin and clindamycin against four strains of *Streptococcus pyogenes*. *Antimicrob. Agents Chemother.* 42, 1266–1268. doi: 10.1128/AAC.42.5.1266

Stevens, D. L., Maier, K. A., Laine, B. M., and Mitten, J. E. (1987). Comparison of clindamycin, rifampin, tetracycline, metronidazole, and penicillin for efficacy

in prevention of experimental gas gangrene due to *Clostridium perfringens*. *J. Infect. Dis.* 155, 220–228. doi: 10.1093/infdis/155.2.220

Stevens, D. L., Tanner, M. H., Winship, J., Swarts, R., Ries, K. M., Schlievert, P. M., et al. (1989). Severe group A streptococcal infections associated with a toxic shock-like syndrome and scarlet fever toxin A. *N. Engl. J. Med.* 321, 1–7. doi: 10.1056/NEJM198907063210101

Sunderkötter, C., Becker, K., Eckmann, C., Graninger, W., Kujath, P., and Schöfer, H. (2019). S2k guidelines for skin and soft tissue infections Excerpts from the S2k guidelines for "calculated initial parenteral treatment of bacterial infections in adults – update 2018". *J. Dtch Dermatol. Ges.* 17, 345–369. doi: 10.1111/ddg.13790

Sutcliffe, J., Tait-Kamradt, A., and Wondrack, L. (1996). *Streptococcus pneumoniae* and *Streptococcus pyogenes* resistant to macrolides but sensitive to clindamycin: a common resistance pattern mediated by an efflux system. *Antimicrob. Agents Chemother.* 40, 1817–1824. doi: 10.1128/AAC.40.8.1817

Tarnutzer, A., Andreoni, F., Keller, N., Zürcher, C., Norrby-Teglund, A., Schüpbach, R. A., et al. (2019). Human polyspecific immunoglobulin attenuates group A streptococcal virulence factor activity and reduces disease severity in a murine necrotizing fasciitis model. *Clin. Microbiol. Infect.* 25, 512.e7-512.e13. doi: 10.1016/j.cmi.2018.07.007

Thabit, A. K., Fatani, D. F., Bamakhrama, M. S., Barnawi, O. A., Basudan, L. O., and Alhejaili, S. F. (2019). Antibiotic penetration into bone and joints: an updated review. *Int. J. Infect. Dis.* 81, 128–136. doi: 10.1016/j.ijid.2019.02.005

Vannice, K. S., Ricaldi, J., Nanduri, S., Fang, F. C., Lynch, J. B., Bryson-Cahn, C., et al. (2020). *Streptococcus pyogenes* pbp2x mutation confers reduced susceptibility to β-Lactam antibiotics. *Clin. Infect. Dis.* 71, 201–204. doi: 10.1093/cid/ciz1000

Vyas, H. K. N., Indraratna, A. D., Everest-Dass, A., Packer, N. H., De Oliveira, D. M. P., Ranson, M., et al. (2020). Assessing the role of pharyngeal cell surface glycans in group A streptococcus biofilm formation. *Antibiotics* 9:775. doi: 10.3390/antibiotics9110775

Walker, M. J., Barnett, T. C., McArthur, J. D., Cole, J. N., Gillen, C. M., Henningham, A., et al. (2014). Disease manifestations and pathogenic mechanisms of group A streptococcus. *Clin. Microbiol. Rev.* 27, 264–301. doi: 10.1128/CMR.00101-13

Weiser, J. N., Ferreira, D. M., and Paton, J. C. (2018). *Streptococcus pneumoniae*: transmission, colonization and invasion. *Nat. Rev. Microbiol.* 16, 355–367. doi: 10.1038/s41579-018-0001-8

Wilde, S., Johnson, A. F., and LaRock, C. N. (2021a). Playing with fire: proinflammatory virulence mechanisms of group A streptococcus. *Front. Cell Infect. Microbiol.* 11:704099. doi: 10.3389/fcimb.2021.704099

Wilde, S., Olivares, K. L., Nizet, V., Hoffman, H. M., Radhakrishna, S., and LaRock, C. N. (2021b). Opportunistic invasive infection by group A streptococcus during anti-interleukin-6 immunotherapy. *J. Infect. Dis.* 223, 1260–1264. doi: 10.1093/infdis/jiaa511

Wilke, M. S., Lovering, A. L., and Strynadka, N. C. (2005). β-Lactam antibiotic resistance: a current structural perspective. *Curr. Opin. Microbiol.* 8, 525–533. doi: 10.1016/j.mib.2005.08.016

Wilkins, A. L., Steer, A. C., Smeesters, P. R., and Curtis, N. (2017). Toxic shock syndrome–the seven Rs of management and treatment. *J. Infect.* 74(Suppl. 1), S147–S152. doi: 10.1016/S0163-4453(17)30206-2

Wolf, A. J., Liu, G. Y., and Underhill, D. M. (2017). Inflammatory properties of antibiotic-treated bacteria. *J. Leukoc. Biol.* 101, 127–134. doi: 10.1189/jlb.4MR0316-153RR

Zarandi, E. R., Mansouri, S., Nakhaee, N., Sarafzadeh, F., and Moradi, M. (2017). Toxin production of Clostridium difficile in sub-MIC of vancomycin and clindamycin alone and in combination with ceftazidime. *Microb. Pathog.* 107, 249–253. doi: 10.1016/j.micpath.2017.03.002

Conflict of Interest: The authors declare that the research was conducted in the absence of any commercial or financial relationships that could be construed as a potential conflict of interest.

Publisher's Note: All claims expressed in this article are solely those of the authors and do not necessarily represent those of their affiliated organizations, or those of the publisher, the editors and the reviewers. Any product that may be evaluated in this article, or claim that may be made by its manufacturer, is not guaranteed or endorsed by the publisher.

frontiers in Microbiology

ORIGINAL RESEARCH
published: 23 December 2021
doi: 10.3389/fmicb.2021.802532

Phylogenomic Reappraisal of Fatty Acid Biosynthesis, Mycolic Acid Biosynthesis and Clinical Relevance Among Members of the Genus *Corynebacterium*

Lynn G. Dover, Amy R. Thompson, Iain C. Sutcliffe and Vartul Sangal*

Faculty of Health and Life Sciences, Northumbria University, Newcastle upon Tyne, United Kingdom

The genus *Corynebacterium* encompasses many species of biotechnological, medical or veterinary significance. An important characteristic of this genus is the presence of mycolic acids in their cell envelopes, which form the basis of a protective outer membrane (mycomembrane). Mycolic acids in the cell envelope of *Mycobacterium tuberculosis* have been associated with virulence. In this study, we have analysed the genomes of 140 corynebacterial strains, including representatives of 126 different species. More than 50% of these strains were isolated from clinical material from humans or animals, highlighting the true scale of pathogenic potential within the genus. Phylogenomically, these species are very diverse and have been organised into 19 groups and 30 singleton strains. We find that a substantial number of corynebacteria lack FAS-I, i.e., have no capability for *de novo* fatty acid biosynthesis and must obtain fatty acids from their habitat; this appears to explain the well-known lipophilic phenotype of some species. In most species, key genes associated with the condensation and maturation of mycolic acids are present, consistent with the reports of mycolic acids in their species descriptions. Conversely, species reported to lack mycolic acids lacked these key genes. Interestingly, *Corynebacterium ciconiae*, which is reported to lack mycolic acids, appears to possess all genes required for mycolic acid biosynthesis. We suggest that although a mycolic acid-based mycomembrane is widely considered to be the target for interventions by the immune system and chemotherapeutics, the structure is not essential in corynebacteria and is not a prerequisite for pathogenicity or colonisation of animal hosts.

Keywords: *Corynebacterium*, fatty acid chains, mycolic acid biosynthesis, phylogenomic diversity, virulence

OPEN ACCESS

Edited by:
Ana Luíza Mattos Guaraldi, Rio de Janeiro State University, Brazil

Reviewed by:
Andreas Burkovski, University of Erlangen Nuremberg, Germany
Elisabete Cappelli, University of Porto, Portugal

***Correspondence:**
Vartul Sangal
vartul.sangal@northumbria.ac.uk

Specialty section:
This article was submitted to Antimicrobials, Resistance and Chemotherapy, a section of the journal Frontiers in Microbiology

Received: *26 October 2021*
Accepted: *30 November 2021*
Published: *23 December 2021*

Citation:
Dover LG, Thompson AR, Sutcliffe IC and Sangal V (2021) Phylogenomic Reappraisal of Fatty Acid Biosynthesis, Mycolic Acid Biosynthesis and Clinical Relevance Among Members of the Genus Corynebacterium. Front. Microbiol. 12:802532. doi: 10.3389/fmicb.2021.802532

INTRODUCTION

Corynebacterium is a diverse genus that encompass multiple species of industrial, medical or veterinary importance (Bernard and Funke, 2015; Oliveira et al., 2017; Sangal and Burkovski, 2020). A number of corynebacterial species are commensals (Brugger et al., 2016; Treerat et al., 2020) but some are notable pathogens including the human pathogen *Corynebacterium*

diphtheriae and *Corynebacterium pseudotuberculosis*, which is not only primarily pathogenic to sheep but can also infect other animals (Tauch and Burkovski, 2015). *Corynebacterium ulcerans* is a zoonotic pathogen, often acquired by humans from canine pets (Sangal et al., 2014). More recently, several new *Corynebacterium* species that are pathogenic to humans or animals have been identified (Oliveira et al., 2017; Möller et al., 2020; Boxberger et al., 2021; Saunderson et al., 2021). *Corynebacterium glutamicum* is an industrially important member of the genus that is used in large-scale production of several amino acids and aromatic compounds (Ikeda and Takeno, 2013; Kallscheuer and Marienhagen, 2018).

Corynebacteria are Gram-positive bacteria with a complex cell envelope architecture, where corynomycolates (short-chain α-branched, β-hydroxy fatty acids) are esterified to an arabinogalactan polysaccharide that is, in turn, covalently bound to the peptidoglycan cell wall core, forming a mycolyl-arabinogalactan–peptidoglycan complex (Dover et al., 2004; Marrakchi et al., 2014; Burkovski, 2018). These cell-bound mycolic acids form the basis of the inner leaflet of a distinctive outer 'mycomembrane', that is completed by intercalation with mycolic acid-containing glycolipids based on trehalose, and other free lipids (Puech et al., 2001; Marchand et al., 2012; Laneelle et al., 2013; Vincent et al., 2018). Thus, the presence of mycolic acids in the cell envelope is associated with stress resistance and pathogenicity both in *Corynebacterium* and *Mycobacterium* strains (Moreira et al., 2008; Vander Beken et al., 2011; Nataraj et al., 2015; Tauch and Burkovski, 2015).

Most knowledge of the roles of mycolic acids in virulence is based on the studies of the human pathogen, *Mycobacterium tuberculosis*. Mycolic acids are involved in the formation of biofilms, affect susceptibility to antibiotics and, in the mycobacteria, play important roles in manipulating the host immune system during the infection (Korf et al., 2005; Dao et al., 2008; Vander Beken et al., 2011; Marrakchi et al., 2014; Nataraj et al., 2015; Batt et al., 2020). T cells specific to mycolic acid offer protection from *M. tuberculosis* infection (Zhao et al., 2015) and an absence of mycolic acid in the cell attenuates the pathogen and modulates cytokine production (Dao et al., 2008; Barkan et al., 2012). However, it should be noted that the size and structural complexity of the mycobacterial mycolic acids is significant here; although the short-chain mycolic acids possessed by corynebacteria can be bound by the CD1 antigen presentation system, they may not activate T-cells (Moody, 2017).

Although all mycolic acids are α-alkyl-β-hydroxy fatty acids, those in *Corynebacterium* species (corynomycolates) differ structurally from those of *Mycobacterium* (Dover et al., 2004; Marrakchi et al., 2014). These corynomycolates have 22–36 carbon atoms in total with short α-branch chains (C_8–C_{18}) whereas the total carbon atoms in mycobacteria varies between 60 and 90 with longer chain (C_{22}–C_{24}) α-alkyl branches and more complex chain modifications (Marrakchi et al., 2014) of the extended meromyoclate chain (**Figure 1**).

Fatty acids are the direct precursors of mycolic acids and the differences in the length of the meromycolate chains are attributed to the variation in the fatty acid biosynthesis pathways between the two genera. Mycobacterial meromycolate synthesis involves two fatty acid synthases, a eukaryotic-like multifunctional FAS-I that produces a bimodal population of fatty acids of chain lengths C_{16}–C_{18} or C_{24}–C_{26} (Marrakchi et al., 2014), and a second bacterial-like FAS-II, that elongates these fatty acids to form meromycolate chains (Dover et al., 2004, 2007; Marrakchi et al., 2014). Only FAS-I has been reported in corynebacteria (Dover et al., 2004, 2007; Marrakchi et al., 2014). However, two functional copies of FAS-I, *fasA* and *fasB*, have been reported in *Corynebacterium glutamicum* and *Corynebacterium efficiens* (Stuible et al., 1997; Radmacher et al., 2005).

Given the importance of mycolic acid in the biology of the corynebacteria and the cell envelope in host-bacterium interactions, we have investigated the conservation of genes involved in mycolic acid biosynthesis across the genus *Corynebacterium*. We also attempted to establish an association between the mycolic acid biosynthetic capacities and clinical relevance of the corynebacterial strains.

MATERIALS AND METHODS

Corynebacterium Genomes

The genome sequences of 140 representative *Corynebacterium* strains, including 110 validly named species (104 type strains), 15 species with effectively published names and a novel *Corynebacterium* sp. that is pathogenic to yellow-eyed penguins (Saunderson et al., 2021) were obtained from GenBank (**Supplementary Table 1**). The data included two *Corynebacterium diphtheriae* strains, the type strain DSM 44123^T and the extensively studied NCTC 13129 strain. We also included both available assemblies of the type strains of *Corynebacterium imitans*, *Corynebacterium jeikeium*, *Corynebacterium pilosum* and *Corynebacterium renale*, and three assemblies of the type strain of *Corynebacterium minutissimum*. One representative each from the two lineages of *Corynebacterium ulcerans* (Subedi et al., 2018) was included. Type strains of *Corynebacterium hadale* and *Corynebacterium godavarianum*, both heterotypic synonyms of *Corynebacterium gottingense*, were included (Bernard et al., 2020) along with a '*Corynebacterium crenatum*' strain that is considered to be a subspecies of *Corynebacterium glutamicum* (Man et al., 2016). The genome sequences of the type strains of *Corynebacterium accolens* and *Corynebacterium segmentosum*, which were recently found to belong to the same species, were also included (Sagerfors et al., 2021). We also included the type strain of *Corynebacterium xerosis* ATCC 373 isolated from the ear discharge of a child (Bernard and Funke, 2015) and strain GS1 isolated from a caseous nodule from liver of a yak (Wen et al., 2019). Information on the presence of mycolic acids and on host and clinical relevance (importance, source of isolation) was obtained from Bernard and Funke (2015) or the original citations accessed from the LSPN database (**Supplementary Table 1**).[1]

[1]https://lpsn.dsmz.de/genus/corynebacterium

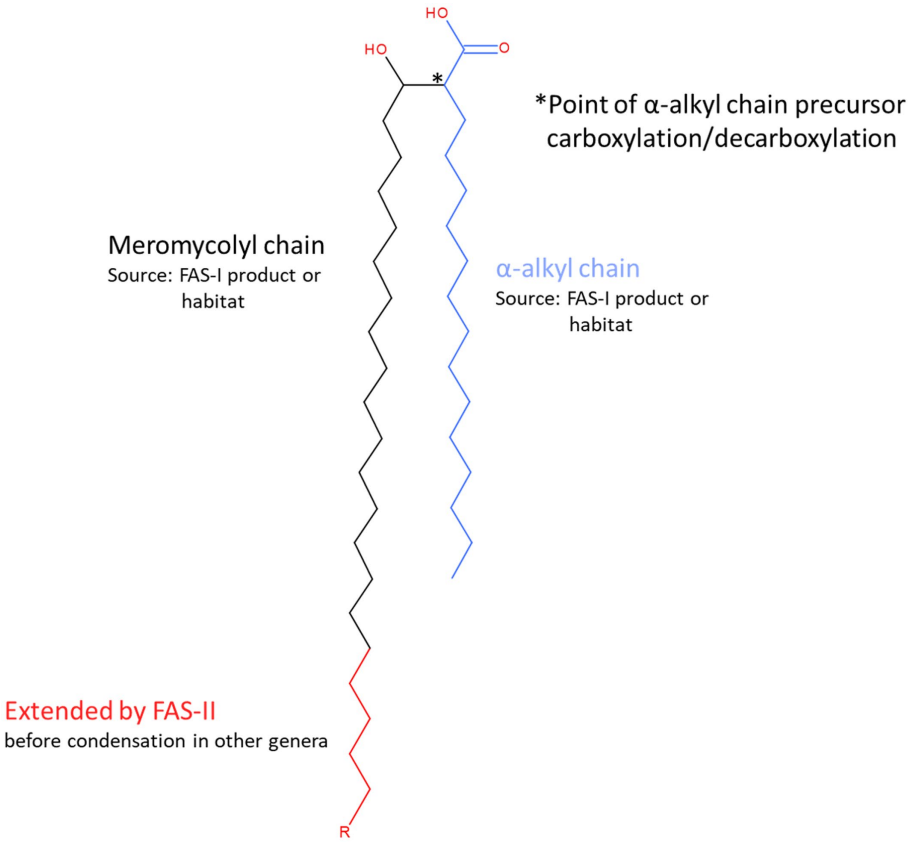

FIGURE 1 | Structural features and sources of mycolic acid components. Mycolic acids are α-alkyl, β-hydroxy branched fatty acids that form the basis of the outer wall permeability barrier or 'mycomembrane' that is the defining characteristic feature of the cell wall model originally proposed by Minnikin (1982) for the mycobacteria and other genera that belong to the order *Mycobacteriales*. Briefly, mycolic acids are generated from the condensation of two fatty acyl chains, known as α-and meromycolyl chains. The α-chain (blue) precursor is activated by carboxylation (position indicated by * and see **Figure 5**). It then participates in a decarboxylative condensation reaction with the carboxylate group of the meromycolyl chain, the residue of which forms a β-keto group that is subsequently reduced to form the characteristic β-hydroxy group of the mature mycolic acid. There are two potential sources of the fatty acid components of mycolic acids. The bacterium may synthesise them *de novo* using fatty acid synthase I or acquire them from its habitat. Corynebacteria produce relatively short corynomycolic acids; fatty acids of approx. 16 C chain lengths are used to form both branches. However, in most other genera in *Mycobacteriales*, the meromycolyl chain is extended by fatty acid synthase II (red chain; the length of R is highly variable but distinctive for each genus and may also contain various structural modifications including double bonds, cyclopropane rings, hydroxy, methoxy, epoxy, wax ester and ketone groups).

Genomic Analyses

The quality of genome assemblies was assessed using CheckM (Parks et al., 2015). All genome sequences that showed more than 90% completeness and less than 5% contamination were considered to be suitable for analysis. These assemblies were automatically annotated using Prokka v 1.13 (Seemann, 2014) and were compared using Roary v 3.12 (Tange, 2011; Page et al., 2015). A protein sequence alignment of 131 core proteins present across all 140 genomes was used to generate a maximum-likelihood tree using IQ-tree v 1.6 using 100,000 ultrafast bootstraps and 100,000 SH-aLRT tests (Nguyen et al., 2015) after removing sites with gaps. Phylogenomic clades with two or more genomes and an average distance from nodes to their leaves <0.15 were assigned a group designation and the remaining strains were treated as singletons.

Protein BLAST searches (Camacho et al., 2009) of 22 gene products from the FAS-I and FAS-II pathways from *M. tuberculosis* strain H37Rv (**Table 1**) were carried out with an e-value cut-off of 1×10^{-5} to determine the presence of these genes among *Corynebacterium* strains. Much of the extant knowledge relating to mycolic acid biosynthesis has been drawn from a large body of experimental evidence from various bacterial models including, among others, *M. tuberculosis*, *Mycolicibacterium smegmatis* and *Corynebacterium glutamicum*. As the corynebacteria are known to produce short chain-length 'corynomycolates', they would be expected to lack genes encoding fatty acid synthase-II (FAS-II), which extends the meromycolate components of mycolic acids in other genera. In order to detect any atypical strains of *Corynebacterium* that might possess FAS-II, we chose query sequences from the well-studied *M. tuberculosis* H37Rv strain; there is strong precedent for significant homology and often

TABLE 1 | List of mycobacterial genes involved in mycolic acid biosynthesis.

System	Gene	Locus	Gene (bp)	Uniprot Accession	Description
	acpS	Rv2523c	393	p0a4w8	Holo-[acyl-carrier protein] synthase; 4′-phosphopantetheinyl transferase
FAS-I	*fas-I*	Rv2524c	9,210	p95029	Fatty acid synthase
	pptT	Rv2794c	684	O33336	4′-phosphopantetheinyl transferase
	fabH	Rv0533c	1,008	p9wng3	β-Ketoacyl-[acyl-carrier-protein] synthase
FAS-II	*fabD*	Rv2243	909	p63458	Malonyl Coa-acyl carrier protein transacylase
FAS-II	*acpM*	Rv2244	348	p9wqf3	Meromycolate extension acyl carrier protein
FAS-II	*kasA*	Rv2245	1,251	p9wqd9	β-Ketoacyl-[acyl-carrier protein] synthase 1
FAS-II	*kasB*	Rv2246	1,317	p9wqd7	β-Ketacyl-[acyl-carrier protein] synthase 2
FAS-II	*accD6*	Rv2247	1,422	p9wqh5	Acetyl/propionyl-Coa carboxylase (beta subunit)
FAS-II	*fabG1*	Rv1483	744	p9wgt3	β-Ketoacyl-[acyl-carrier protein] reductase
FAS-II	*inhA*	Rv1484	810	p9wgr1	NADH-dependent enoyl-[acyl-carrier-protein] reductase
FAS-II	*hadA*	Rv0635	477	p9wfk1	β-Hydroxyacyl-acp dehydratase subunit
FAS-II	*hadB*	Rv0636	429	p96927	β-Hydroxyacyl-acp dehydratase subunit
FAS-II	*hadC*	Rv0637	501	p9wfj9	β-Hydroxyacyl-acp dehydratase subunit
MA condensation	*accD4*	Rv3799c	1,569	o53578	Biotin-dependent long chain acyl-amp carboxylase beta4 subunit
MA condensation	*pks13*	Rv3800c	5,202	o53579	Polyketide synthase
MA condensation	*fadD32*	Rv3801c	1914	o53580	Long-chain-fatty-acid-amp ligase
MA condensation	*accD5*	Rv3280	1,647	p9wqh7	Biotin-dependent acetyl–/propionyl-coenzyme a carboxylase beta5 subunit
MA condensation		Rv3281	534	p96886	Conserved hypothetical protein
MA condensation	*accA3*	Rv3285	1803	p96890	Bifunctional protein acetyl–/propionyl-coenzyme a carboxylase (α-chain)
MA condensation	*accE**		249		Biotin-dependent acetyl–/propionyl-coenzyme A carboxylase ε subunit
MA reduction	*cmrA*	Rv2059	807	i6y9i3	Dehydrogenase (putative oxidoreductase)

MA, mycolic acid.
**accE gene was used from Corynebacterium glutamicum.*

synteny when comparing the genetics of multiple aspects of cell wall biosynthesis in corynebacterial genomes with this model.

Duplicate hits with multiple queries were removed and the single best hit with the highest score was retained. We also excluded the hits with sequence identity below 30%. These exclusions were reconsidered where significant absences were noted. The presence of a gene and additional copies (homologues) were manually curated based on the query coverage and sequence identity (**Supplementary Table 2**). The secondary hits for the protein Rv3285 (encoded by *accA3*) where query or target coverage was <75%, and proteins were 100 amino acids (aa) smaller or larger in size were excluded (**Supplementary Table 2**). Some hits for the Rv1483 protein (encoded by *fabG1*) were significant but were excluded by reciprocal BLAST searches. In some cases, the presence of conserved gene clusters was considered in prioritising equivocal identifications.

RESULTS

Corynebacterium Strains and Clinical Importance

The *Corynebacterium* strains studied herein were isolated from diverse sources: 71 from humans, 32 from other mammals and reptiles (antelopes, bharal, cattle, dogs, rodents, seal, tapir, tortoise, etc.), 12 from birds (storks, eagle, geese, ibis and penguins), 20 from environmental sources (including coral, cosmetic dye, fermentation starter, fuel cell, heather, lubricant, river water, marine sediment, sand, soil and sewage) and five from food (banana and dairy products; **Supplementary Table 1**).

Corynebacterial strains of 54 species that were isolated from humans are clinically important, i.e., are associated with various infections/conditions, two are listed as commensals and two are considered opportunistic human pathogens. *Corynebacterium*

ulcerans and *Corynebacterium kutscheri* strains are often isolated from animals and can cause zoonotic infections among humans. Thirteen corynebacterial species are reported to be pathogenic to animals, particularly *Corynebacterium pseudotuberculosis*, *Corynebacterium renale*, *Corynebacterium cystitidis*, *Corynebacterium endometrii*, *Corynebacterium ulceribovis*, *Corynebacterium capitovis*, *Corynebacterium camporealensis* and *Corynebacterium mastitidis* that are pathogenic to cattle and other farm animals (**Supplementary Table 1**). However, some of these species, such as *Corynebacterium pseudotuberculosis* and *Corynebacterium mastitidis*, can also infect humans (Peel et al., 1997). Therefore, a large proportion of corynebacterial species are either directly associated with infections in humans and animals or are opportunistic pathogens (**Supplementary Table 1**).

Phylogenomic Diversity

The average size of the corynebacterial genomes is 2.6 Mb, with the smallest genome reported for *Corynebacterium caspium* (1.8 Mb) and largest for *Corynebacterium glyciniphilum* (3.6 Mb). These genomes are annotated with 1,630–3,316 coding sequences (**Supplementary Table 1**). Similarly, the GC content is highly variable between the *Corynebacterium* species, varying between 46.5 mol% for *Corynebacterium kutscheri* to 74.7 mol% for *Corynebacterium sphenisci*; overall the mean GC content was 61.3 mol%. The number of rRNA genes varies between 2 and 21 among these genomes with an inverse correlation with the number of contigs: nine or more rRNA genes were identified in 81/84 (96%) genome assemblies with up to five contigs, whereas 51/56 (91%) of assemblies with six or more contigs have 2–7 rRNA genes (**Supplementary Table 1**). Draft genomes with multiple contigs have lower numbers of rRNA genes annotated, potentially caused by assembly errors due to the repetitive nature of rRNA genes. Likewise, the number of tRNA and tmRNA sequences varied between 45 and 64 and 1 and 2, respectively (**Supplementary Table 1**).

A comparative analysis revealed a large and open pangenome of 114,775 genes within the dataset with 112,680 (98%) genes identified as the 'cloud' genes, i.e., those present in ≤15% of the genomes in the dataset, 1846 shell genes (present in 15–95% of the genomes), 74 soft core genes (present in 95–99% of the genomes) and 175 were identified as core that were present among 99–100% of the genomes. Of the 175 core genes, 131 genes were present among all 140 strains and protein sequences of these genes were concatenated for phylogenetic analyses. *Corynebacterium* isolates were defined into 19 clades (groups A–S) and 30 species-level singletons that did not group with any other strains (**Figure 2**). Both the independent genome assemblies of the type strain of *Corynebacterium renale*, associated with infection in cattle grouped together and were treated as a singleton (**Figure 2**; **Supplementary Table 1**).

Nine major phylogenetic groups (A, B, C, F, I, K, L, Q and S) encompassed five or more species (**Figure 2**). Although group M contained five strains, two of them were assemblies of *Corynebacterium xerosis* strains, and hence, it was considered as a minor group (**Supplementary Table 1**). More than 50% of the strains in groups A, B, C, F and K were isolated from humans, mostly associated with clinical infections (**Figures 2, 3A**; **Supplementary Table 1**). All five species in group C were isolated from humans with clinical associations (**Supplementary Table 1**; **Figure 3A**) except for *Corynebacterium urinipleomorphum*, which was isolated from urine of an infant with rotavirus gastroenteritis (Niang et al., 2019). *Corynebacterium urinipleomorphum* strains have also been isolated from other clinical sources, e.g., from a patient with gallbladder infection along with other bacterial species (Backert et al., 2018). Most of the important human and animal pathogens, including *Corynebacterium diphtheriae*, *Corynebacterium ulcerans*, *Corynebacterium silvaticum*, *Corynebacterium pseudotuberculosis* and *Corynebacterium rouxii*, are grouped in clade Q along with *Corynebacterium pelargi*, *Corynebacterium pseudopelargi* and *Corynebacterium gerontici*. The latter three species were isolated from avian hosts but were not associated with clinical infections (**Figure 2**; **Supplementary Table 1**). Approximately 80% of strains in group I and S were isolated from environmental sources. The type strain of *Corynebacterium testudinoris*, clustered in group I, was isolated from necrotic oral lesions in a tortoise along with *Escherichia coli*, a *Streptococcus* species and a *Pseudomonas* species strain; the role of this strain in the infection is unclear (Collins et al., 2001). Group S includes the industrially important species *Corynebacterium glutamicum* and '*Corynebacterium crenatum*' (Ikeda and Takeno, 2013; Man et al., 2016; Kallscheuer and Marienhagen, 2018), originally isolated from sewage and soil, respectively. *Corynebacterium* strains in group L were isolated from diverse sources (human, food or soil) without any clear clinical associations (**Figures 2, 3A**; **Supplementary Table 1**).

Among the minor groups, most of human isolates in groups M, J, O and P were from clinical sources. *Corynebacterium freiburgense* and *Corynebacterium canis* strains in group P were isolated from patients' wounds caused by dog bites and are likely canine in origin (**Supplementary Table 1**). Three of the four strains in group R are of animal origin, two associated with infections (**Figure 3A**; **Supplementary Table 1**). *Corynebacterium kutscheri* was isolated from a rodent but can cause infection in humans (**Supplementary Table 1**). The four strains in group D belong to three species, two potential pathogens *Corynebacterium pilosum* and *Corynebacterium cystitidis* isolated from bovine hosts, and *Corynebacterium lubricantis* which was isolated from a coolant lubricant (**Supplementary Table 1**). The close phylogenetic relatedness of human clinical and non-clinical strains in some groups potentially indicates that *Corynebacterium* strains from the latter sources may be able to cause opportunistic infections in humans. Thirty strains designated as singletons were scattered around the tree and were isolated from animals, environment, food and human samples including clinical isolates.

Most of the groups with a higher proportion of clinical strains (except for groups M and P) have genome sizes below the genus average (2.6 Mb; **Figure 3B**; **Supplementary Table 1**), whereas the genome size of strains in environmental group S are above the genus average. In contrast, Group I is notable in that most of the isolates are environmental yet have with genome sizes ranging closely around the genus average (2.3–2.7 Mb). There is no clear association between the

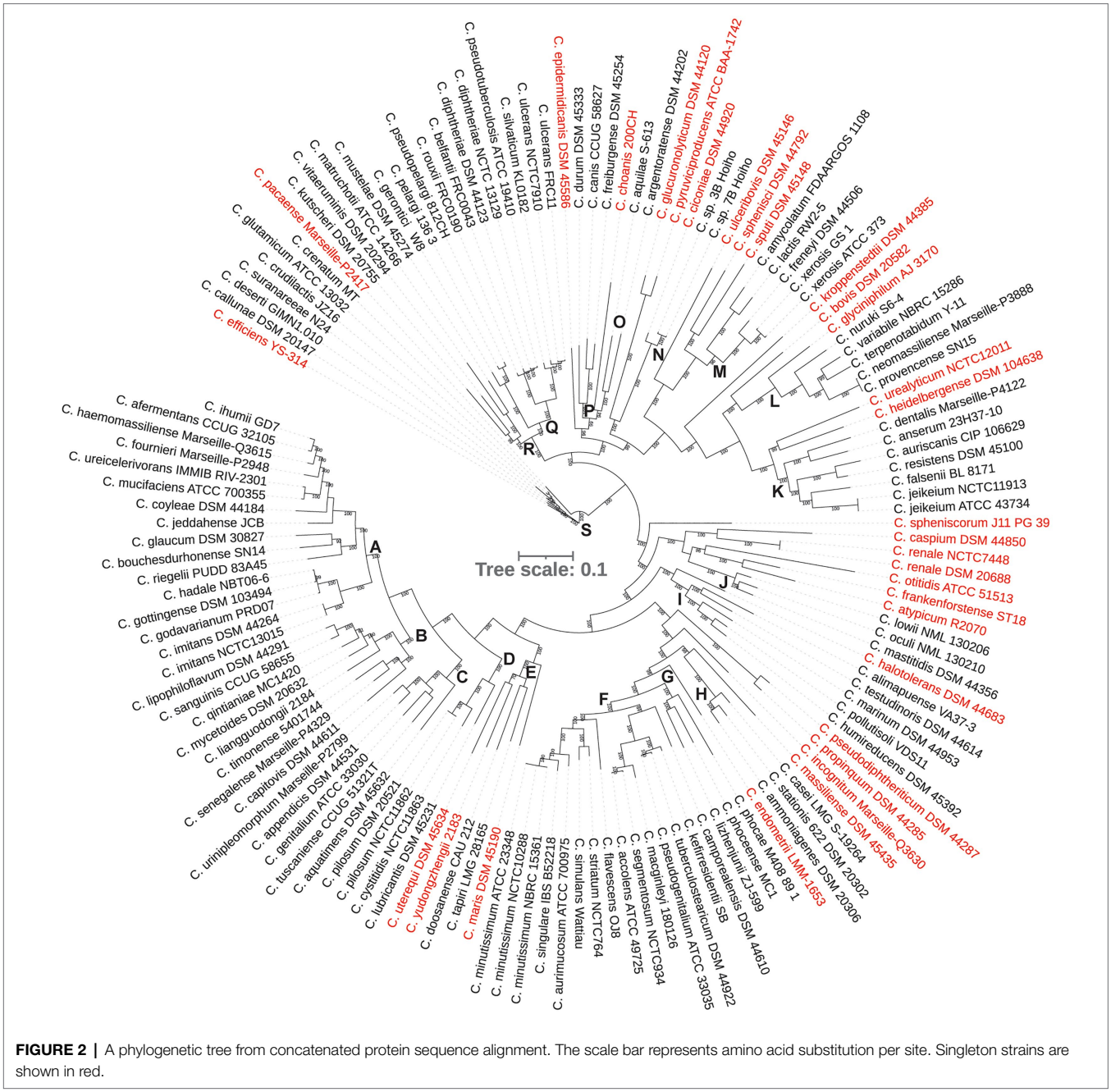

FIGURE 2 | A phylogenetic tree from concatenated protein sequence alignment. The scale bar represents amino acid substitution per site. Singleton strains are shown in red.

distribution of GC content and the clinical or environmental source of isolation of phylogenetic clades (**Figure 3C**; **Supplementary Table 1**).

Consistent with the recent re-classification of *Corynebacterium hadale* and *Corynebacterium godavarianum* as *Corynebacterium gottingense* (Bernard et al., 2020), all three strains clustered very closely in the phylogenomic tree as did strains of *Corynebacterium accolens* and *Corynebacterium segmentosum* (Sagerfors et al., 2021; **Figure 2**). Similarly, independent assemblies of the genomes of the type strains of *Corynebacterium imitans*, *Corynebacterium jeikeium*, *Corynebacterium minutissimum*, *Corynebacterium pilosum* and *Corynebacterium renale* were indistinguishable in the core genome tree (**Figure 2**), demonstrating reproducibility and robustness of the genome sequencing and compilation by different laboratories.

Mycolic Acid Biosynthesis

Based on the original species descriptions, mycolic acids are absent from the cell envelopes of six corynebacterial species: *Corynebacterium amycolatum*, *Corynebacterium caspium*, *Corynebacterium ciconiae*, *Corynebacterium kroppenstedtii*, *Corynebacterium lactis* and *Corynebacterium otitidis* (**Supplementary Table 3**). *Corynebacterium atypicum* was

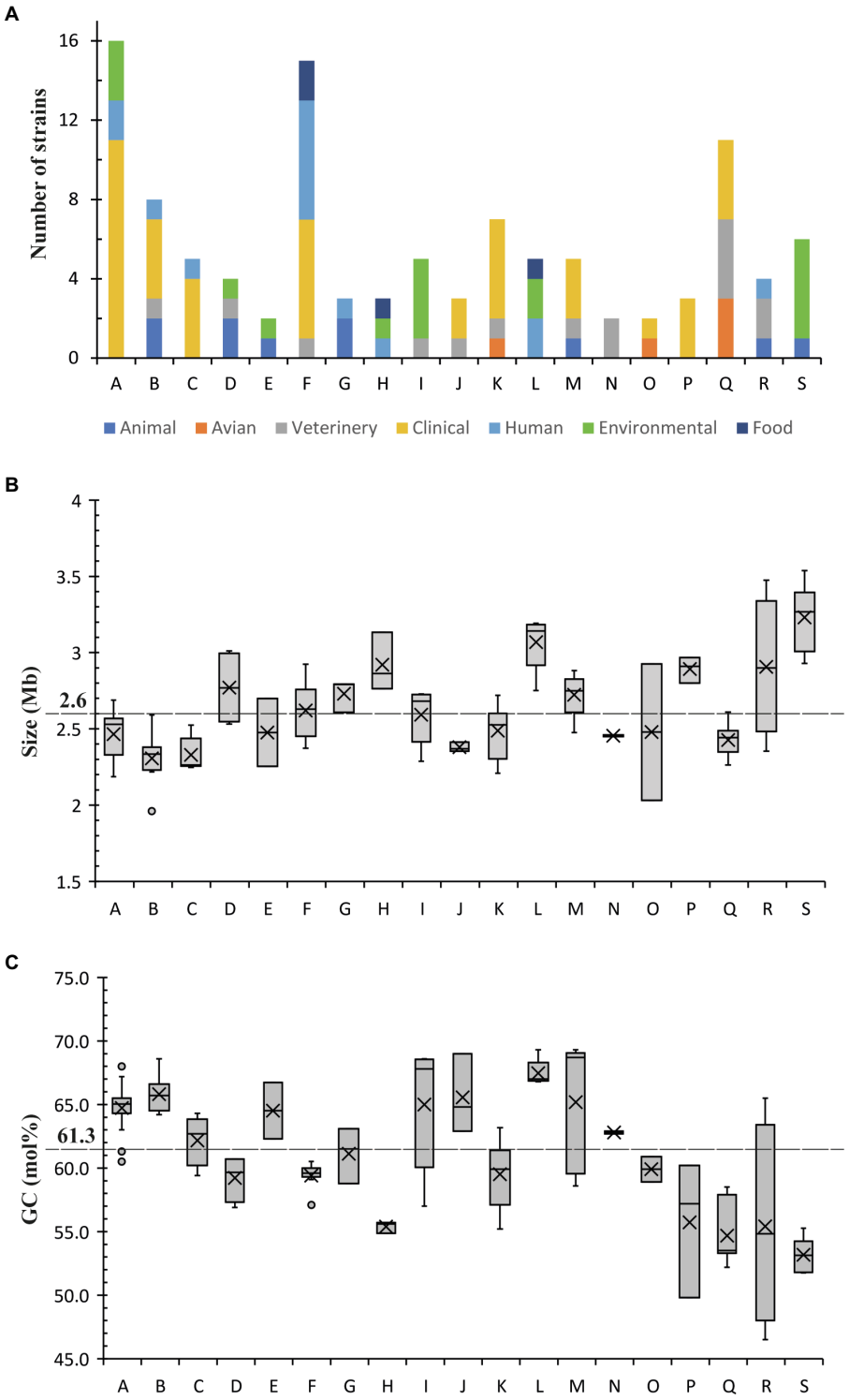

FIGURE 3 | The distribution of **(A)** strains from different sources, **(B)** genome sizes and **(C)** GC content among different phylogenetic groups. Average size and GC content within the genus are highlighted.

originally reported to be lacking mycolic acid based on chemotaxonomic characterisation (Hall et al., 2003) but was found to produce mycolic acids by another study (Wiertz et al., 2013). Of our panel, 85 *Corynebacterium* species were reported to produce mycolic acids; no information was available on the remaining 34 species (**Supplementary Table 3**).

Notable Gene Absences in Meromycolate Extension

We used BLASTP to identify homologues of proteins involved in mycolic acid biosynthesis. For consistency and to detect atypical strains that might possess FAS-II, we used a set of query sequences derived from *M. tuberculosis* H37Rv. Of the proteins involved in mycolic acid biosynthesis in *M. tuberculosis* (**Table 1**; **Figure 4**), Rv0533c (FabH), Rv2243 (FabD), Rv2244 (AcpM), Rv2245 (KasA), Rv2246 (KasB), Rv1483 (FabG1/MabA), Rv1484 (InhA), Rv0635 (HadA), Rv0636 (HadB), Rv0637 (HadC) and Rv3281 (AccE5) were absent among all *Corynebacterium* strains (**Supplementary Table 2**). Most of these gene absences are expected as they encode components of FAS-II which provides for extended meromycolate chains characteristic of some genera. Similarly, FabH links the FAS-I and FAS-II systems (Brown et al., 2005; Marrakchi et al., 2014). All descriptions of mycolic acid lengths in *Corynebacterium* are consistent with the genus lacking the FAS-II that elongates the meromycolate chain. Our genomic analysis is in complete accord with others in this respect (Dover et al., 2004, 2007; Marrakchi et al., 2014).

Carboxylase Complexes for Providing Fatty Acid and Polyketide Extension Substrates and Activating the α-Chain Component for Mycolate Synthesis

Critical Claisen-like condensation reactions drive the extension of polyketides, fatty acids (including meromycolates) and the condensation of the α and meromycolate chains of mycolic acids. These share a decarboxylative mechanism that requires a substrate with a carboxylic acid leaving group (**Figure 5**). In mycobacteria, three members of the AccD family of acyl coenzyme A carboxylase β subunits have been associated with fatty acid and polyketide synthesis (including mycolic acid). These are AccD4, AccD5 and AccD6 and these can each form a variety of heterooligomeric complexes with AccA3 and sometimes AccE5 to adapt the catalytic specificity of the acyl carboxylases (Gago et al., 2006).

The biotinylated α subunit of these acyl carboxylases, AccA3, is conserved among all strains and in some cases, strains possessed up to two additional α subunit genes (**Supplementary Tables 2** and **3**). The simplest substrate generated by these complexes is malonyl CoA which is used in the extension of fatty acids and polyketides by a C_2H_4 unit. Malonyl CoA is formed by the complex that contains AccA3

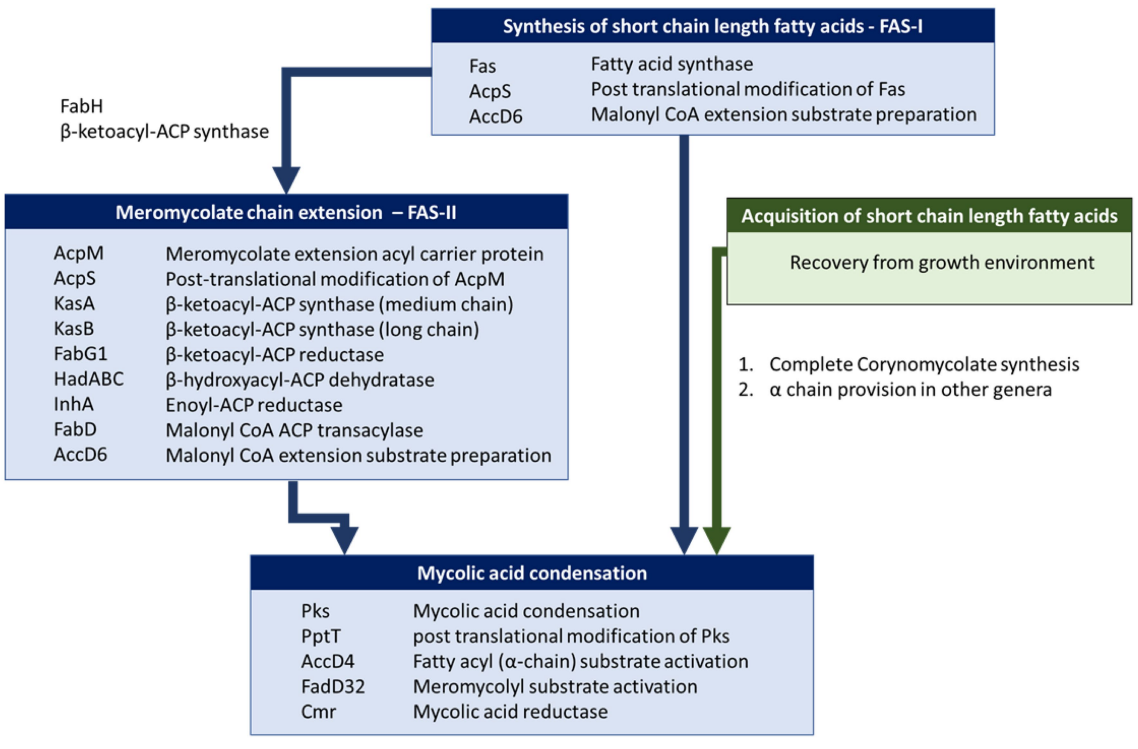

FIGURE 4 | Mycolic acid biosynthetic pathway in *Mycobacterium* and *Corynebacterium*. Briefly, mycolic acid biosynthesis proceeds *via* the activation and condensation of two fatty acyl chains (key enzymes indicated in lower blue box) that ultimately contribute the meromycolyl and α-alkyl chains (see **Figure 1**). Corynebacteria are unusual in that they do not extend the meromycolyl chain *via* fatty acid synthase II (FAS-II, key enzymes indicated in middle blue box), but rather condense two short fatty acyl chains that may be generated metabolically *via* Fatty Acid Synthase I (key enzymes indicated in upper blue box) or taken up from their habitat (route highlighted in green).

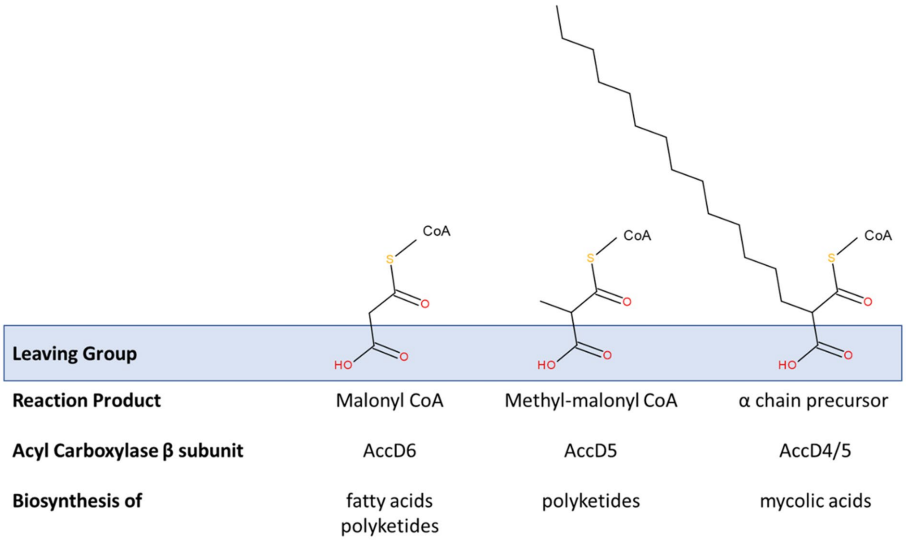

FIGURE 5 | Modification of acyl carboxylase activity by β subunit recruitment. Three acyl carboxylase activities are relevant to the production of fatty acids, polyketides and mycolic acids in studied species of *Mycobacteriales*. All of these are founded on a common α-subunit (AccA3) in a complex with various β-subunits. Those containing the β-subunits AccD4 or AccD5 also contain an ε subunit (AccE5). These acyl carboxylases essentially activate suitable acyl primers to generate substrates for these key biosynthetic processes. A common theme is their involvement in decarboxylative condensation reactions; the carboxyl group is added to promote these reactions and acts as a suitable leaving group (see blue box) that exposes a reactive carbanion that drives the synthetic reaction. The sequence homology shared by these specificity-defining β-subunits is extensive. Their individual functions have been defined through a combination of complex reconstitution and mutagenesis studies. AccD6 prefers an acetyl CoA primer *in vitro* and the carboxylation reaction provides malonyl CoA, an extension substrate used in the synthesis of fatty acids (including *de novo* fatty acid synthesis by FAS-I and meromycolyl chain extension by FAS-II) and polyketides. Acyl carboxylase reconstituted with AccD5 and AccE5 prefers a propionyl CoA primer and forms methyl-malonyl CoA which is used in the synthesis of polyketide molecules. The extent of these substrate preferences may vary and appears to influence the conditional essentiality of AccD6; i.e., acyl carboxylase containing AccD5 may be able to generate enough malonyl CoA to support fatty acid biosynthesis in the absence of *accD6*. AccD4 (likely supported by AccD5 in a heterologous β-subunit complex and AccE5) is responsible for the activation of the α-chain precursor to enable the mycolic condensation (also see **Figure 4**).

and AccD6 (Rv2247) using an acetyl-CoA primer (Dover et al., 2004; Marrakchi et al., 2014). Some polyketides incorporate methyl-branches by inclusion of a C_3H_7 unit derived from methyl-malonyl CoA. AccD5 appears to favour carboxylation of propionyl CoA over acetyl CoA *in vitro*, indicating its primary role may be in producing methyl-malonyl CoA. Although its deletion has been shown to impact upon mycolic acid production, it is likely that it plays a secondary role in mycolic acid biosynthesis.

The gene encoding AccD4 is part of the *accD4-pks13-fadD32* gene cluster. This acyl carboxylase component is required for the carboxylation of FAS-I products that ultimately form the α-chain in the mycolic acid condensation reaction (Gande et al., 2007). Complexes of AccD5 and AccD4 with AccA3 require the participation of AccE, as presumably this allows for the efficient binding of the larger and branched substrates.

There is extensive homology between each of these β subunits, especially between AccD5 and AccD6, which is consistent with their interactions with the common acyl carboxylase components and their similar substrates. The AccD6 (Rv2247) was found to be absent among *Corynebacterium* strains based on the BLAST similarity criteria (**Supplementary Table 2**). However, multiple AccD5 homologues were detected and most of them also with significant sequence similarities to AccD6 (Rv2247) and so one of these copies may substitute for AccD6 or participate in other carboxylation reactions. Therefore, we believe that most *Corynebacterium* strains possess between two and four AccD5/AccD6 homologues (**Supplementary Tables 2** and **3**).

It is conceivable that corynebacteria may be able to satisfy the need for both malonyl and methyl-malonyl extension substrates through only one of these proteins. Both homologues were shown to be able to carboxylate acetyl and proprionyl primers *in vitro* (Daniel et al., 2007) and Pawelczyk et al. demonstrated that, in some mycobacteria, the ability of the AccD5 complex to utilise acetyl CoA as well as proprionyl CoA can influence the essentiality of *accD6* (Pawelczyk et al., 2017).

We could not detect a homologue of the acyl carboxylase ε subunit AccE5 using the *M. tuberculosis* query but were aware from previous studies that an orthologue was present in *Corynebacterium glutamicum* (Gande et al., 2007). Therefore, we used the *Corynebacterium glutamicum* AccE as a query and found that an AccE homologue could be detected in the majority of strains and often clustered alongside an AccD5 homologue, as in *M. tuberculosis*. As the ε subunit appears to be relevant to reactions with branched extension substrates (i.e., with AccD4 and AccD5) and considering the synteny in *M. tuberculosis*, we provisionally assigned the *accD* gene neighbouring *accE* as *accD5*. However, AccE was absent in 19 strains representing 17 species reported to make mycolic acids; two possible explanations are apparent, either this carboxylase subunit is not necessary for

corynomycolate biosynthesis in all corynebacteria or the protein exhibits such sequence variation that all orthologues were not detectable using the *Corynebacterium glutamicum* query. This latter scenario is plausible when we consider the small size of the subunit and that the *M. tuberculosis* query detected no homologues despite the robust detection of other gene products.

AccD4 is present among all the corynebacterial strains examined, except for three species *Corynebacterium otitidis*, *Corynebacterium lactis* and *Corynebacterium kroppenstedtii* that do not produce mycolic acids. An additional copy of AccD4 is present in *Corynebacterium ulceribovis*, *Corynebacterium sputi* and *Corynebacterium epidermidicanis*.

Mycolic Condensation

Alongside AccD4, the gene products of *pks13* and *fadD32* (Rv3801c) form a mycolic condensation system, where FadD32 activates long-chain fatty acids (Le et al., 2016), which are transferred to the phosphopantetheine arm of PKS13 for the final condensation step (Portevin et al., 2004; Gavalda et al., 2014). Subsequently, CmrA (Rv2509) reduces the β-keto group of the product from the mycolic condensation to produce mature mycolic acids, i.e., α-alkyl, β-hydroxy fatty acids (Bhatt et al., 2008; Javid et al., 2020). Additionally, the *pptT* gene product (phosphopantetheine transferase, Rv2794c) is also involved in post-translational modification of type-I polyketide synthases including PKS13 and is thus essential for its activity (Chalut et al., 2006). This gene is also present in most of the strains studied with two copies in '*Corynebacterium neomassiliense*' but is absent from three strains *Corynebacterium amycolatum*, *Corynebacterium lactis* and *Corynebacterium otitidis* (**Supplementary Table 3**) that do not produce mycolic acids. Some species, for example, *Corynebacterium choanae* and "*Corynebacterium neomassiliense*" have two homologues of FadD32 (**Supplementary Table 3**).

As expected, four of the six corynebacterial species reported to lack mycolates are missing crucial genes for mycolic acid biosynthesis (**Supplementary Table 3**), as observed previously for *Corynebacterium amycolatum*, *Corynebacterium kroppenstedtii*, *Corynebacterium lactis* and *Corynebacterium otitidis* (Tauch et al., 2008a; Baek et al., 2018). However, whereas these four genomes lack the *fadD32-pks13-accD4* operon, this locus is present in *Corynebacterium caspium* and *Corynebacterium ciconiae*. Interestingly, an AccE homologue was not detected in *Corynebacterium caspium*; however, we refer to our earlier comments on the reliability of AccE detection. Given these caveats, we consider that *Corynebacterium caspium* and *Corynebacterium ciconiae* are likely to be capable of mycolic acids synthesis, as suggested previously (Baek et al., 2018). Intriguingly, *Corynebacterium bovis*, *Corynebacterium fournieri*, and one of the two *Corynebacterium xerosis* genomes apparently lacks *pks13* gene. *Corynebacterium bovis* has previously been noted to produce distinctively short alkyl-branches (C6-C8; (Collins et al., 1982), whilst no analysis for mycolic acids was carried out when *Corynebacterium fournieri* was described (Diop et al., 2018).

Provision of Fatty Acyl Precursors for Mycolic Condensation

In *Corynebacterium* strains, *de novo* fatty acid biosynthesis is carried out by Fatty Acid Synthase I. Interestingly, 40 strains belonging to 35 species have an additional copy of *fas* gene (**Supplementary Table 3**), as previously reported for *Corynebacterium glutamicum* (Radmacher et al., 2005) where one is essential despite the apparent redundancy. Surprisingly, 29 corynebacterial species (30 strains) lack the *fas* gene including 27 that also lack the proximal *acpS* gene responsible for the essential post-translational modification of FAS-I with phosphopantetheine (**Table 2**). As discussed below, many of these species are reported to be lipophilic, suggesting that these strains must acquire fatty acids from their habitat. Included in this group are all the reported mycolate-lacking strains.

Overall, 82 genomes belonging to 75 species have all mycolic acid biosynthetic genes present, whilst in 24 genomes (21 species) we detected all genes except AccE, including 19 strains from 17 species that are reported to produce mycolates. Thirty-four genomes (32 species) have at least one key missing gene involved in fatty acid and/or mycolic acid biosynthesis (**Table 2**; **Supplementary Table 3**). Of those 32 species, 12 (13 strains) that lack Fas (10 also lacking AcpS) without further absences are likely to be able to generate mycolic acids using exogenous fatty acids. Notably, mycolates have been reported in 8 of these species. Similarly, additional 12 species (13 strains) that lack Fas/AcpS with AccE undetected are also likely to be able to make mycolates from exogenous fatty acids, as reported for six of these species. Five species lacking some or all of the *accD4*, *fadD32* and *pks13* genes are likely to be unable to produce corynomycolates. Some of these genes also appears to be absent in *Corynebacterium atypicum*, *Corynebacterium bovis* and *Corynebacterium xerosis*, potentially due to the assembly/annotation errors, which is discussed below.

DISCUSSION

Genomic Diversity and Virulence

It is well-known that the genus *Corynebacterium* comprises species of industrial, medical or veterinary importance, in addition to human and animal commensals (Bernard and Funke, 2015; Sangal and Burkovski, 2020). Currently, 133 validly named species (excluding synonyms) are listed in the LSPN database (https://lpsn.dsmz.de/genus/corynebacterium; accessed on September 30, 2021). In this study, we have analysed the genome sequences of a collection of corynebacterial genomes with a good representation of the species diversity (126 species, including 15 with effectively published names and one unnamed species from yellow-eyed penguins) from diverse sources including animals, environment, food and humans (**Supplementary Table 1**). Interestingly, more than 50% of these species (69/126) are associated with clinical conditions/symptoms, including opportunistic infections in humans and/or animals (**Supplementary Table 1**). Whilst *Corynebacterium diphtheriae*, *Corynebacterium ulcerans* and *Corynebacterium pseudotuberculosis* are the most notable pathogenic species

TABLE 2 | Presence of mycolic acid biosynthetic genes among corynebacteria, where the Fas protein is absent.

Strain	Lipo[1]	MA[2]	AcpS	CmrA	PptT	AccD5/6	AccA3	AccD4	PKS	FadD32	AccE
Corynebacterium accolens ATCC 49725	Yes	Yes									
Corynebacterium afermentans CCUG 32105	Yes	Yes									
Corynebacterium appendicis DSM 44531	Yes	Yes									
Corynebacterium aquatimens DSM 45632	Yes	Yes									
Corynebacterium bovis DSM 20582	Yes	Yes									
Corynebacterium fournieri Marseille-P2948											
Corynebacterium jeddahense JCB											
Corynebacterium jeikeium ATCC 43734	Yes	Yes									
Corynebacterium jeikeium NCTC11913	Yes	Yes									
Corynebacterium kroppenstedtii DSM 44385		No									
Corynebacterium lipophiloflavum DSM 44291	Yes	Yes									
Corynebacterium lowii NML 130206	Yes										
Corynebacterium macginleyi 180,126	Yes	Yes									
Corynebacterium mastitidis DSM 44356	Yes	Yes									
Corynebacterium oculi NML 130210	Yes										
Corynebacterium pyruviciproducens ATCC BAA-1742	Yes	Yes									
Corynebacterium resistens DSM 45100	Yes										
Corynebacterium segmentosum NCTC934											
Corynebacterium tuberculostearicum DSM 44922	Yes	Yes									
Corynebacterium tuscaniense CCUG 51321	No	Yes									
Corynebacterium urealyticum NCTC12011	Yes	Yes									
Corynebacterium ureicelerivorans IMMIB RIV-2301	Yes	Yes									
Corynebacterium xerosis ATCC 373	No	Yes									
"*Corynebacterium bouchesdurhonense*" SN14											
"*Corynebacterium dentalis*" Marseille-P4122											
"*Corynebacterium genitalium*" ATCC 33030											
"*Corynebacterium heidelbergense*" DSM 104638	Yes	Yes									
"*Corynebacterium kefirresidentii*" SB											
"*Corynebacterium pseudogenitalium*" ATCC 33035											
"*Corynebacterium uriniplasmorphum*" Marseille-P2799											

An absence of protein is shown in white, presence in green, two copies in blue and three copies of a protein is shown in pink. The effectively published names are mentioned in quotation marks. Purple, see section "Discussion" for consideration of these genomes.

[1]*Lipophilic.*

[2]*Mycolic acids reported.*

within the genus, this study highlights the true scale of the pathogenic potential of corynebacteria, both for humans and animals, which has not been previously appreciated.

Corynebacterium is very diverse phylogenomically; this study defines 19 clades with a further 30 singleton strains (**Figure 2**; **Supplementary Table 1**). With respect to the range of genome sizes reported, the largest is 2-fold larger than the smallest with a proportionate number of coding sequences (*Corynebacterium caspium*: 1.8 Mb and 1,630 CDS and *Corynebacterium glyciniphilum*: 3.6 Mb and 3,316 CDS) and their GC contents vary from 46.5 mol% for *Corynebacterium kutscheri* to 74.7 mol% for *Corynebacterium sphenisci* (**Supplementary Table 1**). Most of the groups with a higher proportion of clinical isolates have smaller genome sizes (with a few exceptions; **Figure 3A**), which may indicate reductive genome evolution associated with adaptation to a pathogenic lifestyle (Weinert and Welch, 2017). Interestingly, all bar one of the major clades (i.e., those with >5 strains) include isolates from multiple animal hosts/sources including those of clinical origin. The exception is group S, where most strains have an environmental origin. Group Q includes human pathogens, such as *Corynebacterium diphtheriae* and *Corynebacterium rouxii*, and animal pathogens, such as *Corynebacterium ulcerans* and *Corynebacterium pseudotuberculosis*. The latter species are also able to infect humans. Therefore, this indicates the possibility that other isolates from non-human species may also be able to infect humans.

Mycolic Acid Biosynthesis in Corynebacteria

The analysis for the presence of genes involved in mycolic acid biosynthesis among corynebacteria has been informative (**Figure 4**). As expected, the data confirm an absence of FAS-II biosynthetic pathway within the genus *Corynebacterium* (Dover et al., 2004, 2007; Marrakchi et al., 2014). The presence of all the other genes recognised as essential for mycolic acid biosynthesis is demonstrated among strains of 67 species that are reported to produce mycolic acid and additional 24 species where phenotypic data is not available (**Supplementary Table 3**). The study revealed the absence of key genes in *Corynebacterium amycolatum*, *Corynebacterium kroppenstedtii*, *Corynebacterium lactis* and *Corynebacterium otitidis* that is consistent with the documented absence of corynomycolates in their cell envelopes (**Supplementary Table 3**). *Corynebacterium fournieri* may be an additional corynebacterial species that lacks mycolates as PKS is not detected. Conversely, all required genes for mycolic acid biosynthesis are present in *Corynebacterium ciconiae* but it is reported to lack mycolic acids (Bernard and Funke, 2015), which potentially reflect errors in phenotypic characterisation.

We also noted 15 species that are phenotypically reported to produce mycolates but lack FAS-I (**Table 2**). Most of these species are reported to be lipophilic (except for *Corynebacterium tuscaniense*; **Table 2; Supplementary Table 1**) with AcpS protein also being absent. AcpS is associated with the crucial phosphopantetheinyl post-translational modification of FAS-I (Chalut et al., 2006; Gokulan et al., 2011), a function which is no longer needed if the latter is missing. Thus, it is likely that corynebacterial strains with the *fas* and *acpS* genes missing, are able to use exogenous fatty acids to synthesise mycolic acids, unless additional gene deletions in the mycolate biosynthesis pathway are present (as in *Corynebacterium kroppenstedtii* and *Corynebacterium otitidis*). Of the 29 corynebacterial species (30 strains) that lack the *fas* gene, 18 are reported to be lipophilic (**Table 2**). The corelation between lack of FAS-I and lipophilism provides a clear explanation for the origin of this phenotype, as suggested previously from observations on selected species (Tauch et al., 2008a,b; Tauch and Burkovski, 2015). Interestingly, *Corynebacterium godavarianum*, *Corynebacterium sanguinis*, *Corynebacterium endometrii* and *Corynebacterium sputi* strains are also reported to be lipophilic but possess *acpS* and *fas* genes (**Supplementary Table 3**). As mentioned before, *Corynebacterium godavarianum* has been reclassified as *Corynebacterium gottingense* and the latter is reported to be non-lipophilic and produces mycolates. These discrepancies may reflect difference in culture and/or methodology for assessing lipophilism.

This study also reports the absence of multiple genes including *fas* and *pks13* in the type strain of *Corynebacterium xerosis* ATCC 373 whereas all mycolic acid biosynthesis genes are present in another isolate of this species, GS1 (**Supplementary Table 3**). *Corynebacterium xerosis* ATCC 373 has been reported to produce mycolic acids (Collins et al., 1982; Bernard and Funke, 2015). Two smaller putative proteins mapped partially on PKS13 and four on parts of FAS-I (data not shown), potentially indicating that both the genes are pseudogenes or the multiple gaps (poor/incomplete genome quality) likely contributed to the discrepancy with phenotypic characterisation of mycolates in this strain. Similarly, despite the apparent absence of PKS13 in *Corynebacterium bovis*, we found two smaller genes, GCA_000183325.2_01024 (encoding 71 aa) and GCA_000183325.2_01025 (encoding 319 aa), showing significant similarities with parts of PKS13. This genome has 503 contigs and the higher number of gaps may be responsible for only partial detection of this gene, given it is reported to make mycolic acids (Collins et al., 1982). *Corynebacterium atypicum* R-2070 (=DSM 44849) may lack *fadD32* (**Supplementary Table 3**), although it is noted that Tippelt et al. (2014) reported a complete mycolate biosynthesis pathway in *Corynebacterium atypicum* DSM 44849 (Tippelt et al., 2014), so the absence of *fadD32* noted here may reflect the use of different annotation pipelines. The thin-layer chromatographic identification of mycolates in the study of Wiertz et al. (2013) is also consistent with this conclusion and suggests that the original description of this species as lacking mycolates is incorrect.

This study also shows a presence of second copy of the *fas* gene in 35 corynebacterial species but there is no obvious association to any phylogenetic group (**Supplementary Table 3**). Two copies of *fas* gene, *fasA* and *fasB*, have been characterised in *Corynebacterium glutamicum* where *fasA* was shown to be the essential fatty acid synthase, and the non-essential *fasB* has a supplementary role. Although deletion of *fasB* gene did alter the cornomycolate profile, it was shown to be associated with supplying palmitate and enhanced growth of the bacterium (Radmacher et al., 2005). Deletion of *fasA* resulted in fatty acid auxotrophy which

is consistent with our hypothesis that loss of this gene creates the lipophilic phenotype among *Corynebacterium* strains.

Role of Mycolic Acids in Virulence

Mycolic acids in the mycobacterial cell envelope are known to help bacteria in resisting environmental stresses such as antibiotics and in virulence by manipulating the host immune system (Korf et al., 2005; Dao et al., 2008; Vander Beken et al., 2011; Marrakchi et al., 2014; Nataraj et al., 2015). However, the effects of the more complex mycobacterial mycolates on virulence are primarily linked to modifications (such as cyclopropanation; Barkan et al., 2012) that are not features of the simpler corynomycolates (**Figure 1**).

Early work demonstrated that lipid extracts from *Corynebacterium pseudotuberculosis* had cytotoxic effects on mouse macrophages, but these phenomena were host dependent and the effects were not observed with guinea pig or rabbit macrophages (Hard, 1975). Trehalose mycolate glycolipids from non-pathogenic *Corynebacterium glutamicum* can also activate mouse macrophages (Chami et al., 2002) and this family of glycolipids are well-established as immunopotentiators (Schick et al., 2017; Burkovski, 2018). Intradermal injection of extracts containing corynomycolates from *Corynebacterium pseudotuberculosis* induced mild histopathological lesions in female goats (Jesse et al., 2020) but these extracts may also contain other immunogenic lipids. Interestingly, *Corynebacterium diphtheriae* strains delayed the maturation of phagolysosomes after internalisation in murine and human cell lines, but this was also observed with a strain which lacks corynomycolates (Ott et al., 2017). In addition, induction of cytokines appears to be a mycolate-independent mechanism in *Corynebacterium diphtheriae* strains (Ott et al., 2017; Schick et al., 2017). However, the mycolate-free strain showed increased susceptibility to several classes of antibiotics, consistent with the role of mycolates in presenting an outer membrane permeability barrier.

Notably, several corynebacterial species that lack mycolic acid biosynthetic genes are human clinical isolates (**Supplementary Table 3**). The loss of *pks13* in *Corynebacterium glutamicum* did not affect the viability of the strain but compromised the growth rate and the ability to grow at temperatures above 30°C (Portevin et al., 2004). Therefore, we suggest that the presence of mycolic acids in the cell envelope is a fundamental structural feature that affects strain fitness and helps them to resist environmental stresses such as antibiotic action but is not directly involved in virulence.

DATA AVAILABILITY STATEMENT

The original contributions presented in the study are included in the article/**Supplementary Material**, further inquiries can be directed to the corresponding author.

AUTHOR CONTRIBUTIONS

VS conceived the study. VS, LD, and IS contributed to the design of the study and were involved in data interpretation and drafting of the manuscript. LD, AT, and VS performed data analyses. All authors contributed to the article and approved the submitted version.

SUPPLEMENTARY MATERIAL

The Supplementary Material for this article can be found online at: https://www.frontiersin.org/articles/10.3389/fmicb.2021.802532/full#supplementary-material

REFERENCES

Backert, S., Tegtmeyer, N., Oyarzabal, O. A., Osman, D., Rohde, M., Grutzmann, R., et al. (2018). Unusual manifestation of live *Staphylococcus saprophyticus*, *Corynebacterium urinapleomorphum*, and *Helicobacter pylori* in the gallbladder with Cholecystitis. *Int. J. Mol. Sci.* 19:1826. doi: 10.3390/ijms19071826

Baek, I., Kim, M., Lee, I., Na, S. I., Goodfellow, M., and Chun, J. (2018). Phylogeny trumps chemotaxonomy: a case study involving *Turicella otitidis*. *Front. Microbiol.* 9:834. doi: 10.3389/fmicb.2018.00834

Barkan, D., Hedhli, D., Yan, H. G., Huygen, K., and Glickman, M. S. (2012). *Mycobacterium tuberculosis* lacking all mycolic acid cyclopropanation is viable but highly attenuated and hyperinflammatory in mice. *Infect. Immun.* 80, 1958–1968. doi: 10.1128/IAI.00021-12

Batt, S. M., Minnikin, D. E., and Besra, G. S. (2020). The thick waxy coat of mycobacteria, a protective layer against antibiotics and the host's immune system. *Biochem. J.* 477, 1983–2006. doi: 10.1042/BCJ20200194

Bernard, K. A., and Funke, G. (2015). "Corynebacterium," in *Bergey's Manual of Systematics of Archaea and Bacteria*. eds. W. B. Whitman, F. Rainey, P. Kämpfer, M. Trujillo, J. Chun, P. Devos, et al. (John Wiley & Sons, Inc), 1–70.

Bernard, K. A., Pacheco, A. L., Burdz, T., Wiebe, D., and Bernier, A. M. (2020). *Corynebacterium godavarianum* Jani et al. 2018 and *Corynebacterium hadale* Wei et al. 2018 are both later heterotypic synonyms of *Corynebacterium gottingense* Atasayar et al. 2017, proposal of an emended description of *Corynebacterium gottingense* Atasayar et al. 2017. *Int. J. Syst. Evol. Microbiol.* 70, 3534–3540. doi: 10.1099/ijsem.0.004153

Bhatt, A., Brown, A. K., Singh, A., Minnikin, D. E., and Besra, G. S. (2008). Loss of a mycobacterial gene encoding a reductase leads to an altered cell wall containing beta-oxo-mycolic acid analogs and accumulation of ketones. *Chem. Biol.* 15, 930–939. doi: 10.1016/j.chembiol.2008.07.007

Boxberger, M., Antezack, A., Magnien, S., Cassir, N., and La Scola, B. (2021). Complete genome and description of *Corynebacterium incognita* sp. nov.: a new bacterium within the *Corynebacterium* genus. *New Microbes New Infect.* 42:100893. doi: 10.1016/j.nmni.2021.100893

Brown, A. K., Sridharan, S., Kremer, L., Lindenberg, S., Dover, L. G., Sacchettini, J. C., et al. (2005). Probing the mechanism of the *Mycobacterium tuberculosis* beta-ketoacyl-acyl carrier protein synthase III mtFabH: factors influencing catalysis and substrate specificity. *J. Biol. Chem.* 280, 32539–32547. doi: 10.1074/jbc.M413216200

Brugger, S. D., Bomar, L., and Lemon, K. P. (2016). Commensal-pathogen interactions along the human nasal passages. *PLoS Pathog.* 12:e1005633. doi: 10.1371/journal.ppat.1005633

Burkovski, A. (2018). The role of corynomycolic acids in *Corynebacterium*-host interaction. *Antonie Van Leeuwenhoek* 111, 717–725. doi: 10.1007/s10482-018-1036-6

Camacho, C., Coulouris, G., Avagyan, V., Ma, N., Papadopoulos, J., Bealer, K., et al. (2009). BLAST+: architecture and applications. *BMC Bioinformatics* 10:421. doi: 10.1186/1471-2105-10-421

Chalut, C., Botella, L., De Sousa-D'auria, C., Houssin, C., and Guilhot, C. (2006). The nonredundant roles of two 4′-phosphopantetheinyl transferases in vital processes of mycobacteria. *Proc. Natl. Acad. Sci. U. S. A.* 103, 8511–8516. doi: 10.1073/pnas.0511129103

Chami, M., Andreau, K., Lemassu, A., Petit, J. F., Houssin, C., Puech, V., et al. (2002). Priming and activation of mouse macrophages by trehalose 6,6′-dicorynomycolate vesicles from *Corynebacterium glutamicum*. *FEMS Immunol. Med. Microbiol.* 32, 141–147. doi: 10.1016/S0928-8244(01)00292-9

Collins, M. D., Goodfellow, M., and Minnikin, D. E. (1982). A survey of the structures of mycolic acids in *Corynebacterium* and related taxa. *J. Gen. Microbiol.* 128, 129–149. doi: 10.1099/00221287-128-1-129

Collins, M. D., Hoyles, L., Hutson, R. A., Foster, G., and Falsen, E. (2001). *Corynebacterium testudinoris* sp. nov., from a tortoise, and *Corynebacterium felinum* sp. nov., from a Scottish wild cat. *Int. J. Syst. Evol. Microbiol.* 51, 1349–1352. doi: 10.1099/00207713-51-4-1349

Daniel, J., Oh, T. J., Lee, C. M., and Kolattukudy, P. E. (2007). AccD6, a member of the Fas II locus, is a functional carboxyltransferase subunit of the acyl-coenzyme A carboxylase in *mycobacterium tuberculosis*. *J. Bacteriol.* 189, 911–917. doi: 10.1128/JB.01019-06

Dao, D. N., Sweeney, K., Hsu, T., Gurcha, S. S., Nascimento, I. P., Roshevsky, D., et al. (2008). Mycolic acid modification by the *mmaA4* gene of *M. tuberculosis* modulates IL-12 production. *PLoS Pathog.* 4:e1000081. doi: 10.1371/journal.ppat.1000081

Diop, K., Nguyen, T. T., Delerce, J., Armstrong, N., Raoult, D., Bretelle, F., et al. (2018). *Corynebacterium fournierii* sp. nov., isolated from the female genital tract of a patient with bacterial vaginosis. *Antonie Van Leeuwenhoek* 111, 1165–1174. doi: 10.1007/s10482-018-1022-z

Dover, L. G., Alderwick, L. J., Brown, A. K., Futterer, K., and Besra, G. S. (2007). Regulation of cell wall synthesis and growth. *Curr. Mol. Med.* 7, 247–276. doi: 10.2174/156652407780598601

Dover, L. G., Cerdeno-Tarraga, A. M., Pallen, M. J., Parkhill, J., and Besra, G. S. (2004). Comparative cell wall core biosynthesis in the mycolated pathogens, *Mycobacterium tuberculosis* and *Corynebacterium diphtheriae*. *FEMS Microbiol. Rev.* 28, 225–250. doi: 10.1016/j.femsre.2003.10.001

Gago, G., Kurth, D., Diacovich, L., Tsai, S. C., and Gramajo, H. (2006). Biochemical and structural characterization of an essential acyl coenzyme A carboxylase from *Mycobacterium tuberculosis*. *J. Bacteriol.* 188, 477–486. doi: 10.1128/JB.188.2.477-486.2006

Gande, R., Dover, L. G., Krumbach, K., Besra, G. S., Sahm, H., Oikawa, T., et al. (2007). The two carboxylases of *Corynebacterium glutamicum* essential for fatty acid and mycolic acid synthesis. *J. Bacteriol.* 189, 5257–5264. doi: 10.1128/JB.00254-07

Gavalda, S., Bardou, F., Laval, F., Bon, C., Malaga, W., Chalut, C., et al. (2014). The polyketide synthase Pks13 catalyzes a novel mechanism of lipid transfer in mycobacteria. *Chem. Biol.* 21, 1660–1669. doi: 10.1016/j.chembiol.2014.10.011

Gokulan, K., Aggarwal, A., Shipman, L., Besra, G. S., and Sacchettini, J. C. (2011). *Mycobacterium tuberculosis* acyl carrier protein synthase adopts two different pH-dependent structural conformations. *Acta Crystallogr. D Biol. Crystallogr.* 67, 657–669. doi: 10.1107/S0907444911020221

Hall, V., Collins, M. D., Hutson, R. A., Lawson, P. A., Falsen, E., and Duerden, B. I. (2003). *Corynebacterium atypicum* sp. nov., from a human clinical source, does not contain corynomycolic acids. *Int. J. Syst. Evol. Microbiol.* 53, 1065–1068. doi: 10.1099/ijs.0.02442-0

Hard, G. C. (1975). Comparative toxic effect of the surface lipid of *Corynebacterium ovis* on peritoneal macrophages. *Infect. Immun.* 12, 1439–1449. doi: 10.1128/iai.12.6.1439-1449.1975

Ikeda, M., and Takeno, S. (2013). "Amino Acid Production by *Corynebacterium glutamicum*," in *Corynebacterium glutamicum: Biology and Biotechnology*. eds. H. Yukawa and M. Inui (Berlin, Heidelberg: Springer), 107–147.

Javid, A., Cooper, C., Singh, A., Schindler, S., Hanisch, M., Marshall, R. L., et al. (2020). The mycolic acid reductase Rv2509 has distinct structural motifs and is essential for growth in slow-growing mycobacteria. *Mol. Microbiol.* 113, 521–533. doi: 10.1111/mmi.14437

Jesse, F. F. A., Odhah, M. N., Abba, Y., Garba, B., Mahmood, Z., Hambali, I. U., et al. (2020). Responses of female reproductive hormones and histopathology in the reproductive organs and associated lymph nodes of Boer does challenged with *Corynebacterium pseudotuberculosis* and its immunogenic corynomycolic acid extract. *Microb. Pathog.* 139:103852. doi: 10.1016/j.micpath.2019.103852

Kallscheuer, N., and Marienhagen, J. (2018). *Corynebacterium glutamicum* as platform for the production of hydroxybenzoic acids. *Microb. Cell Factories* 17:70. doi: 10.1186/s12934-018-0923-x

Korf, J., Stoltz, A., Verschoor, J., De Baetselier, P., and Grooten, J. (2005). The *Mycobacterium tuberculosis* cell wall component mycolic acid elicits pathogen-associated host innate immune responses. *Eur. J. Immunol.* 35, 890–900. doi: 10.1002/eji.200425332

Laneelle, M. A., Tropis, M., and Daffe, M. (2013). Current knowledge on mycolic acids in *Corynebacterium glutamicum* and their relevance for biotechnological processes. *Appl. Microbiol. Biotechnol.* 97, 9923–9930. doi: 10.1007/s00253-013-5265-3

Le, N. H., Molle, V., Eynard, N., Miras, M., Stella, A., Bardou, F., et al. (2016). Ser/Thr phosphorylation regulates the fatty acyl-AMP ligase activity of FadD32, an essential enzyme in mycolic acid biosynthesis. *J. Biol. Chem.* 291, 22793–22805. doi: 10.1074/jbc.M116.748053

Man, Z., Xu, M., Rao, Z., Guo, J., Yang, T., Zhang, X., et al. (2016). Systems pathway engineering of *Corynebacterium crenatum* for improved L-arginine production. *Sci. Rep.* 6:28629. doi: 10.1038/srep28629

Marchand, C. H., Salmeron, C., Bou Raad, R., Meniche, X., Chami, M., Masi, M., et al. (2012). Biochemical disclosure of the mycolate outer membrane of *Corynebacterium glutamicum*. *J. Bacteriol.* 194, 587–597. doi: 10.1128/JB.06138-11

Marrakchi, H., Laneelle, M. A., and Daffe, M. (2014). Mycolic acids: structures, biosynthesis, and beyond. *Chem. Biol.* 21, 67–85. doi: 10.1016/j.chembiol.2013.11.011

Minnikin, D. E. (1982). "Complex lipids, their chemistry biosynthesis and roles," in *The Biology of Mycobacteria. Vol. 1*. London: Academic Press, 95–184.

Möller, J., Musella, L., Melnikov, V., Geissdorfer, W., Burkovski, A., and Sangal, V. (2020). Phylogenomic characterisation of a novel corynebacterial species pathogenic to animals. *Antonie Van Leeuwenhoek* 113, 1225–1239. doi: 10.1007/s10482-020-01430-5

Moody, D. B. (2017). How T cells grasp mycobacterial lipid antigens. *Proc. Natl. Acad. Sci. U. S. A.* 114, 13312–13314. doi: 10.1073/pnas.1719260115

Moreira, L. O., Mattos-Guaraldi, A. L., and Andrade, A. F. (2008). Novel lipoarabinomannan-like lipoglycan (CdiLAM) contributes to the adherence of *Corynebacterium diphtheriae* to epithelial cells. *Arch. Microbiol.* 190, 521–530. doi: 10.1007/s00203-008-0398-y

Nataraj, V., Varela, C., Javid, A., Singh, A., Besra, G. S., and Bhatt, A. (2015). Mycolic acids: deciphering and targeting the Achilles' heel of the tubercle bacillus. *Mol. Microbiol.* 98, 7–16. doi: 10.1111/mmi.13101

Nguyen, L. T., Schmidt, H. A., Von Haeseler, A., and Minh, B. Q. (2015). IQ-TREE: a fast and effective stochastic algorithm for estimating maximum-likelihood phylogenies. *Mol. Biol. Evol.* 32, 268–274. doi: 10.1093/molbev/msu300

Niang, E. H. A., Lo, C. I., Morand, A., Ndongo, S., Raoult, D., Fournier, P. E., et al. (2019). *Corynebacterium urinapleomorphum* sp. nov., a new bacterial species isolated from human urine sample. *New Microbes New Infect* 31:100576. doi: 10.1016/j.nmni.2019.100576

Oliveira, A., Oliveira, L. C., Aburjaile, F., Benevides, L., Tiwari, S., Jamal, S. B., et al. (2017). Insight of genus *Corynebacterium*: ascertaining the role of pathogenic and non-pathogenic species. *Front. Microbiol.* 8:1937. doi: 10.3389/fmicb.2017.01937

Ott, L., Hacker, E., Kunert, T., Karrington, I., Etschel, P., Lang, R., et al. (2017). Analysis of *Corynebacterium diphtheriae* macrophage interaction: dispensability of corynomycolic acids for inhibition of phagolysosome maturation and identification of a new gene involved in synthesis of the corynomycolic acid layer. *PLoS One* 12:e0180105. doi: 10.1371/journal.pone.0180105

Page, A. J., Cummins, C. A., Hunt, M., Wong, V. K., Reuter, S., Holden, M. T., et al. (2015). Roary: rapid large-scale prokaryote pan genome analysis. *Bioinformatics* 31, 3691–3693. doi: 10.1093/bioinformatics/btv421

Parks, D. H., Imelfort, M., Skennerton, C. T., Hugenholtz, P., and Tyson, G. W. (2015). CheckM: assessing the quality of microbial genomes recovered from isolates, single cells, and metagenomes. *Genome Res.* 25, 1043–1055. doi: 10.1101/gr.186072.114

Pawelczyk, J., Viljoen, A., Kremer, L., and Dziadek, J. (2017). The influence of AccD5 on AccD6 carboxyltransferase essentiality in pathogenic and non-pathogenic *mycobacterium*. *Sci. Rep.* 7:42692. doi: 10.1038/srep42692

Peel, M. M., Palmer, G. G., Stacpoole, A. M., and Kerr, T. G. (1997). Human lymphadenitis due to *Corynebacterium pseudotuberculosis*: report of ten cases from Australia and review. *Clin. Infect. Dis.* 24, 185–191. doi: 10.1093/clinids/24.2.185

Portevin, D., De Sousa-D'auria, C., Houssin, C., Grimaldi, C., Chami, M., Daffe, M., et al. (2004). A polyketide synthase catalyzes the last condensation step of mycolic acid biosynthesis in mycobacteria and related organisms. *Proc. Natl. Acad. Sci. U. S. A.* 101, 314–319. doi: 10.1073/pnas.0305439101

Puech, V., Chami, M., Lemassu, A., Laneelle, M. A., Schiffler, B., Gounon, P., et al. (2001). Structure of the cell envelope of corynebacteria: importance of the non-covalently bound lipids in the formation of the cell wall permeability barrier and fracture plane. *Microbiology* 147, 1365–1382. doi: 10.1099/00221287-147-5-1365

Radmacher, E., Alderwick, L. J., Besra, G. S., Brown, A. K., Gibson, K. J. C., Sahm, H., et al. (2005). Two functional FAS-I type fatty acid synthases in *Corynebacterium glutamicum*. *Microbiology* 151, 2421–2427. doi: 10.1099/mic.0.28012-0

Sagerfors, S., Poehlein, A., Afshar, M., Lindblad, B. E., Bruggemann, H., and Soderquist, B. (2021). Clinical and genomic features of *Corynebacterium macginleyi*-associated infectious keratitis. *Sci. Rep.* 11:6015. doi: 10.1038/s41598-021-85336-w

Sangal, V., and Burkovski, A. (2020). "Insights into old and new foes: pan-genomics of *Corynebacterium diphtheriae* and *Corynebacterium ulcerans*," in *Pan-genomics: Applications, Challenges, and Future Prospects*. eds. D. Barh, S. Soares, S. Tiwari and V. Azevedo (London: Academic Press), 81–100.

Sangal, V., Nieminen, L., Weinhardt, B., Raeside, J., Tucker, N. P., Florea, C. D., et al. (2014). Diphtheria-like disease caused by toxigenic *Corynebacterium ulcerans* strain. *Emerg. Infect. Dis.* 20, 1257–1258. doi: 10.3201/eid2007.140216

Saunderson, S. C., Nouioui, I., Midwinter, A. C., Wilkinson, D. A., Young, M. J., Mcinnes, K. M., et al. (2021). Phylogenomic Characterization of a Novel *Corynebacterium* Species Associated with Fatal Diphtheritic Stomatitis in Endangered Yellow-Eyed Penguins. *mSystems* 6:e0032021. doi: 10.1128/mSystems.00320-21

Schick, J., Etschel, P., Bailo, R., Ott, L., Bhatt, A., Lepenies, B., et al. (2017). Toll-Like receptor 2 and Mincle cooperatively sense Corynebacterial Cell Wall glycolipids. *Infect. Immun.* 85:85. doi: 10.1128/IAI.00075-17

Seemann, T. (2014). Prokka: rapid prokaryotic genome annotation. *Bioinformatics* 30, 2068–2069. doi: 10.1093/bioinformatics/btu153

Stuible, H. P., Meurer, G., and Schweizer, E. (1997). Heterologous expression and biochemical characterization of two functionally different type I fatty acid synthases from Brevibacterium ammoniagenes. *Eur. J. Biochem.* 247, 268–273. doi: 10.1111/j.1432-1033.1997.00268.x

Subedi, R., Kolodkina, V., Sutcliffe, I. C., Simpson-Louredo, L., Hirata, R. Jr., Titov, L., et al. (2018). Genomic analyses reveal two distinct lineages of *Corynebacterium ulcerans* strains. *New Microbes New Infect.* 25, 7–13. doi: 10.1016/j.nmni.2018.05.005

Tange, O. (2011). GNU Parallel – The Command-Line Power Tool. login: The USENIX Magazine, 42–47.

Tauch, A., and Burkovski, A. (2015). Molecular armory or niche factors: virulence determinants of *Corynebacterium* species. *FEMS Microbiol. Lett.* 362:fnv185. doi: 10.1093/femsle/fnv185

Tauch, A., Schneider, J., Szczepanowski, R., Tilker, A., Viehoever, P., Gartemann, K. H., et al. (2008a). Ultrafast pyrosequencing of *Corynebacterium kroppenstedtii* DSM44385 revealed insights into the physiology of a lipophilic *Corynebacterium* that lacks mycolic acids. *J. Biotechnol.* 136, 22–30. doi: 10.1016/j.jbiotec.2008.03.004

Tauch, A., Trost, E., Tilker, A., Ludewig, U., Schneiker, S., Goesmann, A., et al. (2008b). The lifestyle of *Corynebacterium urealyticum* derived from its complete genome sequence established by pyrosequencing. *J. Biotechnol.* 136, 11–21. doi: 10.1016/j.jbiotec.2008.02.009

Tippelt, A., Mollmann, S., Albersmeier, A., Jaenicke, S., Ruckert, C., and Tauch, A. (2014). Mycolic acid biosynthesis genes in the genome sequence of *Corynebacterium atypicum* DSM 44849. *Genome Announc.* 2, e00845–e008414. doi: 10.1128/genomeA.00845-14

Treerat, P., Redanz, U., Redanz, S., Giacaman, R. A., Merritt, J., and Kreth, J. (2020). Synergism between *Corynebacterium* and *Streptococcus sanguinis* reveals new interactions between oral commensals. *ISME J.* 14, 1154–1169. doi: 10.1038/s41396-020-0598-2

Vander Beken, S., Al Dulayymi, J. R., Naessens, T., Koza, G., Maza-Iglesias, M., Rowles, R., et al. (2011). Molecular structure of the Mycobacterium tuberculosis virulence factor, mycolic acid, determines the elicited inflammatory pattern. *Eur. J. Immunol.* 41, 450–460. doi: 10.1002/eji.201040719

Vincent, A. T., Nyongesa, S., Morneau, I., Reed, M. B., Tocheva, E. I., and Veyrier, F. J. (2018). The mycobacterial cell envelope: A relict From the past or the result of recent evolution? *Front. Microbiol.* 9:2341. doi: 10.3389/fmicb.2018.02341

Weinert, L. A., and Welch, J. J. (2017). Why might bacterial pathogens have small genomes? *Trends Ecol. Evol.* 32, 936–947. doi: 10.1016/j.tree.2017.09.006

Wen, F., Xing, X., Bao, S., Hu, Y., and Hao, B. C. (2019). Whole-genome sequence of *Corynebacterium xerosis* strain GS1, isolated from yak in Gansu Province, China. *Microbiol. Resour. Announc.* 8, e00845–e008414. doi: 10.1128/MRA.00556-19

Wiertz, R., Schulz, S. C., Muller, U., Kampfer, P., and Lipski, A. (2013). *Corynebacterium frankenforstense* sp. nov. and *Corynebacterium lactis* sp. nov., isolated from raw cow milk. *Int. J. Syst. Evol. Microbiol.* 63, 4495–4501. doi: 10.1099/ijs.0.050757-0

Zhao, J., Siddiqui, S., Shang, S., Bian, Y., Bagchi, S., He, Y., et al. (2015). Mycolic acid-specific T cells protect against *Mycobacterium tuberculosis* infection in a humanized transgenic mouse model. *elife* 4:e08525. doi: 10.7554/eLife.08525

Conflict of Interest: The authors declare that the research was conducted in the absence of any commercial or financial relationships that could be construed as a potential conflict of interest.

The reviewer AB declared a past collaboration with one of the authors VS to the handling editor.

Publisher's Note: All claims expressed in this article are solely those of the authors and do not necessarily represent those of their affiliated organizations, or those of the publisher, the editors and the reviewers. Any product that may be evaluated in this article, or claim that may be made by its manufacturer, is not guaranteed or endorsed by the publisher.

frontiers in Microbiology

ORIGINAL RESEARCH
published: 05 January 2022
doi: 10.3389/fmicb.2021.778985

Antibiotic Resistance and Molecular Biological Characteristics of Non-13-Valent-Pneumococcal Conjugate Vaccine Serogroup 15 *Streptococcus pneumoniae* Isolated From Children in China

*Wei Shi, Qianqian Du, Lin Yuan, Wei Gao, Qing Wang and Kaihu Yao**

Beijing Key Laboratory of Pediatric Respiratory Infection Diseases, Key Laboratory of Major Diseases in Children, Ministry of Education, National Key Discipline of Pediatrics (Capital Medical University), National Clinical Research Center for Respiratory Diseases, National Center for Children's Health, Beijing Pediatric Research Institute, Beijing Children's Hospital, Capital Medical University, Beijing, China

OPEN ACCESS

Edited by:
Rustam Aminov, University of Aberdeen, United Kingdom

Reviewed by:
Anusak Kerdsin, Kasetsart University, Thailand
Lesley McGee, Centers for Disease Control and Prevention (CDC), United States

***Correspondence:**
Kaihu Yao
jiuhu2655@sina.com

Specialty section:
This article was submitted to Antimicrobials, Resistance and Chemotherapy, a section of the journal Frontiers in Microbiology

Received: *17 September 2021*
Accepted: *10 December 2021*
Published: *05 January 2022*

Citation:
Shi W, Du Q, Yuan L, Gao W, Wang Q and Yao K (2022) Antibiotic Resistance and Molecular Biological Characteristics of Non-13-Valent-Pneumococcal Conjugate Vaccine Serogroup 15 Streptococcus pneumoniae Isolated From Children in China. Front. Microbiol. 12:778985. doi: 10.3389/fmicb.2021.778985

Background: The isolation rate of serogroup 15 *Streptococcus pneumoniae* has been increasing since developing countries began administering the 13-valent pneumococcal conjugate vaccine.

Methods: We detected the antibiotic resistance and molecular characteristics of 126 serogroup 15 *S. pneumoniae* strains isolated from children in China. Serotypes were determined via the Quellung reaction. Antibiotic resistance was tested using the *E*-test or disc diffusion method. Sequence types were assigned via multilocus sequence typing. Data were analyzed using WHONET 5.6 software.

Results: The frequencies of *S. pneumoniae* serotypes 15A, 15B, 15C, and 15F were 29.37, 40.48, 28.57, and 1.59%, respectively. Continuous-monitoring data from Beijing showed that the annual isolation rates of serogroup 15 *S. pneumoniae* were 7.64, 7.17, 2.58, 4.35, 3.85, 7.41, and 10.53%, respectively, from 2013 to 2019. All 126 serogroup 15 strains were susceptible to vancomycin and ceftriaxone. The non-susceptibility rate to penicillin was 78.57%. All strains were resistant to erythromycin with high minimum inhibitory concentrations (MICs). The multidrug resistance rate was 78.57%. The most common clonal complexes were CC3397, CC6011, CC10088, CC9785, and ST8589.

Conclusion: Serogroup 15 *S. pneumoniae* is common among children in China, and these strains should be continuously monitored.

Keywords: *Streptococcus pneumoniae*, serotype 15, PCV13, vaccine, antibiotic resistance, children

INTRODUCTION

Streptococcus pneumoniae (*S. pneumoniae*) is among the most important pathogenic bacteria in children. More than 100 serotypes within 46 serogroups have been discovered according to the biochemical structure of the capsular polysaccharide (Ganaie et al., 2020). As of 12 October 2020, the 13-valent pneumococcal conjugate vaccine (PCV13), which protects against 13 serotypes (1, 3, 4, 5, 6A, 6B, 7F, 9V, 14, 18C, 19A, 19F, and 23F) has been incorporated into national immunization programs in 160 countries (World Health Organization, 2020). Research on the efficacy of PCV13 showed that PCV13 can reduce the incidence of pneumococcal disease and cause changes in the serotype distributions of pathogenic *S. pneumoniae* strains (Janoir et al., 2016; Schroeder et al., 2017; Ubukata et al., 2018; Kim et al., 2020). Many regions worldwide have reported increased isolation rates of serogroup 15 *S. pneumoniae* strains after PCV13 use (Linden et al., 2015; Liyanapathirana et al., 2015; Sheppard et al., 2016; Lo et al., 2019; Nakano et al., 2020).

PCV13 was approved in China in November 2016 and was available in the country in May 2017. Because PCV13 is expensive and has not been included in China's national immunization program, the PCV13 vaccination rate among Chinese children is low. Another 23-valent pneumococcal polysaccharide vaccine, PPV23, which protects against serotypes 1, 2, 3, 4, 5, 6B, 7F, 8, 9N, 9V, 10A, 11A, 12F, 14, 15B, 17F, 18C, 19A, 19F, 20, 22F, 23F, and 33F, is available in China for children aged > 2 years. The vaccination rates for both vaccines are low. Recipients are concentrated in cities and are children whose parents can afford to pay for the vaccines. Reports on the vaccination data are scarce, and the vaccine coverage is unclear.

We sought to determine the prevalence of serogroup 15 *S. pneumoniae* among Chinese children as well as the characteristics of these strains. Here, we report the serotype distribution, antibiotic-resistance patterns and molecular biological characteristics of 126 serogroup 15 *S. pneumoniae* strains collected from children in China.

MATERIALS AND METHODS

Bacterial Strains

We collected 126 unduplicated strains of serogroup 15 *S. pneumoniae* from Beijing (Beijing Children's Hospital affiliated to Capital Medical University; hereinafter referred to as Beijing Children's Hospital), Zhongjiang (People's Hospital of Zhongjiang County), Youyang (People's Hospital of Chongqing Youyang County), Wulumuqi (Wulumuqi Children's Hospital) and Shenzhen (Shenzhen Children's Hospital) from 2013 to 2019. **Table 1** lists the detailed clinical information on these children, including age, sex, culture time and specimen type isolated.

Of the 126 strains isolated, 63 were collected via continuous surveillance in Beijing Children's Hospital. Beijing Children's Hospital is a national children's medical center, with more than 3 million outpatients and 70,000 inpatients annually. Since 2013, Beijing Children's Hospital has been monitoring the serotype and antibiotic susceptibility characteristics of *S. pneumoniae* strains isolated from children in the hospital. In this study, the isolation rate of serogroup 15 *S. pneumoniae* strains from Beijing Children's Hospital was used to reflect the isolation of serogroup 15 *S. pneumoniae* in children in China.

A parent and/or legal guardian of each participant signed a written informed consent document before enrollment and before the study procedures were performed. The Ethics Committees of Beijing Children's Hospital affiliated to Capital Medical University, People's Hospital of Zhongjiang County, People's Hospital of Chongqing Youyang County, Wulumuqi Children's Hospital, and Shenzhen Children's Hospital approved the study. No ethical problems were encountered.

Serotyping

Serotypes were determined using the Quellung reaction with Pneumotest kits (Statens Serum Institute, Copenhagen, Denmark). Serotyping was interpreted based on capsular swelling under phase-contrast microscopy with an oil-immersion lens (magnification, 100×), as described previously (Sørensen, 1993).

Antimicrobial Susceptibility Testing

The minimum inhibitory concentrations (MICs) of penicillin, amoxicillin, ceftriaxone, imipenem, vancomycin and erythromycin for each strain were determined using *E*-test strips (AB Biodisk, Solna, Sweden). Disc diffusion tests (Oxoid Ltd., Basingstoke, United Kingdom) were performed to ascertain antimicrobial susceptibilities to tetracycline, sulfamethoxazole-trimethoprim, and chloramphenicol. The results were interpreted in accordance with the Clinical and Laboratory Standards Institute 2019 guidelines, and oral breakpoints (susceptible, $\leq$ 0.06 mg/L; intermediate, 0.12–1.0 mg/L; resistant, $\geq$ 2.0 mg/L) were used for penicillin (Clinical Laboratory Standards Institute [CLSI], 2019). *S. pneumoniae* American Type Culture Collection 49619 was used as the quality-control strain and was included in each test set to ensure accuracy of the results. Multidrug-resistant *S. pneumoniae* (MDRSP) was defined as *S. pneumoniae* isolates that were resistant to three or more kinds of antibiotics tested in this study.

Multilocus Sequence Typing

Strains were characterized using multilocus sequence typing (MLST). Chromosomal DNA was extracted from overnight cultures of *S. pneumoniae* strains grown on 5% trypticase soy agar (Oxoid Ltd.) using the SiMax^{TM} Genomic DNA Extraction Kit (SBS Genetech Co., Ltd., Beijing, China) per the manufacturer's instructions. Seven housekeeping genes (*aroE*, *gdh*, *gki*, *recP*, *spi*, *xpt*, and *ddl*) were amplified via polymerase chain reaction from the chromosomal DNA as described previously (Enrigh and Spratt, 1998). The products were sent to BGI Company (Beijing, China) for sequencing of both strands. The resulting sequences were compared with those of all known alleles at

TABLE 1 | Clinical information on the strains included in this study.

	Beijing ($n = 63$)	Youyang ($n = 27$)	Zhongjiang ($n = 17$)	Wulumuqi ($n = 13$)	Shenzhen ($n = 6$)	Total ($n = 126$)
Age (year)						
≤ 1	32	22	11	7	1	73 (57.94%)
∼2	7	2	1	0	0	10 (7.94%)
∼3	9	1	1	2	3	16 (12.70%)
∼4	3	2	2	1	2	10 (7.94%)
∼5	4	0	2	2	0	8 (6.35%)
>5	8	0	0	1	0	9 (7.14%)
Gender						
Male	36	17	12	6	4	75 (59.52%)
Female	27	10	5	7	2	51 (40.48%)
Collecting year						
2013	11	–	–	–	–	11 (8.73%)
2014	16	2	1	–	–	19 (15.08%)
2015	4	25	16	1	–	46 (36.51%)
2016	6	–	–	2	–	8 (6.35%)
2017	4	–	–	–	–	4 (3.17%)
2018	14	–	–	10	6	30 (23.81%)
2019	8	–	–	–	–	8 (6.35%)
Specimen types						
Nasopharyngeal swabs	12	27	17	3	6	65 (51.59%)
Sputum	29	–	–	10	–	39 (30.95%)
Bronchoalveolar lavage fluid	19	–	–	–	–	19 (15.08%)
Venous blood	2	–	–	–	–	2 (1.59%)
Cerebrospinal fluid	1	–	–	–	–	1 (0.79%)

each locus, as well as with the sequence types (STs) in the pneumococcal MLST database.[1] New alleles and allelic profiles were submitted to the MLST database for name assignment. goeBURST v1.2.1[2] was used to investigate relationships among the strains and assign strains to a clonal complex (CC) based on the stringent group definition of six of the seven shared alleles.

Statistical Analysis

Antimicrobial susceptibility and MLST data were analyzed using WHONET 5.6 as recommended by the World Health Organization.

RESULTS

Serotype Distribution and Antimicrobial Susceptibility

Among the 126 strains, the proportions of serotypes 15A, 15B, 15C, and 15F were 29.37% (37/126), 40.48% (51/126), 28.57% (36/126), and 1.59% (2/126), respectively. **Table 2** shows the antimicrobial susceptibility testing results, including MIC values, for the serotypes. All strains were susceptible to vancomycin and ceftriaxone; none were susceptible to amoxycillin. The non-susceptibility rate to penicillin was 78.57%. All 126 strains were resistant to erythromycin, with high MIC values of 24 mg/L for one strain and > 256 mg/L for all other strains. The resistance rate to tetracycline reached 92.86%.

The multidrug-resistance rate was 78.57% (99/126). **Figure 1** shows the antibiotic-resistance pattern distributions of the MDRSP strains. The most common multidrug-resistance pattern was macrolides-β-lactams-tetracyclines, accounting for 64.65% (64/99) of the MDRSP.

Multilocus Sequence Typing

Thirty-one STs were identified among the 126 strains; the most common were ST3397 ($n = 16$, 12.70%), ST6011 ($n = 16$, 12.70%), ST11972 ($n = 15$, 11.90%), ST7768 ($n = 14$, 11.11%), ST6555 ($n = 11$, 8.73%), ST10088 ($n = 8$, 6.35%), ST8589 ($n = 7$, 5.56%), ST11950 ($n = 7$, 5.56%), and ST9785 ($n = 6$, 4.76%). The 31 STs were assigned to five CCs and nine singletons using goeBURST analysis (**Figure 2**). The most predominant CCs were CC3397 ($n = 60$, 47.62%) and CC6011 ($n = 31$, 24.60%), constituting 72.22% of all strains.

Table 3 shows the CCs/ST distribution by serotype. Each serotype had a predominant CC that included most of the isolates. CC6011 was the main CC for the 15A strains (83.78%, 31/37). CC3397 was the main CC for 15B and 15C, accounting for 68.63% (35/51) and 66.67% (24/36) of these strains, respectively.

[1] https://pubmlst.org/spneumoniae/

[2] http://www.phyloviz.net/goeburst/

TABLE 2 | Antimicrobial susceptibility pattern of the 126 serogroup 15 *Streptococcus pneumoniae* strains.

Antimicrobial	Parameter	Isolates n (%)				
		Total ($n = 126$)	15A ($n = 37$)	15B ($n = 51$)	15C ($n = 36$)	15F ($n = 2$)
Penicillin	S	27 (21.43)	17 (45.95)	4 (7.84)	5 (13.89)	1 (50.00)
	I	55 (43.65)	18 (48.65)	24 (47.06)	13 (36.11)	0
	R	44 (34.92)	2 (5.41)	23 (45.10)	18 (50.00)	1 (50.00)
	MIC50	1	0.125	1	1	–
	MIC90	2	1	2	2	–
	MIC range	<0.016–4	<0.016–2	<0.016–4	<0.016–4	0.016, 2
Amoxicillin	S	116 (92.06)	37 (100.00)	45 (88.24)	32 (88.89)	2 (100.00)
	I	10 (7.94)	0	6 (11.76)	4 (11.11)	0
	R	0	0	0	0	0
	MIC50	1	0.25	1	2	–
	MIC90	4	1	4	4	–
	MIC range	<0.016–4	<0.016–2	<0.016–4	<0.016–4	0.016, 2
Ceftriaxone	MIC50	0.5	0.125	1	1	–
	MIC90	1	1	1	1	–
	MIC range	0.016–1	0.016–1	0.016–1	0.016–1	0.016, 1
Imipenem	S	44 (34.92)	25 (67.57)	10 (19.61)	8 (22.22)	1 (50.00)
	I	71 (56.35)	12 (32.43)	35 (68.63)	23 (63.89)	1 (50.00)
	R	11 (8.73)	0	6 (11.76)	5 (13.89)	0
	MIC50	<0.016	0.064	0.25	0.25	–
	MIC90	0.5	0.5	1	1	–
	MIC range	<0.016–1	<0.016–0.5	<0.016–1	<0.016–1	0.016, 0.5
Vancomycin	MIC50	0.5	0.5	0.5	0.5	1
	MIC90	1	1	1	1	1
	MIC range	0.5–1	0.5–1	0.5–1	0.5–1	1
Erythromycin	MIC50	> 256	> 256	> 256	> 256	> 256
	MIC90	> 256	> 256	> 256	> 256	> 256
	MIC range	24– > 256	24– > 256	> 256	>256	> 256
Tetracycline	S	6 (4.76)	5 (13.51)	0	0	1 (50.00)
	I	3 (2.38)	1 (2.70)	1 (1.96)	1 (2.78)	0
	R	117 (92.86)	31 (83.78)	50 (98.04)	35 (97.22)	1 (50.00)
Trimethoprim/sulfamethoxazole	S	33 (26.19)	32 (86.49)	0	0	1 (50.00)
	I	4 (3.17)	2 (5.41)	1 (1.96)	1 (2.78)	0
	R	89 (70.63)	3 (8.11)	50 (98.04)	35 (97.22)	1 (50.00)
Chloramphenicol	S	115 (91.27)	35 (94.59)	47 (92.16)	31 (86.11)	2 (100.00)
	I	0	0	0	0	0
	R	11 (8.73)	2 (5.41)	4 (7.84)	5 (13.89)	0

MIC, minimum inhibitory concentrations.

Relationship Between Antimicrobial Susceptibility and Clonal Complexes

Table 4 summarizes the antibiotic-resistance profiles according to CCs. Different CCs showed different antimicrobial-resistance characteristics. No CC3397 strains were susceptible to penicillin or tetracycline, and all were 100% resistant to sulfamethoxazole-trimethoprim and 100% sensitive to chloramphenicol. All CC6011 and CC10088 strains were susceptible to amoxicillin and resistant to imipenem. All CC10088 strains were intermediate to penicillin, resistant to tetracycline and susceptible to chloramphenicol. All CC9785 strains were resistant to penicillin. All ST8589 strains were susceptible to penicillin, amoxicillin, and imipenem and resistant to tetracycline, sulfamethoxazole-trimethoprim, and chloramphenicol.

Fluctuation of Serotypes by Years

We isolated 1029 *S. pneumoniae* strains from Beijing Children's Hospital during the study period, and 63 were determined to be serogroup 15. The proportion of serogroup 15 *S. pneumoniae* strains was 6.12%. **Figure 3** shows the number of *S. pneumoniae* strains collected yearly and the serogroup 15 isolation rates.

In 2014 and 2015, the proportions of serogroup 15 *S. pneumoniae* were 6.67% (2/30) and 12.20% (25/205),

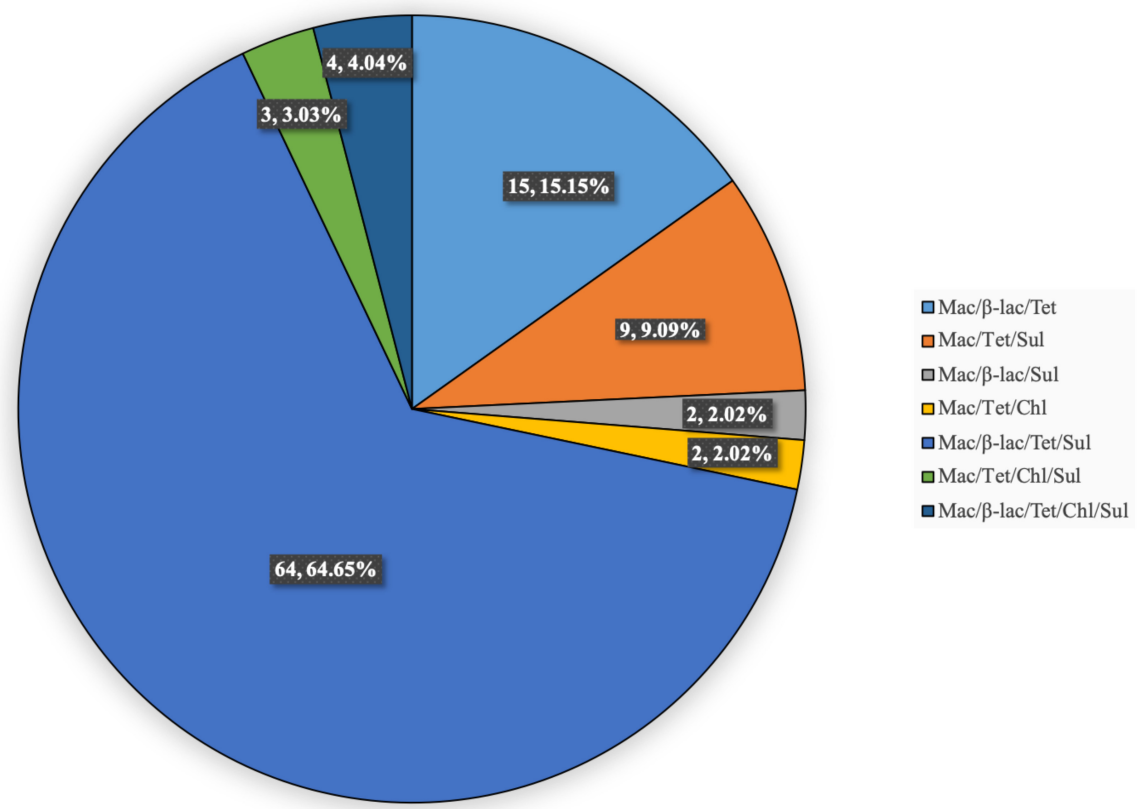

FIGURE 1 | Distribution of antibiotic-resistance patterns of MDRSP strains. Mac, macrolides; β-lac, β-lactams; Tet, tetracyclines; Sul, sulfonamides; Chl, chloramphenicols.

respectively, in Youyang and 6.25% (1/16) and 9.09% (16/176), respectively, in Zhongjiang. In 2015, 2016, and 2018, the proportions of serogroup 15 were 6.25% (1/16), 12.50% (2/16), and 3.88% (10/258), respectively, in Wulumuqi. Six of 66 (9.09%) strains were isolated in Shenzhen in 2018.

DISCUSSION

Since the introduction of PCV13, many countries and regions that included PCV13 in their national immunization programs have reported increased infections from serogroup 15 *S. pneumoniae*, which is not covered by the PCV13 vaccine (Linden et al., 2015; Sheppard et al., 2016; Nakano et al., 2020). Serogroup 15 *S. pneumoniae* strains have caused outbreaks (Katherine et al., 2012) and deaths (Arushothy et al., 2020) among children. China has not yet included PCV13 in the national immunization program, and the PCV13 vaccination rate among Chinese children is low. Additionally, the epidemiological monitoring data for *S. pneumoniae* in Chinese children are inexact; thus, the prevalence of serogroup 15 *S. pneumoniae* and the characteristics of these strains are unclear. Here, we reported the serotype distribution, antibiotic-resistance patterns, and ST characteristics of 126 serogroup 15 *S. pneumoniae* strains isolated from children in China. Half of these strains came from the continuous monitoring of Beijing Children's Hospital, which is one of the few continuous-monitoring data programs in mainland China and can partially reflect the prevalence of *S. pneumoniae* in Chinese children. During the study period, the overall isolation rate of serogroup 15 *S. pneumoniae* in the child population of Beijing Children's Hospital was 6.12%. After PCV13 was launched in China in May 2017, the isolation rates of serogroup 15 *S. pneumoniae* in 2018 and 2019 were 7.41 and 10.53%, respectively, showing an increasing trend.

The Pneumococcal Molecular Epidemiology Network (PMEN)[3] was established in 1997 for global surveillance of antibiotic-resistant *S. pneumoniae* and to standardize the nomenclature and classification of resistant clones. One 15A serotype was included among the 43 drug-resistant clones spread worldwide and published by the PMEN: Sweden^{15A}-25 (ST63). Over the past few years, several studies have reported increasing numbers of serotype 15A-ST63 strains (Ho et al., 2015; Sheppard et al., 2016; Nakano et al., 2018, 2019, 2020). In this study, ST63 accounted for 5.41% (2/37) of the serotype 15A strains, which was far lower than the 88.24% reported in Hong Kong (Ho et al., 2015) and the 98.28% reported in Japan (Nakano et al., 2020). Some studies

[3]https://www.pneumogen.net/pmen

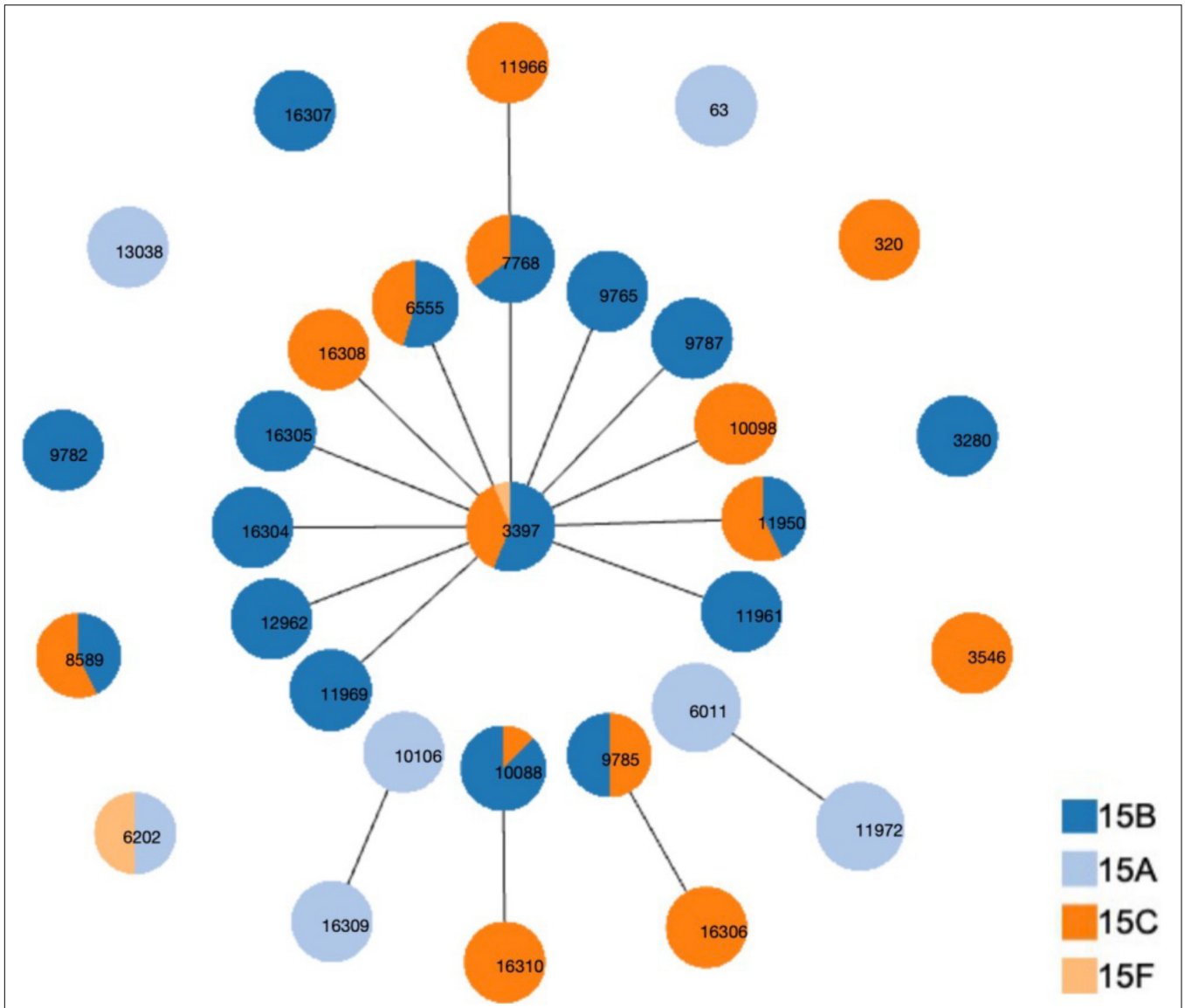

FIGURE 2 | Distribution of sequence types (STs) amongst the clonal complexes of serogroup 15 *Streptococcus pneumoniae* strains. goeBURST analysis was performed on the multilocus sequence typing data generated from all 126 strains analyzed. STs linked by a line belong to the same cluster.

TABLE 3 | CC/ST distribution of serogroup 15 *S. pneumoniae* by serotype.

Serotypes	No.	CC3397	CC6011	CC10088	CC9785	ST8589	Others
15A	37	0	31 (83.78%)	0	0	0	6 (16.22%)
15B	51	35 (68.63%)	0	7 (13.73%)	3 (5.88%)	3 (5.88%)	3 (5.88%)
15C	36	24 (66.67%)	0	2 (5.56%)	4 (11.11%)	4 (11.11%)	2 (5.56%)
15F	2	1 (50.00%)	0	0	0	0	1 (50.00%)
Total	126	60	31	9	7	7	12

%, number of serotypes divided by number of CCs/STs.

reported that ST63 showed high multidrug-resistance rates (Sheppard et al., 2016; Nakano et al., 2018). Both ST63 strains in this study were resistant to erythromycin; one of these was also resistant to tetracycline, and the other was non-susceptible to imipenem, but both strains were sensitive to other antibiotics. The significant differences in isolation

TABLE 4 | Antimicrobial susceptibility of the 126 strains by clonal complex.

Antimicrobial	Parameter	Isolates n (%)						
		Total (*n* = 126)	**CC3397 (*n* = 60)**	**CC6011 (*n* = 31)**	**CC10088 (*n* = 9)**	**CC9785 (*n* = 7)**	**ST8589 (*n* = 7)**	**Others (*n* = 12)**
Penicillin	S	27 (21.43)	0	15 (48.39)	0	0	7 (100.00)	5 (41.67)
	I	55 (43.65)	27 (45.00)	15 (48.39)	9 (100.00)	0	0	4 (33.33)
	R	44 (34.92)	33 (55.00)	1 (3.33)	0	7 (100.00)	0	3 (25.00)
	MIC50	1	2	0.125	1	2	<0.016–0.064	0.125
	MIC90	2	2	1	1	4	0.032	2
	MIC Range	<0.016–4	0.094–2	<0.016–2	0.5–1	2–4	0.064	<0.016–2
Amoxycillin	S	116 (92.06)	51 (85.00)	31 (100.00)	9 (100.00)	7 (100.00)	7 (100.00)	11 (91.67)
	I	10 (7.94)	9 (15.00)	0	0	0	0	1 (8.33)
	R	0	0	0	0	0	0	0
	MIC50	1	2	0.5	0.125	2	<0.016	0.023
	MIC90	4	4	1	0.25	2	<0.016	2
	MIC Range	<0.016–4	<0.016–4	<0.016–1	0.125–0.25	1–2	<0.016	<0.016–4
Ceftriaxone	MIC50	0.5	1	0.25	0.5	1	0.032	0.064
	MIC90	1	1	1	0.5	1	0.032	1
	MIC Range	0.016–1	0.5–1	0.016–1	0.25–0.5	0.5–1	0.016–0.032	0.016–1
Imipenem	S	44 (34.92)	2 (3.33)	20 (64.52)	6 (66.67)	1 (14.29)	7 (100.00)	8 (66.67)
	I	71 (56.35)	50 (83.33)	11 (35.48)	3 (33.33)	3 (42.86)	0	4 (33.33)
	R	11 (8.73)	8 (13.33)	0	0	3 (42.86)	0	0
	MIC50	<0.016	0.5	0.125	0.125	1	<0.016	0.064
	MIC90	0.5	1	0.5	0.25	1	<0.016	0.25
	MIC Range	<0.016–1	<0.016–1	<0.016–0.5	0.064–0.25	0.125–1	<0.016	<0.016–0.5
Vancomycin	MIC50	0.5	1	0.5	0.5	0.5	1	0.5
	MIC90	1	1	1	1	1	1	1
	MIC Range	0.5–1	0.5–1	0.5–1	0.5–1	0.5–1	0.5–1	0.5–1
Erythromycin	MIC50	> 256	> 256	> 256	> 256	> 256	> 256	> 256
	MIC90	> 256	> 256	> 256	> 256	> 256	> 256	> 256
	MIC Range	24– > 256	> 256	>256	> 256	>256	> 256	24– > 256
Tetracycline	S	6 (4.76)	0	3 (9.68)	0	0	0	3 (25.00)
	I	3 (2.38)	1 (1.67)	1 (3.23)	0	1 (14.29)	0	0
	R	117 (92.86)	59 (98.33)	27 (87.10)	9 (100.00)	6 (85.71)	7 (100.00)	9 (75.00)
Trimethoprim/sulfamethoxazole	S	33 (26.19)	0	29 (93.55)	0	0	0	4 (33.33)
	I	4 (3.17)	0	1 (3.23)	1 (11.11)	0	0	2 (16.67)
	R	89 (70.63)	60 (100.00)	1 (3.23)	8 (88.89)	7 (100.00)	7 (100.00)	6 (50.00)
Chloramphenicol	S	115 (91.27)	60 (100.00)	30 (96.77)	9 (100.00)	7 (100.00)	0	9 (75.00)
	I	0	0	0	0	0	0	0
	R	11 (8.73)	0	1 (3.23)	0	0	7 (100.00)	3 (25.00)

MIC, minimum inhibitory concentrations.

rates and antibiotic susceptibility characteristics of ST63 between our study and the other studies may be due to regional differences.

In the present study, most of the serotype 15A strains belonged to CC6011, which was composed of ST6011 and ST11972. ST6011 was popular in both serotype 3 (Ho et al., 2019) and serogroup 15 strains. There were 28 ST6011 strains recorded in the MLST database,[4] among which 22 were serotype 3, 5 were serotype 15A, and 1 strain was serotype 15B/15C. Both serotype 3 and serogroup 15 are non-PCV13 vaccine serotypes, and have an increasing trend in recent years (Linden et al., 2015; Liyanapathirana et al., 2015; Sheppard et al., 2016; LeBlanc et al., 2019; Lo et al., 2019; Goettler et al., 2020; Nakano et al., 2020). Therefore, close attention should be paid to ST6011 prevalent in these two serotypes.

We found that serogroup 15 *S. pneumoniae* strains showed good sensitivity to common antibiotics. However, the most common CC, CC3397, was 100% non-susceptible to penicillin. We wondered whether the prevalence of CC3397 in serogroup

[4]https://pubmlst.org

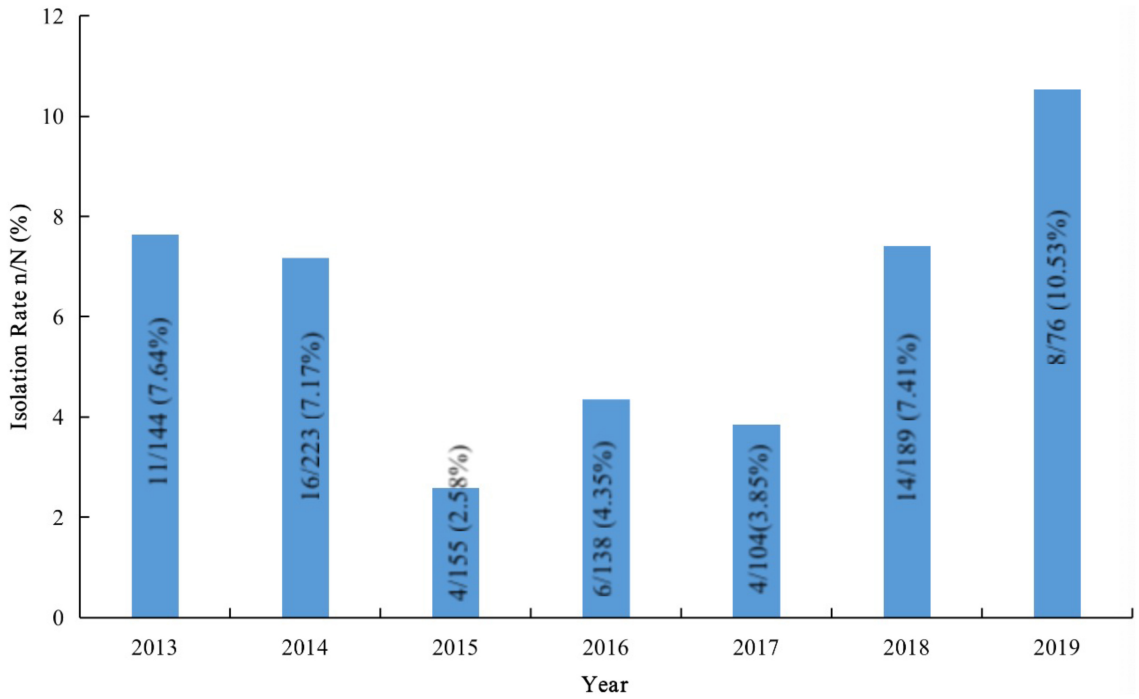

FIGURE 3 | Isolation rates of serogroup 15 *Streptococcus pneumoniae* strains in samples from Beijing Children's Hospital.

15 *S. pneumoniae* results from antibiotic pressure. Many studies have reported clonal shift phenomena in other serotypes, as CC271 replaced CC983 among serotype 19F strains (Li et al., 2013), ST81 replaced ST342 amongst serotype 23F pneumococcal isolates (Ma et al., 2013), CC320 replaced CC230 in 19A strains (Beall et al., 2011; Golden et al., 2015; Mayanskiy et al., 2017), and CC876 replaced CC875 in serotype 14 strains (He et al., 2015). These examples of clonal shift phenomena in the same serotype may be caused by antibiotic pressure, as they followed the principle that CCs/STs expressing high antibiotic resistance will replace CCs/STs with lower antibiotic resistance. Presently, the epidemiological characteristics of serogroup 15 *S. pneumoniae* are not being continuously monitored to access the changes in CC/ST prevalence in China. Whether CC3397 is the most drug-resistant of the serogroup 15 *S. pneumoniae* clones or whether CC3397 will be replaced by more drug-resistant clones in the future is unclear. Therefore, clinicians must strengthen surveillance of the antibiotic resistance and other epidemiological characteristics of serogroup 15 *S. pneumoniae*.

CONCLUSION

Serogroup 15 *S. pneumoniae* is common among children in China. Because CC3397, the main CC of serogroup 15 *S. pneumoniae*, showed high non-susceptibility to penicillin, long-term monitoring of antibiotic susceptibility and other epidemiological characteristics of serogroup 15 *S. pneumoniae* is essential.

DATA AVAILABILITY STATEMENT

The original contributions presented in the study are included in the article/supplementary material, further inquiries can be directed to the corresponding author/s.

AUTHOR CONTRIBUTIONS

WS, QD, LY, and WG conducted the experiments. WS and QW were responsible for the laboratory analysis. WS and KY designed the study, collected the data, analyzed the data, interpreted the results, and drafted the manuscript. All authors reviewed and revised the manuscript and approved the final version.

FUNDING

This study was supported by the Beijing Natural Science Foundation (L202004).

ACKNOWLEDGMENTS

We sincerely thank the staff of the following esteemed institutions for providing isolates during the several collection programs: Beijing Children's Hospital affiliated to Capital Medical University (Fang Dong), People's Hospital of Zhongjiang County (Denian Wen), People's Hospital of Chongqing Youyang County (Changhui Chen), Wulumuqi Children's Hospital (Juling Tian), and Shenzhen Children's Hospital (Jikui Deng).

REFERENCES

Arushothy, R., Ramasamy, H., Hashim, R., Raj, A. S. S., Amran, F., Samsuddin, N., et al. (2020). Multidrug-resistant *Streptococcus pneumoniae* causing invasive pneumococcal disease isolated from a paediatric patient. *Int. J. Infect. Dis.* 90, 219–222. doi: 10.1016/j.ijid.2019.10.037

Beall, B. W., Gertz, R. E., Hulkower, R. L., Whitney, C. G., Moore, M. R., and Brueggemann, A. B. (2011). Shifting genetic structure of invasive serotype 19A pneumococci in the United States. *J. Infect. Dis.* 203, 1360–1368. doi: 10.1093/infdis/jir052

Clinical Laboratory Standards Institute [CLSI] (2019). *Performance Standards for Antimicrobial Susceptibility Testing. In: Twenty-Ninth Informational Supplement. M100-S29*. Wayne, PA: Clinical and Laboratory Standards Institute.

Enrigh, M. C. T., and Spratt, B. G. (1998). A multilocus sequence typing scheme for *Streptococcus pneumoniae*: identification of clone associated with serious invasive disease. *Microbiology* 144(Pt. 11), 3049–3060. doi: 10.1099/00221287-144-11-3049

Ganaie, F., Saad, J. S., McGee, L., van Tonder, A. J., Bentley, S. D., Lo, S. W., et al. (2020). A new pneumococcal capsule type, 10D, is the 100th serotype and has a large cps fragment from an oral *streptococcus*. *mBio* 11:e00937-20. doi: 10.1128/mBio.00937-20

Goettler, D., Streng, A., Kemmling, D., Schoen, C., von Kries, R., Rose, M. A., et al. (2020). Increase in *Streptococcus pneumoniae* serotype 3 associated parapneumonic pleural effusion/empyema after the introduction of PCV13 in Germany. *Vaccine* 38, 570–577. doi: 10.1016/j.vaccine.2019.10.056

Golden, A. R., Rosenthal, M., Fultz, B., Nichol, K. A., Adam, H. J., Gilmour, M. W., et al. (2015). Characterization of MDR and XDR *Streptococcus pneumoniae* in Canada, 2007–13. *J. Antimicrob. Chemother.* 70, 2199–2202.

He, M., Yao, K., Shi, W., Gao, W., Yuan, L., Yu, S., et al. (2015). Dynamic of serotype 14 *Streptococcus pneumoniae* population causing acute respiratory infections among children in China (1997-2012). *BMC Infect. Dis.* 15:266. doi: 10.1186/s12879-015-1008-7

Ho, P. L., Chiu, S. S., Law, P. Y., Chan, E. L., Lai, E. L., and Chow, K. H. (2015). Increase in the nasopharyngeal carriage of non-vaccine serogroup 15 *Streptococcus pneumoniae* after introduction of children pneumococcal conjugate vaccination in Hong Kong. *Diagn. Microbiol. Infect. Dis.* 81, 145–148. doi: 10.1016/j.diagmicrobio.2014.11.006

Ho, P. L., Law, P. Y., and Chiu, S. S. (2019). Increase in incidence of invasive pneumococcal disease caused by serotype 3 in children eight years after the introduction of the pneumococcal conjugate vaccine in Hong Kong. *Hum. Vaccin. Immunother.* 15, 455–458. doi: 10.1080/21645515.2018.1526555

Janoir, C., Lepoutre, A., Gutmann, L., and Varon, E. (2016). Insight into resistance phenotypes of emergent non 13-valent pneumococcal conjugate vaccine type pneumococci isolated from invasive disease after 13-valent pneumococcal conjugate vaccine implementation in France. *Open Forum Infect. Dis.* 3:ofw020. doi: 10.1093/ofid/ofw020

Katherine, F. D., Chukwuma, M., Ruth, L. G., Alexander, N., Guh, A., Forbes, E., et al. (2012). *Streptococcus pneumoniae* serotype 15A in psychiatric unit, Rhode Island, USA, 2010–2011. *Emerg. Infect. Dis.* 18, 1889–1893. doi: 10.3201/eid1811.120454

Kim, S. H., Chung, D. R., Song, J.-H., Baek, J. Y., Thamlikitkul, V., Wang, H., et al. (2020). Changes in serotype distribution and antimicrobial resistance of *Streptococcus pneumoniae* isolates from adult patients in Asia: emergence of drug-resistant non-vaccine serotypes. *Vaccine* 38, 6065–6073. doi: 10.1016/j.vaccine.2019.09.065

LeBlanc, J. J., ElSherif, M., Ye, L., MacKinnon-Cameron, D., Ambrose, A., Hatchette, T. F., et al. (2019). *Streptococcus pneumoniae* serotype 3 is masking PCV13-mediated herd immunity in Canadian adults hospitalized with community acquired pneumonia: a study from the Serious Outcomes Surveillance (SOS) Network of the Canadian immunization research Network (CIRN). *Vaccine* 37, 5466–5473. doi: 10.1016/j.vaccine.2019.05.003

Li, Q. H., Yao, K. H., Yu, S. J., Ma, X., He, M. M., Shi, W., et al. (2013). Spread of multidrug-resistant clonal complex 271 of serotype 19F *Streptococcus pneumoniae* in Beijing, China: characterization of serotype 19F. *Epidemiol. Infect.* 141, 2492–2496. doi: 10.1017/S0950268813000514

Linden, M., Perniciaro, S., and Imöhl, M. (2015). Increase of serotypes 15A and 23B in IPD in Germany in the PCV13 vaccination era. *BMC Infect. Dis.* 15:207. doi: 10.1186/s12879-015-0941-9

Liyanapathirana, V., Nelson, E. A., Ang, I., Subramanian, R., Ma, H., and Ip, M. (2015). Emergence of serogroup 15 *Streptococcus pneumoniae* of diverse genetic backgrounds following the introduction of pneumococcal conjugate vaccines in Hong Kong. *Diagn. Microbiol. Infect. Dis.* 81, 66–70. doi: 10.1016/j.diagmicrobio.2014.09.028

Lo, S. W., Gladstone, R. A., van Tonder, A. J., Lees, J. A., du Plessis, M., Benisty, R., et al. (2019). Pneumococcal lineages associated with serotype replacement and antibiotic resistance in childhood invasive pneumococcal disease in the post-PCV13 era: an international whole-genome sequencing study. *Lancet Infect. Dis.* 19, 759–769. doi: 10.1016/S1473-3099(19)30297-X

Ma, X., Yao, K. H., Yu, S. J., Zhou, L., Li, Q. H., Shi, W., et al. (2013). Genotype replacement within serotype 23F *Streptococcus pneumoniae* in Beijing, China: characterization of serotype 23F. *Epidemiol. Infect.* 141, 1690–1696. doi: 10.1017/S0950268812002269

Mayanskiy, N., Savinova, T., Alyabieva, N., Ponomarenko, O., Brzhozovskaya, E., Lazareva, A., et al. (2017). Antimicrobial resistance, penicillin-binding protein sequences, and pilus islet carriage in relation to clonal evolution of *Streptococcus pneumoniae* serotype 19A in Russia, 2002–2013. *Epidemiol. Infect.* 145, 1708–1719. doi: 10.1017/S0950268817000541

Nakano, S., Fujisawa, T., Ito, Y., Chang, B., Matsumura, Y., Yamamoto, M., et al. (2020). Nationwide surveillance of paediatric invasive and non-invasive pneumococcal disease in Japan after the introduction of the 13-valent conjugated vaccine, 2015–2017. *Vaccine* 38, 1818–1824. doi: 10.1016/j.vaccine.2019.12.022

Nakano, S., Fujisawa, T., Ito, Y., Chang, B., Matsumura, Y., Yamamoto, M., et al. (2019). Whole-genome sequencing analysis of lultidrug-resistant serotype 15A *Streptococcus pneumoniae* in Japan and the emergence of a highly resistant serotype 15A-ST9084 clone. *Antimicrob. Agents Chemother.* 63:e02579-18. doi: 10.1128/AAC.02579-18

Nakano, S., Fujisawa, T., Ito, Y., Chang, B., Matsumura, Y., Yamamoto, M., et al. (2018). Spread of meropenem-resistant *Streptococcus pneumoniae* serotype 15A-ST63 clone in Japan, 2012–2014. *Emerg. Infect. Dis.* 24, 275–283. doi: 10.3201/eid2402.171268

Schroeder, M. R., Chancey, S. T., Thomas, S., Kuo, W. H., Satola, S. W., Farley, M. M., et al. (2017). A population-based assessment of the impact of 7- and 13-valent pneumococcal conjugate vaccines on macrolide-resistant invasive pneumococcal disease: emergence and decline of *Streptococcus pneumoniae* serotype 19A (CC320) with dual macrolide resistance mechanisms. *Clin. Infect. Dis.* 65, 990–998. doi: 10.1093/cid/cix446

Sheppard, C., Fry, N. K., Mushtaq, S., Woodford, N., Reynolds, R., Janes, R., et al. (2016). Rise of multidrug-resistant non-vaccine serotype 15A *Streptococcus pneumoniae* in the United Kingdom, 2001 to 2014. *Euro Surveill.* 21: 30423.

Sørensen, U. B. (1993). Typing of pneumococci by using 12 pooled antisera. *J. Clin. Microbiol.* 31, 2097–2100. doi: 10.1128/jcm.31.8.2097-2100.1993

Ubukata, K., Takata, M., Morozumi, M., Chiba, N., Wajima, T., Hanada, S., et al. (2018). Effects of pneumococcal conjugate vaccine on genotypic penicillin resistance and serotype changes, Japan, 2010–2017. *Emerg. Infect. Dis.* 24, 2010–2020. doi: 10.3201/eid2411.180326

World Health Organization (2020). *WHO Vaccine-Preventable Diseases: Monitoring System. 2020 Global Summary*. Geneva: World Health Organization

Conflict of Interest: The authors declare that the research was conducted in the absence of any commercial or financial relationships that could be construed as a potential conflict of interest.

frontiers in Microbiology

ORIGINAL RESEARCH
published: 10 January 2022
doi: 10.3389/fmicb.2021.804935

Corynebacterium Species Inhibit *Streptococcus pneumoniae* Colonization and Infection of the Mouse Airway

*Kadi J. Horn[1], Alexander C. Jaberi Vivar[1,2], Vera Arenas[1,3], Sameer Andani[1], Edward N. Janoff[4,5] and Sarah E. Clark[1]**

[1] Department of Otolaryngology Head and Neck Surgery, University of Colorado School of Medicine, Aurora, CO, United States, [2] Department of Developmental Biology, Washington University in St. Louis, St. Louis, MO, United States, [3] Department of Molecular, Cell, and Developmental Biology, University of California, Los Angeles, Los Angeles, CA, United States, [4] Division of Infectious Diseases, University of Colorado School of Medicine, Aurora, CO, United States, [5] Denver Veterans Affairs Medical Center, Aurora, CO, United States

OPEN ACCESS

Edited by:
Rustam Aminov, University of Aberdeen, United Kingdom

Reviewed by:
Anders P. Hakansson, Lund University, Sweden
Cassius Souza, Rio de Janeiro State University, Brazil

***Correspondence:**
Sarah E. Clark
sarah.e.clark@cuanschutz.edu

Specialty section:
This article was submitted to Antimicrobials, Resistance and Chemotherapy, a section of the journal Frontiers in Microbiology

Received: *29 October 2021*
Accepted: *03 December 2021*
Published: *10 January 2022*

Citation:
Horn KJ, Jaberi Vivar AC, Arenas V, Andani S, Janoff EN and Clark SE (2022) Corynebacterium Species Inhibit Streptococcus pneumoniae Colonization and Infection of the Mouse Airway. Front. Microbiol. 12:804935. doi: 10.3389/fmicb.2021.804935

The stability and composition of the airway microbiome is an important determinant of respiratory health. Some airway bacteria are considered to be beneficial due to their potential to impede the acquisition and persistence of opportunistic bacterial pathogens such as *Streptococcus pneumoniae*. Among such organisms, the presence of *Corynebacterium* species correlates with reduced *S. pneumoniae* in both adults and children, in whom *Corynebacterium* abundance is predictive of *S. pneumoniae* infection risk. Previously, *Corynebacterium accolens* was shown to express a lipase which cleaves host lipids, resulting in the production of fatty acids that inhibit growth of *S. pneumoniae in vitro*. However, it was unclear whether this mechanism contributes to *Corynebacterium-S. pneumoniae* interactions *in vivo*. To address this question, we developed a mouse model for *Corynebacterium* colonization in which colonization with either *C. accolens* or another species, *Corynebacterium amycolatum*, significantly reduced *S. pneumoniae* acquisition in the upper airway and infection in the lung. Moreover, the lungs of co-infected mice had reduced pro-inflammatory cytokines and inflammatory myeloid cells, indicating resolution of infection-associated inflammation. The inhibitory effect of *C. accolens* on *S. pneumoniae in vivo* was mediated by lipase-dependent and independent effects, indicating that both this and other bacterial factors contribute to *Corynebacterium*-mediated protection in the airway. We also identified a previously uncharacterized bacterial lipase in *C. amycolatum* that is required for inhibition of *S. pneumoniae* growth *in vitro*. Together, these findings demonstrate the protective potential of airway *Corynebacterium* species and establish a new model for investigating the impact of commensal microbiota, such as *Corynebacterium*, on maintaining respiratory health.

Keywords: *Corynebacterium*, *Streptococcus pneumoniae*, nasopharyngeal colonization, lung infection, pneumonia, pneumococcus, bacterial lipases

INTRODUCTION

Respiratory tract infections are a prominent a global health problem. Pneumonia, or lung infection, is a major source of mortality as the 4th most common cause of death worldwide (World Health Organization [WHO], 2021). Children are particularly vulnerable, as pneumonia is the leading cause of death in people under 5 years old (Centers for Disease Control and Prevention, 2019). In the United States, over one million emergency room visits are due to pneumonia every year (Centers for Disease Control and Prevention, 2019). The most common bacterial cause of pneumonia is the Gram-positive bacterial pathogen *Streptococcus pneumoniae*, also known as the pneumococcus (Jose et al., 2015; Torres et al., 2018). *S. pneumoniae* vaccines are extremely effective against invasive pneumococcal disease but are substantially less protective against pneumococcal pneumonia (Cutts et al., 2005; Pilishvili and Bennett, 2015), highlighting the need for new therapeutic strategies to reduce the burden of disease. *S. pneumoniae* is an opportunistic pathogen, as colonization in the nasopharynx of the upper airway is asymptomatic and susceptibility to infection differs among individuals. While this variation is not completely understood, the composition and function of the airway microbiome have emerged as important contributing factors (Clark, 2020). The disruption of the airway microbiome following antibiotic therapy correlates with an increased risk of *S. pneumoniae* acquisition (Biesbroek et al., 2014; Teo et al., 2015). Closely related *Streptococcus* commensals produce factors such as bacteriocins that kill *S. pneumoniae*, and serial administration of such commensals has shown some efficacy in reducing the incidence of pneumococcal-associated infections including otitis media in children (Marchisio et al., 2015; La Mantia et al., 2017). However, the contributions of other members of the commensal airway microbiome, particularly non-streptococcal species, to protection against *S. pneumoniae* are poorly understood.

Next-generation microbiome sequencing studies have identified additional members of the airway microbiome which are proposed to improve protection against pathogens including *S. pneumoniae*. Carriage of *Corynebacteriu*m, frequently together with *Dolosigranulum*, is associated with fewer upper and lower respiratory tract infections in both children and adults (Chonmaitree et al., 2017; Hasegawa et al., 2017; Copeland et al., 2018; Lappan et al., 2018; Man et al., 2019). *Corynebacterium* species are Gram-positive bacteria which frequently colonize the skin and upper airway. While *Corynebacterium diphtheriae*, the causative agent of diphtheria, is an important pathogen (Bernard, 2012), other *Corynebacterium* species are rarely associated with disease. Case reports have identified some *Corynebacterium* species associated with pneumonia, most frequently *Corynebacterium pseudodiphtheriticum* (Yang et al., 2018), indicating opportunistic infections may occur. However, non-*C. diphtheriae* species are more often associated with respiratory health, as the abundance of *Corynebacterium* species in nasopharynx correlates with reduced *S. pneumoniae* colonization and infection in several studies (Laufer et al., 2011; Pettigrew et al., 2012; Bomar et al., 2016; Kelly et al., 2017; Xu et al., 2021). Longitudinal studies tracking upper airway microbiome dynamics in children over time indicate that *Corynebacterium* abundance is predictive of both *S. pneumoniae* carriage and risk of respiratory tract infection (Biesbroek et al., 2014; Teo et al., 2015; Bosch et al., 2017; Kelly et al., 2021). Both children and adults with a higher abundance of *Corynebacterium* also have more stable airway microbiomes, compared to those with a predominance of opportunistic pathogens including *S. pneumoniae* (Bosch et al., 2017; Piters et al., 2019; Kelly et al., 2021). Together, these studies indicate that *Corynebacterium* species may play an important role in microbiome-mediated protection against pathogens such as *S. pneumoniae*, thereby reducing susceptibility to pneumonia.

Interruption of the potential protective benefit of *Corynebacterium* species in the airway is of particular concern for patients receiving antibiotics, as antibiotic therapy selectively reduces the *Corynebacterium* population while pathogens including *S. pneumoniae* are enriched (Teo et al., 2015; Prevaes et al., 2016; Kelly et al., 2021). Mechanistically, several *Corynebacterium* species can directly inhibit growth of *S. pneumoniae in vitro* (Bomar et al., 2016; Kelly et al., 2021; Xu et al., 2021). Among these, *Corynebacterium accolens* inhibits *S. pneumoniae* growth by expression of a bacterial lipase called LipS1, which hydrolyses host triacylglycerols, releasing free fatty acids that kill *S. pneumoniae* (Bomar et al., 2016). Fatty acids (FAs) are long-chain hydrocarbons with a terminal carboxyl group which are a major component of lipids. *Corynebacterium* species use fatty acids for growth, and lipophilic species including *C. accolens* require exogenous lipids to survive (Bernard, 2012; Tchoupa et al., 2021). Two non-lipophilic *Corynebacterium* species, which do not require host lipids for growth, were recently shown to inhibit *S. pneumoniae in vitro*, though the mechanisms were not identified (Xu et al., 2021). Another non-lipophilic species, *Corynebacterium amycolatum*, is frequently isolated from the human nasopharynx (Kaspar et al., 2016; Kelly et al., 2021) but is unusual in that it lacks mycolic acid, a long chain fatty acid which is a major component of the cell wall in almost all other *Corynebacterium* (Collins et al., 1988; Marrakchi et al., 2014). It is unclear whether FA production by bacterial lipases are universally required for *Corynebacterium*-mediated inhibition of *S. pneumoniae*, or whether diverse *Corynebacterium* species, including those less dependent on exogenous lipids, utilize similar mechanisms.

Understanding the host and bacterial requirements for *Corynebacterium*-mediated protection against *S. pneumoniae* is hampered by the lack of animal models for *Corynebacterium* colonization. Two related studies employing a five-dose serial inoculation of *C. pseudodiphtheriticum* in infant mice found that this strategy improves protection against *S. pneumoniae* (Moyano et al., 2020) as well as secondary pneumococcal infection in Respiratory Syncytial Virus (RSV)-infected mice (Kanmani et al., 2017). However, unknown is whether *C. pseudodiphtheriticum* actually colonizes the infant mouse airway in this model or if other *Corynebacterium* species can be used in a similar approach. For this study, we developed a mouse model to investigate the impact of two distinct species, *C. accolens* and *C. amycolatum*, on protection against *S. pneumoniae in vitro* and *in vivo*. Our

findings indicate that both *C. accolens* and *C. amycolatum* can colonize the airways of antibiotic treated mice, and that pre-exposure to these *Corynebacterium* species protects against *S. pneumoniae* colonization of the upper airway as well as infection and inflammation in the lung. We envision that this co-infection model can be used to further understand how exposure to different *Corynebacterium* species in the airway influences pneumococcal colonization and disease.

MATERIALS AND METHODS

Bacterial Strains

Corynebacterium accolens strain ATCC® 49726™ was obtained from the American Type Culture Collection. *Corynebacterium amycolatum* strain SK46, HM-109 was obtained through BEI Resources, NIAID, NIH as part of the Human Microbiome Project. *Corynebacterium* strains were grown from glycerol stocks on BHI agar plates (BD Difco™ Bacto™ Brain Heart Infusion, Thermo Fisher Scientific) aerobically at 37°C overnight. Growth from fresh plates was used to inoculate BHI broth cultures, which were grown overnight aerobically at 37°C with shaking at 200 rpm in preparation for *in vitro* assays and *in vivo* infections. BHI plates and broth were supplemented with 1% Tween® 80 (polysorbate, VWR) to provide an exogenous lipid source, unless otherwise specified. When indicated, 180 mg/mL triolein or oleic acid (VWR) were added to plates or broth cultures.

Streptomycin resistant variants of *Streptococcus pneumoniae* serotype 2 strain D39 and serotype 4 strain TIGR4 were kind gifts from Dr. Jeffrey N. Weiser (New York University). *S. pneumoniae* serotype 3 strain ATCC® 6303™ from the American Type Culture Collection was also used. *S. pneumoniae* was grown in Todd Hewitt Broth supplemented with 5% Yeast Extract (BD Bacto™) and 50 μg/mL streptomycin (MilliporeSigma) for streptomycin^R strains. For all experiments, *S. pneumoniae* cultures were grown from frozen stocks at 37°C with 5% CO_2 without shaking to mid-log phase, centrifuged at ≥ 20,000 × g for 10 min, and resuspended in phosphate-buffered saline (PBS). *S. pneumoniae* CFUs were determined by serial dilution plating on Tryptic Soy Broth agar (TSB, MP Biomedicals) supplemented with neomycin 5 μg/mL, streptomycin 50 μg/mL (streptomycin^R strains), and fresh catalase (5,000 Units/plate, Worthington Biomedical Corporation Lakewood, NJ) at 37°C with 5% CO_2 overnight.

Inhibition of *S. pneumoniae* Growth by Supernatant From *Corynebacterium* Species

For supernatant inhibition assays, *C. accolens* and *C. amycolatum* were grown on BHI agar supplemented with or without 1% Tween 80 and 180 mg/mL triolein. Triolein was emulsified in 100% ethanol for spreading onto plates, and plates were dried to evaporate ethanol prior to inoculation. Plates were incubated under aerobic conditions at 37°C overnight. Cultures were inoculated from fresh plates in BHI broth with or without 1% Tween 80 and 180 mg/mL triolein and grown aerobically at 37°C overnight with shaking at 200 rpm. OD_{600} was measured to standardize starting inocula, and cultures were centrifuged at ≥ 20,000 × g for 10 min to pellet bacterial cells. Cell-free supernatants (200 μL/plate) were spread onto TSB agar plates containing neomycin 5 μg/mL, streptomycin 50 μg/mL (streptomycin^R strains), and fresh catalase (5,000 Units/plate) and allowed to dry completely prior to *S. pneumoniae* serial dilution plating. For the dose response curve, supernatants were diluted in BHI broth (100–1.6% supernatant) prior to plating. *S. pneumoniae* serial dilutions were completed in PBS, with 10 μL spotted onto culture plates per dilution, plated in duplicate. Plates were incubated at 37°C with 5% CO_2 overnight for *S. pneumoniae* CFU enumeration.

Construction of *Corynebacterium* Mutant Strains

Mutation of the lipase encoding *lipS1* in *C. accolens* was performed as described previously (Bomar et al., 2016). Briefly, ∼1 kb regions flanking the coding sequence region for WP_005285206.1 in *C. accolens* ATCC 49726 (nucleotides 2,348,522–2,349,946) were amplified using Q5 high fidelity DNA polymerase (NEB) with primers designed to add a 21 bp scar sequence on the end of the 5′ fragment and beginning of the 3′ fragment, respectively, in addition to a stop codon at the end of the 3′ fragment (see **Supplementary Table 1** for primer sequences). PCR products were purified using the Monarch PCR and DNA cleanup kit (NEB). We used the plasmid pKO (KAN) as a suicide vector for *lips1* cloning. pKO (KAN) was a gift from Markus Seeger (Addgene #110086; RRID:Addgene_110086).[1] pKO was digested with *Pst*I and treated with calf intestinal phosphatase according to manufacturer's instructions (NEB) and purified using the GeneJET plasmid miniprep kit (Thermo Fisher Scientific). Purified plasmid and PCR products were assembled by Gibson assembly using the HiFi DNA Assembly Cloning Kit (NEB), and the assembled sequence was transformed into high efficiency NEB 5-alpha competent *E. coli* (NEB). Clones containing the assembly sequence inserted into pKO were identified by sequencing (Quintara Biosciences, Hayward CA). Competent cells of *C. accolens* were prepared and pKO containing the *lipS1* flanking regions was introduced by electroporation as previously described for *Corynebacterium glutamicum* (Eggeling et al., 2005). Electroporated cells were resuspended in BHI Tween 80 broth containing sorbitol (9.1 g/100 mL) and heat shocked at 46°C for 6 min followed by incubation at 37°C for 1 h prior to plating on selective media. Transformants were grown on BHI agar supplemented with Tween 80, sorbitol, and kanamycin 20 μg/mL to select for clones which integrated the *lipS1* flanking regions and kanamycin resistance gene from the modified pKO plasmid into the *C. accolens* genome by homologous recombination (kanamycin^R) followed by 5% sucrose to select for clones which lost the plasmid vector backbone (sucrose selection against *sacB* in pKO). Deletions in *lipS1* were confirmed by PCR amplification and sequencing (Quintara Biosciences, Hayward CA). The same process was used to construct an in-frame deletion in the

[1] https://www.addgene.org/110086/

coding sequence region for WP_005510233.1 in *C. amycolatum* (nucleotides 16,770–17,957) using primers specific for the flanking sequence regions (**Supplementary Table 1**).

Animals

Male and female 6–12 week old C57BL/6J (WT) mice, purchased from The Jackson Laboratory (RRID:IMSR_JAX:000664), were bred in-house. Mouse colonies were maintained in the University of Colorado Office of Laboratory Animal Resources.

Infections

All mice were treated with ingested broad-spectrum antibiotics (ampicillin 1 g/L, neomycin 1 g/L, metronidazole 1 g/L, vancomycin 0.5 g/L, MilliporeSigma and McKesson) *ad libitum* for 7 days until 48 h prior to infection. Bacterial loads in the stool pre- vs. post-antibiotic treatment were detected by qPCR as described previously (Ricchi et al., 2017). Briefly, stools were weighed and genomic DNA was extracted using the PureLink™ Genomic DNA Mini Kit (Thermo Fisher Scientific). Quantitative PCR was performed using iTaq™ Universal SYBR® Green Supermix (BioRad) together with 200 nM forward and reverse primers (**Supplementary Table 1**; Jimeno et al., 2018) and 2.5 μL template DNA. Reactions were performed using a CFX Connect™ Real-Time System (BioRad) with cycling conditions of: (1) 94°C for 4 min; (2) 40 cycles of 15 s at 95°C, 30 s at 60°C, and (3) 72°C for 10 min. A standard curve was generated using a known concentration of *S. pneumoniae* D39 gDNA, which together with the input ng/μL DNA and Ct values was used to calculate total 16S rRNA gene copy number as described previously (Gomes-Neto et al., 2017). qPCR data was analyzed using CFX Manager Software (version 2.1, BioRad). Nasal lavages, which can only be collected upon sacrifice, were obtained from separate groups of mice with and without antibiotic treatment for quantification of bacterial load by qPCR as above. Lavages were performed by the instillation of 200 μL PBS into cannulated trachea through the nasal cavity and collected from the nares.

Mice were infected with *C. accolens*, *C. amycolatum*, and/or *S. pneumoniae*, as indicated, at 10^7 CFU/mouse i.n. under inhaled isoflurane anesthesia. Nasal lavages were collected as above. Lungs were homogenized using a Bullet Blender tissue homogenizer (Stellar Scientific, Baltimore, MD). *S. pneumoniae* nasal lavage and lung CFUs were calculated following serial dilution and growth on Tryptic Soy agar plates containing neomycin (5 μg/mL, MilliporeSigma) and streptomycin (50 μg/mL, only streptomycin^R strains), supplemented with fresh catalase (5,000 Units/plate, Worthington Biochemical Corporation, Lakewood, NJ) grown overnight at 37°C with 5% CO_2. *Corynebacterium* CFUs were calculated following serial dilution and growth on BHI plates containing 1% Tween 80 grown overnight aerobically at 37°C. In co-infected mice, *Corynebacterium* CFUs were determined by subtracting *S. pneumoniae* CFUs (on streptomycin plates) from total growth (on non-selective BHI plates).

Flow Cytometry

Single cells were prepared from lungs following transcardial perfusion with PBS as described previously (Clark et al., 2020). Briefly, lungs were minced and digested with DNAseI (30 μg/mL, MilliporeSigma) and type 4 collagenase (1 mg/mL, Worthington Biochemical Corporation). Lung preparations were filtered with a 70 μM strainer prior to lysis of red blood cells by brief (1 min) incubation in RBC lysis buffer (0.15M NH_4Cl, 10 mM KHCO3, 0.1 mM Na_2EDTA, pH 7.4). Cell Fc receptors were blocked with anti-CD16/32 2.4G2 hybridoma supernatant prior to staining in FACS buffer (1% BSA, 0.01% NaN_3 in PBS). Cells were fixed in 1% paraformaldehyde. Antibodies used included: Siglec F (clone E50-2440), MHCII (clone M5/114.15.2), Ly6G (clone 1A8), Ly6C (clone HK1.4), CD45.2 (clone 104), CD11c (clone N418), CD11b (clone M1/70), CD64 (clone X54-5/7.1), and CD103 (clone 2E7). Antibodies were purchased from eBioscience, BD, BioLegend, or Thermo Fisher Scientific. Flow cytometry was performed using an LSRII (BD) in the Rocky Mountain Regional VAMC Research Core, Aurora CO and data were analyzed using FlowJo™ v10.8 Software (BD Life Sciences).

Cytokine and Chemokine Analysis

BAL cytokines and chemokines were measured using a LEGENDplex™ Mouse Inflammation Panel, and data were analyzed using the LEGENDplex™ Data Analysis Software Suite (BioLegend). Analytes were detected on the LSR Fortessa X-20 in the ImmunoMicro Flow Cytometry Shared Resource Laboratory at the University of Colorado Anschutz Medical Campus (RRID:SCR_021321). Serum cytokines were measured using mouse TNFα and IFNγ ELISA kits (BD), with analytes detected on a Synergy™ HT Microplate Reader (BioTek).

Mass Spectrometry for Detection of Fatty Acids

Samples were analyzed via ultra-high pressure liquid chromatography coupled to mass spectrometry (UHPLC-MS) at the University of Colorado School of Medicine Metabolomics Core. Nasal lavages were vigorously vortexed to homogenize, then diluted 1:1 in Optima LC-MS (Fisher) grade ice-cold MeOH and vortexed briefly again. Next, samples were incubated at –20°C for 30 min, then centrifuged at 4°C, 30,130 × g for 10 min to remove remaining solids as previously described (Nemkov et al., 2017; Reisz et al., 2019). Supernatants were transferred to pre-cooled autosampler vials, randomized, and analyzed on a Vanquish UHPLC coupled to a Q Exactive MS (Thermo Fisher Scientific, San Jose, CA, United States). Extracts (15 μL) were resolved with flow rate of 300–400 μL/min over an Acuity HSS T3 column (150 × 2.1 mm, 1.8 μm, Waters, Milford, MA, United States) with a 17-min gradient in negative ion polarity mode as previously described (Reisz et al., 2019). Samples were introduced to the MS via electrospray ionization with the MS scanning in full MS mode over the range of 150–1,500 m/z. As a quality control measure, technical replicates were injected every six samples to verify instrument stability (Nemkov et al., 2019). Fatty acids were annotated and integrated with Maven (Princeton University) in reference to the KEGG database. Peak quality was validated using

blanks, technical mixes, and ^{13}C natural isotope abundance (Nemkov et al., 2015).

Study Approval

These studies were approved by the Animal Care and Use Committee (Protocol #00927) and the Institutional Biosafety Committee (Protocol #1418) of the University of Colorado School of Medicine.

Statistical Analysis

Graphing and statistical analysis were completed using GraphPad Prism (Version 8.4.3, GraphPad Software, LLC, San Diego, CA). Statistical tests included *t*-tests for single comparisons, ANOVA with multiple group comparisons of normally distributed data and Kruskal-Wallis tests with multiple group comparisons of non-normal (non-Gaussian) distributions of infectious burden data (due to the limit of detection cut-off). For all statistical tests $p < 0.05$ was considered significant. All *in vivo* infections were conducted with 3–6 mice per group and repeated 3 times. For *in vitro* assays, experiments were completed with 2–3 technical replicates per condition and repeated 3 times.

RESULTS

Inhibition of *S. pneumoniae* Growth *in vitro* by Lipophilic and Non-lipophilic *Corynebacterium* Species

A recent survey of morphologically distinct *Corynebacterium* strains collected from infants showed that cell-free supernatants from four different lipophilic species, including *C. accolens*, inhibited *S. pneumoniae* growth *in vitro* (Kelly et al., 2021). However, supernatants from only 20% of the *Corynebacterium* isolates tested in this study were inhibitory, indicating that not all *Corynebacterium* strains mediate *S. pneumoniae* growth restriction *in vitro*. We considered whether *C. amycolatum*, which unlike *C. accolens* does not require exogenous FAs for either growth or mycolic acid production, inhibits *S. pneumoniae* growth *in vitro*. Cell-free supernatants from *C. accolens* or *C. amycolatum* were spread onto culture plates prior to *S. pneumoniae* inoculation, and *S. pneumoniae* colony forming units (CFUs) were determined following overnight incubation (**Figure 1A**). In contrast to robust growth of type 2 *S. pneumoniae* (strain D39) on untreated culture plates, no growth of *S. pneumoniae* was detected on plates pre-treated with supernatants from either *C. accolens* or *C. amycolatum* (**Figure 1B** and **Supplementary Figure 1A**). *S. pneumoniae* growth was also not detected on plates treated with oleic acid, a FA that kills *S. pneumoniae* (Clementi et al., 2013), included as a positive control. Supernatants from both *C. accolens* and *C. amycolatum* demonstrated similar inhibition of type 4 and type 3 *S. pneumoniae* strains (**Figures 1C,D**), indicating that multiple serotypes of *S. pneumoniae* are vulnerable to *C. accolens* and *C. amycolatum*-mediated growth restriction. Thus, both *C. accolens* and the non-lipophilic *C. amycolatum* inhibit *S. pneumoniae* growth *in vitro*.

We next considered whether the source or amount of FAs determined *Corynebacterium*-mediated inhibition of *S. pneumoniae* growth. In the supernatant assays described above, *Corynebacterium* cultures were supplemented with the synthetic surfactant Tween 80 and triolein, a naturally occurring triacylglycerol. Both Tween 80 and triolein are hydrolyzed by bacterial enzymes, resulting in the release of oleic acid, which is used by *Corynebacterium* as a carbon source for growth (Plou et al., 1998; Taoka et al., 2011). Triolein is hydrolyzed by bacterial lipases, while Tween 80 can be hydrolyzed by both lipases and esterases (Plou et al., 1998). As a result, the bacterial lipase LipS1 is required for growth of lipophilic *C. accolens* in triolein as the sole source of FAs, whereas other enzymes suffice for growth in Tween 80 (Bomar et al., 2016). To compare the relative importance of Tween 80 vs. triolein for *Corynebacterium*-mediated inhibition of *S. pneumoniae* growth, we investigated the inhibitory capacity of supernatants from *Corynebacterium* grown in BHI supplemented with none, one, or both of these lipid sources. For *C. accolens*, the addition of Tween 80 to cultures was sufficient for supernatant inhibition of *S. pneumoniae*. In contrast, *C. amycolatum* inhibition required the addition of both Tween 80 and triolein (**Figure 1E**). Titration of the amount of *Corynebacterium* supernatants added to culture plates revealed that at lower concentrations, *C. accolens* supernatants from cultures with triolein were more inhibitory than those without triolein (**Supplementary Figure 1B**). For *C. amycolatum*, triolein was required for inhibition, which only occurred when supernatants were added above a threshold concentration (**Supplementary Figure 1B**). We also confirmed that BHI alone, supplemented with Tween 80 or Tween 80 and triolein, was not inhibitory (**Supplementary Figure 1B**). These results indicate a dose-dependence for *C. accolens* and *C. amycolatum*-mediated inhibition of *S. pneumoniae*. In both cases, the inclusion of triolein increased the inhibitory effect, although the efficiency of *C. amycolatum*-mediated inhibition was lower than that of *C. accolens,* which was inhibitory in the presence of Tween 80 alone. This difference in substrate usage likely relates to the composition and expression of bacterial lipases and esterases responsible for triolein vs. Tween 80 cleavage in *C. amycolatum* compared with *C. accolens*. Therefore, despite the ability of *C. amycolatum* to grow without an external source of FAs, these are required for the inhibitory effect on *S. pneumoniae*. In aggregate, these results confirm and extend the importance of FA release following lipid hydrolysis for *Corynebacterium*-mediated inhibition of *S. pneumoniae in vitro* and identify differential requirements in distinct *Corynebacterium* species.

Corynebacterium Species Colonize the Upper and Lower Airway of Antibiotic Treated Mice

In order to investigate whether *Corynebacterium* species mediate inhibition of *S. pneumoniae in vivo*, we first established a model of short-term *Corynebacterium* colonization. Mice were treated for 1 week with water containing an antibiotic cocktail to reduce the endogenous flora. One week of antibiotic treatment significantly decreased the total microbial burden in both

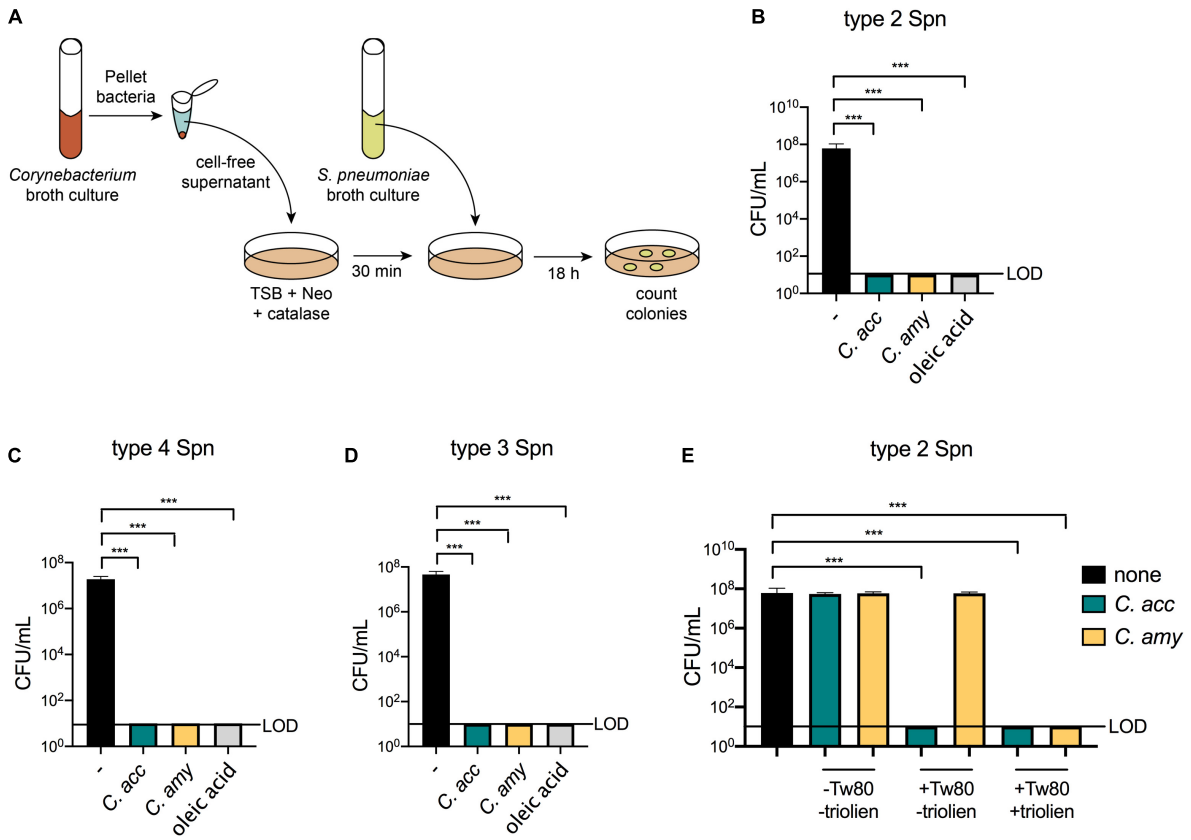

FIGURE 1 | Inhibition of *S. pneumoniae* growth *in vitro* by lipophilic and non-lipophilic *Corynebacterium* species. Supernatant inhibition assay schematic using tryptic soy broth (TSB), neomycin (Neo), and catalase plates **(A)**. Growth of type 2 *S. pneumoniae* (Spn), **(B)**, type 4 Spn **(C)**, and type 3 Spn **(D)** on untreated plates (–) or on plates pre-treated with supernatants from *C. accolens* (*C. acc*) or *C. amycolatum* (*C. amy*) or with 180 mg/mL oleic acid. Growth of type 2 Spn on untreated plates (–) or on plates pre-treated with supernatants from *C. acc* or *C. amy* grown in BHI with or without 1% Tween 80 and 180 mg/mL triolein **(E)**. Limit of detection (LOD) is indicated. Data are pooled from three independent experiments in duplicate. ***$p < 0.001$, ANOVA.

the upper airway and gut (**Supplementary Figure 2**). Mice were taken off antibiotics 2 days prior to intranasal (i.n.) infection with *C. accolens*, *C. amycolatum*, or PBS (control), and *Corynebacterium* burdens were determined 2 days following infection (**Figure 2A**). Both *C. accolens* and *C. amycolatum* were detected in the upper airway (nasal lavage) and lungs of mice 48 h post-infection as measured by live CFU counts from nasal lavage fluid and homogenized lung tissue of mice infected with *Corynebacterium* species, but not PBS-treated controls (**Figure 2B**). Both sites were successfully colonized, albeit with generally higher numbers in the lungs than in the upper airway. These data indicate that both lipophilic and non-lipophilic *Corynebacterium* species can successfully colonize the airway of antibiotic-treated mice. In order to determine the availability of FAs in the murine upper airway, as well as whether *Corynebacterium* colonization influenced FA content, nasal lavage fluids were analyzed by mass spectrometry (MS). Several FAs were detected in the nasal lavage fluid, including oleic acid, myristic acid, and palmitoleic acid (**Figure 2C**), all of which are also present in human nasal lavage fluid (Do et al., 2008). These data are consistent with the presence of FAs in the upper airway of mice which are capable of supporting *Corynebacterium* growth. However, *Corynebacterium* colonization did not significantly alter the relative abundances of any of the FAs detected (**Figure 2C**). These data suggest that either short-term colonization is not sufficient to alter the FA landscape, or that FA turnover by host or bacterial metabolic processes obscured any temporal changes. This model for short-term *Corynebacterium* colonization of the murine airway provided the opportunity to characterize the physiologic and pathologic impact of these commensals on pneumococcal infection.

Inflammatory Myeloid Cells Are Recruited to the Lungs of *Corynebacterium*-Colonized Mice

We next interrogated the impact of short-term *Corynebacterium* colonization on local and systemic cytokine production as well as the recruitment of inflammatory myeloid cells to the lung. Both *C. accolens* and *C. amycolatum* induced a significant increase in systemic levels of the pro-inflammatory cytokines TNFα and IFNγ, compared with PBS-treated mice (**Figure 3A**). In the lung, however, we found that *Corynebacterium* colonization

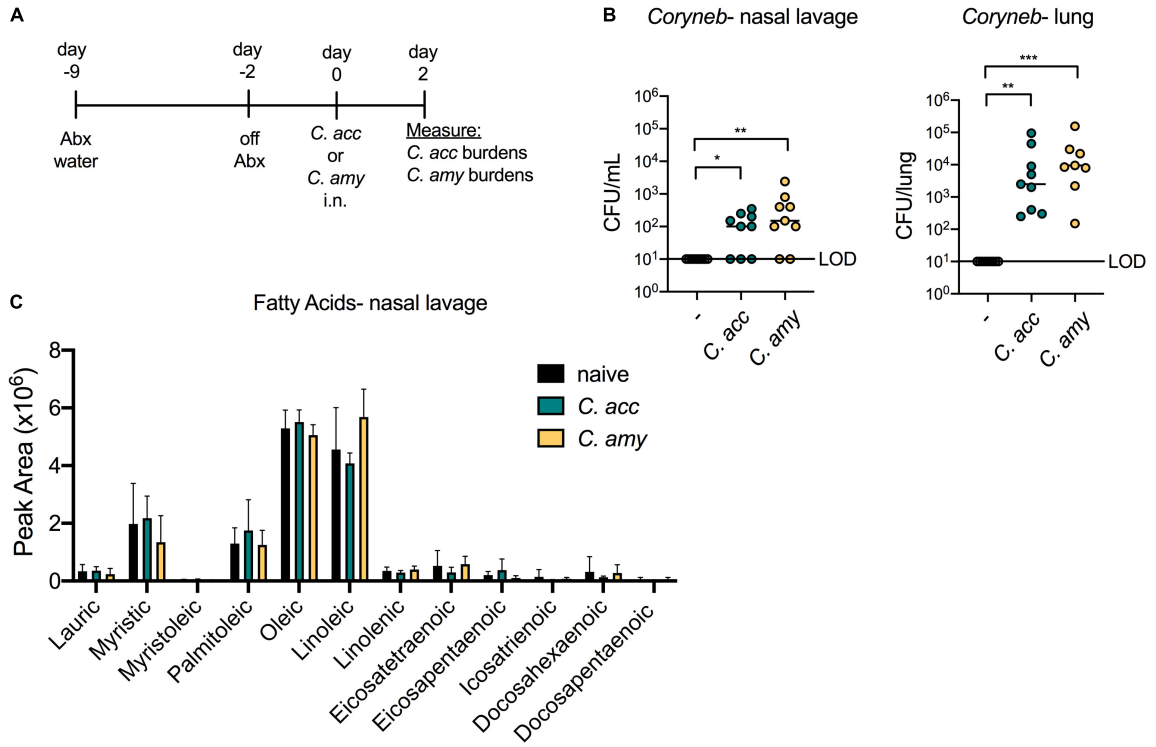

FIGURE 2 | *Corynebacterium* species colonize the upper and lower airway of antibiotic treated mice. Timeline for antibiotic treatment followed by infection with *C. acc* or *C. amy* **(A)**. Burden of *Corynebacterium* (*Coryneb*) in the nasal lavage fluid and lungs of mice 48 h post-infection with *C. acc*, *C. amy*, or PBS (–) detected by live growth **(B)**. Relative abundance of fatty acids detected in the nasal lavage fluid of naïve mice and mice 48 h post-infection with *C. acc* or *C. amy* **(C)**. Data are pooled from three independent experiments with 3–6 mice per group. No significant differences detected in relative FA abundances between groups, ANOVA. $^{*}p < 0.05$, $^{**}p < 0.01$, $^{***}p < 0.001$, Kruskal-Wallis test.

had little impact on cytokine expression in the bronchoalveolar lavage fluid (BAL) at 48 h post-infection, as measured by a 13-plex inflammatory cytokine/chemokine array. Of the 13 cytokines and chemokines tested, only MCP-1 (CCL2), an important chemokine for monocyte and macrophage recruitment (Gschwandtner et al., 2019), was significantly upregulated in the BAL of *C. accolens* and *C. amycolatum*-colonized mice (**Figure 3B** and not shown). These findings indicate that *Corynebacterium* colonization is associated with increased circulating pro-inflammatory cytokines, but a minimal such response in the lung.

We determined the impact of *Corynebacterium* colonization on lung innate immune cell populations by flow cytometry (see gating strategy, **Supplementary Figure 3**). *Corynebacterium* colonization was associated with an increase of both neutrophils ($CD45^+Ly6G^+CD11b^+$ cells) and inflammatory monocytes ($CD45^+Ly6G^-Ly6C^+CD11b^+$ cells) in the lung (**Figures 3C,D**). These increases parallel the elevated MCP-1, which mobilizes the recruitment of inflammatory monocytes from the bone marrow (Gschwandtner et al., 2019), detected in the BAL of *Corynebacterium*-infected mice. Neutrophils are also recruited to the lung from the bone marrow, though responses to other chemokines such as MIP-1 (CXCL2) (Lin and Fessler, 2021) were not measured here. In contrast, the lungs of mice infected with *C. accolens* or *C. amycolatum* had reduced alveolar macrophages (AMs, $CD45^+SiglecF^+CD11b^{low}CD11c^+$ cells), compared with PBS treated controls (**Figure 3E**). Unlike neutrophils and inflammatory monocytes, AMs are largely self-renewing locally in the lung. As the first immune cell to encounter inhaled particles, AMs frequently undergo cell death following bacterial uptake (FitzGerald et al., 2020), consistent with our observation of reduced AMs in the lungs of *Corynebacterium* infected mice. We detected no changes in $CD103^+$ dendritic cells (DCs, $CD45^+MHCII^+SiglecF^-CD11c^+CD64^-$ cells) or $CD11b^{hi}$ DCs, or the expression of MHCII in either population as an indicator of activation, in *Corynebacterium*-infected mice compared with PBS-treated controls (**Supplementary Figure 4**). Collectively, these data indicate that *Corynebacterium* colonization is associated with selective mucosal responses, including increased chemokine-associated myeloid cell recruitment to the lung but minimal changes to the local pro-inflammatory cytokine landscape.

Colonization With *Corynebacterium* Inhibits Colonization and Infection With *S. pneumoniae in vivo*

Our goal in establishing a model for *Corynebacterium* colonization was to evaluate whether *Corynebacterium* species inhibit the acquisition and growth of *S. pneumoniae*

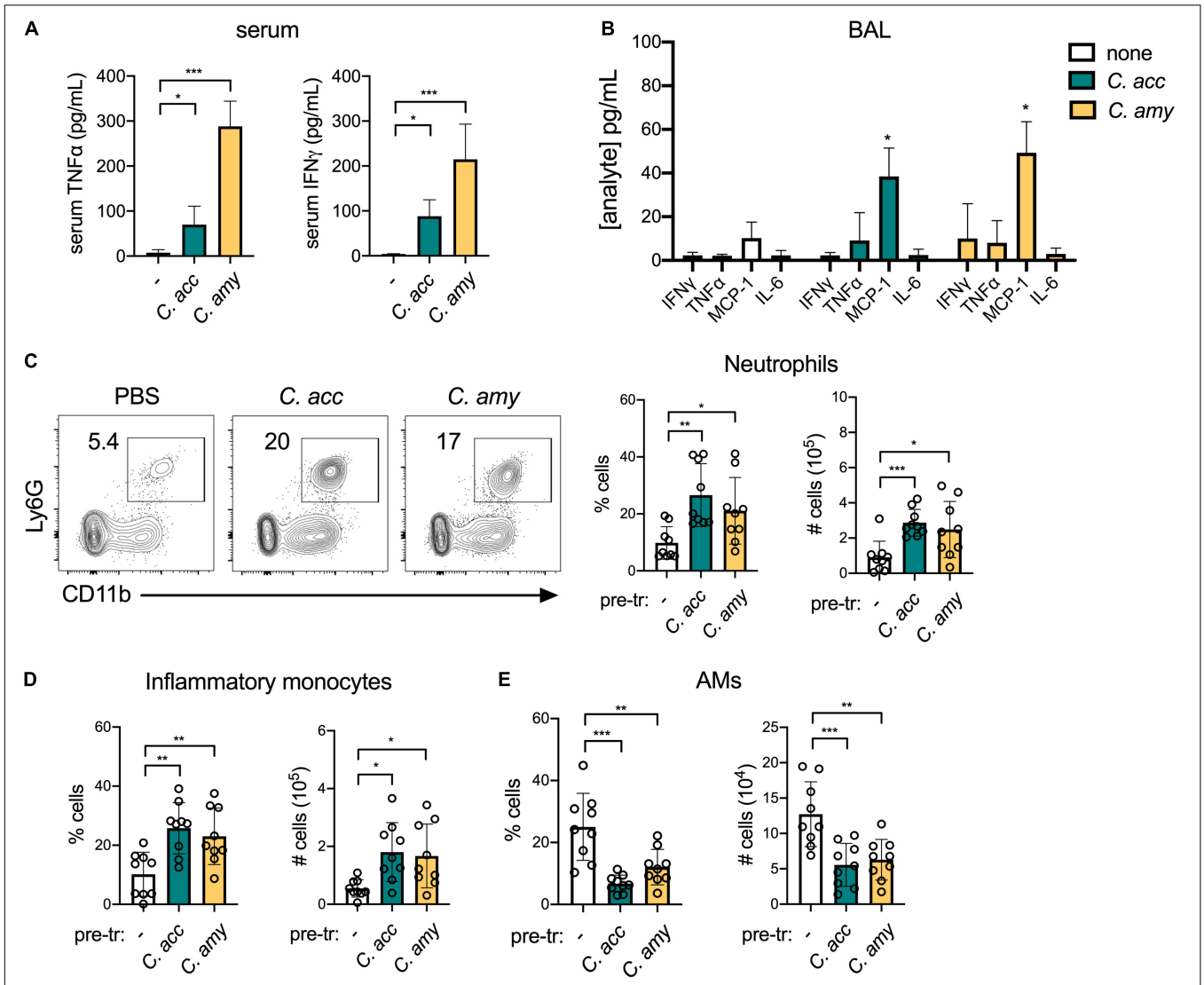

FIGURE 3 | Inflammatory myeloid cells are recruited to the lungs of *Corynebacterium*-colonized mice. Systemic TNFα and IFNγ detected in mice 48 h post-infection with *C. acc*, *C. amy*, or PBS (–) **(A)**. Cytokines and chemokines detected in lung BAL in mice 48 h post-infection with *C. acc* or *C. amy* **(B)**, with significance indicated relative to mice pre-exposed to PBS (none). Percentage and total number of neutrophils ($CD45^+SiglecF^-Ly6G^+CD11b^+$ cells) **(C)**, inflammatory monocytes ($CD45^+$ $Ly6G^-Ly6C^+CD11b^+$ cells) **(D)**, and alveolar macrophages (AMs, $CD45^+SiglecF^+CD11b^{low}CD11c^+$ cells) **(E)** detected by flow cytometry in the lungs of mice 48 h post-infection with *C. acc*, *C. amy,* or PBS (–). Data are pooled from three independent experiments with 3–6 mice per group. $^*p < 0.05$, $^{**}p < 0.01$, $^{***}p < 0.001$, ANOVA.

in vivo, similar to *Corynebacterium*-mediated inhibition of *S. pneumoniae* observed by our group and others *in vitro*. We exposed antibiotic-treated mice to *C. accolens* or *C. amycolatum* 1 day prior to intranasal infection with streptomycin-resistant type 2 *S. pneumoniae* and plated nasal lavage contents and lung homogenates on selective media containing streptomycin 1 day later (**Figure 4A**). Compared with mice pre-exposed to PBS, colonization with either *C. accolens* or *C. amycolatum* significantly reduced the burden of *S. pneumoniae* in both the upper airway (nasal lavage) and lung by 24 h post-infection (**Figure 4B**). In mice pre-exposed to *Corynebacterium*, *S. pneumoniae* burdens were reduced by ∼1 log in the upper airway, and *S. pneumoniae* was not detected in the lungs of 50–60% of the animals in each *Corynebacterium* exposure group. *C. accolens* and *C. amycolatum* burdens remained detectable following growth in non-selective media in the majority of co-infected mice at this timepoint (**Figure 4C**). Further, mice with the highest *Corynebacterium* burdens had the lowest, frequently undetectable, *S. pneumoniae* burdens in the lung (**Supplementary Figures 5A,B**). Our data are consistent with longitudinal microbiome sequencing studies which suggest that *Corynebacterium* abundance predicts *S. pneumoniae* acquisition and infection risk in children (Biesbroek et al., 2014; Teo et al., 2015;

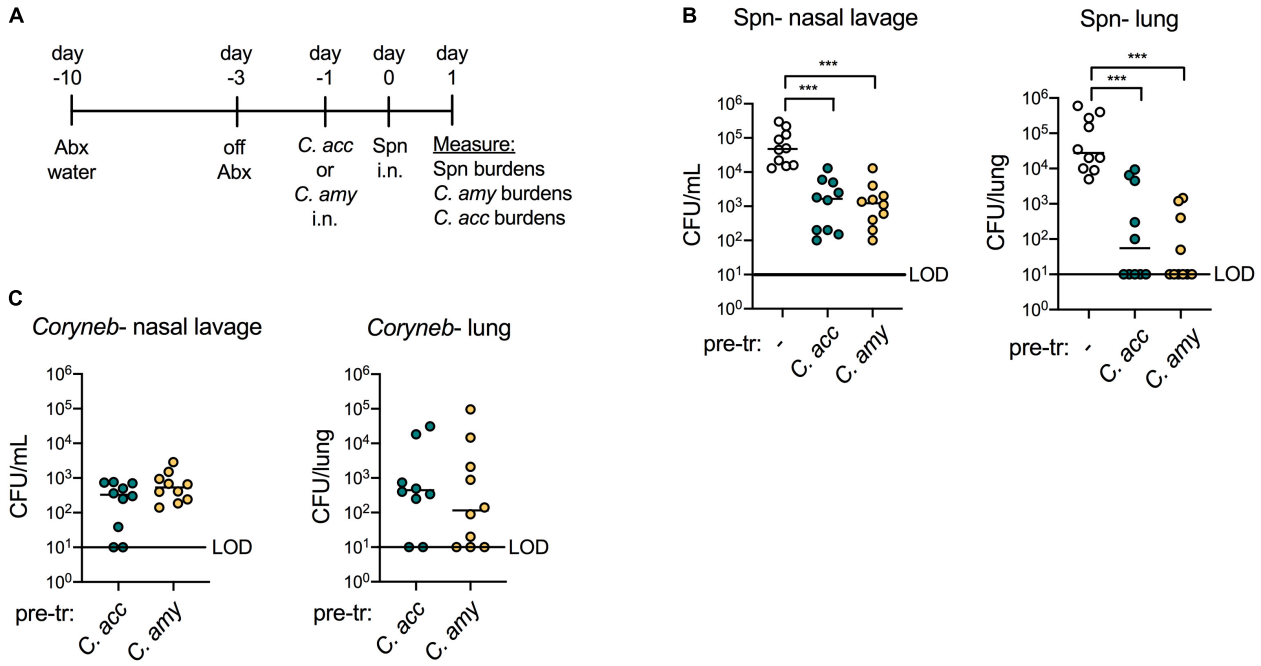

FIGURE 4 | Colonization with *Corynebacterium* inhibits colonization and infection with *S. pneumoniae in vivo*. Timeline for antibiotic treatment followed by pre-exposure to PBS (–), *C. acc* or *C. amy* prior to infection with *S. pneumoniae* (Spn) **(A)**. Burden of Spn **(B)** or *Corynebacterium* (*Coryneb*) **(C)** in nasal lavage fluid and lungs of mice pre-exposed to PBS (–), *C. acc* or *C. amy* at 24 h post-Spn infection detected by live growth. Limit of detection (LOD) is indicated. Data are pooled from three independent experiments with 3–5 mice per group. ***$p < 0.001$, Kruskal-Wallis test.

Bosch et al., 2017; Kelly et al., 2021). Of particular note, these studies demonstrate the potential for live animal modeling of *Corynebacterium-S. pneumoniae* dynamics *in vivo* in order to elucidate the bacterial and host requirements for *Corynebacterium*-mediated protection against respiratory tract infection.

Reduced Inflammation and Inflammatory Myeloid Cell Recruitment in the Lungs of *Corynebacterium-S. pneumoniae* Co-infected Mice

Corynebacterium co-infected mice also had a reduced inflammatory response in the lung compared to mice infected with *S. pneumoniae* alone. In contrast to *S. pneumoniae* challenged mice pre-exposed to PBS, systemic TNFα and IFNγ were reduced in mice pre-exposed to *C. accolens* or *C. amycolatum* (**Figure 5A**). Similarly, in the BAL of co-infected mice, levels of several pro-inflammatory cytokines including TNFα, IFNγ, and IL-6 as well as the chemokine MCP-1 were reduced in mice pre-exposed to *Corynebacterium* compared to mice infected with *S. pneumoniae* alone (**Figure 5B**), while 9 other cytokines were not affected (not shown). Total neutrophils and inflammatory monocytes in the lungs of co-infected mice were also reduced compared with mice infected with *S. pneumoniae* alone (**Figures 5C,D**). In contrast, AMs were increased in co-infected mice (**Figure 5E**). Overall populations of lung DCs, which are important for mobilizing the adaptive immune response but may also facilitate pneumococcal dissemination (Rosendahl et al., 2013), remained the same, although $CD103^+$ DC expression of the activation marker MHCII was significantly reduced in *Corynebacterium* co-infected mice compared to mice infected with *S. pneumoniae* alone (**Supplementary Figure 6**). The reduction in inflammatory myeloid cells together with the recovery of AMs, which are important for the resolution of inflammation in the lung, is consistent with a pro-resolving immune response in the lungs of co-infected mice. We conclude that colonization with either *C. accolens* or *C. amycolatum* improves early clearance of *S. pneumoniae* from the upper and lower airways of mice, in association with reduced, rather than enhanced, inflammation in the lung, likely limiting lung injury.

Corynebacterium Lipases Contribute to, but Are Not Required for, Protection Against *S. pneumoniae in vivo*

We next sought to confirm the importance of the lipase LipS1 for *C. accolens*-mediated inhibition of *S. pneumoniae* growth *in vitro* and to determine whether *C. amycolatum* expresses a lipase with similar activity. We first constructed a *lipS1* mutant in our strain of *C. accolens* by in-frame gene deletion. As described for the original Δ*lipS1 C. accolens*, our Δ*lipS1 C. accolens* grew poorly in triolein as the sole source of FAs (Bomar et al., 2016), indicating LipS1 as critical for lipase-mediated hydrolysis and growth in *C. accolens* (**Supplementary Figure 7A**). In contrast, growth of

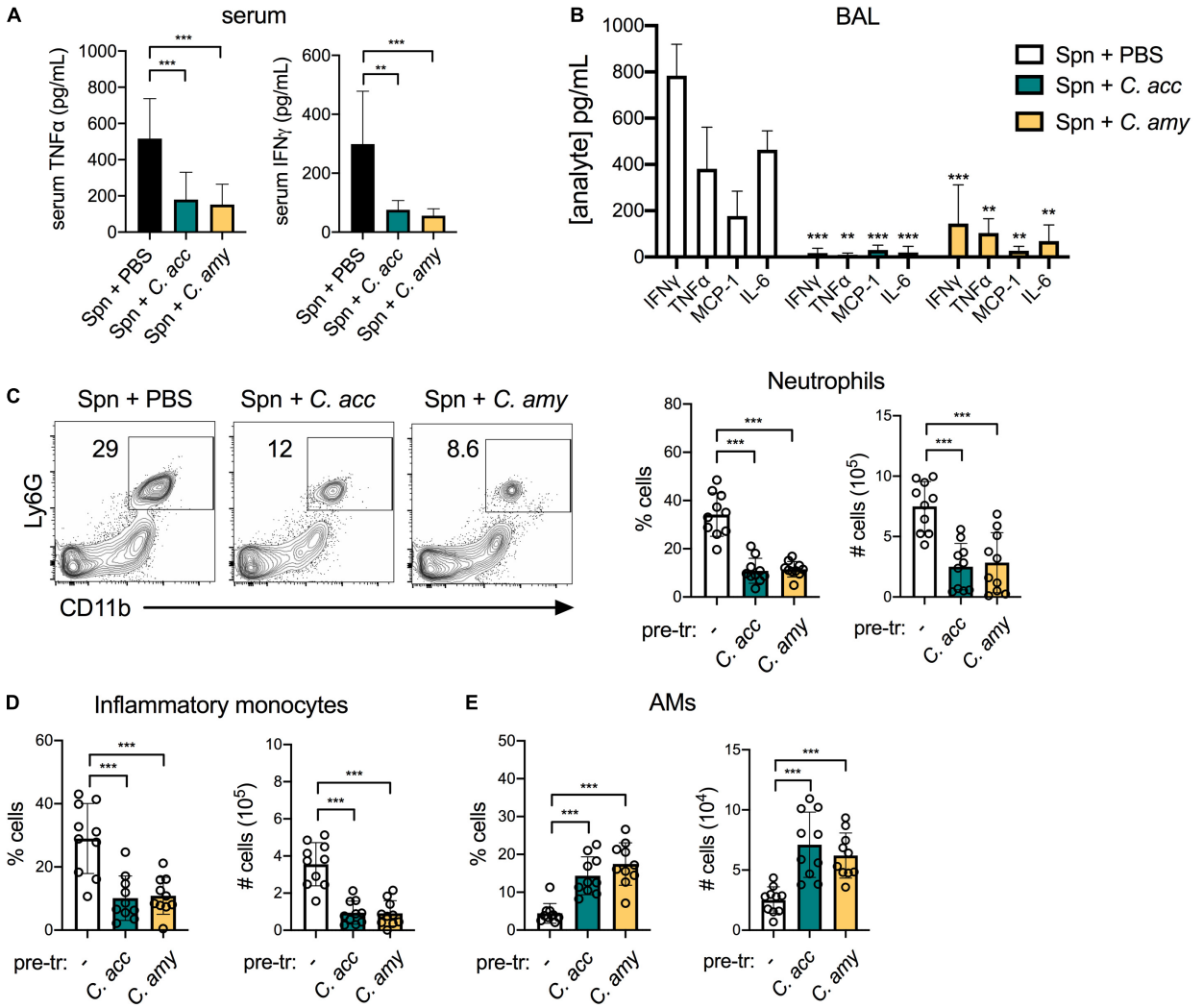

FIGURE 5 | Reduced inflammation and inflammatory myeloid cell recruitment in the lungs of *Corynebacterium-S. pneumoniae* co-infected mice. Systemic TNFα and IFNγ detected in mice pre-exposed to PBS (–), *C. acc* or *C. amy* at 24 h post-*S. pneumoniae* (Spn) infection **(A)**. Cytokines and chemokines detected in lung BAL in mice pre-exposed to PBS (–), *C. acc* or *C. amy* at 24 h post-Spn infection **(B)**, significance indicated relative to mice pre-exposed to PBS (none). Percentage and total number of neutrophils **(C)**, inflammatory monocytes **(D)**, and alveolar macrophages (AMs) **(E)** detected by flow cytometry in the lungs of mice pre-exposed to PBS (–), *C. acc* or *C. amy* at 24 h post-Spn infection. Data are pooled from three independent experiments with 3–5 mice per group. $^{**}p < 0.01$, $^{***}p < 0.001$, ANOVA.

Δ*lipS1 C. accolens* in Tween 80 was not impaired relative to wild-type (WT) *C. accolens*, presumably due to the hydrolysis of Tween 80 by bacterial esterases.

Bacterial lipases in both *C. accolens* and *C. amycolatum* are essential for *Corynebacterium*-mediated inhibition of *S. pneumoniae* growth *in vitro* but have distinct characteristics. Supernatants from Δ*lipS1 C. accolens* did not inhibit *S. pneumoniae* growth *in vitro*, whereas those from WT *C. accolens* did (**Figure 6A**), confirming the importance of LipS1 for *S. pneumoniae* inhibition *in vitro*. A search for similar bacterial lipases in *C. amycolatum* in the NCBI database identified the protein WP_005510233.1 as sharing the greatest homology with that of *C. accolens* LipS1 (WP_005285206.1). Though overall protein sequence homology to *C. accolens* LipS1 was low (36%), the NCBI Conserved Domain Database (CDD, version cdd.v.3.19) (Lu et al., 2019) classified WP_005510233.1 as a member of the LIP family of secretory lipases with an *E*-value of $2.94e^{-33}$, similar to *C. accolens* LipS1. *C. amycolatum* WP_005510233.1 also contains the lipase motif G-X-S-X-G with a predicted active site serine residue (Jaeger et al., 1994), a shared feature among bacterial lipases. Analysis using the SignalP program (version 5.0) (Petersen et al., 2011) indicated that while both *C. accolens* LipS1 and *C. amycolatum* WP_005510233.1 are predicted to be secreted by the general secretion pathway (Sec), LipS1 contains an SP1 cleavage site, whereas *C. amycolatum* WP_005510233.1 contains an SPII cleavage site. Based on this analysis, we generated an in-frame deletion of WP_005510233.1 in *C. amycolatum*, referred to

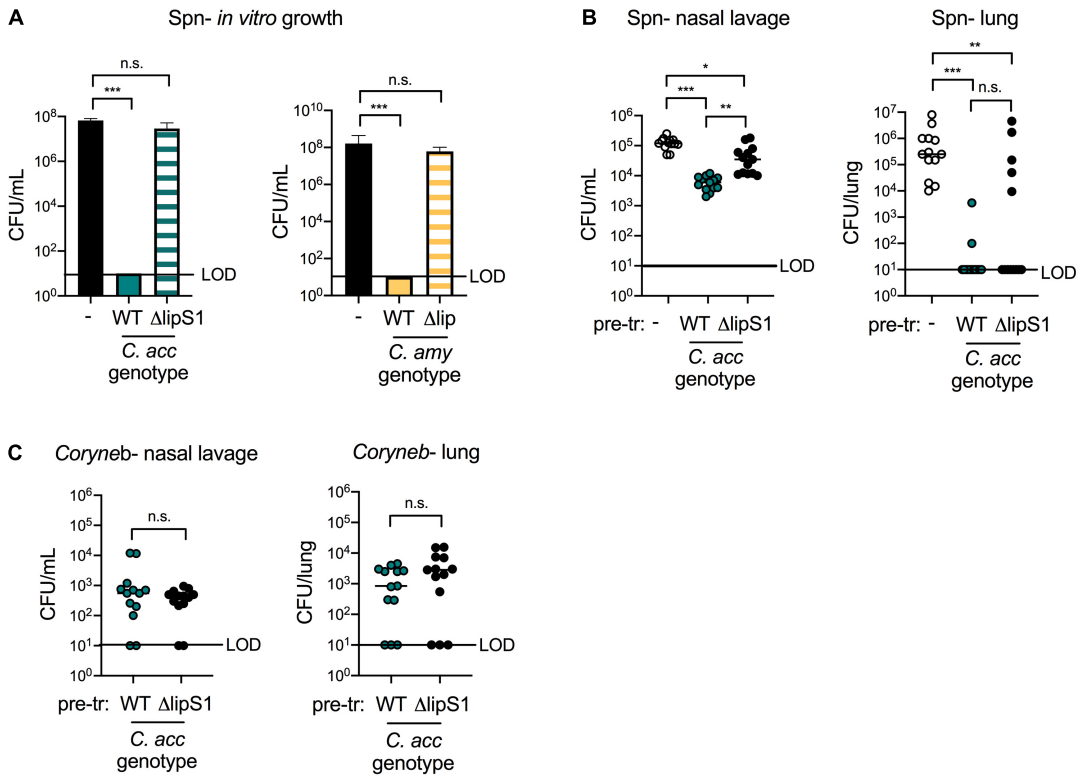

FIGURE 6 | *Corynebacterium* lipases contribute to, but are not required for, protection against *S. pneumoniae in vivo*. Growth of type 2 *S. pneumoniae* (Spn) on untreated plates (–) or on plates pre-treated with supernatants from WT vs. Δ*lipS1 C. acc* or WT vs. Δ*lip C. amy* grown in BHI with 1% Tween 80 and 180 mg/mL triolein **(A)**. Burden of Spn **(B)** or *Corynebacterium* (*Coryneb*) **(C)** in nasal lavage fluid and lungs of mice pre-exposed to PBS (–), WT *C. acc* or Δ*lipS1 C. acc* at 24 h post-Spn infection detected by live growth. Limit of detection (LOD) is indicated. Data are pooled from three independent experiments with 3–5 mice per group. $^{*}p < 0.05$, $^{**}p < 0.01$, $^{***}p < 0.001$, ANOVA **(A)** or Kruskal-Wallis test **(B,C)**.

as Δ*lip C. amycolatum*, to determine whether this putative lipase contributes to *C. amycolatum*-mediated inhibition of *S. pneumoniae* growth. As *C. amycolatum* is non-lipophilic, Δ*lip C. amycolatum* grew similarly to WT in either Tween 80 or triolein (**Supplementary Figure 7B**). However, supernatant from Δ*lip C. amycolatum* no longer inhibited *S. pneumoniae* growth *in vitro* (**Figure 6A**), suggesting that this lipase is critical for *C. amycolatum*-mediated inhibition *in vitro*.

Lipases such as LipS1 and/or other bacterial factors may contribute to *Corynebacterium*-mediated protection against *S. pneumoniae in vivo*. Using our co-infection animal model, we compared the impact of pre-exposure to WT vs. Δ*lipS1 C. accolens* on *S. pneumoniae* colonization and infection. *S. pneumoniae* burdens in the upper airway (nasal lavage) were higher in mice pre-exposed to Δ*lipS1 C. accolens* compared to mice pre-exposed to WT *C. accolens* (**Figure 6B**). However, there was still a significant reduction in upper airway *S. pneumoniae* burdens in mice pre-exposed to Δ*lipS1 C. accolens* compared to mice infected with *S. pneumoniae* alone. These findings indicate that *C. accolens* expression of LipS1 contributes to, but is not solely required for, inhibition of *S. pneumoniae* colonization in the upper airway. In the lungs, mice pre-exposed to either Δ*lipS1* or WT *C. accolens* had significantly reduced burdens of *S. pneumoniae* compared with mice infected with *S. pneumoniae* alone (**Figure 6B**). There was a slight increase in the percentage of mice with detectable *S. pneumoniae* burdens in the lung following pre-exposure to Δ*lipS1 C. accolens* (38%) vs. WT *C. accolens* (15%), similar to the upper airway, however, this difference was not statistically significant. Burdens of WT and Δ*lipS1 C. accolens* in the nasal lavage and lungs of co-infected mice were similar (**Figure 6C**), indicating no colonization defect for Δ*lipS1 C. accolens*. Also, mice with the highest burdens of either WT or Δ*lipS1 C. accolens* correlated with lower and frequently undetectable burdens of *S. pneumoniae* in the lung (**Supplementary Figure 5C**), confirming a relationship between *C. accolens* abundance and reduced *S. pneumoniae* infection of the lung. These data indicate that multiple mechanisms, both LipS1-dependent and independent, contribute to *Corynebacterium*-mediated protection against *S. pneumoniae in vivo*.

DISCUSSION

Our findings provide novel evidence in support of the potential benefit of *Corynebacterium* abundance in the airway. Both *C. accolens* and *C. amycolatum* inhibited *S. pneumoniae* growth *in vitro*, observations corroborated by protection *in vivo*

using a new co-infection model. The only mechanism for *Corynebacterium*-mediated protection against *S. pneumoniae* described thus far is the liberation of host FAs by LipS1 in *C. accolens* (Bomar et al., 2016), as confirmed herein both *in vitro* and *in vivo*. Beyond direct killing of *S. pneumoniae*, FAs induce expression of the antimicrobial peptide β-defensin-2 by human sebocytes (Nakatsuji et al., 2010), which may further enhance protection against *S. pneumoniae* in the airway. We demonstrate that FAs are present in the upper airway of mice, as in humans (Do et al., 2008), consistent with their availability to serve as a nutrient source for lipophilic *Corynebacterium* such as *C. accolens*. The finding that *Corynebacterium* colonization did not influence FA abundance may result from a lack of accessible triacylglycerols for FA production, as has been suggested (Bomar et al., 2016), metabolic turnover, or temporal fluctuations which were missed. Alternatively, we did not determine whether the expression of LipS1 is upregulated in co-infected mice. Regardless, the observation that LipS1-deficient *C. accolens* is less protective against *S. pneumoniae* suggests that lipase activity contributes to *S. pneumoniae* killing *in vivo*. Others have confirmed that the mouse airway can be colonized with endogenous *Corynebacterium*, which becomes the dominant genus following treatment with the antibiotic neomycin (Ichinohe et al., 2011). This finding indicates that competition with the resident microbiota limits *Corynebacterium* colonization, consistent with our inability to establish *Corynebacterium* colonization in non-antibiotic-treated mice (not shown). Thus, while host lipids, including FAs, are present in the mouse airway, microbial depletion is likely a requirement for modeling *Corynebacterium* colonization.

The partial protective effect of LipS1-deficient *C. accolens* indicates a role for additional mechanisms of *Corynebacterium*-mediated protection *in vivo*. *S. pneumoniae* and other opportunistic pathogens are enriched following antibiotic therapy in children, whereas *Corynebacterium* are reduced (Teo et al., 2015; Kelly et al., 2021), suggesting that *S. pneumoniae* is better equipped for expansion into the microbiome-depleted airway. We found that colonizing mice with *Corynebacterium* prior to *S. pneumoniae* exposure is sufficient to reverse this expansion. In addition to competition with pathogens through the expression of bacterial lipases, some *Corynebacterium* species produce siderophores, which reduce growth of the pathogen *Staphylococcus aureus* in iron-limiting environments (Stubbendieck et al., 2019), although the potential impact on *S. pneumoniae* is not known. Beyond competition for niche space and nutrients, interactions between *Corynebacterium* and airway epithelial cells may contribute to enhanced protection against *S. pneumoniae in vivo*. For example, some species of *Corynebacterium* express the molecule phosphorylcholine (ChoP) (Gillespie et al., 1996), which binds to platelet activating factor receptor (PAFR), a critical adherence receptor for *S. pneumoniae* (Rijneveld et al., 2004). ChoP expression by selected *Corynebacterium* species may therefore interfere with *S. pneumoniae* access to PAFR, reducing *S. pneumoniae* acquisition and infection. Moreover, *Corynebacterium* activation of airway epithelial cells may enhance their production of antimicrobial peptides in a FA-independent manner, as with other airway commensals (Liu et al., 2019). Finally, *Corynebacterium*-mediated recruitment of inflammatory myeloid cells, as we observed in the lung, may serve as an immune priming signal to enhance clearance of *S. pneumoniae*, as neutrophils and inflammatory monocytes are critical for early *S. pneumoniae* killing (Calbo and Garau, 2010). The development of an animal model for *Corynebacterium* colonization, which mirrors the relationship between *Corynebacterium* abundance and risk of *S. pneumoniae* acquisition observed in humans, should facilitate investigation of these and other mechanisms in future studies. However, translation of such findings in mice into novel therapeutic approaches will require verification that similar effects are active during human colonization with *Corynebacterium*.

In these studies, two morphologically and metabolically distinct species of *Corynebacterium* protected against *S. pneumoniae* growth. The non-lipophilic *C. amycolatum* was only inhibitory *in vitro* upon the addition of multiple FA sources, indicating that screens which do not incorporate enough exogenous lipids may miss the inhibitory potential of additional *Corynebacterium* clinical isolates. Indeed, while airway microbiome sequencing studies indicate a broadly protective role for *Corynebacterium* species against respiratory tract infections and *S. pneumoniae*, mechanistic studies have revealed heterogeneity among different *Corynebacterium*-pathogen pairs. For example, both *C. pseudodiphtheriticum* and *Corynebacterium striatum* inhibit growth of the pathogen *S. aureus*, whereas *C. accolens* instead promotes *S. aureus* growth *in vitro* (Yan et al., 2013; Ramsey et al., 2016). *C. pseudodiphtheriticum* mediates a broadly protective effect against primary and secondary *S. pneumoniae* infections (Kanmani et al., 2017; Moyano et al., 2020) and also inhibits growth of another pathogen, *Moraxella catarrhalis*, *in vitro* (Lappan and Peacock, 2019). The potential therapeutic effect of *C. pseudodiphtheriticum* has been evaluated in humans, where delivery by nasal spray was shown to reduce colonization with *S. aureus* in healthy adults (Kiryukhina et al., 2013). While this was only tested in four subjects, another *Corynebacterium* designated as strain Co304 had a similar effect in another 17 subjects (Uehara et al., 2000). The impact of other *Corynebacterium* species, including those such as *C. accolens* which may inhibit some pathogens but promote others, on a broader infection profile will be important to determine in future studies.

Colonization of mice by both species of *Corynebacterium* (*C. accolens* and *C. amycolatum*) elicited comparably robust myeloid cell responses in the lung in parallel with elevations in the chemotactic protein MCP-1. However, neither species induced appreciable expression of pro-inflammatory cytokines in lung BAL. As reported following colonization with *C. pseudodiphtheriticum* in infant mice (Kanmani et al., 2017), both TNFα and IFNγ were increased in the serum, as in our study, but, unlike our results, several pro-inflammatory cytokines were also increased in the BAL, highlighting the importance of investigating species-specific outcomes. Colonization at different host sites may also induce distinct immune activation profiles. We did not detect an IL-17A response in the lungs of *Corynebacterium*-exposed mice, whereas skin colonization with

C. accolens, but not *C. amycolatum*, was associated with the induction of a γδT cell IL-17A response (Ridaura et al., 2018). The lung is particularly sensitive to the detrimental effects of inflammation, which causes damage to the integrity of the barrier, reducing oxygen exchange (Muller-Redetzky et al., 2014). *S. pneumoniae* co-infections, particularly with viral pathogens, are associated with an enhanced inflammatory response, promoting inflammation-mediated damage in the co-infected lung and leading to increased morbidity and mortality (Kash et al., 2011; Aguilera and Lenz, 2020). In contrast, we find that, unlike with respiratory viral and other pathogens, co-infection with *Corynebacterium* tempers the inflammatory response to *S. pneumoniae*, as described for *C. pseudodiphtheriticum* in the context of sterile lung injury (Kanmani et al., 2017; Moyano et al., 2020), along with *S. pneumoniae* clearance, indicating the potential to improve lung recovery from infection and injury.

A limitation of this study is that we did not investigate co-colonization with *Dolosigranulum*, which frequently associates with *Corynebacterium* in the human upper airway of humans (Bogaert et al., 2011; Laufer et al., 2011; Copeland et al., 2018). Abundances of several different *Corynebacterium* species are increased in both child and adult carriers of *Dolosigranulum* (Brugger et al., 2020). *In vitro*, these authors demonstrated that some *Corynebacterium* species support growth of *Dolosigranulum pigrum*, although not consistently (Brugger et al., 2020). Further, *S. pneumoniae* growth was inhibited *in vitro* by *D. pigrum* and *C. pseudodiphtheriticum*, neither of which were inhibitory on their own under the assay conditions used (Brugger et al., 2020). This study alludes to greater complexity in the human airway, where *Corynebacterium*-pathogen interactions are likely influenced by the presence of other commensal species including *Dolosigranulum*. In addition, *Corynebacterium* and *Dolosigranulum* must themselves compete with other airway commensals. For example, *Staphylococcus epidermidis* can inhibit both *D. pilgrim* and *C. pseudodiphtheriticum* growth *in vitro* (Janek et al., 2016). These findings highlight the importance of considering multiple commensal-pathogen dynamics in the airway, beyond interactions between specific commensal-pathogen pairs.

In summary, these studies identify *C. accolens* and *C. amycolatum* as *Corynebacterium* species which are capable of short-term colonization in antibiotic treated mice. Further, pre-exposure to either of these *Corynebacterium* species significantly reduces *S. pneumoniae* infection while mitigating lung inflammation. Although the host and bacterial requirements for *Corynebacterium*-mediated protection against *S. pneumoniae* are not fully resolved, both *C. accolens* and *C. amycolatum* express bacterial lipases which contribute to growth inhibition *in vitro*, a mechanism responsible, in part, for *C. accolens*-mediated protection *in vivo*. These findings indicate that therapeutic strategies to enhance *Corynebacterium* colonization may reduce the risk of *S. pneumoniae* acquisition and infection. We envision that such approaches would be particularly beneficial following antibiotic therapy, when the endogenous airway microbiome is disrupted. However, it is also important to consider potential adverse effects associated with enhanced *Corynebacterium* colonization, as some species may serve as a source of opportunistic infections. Improved understanding of the mechanisms of *Corynebacterium*-mediated protection will therefore facilitate harnessing the potential therapeutic benefit of these endogenous "protector" bacteria.

DATA AVAILABILITY STATEMENT

The original contributions presented in the study are included in the article/**Supplementary Material**, further inquiries can be directed to the corresponding author/s.

ETHICS STATEMENT

Animal studies were reviewed and approved by the Animal Care and Use Committee of the University of Colorado School of Medicine.

AUTHOR CONTRIBUTIONS

SC conceived the study and designed the experiments together with VA, EJ, and SA. SC, KH, VA, and SA performed the experiments. SC wrote the manuscript. SC and EJ edited the manuscript. All authors contributed to the article and approved the submitted version.

FUNDING

This work was funded by a Career Transition Award K22AI143922 (SC) and an R21 award AI146295 (EJ) from the National Institute of Allergy and Infectious Diseases of the National Institutes of Health, an American Lung Association Innovation Award (SC), the Boettcher Foundation Webb-Waring Biomedical Research Award (SC), and the Veterans Affairs Research Service (Merit Review I01BX004320) (EJ). AJ was supported by the MARC U-STAR T34 Program grant GM141639.

ACKNOWLEDGMENTS

We wish to acknowledge members of the University of Colorado School of Medicine Metabolomics Core, including Micaela Roy and Julie Haines, for their contributions to this manuscript. We also acknowledge the National Summer Undergraduate Research Project (NSURP) and the Colorado Undergraduate Summer Research Program (CUSP) for programmatic support of VA and AJ, respectively. Finally, we thank their colleagues in the Department of Otolaryngology and Department of Immunology and Microbiology for contributing to critical analysis and discussions of these data.

SUPPLEMENTARY MATERIAL

The Supplementary Material for this article can be found online at: https://www.frontiersin.org/articles/10.3389/fmicb.2021.804935/full#supplementary-material

REFERENCES

Aguilera, E. R., and Lenz, L. L. (2020). Inflammation as a modulator of host susceptibility to pulmonary influenza, pneumococcal, and co-infections. *Front. Immunol.* 11:105. doi: 10.3389/fimmu.2020.00105

Bernard, K. (2012). The genus *Corynebacterium* and other medically relevant coryneform-like bacteria. *J. Clin. Microbiol.* 50, 3152–3158. doi: 10.1128/JCM.00796-12

Biesbroek, G., Tsivtsivadze, E., Sanders, E. A. M., Montijn, R., Veenhoven, R. H., Keijser, B. J. F., et al. (2014). Early respiratory microbiota composition determines bacterial succession patterns and respiratory health in children. *Am. J. Respir. Crit. Care Med.* 190, 1283–1292. doi: 10.1164/rccm.201407-1240OC

Bogaert, D., Keijser, B., Huse, S., Rossen, J., Veenhoven, R., van Gils, E., et al. (2011). Variability and diversity of nasopharyngeal microbiota in children: a metagenomic analysis. *PLoS One* 6:e17035. doi: 10.1371/journal.pone.0017035

Bomar, L., Brugger, S. D., Yost, B. H., Davies, S. S., and Lemon, K. P. (2016). *Corynebacterium accolens* Releases antipneumococcal free fatty acids from human nostril and skin surface triacylglycerols. *mBio* 7:e01725-15.

Bosch, A. A. T. M., Piters, W. A. A., de, S., van Houten, M. A., Chu, M. L. J. N., Biesbroek, G., et al. (2017). Maturation of the infant respiratory microbiota, environmental drivers, and health consequences. a prospective cohort study. *American J. Respir. Crit. Care Med.* 196, 1582–1590.

Brugger, S. D., Eslami, S. M., Pettigrew, M. M., Escapa, I. F., Henke, M. T., Kong, Y., et al. (2020). *Dolosigranulum pigrum* cooperation and competition in human nasal microbiota. *mSphere* 5:e00852-20. doi: 10.1128/mSphere.00852-20

Calbo, E., and Garau, J. (2010). Of mice and men: innate immunity in pneumococcal pneumonia. *Int. J. Antimicrob. Agents* 35, 107–113. doi: 10.1016/j.ijantimicag.2009.10.002

Centers for Disease Control and Prevention (2019). Deaths: final data for 2017. *Natl. Vital Stat. Rep.* 68, 1–80.

Chonmaitree, T., Jennings, K., Colovko, G., Khanipov, K., Pimenova, M., Patel, J. A., et al. (2017). Nasopharyngeal microbiota in infants and changes during viral upper respiratory tract infection and acute otitis media. *PLoS One* 12:e0180630. doi: 10.1371/journal.pone.0180630

Clark, S. E. (2020). Commensal bacteria in the upper respiratory tract regulate susceptibility to infection. *Curr. Opin. Immunol.* 66, 42–49. doi: 10.1016/j.coi.2020.03.010

Clark, S. E., Schmidt, R. L., Aguilera, E. R., and Lenz, L. L. (2020). IL-10-producing NK cells exacerbate sublethal *Streptococcus pneumoniae* infection in the lung. *Transl. Res.* 226, 70–82. doi: 10.1016/j.trsl.2020.07.001

Clementi, E. A., Wilhelm, K. R., Schleucher, J., Morozova-Roche, L. A., and Hakansson, A. P. (2013). A complex of equine lysozyme and oleic acid with bactericidal activity against *Streptococcus pneumoniae*. *PLoS One* 8:e80649. doi: 10.1371/journal.pone.0080649

Collins, M. D., Burton, R. A., and Jones, D. (1988). *Corynebacterium amycolatum* sp. nov. a new mycolic acid-less *Corynebacterium* species from human skin. *FEBS Microbiol. Lett.* 49, 349–352. doi: 10.1111/j.1574-6968.1988.tb02755.x

Copeland, E., Leonard, K., Carney, R., Kong, J., Forer, M., Naidoo, Y., et al. (2018). Chronic rhinosinusitis: potential role of microbial dysbiosis and recommendations for sampling sites. *Front. Cell. Infect. Microbiol.* 8:57. doi: 10.3389/fcimb.2018.00057

Cutts, F. T., Zaman, S. M. A., Enwere, G., Jaffar, S., Levine, O. S., Okoko, J. B., et al. (2005). Efficacy of nine-valent pneumococcal conjugate vaccine against pneumonia and invasive pneumococcal disease in The Gambia: randomised, double-blind, placebo-controlled trial. *Lancet* 365, 1139–1146. doi: 10.1016/S0140-6736(05)71876-6

Do, T. Q., Moshkani, S., Castillo, P., Anunta, S., Pogosyan, A., Cheung, A., et al. (2008). Lipids including cholesteryl linoleate and cholesteryl arachidonate contribute to the inherent antibacterial activity of human nasal fluid. *J. Immunol.* 181, 4177–4187. doi: 10.4049/jimmunol.181.6.4177

Eggeling, L., Bott, M., and Daffe, M. (2005). *Handbook of Corynebacterium glutamicum*. Boca Raton, FL: Taylor & Francis Group, LLC.

FitzGerald, E. S., Luz, N. F., and Jamieson, A. M. (2020). Competitive cell death interactions in pulmonary infection: host modulation versus pathogen manipulation. *Front. Immunol.* 11:814. doi: 10.3389/fimmu.2020.00814

Gillespie, S. H., Ainscough, S., Dickens, A., and Lewin, J. (1996). Phosphorylcholine-containing antigens in bacteria from the mouth and respiratory tract. *J. Med. Microbiol.* 44, 35–40. doi: 10.1099/00222615-44-1-35

Gomes-Neto, J. C., Mantz, S., Held, K., Sinha, R., Munoz, R. R. S., Schmaltz, R., et al. (2017). A real-time PCR assay for accurate quantification of the individual members of the Altered Shaedler Flora microbiota in gnotobiotic mice. *J. Microbiol. Methods* 135, 52–62. doi: 10.1016/j.mimet.2017.02.003

Gschwandtner, M., Derler, R., and Midwood, K. S. (2019). More than just attractive: how CCL2 influences myeloid cell behavior beyond chemotaxis. *Front. Immunol.* 10:2759. doi: 10.3389/fimmu.2019.02759

Hasegawa, K., Linnemann, R. W., Mansbach, J. M., Ajami, N. J., Espinola, J., Petrosino, J., et al. (2017). Nasal airway microbiota profile and severe bronchiolitis in infants a case-control study. *Pediatr. Infect. Dis. J.* 36, 1044–1051. doi: 10.1097/INF.0000000000001500

Ichinohe, T., Pang, I. K., Kumamoto, Y., Peaper, D. R., Ho, J. H., Murray, T. S., et al. (2011). Microbiota regulates immune defense against respiratory tract influenza A virus infection. *Proc. Natl. Acad. Sci. U.S.A.* 108, 5354–5359. doi: 10.1073/pnas.1019378108/-/DCSupplemental/pnas.201019378SI.pdf

Jaeger, K.-E., Ransac, S., Dijkstra, B. W., Colson, C., van Heuvel, M., and Misset, O. (1994). Bacterial lipases. *FEMS Microbiol. Rev.* 15, 29–63.

Janek, D., Zipperer, A., Kulik, A., Krismer, B., and Peschel, A. (2016). High frequency and diversity of antimicrobial activities produced by nasal *Staphylococcus* strains against bacterial competitors. *PLoS Pathog.* 12:e1005812. doi: 10.1371/journal.ppat.1005812

Jimeno, R., Brailey, P. M., and Barral, P. (2018). Quantitative polymerase chain reaction-based analyses of murine intestinal microbiota after oral antibiotic treatment. *J. Vis. Exp.* 141:e58481. doi: 10.3791/58481

Jose, R. J., Periselneris, J. N., and Brown, J. S. (2015). Community-acquired pneumonia. *Curr. Opin. Pulm. Med.* 21, 212–218. doi: 10.1097/MCP.0000000000000150

Kanmani, P., Clua, P., Vizoso-Pinto, M. G., Rodriguez, C., Alvarez, S., Melnikov, V., et al. (2017). Respiratory commensal bacteria *Corynebacterium pseudodiphtheriticum* improves resistance of infant mice to respiratory syncytial virus and *Streptococcus pneumoniae* superinfection. *Front. Microbiol.* 8:1613.

Kash, J. C., Walters, K.-A., Davis, A. S., Sandouk, A., Schwartzman, L. M., Jagger, B. W., et al. (2011). Lethal synergism of 2009 pandemic H1N1 influenza virus and *Streptococcus pneumoniae* coinfection is associated with loss of murine lung repair responses. *mBio* 2:e00172-11. doi: 10.1128/mBio.00172-11

Kaspar, U., Kriegeskorte, A., Schubert, T., Peters, G., Rudack, C., Pieper, D. H., et al. (2016). The culturome of the human nose habitats reveals individual bacterial fingerprint patterns. *Environ. Microbiol.* 18, 2130–2142. doi: 10.1111/1462-2920.12891

Kelly, M. S., Plunkett, C., Yu, Y., Aquino, J. N., Patel, S. M., Hurst, J. H., et al. (2021). Non-diphtheriae *Corynebacterium* species are associated with decreased risk of pneumococcal colonization during infancy. *ISME J.* 1–11. doi: 10.1038/s41396-021-01108-4 [Epub ahead of print].

Kelly, M. S., Surette, M. G., Smieja, M., Pernica, J. M., Rossi, L., Luinstra, K., et al. (2017). The nasopharyngeal microbiota of children with respiratory infections in Botswana. *Pediatr. Infect. Dis. J.* 36, e211–e218.

Kiryukhina, N. V., Melnikov, V. G., Suvorov, A. V., Morozova, Y. A., and Ilyin, V. K. (2013). Use of *Corynebacterium pseudodiphtheriticum* for elimination of *Staphylococcus aureus* from the nasal cavity in volunteers exposed to abnormal microclimate and altered gaseous environment. *Probiot. Antimicrob. Proteins* 5, 233–238. doi: 10.1007/s12602-013-9147-x

La Mantia, I., Varricchio, A., and Ciprandi, G. (2017). Bacteriotherapy with Streptococcus salivarius 24SMB and Streptococcus oralis 89a nasal spray for preventing recurrent acute otitis media in children: a real-life clinical experience. *Int. J. Gen. Med.* 10, 171–175. doi: 10.2147/IJGM.S137614

Lappan, R., and Peacock, C. S. (2019). *Corynebacterium* and *Dolosigranulum*: future probiotic candidates for upper respiratory tract infections. *Microbiol. Austr.* 40, 172–177. doi: 10.1111/1469-0691.12373

Lappan, R., Imbrogno, K., Sikazwe, C., Anderson, D., Mok, D., Coates, H., et al. (2018). A microbiome case-control study of recurrent acute otitis media identified potentially protective bacterial genera. *BMC Microbiol.* 18:13. doi: 10.1186/s12866-018-1154-3

Laufer, A. S., Metlay, J. P., Gent, J. F., Fennie, K. P., Kong, Y., and Pettigrew, M. M. (2011). Microbial communities of the upper respiratory tract and otitis media in children. *mBio* 2:e00245-10. doi: 10.1128/mBio.00245-10

Lin, W.-C., and Fessler, M. B. (2021). Regulatory mechanisms of neutrophil migration from the circulation to the airspace. *Cell. Mol. Life Sci.* 78, 4095–4124. doi: 10.1007/s00018-021-03768-z

Liu, Q., Liu, Q., Meng, H., Lv, H., Liu, Y., Liu, J., et al. (2019). *Staphylococcus epidermidis* contributes to healthy maturation of the nasal microbiome by stimulating antimicrobial peptide production. *Cell Host Microbe* 27, 68–78.e5.

Lu, S., Wang, J., Chitsaz, F., Derbyshire, M. K., Geer, R. C., Gonzales, N. R., et al. (2019). CDD/SPARCLE: the conserved domain database in 2020. *Nucleic Acids Res.* 48, D265–D268. doi: 10.1093/nar/gkz991

Man, W. H., van Houten, M. A., Mérelle, M. E., Vlieger, A. M., Chu, M. L. J. N., Jansen, N. J. G., et al. (2019). Bacterial and viral respiratory tract microbiota and host characteristics in children with lower respiratory tract infections: a matched case-control study. *Lancet Respir. Med.* 7, 417–426.

Marchisio, P., Santagati, M., Scillato, M., Baggi, E., Fattizzo, M., Rosazza, C., et al. (2015). *Streptococcus salivarius* 24SMB administered by nasal spray for the prevention of acute otitis media in otitis-prone children. *Eur. J. Clin. Microbiol. Infect. Dis.* 34, 2377–2383. doi: 10.1007/s10096-015-2491-x

Marrakchi, H., Lanéelle, M.-A., and Daffé, M. (2014). Mycolic acids: structures, biosynthesis, and beyond. *Chem. Biol.* 21, 67–85.

Moyano, R. O., Tonetti, F. R., Tomokiyo, M., Kanmani, P., Vizoso-Pinto, M. G., Kim, H., et al. (2020). The ability of respiratory commensal bacteria to beneficial modulate the lung innate immune response is a strain dependent characteristic. *Microorganisms* 8:727. doi: 10.3390/microorganisms8050727

Muller-Redetzky, H. C., Suttorp, N., and Witzenrath, M. (2014). Dynamics of pulmonary endothelial barrier function in acute inflammation: mechanisms and therapeutic perspectives. *Cell Tissue Res.* 355, 657–673. doi: 10.1007/s00441-014-1821-0

Nakatsuji, T., Kao, M. C., Zhang, L., Zouboulis, C. C., Gallo, R. L., and Huang, C.-M. (2010). Sebum free fatty acids enhance the innate immune defense of human sebocytes by upregulating β-defensin-2 expression. *J. Investig. Dermatol.* 130, 985–994. doi: 10.1038/jid.2009.384

Nemkov, T., D'Alessandro, A., and Hansen, K. C. (2015). Three-minute method for amino acid analysis by UHPLC and high-resolution quadrupole orbitrap mass spectrometry. *Amino Acids* 47, 2345–2357. doi: 10.1007/s00726-015-2019-9

Nemkov, T., Hansen, K. C., and D'Alessandro, A. (2017). A three-minute method for high-throughput quantitative metabolomics and quantitative tracing experiments of central carbon and nitrogen pathways. *Rapid Commun. Mass. Spectrom.* 31, 663–673. doi: 10.1002/rcm.7834

Nemkov, T., Reisz, J. A., Gehrke, S., Hansen, K. C., and D'Alessandro, A. (2019). High-throughput metabolomics: isocratic and gradient mass spectrometry-based methods. *Methods Mol. Biol.* 1978, 13–26.

Petersen, T. N., Brunak, S., von Heijne, G., and Nielsen, H. (2011). SignalP 4.0: discriminating signal peptides from transmembrane regions. *Nat. Methods* 8, 785–786. doi: 10.1038/nmeth.1701

Pettigrew, M. M., Laufer, A. S., Gent, J. F., Kong, Y., Fennie, K. P., and Metlay, J. P. (2012). Upper respiratory tract microbial communities, acute otitis media pathogens, and antibiotic use in healthy and sick children. *Appl. Environ. Microbiol.* 78, 6262–6270. doi: 10.1128/AEM.01051-12

Pilishvili, T., and Bennett, N. M. (2015). Pneumococcal disease prevention among adults: strategies for the use of pneumococcal vaccines. *Vaccine* 33, D60–D65.

Piters, W. A. A. S., Jochems, S. P., Mitsi, E., Rylance, J., Pojar, S., Nikolaou, E., et al. (2019). Interaction between the nasal microbiota and *S. pneumoniae* in the context of live-attenuated influenza vaccine. *Nat. Commun.* 10:2981. doi: 10.1038/s41467-019-10814-9

Plou, F. J., Ferrer, M., Nuero, O. M., Calvo, M. V., Alcalde, M., Reyes, F., et al. (1998). Analysis of tween 80 as an esterase/ lipase substrate for lipolytic activity assay. *Biotechnol. Techniq.* 12, 183–186. doi: 10.1023/A:1008809105270

Prevaes, S. M. P. J., de Winter-de Groot, K. M., Janssens, H. M., de Steenhuijsen Piters, W. A. A., Tramper-Stranders, G. A., Wyllie, A. L., et al. (2016). Development of the nasopharyngeal microbiota in infants with cystic fibrosis. *American J. Respir. Crit. Care Med.* 193, 504–515.

Ramsey, M. M., Freire, M. O., Gabrilska, R. A., Rumbaugh, K. P., and Lemon, K. P. (2016). *Staphylococcus aureus* shifts toward commensalism in response to *Corynebacterium* Species. *Front. Microbiol.* 7:1230.

Reisz, J. A., Zheng, C., D'Alessandro, A., and Nemkov, T. (2019). "Untargeted and semi-targeted lipid analysis of biological samples using mass spectrometry-based metabolomics," in *High-Throughput Metabolomics: Methods and Protocols*, ed. A. D'Alessandro (New York, NY: Springer), 121–135.

Ricchi, M., Bertasio, C., Boniotti, M. B., Vicari, N., Russo, S., Tilola, M., et al. (2017). Comparison among the quantification of bacterial pathogens by qPCR, dPCR, and cultural methods. *Front. Microbiol.* 8:1174. doi: 10.3389/fmicb.2017.01174

Ridaura, V. K., Bouladoux, N., Claesen, J., Chen, Y. E., Byrd, A. L., Constantinides, M. G., et al. (2018). Contextual control of skin immunity and inflammation by Corynebacterium. *J. Exp. Med.* 215, 785–799.

Rijneveld, A. W., Weijer, S., Florquin, S., Speelman, P., Shimizu, T., Ishii, S., et al. (2004). Improved host defense against pneumococcal pneumonia in platelet-activating factor receptor–deficient mice. *J. Infect. Dis.* 189, 711–716. doi: 10.1086/381392

Rosendahl, A., Bergmann, S., Hammerschmidt, S., Goldmann, O., and Medina, E. (2013). Lung dendritic cells facilitate extrapulmonary bacterial dissemination during pneumococcal pneumonia. *Front. Cell. Infect. Microbiol.* 3:21. doi: 10.3389/fcimb.2013.00021/abstract

Stubbendieck, R. M., May, D. S., Chevrette, M. G., Temkin, M. I., Wendt-Pienkowski, E., Cagnazzo, J., et al. (2019). Competition among nasal bacteria suggests a role for siderophore-mediated interactions in shaping the human nasal microbiota. *Appl. Environ. Microbiol.* 85:e02406-18. doi: 10.1128/AEM.02406-18

Taoka, Y., Nagano, N., Okita, Y., Izumida, H., Sugimoto, S., and Hayashi, M. (2011). Effect of Tween 80 on the growth, lipid accumulation and fatty acid composition of *Thraustochytrium aureum* ATCC 34304. *J. Biosci. Bioeng.* 111, 420–424. doi: 10.1016/j.jbiosc.2010.12.010

Tchoupa, A. K., Eijkelkamp, B. A., and Peschel, A. (2021). Bacterial adaptation strategies to host-derived fatty acids. *Trends Microbiol.* 1–13. doi: 10.1016/j.tim.2021.06.002 [Epub ahead of print].

Teo, S. M., Mok, D., Pham, K., Kusel, M., Serralha, M., Troy, N., et al. (2015). The infant nasopharyngeal microbiome impacts severity of lower respiratory infection and risk of asthma development. *Cell Host Microbe* 17, 704–715. doi: 10.1016/j.chom.2015.03.008

Torres, A., Cillóniz, C., Blasi, F., Chalmers, J. D., Gaillat, J., Dartois, N., et al. (2018). Burden of pneumococcal community-acquired pneumonia in adults across Europe: a literature review. *Respir. Med.* 137, 6–13. doi: 10.1016/j.rmed.2018.02.007

Uehara, Y. E. A., Nakama, H., Agematsu, K., Uchida, M., Kawakami, Y., Fattah, A. S. M. A., et al. (2000). Bacterial interference among nasal inhabitants: eradication of *Staphylococcus aureusfrom* nasal cavities by artificial implantation of *Corynebacterium* sp. *J. Hosp. Infect.* 44, 127–133. doi: 10.1053/jhin.1999.0680

World Health Organization [WHO] (2021). *World Health Statistics 2021: Monitoring Health for the SDGs, Sustainable Development Goals*. Geneva: World Health Organization, 1–136.

Xu, L., Earl, J., and Pichichero, M. E. (2021). Nasopharyngeal microbiome composition associated with *Streptococcus pneumoniae* colonization suggests a protective role of *Corynebacterium* in young children. *PLoS One* 16:e0257207. doi: 10.1371/journal.pone.0257207

Yan, M., Pamp, S. J., Fukuyama, J., Hwang, P. H., Cho, D.-Y., Holmes, S., et al. (2013). Nasal microenvironments and interspecific interactions influence nasal microbiota complexity and *S. aureus* carriage. *Cell Host Microbe* 14, 631–640. doi: 10.1016/j.chom.2013.11.005

Yang, K., Kruse, R. L., Lin, W. V., and Musher, D. M. (2018). Corynebacteria as a cause of pulmonary infection: a case series and literature review. *Pneumonia* 10:10. doi: 10.1186/s41479-018-0054-5

Conflict of Interest: The authors declare that the research was conducted in the absence of any commercial or financial relationships that could be construed as a potential conflict of interest.

Publisher's Note: All claims expressed in this article are solely those of the authors and do not necessarily represent those of their affiliated organizations, or those of the publisher, the editors and the reviewers. Any product that may be evaluated in this article, or claim that may be made by its manufacturer, is not guaranteed or endorsed by the publisher.

frontiers in Microbiology

ORIGINAL RESEARCH
published: 13 January 2022
doi: 10.3389/fmicb.2021.798750

Serotype Distribution, Antimicrobial Susceptibility, Multilocus Sequencing Type and Virulence of Invasive *Streptococcus pneumoniae* in China: A Six-Year Multicenter Study

Menglan Zhou[1,2†], Ziran Wang[1,2†], Li Zhang[3†], Timothy Kudinha[4,5], Haoran An[6,7], Chenyun Qian[6,7], Bin Jiang[8], Yao Wang[1,2], Yingchun Xu[1,2], Zhengyin Liu[3], Hong Zhang[9*] and Jingren Zhang[5,6*]*

[1] State Key Laboratory of Complex Severe and Rare Diseases, Department of Clinical Laboratory, Peking Union Medical College Hospital, Chinese Academy of Medical Sciences and Peking Union Medical College, Beijing, China, [2] Beijing Key Laboratory for Mechanisms Research and Precision Diagnosis of Invasive Fungal Diseases, Beijing, China, [3] Department of Infectious Disease, Peking Union Medical College Hospital, Chinese Academy of Medical Sciences, Beijing, China, [4] School of Biomedical Sciences, Charles Sturt University, Orange, NSW, Australia, [5] NSW Health Pathology, Regional and Rural, Orange Hospital, Orange, NSW, Australia, [6] Department of Basic Medical Science, School of Medicine, Tsinghua University, Beijing, China, [7] Tsinghua-Peking Center for Life Sciences, Tsinghua University, Beijing, China, [8] Department of Clinical Laboratory, Hunan Provincial People's Hospital, The First Affiliated Hospital of Hunan Normal University, Changsha, China, [9] Department of Clinical Laboratory, Shanghai Children's Hospital, Shanghai Jiao Tong University, Shanghai, China

Background: *Streptococcus pneumoniae* is an important human pathogen that can cause severe invasive pneumococcal diseases (IPDs). The aim of this multicenter study was to investigate the serotype and sequence type (ST) distribution, antimicrobial susceptibility, and virulence of *S. pneumoniae* strains causing IPD in China.

Methods: A total of 300 invasive *S. pneumoniae* isolates were included in this study. The serotype, ST, and antimicrobial susceptibility of the strains, were determined by the Quellung reaction, multi-locus sequence typing (MLST) and broth microdilution method, respectively. The virulence level of the strains in the most prevalent serotypes was evaluated by a mouse sepsis model, and the expression level of well-known virulence genes was measured by RT-PCR.

Results: The most common serotypes in this study were 23F, 19A, 19F, 3, and 14. The serotype coverages of PCV7, PCV10, PCV13, and PPV23 vaccines on the strain collection were 42.3, 45.3, 73.3 and 79.3%, respectively. The most common STs were ST320, ST81, ST271, ST876, and ST3173. All strains were susceptible to ertapenem, levofloxacin, moxifloxacin, linezolid, and vancomycin, but a very high proportion (>95%) was resistant to macrolides and clindamycin. Based on the oral, meningitis and non-meningitis breakpoints, penicillin non-susceptible *Streptococcus pneumoniae* (PNSP) accounted for 67.7, 67.7 and 4.3% of the isolates, respectively. Serotype 3 strains were characterized by high virulence levels and low antimicrobial-resistance rates, while strains of serotypes 23F, 19F, 19A, and 14, exhibited low virulence and high resistance

OPEN ACCESS

Edited by:
Mattias Collin,
Lund University, Sweden

Reviewed by:
Luchang Zhu,
Houston Methodist Research Institute, United States
Haijian Zhou,
National Institute for Communicable Disease Control and Prevention, China CDC, China

***Correspondence:**
Zhengyin Liu
zhengyinl@hotmail.com
Hong Zhang
zhanghong3010@vip.126.com
Jingren Zhang
zhanglab@mail.tsinghua.edu.cn

[†] These authors have contributed equally to this work

Specialty section:
This article was submitted to Antimicrobials, Resistance and Chemotherapy, a section of the journal Frontiers in Microbiology

Received: 20 October 2021
Accepted: 08 December 2021
Published: 13 January 2022

Citation:
Zhou M, Wang Z, Zhang L, Kudinha T, An H, Qian C, Jiang B, Wang Y, Xu Y, Liu Z, Zhang H and Zhang J (2022) Serotype Distribution, Antimicrobial Susceptibility, Multilocus Sequencing Type and Virulence of Invasive Streptococcus pneumoniae in China: A Six-Year Multicenter Study. Front. Microbiol. 12:798750. doi: 10.3389/fmicb.2021.798750

rates to antibiotics. Capsular polysaccharide and non-capsular virulence factors were collectively responsible for the virulence diversity of *S. pneumoniae* strains.

Conclusion: Our study provides a comprehensive insight into the epidemiology and virulence diversity of *S. pneumoniae* strains causing IPD in China.

Keywords: *Streptococcus pneumoniae*, serotype distribution, molecular epidemiology, antimicrobial susceptibility, virulence

INTRODUCTION

Streptococcus pneumoniae is a common Gram-positive coccus that can cause serious invasive pneumococcal diseases (IPDs) such as pneumonia, meningitis, and sepsis, especially in children and the elderly. It is estimated that IPD is responsible for approximately 826,000 deaths in children aged 1–59 months annually worldwide (O'Brien et al., 2009). Furthermore, the incidence of IPD increases with age, and with higher mortality reported in people over 65 years of age (Marrie et al., 2018).

The capsular polysaccharides of *S. pneumoniae* play an important role in pneumococcal disease pathogenesis, and at least 100 serotypes have been identified based on the capsule synthesis locus (*cps*) gene differences (Ganaie et al., 2020). The use of vaccines targeting specific serotypes has significantly reduced the morbidity and mortality of pneumococcal disease. *S. pneumoniae* vaccines PPV23 (covering serotypes 1–5, 6B, 7F, 8, 9 N, 9V, 10A, 11A, 12F, 14, 15B, 17F, 18C, 19A, 19F, 20, 22F, 23F, and 33F), PCV7 (covering serotypes 4, 6B, 9 V, 14, 18C, 19F, and 23F), PCV10 (covering PCV7 serotypes plus serotypes 1, 5, and 7F) and PCV13 (covering PCV10 serotypes plus serotypes 3, 6A, and 19A) were commercially introduced in the United States of America (USA) as early as 1983, 2000, 2008, and 2009 (Kim et al., 2020). At present, developed countries in Europe and the United States have already included PCV and PPV vaccines in their national vaccination programs, greatly reducing IPD caused by serotypes covered by these vaccines (Richter et al., 2013; Esposito et al., 2014). In China, several vaccines such as PCV7, PCV13, and PPV23 are currently available, but vaccination rates are still low due to the high cost of the vaccines (Boulton et al., 2016; Liang et al., 2016; Chen et al., 2018). However, the use of vaccines results in a shift in *S. pneumoniae* serotype distribution, a phenomenon known as "serotype replacement", in which the prevalence of serotypes covered in the vaccines decrease whilst that of serotypes not included in the vaccines increase (Geno et al., 2015). Besides, *S. pneumoniae* can undergo efficient intra- and interspecies DNA recombination, leading to changes in the capsule composition, molecular typing, antibiotic resistance, and virulence factors (Varghese et al., 2019). These phenomena present great challenges to the prevention and treatment of pneumococcal diseases.

There is still a scarcity of comprehensive studies on the epidemiological characteristics as well as the virulence levels of *S. pneumoniae* causing invasive infections in China. The aim of this multicenter study was to investigate the serotype and sequence type (ST) distribution, antimicrobial susceptibility, and virulence of *S. pneumoniae* isolates causing IPD in China.

MATERIALS AND METHODS

Isolates Collection

A total of 300 invasive *S. pneumoniae* isolates from 27 teaching hospitals in 13 provinces in China, collected during the period January 2010–October 2015, were included in this study (**Supplementary Figure 1**). All isolates were non-replicate and obtained from sterile sites, with only the first isolate selected from the same patient. The majority (141/300, 47%) of the isolates were isolated from younger children (0 to 5 years), whilst 29 (9.7%) were from older children (5 to 18 years), 92 (30.7%) from adults aged 18 to 65 years, and 38 (12.7%) from patients >65 years old. The major specimen type was blood (72.7%, 218/300), followed by cerebrospinal fluid (CSF) (19.0%, 57/300), and then pleural effusion (5.7%, 17/300). Other specimen types included ascetic fluid (n = 4), joint tissue (n = 2), thoracic drainage fluid (n = 1) and lung tissue (n = 1). All isolates were identified as *S. pneumoniae* using Vitek MS system (BioMerieux, Rhône, France) and optochin susceptibility test.

Serotyping

All the isolates were serotyped by the Quellung reaction, which was considered the gold standard for serotyping. Firstly, the *S. pneumoniae* serogroup/type was preliminarily determined by latex agglutination test using the checkerboard typing system (Lalitha et al., 1999). Then specific antiserum was mixed with the bacterial suspension and capsular swelling was observed under the microscope. If the Quellung reaction was negative with all antisera, it was classified as non-typeable (NT) type.

Multi-Locus Sequence Typing

The DNA of the *S. pneumoniae* isolates was extracted using the AxyGenamp DNA Mini Extraction Kit (Axygen, United States) according to the manufacturer's instructions. Using the extracted DNA as the template, the seven housekeeping genes (*aroE, gdh, gki, recP, spi, xpt, ddl*) were amplified using polymerase chain reaction (PCR). The primer sequences used are detailed in **Supplementary Table 1**. The amplified products were sequenced and aligned with the sequences on the MLST website to determine the sequence type (ST) of the isolate. If a new allele combination was obtained, the corresponding sequence and strain-related information were submitted to the MLST databases[1] for assigning of a new ST accession number after approval.

[1]https://pubmlst.org

Antimicrobial Susceptibility Testing

The minimum inhibitory concentrations (MICs) of *S. pneumoniae* isolates against penicillin (P), amoxicillin/clavulanic (AMC), cefuroxime (CXM), ceftriaxone (CRO), and several other antibiotics (cefepime, ertapenem, imipenem, meropenem, levofloxacin, trimethoprim/sulfamethoxazole, clindamycin, clarithromycin, erythromycin, linezolid and vancomycin), were determined by broth microdilution method. *S. pneumoniae* ATCC 49619 and *Escherichia coli* ATCC25922 were used as quality control strains. Each batch of isolates was tested simultaneously with the quality control strains, and the results were considered valid when the MIC values of both strains were within the expected quality control range. The antimicrobial susceptibility testing results were interpreted according to CLSI, 2019 document (CLSI, 2019).

Virulence Test *in vivo*

This study was approved by the Medical Ethics Committee of Peking Union Medical College Hospital (No. S-263). The strains from the most prevalent serotypes in this study, and all serogroup six strains, were tested for virulence using a mouse sepsis model. Overall, 65 *S. pneumoniae* isolates were tested in this model, including serotypes 23F ($n = 8$), 19F ($n = 8$), 19A ($n = 8$), 3 ($n = 8$), 14 ($n = 8$), 6A ($n = 12$), 6B ($n = 11$), and 6C ($n = 2$).

We established an intraperitoneal infection model for *S. pneumoniae* using 6-week-old outbred CD-1 female mice (obtained from Beijing Vital River Laboratory Animal Technology Co. Ltd). For each isolate tested, a group of six mice were inoculated intraperitoneally with 200 μl of bacterial suspension containing approximately 1×10^4 CFU of *S. pneumoniae* per mouse. The mortality of the mice was assessed daily until the 7th day. Isoflurane (Sigma-Aldrich, United States) was used at a dose of 6 mg/kg of the mouse weight for anesthetization at the time of blood collection. Orbital vein blood samples were obtained every 12 h for the first 2 days after inoculation and then daily for the next 5 days. Quantification of bacteria in the blood was determined by serial dilution and plating on trypticase soy agar with 3% sheep blood.

Analysis of Virulence Gene Expression

RNA from 25 strains of serogroup 6 was extracted using Magen RNA Extraction Kit (Magen Bio, China) according to manufacturer's instructions. Reverse transcription of the RNA was performed using the FastKing RT Kit (Tiangen Bio, China). Quantitative PCR reactions were performed using the SYBR Premix ExTaq^{TM} PCR kit (Takara Bio, Japan) on a LightCycler 480 instrument (Roche Molecular Diagnostics, Rotkreuz, Switzerland). Using 16S rRNA as an internal reference gene, the expression of six non-capsule-associated virulence genes (*ply, lytA, nanA, psaA, pspA, and HylA*) (Ogunniyi et al., 2002; LeMessurier et al., 2006) was calculated using the $2^{-\Delta\Delta Ct}$ method. The primer sequences used are detailed in **Supplementary Table 1**.

Statistical Analysis

Data on the distribution of different serotypes and vaccine coverage was analysed using Excel 2019 software (Microsoft Inc., United States). Differences in antimicrobial susceptibility were analyzed by MIC range, MIC_{50} and MIC_{90}, and statistical analysis was performed by chi-square test or Fisher's exact probability test using SPSS software (version 22.0, SPSS Inc., Chicago, IL, United States). Differences in survival time and gene expression between and within groups were analyzed by independent sample *t*-test and one-way ANOVA. *P*-values < 0.05 were considered statistically significant.

RESULTS

Serotype Distribution

The serotypes of 299 *S. pneumoniae* strains were accurately identified by Quellung reaction, and the remaining one isolate was considered as non-typeable (NT). Overall, 40 serotypes were identified, with the 5 commonest being 23F (14.3%, 43/300), 19F (13.7%, 41/300), 19A (13.7%, 41/300), 3 (10.3%, 31/300), and 14 (9.0%, 27/300) (**Supplementary Table 2**). Based on the specific serotypes included in the vaccines, the coverage rates of PCV7, PCV10, PCV13, and PPV23 vaccines on this bacterial collection were 42.3% (127/300), 45.3% (136/300), 73.3% (220/300), and 79.3% (238/300), respectively (**Figure 1A**). The most prevalent serotypes isolated in the adult and children's groups were similar. In the adult group, serotypes 23F (16.9%) and 19A (16.9%) were dominant, followed by 19F (14.6%), 14 (7.7%), and 3 (6.15%), whereas in the children group, serotype 3 was dominant (13.5%), followed by 19F (12.9%), 23F (12.4%), 19A (11.2%), and 14 (10.0%). There was no significant difference in the distribution of vaccine coverage between the adult and children's groups: PCV7 (43.8% vs 41.2%) ($P = 0.7386$), PCV10 (47.7% vs 43.5%) ($P = 0.5438$), PCV13 (74.6% vs 72.4%) ($P = 0.4224$) and PPV23 (79.2% vs79.4%) ($P = 0.9192$) (**Figure 1B**).

Serotypes 23F, 19F, 19A, 3, and 14 were dominant from 2010 to 2015, ranging from 52.0 to 76.4%, albeit slight yearly variation in the distribution. In contrast, from the year 2010–2015, there was a decrease in the isolation rates of serotypes 23F, 19A, and 14, while that of 19F, 3, 6A, and 6B increased, although the differences were not statistically significant (**Supplementary Figure 2**). Noticeably, for both PCV13 and PPV23 vaccines, the vaccine serotype coverage among the isolates showed a decreasing trend from 2010 to 2015 (PCV13: 85.3 to 68%; PPV23: 91.2 to 72%), while the proportion of non-vaccine covered serotypes increased (non-PCV13: 14.7 to 32%; non-PPV23: 8.8 to 28%), though the difference was not statistically significant ($P = 0.2053$ for PCV13 and $P = 0.1114$ for PPV23) (**Figures 1C,D**).

Multi-Locus Sequence Typing

Among the 300 isolates studied, 123 STs were identified by MLST analysis (**Supplementary Table 3**). Of these, ST320 (11.3%, 34/300) predominated, followed closely by ST81 (9.3%, 28/300), ST271 (8.7%, 26/300), ST876 (8.7%, 26/300) and ST3173 (2.7%, 8/300). There were 33 STs identified for

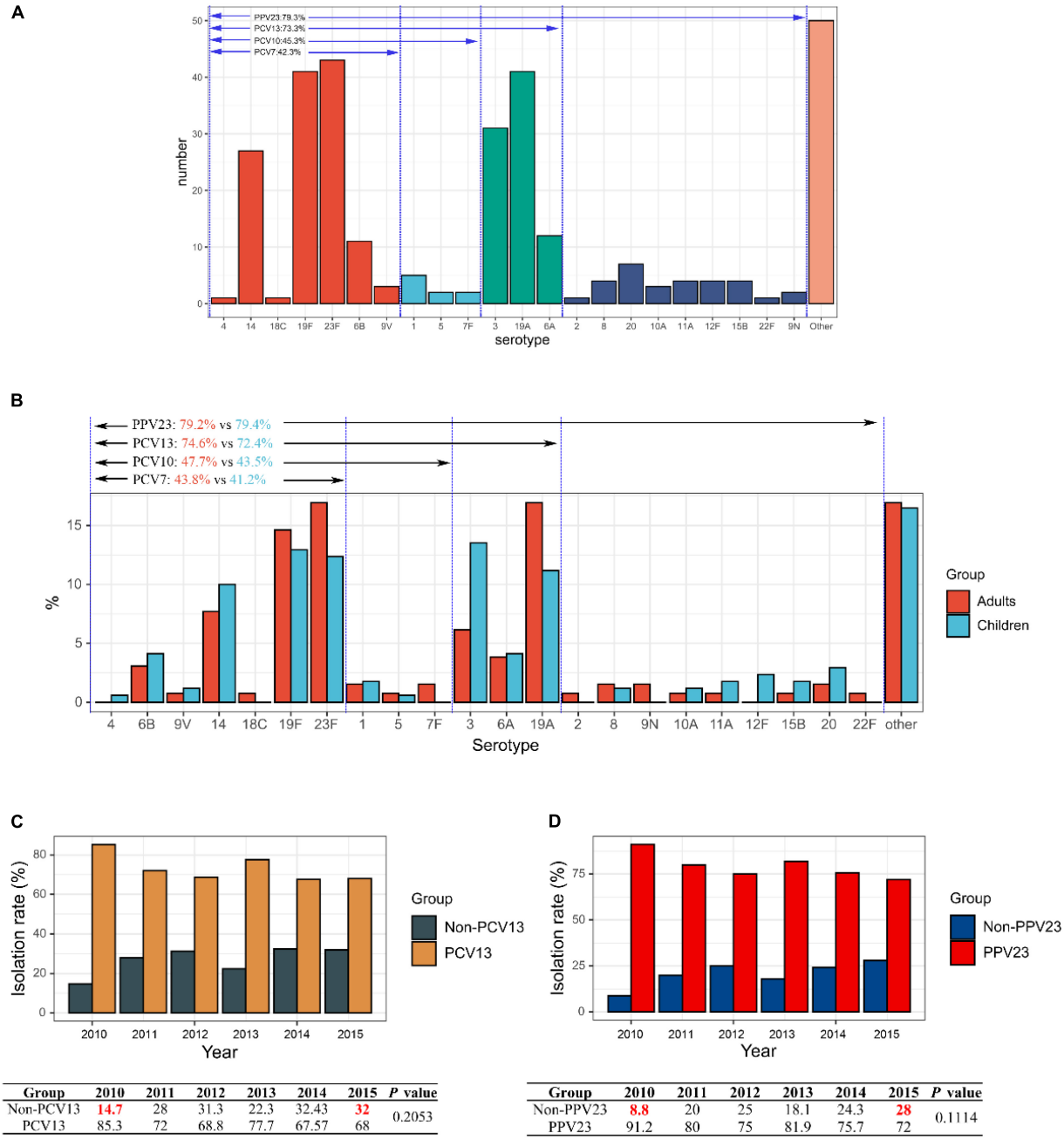

Group	2010	2011	2012	2013	2014	2015	*P* value
Non-PCV13	**14.7**	28	31.3	22.3	32.43	**32**	0.2053
PCV13	85.3	72	68.8	77.7	67.57	68	

Group	2010	2011	2012	2013	2014	2015	*P* value
Non-PPV23	**8.8**	20	25	18.1	24.3	**28**	0.1114
PPV23	91.2	80	75	81.9	75.7	72	

FIGURE 1 | Serotype distribution of 300 invasive *S. pneumoniae* isolates. **(A)** Vaccine coverage *S. pneumoniae* isolates involved in this study. **(B)** Serotype distribution of isolates in different age groups in adult and children. **(C)** Changes in isolation rates of PCV13 and non-PCV13 covered serotypes strains during the study period 2010–2015. **(D)** Changes in isolation rates of PCV23 and non-PCV23 covered serotypes strains during the study period 2010–2015.

the first time here, including ST12901-ST12920, ST13199-ST13200, ST14346-ST14351, ST14705-ST14707, and ST14726-ST14727.

A phylogenetic tree was constructed based on single-locus variants (SLV) in seven housekeeping genes, and a total of 18 clonal complexes (CC) and 65 singletons were identified (**Figure 2**). The most common clonal complex was CC320 (13.3%), followed by CC271 (12.3%), CC81 (11.0%), CC876 (6.7%), and CC1263 (3.3%) (**Table 1**). Based on the Pneumococcal Molecular Epidemiology Network database (PMEN), seven international resistance clones containing 46 strains were identified in this study, including Spain^{23F}-1 (ST81, n = 28), Netherlands^{3}-31 (ST180, n = 6), Taiwan^{19F}-14 (ST236, n = 4), Spain^{6B}-2 (ST90, n = 4), Taiwan^{23F}-15 (ST242, n = 2), Denmark^{14}-32 (ST230, n = 1), and Colombia^{23F}-26 (ST338, n = 1) (**Supplementary Table 4**).

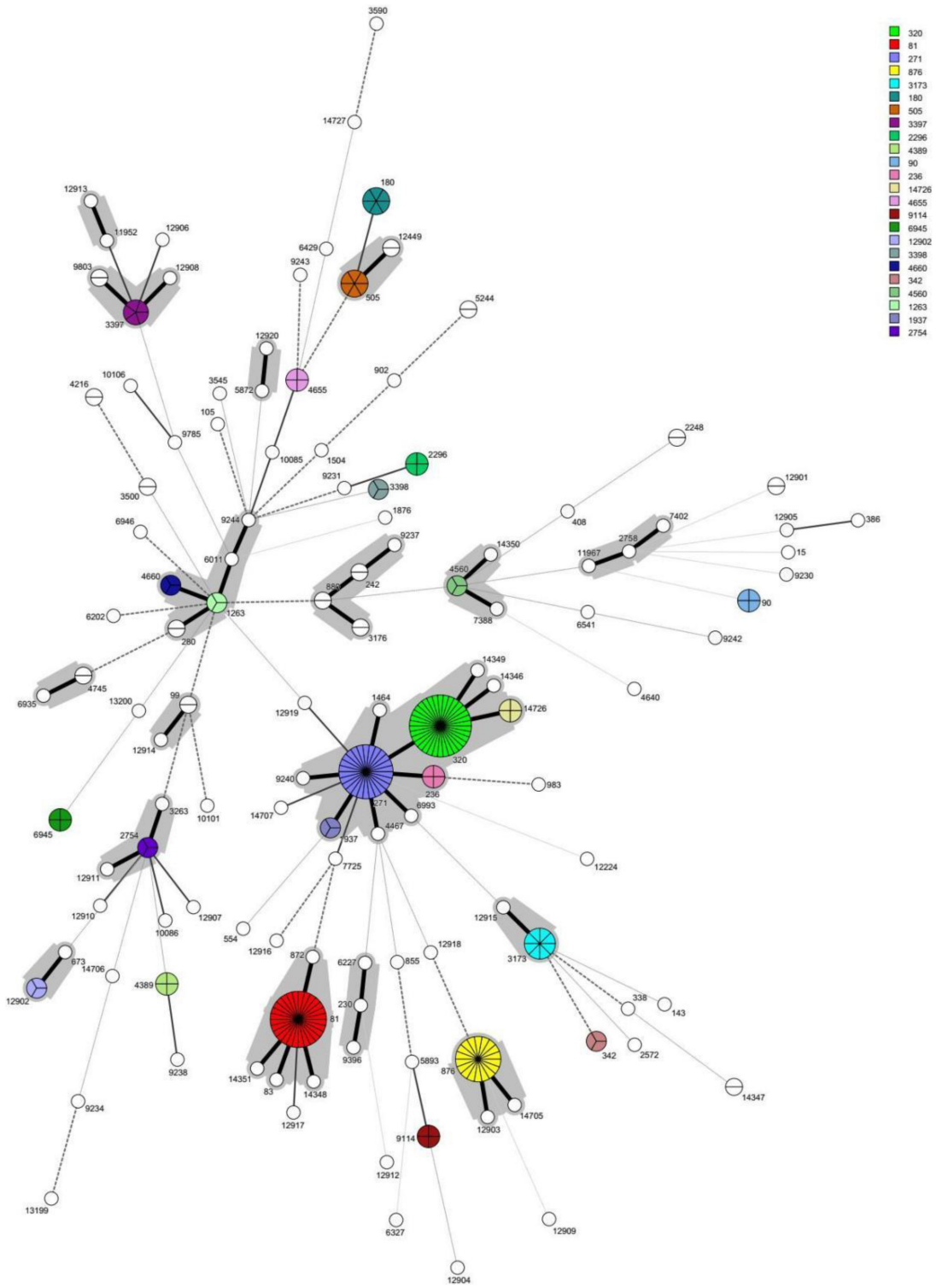

FIGURE 2 | The minimun spanning tree (MST) of the 300 invasive *S. pneumoniae* isolates based on MLST. Note: Each circle corresponds to a sequence type (ST). The number besides the circle represents ST number. The circle size represents the number of strains. The circle color represents different ST categories with isolate number ≥3. The lines between circles indicate the similarity between profiles: bold solid line, six of seven MLST alleles in common; normal solid line, five alleles in common; dashed line, four alleles in common; dotted line, ≤3 alleles. The gray halo surrounding the STs in Figure denotes STs belonging to different MLST clusters/clonal complexes.

TABLE 1 | Summary of clonal complexes of 300 invasive *S. pneumoniae* isolates involved in this study.

CC/ Singletons	No of isolates	Percentage (%)	Sequence types (STs)
CC320	40	13.3	ST320 (*n* = 34), ST14346 (*n* = 1), ST14349 (*n* = 1), ST14726 (*n* = 4)
CC271	37	12.3	ST271 (*n* = 26), ST236 (*n* = 4), ST1464 (*n* = 1), ST1937 (*n* = 3), ST4467 (*n* = 1), ST6993 (*n* = 1), ST9240 (*n* = 1)
CC81	33	11.0	ST81 (*n* = 28), ST83 (*n* = 1), ST872 (*n* = 1), ST12917 (*n* = 1), ST14348 (*n* = 1), ST14351 (*n* = 1)
CC876	20	6.7	ST876 (*n* = 18), ST12903 (*n* = 1), ST14705 (*n* = 1)
CC1263	10	3.3	ST280 (*n* = 2), ST1263 (*n* = 3), ST4660 (*n* = 3), ST6011 (*n* = 1), ST9244 (*n* = 1)
CC3173	9	3.0	ST3173 (*n* = 8), ST12915 (*n* = 1)
CC505	8	2.7	ST505 (*n* = 6), ST12449 (*n* = 2)
CC3397	8	2.7	ST3397 (*n* = 5), ST9803 (*n* = 2), ST12908 (*n* = 1)
CC880	7	2.3	ST880 (*n* = 2), ST242 (*n* = 2), ST3176 (*n* = 2), ST9237 (*n* = 1)
CC2754	5	1.7	ST2754 (*n* = 3), ST3263 (*n* = 1), ST12911 (*n* = 1)
CC4560	5	1.7	ST4560 (*n* = 3), ST7388 (*n* = 1), ST14350 (*n* = 1)
CC673	4	1.3	ST673 (*n* = 1), ST12902 (*n* = 3)
CC99	3	1.0	ST99 (*n* = 2), ST12914 (*n* = 1)
CC4745	3	1.0	ST4745 (*n* = 2), ST6935 (*n* = 1)
CC2758	3	1.0	ST2758 (*n* = 1), ST7402 (*n* = 1), ST11967 (*n* = 1)
CC230	3	1.0	ST230 (n = 1), ST6227 (*n* = 1), ST9396 (*n* = 1)
CC5872	2	0.7	ST5872 (*n* = 1), ST12920 (*n* = 1)
CC11952	2	0.7	ST11952 (*n* = 1), ST12913 (*n* = 1)
Singletons	98	32.7	ST180 (*n* = 6), ST4389 (*n* = 4), ST90 (*n* = 4), ST465 (*n* = 4)5, ST9114 (*n* = 4), ST2296 (*n* = 4), ST6945 (*n* = 4), ST3398 (*n* = 3), ST342 (*n* = 3), ST4216 (*n* = 2), ST12901 (*n* = 2), ST5244 (*n* = 2), ST2248 (*n* = 2), ST3500 (*n* = 2), ST14347 (*n* = 2), ST10106 (*n* = 1), ST9234 (*n* = 1), ST12910 (*n* = 1), ST143 (*n* = 1), ST9785 (*n* = 1), ST2572 (*n* = 1), ST12905 (*n* = 1), ST408 (*n* = 1), ST12919 (*n* = 1), ST902 (*n* = 1), ST9242 (*n* = 1), ST3545 (*n* = 1), ST10086 (*n* = 1), ST3590 (*n* = 1), ST1876 (*n* = 1), ST983 (*n* = 1), ST12907 (*n* = 1), ST105 (*n* = 1), ST12916 (*n* = 1), ST4640 (*n* = 1), ST855 (*n* = 1), ST338 (*n* = 1), ST9238 (*n* = 1), ST1504 (*n* = 1), ST9243 (*n* = 1), ST5893 (*n* = 1), ST10085 (*n* = 1), ST6202 (*n* = 1), ST10101 (*n* = 1), ST6327 (*n* = 1), ST12224 (*n* = 1), ST6429 (*n* = 1), ST12904 (*n* = 1), ST6541 (*n* = 1), ST12906 (*n* = 1), ST15 (*n* = 1), ST12909 (*n* = 1), ST6946 (*n* = 1), ST12912 (*n* = 1), ST13200 (*n* = 1), ST12918 (*n* = 1), ST14706 (*n* = 1), ST13199 (*n* = 1), ST14727 (*n* = 1), ST9231 (*n* = 1), ST7725 (*n* = 1), ST14707 (*n* = 1), ST386 (*n* = 1), ST554 (*n* = 1), ST9230 (*n* = 1)

In terms of annual distribution, ST320 dominated in 2010 (26.5%; 9/34), 2011 (12%, 3/25) and 2013 (12.8%, 12/94). Likewise, ST271 dominated in 2012, accounting for 12.5% (6/48) of the isolates, whilst ST81 (10.8%, 8/74), ST320 (12.0%, 3/25) and ST271 (12.0%, 3/25) dominated in 2014 and 2015, respectively. A declining trend in the prevalence of ST320 (from 26.5% in 2010 to 12% in 2015) and ST81 (from 14.7% in 2010 to 4% in 2015) was observed as can be seen in **Supplementary Figure 3**, whilst an increasing trend is obvious for ST271 (from 8.8% in 2010 to 12% in 2015) and ST876 (from 2.9% in 2010 to 10.8% in 2014) (**Supplementary Figure 3**).

The distribution of STs among the different serotypes is shown in **Figure 3**. Only one ST was described in each of the following serotypes; 12F (*n* = 4), 28F (*n* = 3), 28A (*n* = 2), 4, 25F, 22F, 17, 2, 17A, and 18C (all *n* = 1, each). However, other serotypes showed diverse ST distribution. Serotype 23F was dominated by ST81 (63.0%, 27/43), whilst serotype 19F was dominated by ST271 (63.4%, 26/41) and serotypes 19A by ST320 (80.5%, 33/41). In addition, serotype 3 was dominated by ST505 (19.4%, 6/31) and ST180 (19.4%, 6/31), and serotype 14 by ST876 (66.7%, 18/27).

Antimicrobial Susceptibility

Antimicrobial susceptibility results of the 300 invasive *S. pneumoniae* isolates are shown in **Table 2**. All the isolates were susceptible to ertapenem, levofloxacin, moxifloxacin, linezolid, and vancomycin, with MIC_{90} values of 0.25 μg/ml, 1 μg/ml, 0.125 μg/ml, 1 μg/ml and 0.5 μg/ml, respectively. This was closely followed by amoxicillin/clavulanic acid with a susceptible rate of 97.7% among the isolates. Over 90% of the strains were resistant to azithromycin, clarithromycin, erythromycin, clindamycin, tetracycline, and chloramphenicol. Notably, MIC_{50} and MIC_{90} values for azithromycin, clarithromycin and erythromycin were higher than 1024 μg/ml each. Based on the non-meningitis ($R \geq 8$ μg/ml) breakpoint for penicillin, no resistant strains were observed among the isolates for this antibiotic, but only an intermediate rate of 4.3%. However, based on the meningitis ($R \geq 0.12$ μg/ml) and oral ($R \geq 2$ μg/ml) breakpoints for penicillin, the resistance rates for this antibiotic among the isolates were 67.7 and 44.7%, respectively. The resistance rate of the isolates to trimethoprim/sulfamethoxazole, cefuroxime and cefaclor was ≥60% each, with similar MIC_{90} values for ceftriaxone and cefepime at 2 μg/ml each. As per the meningitis breakpoint for cefepime, the resistance rate for cefepime was slightly higher than that of ceftriaxone (29.7% vs 25.7%), but slightly lower than that of ceftriaxone (4.0% vs 7.3%) when based on the non-meningitis breakpoint. A very small proportion of the isolates was resistant to imipenem (3.7%) and meropenem (2.7%), but the intermediate rate was higher at 37.7% (imipenem) and 46.0% (meropenem).

The susceptibility profiles of several predominant serotypes to different antimicrobial agents are shown in **Table 3**. Overall, serotypes 23F, 19F, 19A, and 14 exhibited a higher resistance rate to all the antimicrobials tested, while serotype 3 had a relatively lower resistance rate. All serotypes showed high resistance rates to macrolides (87.1–100%), chloramphenicol

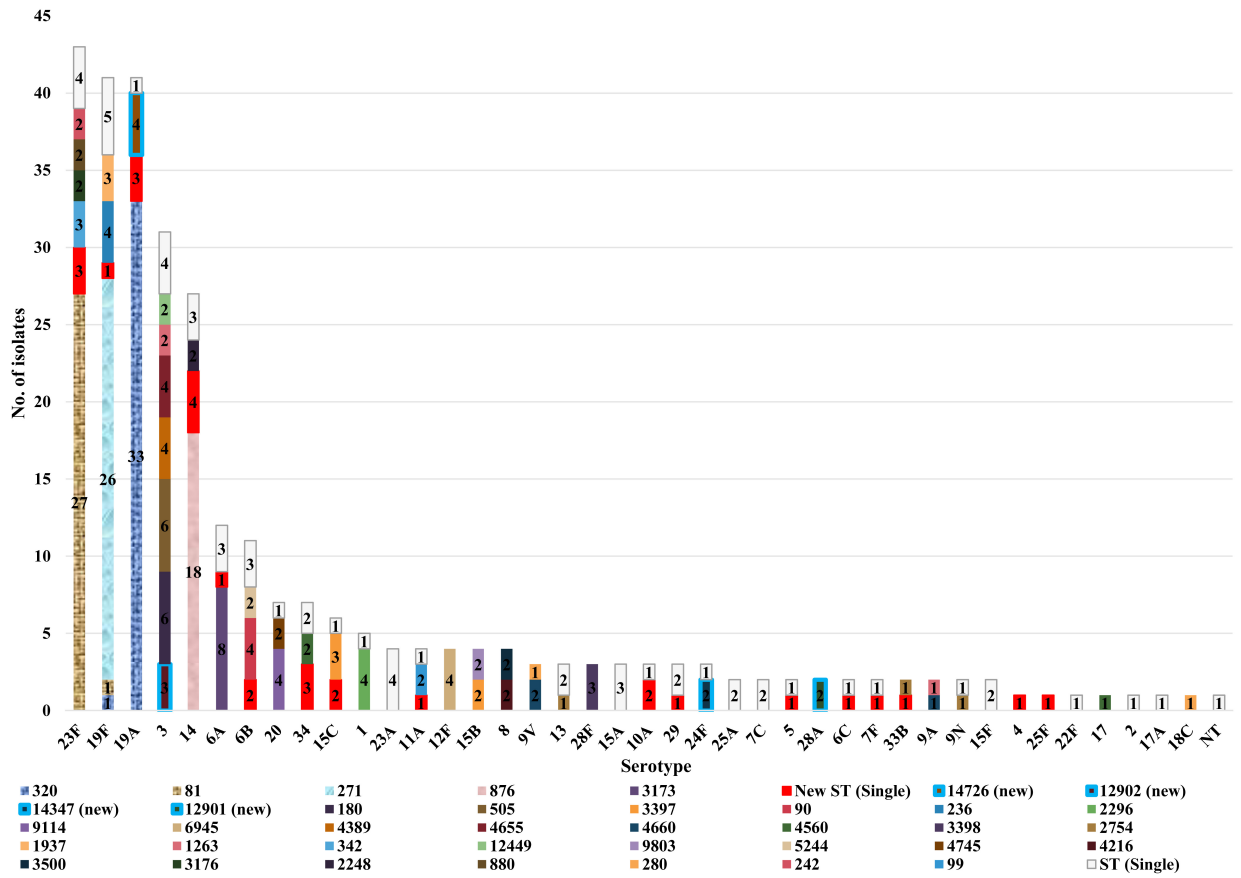

FIGURE 3 | Sequence type distribution of 300 invasive *S. pneumoniae* isolates among different serotypes.

(87.8–100%) and tetracycline (83.9–100%). Furthermore, all serotypes except serotype 3, exhibited high resistance rates to penicillin (meningitis and oral breakpoint), cefuroxime (63.6–100%) and cefaclor (72.7–100%). Serotype 19F had higher resistance rates to ceftriaxone (39.0% based on the non-meningitis breakpoint and 75.6% based on the meningitis breakpoint) and cefepime (14.6% based on the non-meningitis breakpoint and 78.0% based on the meningitis breakpoint) compared to other serotypes.

Serotype 14 showed a high rate of resistance to imipenem (7.4%), serotype 6B showed a high rate of resistance to meropenem (9.1%), whereas serotype 6A exhibited a low level of resistance to trimethoprim/sulfamethoxazole (25.0%). We also observed that both PCV and PPV23 vaccine-covered serotype strains showed higher resistance rates to most antimicrobial drugs than the corresponding non-vaccine-covered serotype strains, including for penicillin, cefuroxime, ceftriaxone, cefepime (meningitis breakpoint), and cefaclor (**Supplementary Table 5**). In addition, a higher proportion of PCV-covered serotype strains were resistant to clindamycin than non-covered strains (97.3% vs 91.2%, P = 0.0482). Likewise, a higher percentage of PPV23-covered serotype strains were resistant to cotrimoxazole than non-covered serotype strains (68.9% vs 51.6%, P = 0.0164).

An analysis of overall resistance rates of the isolates to different antimicrobial drugs by year is shown in **Table 4**. Collectively, over the six-year study period, a decreasing trend in antibiotic resistance rates to penicillin, cefuroxime, ceftriaxone, cefepime, cefaclor and trimethoprim/sulfamethoxazole, was observed. However, the resistance rates for ertapenem, levofloxacin, moxifloxacin, linezolid, and vancomycin remained at zero. On the other hand, clindamycin, azithromycin, clarithromycin, erythromycin, chloramphenicol, and tetracycline, maintained high levels of resistance rates (81.2–100%) across the six-year period. The resistance rate of imipenem also underwent a fluctuation (2.9% in 2010, 0% in 2011 and 2012, and then 8.1 and 8.0% in 2014 and 2015) during the 6 years. For other antibiotics, such as amoxicillin/clavulanic acid and meropenem, resistant strains have emerged but the overall resistance rate was still no more than 5%.

The Virulence Levels of Predominant Serotypes

The results of the virulence level assessment among the predominant serotype strains are shown in **Figure 4A**. We observed extremely low virulence levels for *S. pneumoniae* strains in serotypes 23F, 19A, 19F, and 14, with an average mice survival

TABLE 2 | Antimicrobial susceptibility results of the 300 *S. pneumoniae* isolates.

Antibiotics	*R* (%)	*I* (%)	*S* (%)	MIC_{50} (μg/ml)	MIC_{90} (μg/ml)	MIC range (μg/ml)
P[a]	0	4.3	95.7	1	2	≤0.015–4
P[b]	67.7	0	32.3	1	2	≤0.015–4
P[c]	44.7	23	32.3	1	2	≤0.015–4
AMC[a]	0.3	2	97.7	0.5	2	0.015–8
CXM[d]	64.3	2	33.7	4	16	0.06–64
CXM[c]	60	4.3	35.7	4	16	0.06–64
CRO[a]	7.3	18.3	74.3	0.5	2	0.007–8
CRO[b]	25.7	23.3	51	0.5	2	0.007–8
FEP[a]	4	25.7	70.3	1	2	0.03–8
FEP[b]	29.7	33	37.3	1	2	0.03–8
CEC	64	3	33	32	64	0.25–128
ETP	0	0	100	0.125	0.25	0.004–1
IPM	3.7	37.7	58.7	0.125	0.25	0.008–8
MEM	2.7	46	51.3	0.25	0.5	0.004–1
LEV	0	0	100	0.5	1	0.007–2
MXF	0	0	100	0.125	0.125	0.06–0.25
SXT	65.3	13	21.7	8	16	0.12–128
DA	95.7	1.7	2.7	128	128	0.12–256
AZM	96	0	4	>1024	>1024	0.25–2048
CLR	96	0	4	>1024	>1024	0.06–2048
E	96	0	4	>1024	>1024	0.06–2048
LZD	0	0	100	1	1	0.5–2
VA	0	0	100	0.5	0.5	0.015–1
C	91.7	0	8.3	8	16	0.25–64
TET	93.7	2.7	3.7	16	32	0.12–32

[a]*non-meningitis breakpoint.*
[b]*meningitis breakpoint.*
[c]*oral breakpoint.*
[d]*parenteral breakpoint.*
P, penicillin; AMC, amoxicillin/clavulanic; CXM, cefuroxime; CRO, ceftriaxone; FEP, cefepime; CEC, cefaclor; ETP, ertapenem; IPM, imipenem; MEM, meropenem; LEV, levofloxacin; MXF, moxifloxacin; SXT, trimethoprim/sulfamethoxazole; DA, clindamycin; AZM, azithromycin; CLR, clarithromycin; E, erythromycin; LZD, linezolid; VA, vancomycin; C, chloramphenicol; TET, tetracycline.

TABLE 3 | Antimicrobial susceptibility results of the 300 *S. pneumoniae* isolates with different serotypes in China.

Antibiotics	*R* (%)						
	23F (*n* = 43)	19F (*n* = 41)	19A (*n* = 41)	3 (*n* = 31)	14 (*n* = 27)	6A (*n* = 12)	6B (*n* = 11)
P[a]	0	0	0	0	0	0	0
P[b]	97.7	100	97.6	0	100	100	100
P[c]	81.4	70.7	97.6	0	77.8	66.7	0
AMC[a]	0	2.4	0	0	0	0	0
CXM[d]	86	97.6	100	9.7	92.6	83.3	63.6
CXM[c]	93	100	100	19.4	96.3	83.3	63.6
CRO[a]	4.7	39	7.3	0	0	0	0
CRO[b]	30.2	75.6	39	9.7	22.2	25	27.3
FEP[a]	4.7	14.6	4.9	3.2	0	0	0
FEP[b]	20.9	78	63.4	9.7	25.9	16.7	18.2
CEC	90.7	97.6	100	16.1	92.6	91.7	72.7
ETP	0	0	0	0	0	0	0
IPM	0	7.3	2.4	3.2	7.4	0	0
MEM	0	4.9	7.3	3.2	0	0	9.1
LEV	0	0	0	0	0	0	0
MXF	0	0	0	0	0	0	0
SXT	90.7	95.1	97.6	32.3	33.3	25	45.5
DA	100	100	100	87.1	100	100	100
AZM	100	100	100	87.1	100	100	100
CLR	100	100	100	87.1	100	100	100
E	100	100	100	87.1	100	100	100
LZD	0	0	0	0	0	0	0
VA	0	0	0	0	0	0	0
C	95.3	87.8	90.2	80.6	96.3	100	100
TET	100	97.6	100	83.9	85.2	100	100

[a]*non-meningitis breakpoint.*
[b]*meningitis breakpoint.*
[c]*oral breakpoint.*
[d]*parenteral breakpoint.*
P, penicillin; AMC, amoxicillin/clavulanic; CXM, cefuroxime; CRO, ceftriaxone; FEP, cefepime; CEC, cefaclor; ETP, ertapenem; IPM, imipenem; MEM, meropenem; LEV, levofloxacin; MXF, moxifloxacin; SXT, trimethoprim/sulfamethoxazole; DA, clindamycin; AZM, azithromycin; CLR, clarithromycin; E, erythromycin; LZD, linezolid; VA, vancomycin; C, chloramphenicol; TET, tetracycline.

time uniformly exceeding 7 days. Conversely, 1×10^4 CFU of serotype 3 strains killed all the mice within 2 days, with a mean survival time of 24 h. In addition, the number of bacteria in the blood of mice infected with serotype 3 strains ($n = 8$) increased rapidly to 10^5 CFU/ml in the first 12 h of inoculation, and then increased up to 10^9 CFU/ml at 24 h. For serotypes 23F, 19F, 19A, and 14 strains, the bacterial load remained undetectable over the course of the experiment. These results suggest that the virulence levels of *S. pneumoniae* isolates is somehow dependent on capsular serotypes. For instance, serotype 3 strains were highly virulent in the mouse model whilst serotypes 23F, 19A, 19F, and 14 were lowly virulent. However, for serogroup 6 strains, virulence level variation existed among the strains.

We defined strains with maximal bacterial load in the blood of $\geq 10^5$ CFU/ml and a 7-day survival rate $\leq$20% as high virulent strains (HVS), while those with bacterial blood load of $\leq 10^4$ CFU/ml and a 7-day survival rate $\geq$80%, were defined as low virulence strains (LVS). The remainder was classified as intermediate virulent strains (IVS). Based on this criterion, six (S165, S219, S221, S249, S260, and S292) of the 12 strains of serotype 6A were HVS, two (S142 and S179) were LVS and the rest (S33, S197, S273, S276) IVS (**Figure 4B**). For serotype 6B, only one strain (S78) was classified as HVS, two (S4 and S14) as IVS and the remaining eight (S70, S159, S178, S183, S209, S290, S299, and S300) as LVS (**Figure 4C**). There were only two strains of serotype 6C, and one was classified as HVS (S119) and the other (S227) as LVS (**Figure 4D**).

The virulence level variation among strains within the same serotype suggests that some capsule-independent factors may have contributed to virulence. Thus, the expression levels of six non-capsule-associated virulence genes (*ply*, *lytA*, *nanA*, *psaA*, *pspA*, and *hylA*) were measured by RT-PCR (**Figure 5**). In serotype 6A, strain S292 (HVS) had the highest-level expression of *ply* and *nanA* genes, whilst isolate S260 (HVS) had the highest level of expression of *psaA* and *pspA* genes. Furthermore, isolate

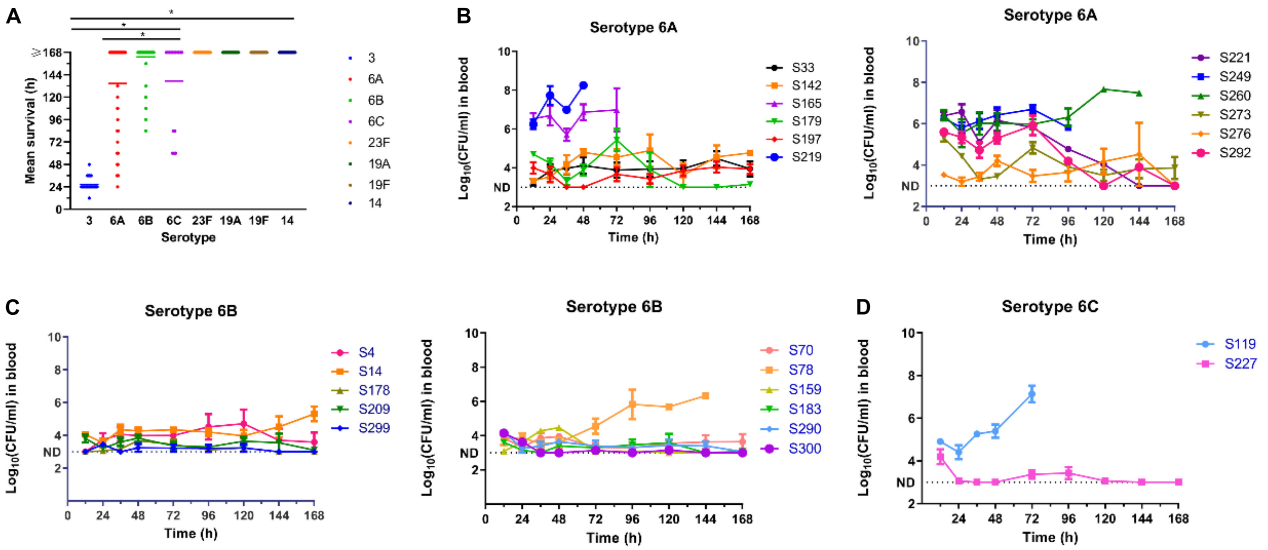

FIGURE 4 | Virulence assessment of pneumococcal isolates in mouse sepsis model. **(A)** Relationship of the virulence levels and the serotypes of *S. pneumoniae*. Virulence level was determined by the mean survival time of mice i.p. infected with pneumococcal isolates. One-way ANOVA was used to compare differences among groups. **(B–D)** Blood burden of bacteria in mice infected with different pneumococcal strains in serotype 6A, 6B, and 6C. *$P < 0.05$.

S219 (HVS) had the highest level of expression of *hylA*, whilst isolate 179 (IVS) had the highest level of expression of *lytA*. In contrast to serotype 6A, all genes were expressed at the highest level in the LVS serotype 6B isolate, save for the *hylA* gene which was expressed at the highest level in the HVS isolate (S78). For serotype 6C, the expression levels of *ply*, *lytA*, *psaA*, and *hylA* genes were higher in the HVS strain (S119) than in the LVS strain (S227), whereas the expression levels of *nanA* and *pspA* were higher in the LVS strain (S227) than in the HVS strain (S119).

Overall, we found great variation in the expression of these virulence genes in different serotypes and even among different strains within the same serotypes. In general, capsular, and non-capsular properties together determined the virulence of *S. pneumoniae* strains. The regulation of virulence levels is complex and elaborate, determined by a variety of virulence genes.

DISCUSSION

The 300 *S. pneumoniae* isolates studied were isolated from 27 teaching hospitals in China, all from sterile body sites, including blood, cerebrospinal fluid, and pleural effusion, which can result in severe IPD. IPD is an aggressive disease with an annual incidence of 6.6–14 per 100,000 people, and a mortality rate of 10–30% (Sousa et al., 2018). Given that *S. pneumoniae* has become a major challenge to public health systems worldwide, a comprehensive understanding of its clinical characteristics is of great importance.

It has been reported that the distribution of *S. pneumoniae* serotypes exhibits association of specific serotypes with geographical locale, attack rate, age, tendency to cause outbreaks, and propensity to acquire antimicrobial resistance genes (Jourdain et al., 2011). Furthermore, the introduction of vaccines covering specific serotypes has been an effective way to prevent IPD caused by *S. pneumoniae*. The five most common serotypes in this study were: 23F (43, 14.3%), 19A (41, 13.7%), 19F (41, 13.7%), 3 (31, 10.3%), and 14 (27, 9.0%). The serotype coverage rates of PCV7, PCV10, PCV13, and PPV23 vaccines on our bacterial collection was 42.3, 45.3, 73.3 and 79.3%, respectively. The distribution of serotypes and vaccine coverage in our study was similar between the children and adult groups.

Based on reports from the Canadian Public Health Laboratory Network (Demczuk et al., 2013), the predominant *S. pneumoniae* serotypes causing IPD in Canada during the years 2010–2012 were 19A, 7F, 3, and 22F, with PCV13 vaccine coverage ranging from 41 to 66%. Among Turkish children, the most common serotypes causing IPD in 2015–2018 were 19F, 1, and 3, with PCV13 serotypes accounting for 56.2%, as reported by Mehmet Ceyhan et al. (Ceyhan et al., 2020). In Japan, an Asian neighbor of China, the most common serotypes in a study that included 177 patients with IPD from September 2016 to April 2018, were 12F, 3, 23, 19F, 10A, 6C, and 22F, while PCV7, PCV13, and PCV23 had 2.8, 28.2 and 61.0% coverage, respectively (Yanagihara et al., 2021). These findings demonstrate that the distribution of *S. pneumoniae* serotypes and vaccine coverage varies by country, time of isolation, age, *etc.*, which may be related to differences in antibiotic use, health conditions, economic situation, and time of vaccine introduction in various regions.

A study from two tertiary children's hospitals in Beijing (2012–2017) showed that the dominant *S. pneumoniae* serotypes in IPD cases in children were 19F, 19A, 14, 23F, and 6B, with PCV13 having a coverage of 90.1% of the strains (Shi et al., 2019). Likewise, in another study carried out at a hospital in Shenyang, a city in northeast China, from 2010 to 2014, the most common *S. pneumoniae* serotypes among isolates from pediatric

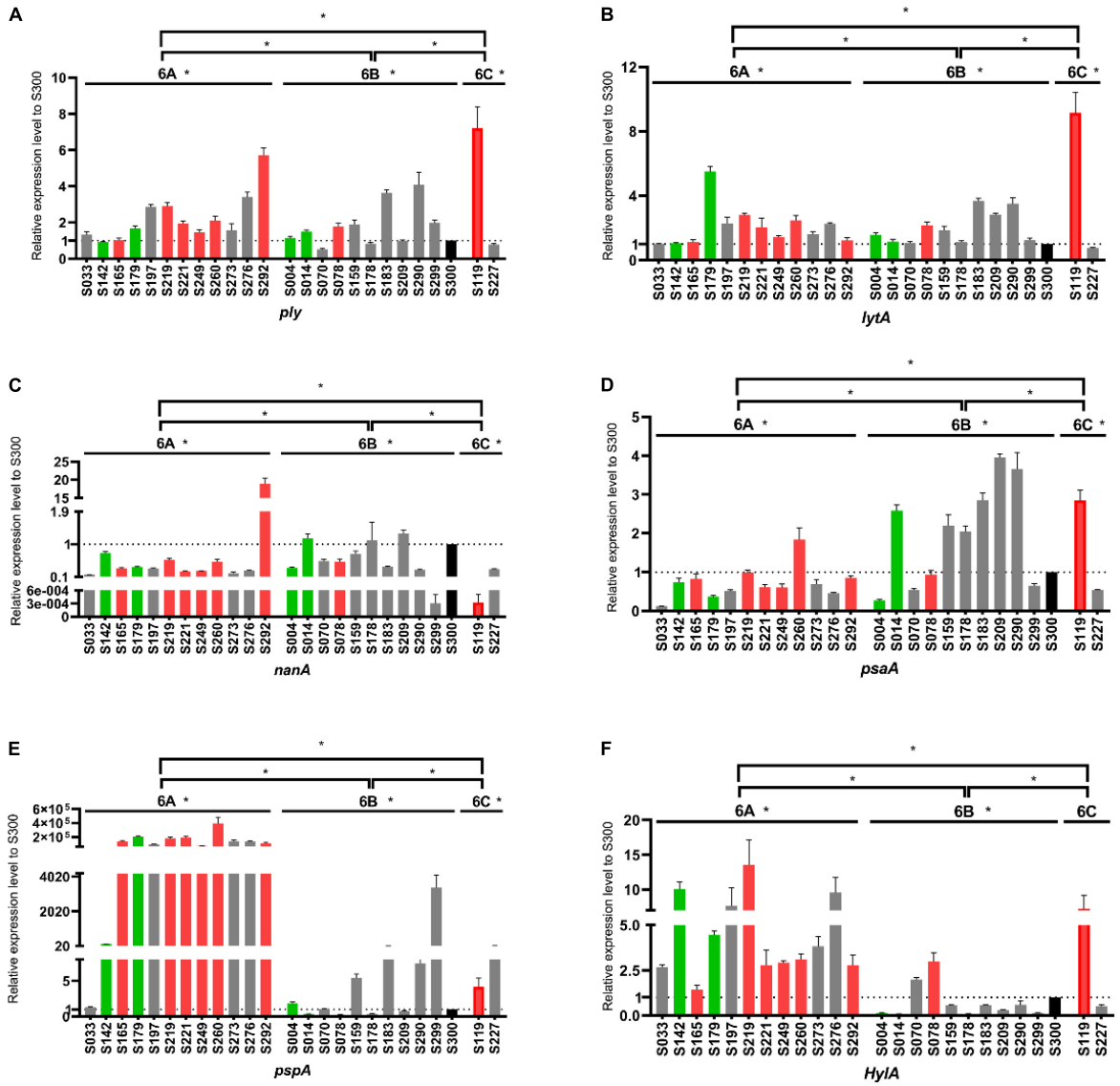

FIGURE 5 | Comparison of virulence gene expression levels among serogroup 6 strains. Expression levels of *ply* **(A)**, *lytA* **(B)**, *nanA* **(C)**, *psaA* **(D)**, *pspA* **(E)** and *hylA* **(F)** were measured and compared with the S300 strain (marked in black) as the control strain. Gray, green and red represent the low virulence strains (LVS), intermediate virulent strains (IVS) and high virulent strains (HVS), respectively. *$P < 0.05$.

IPD cases were 19A, 14, 19F, 23F, and 6B, and the coverage of PCV7, PCV10 and PCV13 vaccines was 53.9, 56.3 and 93.8%, respectively (Zhou et al., 2016). The prevalent serotypes in the two studies mentioned above are similar to ours, but with slightly higher vaccine coverage, which may be due to differences in geographical distribution of the serotypes (Zhou et al., 2016).

PCV7 was introduced in China in 2008, while PCV13 was approved in 2016 and PPV23 was only available for children older than 2 years (Shi et al., 2019). However, vaccination rates of the above-mentioned vaccines are relatively low in most regions of China due to the prohibitive high cost. Hence, many children and elderly people are still vulnerable to the lethal threats of IPD caused by *S. pneumoniae*. Moreover, based on our research, it is worth noting that the serotype coverage of PCV13 has increased significantly relative to PCV7 and PCV10, but not significantly different from that of PPV23. This may be attributed to the continuous rise in the prevalence of PCV13-associated serotypes 19A, 6A, and 3. On this basis, we recommend vaccinating the population in China with PCV13 or PPV23 to reduce the incidence of IPD.

Although the introduction of vaccines has greatly reduced the incidence of IPD for vaccine-covered serotypes, on the other hand, the incidence of IPD caused by non-vaccine-covered serotypes has increased, a phenomenon commonly referred to as "serological replacement". Data from the Danish National Serological Institute from 1999–2014 showed that the incidence of IPD caused by non-vaccine covered serotypes 8, 9N, 11A, 12F, 15A, 20, 22F, 23B, 24F, and 33F, increased for all ages

TABLE 4 | Antimicrobial susceptibility results of the 300 *S. pneumoniae* isolates during the study period in China.

Antibiotics	*R* (%)						*P*-value
	2010 (*n* = 34)	2011 (*n* = 25)	2012 (*n* = 48)	2013 (*n* = 94)	2014 (*n* = 74)	2015 (*n* = 25)	
P[a]	0	0	0	0	0	0	NA
P[b]	76.5	52	70.8	73.4	60.8	64	0.4491
P[c]	61.8	32	41.7	52.1	36.5	36	0.09
AMC[a]	0	0	0	0	1.4	0	NA
CXM[d]	67.6	52	60.4	66	51.4	60	0.7434
CXM[c]	73.5	52	66.7	72.3	51.4	68	0.865
CRO[a]	11.8	8	6.2	6.4	6.8	8	0.967
CRO[b]	44.1	16	29.2	25.5	14.9	36	0.7206
FEP[a]	8.8	4	2.1	4.3	4.1	0	0.3566
FEP[b]	52.9	24	33.3	24.5	23	36	0.3062
CEC	73.5	56	64.6	69.1	52.7	72	0.8664
ETP	0	0	0	0	0	0	NA
IPM	2.9	0	0	2.1	8.1	8	0.7778
MEM	0	0	4.2	4.3	2.7	0	NA
LEV	0	0	0	0	0	0	NA
MXF	0	0	0	0	0	0	NA
SXT	88.2	68	54.2	69.1	55.4	68	0.1148
DA	97.1	100	89.6	95.7	97.3	96	0.6179
AZM	100	100	87.5	95.7	98.6	96	0.8763
CLR	100	100	87.5	95.7	98.6	96	0.8763
E	100	100	87.5	95.7	98.6	96	0.8763
LZD	0	0	0	0	0	0	NA
VA	0	0	0	0	0	0	NA
C	100	88	89.6	88.3	94.6	92	0.3421
TET	100	92	81.2	97.9	93.2	96	0.8763

[a]*non-meningitis breakpoint.*
[b]*meningitis breakpoint.*
[c]*oral breakpoint.*
[d]*parenteral breakpoint.*
NA, not available.
P, penicillin; AMC, amoxicillin/clavulanic; CXM, cefuroxime; CRO, ceftriaxone; FEP, cefepime; CEC, cefaclor; ETP, ertapenem; IPM, imipenem; MEM, meropenem; LEV, levofloxacin; MXF, moxifloxacin; SXT, trimethoprim/sulfamethoxazole; DA, clindamycin; AZM, azithromycin; CLR, clarithromycin; E, erythromycin; LZD, linezolid; VA, vancomycin; C, chloramphenicol; TET, tetracycline.

after the introduction of PCV13 vaccine, compared to the pre-introduction period (Slotved et al., 2016). A review showed that the most common serotypes in European countries before the introduction of the PCV7 vaccine were 14, 6B, 19F, and 23, but after the introduction of this vaccine, the dominant serotypes switched to 1, 19A, 3, 6A, and 7F, which were not covered by PCV7 (Isaacman et al., 2010). In our study, serological replacement was observed for both PCV13 and PPV23 vaccines, although the distribution of prevalent serotypes varied from 2010 to 2015. Therefore, continuous monitoring of the distribution of non-vaccine covered serotypes is essential to assess the effectiveness of vaccine preventative efforts and to effectively control IPD.

Multi-locus sequence typing (MLST) analysis revealed a considerable diversity among the strains, with the most common STs being ST320, ST81, ST271, ST876, and ST3173. Phylogenetic tree analysis revealed that CC320, CC271, CC81, CC876, and CC1263 were the most common clonal complexes. This was consistent with previous studies in which CC320 and CC271 were prevalent complex groups in China (Li et al., 2019). A previous study in Catalonia, Spain, during the year 2009, which consisted of 614 IPD cases, showed that the most common clonal lineages were ST306, CC191, CC230, CC156, ST304, CC1223, and CC180 (Muñoz-Almagro et al., 2011). However, in Singapore, an Asian country, the most common STs causing IPD in children were ST9, ST156, ST236, and ST90 (Jefferies et al., 2011). Therefore, the clonal lineage of *S. pneumoniae* may vary by geographical location.

We observed that the decline in the prevalence of ST320 and ST81 (from 2010–2015) in our study was accompanied by an increase in the prevalence of ST271 and ST876. Given the relationship between serotypes and STs, serotype 19A is dominated by ST320 (80.5%). *S. pneumoniae* strain 19A ST320, derived from an international Taiwan (19F)-14 (ST236) clone, has been reported to be more competitive than its ancestral clone (Hsieh et al., 2013; Chen et al., 2019). Meanwhile, in the current study, serotype 19A ST320 had a higher rate of drug resistance than other STs, and is often associated with multidrug resistance in Asian countries (Shin et al., 2011). Despite a gradual decline (2011–2015) in the isolation rate of serotype 19A ST320 in our study, possibly owing to vaccine pressure, it remained the predominant ST in 2015. In view of its notoriety, the dissemination and sequence type switching of serotype 19A still requires continuous monitoring in China and elsewhere.

In the present study, ST81 was mainly associated with serotype 23F, accounting for 63% of this serotype. The *S. pneumoniae* 23F ST81 lineage was one of the first pandemic clones identified, and was implicated in nearly 40% of penicillin-resistant pneumococcal infections in the United States in the late 1990s (Muñoz et al., 1991). Since then, a study from Beijing raised an alarm that serotype 23F ST81 was non-susceptible to β-lactam antibiotics and was on the rise (Ma et al., 2013). In the present study, although the isolation rate of 23F ST81 went from 14.7% in 2010 to 4% in 2015, the isolation rate in 2014 was still relatively high (10.8%). The discrepancy may be explained by variation in the number of isolates between the years or by a shift in the ST under vaccine pressure. Hence, the distribution of serotype 23F ST81 deserves continuous attention.

ST271 and ST876 were correlated with serotypes 19F and 14, respectively, and were in a rising trend (2010–2015). A previous study demonstrated a worrying rising trend in the 19F CC271 lineage among *S. pneumoniae* strains from acute respiratory infections in Chinese children, from 14.3% in 1997–1998 to 92% in 2010, and was responsible for the increased non-susceptibility rate to β-lactam antibiotics of serotype 19F (Li et al., 2013). Although serotype 19F has been included in the PCV7 vaccine, it presented huge challenges in its manipulation to elicit a satisfactory protective immune response in the human host as it is more resistant to C3 deposition and less sensitive to opsono-phagocytosis (Melin et al., 2009; Poolman et al., 2011). In agreement with this, the isolation rate of serotype 19F in the present study increased from 11.8% in 2010 to 16% in 2015. Thus, trends in serotype 19F and ST271 distribution need to be

monitored continuously in the future, especially after the vaccine becomes more widely available.

The isolation rate for ST876 in the present study was relatively low, although it increased alarmingly from 2.9% in 2010 to 10.8% in 2014. Previous studies reported very dramatic increases in the detection rate of *S. pneumoniae* serotype 14 CC876 lineage, increasing notably from 0% in 1997–2000 to 96.4% in 2010 in children with acute respiratory infections in China, completely replacing the previously dominant clonal group CC875 (from 84.2 to 0%) and exhibiting a high level of non-susceptibility rates to β-lactam antibiotics (He et al., 2015). While serotype 14-ST876 did not currently dominate in this study, the increasing isolation rate, and the potent clonal expansiveness of ST876 still sounded alarm bells.

Interestingly, 10 serotypes (12F, 28F, 28A, 4, 25F, 22F, 17, 2, 17A, and 18C) matched only one ST each, implying that the non-vaccine covered serotypes may have a lower clonal diversity. As discussed above, the numbers of non-vaccine covered serotypes are growing and therefore further molecular typing studies of the non-vaccine covered serotypes are needed in the future to assess the effects of vaccines on the epidemiology of *S. pneumoniae.* In addition to this, seven groups of internationally resistance clones such as Spain23F-1, were detected in the present study by sequence alignment with those on the PMEN website. It can be assumed that the increasing international interactions have led to the widespread dissemination of these resistant clones worldwide.

The use of antibiotics is the mainstay of IPD treatment, so it is particularly important to choose effective antimicrobial drugs. All strains in the present study were susceptible to ertapenem, levofloxacin, moxifloxacin, linezolid, and vancomycin, which is in line with most studies in China and elsewhere (Xue et al., 2010; Cai et al., 2018; Golden et al., 2019). These antimicrobial agents may be a valuable reference for empirical medication in IPD treatment.

Penicillin has been recognized as an important choice for the treatment of invasive *S. pneumoniae* infections, but the rising rate of resistance among strains in recent years has sparked concern. In our study, we found that the proportion of PNSP based on the oral breakpoint was 67.7%, compared to 67.7 and 4.3% based on the meningitis and non-meningitis breakpoints, respectively. An analysis involving 1517 invasive *S. pneumoniae* strains from children in Germany between 1997 and 2004, showed that only 5.1 and 1.1% of the isolates were penicillin-intermediate and resistant, respectively (Reinert et al., 2007).

In China's bordering country, Cambodia, 46% of *S. pneumoniae* strains from children with invasive infections (2007–2012) were PNSP based on the meningitis breakpoint (Moore et al., 2016). The proportion of PNSP in our study was significantly higher than those in the two studies mentioned above, which may be explained by variation in the population included and the misuse of these over-the-counter antibiotics in China due to their availability and convenience from numerous licensed and non-licensed sources (Troy, 1992). Furthermore, the present study included isolates from both adults and children whereas the previous studies only focused on the pediatric population. In general, the adult population tends to be exposed to antibiotics more than children, resulting in an increased overall non-susceptibility rate.

Notably, most of the studied isolates (over 95%) were resistant to macrolides (azithromycin, clarithromycin, erythromycin) and clindamycin. This may be related to the frequent clinical use of these antibiotics during the past years, and imply that these antibiotics should no longer be recommended for treating *S. pneumoniae* infections. The widespread clinical use of macrolide antibiotics was strongly associated with the rise in resistance, and the major resistance mechanism is the acquisition of the *erm*(B) gene encoding a 23S methylase or the *mef* gene encoding an active (proton dependent) efflux pump (Cornick and Bentley, 2012). Besides, the high resistance rate of *S. pneumoniae* to clindamycin is noteworthy and further studies are needed to elucidate the exact resistance mechanism involved.

In terms of the distribution of antibiotic drug resistance across serotypes, serotypes 23F, 19F, 19A, and 14, exhibited higher resistance rates, while serotype 3 exhibited a relatively lower resistance rate. As previously mentioned, high levels of resistance in serotypes 23F, 19F, 19A, and 14 may be associated with the widespread international spread of ST81, ST271, ST320, and ST876, respectively. As for serotype 3, a similar resistance pattern was observed in Mexico, where 196 *S. pneumoniae* strains were susceptible to almost all the antibiotics tested, the predominant clonal complex group being CC180 (71.4%) (Echániz-Aviles et al., 2019). In our study, serotype 3 had a highly clonal diversity, dominated by ST505 (19.4%) and ST180 (19.4%). By whole genome sequencing of 616 strains of serotype 3 from England and Wales over a 15-year period, Groves et al. found that the composition of their clade changed along with shifts in antibiotic resistance (Groves et al., 2019). Thus, the clonal lineage and resistance pattern of serotype 3 should be closely monitored.

Another noticeable finding in this study was that the resistance rates of vaccine-covered serotypes were generally higher than those of non-vaccine-covered serotypes, which is in agreement with a previous report (Zhao et al., 2020). With the increasing number of non-vaccines covered serotypes causing IPD, the resistance levels of these serotypes should be carefully monitored under the dual pressure of antibiotics and vaccines.

An analysis of the annual antibiotic resistance rates showed a decrease from 2010 to 2015 for penicillin, cefuroxime, ceftriaxone, cefepime, cefaclor and trimethoprim/sulfamethoxazole. Regarding penicillin, we speculated that this phenomenon may be related to the penicillin breakpoint update in 2008 and the introduction of the PCV7 vaccine. Karlowsky et al. (2018) reported that 6001 *S. pneumoniae* isolates from Canada showed a small increase ($P < 0.05$) in susceptibility to penicillin and ceftriaxone during the period 2011–2015. In our study, the increased susceptibility of *S. pneumoniae* to cephalosporin antibiotics may be due to a decrease in serotypes 19A and 23F, which were resistant to a variety of antibiotics, including cephalosporins. Furthermore, a 20-year continuous global monitoring by the SENTRY Antimicrobial Surveillance Program (1997–2016) found that the susceptibility rates of ceftriaxone, erythromycin, clindamycin, tetracycline, and trimethoprim-sulfamethoxazole decreased in the first 12–14 years, and increased thereafter in

the last 6–8 years (Sader et al., 2019). From a long-term point of view, a global collaboration with large samples and a prolonged time scale will help elucidate the current and changing trends of drug resistance to combat invasive infections caused by *S. pneumoniae* effectively.

Virulence is a key indicator for evaluating pathogenicity. We performed *in vivo* animal experiments to assess the virulence levels of the prevalent serotypes using the intraperitoneal infection model. Our study showed that serotypes 23F, 19A, 19F, and 14 strains were the prevalent avirulent serotypes while serotype 3 exhibited high virulence levels. However, the virulence levels of strains in serogroup 6 varied among serotypes and strains. A previous meta-analysis consisting of nine studies showed that the outcome of IPD was strongly associated with the serotype (Weinberger et al., 2010). In that study, serotypes 1, 7F, and 8 were associated with decreased risk ratio (RR) while serotypes 3, 6A, 6B, 9N, and 19F, were associated with increased relative risk (RR). Another study (Briles et al., 1992) demonstrated the strong association between capsular serotypes and virulence of the *S. pneumoniae* strains through *in vivo* virulence experiments in mice. Based on their observation, all serotype 4 strains, 40% of serotype 3 and 60% of serogroup 6, were virulent for mice, whilst strains of serogroups/types 14, 19, and 23, were avirulent. This was partly in line with our findings. Furthermore, according to our investigations, all serotype 3 strains from various clonal origins were virulent while all strains of serotypes 23F, 19F, 19A, and 14 from diverse clonal origins were avirulent, suggesting that the different capsular polysaccharides conferred pneumococci with intrinsically different virulence properties. Intriguingly, we found that strains of serotype 3 were characterized by high virulence and low resistance, while strains of serotypes 23F, 19F, 19A, and 14 were of low virulence and high resistance. Our findings are similar to those of Azoulay-Dupuis et al. (2000). In addition, a case-control study also showed that the clinical presentation of adult pneumonia caused by PNSP was milder than that of PSSP, suggesting that it is possible that resistance "carries a cost" (Einarsson et al., 1998). We speculated that strains of low virulent serotypes may be more prone to long-term colonization to acquire resistance through exposure to more antibiotics.

The virulence level of strains in serogroup 6 as per our mouse sepsis model was considerably complicated and complex, with great variation observed in the virulence levels of different strains within the same serotype (6A, 6B or 6C). Previous research (Briles et al., 1992) has shown that only 60% of strains in serogroup 6 were virulent for mice, which reinforced the heterogeneity of the virulence of serogroup 6 pneumococci. The fact that strains with the same serotype exhibit different virulence levels suggest presence of virulence determinants other than capsular polysaccharides. It is also worth noting that several studies (Polissi et al., 1998; Lau et al., 2001) using signature-tagged mutagenesis have unveiled a large set of genes that can influence the virulence of *S. pneumoniae*. Numerous non-capsular virulence genes, including *ply*, *lytA*, *nanA*, *psaA*, *pspA* and *hylA*, have been shown to be involved in the regulation of pneumococcal virulence (Ogunniyi et al., 2002; LeMessurier et al., 2006). *Ply* encoding pneumolysin, which can contribute to the early development of IPD by facilitating the invasion of *S. pneumoniae* from the lung into the bloodstream. Significantly, pneumolysin is a multifunctional toxin exhibiting both hemolytic and complement activities, and its deficiency would lead to a reduction in the virulence of the *S. pneumoniae* strain (Rubins et al., 1996). *LytA*, encoding an amidase with autolytic activity, exerts its virulence by releasing pneumolysin and inflammatory peptidoglycan from lysing bacteria (Kadioglu et al., 2008). It was reported that *LytA*-negative *S. pneumoniae* exhibited a lower virulence level through murine models of pneumonia and bacteremia (Canvin et al., 1995). All *S. pneumoniae* strains express *nanA* which encoding neuraminidase, it is essential for promoting *S. pneumoniae* adhesion to and invasion of uman brain microvascular endothelial cells (Uchiyama et al., 2009). *PsaA* is thought to encode a pneumococcal adhesin. In murine models of pneumonia, bacteremia and colonization, knockout of *psaA* abolished the virulence of *S. pneumoniae* (Marra et al., 2002). *PspA* impairs the fixation of complement component C3 on the surface of pneumococcal cells, thereby inhibiting complement-mediated opsonization. In addition, *pspA* encodes a lactoferrin-binding protein that protects bacteria from being killed by apolactoferrin (Kadioglu et al., 2008). *HylA* encodes the hyaluronate lyase enzyme which degrades hyaluronan, then destroying the structure of the connective tissue and exposing it to endo- and exogenous factors, including various bacterial toxins (Jedrzejas et al., 2002).

Therefore, the expression level of above genes amongst serogroup 6 strains was measured and compared. Our results revealed that the expression of virulence genes varied among these strains, but did not correspond significantly to the virulence phenotype of the *in vivo* experiments. This prompted us to think that pneumococcal virulence may be collaboratively regulated by multiple virulence genes, and that this regulation is highly complex and multifactorial. Robinson et al. (2002) identified the major clones of 212 *S. pneumoniae* strains from 39 countries by MLST, and the results indicated that the virulent serogroup 6 strains originated from the avirulent ancestral clones and went through multiple evolution to become virulent. It is possible that horizontal recombination or evolution of virulence genes between strains contributed to a diversity in virulence. Overall, our study suggests that capsular polysaccharide and non-capsular virulence genes are collectively responsible for the virulence diversity of *S. pneumoniae* strains.

This study has several limitations. Firstly, the strains collected in this study were from different time periods, which could lead to bias in the results. Secondly, the strains were mainly from tertiary teaching hospitals in China; samples from remote and rural areas were not included. Thirdly, the virulence of some of the rarer serotypes and non-vaccine covered serotypes were not evaluated.

CONCLUSION

Overall, our study provides a comprehensive insight into the epidemiological and virulence diversity of *S. pneumoniae* strains causing IPD in China. The most common serotypes in this

study were 23F, 19A, 19F, 3, and 14. The serotype coverages of PCV7, PCV10, PCV13, and PPV23 vaccines on the bacterial collection were 42.3, 45.3, 73.3 and 79.3%, respectively. The most common STs were ST320, ST81, ST271, ST876, and ST3173. All strains were susceptible to ertapenem, levofloxacin, moxifloxacin, linezolid, and vancomycin, but highly resistant to macrolides and clindamycin (>95%). Serotype 3 strains were characterized by high virulence levels and low antimicrobial-resistance rates, while strains of serotypes 23F, 19F, 19A, and 14, exhibited low virulence and high resistance rates to antibiotics.

DATA AVAILABILITY STATEMENT

The original contributions presented in the study are included in the article/**Supplementary Material**, further inquiries can be directed to the corresponding author/s.

ETHICS STATEMENT

The animal study was reviewed and approved by the Medical Ethics Committee of Peking Union Medical College Hospital (No. S-263).

AUTHOR CONTRIBUTIONS

ZL, HZ, YX, and JZ conceived and designed the work. MZ, HA, CQ, BJ, and YW performed the experiments. MZ, ZW, LZ, and TK performed the data analysis and wrote the manuscript. All authors read and approved the final manuscript.

FUNDING

This work was supported by Special Foundation for National Science and Technology Basic Research Program of China (grant No. 2019FY101200), Beijing Key Clinical Specialty for Laboratory Medicine–Excellent Project (grant No. ZK201000), Graduate Innovation Fund of Peking Union Medical College (grant No. 2017-1002-1-21).

SUPPLEMENTARY MATERIAL

The Supplementary Material for this article can be found online at: https://www.frontiersin.org/articles/10.3389/fmicb.2021.798750/full#supplementary-material

REFERENCES

Azoulay-Dupuis, E., Rieux, V., Muffat-Joly, M., Bédos, J. P., Vallée, E., Rivier, C., et al. (2000). Relationship between capsular type, penicillin susceptibility, and virulence of human *Streptococcus pneumoniae* isolates in mice. *Antimicrob. Agents Chemother.* 44, 1575–1577. doi: 10.1128/aac.44.6.1575-1577.2000

Boulton, M. L., Ravi, N. S., Sun, X., Huang, Z., and Wagner, A. L. (2016). Trends in childhood pneumococcal vaccine coverage in Shanghai, China, 2005-2011: a retrospective cohort study. *BMC Public Health* 16:109. doi: 10.1186/s12889-016-2785-7

Briles, D. E., Crain, M. J., Gray, B. M., Forman, C., and Yother, J. (1992). Strong association between capsular type and virulence for mice among human isolates of *Streptococcus pneumoniae*. *Infect. Immun.* 60, 111–116. doi: 10.1128/iai.60.1.111-116.1992

Cai, K., Wang, Y., Guo, Z., Xu, X., Li, H., and Zhang, Q. (2018). Clinical characteristics and antimicrobial resistance of pneumococcal isolates of pediatric invasive pneumococcal disease in China. *Infect. Drug Resist.* 11, 2461–2469. doi: 10.2147/idr.S183916

Canvin, J. R., Marvin, A. P., Sivakumaran, M., Paton, J. C., Boulnois, G. J., Andrew, P. W., et al. (1995). The role of pneumolysin and autolysin in the pathology of pneumonia and septicemia in mice infected with a type 2 pneumococcus. *J. Infect. Dis.* 172, 119–123. doi: 10.1093/infdis/172.1.119

Ceyhan, M., Aykac, K., Gurler, N., Ozsurekci, Y., Öksüz, L., Altay Akısoglu, Ö, et al. (2020). Serotype distribution of *Streptococcus pneumonia* in children with invasive disease in Turkey: 2015-2018. *Hum. Vaccin. Immunother.* 16, 2773–2778. doi: 10.1080/21645515.2020.1747931

Chen, K., Zhang, X., Shan, W., Zhao, G., and Zhang, T. (2018). Serotype distribution of *Streptococcus pneumoniae* and potential impact of pneumococcal conjugate vaccines in China: a systematic review and meta-analysis. *Hum. Vaccin. Immunother.* 14, 1453–1463. doi: 10.1080/21645515.2018.1435224

Chen, Y. Y., Wang, J. T., Lin, T. L., Gong, Y. N., Li, T. H., Huang, Y. Y., et al. (2019). Prophage excision in *Streptococcus pneumoniae* serotype 19A ST320 promote colonization: insight into its evolution from the Ancestral Clone Taiwan 19F-14 (ST236). *Front. Microbiol.* 10:205. doi: 10.3389/fmicb.2019.00205

CLSI (2019). *Performance Standards for Antimicrobial Susceptibility Testing, 29th Edn, CLSI Supplement M100*. Wayne, PA: Clinical and Laboratory Standards Institute.

Cornick, J. E., and Bentley, S. D. (2012). *Streptococcus pneumoniae*: the evolution of antimicrobial resistance to beta-lactams, fluoroquinolones and macrolides. *Microbes Infect.* 14, 573–583. doi: 10.1016/j.micinf.2012.01.012

Demczuk, W. H., Martin, I., Griffith, A., Lefebvre, B., McGeer, A., Lovgren, M., et al. (2013). Serotype distribution of invasive *Streptococcus pneumoniae* in Canada after the introduction of the 13-valent pneumococcal conjugate vaccine, 2010-2012. *Can. J. Microbiol.* 59, 778–788. doi: 10.1139/cjm-2013-0614

Echániz-Aviles, G., Guerreiro, S. I., Silva-Costa, C., Mendes, C. I., Carriço, J. A., Carnalla-Barajas, M. N., et al. (2019). *Streptococcus pneumoniae* serotype 3 in Mexico (1994 to 2017): decrease of the unusual clonal complex 4909 lineage following PCV13 introduction. *J. Clin. Microbiol.* 57:e01354-18. doi: 10.1128/jcm.01354-18

Einarsson, S., Kristjansson, M., Kristinsson, K. G., Kjartansson, G., and Jonsson, S. (1998). Pneumonia caused by penicillin-non-susceptible and penicillin-susceptible pneumococci in adults: a case-control study. *Scand. J. Infect. Dis.* 30, 253–256. doi: 10.1080/00365549850160882

Esposito, S., Principi, N., and Cornaglia, G. (2014). Barriers to the vaccination of children and adolescents and possible solutions. *Clin. Microbiol. Infect.* 20 Suppl 5, 25–31. doi: 10.1111/1469-0691.12447

Ganaie, F., Saad, J. S., McGee, L., van Tonder, A. J., Bentley, S. D., Lo, S. W., et al. (2020). A new pneumococcal capsule type, 10D, is the 100th serotype and has a large cps fragment from an oral streptococcus. *mBio* 11:e00937-20. doi: 10.1128/mBio.00937-20

Geno, K. A., Gilbert, G. L., Song, J. Y., Skovsted, I. C., Klugman, K. P., Jones, C., et al. (2015). Pneumococcal capsules and their types: past, present, and future. *Clin. Microbiol. Rev.* 28, 871–899. doi: 10.1128/cmr.00024-15

Golden, A. R., Baxter, M. R., Davidson, R. J., Martin, I., Demczuk, W., Mulvey, M. R., et al. (2019). Comparison of antimicrobial resistance patterns in *Streptococcus pneumoniae* from respiratory and blood cultures in Canadian hospitals from 2007-16. *J. Antimicrob. Chemother.* 74(Suppl 4), iv39–iv47. doi: 10.1093/jac/dkz286

Groves, N., Sheppard, C. L., Litt, D., Rose, S., Silva, A., Njoku, N., et al. (2019). Evolution of *Streptococcus pneumoniae* serotype 3 in England and Wales: a major vaccine evader. *Genes (Basel)* 10:845. doi: 10.3390/genes10110845

He, M., Yao, K., Shi, W., Gao, W., Yuan, L., Yu, S., et al. (2015). Dynamics of serotype 14 *Streptococcus pneumoniae* population causing acute respiratory infections among children in China (1997-2012). *BMC Infect. Dis.* 15:266. doi: 10.1186/s12879-015-1008-7

Hsieh, Y. C., Lin, T. L., Chang, K. Y., Huang, Y. C., Chen, C. J., Lin, T. Y., et al. (2013). Expansion and evolution of *Streptococcus pneumoniae* serotype 19A ST320 clone as compared to its ancestral clone, Taiwan19F-14 (ST236). *J. Infect. Dis.* 208, 203–210. doi: 10.1093/infdis/jit145

Isaacman, D. J., McIntosh, E. D., and Reinert, R. R. (2010). Burden of invasive pneumococcal disease and serotype distribution among *Streptococcus pneumoniae* isolates in young children in Europe: impact of the 7-valent pneumococcal conjugate vaccine and considerations for future conjugate vaccines. *Int. J. Infect. Dis.* 14, e197–e209. doi: 10.1016/j.ijid.2009.05.010

Jedrzejas, M. J., Mello, L. V., de Groot, B. L., and Li, S. (2002). Mechanism of hyaluronan degradation by *Streptococcus pneumoniae* hyaluronate lyase. Structures of complexes with the substrate. *J. Biol. Chem.* 277, 28287–28297. doi: 10.1074/jbc.M112009200

Jefferies, J. M. C., Tee, W. S. N., and Clarke, S. C. (2011). Molecular analysis of *Streptococcus pneumoniae* clones causing invasive disease in children in Singapore. *J. Med. Microbiol.* 60(Pt 6), 750–755. doi: 10.1099/jmm.0.030007-0

Jourdain, S., Drèze, P. A., Vandeven, J., Verhaegen, J., Van Melderen, L., and Smeesters, P. R. (2011). Sequential multiplex PCR assay for determining capsular serotypes of colonizing *S. pneumoniae*. *BMC Infect. Dis.* 11:100. doi: 10.1186/1471-2334-11-100

Kadioglu, A., Weiser, J. N., Paton, J. C., and Andrew, P. W. (2008). The role of *Streptococcus pneumoniae* virulence factors in host respiratory colonization and disease. *Nat. Rev. Microbiol.* 6, 288–301. doi: 10.1038/nrmicro1871

Karlowsky, J. A., Adam, H. J., Golden, A. R., Baxter, M. R., Nichol, K. A., Martin, I., et al. (2018). Antimicrobial susceptibility testing of invasive isolates of *Streptococcus pneumoniae* from Canadian patients: the SAVE study, 2011-15. *J. Antimicrob. Chemother.* 73(suppl_7), vii5–vii11. doi: 10.1093/jac/dky156

Kim, S. H., Chung, D. R., Song, J. H., Baek, J. Y., Thamlikitkul, V., Wang, H., et al. (2020). Changes in serotype distribution and antimicrobial resistance of *Streptococcus pneumoniae* isolates from adult patients in Asia: emergence of drug-resistant non-vaccine serotypes. *Vaccine* 38, 6065–6073. doi: 10.1016/j.vaccine.2019.09.065

Lalitha, M. K., Thomas, K., Kumar, R. S., and Steinhoff, M. C. (1999). Serotyping of *Streptococcus pneumoniae* by coagglutination with 12 pooled antisera. *J. Clin. Microbiol.* 37, 263–265. doi: 10.1128/jcm.37.1.263-265.1999

Lau, G. W., Haataja, S., Lonetto, M., Kensit, S. E., Marra, A., Bryant, A. P., et al. (2001). A functional genomic analysis of type 3 *Streptococcus pneumoniae* virulence. *Mol. Microbiol.* 40, 555–571. doi: 10.1046/j.1365-2958.2001.02335.x

LeMessurier, K. S., Ogunniyi, A. D., and Paton, J. C. (2006). Differential expression of key pneumococcal virulence genes in vivo. *Microbiology (Reading)* 152(Pt 2), 305–311. doi: 10.1099/mic.0.28438-0

Li, Q. H., Yao, K. H., Yu, S. J., Ma, X., He, M. M., Shi, W., et al. (2013). Spread of multidrug-resistant clonal complex 271 of serotype 19F *Streptococcus pneumoniae* in Beijing, China: characterization of serotype 19F. *Epidemiol. Infect.* 141, 2492–2496. doi: 10.1017/s0950268813000514

Li, X. X., Xiao, S. Z., Gu, F. F., Zhao, S. Y., Xie, Q., Sheng, Z. K., et al. (2019). Serotype distribution, antimicrobial susceptibility, and Multilocus Sequencing Type (MLST) of *Streptococcus pneumoniae* from adults of three hospitals in Shanghai, China. *Front. Cell. Infect Microbiol.* 9:407. doi: 10.3389/fcimb.2019.00407

Liang, Q., Li, G. F., and Zhu, F. C. (2016). Vaccine profile of PPV23: Beijing Minhai Biotech 23-valent pneumococcal vaccine. *Expert. Rev. Vaccines* 15, 1351–1359. doi: 10.1080/14760584.2016.1239536

Ma, X., Yao, K. H., Yu, S. J., Zhou, L., Li, Q. H., Shi, W., et al. (2013). Genotype replacement within serotype 23F *Streptococcus pneumoniae* in Beijing, China: characterization of serotype 23F. *Epidemiol. Infect.* 141, 1690–1696. doi: 10.1017/s0950268812002269

Marra, A., Lawson, S., Asundi, J. S., Brigham, D., and Hromockyj, A. E. (2002). In vivo characterization of the psa genes from *Streptococcus pneumoniae* in multiple models of infection. *Microbiology (Reading)* 148(Pt 5), 1483–1491. doi: 10.1099/00221287-148-5-1483

Marrie, T. J., Tyrrell, G. J., Majumdar, S. R., and Eurich, D. T. (2018). Effect of age on the manifestations and outcomes of invasive pneumococcal disease in adults. *Am. J. Med.* 131, 100.e1–100.e7. doi: 10.1016/j.amjmed.2017.06.039

Melin, M., Jarva, H., Siira, L., Meri, S., Käyhty, H., and Väkeväinen, M. (2009). *Streptococcus pneumoniae* capsular serotype 19F is more resistant to C3 deposition and less sensitive to opsonophagocytosis than serotype 6B. *Infect. Immun.* 77, 676–684. doi: 10.1128/iai.01186-08

Moore, C. E., Giess, A., Soeng, S., Sar, P., Kumar, V., Nhoung, P., et al. (2016). Characterisation of invasive *Streptococcus pneumoniae* isolated from Cambodian children between 2007 – 2012. *PLoS One* 11:e0159358. doi: 10.1371/journal.pone.0159358

Muñoz, R., Coffey, T. J., Daniels, M., Dowson, C. G., Laible, G., Casal, J., et al. (1991). Intercontinental spread of a multiresistant clone of serotype 23F *Streptococcus pneumoniae*. *J. Infect. Dis.* 164, 302–306. doi: 10.1093/infdis/164.2.302

Muñoz-Almagro, C., Ciruela, P., Esteva, C., Marco, F., Navarro, M., Bartolome, R., et al. (2011). Serotypes and clones causing invasive pneumococcal disease before the use of new conjugate vaccines in Catalonia. *Spain. J. Infect.* 63, 151–162. doi: 10.1016/j.jinf.2011.06.002

O'Brien, K. L., Wolfson, L. J., Watt, J. P., Henkle, E., Deloria-Knoll, M., McCall, N., et al. (2009). Burden of disease caused by *Streptococcus pneumoniae* in children younger than 5 years: global estimates. *Lancet* 374, 893–902. doi: 10.1016/S0140-6736(09)61204-6

Ogunniyi, A. D., Giammarinaro, P., and Paton, J. C. (2002). The genes encoding virulence-associated proteins and the capsule of *Streptococcus pneumoniae* are upregulated and differentially expressed in vivo. *Microbiology (Reading)* 148(Pt 7), 2045–2053. doi: 10.1099/00221287-148-7-2045

Polissi, A., Pontiggia, A., Feger, G., Altieri, M., Mottl, H., Ferrari, L., et al. (1998). Large-scale identification of virulence genes from *Streptococcus pneumoniae*. *Infect. Immun.* 66, 5620–5629. doi: 10.1128/iai.66.12.5620-5629.1998

Poolman, J., Frasch, C., Nurkka, A., Käyhty, H., Biemans, R., and Schuerman, L. (2011). Impact of the conjugation method on the immunogenicity of *Streptococcus pneumoniae* serotype 19F polysaccharide in conjugate vaccines. *Clin. Vaccine Immunol.* 18, 327–336. doi: 10.1128/cvi.00402-10

Reinert, R. R., van der Linden, M., Seegmüller, I., Al-Lahham, A., Siedler, A., Weissmann, B., et al. (2007). Molecular epidemiology of penicillin-non-susceptible *Streptococcus pneumoniae* isolates from children with invasive pneumococcal disease in Germany. *Clin. Microbiol. Infect.* 13, 363–368. doi: 10.1111/j.1469-0691.2006.01676.x

Richter, S. S., Heilmann, K. P., Dohrn, C. L., Riahi, F., Diekema, D. J., and Doern, G. V. (2013). Pneumococcal serotypes before and after introduction of conjugate vaccines, United States, 1999-2011(1.). *Emerg. Infect. Dis.* 19, 1074–1083. doi: 10.3201/eid1907.121830

Robinson, D. A., Briles, D. E., Crain, M. J., and Hollingshead, S. K. (2002). Evolution and virulence of serogroup 6 pneumococci on a global scale. *J. Bacteriol.* 184, 6367–6375. doi: 10.1128/jb.184.22.6367-6375.2002

Rubins, J. B., Charboneau, D., Fasching, C., Berry, A. M., Paton, J. C., Alexander, J. E., et al. (1996). Distinct roles for pneumolysin's cytotoxic and complement activities in the pathogenesis of pneumococcal pneumonia. *Am. J. Respir. Crit. Care Med.* 153(4 Pt 1), 1339–1346. doi: 10.1164/ajrccm.153.4.8616564

Sader, H. S., Mendes, R. E., Le, J., Denys, G., Flamm, R. K., and Jones, R. N. (2019). Antimicrobial susceptibility of *Streptococcus pneumoniae* from North America, Europe, Latin America, and the Asia-Pacific Region: results from 20 years of the SENTRY antimicrobial surveillance program (1997–2016). *Open Forum Infect. Dis.* 6(Suppl 1), S14–S23. doi: 10.1093/ofid/ofy263

Shi, W., Li, J., Dong, F., Qian, S., Liu, G., Xu, B., et al. (2019). Serotype distribution, antibiotic resistance pattern, and multilocus sequence types of invasive *Streptococcus pneumoniae* isolates in two tertiary pediatric hospitals in Beijing prior to PCV13 availability. *Expert. Rev. Vaccines* 18, 89–94. doi: 10.1080/14760584.2019.1557523

Shin, J., Baek, J. Y., Kim, S. H., Song, J. H., and Ko, K. S. (2011). Predominance of ST320 among *Streptococcus pneumoniae* serotype 19A isolates from 10 Asian countries. *J. Antimicrob. Chemother.* 66, 1001–1004. doi: 10.1093/jac/dkr048

Slotved, H. C., Dalby, T., and Hoffmann, S. (2016). The effect of pneumococcal conjugate vaccines on the incidence of invasive pneumococcal disease caused by ten non-vaccine serotypes in Denmark. *Vaccine* 34, 769–774. doi: 10.1016/j.vaccine.2015.12.056

Sousa, A., Pérez-Rodríguez, M. T., Nodar, A., Martínez-Lamas, L., Vasallo, F. J., Álvarez-Fernández, M., et al. (2018). Clinical and microbiological

characteristics of unusual manifestations of invasive pneumococcal disease. *Enferm. Infecc. Microbiol. Clin.* 36, 284–289. doi: 10.1016/j.eimc.2017.05.003

Troy, F. A. II (1992). Polysialylation: from bacteria to brains. *Glycobiology* 2, 5–23.

Uchiyama, S., Carlin, A. F., Khosravi, A., Weiman, S., Banerjee, A., Quach, D., et al. (2009). The surface-anchored NanA protein promotes pneumococcal brain endothelial cell invasion. *J. Exp. Med.* 206, 1845–1852. doi: 10.1084/jem.20090386

Varghese, R., Neeravi, A., Subramanian, N., Pavithra, B., Kavipriya, A., Kumar, J. L., et al. (2019). Clonal similarities and sequence-type diversity of invasive and carriage *Streptococcus pneumoniae* in India among children under 5 years. *Indian J. Med. Microbiol.* 37, 358–362. doi: 10.4103/ijmm.IJMM_19_348

Weinberger, D. M., Harboe, Z. B., Sanders, E. A., Ndiritu, M., Klugman, K. P., Rückinger, S., et al. (2010). Association of serotype with risk of death due to pneumococcal pneumonia: a meta-analysis. *Clin. Infect. Dis.* 51, 692–699. doi: 10.1086/655828

Xue, L., Yao, K., Xie, G., Zheng, Y., Wang, C., Shang, Y., et al. (2010). Serotype distribution and antimicrobial resistance of *Streptococcus pneumoniae* isolates that cause invasive disease among Chinese children. *Clin. Infect. Dis.* 50, 741–744. doi: 10.1086/650534

Yanagihara, K., Kosai, K., Mikamo, H., Mukae, H., Takesue, Y., Abe, M., et al. (2021). Serotype distribution and antimicrobial susceptibility of *Streptococcus pneumoniae* associated with invasive pneumococcal disease among adults in Japan. *Int. J. Infect. Dis.* 102, 260–268. doi: 10.1016/j.ijid.2020.10.017

Zhao, C., Xie, Y., Zhang, F., Wang, Z., Yang, S., Wang, Q., et al. (2020). Investigation of antibiotic resistance, serotype distribution, and genetic characteristics of 164 invasive *Streptococcus pneumoniae* from North China between April 2016 and October 2017. *Infect. Drug Resist.* 13, 2117–2128. doi: 10.2147/idr.S256663

Zhou, X., Liu, J., Zhang, Z., Liu, Y., Wang, Y., and Liu, Y. (2016). Molecular characteristics of penicillin-binding protein 2b, 2x and 1a sequences in *Streptococcus pneumoniae* isolates causing invasive diseases among children in Northeast China. *Eur. J. Clin. Microbiol. Infect. Dis.* 35, 633–645. doi: 10.1007/s10096-016-2582-3

Conflict of Interest: The authors declare that the research was conducted in the absence of any commercial or financial relationships that could be construed as a potential conflict of interest.

Publisher's Note: All claims expressed in this article are solely those of the authors and do not necessarily represent those of their affiliated organizations, or those of the publisher, the editors and the reviewers. Any product that may be evaluated in this article, or claim that may be made by its manufacturer, is not guaranteed or endorsed by the publisher.

frontiers in Microbiology

PERSPECTIVE
published: 20 January 2022
doi: 10.3389/fmicb.2022.806576

Beyond to the Stable: Role of the Insertion Sequences as Epidemiological Descriptors in *Corynebacterium striatum*

*Benjamín Leyton-Carcaman and Michel Abanto**

Genomics and Bioinformatics Unit, Scientific and Technological Bioresource Nucleus (BIOREN), Universidad de La Frontera, Temuco, Chile

In recent years, epidemiological studies of infectious agents have focused mainly on the pathogen and stable components of its genome. The use of these stable components makes it possible to know the evolutionary or epidemiological relationships of the isolates of a particular pathogen. Under this approach, focused on the pathogen, the identification of resistance genes is a complementary stage of a bacterial characterization process or an appendix of its epidemiological characterization, neglecting its genetic components' acquisition or dispersal mechanisms. Today we know that a large part of antibiotic resistance is associated with mobile elements. *Corynebacterium striatum*, a bacterium from the normal skin microbiota, is also an opportunistic pathogen. In recent years, reports of infections and nosocomial outbreaks caused by antimicrobial multidrug-resistant *C. striatum* strains have been increasing worldwide. Despite the different existing mobile genomic elements, there is evidence that acquired resistance genes are coupled to insertion sequences in *C. striatum*. This perspective article reviews the insertion sequences linked to resistance genes, their relationship to evolutionary lineages, epidemiological characteristics, and the niches the strains inhabit. Finally, we evaluate the potential of the insertion sequences for their application as a descriptor of epidemiological scenarios, allowing us to anticipate the emergence of multidrug-resistant lineages.

Keywords: insertion sequences, epidemiological markers, *Corynebacterium striatum*, emerging pathogen, multi-drug resistance, mobile elements, AMR, machine-learning

OPEN ACCESS

Edited by:
Rustam Aminov, University of Aberdeen, United Kingdom

Reviewed by:
Louisy Santos, Rio de Janeiro State University, Brazil
Antony T. Vincent, Laval University, Canada

****Correspondence:***
Michel Abanto
mfabanto@gmail.com

Specialty section:
This article was submitted to Antimicrobials, Resistance and Chemotherapy, a section of the journal Frontiers in Microbiology

Received: *01 November 2021*
Accepted: *04 January 2022*
Published: *20 January 2022*

Citation:
Leyton-Carcaman B and Abanto M (2022) Beyond to the Stable: Role of the Insertion Sequences as Epidemiological Descriptors in Corynebacterium striatum. Front. Microbiol. 13:806576. doi: 10.3389/fmicb.2022.806576

INTRODUCTION

Genomic publications in recent years have reinforced the essential role of the niche in the genomic structure of bacteria (Matlock et al., 2021; Shaw et al., 2021). The evolution of bacteria in the different niches is mainly driven by two factors, vertical gene transfer (VGT), and horizontal gene transfer (HGT), due to transduction, transformation, or conjugation events (Lawrence, 2005). The effect of mutations on the evolution of microorganisms is well known, but mobile genetic elements (MGEs) are also important components driving the bacteria evolution. MGEs are the main evolutionary source of pathogenic bacteria in the hospital environment (Djordjevic et al., 2013). However, despite its evolutionary importance, the role

of these genomic elements as a whole and their potential use from an epidemiological perspective has been little explored and applied.

Insertion sequences (IS) are small, simple, autonomous, and widely distributed MGE in bacterial genomes. Their size ranges from 700 to 2,500 bp, and they contain a sequence that codes for a transposase flanked by two inversely repeated sequences (IR; Mahillon and Chandler, 1998). Initially, they were considered as "harmful genomic parasites" (Kalia et al., 2004; Vandecraen et al., 2017); however, they are currently considered mutagenic agents that allow the host to adapt to new environmental challenges and colonize new niches (Siguier et al., 2014). In addition, IS are important elements in the formation of other mobile elements such as transposons and plasmids, which is why they are responsible for the mobilization of many genes that confer resistance to antibiotics (ARG) and virulence (Partridge et al., 2018; Razavi et al., 2020).

Corynebacterium striatum is a member of the skin and nasal mucosal microbiota in humans; however, its role as an etiological agent of nosocomial and community-acquired diseases is increasingly recurrent due to its multi-drug resistance and biofilm formation capacity (Silva-Santana et al., 2021). Resistance to antibiotics in *C. striatum* has been mainly associated with transposons and plasmids (Olender, 2012) which are part of its resistome, i.e., the total repertoire of genes that contribute to resistance. Recently, the richness of the resistome in *C. striatum* has been evidenced, mainly associated with MGE, where the vast presence of IS in the genomic context of several ARGs was highlighted and underlined the importance of IS in the formation of the resistome in *C. striatum* (Leyton et al., 2021). Whereas insertion sequences have been associated with genes that confer advantageous phenotypes, including resistance genes, studying and relating them could help to better understand the emergence, spread, and persistence of resistance in *C. striatum*, thus making the IS important epidemiological descriptors.

WHY SHOULD INSERTION SEQUENCES BE AN EPIDEMIOLOGICAL DESCRIPTOR?

Classical epidemiology determines the clinical and environmental factors in which disease occurs or relates the routes of transmission and spread of a pathogen. However, with the emergence of molecular epidemiology more than 10 years ago, it has become possible to characterize and determine genetic and environmental factors associated with infectious diseases' emergence, spread, and pathogenesis. In this context, phylogenetic analyses have made it possible to identify disease lineages and establish the epidemiological links related to infectious diseases. On the other hand, the study of the differential content of genes in strains from different isolation sources has demonstrated the genomic plasticity of these bacteria, suggesting their role in the exploration and establishment of specific niches. Like phylogenetic analyses and differential content analyses, we believe that the IS should be incorporated into the characterization of pathogens such as *C. striatum*, which could help to better understand its pathogenicity, persistence, and transmission dynamics. Here, we explain the reasons why we must consider them epidemiological descriptors.

Reason 1: *Corynebacterium striatum* Is a Ubiquitous Bacterium

Bacteria ubiquity is explained in part due to their genome size and metabolic capacity (Barberán et al., 2014). *Corynebacterium striatum* has been described as a ubiquitous microorganism; however, the relationships of the adaptative capacity with genomic content are still not entirely clear. The old Baas Becking statement "everything is everywhere, but the environment selects" (O'Malley, 2008) suggests that there are adaptative mechanisms of bacteria related to the niche. *Corynebacterium striatum* has shown a wide range of resistance to antibiotics, and this resistance has probably been obtained and developed in nosocomial settings (Renom et al., 2007; Alibi et al., 2017), leading to the emergence and persistence of antibiotic resistance genes from high their mobility and evolutionary forces (Fondi et al., 2016).

The adaptation and evolution of *C. striatum* can be explained by the insertion sequences. In *Escherichia coli*, it has been suggested that IS could be associated with the genome evolution, fitness, and the formation of new operons (Gaffé et al., 2011; Consuegra et al., 2021; Kanai et al., 2021). This raises the question if the presence of IS would explain the transition of *C. striatum* lineages from normal microbiota to the generation of pathogenic lineages, and whether it would also be related to the role of the environment in the evolution of its pathogenicity. The impact of insertion sequences on the evolution of lineages has been seen in *Shigella* spp., which represents specialized lineages of *E. coli* (Hawkey et al., 2020). Hawkey et al. (2020) pointed out that a part of the historical loss of the metabolic function of *Shigella* spp. is due to the activity of IS and that they continue to play a central role in the ongoing evolution of *Shigella* spp.

Here, we suppose that the IS provide a way of adapting to the niche in *C. striatum*. It has been suggested that IS abundance is positively related to genome size and HGT events (Touchon and Rocha, 2007). Moreover, through "transposition bursts," the IS arise in environmental stress; IS can persist or become extinct in the host, depending on the adaptive regulation that the host possesses (Wu et al., 2015). This suggests that the dynamics of the IS are variable, and they can provide information on the evolutionary state of bacteria like *C. striatum*. In this perspective, we propose that the evolution of *C. striatum* into opportunistic states or pathogenic lineages is the product of the selective pressure of the environment, reflecting mainly the presence and abundance of IS. Therefore, we suggest the role of the IS as epidemiological descriptors in *C. striatum*.

Reason 2: The Presence of Plasmids in *Corynebacterium striatum* Is Rare

Historically, the pathogenicity of bacteria has been associated with large MGEs, such as bacteriophages and plasmids. It is

known that plasmids are increasingly persistent in a bacterial community (Alonso-del Valle et al., 2021), and there are approaches such as plasmid classification and typing proposed to monitor antibiotic resistance (Orlek et al., 2017). Yet despite the approaches to applying plasmids as surveillance in the epidemiology of certain bacteria such as *Klebsiella pneumoniae* (Ramirez et al., 2019), in *C. striatum* seems to be difficult due to difficulties in determining the presence of plasmids. As of the writing of this manuscript, four plasmids have been registered in *C. striatum* (pTP10: NC_004939.1, FDAARGOS_1197 plasmid unnamed: CP069515.1, pCs-Na-1: CP021253.1, and pCs-Na-2: NZ_CP021254.1). The plasmid pTP10 is the best known: it was reported in *C. striatum* M82B, a strain dated approximately 1983 (Kono et al., 1983; Tauch et al., 2000). However, there are no studies related to the other three plasmids. Although there have been attempts to find plasmids (Ramos et al., 2018), to date, no other plasmids have been reported (08-12-2021), probably because they do not exist or because the pTP10 or related plasmids have been integrated into the genome of *C. striatum*. This latter idea is reinforced by two of the four known plasmids corresponding to strains from approximately 40 years ago, whereas the other two plasmids correspond to a strain isolated from *Neophocaena asiaeorientalis*, a fresh water cetacean, and which represents a very different environment from the nosocomial setting.

The plasmids in bacteria provide a positive platform to capture and spread a variety of ARG. In corynebacteria of clinical importance, several plasmids are known to confer resistance (Deb and Nath, 1999; Leyton et al., 2021), such as pTP10 of *C. striatum*, pNG2 of *Corynebacterium diphtheriae*, and pJA144188 of *Corynebacterium resistens*. They also include a significant content of insertion sequences (Tauch et al., 2003; Schröder et al., 2012), suggesting a relation between IS, plasmids, and *C. striatum*. Furthermore, this extends to other plasmids and other bacteria; for example, Che et al. (2021) showed that IS contribute to the acquisition and transfer of ARG in conjugative plasmids. Regardless of the existence of plasmids, something that is quite clear is the relationship of IS with antibiotic resistance in *C. striatum* (Wang et al., 2020; Leyton et al., 2021). Therefore, the increase in resistance in *C. striatum* strains would be mainly associated with these mobile elements.

Reason 3: Analysis of the Content of Insertion Sequences in *Corynebacterium striatum* Isolates Shows Relationships With Epidemiological Factors

To determine the diversity of the insertion sequences in *C. striatum*, we recovered 268 genomes from *C. striatum*, identified the lineages, and looked for clustering patterns using constrained principal coordinate analysis (CPCoA) from a large dataset (**Supplementary Data 1**). Despite the definition of IS, to perform the analyses in this study, we defined the IS in terms of their transposase. This dataset includes the presence and abundance of insertion sequences detected by Prokka (Seemann, 2014) and grouped by Panaroo (Tonkin-Hill et al., 2020). The details and code used for this methodological approach are available on GitHub.[1] We found a relationship between epidemiological factors and the composition of insertion sequences (**Figure 1**; ANOVA-like permutation analysis, value of $p < 0.0004$). Thus, we found an association between lineages and IS composition (**Figure 1B**); this suggests an adaptation and a population cohesion around the content and abundance of IS. Subsequently, we evaluated the abundance of ARGs in the lineages and IS patterns. Interestingly, we found lineages with a more significant number of ARGs (**Figure 1C**). Moreover, these lineages, including CS-2 and CS-3, are phylogenetically distant from the rest, indicating a specialization of the lineages according to their IS content.

To determine the importance of the IS content in epidemiological characteristics analyzed in this study, we performed a random forest (RF) analysis. Since its development in 2001, RF has become a popular tool in omics research (Dutilh et al., 2014). RF has the advantage of incorporating a vast and diverse amount of data to predict characteristics. We consider that RF can provide a potential application to classify epidemiological features in *C. striatum*. IS, being abundant and diverse mobile elements, become difficult to analyze. Thus, we built a RF model for each characteristic evaluated in this study (**Figure 2**). We found that there are families (IS6 and ISL3) associated with the lineage. In addition, we found that the IS corresponding to the IS30, IS481, IS3, IS21, and IS256 families have great importance in the classification in the three epidemiological categories studied. In addition, IS380 and IS5 are not important for the RF classification. Interestingly, a member of the IS30 family associated with daptomycin resistance was recently reported (Gotoh et al., 2021), which together with this perspective highlights the importance of IS as evolutionary triggers in *C. striatum*.

DISCUSSION

The use of insertion sequences is not new in bacterial pathogen studies, having been used as epidemiological markers in some species. A specific example is IS6110 in the genus *Mycobacterium*, where this IS has been used as a typing tool. The number of copies of this element would be related to the species identification and the strain typing, demonstrating an essential value in the epidemiology of *Mycobacterium* spp. (van Soolingen et al., 1991; Suffys et al., 1997; Roychowdhury et al., 2015). We propose that the importance of insertion sequences lies in describing the environment or niche in which the pathogen is found. In a nosocomial environment, MGEs play a fundamental role in the emergence of pathogens due to genes that confer resistance to antibiotics or virulence and, therefore, with differing levels of fitness. Several studies have identified the presence of IS and addressed the role of larger genomic elements, such as plasmids and integrons, in the epidemiology of some pathogens (Rozwandowicz et al., 2018; Ramirez et al., 2019; Hawkey et al., 2020; Leal et al., 2020; Mbelle et al., 2020). Recently, a high presence of IS has been evidenced, composing conjugative plasmids, and that would be overrepresented in the presence

[1]https://github.com/Leytoncito/IS_Prokka_Panaroo

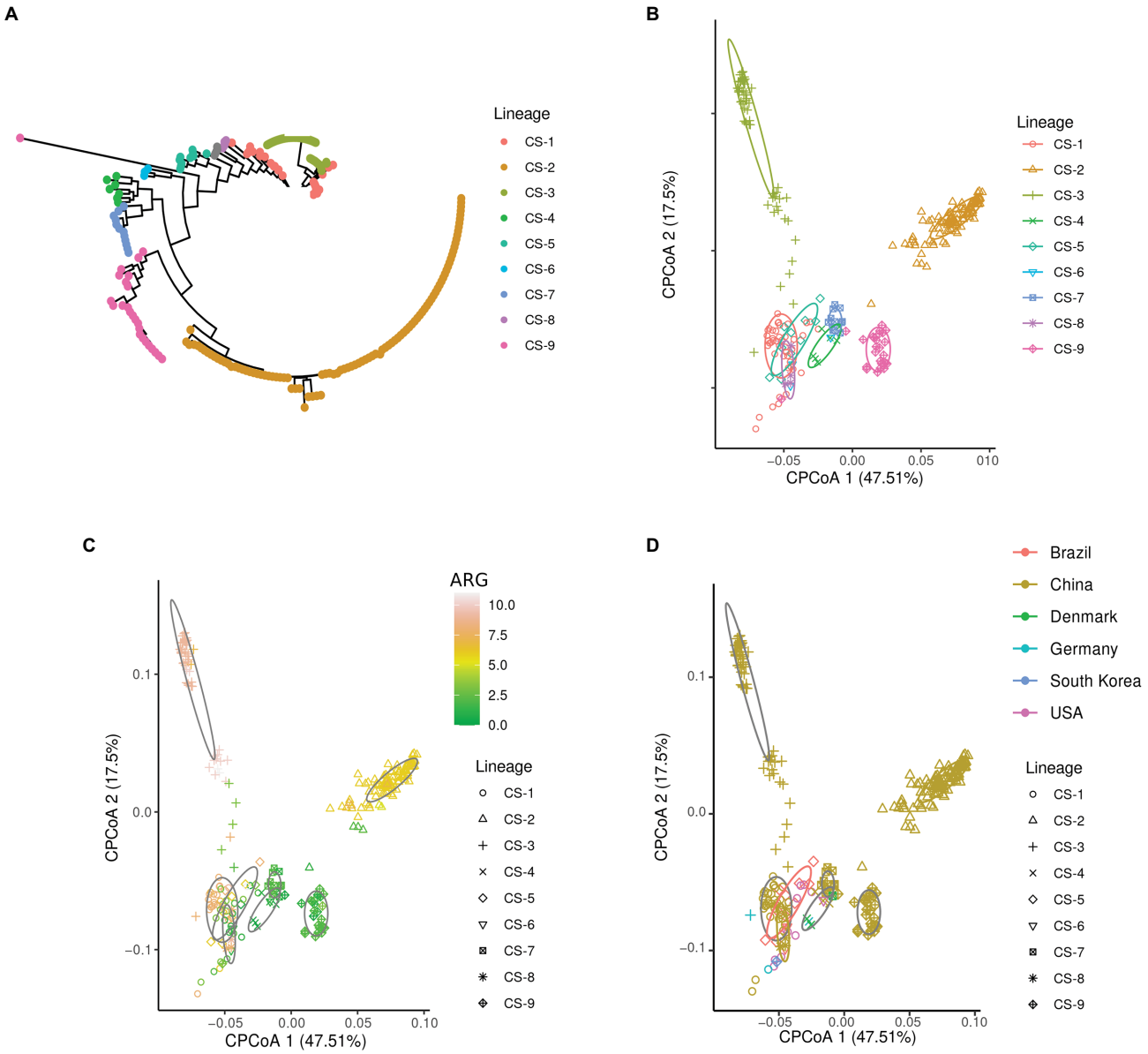

FIGURE 1 | Relationship of IS with epidemiological characteristics. **(A)** Lineages of *Corynebacterium striatum*. **(B–D)** Constrained principal coordinate analysis (CPCoA analysis). Lineages were determined using the R package, RhierBAPS (Tonkin-Hill et al., 2018) using a masked alignment generated by Gubbins (Croucher et al., 2015), and phylogenetic tree generated by IQ-TREE (Nguyen et al., 2015). The CPCoA analyses (ANOVA-like permutation analysis, value of $p < 0.0004$, and 24.9% of variance) were constructed from the presence and abundance of IS in the *C. striatum* genomes and explored according to the metadata available and retrieved from different sources in this study. Briefly, we obtained the *C. striatum* genomes available at NCBI (07/26/2021), made the annotation with Prokka (Seemann, 2014) and constructed its pangenome with Panaroo (Tonkin-Hill et al., 2020). The presence and abundance of insertion sequences were extracted from the pangenome. For phylogenetic reconstruction, we align the core-genome using Parsnp (Treangen et al., 2014), and we build a tree based on core-genome alignment using IQ-TREE. The presence of resistance genes was extracted from the metadata available from the NCBI, a database that annotates the genomes using AMRFinderPlus (Feldgarden et al., 2021). Finally, the visualization of the CPCoA analyzes was used BIC (http://www.ehbio.com/Cloud_Platform/front/#).

of ARG (Che et al., 2021). We propose that attention focus on IS assumed to be mobile functional monomers capable of being part of larger mobile elements. Furthermore, we think that IS could be an indicator of risk or alarm because the presence of IS could provide information on the pathogenic evolution of the bacteria that inhabit the nosocomial niche.

Based on our results, the IS profile could be a framework for assessing the health risk of antimicrobial resistance genes. The diversity and abundance of ARGs associated with IS, allowed us to infer high-risk lineages such as the CS-2 and CS-3 lineages compared to other lower risk lineages due to having fewer ARGs. According to the analyzed data, most of

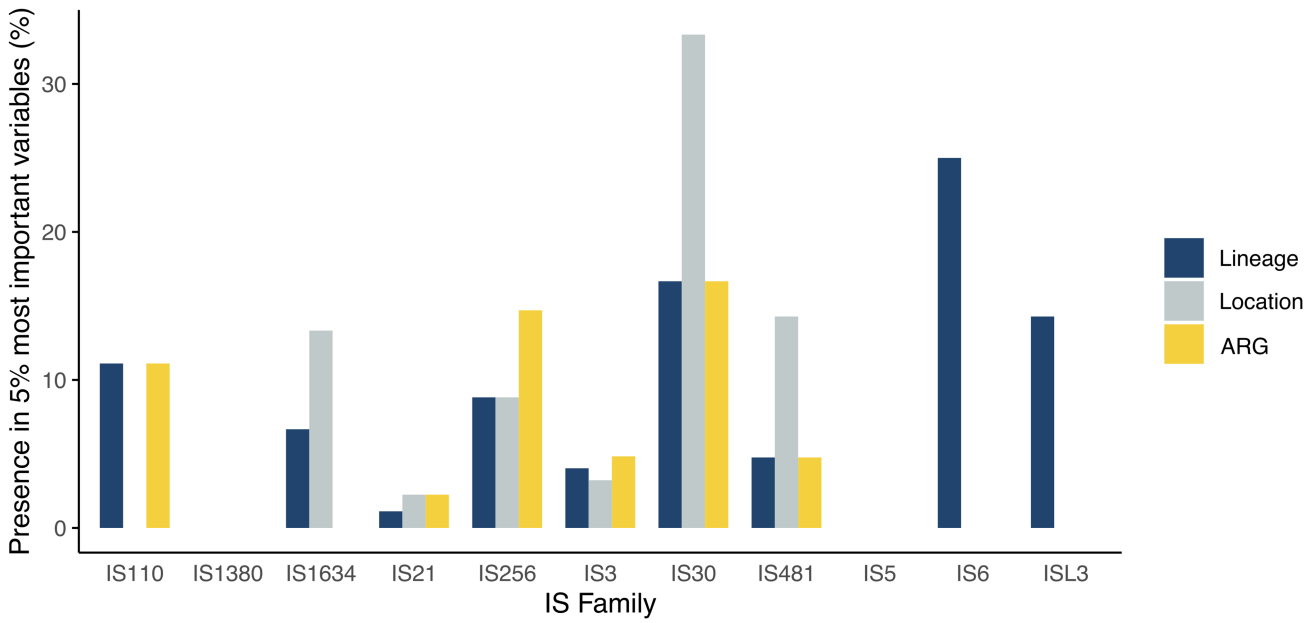

FIGURE 2 | The importance of IS Families in each epidemiological variable. Presence of 5% of the most important functionally annotated insertion sequences for Random Forest (RF) in each epidemiological variable evaluated. All RFs consisted of 501 trees each and were calculated using the random forest 4.6-14 package (Breiman, 2001; default parameters) in version R 4.1.0 (The R Project for Statistical Computing; http://www.r-project.org). For RFs validation, a *k*-Fold Cross Validation test (*k*-fold = 100), and a Kappa concordance test were carried out (for lineage classification, $k = 0.963$, value of $p < 0.0001$; for Location classification, $k = 0.597$, value of $p < 0.0001$; for ARG classification, $k = 0.786$, value of $p < 0.0001$). Finally, the importance of each variable was based on the mean decrease Gini index respecting the pathline described by Dutilh et al. (2014).

the available sequences of *C. striatum* are from China (**Figure 1D**), and a recent epidemiology study found that isolates from various cities in China were separated into four lineages, which would have originated more than 20 years ago (Wang et al., 2020). Interestingly, the IS patterns generated in our analysis identified that the Chinese isolates were separated into six clusters, of which CS-1, CS-2, CS-3, and CS-9 would be more specialized in terms of IS. Moreover, our results suggest that the IS profile allows a fine-tuned lineage characterization related to the presence of a more significant number of ARGs.

In this study, 16,360 copies of IS were found, grouped into 323 clusters of gene families. From the results obtained, we found that the abundance of IS could explain the capacity of *C. striatum* to acquire antibiotic resistance. Yet a high abundance of IS not strictly synonymous with HGT (Touchon and Rocha, 2007); rather, a high transposition of IS tends to be detrimental to the host (Wu et al., 2015). This does not seem to be the case for *C. striatum*, however, which suggests there must be regulation mechanisms in *C. striatum* to obtain the persistence of the IS and of the bacterium itself. To explore whether the transposition of the IS has been affecting the evolution of *C. striatum*, we explored the dynamics of recombination and mutation of the genomes analyzed using ClonalFrameML (Didelot and Wilson, 2015). We estimated the relative impact of recombination around four times more than to mutation in genomic diversification ($r/m = 4.4$), suggesting a clear role of homologous recombination events in genomic plasticity and evolution in *C. striatum*. Strictly, not all recombination events can be attributed to the IS activity; however, in the absence of other mobile elements, the IS could play an important role in *C. striatum*. For example, the r/m value of *C. striatum* is lower than that reported in a *C. diphtheriae* population ($r/m = 5$; Hennart et al., 2020). Moreover, the recombination of *C. diphtheriae* is influenced by other larger MGEs such as plasmids and integrons (Tauch et al., 2003; Barraud et al., 2011; Hennart et al., 2020).

Genetic determinism has tended to follow the simplistic idea that single genes control a disease (Ahn et al., 2006; Loscalzo et al., 2007; Williams and Auwerx, 2015). Based on this assumption, it has probably led us to look for single gene markers, and why IS as unique genes and markers have not generated much interest. However, considering the current microbial genomics scenario where we can now obtain whole-genome information, we propose that the study of the IS composition should be used as an epidemiological descriptor of *C. striatum*.

Limitations and Future Approaches

In addition to what we have explored in this study, another important point to be explored would be the association of IS with genes in their genomic context in order to achieve a greater understanding of the functional role of IS. Nevertheless, due to the structure and genomic context of IS, their characterization and their genomic context could be affected by short-read sequencing technologies that produce

fragmented genome assemblies, which could be a limitation for the recovery of IS and the characterization of their genomic context. To overcome this limitation, the use of long-read sequencing technologies such as nanopore or PacBio, alone or in combination with short-reads technologies, could help produce complete genomic assemblies and thus perform a better characterization of ISs. In addition, it is crucial to evaluate the entire repertoire of ISs, which would most convincingly explain the niche or the environments that host them.

Our study based on IS composition identified genomes clustered according to the phylogenetic lineages, a potential application of insertion sequences as epidemiological descriptors. To study a large number of genes to describe epidemiological features could be a hard task to undertake. Implementation of integrative approaches such as machine learning and deep learning in microbiology and genomics has gradually increased due to the large amounts of data generated by high-throughput sequencing technology (Libbrecht and Noble, 2015; Qu et al., 2019). Our analyses show specific patterns of the presence and abundance of IS with the detected lineages or related to ARG composition. Classification techniques such as Random Forest (as described in this study) and Super Vector Machine (SVG) could be valuable for classifying epidemiological features related to *C. striatum* based on its IS composition. Moreover, unsupervised machine-learning techniques could help find new IS patterns in *C. striatum*.

Currently, there is an inclination to "dissect" deep learning models (Bau et al., 2017). Unveiling neural layer learning, a concept is known as "opening the black-box," consists of obtaining a better interpretation of how deep learning models work (Shwartz-Ziv and Tishby, 2017). In this sense, a future application would be to train the IS patterns by deep learning and then dissect these models to identify the role of certain IS in different epidemiological scenarios of *C. striatum*.

On the other hand, microbial genome-wide association studies (mGWAS) are a new field that seeks to understand how variations in microbial genomes affect the phenotype of a pathogen, such as drug resistance and virulence (Power et al., 2017; San et al., 2020). mGWAS bioinformatics tools use machine learning intrinsically in their algorithms, such as PySEER and Kover, for phenotype prediction (San et al., 2020). Therefore, mGWAS becomes a promising alternative for studying insertion sequences and their relationship with phenotypes in *C. striatum*. All these approaches must be considered due to the currently available genomic data, which can be a way forward to understanding the epidemiology and evolution of emerging pathogens such as *C. striatum*.

In conclusion, taken together, we propose the use of the IS composition as epidemiological descriptors, i.e., as a set of genomic data that can describe epidemiological features. Descriptions could include the transient or persistent state of *C. striatum*, the relationship with the lineage to which they belong (and the role of the IS in the establishment of these lineages in the face of the selective pressures of the environment); as well its use in surveillance and emergence of new lineages. Finally, the study of the composition of ISs through exploratory and integrative big-data approaches could facilitate the ecological and evolutionary understanding of antibiotic resistance in *C. striatum*.

DATA AVAILABILITY STATEMENT

The original contributions presented in the study are included in the article/**Supplementary Material**, further inquiries can be directed to the corresponding author.

AUTHOR CONTRIBUTIONS

BL-C performed the data curation, formal analysis, investigation, visualization, and writing the original draft. MA performed the conceptualization of the study, investigation, supervision, and writing – review and editing of the manuscript. All authors contributed to the article and approved the submitted version.

SUPPLEMENTARY MATERIAL

The Supplementary Material for this article can be found online at: https://www.frontiersin.org/articles/10.3389/fmicb.2022.806576/full#supplementary-material

Supplementary Data 1 | Data collected from NCBI and data generated in this study. This material contains the list of genomes studies, annotation of insertion sequences, and a matrix with the presence and abundance of insertion sequences per genome.

REFERENCES

Ahn, A. C., Tewari, M., Poon, C.-S., and Phillips, R. S. (2006). The limits of reductionism in medicine: could systems biology offer an alternative? *PLoS Med.* 3:e208. doi: 10.1371/journal.pmed.0030208

Alibi, S., Ferjani, A., Boukadida, J., Cano, M. E., Fernández-Martínez, M., Martínez-Martínez, L., et al. (2017). Occurrence of *Corynebacterium striatum* as an emerging antibiotic-resistant nosocomial pathogen in a Tunisian hospital. *Sci. Rep.* 7:9704. doi: 10.1038/s41598-017-10081-y

Alonso-del Valle, A., León-Sampedro, R., Rodríguez-Beltrán, J., DelaFuente, J., Hernández-García, M., Ruiz-Garbajosa, P., et al. (2021). Variability of plasmid fitness effects contributes to plasmid persistence in bacterial communities. *Nat. Commun.* 12:2653. doi: 10.1038/s41467-021-22849-y

Barberán, A., Ramirez, K. S., Leff, J. W., Bradford, M. A., Wall, D. H., and Fierer, N. (2014). Why are some microbes more ubiquitous than others? Predicting the habitat breadth of soil bacteria. *Ecol. Lett.* 17, 794–802. doi: 10.1111/ele.12282

Barraud, O., Badell, E., Denis, F., Guiso, N., and Ploy, M.-C. (2011). Antimicrobial drug resistance in *Corynebacterium diphtheriae* mitis. *Emerg. Infect. Dis.* 17, 2078–2080. doi: 10.3201/eid1711.110282

Bau, D., Zhou, B., Khosla, A., Oliva, A., and Torralba, A. (2017). "Network dissection: quantifying interpretability of deep visual representations." in *2017 IEEE Conference on Computer Vision and Pattern Recognition (CVPR)*; July 21–26, 2017; 3319–3327.

Breiman, L. (2001). Random forests. *Mach. Learn.* 45, 5–32. doi: 10.1023/A:1010933404324

Che, Y., Yang, Y., Xu, X., Břinda, K., Polz, M. F., Hanage, W. P., et al. (2021). Conjugative plasmids interact with insertion sequences to shape the horizontal

transfer of antimicrobial resistance genes. *Proc. Natl. Acad. Sci.* 118:e2008731118. doi: 10.1073/pnas.2008731118

Consuegra, J., Gaffé, J., Lenski, R. E., Hindré, T., Barrick, J. E., Tenaillon, O., et al. (2021). Insertion-sequence-mediated mutations both promote and constrain evolvability during a long-term experiment with bacteria. *Nat. Commun.* 12:980. doi: 10.1038/s41467-021-21210-7

Croucher, N. J., Page, A. J., Connor, T. R., Delaney, A. J., Keane, J. A., Bentley, S. D., et al. (2015). Rapid phylogenetic analysis of large samples of recombinant bacterial whole genome sequences using Gubbins. *Nucleic Acids Res.* 43:e15. doi: 10.1093/nar/gku1196

Deb, J. K., and Nath, N. (1999). Plasmids of corynebacteria. *FEMS Microbiol. Lett.* 175, 11–20. doi: 10.1111/j.1574-6968.1999.tb13596.x

Didelot, X., and Wilson, D. J. (2015). ClonalFrameML: efficient inference of recombination in whole bacterial genomes. *PLoS Comput. Biol.* 11:e1004041. doi: 10.1371/journal.pcbi.1004041

Djordjevic, S. P., Stokes, H. W., and Chowdhury, P. R. (2013). Mobile elements, zoonotic pathogens and commensal bacteria: conduits for the delivery of resistance genes into humans, production animals and soil microbiota. *Front. Microbiol.* 4:86. doi: 10.3389/fmicb.2013.00086

Dutilh, B. E., Thompson, C. C., Vicente, A. C., Marin, M. A., Lee, C., Silva, G. G., et al. (2014). Comparative genomics of 274 vibrio cholerae genomes reveals mobile functions structuring three niche dimensions. *BMC Genomics* 15:654. doi: 10.1186/1471-2164-15-654

Feldgarden, M., Brover, V., Gonzalez-Escalona, N., Frye, J. G., Haendiges, J., Haft, D. H., et al. (2021). AMRFinderPlus and the reference gene catalog facilitate examination of the genomic links among antimicrobial resistance, stress response, and virulence. *Sci. Rep.* 11:12728. doi: 10.1038/s41598-021-91456-0

Fondi, M., Karkman, A., Tamminen, M. V., Bosi, E., Virta, M., Fani, R., et al. (2016). "Every gene is everywhere but the environment selects": global geolocalization of gene sharing in environmental samples through network analysis. *Genome Biol. Evol.* 8, 1388–1400. doi: 10.1093/gbe/evw077

Gaffé, J., McKenzie, C., Maharjan, R. P., Coursange, E., Ferenci, T., and Schneider, D. (2011). Insertion sequence-driven evolution of *Escherichia coli* in Chemostats. *J. Mol. Evol.* 72, 398–412. doi: 10.1007/s00239-011-9439-2

Gotoh, K., Mayura, I. P. B., Enomoto, Y., Iio, K., Matsushita, O., Otsuka, F., et al. (2021). Detection of in-frame mutation by IS30-family insertion sequence in the phospholipid phosphatidylglycerol synthase gene (pgsA2) of high-level daptomycin-resistant *Corynebacterium striatum*. *Eur. J. Clin. Microbiol. Infect. Dis.* doi: 10.1007/s10096-021-04369-1 [Epub ahead of print].

Hawkey, J., Monk, J. M., Billman-Jacobe, H., Palsson, B., and Holt, K. E. (2020). Impact of insertion sequences on convergent evolution of Shigella species. *PLoS Genet.* 16:e1008931. doi: 10.1371/journal.pgen.1008931

Hennart, M., Panunzi, L. G., Rodrigues, C., Gaday, Q., Baines, S. L., Barros-Pinkelnig, M., et al. (2020). Population genomics and antimicrobial resistance in *Corynebacterium diphtheriae*. *Genome Med.* 12:107. doi: 10.1186/s13073-020-00805-7

Kalia, A., Mukhopadhyay, A. K., Dailide, G., Ito, Y., Azuma, T., Wong, B. C. Y., et al. (2004). Evolutionary dynamics of insertion sequences in *helicobacter pylori*. *J. Bacteriol.* 186, 7508–7520. doi: 10.1128/JB.186.22.7508-7520.2004

Kanai, Y., Tsuru, S., and Furusawa, C. (2021). Operon formation by insertion sequence IS3 in *Escherichia coli*. bioRxiv [Preprint]. doi: 10.1101/2021.11.02.466885

Kono, M., Sasatsu, M., and Aoki, T. (1983). R plasmids in *Corynebacterium xerosis* strains. *Antimicrob. Agents Chemother.* 23, 506–508. doi: 10.1128/AAC.23.3.506

Lawrence, J. G. (2005). "Horizontal and vertical gene transfer: the life history of pathogens," in *Concepts in Bacterial Virulence*. eds. W. Russell and H. Herwald (Basel: KARGER), 255–271.

Leal, N. C., Campos, T. L., Rezende, A. M., Docena, C., Mendes-Marques, C. L., de Sá Cavalcanti, F. L., et al. (2020). Comparative genomics of *Acinetobacter baumannii* clinical strains from Brazil reveals polyclonal dissemination and selective exchange of mobile genetic elements associated with resistance genes. *Front. Microbiol.* 11:1176. doi: 10.3389/fmicb.2020.01176

Leyton, B., Ramos, J. N., Baio, P. V. P., Veras, J. F. C., Souza, C., Burkovski, A., et al. (2021). Treat me well or will resist: uptake of mobile genetic elements determine the resistome of *Corynebacterium striatum*. *Int. J. Mol. Sci.* 22:7499. doi: 10.3390/ijms22147499

Libbrecht, M. W., and Noble, W. S. (2015). Machine learning applications in genetics and genomics. *Nat. Rev. Genet.* 16, 321–332. doi: 10.1038/nrg3920

Loscalzo, J., Kohane, I., and Barabasi, A. (2007). Human disease classification in the postgenomic era: a complex systems approach to human pathobiology. *Mol. Syst. Biol.* 3:124. doi: 10.1038/msb4100163

Mahillon, J., and Chandler, M. (1998). Insertion sequences. *Microbiol. Mol. Biol. Rev.* 62, 725–774. doi: 10.1128/MMBR.62.3.725-774.1998

Matlock, W., Chau, K. K., AbuOun, M., Stubberfield, E., Barker, L., Kavanagh, J., et al. (2021). Genomic network analysis of environmental and livestock F-type plasmid populations. *ISME J.* 15, 2322–2335. doi: 10.1038/s41396-021-00926-w

Mbelle, N. M., Feldman, C., Sekyere, J. O., Maningi, N. E., Modipane, L., and Essack, S. Y. (2020). Pathogenomics and evolutionary epidemiology of multi-drug resistant clinical *Klebsiella pneumoniae* isolated from pretoria, South Africa. *Sci. Rep.* 10:1232. doi: 10.1038/s41598-020-58012-8

Nguyen, L.-T., Schmidt, H. A., von Haeseler, A., and Minh, B. Q. (2015). IQ-TREE: a fast and effective stochastic algorithm for estimating maximum-likelihood phylogenies. *Mol. Biol. Evol.* 32, 268–274. doi: 10.1093/molbev/msu300

O'Malley, M. A. (2008). 'Everything is everywhere: but the environment selects': ubiquitous distribution and ecological determinism in microbial biogeography. *Stud. Hist. Phil. Biol. Biomed. Sci.* 39, 314–325. doi: 10.1016/j.shpsc.2008.06.005

Olender, A. (2012). "Mechanisms of antibiotic resistance in *Corynebacterium* spp. causing infections in people," in *Antibiotic Resistant Bacteria—A Continuous Challenge in the New Millennium*. ed. M. Pana (Rijeka: InTech), 387–402.

Orlek, A., Stoesser, N., Anjum, M. F., Doumith, M., Ellington, M. J., Peto, T., et al. (2017). Plasmid classification in an era of whole-genome sequencing: application in studies of antibiotic resistance epidemiology. *Front. Microbiol.* 8:182. doi: 10.3389/fmicb.2017.00182

Partridge, S. R., Kwong, S. M., Firth, N., and Jensen, S. O. (2018). Mobile genetic elements associated with antimicrobial resistance. *Clin. Microbiol. Rev.* 31, e00088–e00017. doi: 10.1128/CMR.00088-17

Power, R. A., Parkhill, J., and de Oliveira, T. (2017). Microbial genome-wide association studies: lessons from human GWAS. *Nat. Rev. Genet.* 18, 41–50. doi: 10.1038/nrg.2016.132

Qu, K., Guo, F., Liu, X., Lin, Y., and Zou, Q. (2019). Application of machine learning in microbiology. *Front. Microbiol.* 10:827. doi: 10.3389/fmicb.2019.00827

Ramirez, M. S., Iriarte, A., Reyes-Lamothe, R., Sherratt, D. J., and Tolmasky, M. E. (2019). Small *Klebsiella pneumoniae* plasmids: neglected contributors to antibiotic resistance. *Front. Microbiol.* 10:2182. doi: 10.3389/fmicb.2019.02182

Ramos, J. N., Rodrigues, I. D. S., Baio, P. V. P., Veras, J. F. C., Ramos, R. T. J., Pacheco, L. G., et al. (2018). Genome sequence of a multidrug-resistant *Corynebacterium striatum* isolated from bloodstream infection from a nosocomial outbreak in Rio de Janeiro, Brazil. *Mem. Inst. Oswaldo Cruz.* 113:e180051. doi: 10.1590/0074-02760180051

Razavi, M., Kristiansson, E., Flach, C.-F., and Larsson, D. G. J. (2020). The association between insertion sequences and antibiotic resistance genes. *mSphere* 5, e00418–e00420. doi: 10.1128/mSphere.00418-20

Renom, F., Garau, M., Rubi, M., Ramis, F., Galmes, A., and Soriano, J. B. (2007). Nosocomial outbreak of *Corynebacterium striatum* infection in patients with chronic obstructive pulmonary disease. *J. Clin. Microbiol.* 45, 2064–2067. doi: 10.1128/JCM.00152-07

Roychowdhury, T., Mandal, S., and Bhattacharya, A. (2015). Analysis of IS6110 insertion sites provide a glimpse into genome evolution of *Mycobacterium tuberculosis*. *Sci. Rep.* 5:12567. doi: 10.1038/srep12567

Rozwandowicz, M., Brouwer, M. S. M., Fischer, J., Wagenaar, J. A., Gonzalez-Zorn, B., Guerra, B., et al. (2018). Plasmids carrying antimicrobial resistance genes in Enterobacteriaceae. *J. Antimicrob. Chemother.* 73, 1121–1137. doi: 10.1093/jac/dkx488

San, J. E., Baichoo, S., Kanzi, A., Moosa, Y., Lessells, R., Fonseca, V., et al. (2020). Current affairs of microbial genome-wide association studies: approaches, bottlenecks and analytical pitfalls. *Front. Microbiol.* 10:3119. doi: 10.3389/fmicb.2019.03119

Schröder, J., Maus, I., Meyer, K., Wördemann, S., Blom, J., Jaenicke, S., et al. (2012). Complete genome sequence, lifestyle, and multi-drug resistance of the human pathogen *Corynebacterium resistens* DSM 45100 isolated from

blood samples of a leukemia patient. *BMC Genomics* 13:141. doi: 10.1186/1471-2164-13-141

Seemann, T. (2014). Prokka: rapid prokaryotic genome annotation. *Bioinformatics* 30, 2068–2069. doi: 10.1093/bioinformatics/btu153

Shaw, L. P., Chau, K. K., Kavanagh, J., AbuOun, M., Stubberfield, E., Gweon, H. S., et al. (2021). Niche and local geography shape the pangenome of wastewater- and livestock-associated Enterobacteriaceae. *Sci. Adv.* 7:eabe3868. doi: 10.1126/sciadv.abe3868

Shwartz-Ziv, R., and Tishby, N. (2017). Opening the Black Box of Deep Neural Networks via Information. ArXiv [Preprint].

Siguier, P., Gourbeyre, E., and Chandler, M. (2014). Bacterial insertion sequences: their genomic impact and diversity. *FEMS Microbiol. Rev.* 38, 865–891. doi: 10.1111/1574-6976.12067

Silva-Santana, G., Silva, C. M. F., Olivella, J. G. B., Silva, I. F., Fernandes, L. M. O., Sued-Karam, B. R., et al. (2021). Worldwide survey of *Corynebacterium striatum* increasingly associated with human invasive infections, nosocomial outbreak, and antimicrobial multidrug-resistance, 1976–2020. *Arch. Microbiol.* 203, 1863–1880. doi: 10.1007/s00203-021-02246-1

Suffys, P. N., De Araujo, M. E. I., and Degrave, W. M. (1997). The changing face of the epidemiology of tuberculosis due to molecular strain typing: a review. *Mem. Inst. Oswaldo Cruz* 92, 297–316. doi: 10.1590/S0074-02761997000300001

Tauch, A., Bischoff, N., Brune, I., and Kalinowski, J. (2003). Insights into the genetic organization of the *Corynebacterium diphtheriae* erythromycin resistance plasmid pNG2 deduced from its complete nucleotide sequence. *Plasmid* 49, 63–74. doi: 10.1016/S0147-619X(02)00115-4

Tauch, A., Krieft, S., Kalinowski, J., and Pühler, A. (2000). The 51,409-bp R-plasmid pTP10 from the multiresistant clinical isolate *Corynebacterium striatum* M82B is composed of DNA segments initially identified in soil bacteria and in plant, animal, and human pathogens. *Mol. Gen. Genet.* 263, 1–11. doi: 10.1007/PL00008668

Tonkin-Hill, G., Lees, J. A., Bentley, S. D., Frost, S. D. W., and Corander, J. (2018). RhierBAPS: An R implementation of the population clustering algorithm hierBAPS. *Wellcome Open Res.* 3:93. doi: 10.12688/wellcomeopenres.14694.1

Tonkin-Hill, G., MacAlasdair, N., Ruis, C., Weimann, A., Horesh, G., Lees, J. A., et al. (2020). Producing polished prokaryotic pangenomes with the Panaroo pipeline. *Genome Biol.* 21:180. doi: 10.1186/s13059-020-02090-4

Touchon, M., and Rocha, E. P. C. (2007). Causes of insertion sequences abundance in prokaryotic genomes. *Mol. Biol. Evol.* 24, 969–981. doi: 10.1093/molbev/msm014

Treangen, T. J., Ondov, B. D., Koren, S., and Phillippy, A. M. (2014). The harvest suite for rapid core-genome alignment and visualization of thousands of intraspecific microbial genomes. *Genome Biol.* 15:524. doi: 10.1186/s13059-014-0524-x

van Soolingen, D., Hermans, P. W., de Haas, P. E., Soll, D. R., and van Embden, J. D. (1991). Occurrence and stability of insertion sequences in mycobacterium tuberculosis complex strains: evaluation of an insertion sequence-dependent DNA polymorphism as a tool in the epidemiology of tuberculosis. *J. Clin. Microbiol.* 29, 2578–2586. doi: 10.1128/jcm.29.11.2578-2586.1991

Vandecraen, J., Chandler, M., Aertsen, A., and Van Houdt, R. (2017). The impact of insertion sequences on bacterial genome plasticity and adaptability. *Crit. Rev. Microbiol.* 43, 709–730. doi: 10.1080/1040841X.2017.1303661

Wang, X., Zhou, H., Du, P., Lan, R., Chen, D., Dong, A., et al. (2020). Genomic epidemiology of *Corynebacterium striatum* from three regions of China: an emerging national nosocomial epidemic. *J. Hosp. Infect.* 110, 67–75. doi: 10.1016/j.jhin.2020.10.005

Williams, E. G., and Auwerx, J. (2015). The convergence of systems and reductionist approaches in complex trait analysis. *Cell* 162, 23–32. doi: 10.1016/j.cell.2015.06.024

Wu, Y., Aandahl, R. Z., and Tanaka, M. M. (2015). Dynamics of bacterial insertion sequences: can transposition bursts help the elements persist? *BMC Evol. Biol.* 15:288. doi: 10.1186/s12862-015-0560-5

Conflict of Interest: The authors declare that the research was conducted in the absence of any commercial or financial relationships that could be construed as a potential conflict of interest.

Publisher's Note: All claims expressed in this article are solely those of the authors and do not necessarily represent those of their affiliated organizations, or those of the publisher, the editors and the reviewers. Any product that may be evaluated in this article, or claim that may be made by its manufacturer, is not guaranteed or endorsed by the publisher.

frontiers in Microbiology

ORIGINAL RESEARCH
published: 31 January 2022
doi: 10.3389/fmicb.2021.777504

F_0F_1-ATPase Contributes to the Fluoride Tolerance and Cariogenicity of *Streptococcus mutans*

Cheng Li[1,2], Cai Qi[1,2], Sirui Yang[1,2], Zhengyi Li[1], Biao Ren[1], Jiyao Li[1,2], Xuedong Zhou[1,2], Huawei Cai[3], Xin Xu[1,2] and Xian Peng[1]**

[1] State Key Laboratory of Oral Diseases and National Clinical Research Center for Oral Diseases, West China Hospital of Stomatology, Sichuan University, Chengdu, China, [2] Department of Cariology and Endodontics, West China Hospital of Stomatology, Sichuan University, Chengdu, China, [3] Laboratory of Nuclear Medicine, Department of Clinical Nuclear Medicine, West China Hospital, Sichuan University, Chengdu, China

The phenotypic traits of *Streptococcus mutans*, such as fluoride tolerance, are usually associated with genotypic alterations. The aim of this study was to identify adaptive mutations of *S. mutans* to gradient fluoride concentrations and possible relationships between the mutations and fluoride tolerance. We identified a highly resistant *S. mutans* strain (FR1000) with a novel single nucleotide polymorphism (SNP, −36G→T) in the promoter region of F_0F_1-ATPase gene cluster (*SMU_1527-SMU_1534*) resistant to 1,000 ppm fluoride using the whole-genome Illumina PE250 sequencing. Thus, a −36G→T F_0F_1-ATPase promoter mutation from the parental strain *S. mutans* UA159 was constructed and named UA159-T. qRT-PCR showed that the F_0F_1-ATPase gene expression of both FR1000 and UA159-T was up-regulated, and fluoride tolerance of UA159-T was significantly improved. Complementation of Dicyclohexylcarbodiimide (DCCD), a specific inhibitor of F_0F_1-ATPase, increased fluoride susceptibility of FR1000 and UA159-T. Intracellular fluoride concentrations of fluoride tolerance strains were higher compared to UA159 strain as demonstrated by ^{18}F analysis. Further validation with rat caries models showed that UA159-T caused more severe caries lesions under fluoride exposure compared with its parental UA159 strain. Overall, the identified −36G→T mutation in the promoter region of F_0F_1-ATPase gene drastically contributed to the fluoride tolerance and enhanced cariogenicity of *S. mutans*. These findings provided new insights into the mechanism of microbial fluoride tolerance, and suggested F_0F_1-ATPase as a potential target for suppressing fluoride resistant strains.

Keywords: ***Streptococcus mutans*, fluoride(s), genomics, caries, antimicrobials**

OPEN ACCESS

Edited by:
Fabian Cieplik,
University Medical Center Regensburg, Germany

Reviewed by:
Guoqing Niu,
Southwest University, China
Sandeep Sharma,
Lovely Professional University, India

***Correspondence:**
Xin Xu
xin.xu@scu.edu.cn
Xian Peng
pengx@scu.edu.cn

Specialty section:
This article was submitted to Antimicrobials, Resistance and Chemotherapy, a section of the journal Frontiers in Microbiology

Received: *15 September 2021*
Accepted: *20 December 2021*
Published: *31 January 2022*

Citation:
Li C, Qi C, Yang S, Li Z, Ren B, Li J, Zhou X, Cai H, Xu X and Peng X (2022) F_0F_1-ATPase Contributes to the Fluoride Tolerance and Cariogenicity of Streptococcus mutans. Front. Microbiol. 12:777504. doi: 10.3389/fmicb.2021.777504

INTRODUCTION

Fluoride is a ubiquitous compound in the environment, which is found in soil, water, and air (Davison and Weinstein, 2004; Jagtap et al., 2012). It is also widely used in many oral hygiene products, such as toothpaste, mouthwash, and gel (Anusavice et al., 2016). *Streptococcus mutans* is the principal causative agent of dental caries in humans (Hudson and Curtiss, 1990) and fluoride is the most widely used chemical agent for controlling the disease (Chansley and Kral, 1989). It is because that fluoride can inhibit oral bacterial growth and metabolism, protect dental enamel from

demineralization and enhance the remineralization process (Buzalaf et al., 2011). The antimicrobial action of fluoride is pH dependent (Sutton et al., 1987). The *pKa* of fluoride is 3.15, and fluoride cannot permeate bacterial cell membranes at pH 7.0. Gutknecht and Walter (1981) reported that the permeability coefficient of synthetic membranes for hydrogen fluoride (HF) was about 1×10^7 times that of fluoride. HF is formed when the oral pH drops as a result of carbohydrate fermentation by *S. mutans*. Then, HF easily crosses the cell membrane and enters the bacterium (Loesche, 1986). Inside the cell, HF dissociates, forming a proton (H^+) and a fluoride ion (F^-) in the relatively alkaline cytoplasm (Hamilton, 1990). F^- acts as an enzyme inhibitor while H^+ acidifies the cytoplasm, and they both reduce protons extruded through the cell membrane by inhibiting F_0F_1-ATPase, which is a membrane channel (Liao et al., 2017). Enolase, an enzyme involved in glycolysis pathway and glucose uptake, is competitively inhibited by F^- (Guha-Chowdhury et al., 1997) and indirectly inhibited by low cytoplasm pH resulting from H^+ accumulation (Belli et al., 1995; Marquis et al., 2003). Inhibition of this enzyme results in a reduction of sugar uptake and glycolysis (Sutton et al., 1987). Moreover, fluoride modulates metabolism by binding to pyrophosphatase in the presence of Mn^{2+} (Marquis et al., 2003). Also, fluoride inhibits alkali production through the inhibition of urease and the arginine deiminase system (ADS), which requires low pH values (Curran et al., 1998; Burne and Marquis, 2000). In summary, the antibacterial effect of fluoride depends on the influx of HF in an acidic environment. The intracellular F^- and H^+ can directly or indirectly affect enzymatic activities and physiological processes, thereby affecting the biological function of *S. mutans*.

Usage of high fluoride concentrations in oral hygiene products results in fluoride-resistant strains, thus effectiveness of these products is greatly comprised. Fluoride resistance can either be classified as transient or permanent. Transient resistance, acquired through phenotypic adaptation, is lost after 1–7 generations in a fluoride-free medium (Streckfuss et al., 1980). Fluoride-resistant strains isolated clinically were likely to have transient fluoride resistance. Transient fluoride-resistant *S. mutans* strains, which can resist to 300–600 ppm fluoride, have been isolated from xerostomia patients (Streckfuss et al., 1980; Brown et al., 1983). Transient fluoride resistance may be the result of environmental adaptation and is related to the horizontal transfer of bacterial plasmids. These strains will lose its plasmid in the absence of fluorine stimulation and revert to fluorine-sensitive strains (Streckfuss et al., 1980). Permanent fluoride resistance results from chromosomal alterations (Mitsuhata et al., 2014; Liao et al., 2015). van Loveren et al. (1991) defined the genotypic fluoride resistance as a stable resistance that can persist for at least 20 generations in a fluoride-free medium. Most laboratory-derived fluoride-resistant strains showed stable fluoride resistance, and were used to study cariogenicity, strain fitness, and mechanisms of acquired fluoride resistance. *In vitro* induction and further artificial selection were used to isolate stable fluoride-resistant strains. van Loveren et al. (1991) directly transferred fluorine-sensitive parent strains *S. mutans* C180-2 from fluoride-free medium to 1,000 ppm fluoride medium to obtain fluoride-resistant strains. Brussock and Kral (1987), Zhu et al. (2012), Liao et al. (2015), and Mieher et al. (2018) cultivated fluorine-sensitive parent strains GS-5, C180-2, Ingbritt, and UA159 on medium containing increasing concentrations of NaF (0−1,000 ppm, in increments of 50 ppm), and then isolated fluoride-resistant strains on plate. Until now, researchers have found SNPs in several genes from isolated fluoride-resistant strains, including *eno* and *pykF* (encoding two glycolytic enzymes, namely enolase and pyruvate kinase), *glpF* (encoding a glycerol uptake facilitator protein), and $eriC^F$ (encoding fluoride antiporters, $EriC^F$) (Liao et al., 2015, 2018). Only $eriC^F$ has been clearly confirmed to be linked to fluoride resistance (Liao et al., 2016; Men et al., 2016; Murata and Hanada, 2016). Mechanisms of fluoride response by cells are still not clear.

F_0F_1-ATPase, a membrane-bound proton translocating ATPase, is a well-known aciduric virulence factor of *S. mutans* (Bender et al., 1986). Previous studies showed that it also has a potential regulatory effect on fluoride resistance. In the fluoride environment, the influx of HF, as well as the inhibition of the proton-extruding F_0F_1-ATPase, leads to the acidification of the cytoplasm and the reduction in acidurance of *S. mutans* (Bender et al., 1986; Marquis, 1990; Van Loveren, 2001). However, F_0F_1-ATPase in a fluoride-resistant strain was found to be insensitive to fluoride at pH 5.0 while the corresponding wild-type strain was sensitive under the same pH condition (Hoelscher and Hudson, 1996). Previous studies on fluoride inhibition of F_0F_1-ATPase were done either with the purified enzyme or in permeabilized cells (Sutton et al., 1987; Marquis, 1995; Pandit et al., 2013). The inhibition of F_0F_1-ATPase in intact cells remains unknown. Vanloveren et al. (2010) speculated that fluoride-resistant strains may have a both fluorine-resistant and acid-resistant F_0F_1-ATPase transport system. On the other hand, F^- can bind to F_0F_1-ATPase as AlF^-, and replaces PO_4^{3-}, which binds to ADP at the active site. Thus, it can inhibit F_0F_1-ATPase by forming an inactive complex. So, Hoelscher and Hudson (1996) speculated that the reason why F_0F_1-ATPase in fluoride-resistant strains is insensitive was that their structure of F_0F_1-ATPase has changed, and fluoride was unable to bind to the active site. Moreover, Miwa et al. (1997) speculated that expression of F_0F_1-ATPase was upregulated in fluoride-resistant strains, which increased the number of the enzyme to antagonize the inhibitory effect of fluoride. However, in previous studies on fluoride-resistant strains, no mutation was found in the *atpHGFEDCBA* operon.

In this study, we found a novel adaptive F_0F_1-ATPases point mutation, which significantly altered fluoride tolerance and cariogenicity. This article provided new insights on mechanisms of microbial fluoride resistance.

MATERIALS AND METHODS

Bacterial Strains and Growth Conditions

S. mutans UA159 strains were provided by State Key Laboratory of Oral Diseases of Sichuan University. Bacteria were grown routinely in Tryptone soya broth (TSB, OXOID, Basingstoke, England) containing 0/300/600/1,000 ppm Sodium Fluoride (NaF, KESHI, Chengdu, China) and in an anaerobic chamber

(10% H_2, 5% CO_2, and 85% N_2; Thermo Fisher Scientific, Inc., Waltham, MA, United States) at 37°C. Tryptone soya agar (TSA, OXOID, Basingstoke, England) containing 300/600/1,000 ppm NaF were used for bacterial plating and isolation. To be specific, first of all, the wild-type strain UA159 was cultivated in fluoride-free TSB in a 15 mL centrifuge tube (NEST, Jiangsu, China) in an anaerobic chamber at 37°C for 16 h. Then, 1 mL bacterial suspension was added to 9 mL TSB (1:10 dilution) and cultivated at the same conditions for 2–3 h until exponential phase (OD_{600} = 0.6). Next, 1 mL exponential-phase UA159 was added and cultivated in 9 mL TSB containing 300 ppm NaF for 16 h until OD_{600} reached 0.6. Then 200 μL bacterial suspension was plated in TSA containing 300 ppm NaF in an anaerobic chamber at 37°C for 48 h. Thus, transient fluoride-resistant strains which can tolerate 300 ppm NaF was isolated. To get stable fluoride-resistant strains, isolates were cultivated in 10 mL fluoride-free TSB in a 15 mL centrifuge tube for 16 h at the same conditions for 20 passages, respectively. At last, stable 300 ppm-fluoride-resistant strains were isolated in TSA plates containing 300 ppm NaF and named FR300. A few (10–20) isolates of FR300 were obtained and one was picked for whole-genome sequencing. Following the same procedure, FR300 was cultivated in TSB containing 600 ppm NaF for 16 h, and then plated in TSA containing 600 ppm NaF. Transient fluoride-resistant strains were cultivated in fluoride-free TSB for 20 passages, and then plated in TSA containing 600 ppm NaF to get stable 600 ppm-fluoride-resistant strains, namely FR600. Similarly, 1,000 ppm-fluoride-resistant strains were derived from FR600 and named FR1000. One isolate of FR600 and FR1000 each was picked for whole-genome sequencing (**Supplementary Figure 1** showed the isolation procedure from gradient fluoride concentrations). Growth conditions (gradient fluoride concentrations of the medium, the anaerobic environment and the temperature) were carefully controlled in all phenotypic experiments. Bacterial strains utilized in this study are listed in **Supplementary Table 3**.

Whole-Genome Sequencing

Genomic DNA was extracted using Wizard® Genomic DNA Purification Kit (Promega) according to the manufacturer's protocol. Purified genomic DNA was quantified with TBS-380 fluorometer (Turner BioSystems Inc., Sunnyvale, CA). High quality DNA (OD260/280 = 1.8–2.0, >1μg) was considered suitable for further experiments.

For Illumina sequencing, at least 1 μg genomic DNA for each strain was used to construct sequencing library. DNA samples were sheared into 400–500 bp fragments using a Covaris M220 Focused Acoustic Shearer following the manufacture's protocol. Illumina sequencing libraries were prepared from the sheared fragments using the NEXTflex™ Rapid DNA-Seq Kit. Briefly, 5′ prime ends were first end-repaired and phosphorylated. Next, the 3′ ends were A-tailed and ligated to sequencing adapters. The next step was the enrichment of the adapters-ligated products using PCR. The prepared libraries were used for paired-end Illumina sequencing (2 × 150 bp) on an Illumina HiSeq X Ten machine.

Raw Illumina paired-end reads were demultiplexed using barcodes and quality trimmed using Trimmomatic (Bolger et al., 2014). Trimmed reads were mapped to reference genome of *S. mutans* UA159 with the updated RefSeq annotation using Burrows-Wheeler Aligner (Li and Durbin, 2009). The resulting SAM files were converted to BAM files and indexed using SAMtools (Li et al., 2009). The platform was used to identify GATK SNPs and INDELs (DePristo et al., 2011) with default parameters except that the minimum phred-scaled confidence threshold was 50, which means only the variants with ≥50% frequency were selected. The whole-genome sequencing data of FR300, FR600, and FR1000 is available on the National Center for Biotechnology Information (NCBI) Sequence Read Archive Database, accession number *SRR13846722, SRR13846723, and SRR13846724*.

Quantitative Real-Time PCR Assays

Standard magnetic bead-based procedures described previously (Osman et al., 2012) were used for tissue homogenization, RNA extraction and quantitative real-time PCR (qRT-PCR). Strains were grown in Brain Heart Infusion (BHI, OXOID, Basingstoke, England) broth until exponential phase (OD_{600} = 0.6). 50 mL culture was centrifuged at 4,000 g for 10 min at 4℃. Pellets were added to fastrep tubes (Betin, Shanghai, China) containing 0.1 mm magnetic beads (Betin, Shanghai, China). Total RNA was extracted by high pressure homogenization using the Genejet RNA kit (Thermo Scientific, MA, United States). Genomic DNA contamination was removed, and cDNA was synthesized using PrimeScript RT reagent Kit with gDNA Eraser (Takara, Shiga, Japan). qRT-PCR analyses were conducted using TB Green Premix Ex TaqII (Tli RNaseH Plus) (Takara, Shiga, Japan). mRNA expression levels of the *atpH* gene were normalized using *gyrA* as an internal control (Min et al., 2009; Hossain and Biswas, 2012). The primers utilized are listed in **Supplementary Table 4**. The experiment was independently repeated three times with four replicates per group (UA159/FR600/FR1000/UA159-T, N = 12 per group). IBM SPSS Statistics 24 was employed for statistical analysis using One-way ANOVA to compared groups. Dunnett's T3 was used for multiple comparisons after ANOVA (heterogeneity of variance). A P-value of 0.05 was considered significant.

Mutant Strain Construction

We constructed a −36G→T F_0F_1-ATPases promoter mutation from *S. mutans* UA159 and named it UA159-T. Specific sequences atpH-pTune were synthesized (TSINGKE, Chengdu, China) and 1 μL of these was added to 300 μL UA159 in early exponential phase (OD_{600} = 0.3) with 1 μL competence stimulating peptide (CSP-18, 1 μg/μL, Peptide Pharmaceutical Technology Co., Ltd, Zhengzhou, China). Then, they were cultivated in a 1.5 mL centrifuge tube (NEST, Jiangsu, China) in an anaerobic chamber at 37°C for 2 h. In the two control groups, UA159 was cultivated without atpH-pTune, or without neither atpH-pTune nor CSP-18. Then 200 μL bacterial suspension of the three groups was plated in TSA containing 1,000 ppm NaF, respectively, and cultivated in an anaerobic chamber at 37°C for 48 h. Thus, fluoride-resistant colonies were isolated in the experimental group. PCR products (Primer atpH-seqFor and atpH-seqRev) were submitted to a sequencing company (TSINGKE, Chengdu, China) to test the validity of sequences. The experiment was

independently repeated three times and three isolates were picked for sequencing each time. Interestingly, all the nine isolates showed one −36G→T promoter point mutation, indicating the point mutation could be critical to fluoride resistance. The primers utilized are listed in **Supplementary Table 4**.

Minimum Inhibitory Concentration Assays

MIC assays were performed as previously described (Suntharalingam et al., 2009) with some modifications. Briefly, strains (UA159/FR600/FR1000/UA159-T) were grown in TSB overnight until exponential phase (OD_{600} = 0.6) and then diluted with TSB in the proportion of 1:100. We subsequently prepared a 96-well culture plate (Corning-Costar, NY, United States) containing 50 μL TSB, supplemented with 3/4-fold serial dilutions of NaF. The concentration of NaF was 8,000 ppm in column 1 and 0 ppm in column 12. Then, 50 μL diluted bacterial suspension was added to each well. Thus, the concentration of NaF became 4,000 ppm in column 1 but that in column 12 was still 0 ppm. After incubation at 37°C in an anaerobic chamber for 24 h, bacterial growth was spectrophotometrically measured with a microtiter plate reader at an absorbance of 600 nm. The OD_{600} readings for the wells with medium only were subtracted to account for background signals. The minimum inhibitory concentration (MIC) value was determined as the concentration that reduces 90% OD_{600} value of the fluoride-free control. The experiment was independently repeated three times with four replicates per group (N = 12 per group and per fluoride concentration).

Fluoride Inhibitory Assays

Fluoride inhibitory assays were designed based on MIC tests with Dicyclohexylcarbodiimide (DCCD, Solarbio, Beijing, China), a specific F_0F_1-ATPase inhibitor. Strains (UA159/UA159-T) were grown in TSB until exponential phase (OD_{600} = 0.6) and then were diluted with TSB at a ratio of 1:100. A 96-well culture plate (Corning-Costar, NY, United States) containing 50 μL TSB, supplemented with DCCD and 1/2-fold serial dilutions of NaF was prepared. Fifty microliter diluted bacterial suspension was added to each well to a final concentration of 0, 125, 250 ppm fluoride and 200 μM DCCD. After incubation at 37°C in an anaerobic chamber for 24 h, bacterial growth was spectrophotometrically measured with a microtiter plate reader at an absorbance of 600 nm. In the control groups, UA159 and UA159-T were cultivated without DCCD. The OD_{600} readings from medium only wells were subtracted to account for background readings. The experiment was independently repeated four times with two replicates per group (N = 8 per group). IBM SPSS Statistics 24 was employed for statistical analysis using independent two-sample t-test (two-tailed test) to compared groups. A P-value of 0.05 was considered significant. In addition, to further study the effect of gradient-concentration fluoride treatment with 200 μM DCCD on *S. mutans* growth, the same MIC procedure was applied for strains (UA159/FR1000/UA159-T) with 3/4-fold serial dilutions of NaF. In the control groups, strains (UA159/FR1000/UA159-T) were cultivated without DCCD at 37°C in an anaerobic chamber for 24 h. The OD_{600} readings from medium-only wells were subtracted to account for background readings. The experiment was independently repeated three times with four replicates per group (N = 12 per group and per fluoride concentration).

Measurement of Relative Intracellular Fluoride Concentration

The relative intracellular fluoride concentration was measured as previously described (Drescher and Suttie, 1972; Quissell and Suttie, 1972; Li et al., 2013) with some modifications. Briefly, strains (UA159/FR600/FR1000/UA159-T) were grown in TSB until exponential phase (OD_{600} = 0.6). A 24-well culture plate (Corning-Costar, NY, United States) containing 1 mL TSB supplemented with 1/2-fold serial dilutions of non-radioactive NaF and ^{18}F (provided by Laboratory of Nuclear Medicine of West China Hospital) was prepared. The concentration of NaF was 8,000 ppm in column 1 and 250 ppm in column 6. The activity of ^{18}F in column 1 was 320 μCi and that in column 6 was 10 μCi. 1 mL bacterial suspension was added to each well. Thus, the concentration of NaF in column 1 became 4,000 ppm and in column 6 became 125 ppm. The activity of ^{18}F was not altered. After incubation at 37°C in an anaerobic chamber for 1 h, the media were removed, and the cells were washed four times through vacuum filtration. Any fluoride not absorbed by the cells was washed away. Cells were then resuspended in 1 mL PBS, and the radiation intensity was measured by scintillation counting using a ^{18}F measurement protocol. Each sample was counted for 1 min, and the decay of ^{18}F during counting was accounted for by using the half-life of 109 min. Hundred microliter of a 1:1,000 dilution of the 320 μCi ^{18}F standard stock (for contrast) was counted alongside the samples (experimental groups: UA159/FR600/FR1000/UA159-T) to determine the specific activity. At the same time, OD_{600} reading of each well, which represents relative number of cells, was measured. The OD_{600} readings from medium only wells were subtracted to account for background readings. The relative concentration of NaF in each cell was determined by dividing the counts by the OD_{600} readings. The experiment was independently repeated three times with two replicates per group (N = 6 per group and per fluoride concentration). IBM SPSS Statistics 24 was employed for statistical analysis using One-way ANOVA to compared groups. Dunnett's T3 was used for multiple comparisons after ANOVA (heterogeneity of variance). A P-value of 0.05 was considered significant.

Rat Caries Models

The *in vivo* effect of *S. mutans* on SPF Wistar rats was assessed using methods previously described (Galvao et al., 2017; Garcia et al., 2017). Twelve 17-days-old male pups free of *S. mutans* were provided by Chengdu Dossy Experimental Animals Co., Ltd. (Chengdu China) and acclimatized for 3 days in our SPF Animal Center. They were randomly divided into two groups with six rats in each group. All animals were provided sterile drinking water containing 0.1% ampicillin, 0.1% chloramphenicol, 0.1% carbenicillin (J&K Chemical, Beijing, China) for 3 days to suppress endogenous flora before the infection of *S. mutans*. Saliva (obtained by sterile cotton swabs) of each rat was plated

on BHI to determine the total cultivable microorganisms and to check whether endogenous flora was effectively suppressed. The rats were orally infected with *S. mutans* UA159 and UA159-T using sterile injection syringes containing mid-exponential bacterial cultures of 10^7 CFU/mL and 0.2 mL per rat for successive days until the oral infection was confirmed 1 week later by PCR (saliva samples obtained by sterile cotton swab, primer atpH-seqFor and atpH-seqRev) and sequencing. See **Supplementary Figure 2** for the detailed comparison results of PCR product sequences. During this period, rats were given highly cariogenic Diet 2000# (Trophic Animal Feed High-Tech Co., Ltd., China) and 5% sucrose water *ad libitum*. The oral-infection experiments were conducted by one group member and the following fluoride-treatment experiments and data analysis work were conducted by another group member without knowing the group label. For treatment experiments, rat molars were flushed with fluoride solution (1,000 ppm) for 1 min daily, using 5-mL-sterile injection syringes. Rats were weighed weekly and killed at 4 weeks with CO_2 asphyxiation. Their maxillas and mandibles were dissected, cleaned and suspended in 0.4% urea amine solution in dark for 12 h for dyeing. All operations were performed in random order to minimize potential confounders.

Caries severities of smooth-surface and sulcal were observed under stereomicroscopy and scored using Keyes method (Keyes, 1958). In the Keyes scoring method, E means the depth of penetration that restricted to enamel only; slight dentinal penetration (Ds) describes penetration overlying enamel and up to one-fourth of the dentin between the enamel and pulp chamber; dentinal penetration between one-fourth and three-fourths is classified as moderate (Dm) while penetration beyond three-fourths is designated as extensive (Dx). Besides cavity depth, cavity extension is another important factor for calculating Keyes' scores. The buccal, lingual, sulcal and proximal surfaces of rat molars were divided into standard units (**Table 1** and **Supplementary Figure 3**). For each lesion severity level (E, Ds, Dm, Dx), lesion extension units were calculated, respectively, in smooth surfaces (**Supplementary Figure 3A**) and sulcal surfaces (**Supplementary Figure 3B**). Linear extent of lesions was judged by eye. And where necessary, lesions were probed to allow estimation. Only whole numbers were used. Group differences were compared by independent two-sample *t*-test (two-tailed test, heterogeneity of variance) using the IBM SPSS Statistics 24. A *P*-value of 0.05 was considered significant. The study conforms to the ARRIVE Guidelines.

TABLE 1 | The standard units of buccal, lingual, sulcal and proximal surfaces of rat molars.

Lesion types	Mandibular			Maxillary		
	1st	2nd	3rd	1st	2nd	3rd
Buccal	6	4	4	6	4	3
Lingual	6	4	4	6	4	3
Sulcal	7	5	2	5	3	2
Proximal	1	2	1	1	2	1

RESULTS

High Fluoride Concentrations Caused Fluoride Tolerance in *Streptococcus mutans* Through Point Mutations

S. mutans fluoride-resistant strains thriving in 300–1,000 ppm fluoride were isolated and named FR300 (*SRR13846724*), FR600 (*SRR13846723*), and FR1000 (*SRR13846722*). Though whole-genome sequencing, three types of variant analyses, including structural variations, insertion-deletion variant (InDel) calling and SNP calling, were carried out on the scaffolds of all strains. The resistant strains showed high homology and no genome rearrangement was observed. InDels in different coding regions in the 3 fluoride-resistant strains were compared with UA159 as listed in **Supplementary Table 1**. The results on SNP analysis, including 4 stopgain single nucleotide variants (SNVs) in 3 Open Reading Frames (ORFs), 1 stoploss SNV, 2 synonymous coding substitutions and 2 non-synonymous coding substitutions, are shown in **Supplementary Table 2**. The organization of gene clusters and their relations to the intergenic SNPs are shown in **Figure 1**. Most prokaryotic promoters share conserved sequences at the putative −10 element (TATAAT) and the putative −35 element (TTGACA). These two sequences form RNA polymerase binding site (Browning and Busby, 2004), and mutations at this region may alter RNA polymerase affinity. Notably, one SNP in FR600 and FR1000 occurred in the −35element of the *SMU_1291c* gene and one SNP in FR1000 occurred in the −10 element of the *atpH (SMU_1534)* gene. Interestingly, the *tpx (SMU_924)* SNP (−10A→T) and the *atpH* SNP (−36G→T) occurred only in FR1000, which was resistant to high fluoride concentrations, but not in FR300 or FR600. And the *atpHGFEDCBA* operon codes for a F_0F_1-ATPase/ATP synthase, which is a proton pump that maintains intracellular pH of bacteria. This highly suggests that F_0F_1-ATPase, whose mutation has not been found even in the renowned fluoride resistant strain UA159FR, could be an important regulation site of bacterial fluoride resistance.

A Novel Point Mutation in F_0F_1-ATPase Promoter Up-Regulated the Expression of *atpH* and Fluoride Resistance

To verify whether F_0F_1-ATPase is associated with fluoride resistance of *S. mutans*. A F_0F_1-ATPase promoter point mutation (UA159-T) was established from the reference strain UA159. Hereafter, *atpH* gene expression of FR600, FR1000, and UA159-T were compared with the parent strain by quantitative real-time PCR (qRT-PCR) using *gyrA* as an internal control. The *atpH* expression of FR600 was 1.79-fold higher ($P < 0.001$), of FR1000 was 3.15-fold higher ($P < 0.001$) and of UA159-T was 3.40-fold higher ($P < 0.001$) than UA159 (**Figure 2A**). There were no significant differences between the *atpH* expression of FR1000 and UA159-T ($P = 0.737$).

The MIC to fluoride of UA159 was 200 ppm; of FR600 was 1,000 ppm; of FR1000 and UA159-T was 4,000 ppm (**Figure 2B**). Apparently, −36G→T mutation in promoter

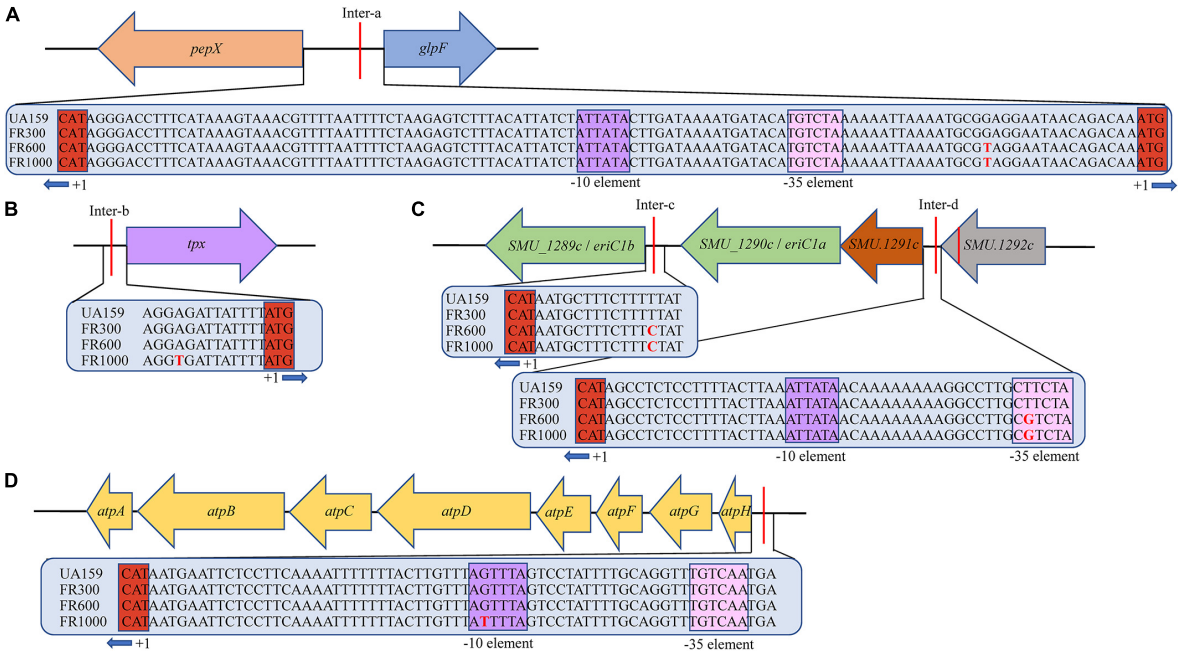

FIGURE 1 | Organization of gene clusters of *S. mutans* and their relation to intergenic SNPs. **(A)** Intergenic SNP upstream of *pepX* and *glpF* gene in FR600/FR1000. **(B)** Intergenic SNP upstream of *tpx* gene in FR1000. The -10A→T promoter mutation occurred in FR1000. **(C)** Intergenic SNP *eriC1a* (*SMU_1290c*) and *eriC1b* (*SMU_1289c*) in FR600 and FR1000. The -13T→C promoter mutation occurred in FR600 and FR1000. Intergenic SNPs of *SMU_1292c* and *SMU_1291c* in FR600 and FR1000. The -44T→G promoter mutation occurred in FR600 and FR1000. **(D)** Intergenic SNPs upstream of *atpHGFEDCBA* in FR1000. The -36G→T promoter mutation occurred in FR600 and FR1000. Sequences of intergenic regions were given in the blue bar. Red letter indicates SNPs; Purple box indicates putative -10 element (Pribnow box, share conserved sequences TATAAT/ATTATA); Pink box indicates putative -35 element (share conserved sequences TTGACA/TGTCAA); Red box indicates translation start site (ATG/CAT) of the operon.

increased F_0F_1-ATPase expression, resulting to the increase in fluoride resistance in *S. mutans*. 5 μL suspension of UA159, FR1000, and UA159-T from the 96-well culture plate of MIC assays, was grown anaerobically on TSA agar for 2 days, respectively. Stereomicroscopy images showing the effect of gradient-concentration fluoride treatment on Colony-Forming Units (CFUs) were shown in **Figure 2C**. After 2 days' incubation in the fluoride free TSA agar, many colonies were seen in cases of FR1000 and UA159-T, which indicates that for these strains, high-fluoride treatment only have antibacterial effect instead of bactericidal effect. In contrast, almost none colonies were seen in the case of parent strain UA159 after the 4,000 ppm fluoride treatment. These findings indicate fluoride resistance of *S. mutans* can be attributed to the one-point mutation at the promoter region of the *atpHGFEDCBA* operon.

Suppression of the F_0F_1-ATPase Activity by Dicyclohexylcarbodiimide Reduced Fluoride Resistance Induced by the Promoter Mutation

To further validate the relationship between the increasing of F_0F_1-ATPase expression and fluoride resistance, the suppression assay was performed. DCCD, a F_0F_1-ATPase specific inhibitor, halts proton translocation across the cell membrane (Belli et al., 1995). In the suppression assay, 200 μM DCCD showed no significant cytotoxic effects in a fluoride-free environment (**Figure 3A**). There were no significant differences between the fluoride-free groups cultivated with and without DCCD (P = 0.370 in the UA159 group; P = 0.910 in the UA159-T group). However, 200 μM DCCD suppressed UA159 and UA159-T growth in 125 and 250 ppm fluoride environment ($P < 0.001$). Interestingly, 200 μM DCCD reduced fluoride resistance in both fluoride sensitive strain UA159 and fluoride resistant strain UA159-T (**Figure 3A**). Addition of 200 μM DCCD reduced the MIC values of FR1000 and UA159-T to the level of UA159 (**Figure 3B**). Thus, the positive effects that over-expression of F_0F_1-ATPase brought about could be offset by suppression of F_0F_1-ATPase.

Fluoride Resistant Strains Tolerated Higher Intracellular Fluoride Concentrations

Relative intracellular fluoride concentration was measured by radioactive ^{18}F and results were shown in **Figure 4**. In all strains, the relative intracellular fluoride concentration increased with the increase of external fluoride concentration. Strains that are resistant to higher fluoride concentrations had accordingly higher intracellular fluoride concentrations (**Figure 4A**). With addition of 4,000 ppm external fluoride, intracellular fluoride levels in fluoride resistant strains were higher compared to UA159 (**Figure 4B**, $P < 0.001$ in FR600/FR1000/UA159-T group

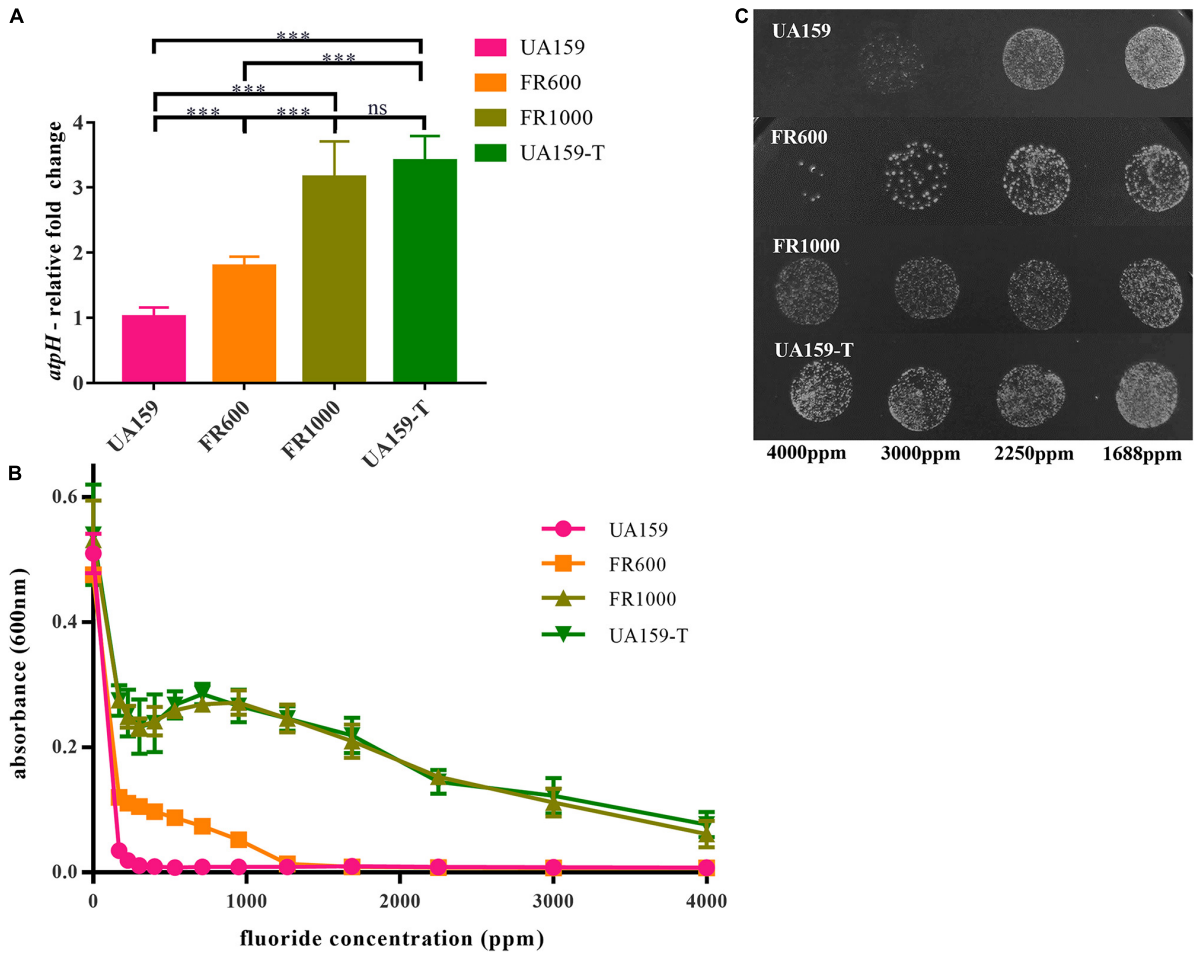

FIGURE 2 | −36G→T point mutation in UA159-T caused up-regulated *atpH* gene expression and fluoride resistance. **(A)** Quantitative real-time PCR of *atpH*: One -36G→T point mutation in F_0F_1-ATPase promoter significantly up-regulated *atpH* gene expression. Overall expression compared to UA159 was presented as average fold change ± SD. The significance level (α) was set at 0.05 (One-way ANOVA, Dunnett's T3, IBeleM SPSS Statistics 24). *** indicates $P < 0.001$. ns indicates no significant difference. $N = 12$ per group. **(B)** Effects of gradient-concentration fluoride treatment on *S. mutans* growth: One -36G→T point mutation in F_0F_1-ATPase promoter significantly increased fluoride resistance. 1:100 diluted overnight suspension of strains was incubated in 96-well culture plates with different concentrations of fluoride (3/4-fold serial) for 24 h. $N = 12$ per group and per fluoride concentration. **(C)** Effects of gradient-concentration fluoride treatment on Colony-Forming Units of *S. mutans*: FR1000 and UA159-T showed higher fluoride tolerance than UA159. Five microliter suspension of the UA159, FR1000, UA159-T from the 96-well culture plate of MIC assays (treated with 3/4-fold serial dilutions of fluoride for 24 h) was incubated on TSA for 2 days. Images were taken by a microscopy.

when compared to UA159). There was no significant difference in intracellular fluoride concentrations of FR1000 and UA159-T ($P = 0.998$). In conclusion, fluoride resistant strains could tolerate higher intracellular fluoride concentrations than fluoride sensitive strains.

−36G→T Mutation in F_0F_1-ATPases Promoter Enhanced the Cariogenicity of *Streptococcus mutans* Under Fluoride Exposure

To examine the cariogenicity of the fluoride resistant strains, we established rat caries models inoculating these strains. Different effects of UA159 and UA159-T on maxillary and mandibular teeth were illustrated in **Figure 5A**. Black arrows showed different severity in the same site of the two groups. As shown in the image, UA159-T caused more severe dental caries than UA159.

Keyes' scores of dental caries on smooth surface were calculated, analyzed and shown in **Figure 5B** and **Supplementary Tables 5**, **6**. Since caries on the smooth surfaces were not severe, the lesion extension was restricted to enamel regions only. Smooth surface scores (E) showed significant differences between UA159 and UA159-T in maxilla ($P = 0.015$), mandibula ($P = 0.033$) and in total ($P = 0.008$). Keyes' scores of dental caries on sulcal surface were calculated, analyzed and presented as graphs (**Figure 5B**). Maxillary, mandibular and accumulated sulcal enamel lesions (E) and slight dentinal lesions (Ds) scores for UA159-T group were significantly higher compared with UA159 group scores ($P = 0.018$ in maxilla/E; $P = 0.020$ in mandibula/E; $P = 0.002$ in total/E; $P = 0.018$ in maxilla/Ds;

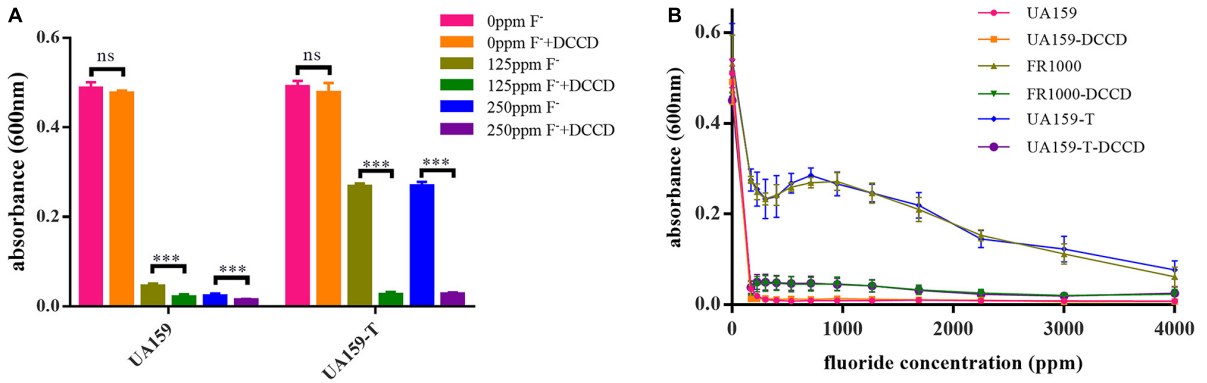

FIGURE 3 | Effects of Dicyclohexylcarbodiimide (DCCD), a specific F_0F_1-ATPase inhibitor, on fluoride resistance of *S. mutans*. **(A)** Fluoride inhibitory assays with 200 μM DCCD: suppression of the F_0F_1-ATPases by DCCD increased fluoride susceptibility of the fluoride-resistant strains in fluoride environment. The significance level (α) was set at 0.05 (independent two-sample *t*-test, two-tailed test, IBM SPSS Statistics 24). *** indicates $P < 0.001$. ns indicates no significant difference. $N = 8$ per group. **(B)** Effects of gradient-concentration fluoride treatment with 200 μM DCCD on *S. mutans* growth ($N = 12$ per group and per fluoride concentration): 200 μM DCCD suppressed F_0F_1-ATPases, increased fluoride susceptibility of the fluoride-resistant strains, and reversed the resistance effects induced by F_0F_1-ATPase over-expression.

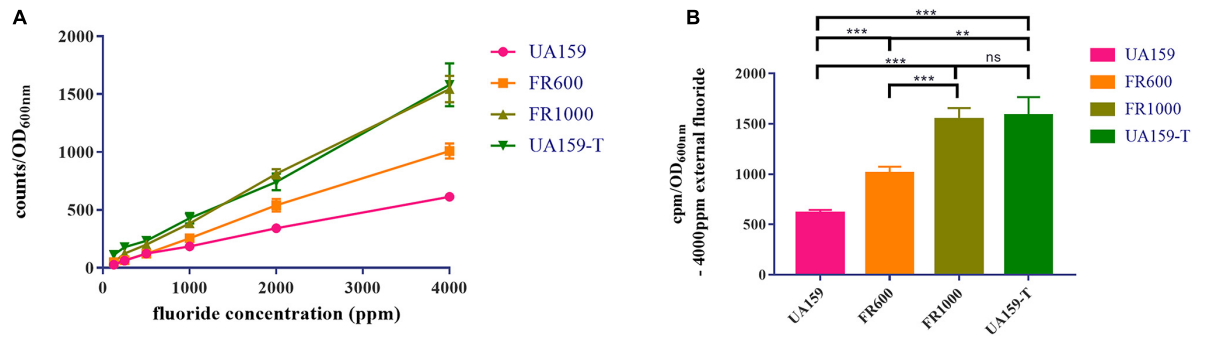

FIGURE 4 | Measurement of relative intracellular fluoride concentration. **(A)** The relative intracellular fluoride concentration increased alongside the external fluoride concentration. **(B)** With the existence of 4,000 ppm external fluoride, relative intracellular fluoride concentrations of fluoride resistant strains (FR1000 and UA159-T) were higher than UA159. The significance level (α) was set at 0.05 (One-way ANOVA, Dunnett's T3, IBM SPSS Statistics 24). $N = 6$ per group. ** indicates $P < 0.01$. *** indicates $P < 0.001$. ns indicates no significant difference.

$P = 0.012$ in mandibula/Ds; $P = 0.002$ in total/Ds). Moderate dentinal (Dm) scores for UA159-T group, though seemed to be higher, were not significantly different from UA159 group scores ($P = 0.838$ in maxilla/Dm; $P = 0.057$ in mandibula/Dm; $P = 0.098$ in total). As for extensive lesions (Dx), as only few animals had Dx lesions probably because animals were reared over a short period. Most animals in both groups had a Dx score of zero. In UA159-T group, a few animals showed Dx scores up to 3. However, Dx scores showed no significance difference in maxilla ($P = 0.363$), mandibula ($P = 0.094$) and in total ($P = 0.066$) between the two groups. From these findings, we conclude that fluoride resistant strains developed by over-expressed F_0F_1-ATPase caused more severe dental caries compared to the reference strain.

DISCUSSION

Fluoride is an abundant element in environment and is added as an anti-caries agent to a variety of oral care products (Anusavice et al., 2016). Fluoride is absorbed by bacterial cells in the form of HF, which dissociates in the cell into F^- and H^+. Intracellular F^- and H^+ directly or indirectly affects physiological processes and enzymatic activities in the cell, such as F_0F_1-ATPase, Enolase, fluoride exporters, pyruvate kinase, pyrophosphatase, urease and the arginine deiminase system (ADS) (Rolla and Melsen, 1975; Bender et al., 1985; Meurman, 1988; Marquis, 1990; Belli et al., 1995; Van Loveren, 2001; Hamilton and Ellwood, 1978). Many microorganisms have developed fluoride resistance (Streckfuss et al., 1980; Mitsuhata et al., 2014; Liao et al., 2015) due to extensive usage of fluoride in oral hygiene products. As a result, these products are not expectedly effective in treatment of dental caries. Stable fluoride resistant strains were isolated and used to study the mechanism of the acquired resistance, which is still unclear.

In this study, the effects of fluoride treatment on *S. mutans* were studied through comparison of functional genomics. Fluoride treatment on *S. mutans* strain UA159 resulted to 4 fluoride-resistant strains (FR300, FR600, FR1000, and UA159-T)

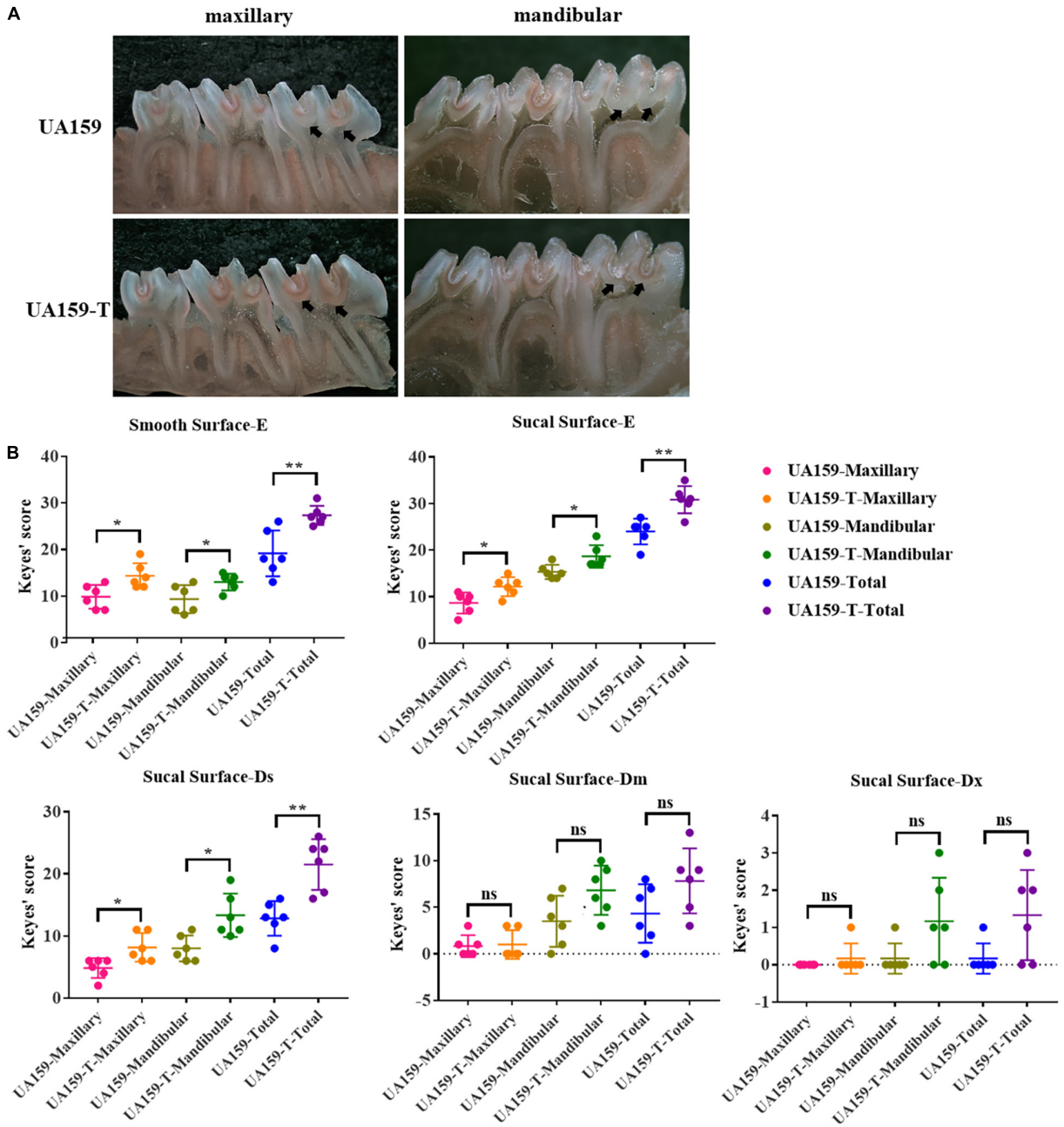

FIGURE 5 | Dental caries conditions and Keyes' scores of rat caries models. **(A)** Stereomicroscopy images of dental caries on maxillary and mandibular bones of rats infected with UA159 and UA159-T. Black arrows point out different severity in the same site of the two groups. UA159-T strains led to severer dental caries than UA159. **(B)** Keyes' scores of smooth surfaces and sulcal surfaces of two group (UA159 and UA159-T) and $N = 6$ per group: UA159-T strains achieved higher Keyes' scores and led to severer dental caries than UA159. The significance level (α) was set at 0.05 (independent two-sample *t*-test, two-tailed test, IBM SPSS Statistics 24). * indicates $P < 0.05$. ** indicates $P < 0.01$. ns indicates no significant difference.

and a site-directed mutagenesis (-36G→T) in the F_0F_1-ATPases promoter region in UA159-T. Two SNPs in FR300, 8 SNPs in FR600 and 9 SNPs in FR1000 were identified through the Illumina PE250 sequencing platform and compared with UA159 (**Supplementary Table 2**).

Notably, a non-synonymous SNP was identified in FR600 and FR1000 in *pykF (SMU_1190)* gene, which encodes pyruvate kinase, an important glycolytic enzyme. Enolase catalyzes the conversion of 2-phosphoglycerate to phosphoenolpyruvate (PEP), while pyruvate kinase converts PEP to pyruvate during glycolysis. Fluoride competitively inhibits enolase enzyme (Guha-Chowdhury et al., 1997). This inhibition is observed both in purified enolase and enolase from permeabilized cells (Curran et al., 1994; Guha-Chowdhury et al., 1997;

van Loveren et al., 2008). In addition, enolase is indirectly inhibited by low cytoplasm pH levels caused by H^+ accumulation (Belli et al., 1995; Marquis et al., 2003). Moreover, enolase catalyzes the production of PEP for glucose uptake through the PEP dependent phosphotransferase system (PTS). Thus, enolase inhibition results in reduction of sugar uptake as well as glycolysis (Sutton et al., 1987). Previous studies (Marquis et al., 2003) reported that inhibition of pyruvate kinase is unlikely to occur in bacterial cells because the inhibitory fluoride concentration for this enzyme was approximately 10–100 times higher than that required for enolase inhibition. Liao et al. (2015, 2018) reports two different SNPs from ours in *S. mutans pykF* gene using whole-genome shotgun sequencing and genome comparisons between C180-2 and C180-2FR. However, qRT-PCR analysis shows similar pyruvate kinase expression levels in C180-2 and C180-2FR. Thus, the role of pyruvate kinase in bacterial fluoride resistance needs further explore.

Genes controlled by promoters in the mutated intergenic regions were identified (**Supplementary Table 2** and **Figure 1**). Firstly, *glpF (SMU_396)* and *pepX (SMU_395)* genes located downstream of the mutated intergenic region were identified (Inter-a, **Figure 1**). *pepX* encodes Xaa-Pro dipeptidyl-peptidase (Q8DVS2), which cleaves N-terminal dipeptides sequentially from polypeptides with unsubstituted N-termini provided that the penultimate residue is proline. *glpF* encodes a putative glycerol uptake facilitator protein, a membrane channel that selectively transports water, small neutral molecules and ions (Fu et al., 2002). In *Escherichia coli*, which uses glycerol as a carbon source, *glpF* mediates glycolysis and lipid biogenesis (Heller et al., 1980). In *Lactococcus lactis*, it mediates the growth of bacterial cells in the presence of glycerol (Froger et al., 2001). In this study, we identified the same SNP in the intergenic region of *pepX* and *glpF* genes as the previously reported SNP by Liao et al. (2015) in *S. mutans* C180-2 and C180-2FR. In their study, Liao et al. (2015) reported lower expression levels of the *glpF* in C180-2FR than C180-2 in early exponential phase. The lower expression levels may be attributed to slower growth rate of the fluoride-resistant strain. In conclusion, *glpF* plays a role in bacterial cell growth but not in fluoride resistance.

A mutation in an intergenic region (**Supplementary Table 2** and Inter-b, **Figure 1**) was located upstream of *tpx* gene, which encodes thiol peroxidase. Thiol-specific peroxidase catalyzes the reduction of hydrogen peroxide and organic hydroperoxides to water and alcohols. It protects cells against oxidative stress by breaking down peroxides (Baker and Poole, 2003; Cha et al., 2004). Interestingly, the -10A→T promoter mutation only occurred in FR1000 but not in FR300 or FR600. Thus, there is a high possibility that this mutation may be implicated in fluoride resistance and further exploration is needed.

Mutations were observed between *SMU_1289c* and *SMU_1290c* genes (**Supplementary Table 2** and Inter-c, **Figure 1**) and between *SMU_1291c* and *SMU_1292c* genes (**Supplementary Table 2** and Inter-d, **Figure 1**). These 3 genes, *SMU_1291c*, *SMU_1290c/eriC1a* and *SMU_1289c/eriC1a* occur in proximity and they encode putative chorismate mutase, putative permease and chloride channel, respectively. Breaker (2012)x and Baker et al. (2012) reported that *crcB* (fungal *FEX* homologs) and $EriC^F$ (ClC-type ion channel protein) gene families play similar biochemical roles. These gene families encode fluoride exporters (Rapp et al., 2006; Baker et al., 2012) and are implicated in fluoride resistance of microorganisms. These genes are divided into three groups: group I, consisting of *eriC1*; group II, *eriC1* and *eriC2*; and group III, *eriC2*, *crcB1*, and *crcB2*. A previous study reported that these genes were highly selective fluoride channels that discriminate against Cl^- by a factor of > 10,000-fold (Stockbridge et al., 2013). Unlike other CLC transporters, which employ two-to-one stoichiometry, the fluoride exporter exchanges F^- with H^+ with one-to-one stoichiometry (Picollo et al., 2012; Stockbridge et al., 2012). *eriC1* in group I is from *S. mutans* and has two $eriC^F$ genes in tandem with the same orientation, namely *eriC1a* and *eriC1b* (Men et al., 2016). The two genes encode proteins with 58% amino acid identity (Liao et al., 2015). Ying Liao reported the same −44T→G SNP in C180-2FR (Liao et al., 2015) as our study (**Supplementary Table 2** and Inter-d, **Figure 1**), and a different -47T→A SNP (Liao et al., 2018) in UA159FR. Expression levels of the three genes was higher in both C180-2FR and UA159FR compared with C180-2 and UA159. A -44T→G mutation in the promoter of strain C180-2 constitutively upregulated *eriC1a* and *eriC1b* expression and conferred fluoride resistance on fluoride sensitive *S. mutans* strain (Liao et al., 2016). Two gene knockout studies demonstrated that *eriC1a* and *eriC1b* genes were implicated in fluoride resistance (Men et al., 2016; Murata and Hanada, 2016). *S. mutans* strains with $eriC^F$ genes knocked out were more susceptible to fluoride in both studies. However, one study showed knocking out either *eriC1a* or *eriC1b* gene can increase fluoride susceptibility (Murata and Hanada, 2016) while another author reported that only *eriC1b* gene was implicated in fluoride resistance (Men et al., 2016). In conclusion, *eriC1a* and *eriC1b* encode H^+-coupled fluoride antiporters $EriC^F$, which extrudes F^- from cell. High expression levels of these two genes protect *S. mutans* fluoride resistant strains from high fluoride concentrations.

Furthermore, a mutated intergenic region (**Supplementary Table 2** and Inter-d, **Figure 1**) located upstream of *atpHGFEDCBA*, which separately encodes ATP synthase subunit proteins, was observed. ATP synthase, also known as F_0F_1-ATPase, is a protein consisting of two domains: F_0 (cytoplasmic) and F_1 (membrane bound). F_0F_1-ATPase hydrolyzes or synthesizes ATP while transporting protons through the F_0 pore in the membrane (Bender et al., 1986). Therefore, F_0F_1-ATPase plays an important role in regulating intracellular pH through proton transporting and is closely related to the acid tolerance of bacteria (Bender et al., 1986). Differences in the pH optima of F_0F_1-ATPase appears to be the main reason why *S. mutans* is more tolerant of low pH values and hence pathogenic. Previous studies have shown that the pH optima of F_0F_1-ATPase of *S. mutans* was approximately 6.0 while that of *Streptococcus sanguis* was approximately 7.0 (Sturr and Marquis, 1992). Thus, the S. *mutans* enzyme is well positioned to continue pumping at pH values below levels at which *S. sanguis* can survive. The expression of F_0F_1-ATPase gene of *S. mutans* is

regulated by pH and will be up-regulated in acidic environment than in neutral environment (Kuhnert et al., 2004). As for fluoride, previous studies found that it can inhibit F_0F_1-ATPases directly by F^- and indirectly by cytoplasm acidification through HF influx (Liao et al., 2017). Inhibiting proton transporting of F_0F_1-ATPases (dissipating pH_i gradients) is one important mechanism of fluoride to prevent dental caries (Dashper and Reynolds, 1992). However, the role of F_0F_1-ATPase in fluoride resistance has never been reported. Researchers speculated that, fluoride-resistant *S. mutans* are able to up-regulate synthesis of its F_0F_1-ATPase (Miwa et al., 1997; Belli and Marquis, 2010; Hamilton and Buckley, 2010). In order to better understand the molecular mechanisms by which *S. mutans* up-regulates its F_0F_1-ATPase, Smith et al. (1996) had previously undertaken the characterization of the *S. mutans atpHGFEDCBA* operon, including its cloning and nucleotide sequence determination. The deduced amino acid sequences for the eight structural genes of the *S. mutans atpHGFEDCBA* operon showed that this enzyme is homologous to the well-characterized *Escherichia coli* ATPase as well as those of other bacteria (Smith et al., 1996). Interestingly, the *S. mutans* operon did not contain an *atpI* gene equivalent upstream of the structural genes but rather contained an intergenic region of 239 bp (Smith et al., 1996). Kuhnert and Quivey (2003) reported that the genetic organization of the operons has been maintained in the oral streptococci and speculated that the large intergenic regions seen upstream of the *S. mutans atpHGFEDCBA* operons may be involved in the regulation of the operon. Primer extension analysis were used to examine the transcriptional start site for the operon. The results of identified a guanine at position −28 bp relative to the initial methionine for the *atpH* gene. Once the start site was identified, sequence analysis of the region immediately upstream suggested a putative Pribnow box (−10 element) with a sequence of TAAACT, which was similar to the *E. coli* consensus sequence of TATAAT (66% homogeneity). A potential −35 element sequence was also identified that was completely identical to the canonical *E. coli* −35 region of TTGACA (Kuhnert and Quivey, 2003). However, in previous studies on fluoride-resistant strains, no mutation was found in the *atpHGFEDCBA* operon.

In our study, a novel −36G→T promoter mutation was observed in the putative Pribnow box/-10 element (**Supplementary Table 2** and **Figure 1**). Pribnow box is an important RNA polymerase binding site (Browning and Busby, 2004), and mutations at this region may alter RNA polymerase affinity. This novel mutation only occurred in FR1000 but not in UA159, FR300 or FR600, highly suggesting that F_0F_1-ATPase could be an important regulation site for bacteria to resist high fluoride concentrations. Quantitative real-time PCR assays showed that *atpH* expression levels were higher in FR600, FR1000 and UA159-T ($P < 0.001$) than in UA159 (qRT-PCR, **Figure 2**). Interestingly, −36G→T point mutation in the promoter increased of F_0F_1-ATPase expression levels (qRT-PCR, **Figure 2**) and conferred fluoride resistance on the fluoride sensitive *S. mutans* strain (MIC assays, **Figure 2**). However, the addition of 200 μM DCCD, a specific inhibitor of F_0F_1-ATPase, reduced the MIC values of FR1000 and UA159-T to the same amount of UA159 (**Figure 3**). This implies that 200 μM DCCD reverses the resistance effects induced by F_0F_1-ATPase over-expression. F_0F_1-ATPase high expression levels may improve fluoride resistance by extruding proton out of the cell thus increasing cytoplasm pH. To be specific, inhibitory effect of fluoride on bacterial intracellular metabolism is modulated by HF influx. Intracellular F^- and H^+ directly or indirectly affects enzymatic activities and physiological processes in the cell. When cells are exposed to high fluoride environment, fluoride antiporters export F^- to extracellular by acting as H^+-coupled antiporters. However, entry of H^+ ions lower cytoplasm pH. In this case, high expression of F_0F_1-ATPase can extrude surplus protons out of cell and increase cytoplasm pH. Thus, F_0F_1-ATPase plays an important role in antagonizing fluoride inhibition effect on *S. mutans* and improving fluoride resistance in *S. mutans*. When proton transporting of F_0F_1-ATPases was inhibited by DCCD, surplus protons cannot be pumped out of the cell, causing acidification of the cytoplasm, and further affecting physiological processes of the cell. What is more, the study founded the relative intracellular fluoride concentration of fluoride resistant strains was higher than in UA159, implying that fluoride resistant strains could tolerate higher intracellular fluoride concentrations than fluoride sensitive strains (**Figure 4**). This finding supported our hypothesis that the increase of fluoride tolerance was caused by increasing H^+ extrusion and cytoplasm pH. Rat caries models under fluoride exposure showed that UA159-T caused more severe dental caries than UA159 (**Figure 5**). In summary, tolerance of *S. mutans* to high fluoride concentrations is speculated to be caused by critical genetic changes. The novel SNP in the F_0F_1-ATPases promoter can greatly increase fluoride resistance and cariogenicity in *S. mutans*. High correlation between F_0F_1-ATPase suppression and fluoride susceptibility makes F_0F_1-ATPase a potential suppression target for fluoride resistant strains.

DATA AVAILABILITY STATEMENT

The datasets presented in this study can be found in online repositories. The names of the repository/repositories and accession number(s) can be found below: NCBI SRA BioProject, accession no: PRJNA706102.

ETHICS STATEMENT

All animal experiments were performed in strict accordance with guidelines from the Institutional Animal Care and Use Committee (IACUC). The animal study was reviewed and approved by Ethics Committee of State Key Laboratory of Oral Diseases, Sichuan University, Chengdu, China (Protocol WCHSIRB-D-2019-184).

AUTHOR CONTRIBUTIONS

CL, XX, and XP contributed to conception, design, data acquisition, analysis, and interpretation, drafted, and critically

revised the manuscript. ZL, CQ, and SY contributed to data acquisition, analysis, and interpretation, and drafted the manuscript. BR, JL, XZ, and HC contributed to design and critically revised the manuscript. All authors gave final approval and agreed to be accountable for all aspects of the work.

FUNDING

This study was supported by the National Natural Science Foundation of China (32070120, 81771099, 81991500, 81991501, and 81700963).

ACKNOWLEDGMENTS

We thank Ning Ji from Animal Laboratory of the State Key Laboratory of Oral Diseases, Sichuan University for his supervision and instructions on animal experiments, welfare and ethics.

SUPPLEMENTARY MATERIAL

The Supplementary Material for this article can be found online at: https://www.frontiersin.org/articles/10.3389/fmicb.2021.777504/full#supplementary-material

REFERENCES

Anusavice, K. J., Zhang, N. Z., and Shen, C. (2016). Effect of caf2 content on rate of fluoride release from filled resins. *J. Dent. Res.* 84, 440–444. doi: 10.1177/154405910508400508

Baker, J. L., Sudarsan, N., Weinberg, Z., Roth, A., Stockbridge, R. B., and Breaker, R. R. (2012). Widespread genetic switches and toxicity resistance proteins for fluoride. *Science* 335, 233–235. doi: 10.1126/science.1215063

Baker, L. M., and Poole, L. B. (2003). Catalytic mechanism of thiol peroxidase from *escherichia coli*. Sulfenic acid formation and overoxidation of essential cys61. *J. Biol. Chem.* 278, 9203–9211. doi: 10.1074/jbc.M209888200

Belli, W. A., Buckley, D. H., and Marquis, R. E. (1995). Weak acid effects and fluoride inhibition of glycolysis by streptococcus mutans gs-5. *Can. J. Microbiol.* 41, 785–791. doi: 10.1139/m95-108

Belli, W. A., and Marquis, R. E. (2010). Catabolite modification of acid tolerance of streptococcus mutans gs-5. *Mol. Oral Microbiol.* 9, 29–34. doi: 10.1111/j.1399-302x.1994.tb00211.x

Bender, G. R., Sutton, S. V., and Marquis, R. E. (1986). Acid tolerance, proton permeabilities, and membrane atpases of oral streptococci. *Infect. Immun.* 53, 331–338. doi: 10.1128/iai.53.2.331-338.1986

Bender, G. R., Thibodeau, E. A., and Marquis, R. E. (1985). Reduction of acidurance of streptococcal growth and glycolysis by fluoride and gramicidin. *J. Dent. Res.* 64, 90–95. doi: 10.1177/00220345850640021701

Bolger, A. M., Lohse, M., and Usadel, B. (2014). Trimmomatic: a flexible trimmer for illumina sequence data. *Bioinformatics* 30, 2114–2120. doi: 10.1093/bioinformatics/btu170

Breaker, R. R. (2012). New insight on the response of bacteria to fluoride. *Caries Res.* 46, 78–81. doi: 10.1159/000336397

Brown, L. R., White, J. O., Horton, I. M., Dreizen, S., and Streckfuss, J. L. (1983). Effect of continuous fluoride gel use on plaque fluoride retention and microbial activity. *J. Dent. Res.* 62, 746–751. doi: 10.1177/00220345830620061201

Browning, D. F., and Busby, S. J. (2004). The regulation of bacterial transcription initiation. *Nat. Rev. Microbiol.* 2, 57–65.

Brussock, S. M., and Kral, T. A. (1987). Effects of ph on expression of sodium fluoride resistance in streptococcus mutans. *J. Dent. Res.* 66:1594. doi: 10.1177/00220345870660101701

Burne, R. A., and Marquis, R. E. (2000). Alkali production by oral bacteria and protection against dental caries. *FEMS Microbiol. Lett.* 193, 1–6. doi: 10.1111/j.1574-6968.2000.tb09393.x

Buzalaf, M. A., Pessan, J. P., Honorio, H. M., and Ten, C. J. (2011). Mechanisms of action of fluoride for caries control. *Monogr. Oral Sci.* 22, 97–114.

Cha, M. K., Kim, W. C., Lim, C. J., Kim, K., and Kim, I. H. (2004). *Escherichia coli* periplasmic thiol peroxidase acts as lipid hydroperoxide peroxidase and the principal antioxidative function during anaerobic growth. *J. Biol. Chem.* 279, 8769–8778. doi: 10.1074/jbc.M312388200

Chansley, P. E., and Kral, T. A. (1989). Transformation of fluoride resistance genes in streptococcus mutans. *Infect. Immun.* 57, 1968–1970. doi: 10.1128/iai.57.7.1968-1970.1989

Curran, T. M., Buckley, D. H., and Marquis, R. E. (1994). Quasi-irreversible inhibition of enolase of streptococcus mutans by fluoride. *FEMS Microbiol. Lett.* 119, 283–288. doi: 10.1111/j.1574-6968.1994.tb06902.x

Curran, T. M., Ma, Y., Rutherford, G. C., and Marquis, R. E. (1998). Turning on and turning off the arginine deiminase system in oral streptococci. *Can. J. Microbiol.* 44, 1078–1085. doi: 10.1139/cjm-44-11-1078

Dashper, S. G., and Reynolds, E. C. (1992). Ph regulation by streptococcus mutans. *J. Dent. Res.* 71:1159. doi: 10.1177/00220345920710050601

Davison, A., and Weinstein, L. H. (2004). *Fluorides in the environment :effects on Plants and Animals*. Wallingford: CABI Pub.

DePristo, M. A., Banks, E., Poplin, R., Garimella, K. V., Maguire, J. R., Hartl, C., et al. (2011). A framework for variation discovery and genotyping using next-generation DNA sequencing data. *Nat. Genet.* 43, 491–498. doi: 10.1038/ng.806

Drescher, M., and Suttie, J. W. (1972). Intracellular fluoride in cultured mammalian cells. *Proc. Soc. Exp. Biol. Med.* 139, 228–230. doi: 10.3181/00379727-139-36115

Froger, A., Rolland, J. P., Bron, P., Lagree, V., Le Caherec, F., Deschamps, S., et al. (2001). Functional characterization of a microbial aquaglyceroporin. *Microbiology* 147, 1129–1135. doi: 10.1099/00221287-147-5-1129

Fu, D., Libson, A., and Stroud, R. (2002). The structure of glpf, a glycerol conducting channel. *Novartis Found Symp.* 245, 51–61. doi: 10.1002/0470868759.ch5

Galvao, L. C., Rosalen, P. L., Rivera-Ramos, I., Franco, G. C., Kajfasz, J. K., Abranches, J., et al. (2017). Inactivation of the spxa1 or spxa2 gene of streptococcus mutans decreases virulence in the rat caries model. *Mol. Oral Microbiol.* 32, 142–153. doi: 10.1111/omi.12160

Garcia, S. S., Blackledge, M. S., Michalek, S., Su, L., Ptacek, T., Eipers, P., et al. (2017). Targeting of streptococcus mutans biofilms by a novel small molecule prevents dental caries and preserves the oral microbiome. *J. Dent. Res.* 96, 807–814. doi: 10.1177/0022034517698096

Guha-Chowdhury, N., Clark, A. G., and Sissons, C. H. (1997). Inhibition of purified enolases from oral bacteria by fluoride. *Oral Microbiol. Immunol.* 12, 91–97. doi: 10.1111/j.1399-302x.1997.tb00623.x

Gutknecht, J., and Walter, A. (1981). Hydrofluoric and nitric acid transport through lipid bilayer membranes. *Biochim. Biophys. Acta.* 644, 153–156. doi: 10.1016/0005-2736(81)90071-7

Hamilton, I. R. (1990). Biochemical effects of fluoride on oral bacteria. *J. Dent. Res.* 69, 660–667. doi: 10.1177/00220345900690S128

Hamilton, I. R., and Buckley, N. D. (2010). Adaptation by streptococcus mutans to acid tolerance. *Oral Microbiol. Immunol.* 6, 65–71. doi: 10.1111/j.1399-302x.1991.tb00453.x

Hamilton, I. R., and Ellwood, D. C. (1978). Effects of fluoride on carbohydrate metabolism by washed cells of streptococcus mutans grown at various pH values in a chemostat. *Infect Immun.* 19, 434–442. doi: 10.1128/iai.19.2.434-442.1978

Heller, K. B., Lin, E. C., and Wilson, T. H. (1980). Substrate specificity and transport properties of the glycerol facilitator of *escherichia coli*. *J. Bacteriol.* 144, 274–278. doi: 10.1128/jb.144.1.274-278.1980

Hoelscher, G. L., and Hudson, M. C. (1996). Characterization of an unusual fluoride-resistant streptococcus mutans isolate. *Curr. Microbiol.* 32, 156–161. doi: 10.1007/s002849900028

Hossain, M. S., and Biswas, I. (2012). An extracelluar protease, sepm, generates functional competence-stimulating peptide in streptococcus mutans ua159. *J. Bacteriol.* 194, 5886–5896. doi: 10.1128/JB.01381-12

Hudson, M. C., and Curtiss, R. R. (1990). Regulation of expression of streptococcus mutans genes important to virulence. *Infect. Immun.* 58, 464–470. doi: 10.1128/iai.58.2.464-470.1990

Jagtap, S., Yenkie, M. K., Labhsetwar, N., and Rayalu, S. (2012). Fluoride in drinking water and defluoridation of water. *Chem. Rev.* 112, 2454–2466. doi: 10.1021/cr2002855

Kuhnert, W. L., and Quivey, R. G. (2003). Genetic and biochemical characterization of the f-atpase operon from streptococcus sanguis 10904. *J. Bacteriol.* 185, 1525–1533. doi: 10.1128/JB.185.5.1525-1533.2003

Kuhnert, W. L., Zheng, G., Faustoferri, R. C., and Quivey, R. G. (2004). The f-atpase operon promoter of streptococcus mutans is transcriptionally regulated in response to external ph. *J. Bacteriol.* 186, 8524–8528. doi: 10.1128/JB.186.24.8524-8528.2004

Li, H., and Durbin, R. (2009). Fast and accurate short read alignment with burrows-wheeler transform. *Bioinformatics* 25, 1754–1760. doi: 10.1093/bioinformatics/btp324

Li, H., Handsaker, B., Wysoker, A., Fennell, T., Ruan, J., Homer, N., et al. (2009). The sequence alignment/map format and samtools. *Bioinformatics* 25, 2078–2079. doi: 10.1093/bioinformatics/btp352

Li, S., Smith, K. D., Davis, J. H., Gordon, P. B., Breaker, R. R., and Strobel, S. A. (2013). Eukaryotic resistance to fluoride toxicity mediated by a widespread family of fluoride export proteins. *Proc. Natl. Acad. Sci.* 110, 19018–19023. doi: 10.1073/pnas.1310439110

Liao, Y., Brandt, B. W., Li, J., Crielaard, W., Van Loveren, C., and Deng, D. M. (2017). Fluoride resistance in streptococcus mutans: a mini review. *J. Oral Microbiol.* 9:1344509. doi: 10.1080/20002297.2017.1344509

Liao, Y., Brandt, B. W., Zhang, M., Li, J., Crielaard, W., van Loveren, C., et al. (2016). A single nucleotide change in the promoter mutp enhances fluoride resistance of streptococcus mutans. *Antimicrob. Agents Chemother.* 60, 7509–7512. doi: 10.1128/AAC.01366-16

Liao, Y., Chen, J., Brandt, B. W., Zhu, Y., Li, J., van Loveren, C., et al. (2015). Identification and functional analysis of genome mutations in a fluoride-resistant streptococcus mutans strain. *PLoS One* 10:e0122630. doi: 10.1371/journal.pone.0122630

Liao, Y., Yang, J., Brandt, B. W., Li, J., Crielaard, W., van Loveren, C., et al. (2018). Genetic loci associated with fluoride resistance in streptococcus mutans. *Front. Microbiol.* 9:3093. doi: 10.3389/fmicb.2018.03093

Loesche, W. J. (1986). Role of streptococcus mutans in human dental decay. *Microbiol. Rev.* 50, 353–380. doi: 10.1128/mr.50.4.353-380.1986

Marquis, R. E. (1990). Diminished acid tolerance of plaque bacteria caused by fluoride. *J. Dent. Res.* 69, 672–675. doi: 10.1177/00220345900690S130

Marquis, R. E., Clock, S. A., and Mota-Meira, M. (2003). Fluoride and organic weak acids as modulators of microbial physiology. *FEMS Microbiol. Rev.* 26, 493–510. doi: 10.1111/j.1574-6976.2003.tb00627.x

Marquis, R. E (1995). Antimicrobial actions of fluoride for oral bacteria. *Can. J. Microbiol.* 41, 955–964. doi: 10.1139/m95-133

Men, X., Shibata, Y., Takeshita, T., and Yamashita, Y. (2016). Identification of anion channels responsible for fluoride resistance in oral streptococci. *PLoS One* 11:e0165900. doi: 10.1371/journal.pone.0165900

Meurman, J. H. (1988). Ultrastructure, growth, and adherence of streptococcus mutans after treatment with chlorhexidine and fluoride. *Caries Res.* 22, 283–287. doi: 10.1159/000261122

Mieher, J. L., Larson, M. R., Schormann, N., Purushotham, S., Wu, R., Rajashankar, K. R., et al. (2018). Glucan binding protein c of streptococcus mutans mediates both sucrose-independent and sucrose-dependent adherence. *Infect. Immunity* 86, e00146–18. doi: 10.1128/IAI.00146-18

Min, Z., Ajdi, D., Yuan, L., Lynch, D., and Merritt, J. (2009). Role of the streptococcus mutans irva gene in gbpc-independent, dextran-dependent aggregation and biofilm formation. *Appl. Environ. Microbiol.* 75, 7037–7043. doi: 10.1128/AEM.01015-09

Mitsuhata, C., Puteri, M. M., Ohara, Y., Tatsukawa, N., and Kozai, K. (2014). Possible involvement of enolase in fluoride resistance in streptococcus mutans. *Pediatric. Dent. J.* 24, 12–16.

Miwa, T., Esaki, H., Umemori, J., and Hino, T. (1997). Activity of h(+)-atpase in ruminal bacteria with special reference to acid tolerance. *Appl. Environ. Microbiol.* 63, 2155–2158. doi: 10.1128/aem.63.6.2155-2158.1997

Murata, T., and Hanada, N. (2016). Contribution of chloride channel permease to fluoride resistance in streptococcus mutans. *FEMS Microbiol. Lett.* 363:fnw101. doi: 10.1093/femsle/fnw101

Osman, F., Olineka, T., Hodzic, E., Golino, D., and Rowhani, A. (2012). Comparative procedures for sample processing and quantitative pcr detection of grapevine viruses. *J. Virol. Methods* 179, 303–310. doi: 10.1016/j.jviromet.2011.11.008

Pandit, S., Kim, H. J., Song, K. Y., and Jeon, J. G. (2013). Relationship between fluoride concentration and activity against virulence factors and viability of a cariogenic biofilm: in vitro study. *Caries Res.* 47, 539–547. doi: 10.1159/000348519

Keyes, P. H. (1958). Dental caries in the molar teeth of rats. Ii. A method for diagnosing and scoring several types of lesions simultaneously. *J. Dent. Res.* 37, 1088–1099. doi: 10.1177/00220345580370060901

Picollo, A., Xu, Y., Johner, N., Berneche, S., and Accardi, A. (2012). Synergistic substrate binding determines the stoichiometry of transport of a prokaryotic h(+)/cl(-) exchanger. *Nat. Struct. Mol. Biol.* 19, 525–31. doi: 10.1038/nsmb.2277

Quissell, D. O., and Suttie, J. W. (1972). Development of a fluoride-resistant strain of l cells: membrane and metabolic characteristics. *Am. J. Physiol.* 223, 596–603. doi: 10.1152/ajplegacy.1972.223.3.596

Rapp, M., Granseth, E., Seppala, S., and von Heijne, G. (2006). Identification and evolution of dual-topology membrane proteins. *Nat. Struct. Mol. Biol.* 13, 112–116. doi: 10.1038/nsmb1057

Rolla, G., and Melsen, B. (1975). Desorption of protein and bacteria from hydroxyapatite by fluoride and monofluorophosphate. *Caries Res.* 9, 66–73. doi: 10.1159/000260144

Smith, A. J., Quivey, R. G., and Faustoferri, R. C. (1996). Cloning and nucleotide sequence analysis of the streptococcus mutans membrane-bound, proton-translocating atpase operon. *Gene* 183, 87–96. doi: 10.1016/s0378-1119(96)00502-1

Stockbridge, R. B., Lim, H. H., Otten, R., Williams, C., Shane, T., Weinberg, Z., et al. (2012). Fluoride resistance and transport by riboswitch-controlled clc antiporters. *Proc. Natl. Acad. Sci.* 109, 15289–15294. doi: 10.1073/pnas.1210896109

Stockbridge, R. B., Robertson, J. L., Kolmakova-Partensky, L., and Miller, C. (2013). A family of fluoride-specific ion channels with dual-topology architecture. *Elife* 2:e01084. doi: 10.7554/eLife.01084

Streckfuss, J. L., Perkins, D., Horton, I. M., Brown, L. R., Dreizen, S., and Graves, L. (1980). Fluoride resistance and adherence of selected strains of streptococcus mutans to smooth surfaces after exposure to fluoride. *J. Dent. Res.* 59, 151–158. doi: 10.1177/00220345800590021501

Sturr, M. G., and Marquis, R. E. (1992). Comparative acid tolerances and inhibitor sensitivities of isolated f-atpases of oral lactic acid bacteria. *Appl. Environ. Microbiol.* 58, 2287–2291. doi: 10.1128/aem.58.7.2287-2291.1992

Suntharalingam, P., Senadheera, M. D., Mair, R. W., Levesque, C. M., and Cvitkovitch, D. G. (2009). The liafsr system regulates the cell envelope stress response in streptococcus mutans. *J. Bacteriol.* 191, 2973–2984. doi: 10.1128/JB.01563-08

Sutton, S. V., Bender, G. R., and Marquis, R. E. (1987). Fluoride inhibition of proton-translocating atpases of oral bacteria. *Infect. Immun.* 55, 2597–2603. doi: 10.1128/iai.55.11.2597-2603.1987

Van Loveren, C. (2001). Antimicrobial activity of fluoride and its in vivo importance: Identification of research questions. *Caries Res.* 35, 65–70. doi: 10.1159/000049114

van Loveren, C., Buys, J. F., de Soet, J. J., de Graaff, J., and Ten, C. J. (1991). Competition between fluoride-resistant and fluoride-sensitive streptococcus mutans in rat dental plaque. *Caries Res.* 25, 424–430. doi: 10.1159/000261405

van Loveren, C., Hoogenkamp, M. A., Deng, D. M., and Ten, C. J. (2008). Effects of different kinds of fluorides on enolase and atpase activity of a fluoride-sensitive

and fluoride-resistant streptococcus mutans strain. *Caries Res.* 42, 429–434. doi: 10.1159/000159606

Vanloveren, C., Vandeplasschesimons, Y. M., Desoet, J. J., Degraaff, J., and Tencate, J. M. (2010). Acidogenesis in relation to fluoride resistance of streptococcus mutans. *Mol. Oral Microbiol.* 6, 288–291. doi: 10.1111/j.1399-302x.1991.tb00494.x

Zhu, L., Zhang, Z., and Liang, J. (2012). Fatty-acid profiles and expression of the fabm gene in a fluoride-resistant strain of streptococcus mutans. *Arch. Oral Biol.* 57, 10–14. doi: 10.1016/j.archoralbio.2011.06.011

Conflict of Interest: The authors declare that the research was conducted in the absence of any commercial or financial relationships that could be construed as a potential conflict of interest.

Publisher's Note: All claims expressed in this article are solely those of the authors and do not necessarily represent those of their affiliated organizations, or those of the publisher, the editors and the reviewers. Any product that may be evaluated in this article, or claim that may be made by its manufacturer, is not guaranteed or endorsed by the publisher.

Advantages of publishing in Frontiers

OPEN ACCESS
Articles are free to read for greatest visibility and readership

FAST PUBLICATION
Around 90 days from submission to decision

HIGH QUALITY PEER-REVIEW
Rigorous, collaborative, and constructive peer-review

TRANSPARENT PEER-REVIEW
Editors and reviewers acknowledged by name on published articles

Frontiers
Avenue du Tribunal-Fédéral 34
1005 Lausanne | Switzerland

Visit us: www.frontiersin.org
Contact us: frontiersin.org/about/contact

REPRODUCIBILITY OF RESEARCH
Support open data and methods to enhance research reproducibility

DIGITAL PUBLISHING
Articles designed for optimal readership across devices

FOLLOW US
@frontiersin

IMPACT METRICS
Advanced article metrics track visibility across digital media

EXTENSIVE PROMOTION
Marketing and promotion of impactful research

LOOP RESEARCH NETWORK
Our network increases your article's readership